



**Chasing “Zampanalogs”:
Advancing the Synthesis of the
Zampanolide Macrocycle**

By

Sophie Geyrhofer MSc

*A thesis submitted to Victoria University of Wellington in fulfilment
of the requirements for the degree of Doctor of Philosophy*

Victoria University of Wellington
School of Chemical and Physical Sciences

(2018)

To be what we are,
and to become what we are capable of becoming,
is the only end of life.

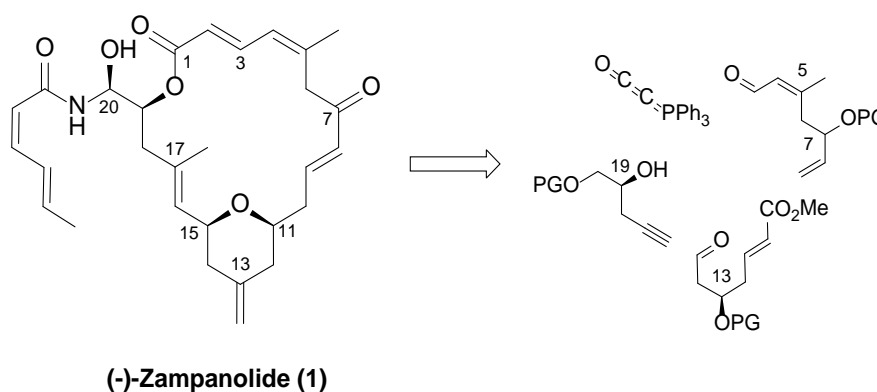
Robert Louis Stevenson

To all those who have supported me
and helped me back on track when I was lost.

You know who you are.

Abstract

(-)-Zampanolide (**1**), a natural product isolated from a marine sponge, is a microtubule-stabilizing agent that exhibits activity in the nanomolar range against various cancer cells, including in P-gp pump overexpressing cells. This attribute makes (-)-zampanolide an interesting target for further investigation. In this work, a new method for a modular and convergent total synthesis of optically pure zampanolide was investigated, which would also allow the generation of “zampanalogs” following the same basic strategy. Their biological activity may then be assessed to allow the elucidation of structure-activity relationships of (-)-zampanolide and its analogs in tubulin binding.



The synthetic plan consisted of the modular combination of four major fragments, which would be connected in the late stages of the synthesis and could therefore be easily exchanged to allow the generation of analogs. The C15-C16 bond would be connected *via* an alkylation reaction, and a subsequent reductive methylation would install the trisubstituted alkene. The connections at C1 and C3 could be achieved through a Bestmann ylide linchpin reaction, while the macrolactonization would be completed using a ring-closing metathesis to form the C8-C9 alkene. The side chain could be attached at C20 using one of the established aza-aldol methods.

The fragments necessary for the formation of the macrocycle were synthesized successfully. The purification strategy throughout the synthetic route was rationalized and provides an improvement with respect to yield and time compared to work previously done in this research group. Alongside these fragments, modified fragments that were originally intended to serve as model systems were synthesized, which could also be used as building blocks in the synthesis of “zampanalogs”.

Several methods for a stereoselective alkynylation at C15 were tested. These led to only meager successes, so an approach using a non-stereoselective alkynylation, followed by oxidation and a stereoselective CBS-reduction, was chosen. For the installation of the trisubstituted alkene a reductive methylation with vitride was tested, but this only led to the reduction of the alkyne without methylation. This product may be employed for the synthesis of C17-desmethyl analogs. The reductive methylation at C16-C17 was ultimately achieved using the Gilman reagent in a similar manner to the installation of the C5 methyl group in the C3-C8 fragment.

A linchpin strategy with the Bestmann ylid simultaneously formed the connectivity at C1 and C3. This process was successfully performed on multiple substrates arising from the model systems used in the alkynylation and reductive methylation reactions, yielding precursors to the ring-closing metathesis and potentially enabling the synthesis of various analogs.

The ring-closing metathesis proved to be difficult in analogs lacking the C17 methyl group and *cis*-tetrahydropyran ring, and due to this tendency further investigations are necessary. Once the macrocycle has been closed, a global

deprotection and oxidation of hydroxy groups is necessary to allow for the installation of the sidechain.

Acknowledgments

Writing a PhD thesis is like climbing a mountain. There are lots of ups and downs. In one moment, you feel like nothing can stop you and you're able to achieve whatever you set out to do, and in the next, you just want to pack it all in, turn around and go home. However, in the end, when you're on top of that mountain and look back on what you've achieved, it's all worth it.

First and foremost, I would like to thank my primary supervisor Dr. Joanne Harvey, who decided to give me the chance to come to New Zealand and work in her research group. I will be forever grateful for this opportunity and all the support and guidance, before, during and after conducting the work and writing this thesis.

Many thanks also go to my secondary supervisor, Dr. Paul Teesdale-Spittle, who helped with words and deeds whenever the need arose, and Monday morning puns which were not needed but much appreciated.

Even though I've nearly seen a complete change of the research group during the course of my thesis, it's still an awesome bunch of people. My thanks to Dr. Jinging Wang, Dr. Kalpani Somarathne, Dr. Hemi Cumming, Dr. Thomas Bevan, Dr. Claire Cuyamendous, Amira Brackovic, Tao Xu, Ethan Woolly, Jordan McCone, Matt Fisk, Dan Phipps, Hedley Stirrat, Loïc Lassueur, Sarah Brown, Ben Durrant, Helena Wong, Jasmin Riesterer, José-Luis Pinedo-Rivera, Chris Orme, James Francis-Taylor, Ash Asbury, Paris Watson and Phoebe Harnos.

Special thanks go to Jingjing, who started this project off, not only for helping me so much during my first few months here, but also for literally climbing a mountain with me. I would also like to thank Amira, who's been my confidant when my relationship with chemistry was going through some rough times, and Jordan McCone for proofreading this thesis and help with some finishing touches.

Several people from outside the group deserve to be thanked as well: Ian Vorster, who, like a firefighter, responded to calls nearly 24/7 to help out with NMR and MS troubles; Teresa Gen, who let me borrow glassware and chemicals and kept reminding all the undergrads that I am not German and therefore helped to preserve my sanity; Struan Cummins for his help with reactions conducted in the glovebox.

Last but not least, I would like to thank my friends and family. Julia P. and Lisa B., you are my squad, no physical distance will ever change that. Julia S. and I have been on the same journey for the last three years, arriving in New Zealand only days apart, and finishing our PhD's in chemistry only a month apart. Your friendship and support was and still is invaluable to me. Sam S., without your support during those last six months I'm not sure I would've finished writing, now or ever. You are my inspiration. My deepest gratitude to my sister Verena, who's always lent me an ear if I had to vent and provided me with plenty of pictures of our family cat to cheer me up. Special thanks go to my mum and dad, who've both supported me unconditionally, from the crib until today. If not for you, I wouldn't be where I am today. Thank you

Table of Contents

Abstract.....	vi
Acknowledgments	ix
Table of Contents	xi
List of Figures.....	1
List of Tables.....	3
List of Schemes	5
Abbreviations	12
Cell Lines	15
Chapter 1: Introduction	16
1.1 Cancer: Motivation for this Work	16
1.2 Classes of Chemotherapeutic Drugs.....	16
1.3 Microtubule-Targeting Agents.....	19
1.3.1 Microtubule Dynamics.....	19
1.3.2 Microtubule-Destabilizing Agents.....	20
1.3.3 Microtubule-Stabilizing Agents: Paclitaxel, Docetaxel and the Epothilones	22
1.4 Zampanolide: A Novel Microtubule-Stabilizing Agent	23
1.4.1 Isolation and Structure Elucidation.....	23
1.4.2 Biological Activity and Binding to Tubulin.....	25
1.5 Analogue and SAR Studies	29
1.5.1 Biological Testing of Uenishi's and Ghosh's Analogs	29
1.5.2 Altmann's Structure-Activity Relationship Studies.....	31
Chapter 2: Previous Synthetic Work and Retrosynthetic Approach.....	35
2.1 Published Syntheses of Zampanolide and Dactylolide	35

2.1.1	Smith's Total Synthesis of (+)-Zampanolide (2001).....	36
2.1.2	Hoye's Total Synthesis of (-)-Dactylolide (2003)	38
2.1.3	Floreancig's Total Synthesis of (+)-Dactylolide (2005)	39
2.1.4	Jennings' Total Synthesis of (-)-Dactylolide (2005)	41
2.1.5	Keck's Total Synthesis of (+)-Dactylolide (2005)	42
2.1.6	McLeod's Total Synthesis of (-)-Dactylolide (2006).....	43
2.1.7	Porco's Total Synthesis of the Macrocyclic Core of (-)-Zampanolide (2008)	43
2.1.8	Uenishi's Total Synthesis of (-)-Zampanolide (2009).....	45
2.1.9	Lee's Total Synthesis of (-)-Dactylolide (2010).....	48
2.1.10	Ghosh's Total Synthesis of (-)-Zampanolide (2011)	49
2.1.11	Hong's Total Synthesis of (+)-Dactylolide (2012).....	51
2.1.12	Altmann's Total Synthesis of (-)-Dactylolide (2010), (-)-Zampanolide And Analogs Thereof (2012).....	52
2.2	Previous Work in the Harvey group	54
2.2.1	Ting's Work on Fragments	54
2.2.2	Gray's Work on Fragments for the Synthesis of Sidechain Analogs	58
2.2.3	Wang's Synthesis of the C5-Desmethyl Fragment	60
2.2.4	Wang's Scope Studies on the Bestmann Ylid Linchpin.....	62
2.3	Aim of This Thesis	64
2.4	First Generation Retrosynthetic Approach Based on Wang's Thesis	65
Chapter 3: Fragment Synthesis and Second Generation Retrosynthetic Approach		68
3.1	Synthesis of the C3-C8 Fragment.....	68
3.2	Synthesis of the C9-C15 Fragment.....	71
3.2.1	Synthesis of the C12 Desmethylene Fragment.....	76
3.3	Synthesis of the C16-C20 Fragment and Model for Alkynylation.....	78

3.4	Second Generation Retrosynthetic Approach.....	81
Chapter 4:	Connecting C15-C16: Alkynylation.....	85
4.1	Stereoselective Alkynylation.....	86
4.1.1	Shibasaki's Method Using Indium Bromide	86
4.1.2	Carreira's Method Using Zinc Triflate	87
4.1.3	Pu's Method Using Diethyl Zinc and BINOL/H8-BINOL	89
4.1.4	Trost's Method using Dialkyl Zinc and Propenol	93
4.2	Non-Stereoselective Alkynylation.....	102
4.3	Summary of Chapter 4: Connecting C15-C16: Alkynylation.....	105
Chapter 5:	Conversion of the C16-C17 Alkyne to an Alkene: Reducti(ve methylati)on	106
5.1	Reductive Methylation of the Propargylic Alcohol.....	107
5.1.1	Jamison's Method Using Vitride®/MeLi/CuCl/RX	107
5.1.2	Corey's Method Using LAH/NaOMe	114
5.1.3	Negishi's Method Using AlMe ₃ /Cl ₂ ZrCp ₂	116
5.2	Reductive Methylation of the Alkynone	119
5.3	Setting the Configuration at C15.....	124
5.4	Protecting Group Adjustments	127
5.5	Summary of Chapter 5: Conversion of the C16-C17 Alkyne to an Alkene: Reducti(ve methylati)on.....	128
Chapter 6:	Formation of the cis-Tetrahydropyran Ring.....	130
6.1	Pd(II)-Catalyzed Tetrahydropyran Formation.....	131
6.2	Tetrahydropyran Formation <i>via</i> <i>O</i> -Michael Reaction.....	136
6.2.1	Cross-metathesis and <i>O</i> -Michael Reaction	140
6.3	Modifications to Prepare for RCM	145
6.4	Summary of Chapter 6	147

Chapter 7: Late Stage Connections: Bestmann Ylid Linchpin and Ring-Closing Metathesis	148
7.1 Analog 1: Non-THP Alkyne Analog	149
7.2 Analog 2: Non-THP C17-Desmethyl C15 Ketone Analog	151
7.3 Analog 3: Non-THP C15 Ketone Analog.....	153
7.4 Analog 4: Non-THP C17-Desmethyl Analog.....	153
Chapter 8: Conclusion and Future Work	156
Chapter 9: Experimental	159
9.1 General Experimental Data	159
9.2 Reagent Synthesis and Purification	160
9.3 General Procedures	162
9.3.1 Oxidations	162
9.3.2 Alkynylations	164
9.3.3 Alkyne Transformations	166
9.4 Chapter 3: Fragment Synthesis and Second Generation Retrosynthetic Approach.....	169
9.5 Chapter 4: Connecting C15-C16: Alkynylation	198
9.6 Chapter 5: Conversion of the C16-C17 Alkyne to an Alkene: Reducti(ve methylati)on	205
9.7 Formation of the cis-Tetrahydropyran Ring.....	216
9.8 Late Stage Connections: Bestmann Ylid Linchpin and Ring-Closing Metathesis	223
References	231
Appendix	241

List of Figures

Figure 1-1 Assembly and disassembly of microtubules from α - and β -tubulin heterodimers. Unpublished. © Jessica Field 2011.	20
Figure 1-2 Chemical structures of halichondrin B (2) and eribulin (3).....	21
Figure 1-3 Chemical structures of paclitaxel (4) and its semi-synthetic analog docetaxel (5). The highlighted regions show the differences between the natural product and the analog.	22
Figure 1-4 Chemical structures of epothilone B (6) and its semi-synthetic analog ixabepilone (7). The highlighted region shows the difference between the parent compound and the analog.....	23
Figure 1-5 Structures of (-)-zampanolide (1 , ZAMP) and (+)-dactylolide (8 , DACT).	24
Figure 1-6 Effects of 10 nM zampanolide (ZAMP) and 10 nM paclitaxel (PAX) on 1A9 human ovarian carcinoma cells after 12 hours. α -Tubulin was stained to visualize microtubules, revealing the formation of microtubule bundles in interphase cells (arrows), and multiple spindle asters in mitotic cells. Adapted with permission from <i>J. Med. Chem.</i> 52 , 7328–7332 (2009). Copyright (2018) American Chemical Society.....	26
Figure 1-7 Crystal structure of the interaction between (-)-zampanolide and the β -tubulin subunit of the α - and β -tubulin heterodimers from two different angles. Hydrogen bonds are depicted with black dashed lines, while the covalent bond to C9 is represented as orange stick. From <i>Science</i> , 339 , 587–590 (2013). Reprinted with permission from AAAS.....	29
Figure 1-8 Structures of the analogs synthesized by Altmann's research group and classified according to their modifications.....	32
Figure 2-1 The main disconnection points utilized in the synthesis of the zampanolide macrocycle and natural product.....	35
Figure 2-2 Chemical structure of the chiral phosphoric acid S-TRIP used by Gosh's group to install the N-acyl hemiaminal functionality of (-)-zampanolide.	51

Figure 2-3 Structures of proposed analogs.	64
Figure 4-1 Comparison of the proton NMR spectra of 155 and 160	91
Figure 5-1 Proton NMR spectrum of 170	111
Figure 5-2 NOESY correlation suggesting the main product is the desired E-isomer 186	122
Figure 5-3 Proton NMR of E-alkene 186 and NOE correlation between H1 and H5.	122
Figure 5-4 Shielding and deshielding effects on the protons in the (S)-(-)-MTPA ester and (R)-(+)-MTPA ester product	125
Figure 5-5 Comparison of the proton NMR spectra of the (S)-(-)-MTPA and (R)-(+)-MTPA product	126
Figure 6-1 Proton and carbon NMR spectra of ketone 194	134
Figure 6-2 By-product of the O-Michael reaction of Uenishi and co-workers....	137
Figure 8-1 Potential analogs resulting from the research conducted in this thesis.	158

List of Tables

Table 1.1 IC ₅₀ values of (-)-zampanolide (natural and synthetic), (-)-dactylolide and paclitaxel in ovarian carcinoma cells A2780 and P-gp overexpressing A2780AD cells. R/S is the relative resistance of the A2780D cell line and is obtained by dividing the IC ₅₀ of the resistant cell line by that of the parental A2780 cell line.	27
Table 1.2 IC ₅₀ values (in nM) of paclitaxel (4), zampanolide (1), the C20 epimer of zampanolide (epi-1) and the bis(N-acyl) product (10) in various cancer cell lines, including the P-gp efflux pump-overexpressing cell line NCI/ADR-RES.....	31
Table 1.3 IC ₅₀ values in nM for zampanolide, dactylolide and analogs synthesized by the Altmann group in four different cell lines, adapted from Ref. ³⁵	33
Table 2.1 Bestmann ylid cascade reaction of the zampanolide fragments 112 and 113 with E-cinnamaldehyde 115 in refluxing THF or toluene. ^a The product was contaminated with the regioisomer resulting from silyl migration and esterification of the primary alcohol.	63
Table 3.1 Optimization conditions for the deprotection of the primary TES group using PPTS in MeOH. ^a The ratio of 140 to 142 was determined by analysis of the ¹ H NMR spectrum of the crude mixture.	75
Table 4.1 Reaction conditions tested for the stereoselective alkynylation following Pu's methodology.	92
Table 4.2 Optimization conditions for the stereoselective alkynylation between 155 and 147	97
Table 4.3 Optimization conditions for the stereoselective alkynylation between 156 and 147	98
Table 4.4 Optimization conditions for the stereoselective alkynylation between 157 and 147	99
Table 4.5 Possible diastereomers generated in the reaction of the diastereomeric mixture of (S,S)- 162 and (S,R)- 162 with (S)- and (R)-MTPA respectively.	100
Table 4.6 Tested substrates for the non-stereoselective alkynylation.	102

Table 4.7 Optimization conditions for the non-stereoselective alkynylation using EE protected alkyne starting material.	104
Table 5.1 Materials tested with Jamison's reductive methylation protocol.....	109
Table 5.2 Different substrates tested in the adapted trans-hydroalumination reaction.....	110
Table 5.3 Different alkyl halides and other additives used for the trans-hydroalumination/alkylation reaction.	112
Table 5.4 Trans-hydroalumination/alkylation reactions performed on EE protected DB product.....	114
Table 5.5 Conditions and substrates used for the reductive iodination reaction with LAH and NaOMe.....	116
Table 5.6 Conditions and substrates tested for the reductive methylation/iodination following Negishi's procedure.....	118
Table 6.1 Cross-metathesis reactions performed to prepare for the O-Michael addition.	141
Table 6.2 Comparison of ¹ H-NMR shifts between Uenishi's cis- and trans-THP compound, and the THP-containing compounds synthesized in this work.....	144

List of Schemes

Scheme 1.1 Uenishi's and Ghosh's formation of zampanolide (1), C20 epimer of zampanolide (epi-1) and the bis(N-acyl) product 10 from the CSA-promoted reaction of dactyloidide (4) with (2Z,4E)-hexa-2,4-dienamide 10	30
Scheme 2.1 Smith's total synthesis of (+)-zampanolide (ent-11), featuring a HWE reaction as macrolactonization step, a Julia-Kocienski reaction to form the C8-C9 bond and a Curtius rearrangement to generate the hemiaminal sidechain.	36
Scheme 2.2 Installation of the sidechain of zampanolide in Smith's synthesis through a Curtius rearrangement and subsequent acylation.	37
Scheme 2.3 Petasis-Ferrier rearrangement leading to the synthesis of the cis-THP ring in Smith's zampanolide synthesis.	37
Scheme 2.4 Hoye's total synthesis of (-)-dactyloidide featuring two distinct macrocyclization strategies: a novel Ti(IV)-mediated macrolactonization of epoxy-acid and a complementary RCM macrocyclization. The cis-THP is formed via an intramolecular Sakurai cyclization.	39
Scheme 2.5 Floreancig's total synthesis of (+)-dactyloidide using a Peterson olefination and Prins reaction to generate the cis-THP ring, and a HWE reaction to close the macrocycle.	40
Scheme 2.6 Formation of the cis-THP ring through a Peterson olefination followed by a Prinsreaction.	40
Scheme 2.7 Formation of acetal intermediate 27 from two advanced synthetic fragments.	41
Scheme 2.8 Jennings' total synthesis of (-)-dactyloidide, using a Yamaguchi esterification to connect building blocks 28 and 29 , and a RCM as ring-closing step.	42
Scheme 2.9 Keck's total synthesis of (+)-dactyloidide using HWE reactions for connecting two major fragments and closing the macrocycle, and a Prins reaction to form the cis-THP ring.	42

Scheme 2.10 McLeod's total synthesis of (-)-dactylolide, featuring a Mitsunobu esterification as ring-closing step. The trisubstituted alkene at C16-C17 was installed through an Ireland-Claisen rearrangement. A hetero-Diels-Alder reaction was used to generate the cis-THP ring.....	43
Scheme 2.11 Porco's total synthesis of (-)-zampanolide. A Stedlich esterification is used to establish the ester moiety at C1, and the macrocycle is closed through a Stille coupling. The cis-THP ring is formed via a Sakurai reaction.	44
Scheme 2.12 Sakurai reaction used in Porco's synthesis of the macrocyclic core of (-)-zampanolide to form the cis-THP ring.	44
Scheme 2.13 a) One of Porco's model compounds, which was used in ¹ H NMR experiments to confirm the existence of a hydrogen bonding network as shown in b). These results strongly suggest the existence of a similar hydrogen-bonding network in (-)-zampanolide, c). Adapted with permission from Troast, D. M. & Porco Jr., J. A., <i>Org. Lett.</i> 4 , 991–994 (2002). Copyright 2018 American Chemical Society.	45
Scheme 2.14 Uenishi's synthesis of (-)-zampanolide, featuring a N-hemiacetalization, an HWE reaction and a new method for the macrolactonization using the Trost-Kita method for esterifications.	46
Scheme 2.15 Uenishi and coworkers employed a Sakurai reaction and subsequent O-Michael reaction to form the cis-THP ring of (-)-zampanolide.....	47
Scheme 2.16 Byproducts formed in the reaction of dactylolide with sidechain 47 , catalyzed by CSA.	47
Scheme 2.17 Lee's total synthesis of (-)-dactylolide featuring a Suzuki coupling to connect building blocks 52 and 53 , and a RCM to close the macrocycle.	48
Scheme 2.18 Formation of boronic half ester 53	49
Scheme 2.19 Lee and coworkers used a RCAER (ruthenium-catalyzed Alder-ene reaction to connect fragments 56 and 57 and to form the exomethylene group, followed by a Pd-catalyzed cyclization to form the cis-THP ring.....	49
Scheme 2.20 Ghosh's total synthesis of (-)-zampanolide. A Yamaguchi esterification was used to connect the two major building blocks 59 and 60 at C1, followed by a RCM to close the macrocycle at C8-C9.....	50
Scheme 2.21 Formation of the cis-THP ring leading to fragment 59	50

Scheme 2.22 Synthesis of Ghosh's C1-C8 fragment 60	51
Scheme 2.23 Hong's total synthesis of (+)-dactylolide, using a NHC-catalyzed reaction as the ring-closing step. The bond between C6-C7 is formed through a cyanohydrin umpolung alkylation. The cis-THP ring is formed through an asymmetric organozinc addition, followed by an O-Michael reaction.	52
Scheme 2.24 Altmann's total synthesis of (-)-dactylolide. Building blocks 69 and 70 are connected via Yamaguchi esterification. A HWE reaction is used to close the macrocycle. The cis-THP is formed through a Prins reaction, followed by iodine displacement olefination and carbostannylation/iodination reaction.	53
Scheme 2.25 Ting's retrosynthetic strategy featuring a NHK-reaction, esterification and RCM as major disconnections.	55
Scheme 2.26 Ting's attempted synthesis of the C1-C8 fragment, using a carboalumination/iodination reaction followed by a Stille coupling.....	55
Scheme 2.27 Ting's alternative synthesis of the top fragment in seven steps. The sequence failed in the last step, the Stille coupling.	56
Scheme 2.28 Ting's strategy for the synthesis of the C16-C20 fragment.....	57
Scheme 2.29 Ting's second attempt at the synthesis of the C16-C20 fragment using glycidol as starting material.	58
Scheme 2.30 Gray's synthesis of sidechain analogs using two different methods.	59
Scheme 2.31 Proposed synthesis for Fragment D.	60
Scheme 2.32 Wang's attempted synthesis of the C5-desmethyl building block. .	60
Scheme 2.33 Wang's successful reactions leading to the desired configuration of the C4-C5 alkene.	61
Scheme 2.34 Different conditions tested by Wang for the oxidation of alcohol 108 to C5-desmethyl fragment 110 and byproduct 111	62
Scheme 2.35 Bestmann ylid cascade reaction to connect the C16-C20- fragment (112 , 113 and 116) with the C3-C8 aldehyde fragment 117	63
Scheme 2.36 Retrosynthetic approach as devised by Wang.	66
Scheme 2.37 Suggested methods to form the pyran ring.....	67
Scheme 3.1 Reaction scheme for the synthesis of fragment 117	68

Scheme 3.2 Transition state of the reductive methylation using Gilman's reagent and OE correlation used to confirm the correct product 132	70
Scheme 3.3 Reaction scheme for the synthesis of compound 139 , which serves as precursor for building block 128	71
Scheme 3.4 Mechanism for the retention of configuration in the Sandmeyer-type reaction of 134 to 135	72
Scheme 3.5 Deprotection and oxidation to convert protected dial 139 into aldehyde 141	73
Scheme 3.6 Proposed mechanisms for acetylation of the hydroxy group in the presence of water.	73
Scheme 3.7 Ozonolysis of 139 to afford fragment 143 ready for stereoselective alkynylation reactions.	76
Scheme 3.8 Oxidation conditions used in this work to oxidize 145 to 144	77
Scheme 3.9 Conditions used for the oxidation of 145 to 144 by Wang and possible mechanisms for the dimerization of the product via aldol reaction.	77
Scheme 3.10 Synthesis for alternative aldehyde 147 through a protection/ozonolysis sequence.....	78
Scheme 3.11 Synthesis of compound 151 which serves as C16-C20 building block and model compounds 153 for alkynylation, as well as the failed synthesis of a model for the sidechain attachment.....	79
Scheme 3.12 Yields for the synthesis of 155 which serves as C16-C20 building block with PMB ether instead of TBDPS ether as protecting group, along with 156 , which was used for subsequent alkynylation studies.	81
Scheme 3.13 Second generation retrosynthetic approach with revised protecting group strategy and order of events.	82
Scheme 3.14 Mechanism of the oxidative cyclization pathway to from PMP acetal 156 , as proposed by Gamboni et al.....	83
Scheme 3.15 Oxidative PMP protection and planned subsequent reactions.	84
Scheme 3.16 Protection of alcohol 116 as acetate (157) or ethoxyethyl ether (158) in excellent yields.	84

Scheme 4.1 The connection at C15 of (-)-zampanolide was envisaged to be performed via a stereoselective alkynylation reaction, also setting the desired stereochemistry at C15.....	85
Scheme 4.2 Shibasaki's alkynylation method using InBr ₃ and BINOL as chiral ligand.....	86
Scheme 4.3 Attempted stereoselective alkynylation using Shibasaki's method..	87
Scheme 4.4 Carreira's alkynylation method.....	87
Scheme 4.5 Attempted stereoselective alkynylation using adaptation of Carreira's method.....	88
Scheme 4.6 Pu's alkynylation method, generating diethyl zinc in situ.....	89
Scheme 4.7 Pu's working hypothesis for the reaction of Zn, EtI, an alkyne and an aldehyde promoted by BINOL-Ti(O ⁱ Pr) ₄	90
Scheme 4.8 Stereoselective alkynylation using Pu's method, generating diethyl zinc in situ.....	90
Scheme 4.9 Trost's stereoselective alkynylation using Me ₂ Zn and ProPhenol...	94
Scheme 4.10 Trost's proposed mechanism for the ProPhenol-catalyzed alkynylation of aldehydes.....	95
Scheme 4.11 Stereoselective alkynylation using Trost's method.	96
Scheme 4.12 Formation of the byproduct formed through TCPC addition to the alcohol under Yamaguchi esterification conditions.....	101
Scheme 4.13 Shielding and de-shielding effects utilized in the Mosher ester analysis.	101
Scheme 5.1 Necessary transformation to install the trans-alkene in zampanolide and C17-desmethyl analogs.	106
Scheme 5.2 Mechanism for trans-hydroalumination step.	108
Scheme 5.3 Goswami's attempt at a trans-hydroalumination/alkylation.....	111
Scheme 5.4 Corey's method for reduction of an alkyne and iodination using LAH and an additive, followed by a quench with iodine.	115
Scheme 5.5 Negishi's method to form trisubstituted alkenes from terminal alkynes using AlMe ₃ and Cl ₂ ZrCp ₂	117
Scheme 5.6 Reaction of ynoates and ynones with Gilman reagent.....	119

Scheme 5.7 Manganese dioxide oxidation of propargylic alcohol to the corresponding ynone.....	120
Scheme 5.8 Reductive methylation of 181 using Gilman reagent.....	120
Scheme 5.9 Attempted deprotection of compounds 182 and 183 resulting in dehydration.....	121
Scheme 5.10 Possible mechanism for the formation of the E-alkene over the Z-alkene via an allene intermediate.....	123
Scheme 5.11 Manganese dioxide oxidation of diastereomeric alcohol (S,S/R)- 174 to ketone (S)- 188 , followed by stereoselective CBS-reduction back to the now single diastereomeric alcohol (S,S)- 174	124
Scheme 5.12 Change of protecting groups to prepare for the Bestmann ylid cascade and subsequent synthesis of non-THP analogs.....	127
Scheme 6.1 Proposed THP ring formation via Pd-catalyzed carboxylative cyclization or O-Michael reaction.....	130
Scheme 6.2 White's Pd-catalyzed carboxylative cyclization to form substituted THP rings.....	132
Scheme 6.3 Two initial attempts at the Pd-catalyzed carboxylative cyclization using PdCl ₂ (Method A) and Pd(OAc) ₂ (Method B).....	133
Scheme 6.4 Ketone 194 formed in the Pd-catalyzed carboxylative cyclization/deprotection sequence.....	133
Scheme 6.5 Proposed mechanism for the formation of Wacker product 195 and deprotection of the formed acetal to give ketone 194	135
Scheme 6.6 Adjusted conditions to avoid the Wacker reaction.....	135
Scheme 6.7 Uenishi's method for the cis-THP formation in the zampanolide system.....	136
Scheme 6.8 Possible options to synthesize RCM precursor 201 from the reductive methylation product 197 via three different pathways using cross-metathesis, cyclization and reduction/oxidation steps.....	138
Scheme 6.9 A. Hong's method for a tandem allylic oxidation/oxa-Michael reaction to form a cis-THP ring. B. Axial interactions leading to the preferred formation of the cis-THP over the trans-THP.....	140

Scheme 6.10 Attempt at a tandem allylic oxidation/O-Michael addition reaction.	141
Scheme 6.11 cis-THP formation using TMEDA and LHMDS.	143
Scheme 6.12 Overview of the transformations of the reduction product 174 to the cis-THP-containing compound cis-213 , including all protection/deprotection steps.	145
Scheme 6.13 Necessary transformation to set up for the subsequent RCM.	146
Scheme 6.14 Reduction of methyl ester 213 to aldehyde 214 in preparation for the Wittig reaction.	146
Scheme 7.1 Synthesis of the Bestmann ylid reagent.	148
Scheme 7.2 Overview of the major late step connections, namely Bestmann ylid linchpin and RCM.	149
Scheme 7.3 Tested conditions for the mono-protection of the alkyne substrate in preparation for the Bestmann ylid coupling.	150
Scheme 7.4 Bestmann ylid linchpin performed on the mono-protected alkyne starting material.	150
Scheme 7.5 Attempted RCM reaction to form Analog 1, a non-THP analog with an alkyne in place.	151
Scheme 7.6 Transformations performed to synthesize the substrate for the Bestmann ylid linchpin.	152
Scheme 7.7 Attempted Bestmann ylid linchpin to form the precursor for Analog 3.	152
Scheme 7.8 Attempted Bestmann ylid linchpin to form the precursor for Analog 4.	153
Scheme 7.9 Bestmann ylid linchpin performed on the mono-protected starting material 191 with the trans-alkene in place.	154
Scheme 7.10 Attempted methods for the RCM reaction to produce the non-THP C17-desmethyl analog.	154
Scheme 7.11 Proposed unraveling of the nearly completed macrocycle into three six-membered rings.	155

Abbreviations

Ac	Acetyl
BAIB.....	(Diacetoxyiodo)benzene
BINOL.....	1,1'-Bi-2-naphthol
Boc	<i>tert</i> Butyloxycarbonyl
BRSM	Based on recovered starting material
CBS.....	Corey-Bakshi-Shibata
CSA.....	Camphorsulfonic acid
DACT.....	Dactylolide
DCC	<i>N,N'</i> Dicyclohexylcarbodiimide
DCE	1,2-Dichloroethane
DCM	Dichloromethane
DDQ.....	2,3-Dichloro-5,6-dicyano-1,4-benzoquinone
DIBAL-H	Diisobutylaluminum hydride
DIPEA	<i>N,N'</i> -Diisopropylethylamine
DMAP	Dimethylaminopyridine
DMB	Dimethoxybenzyl
DMF.....	<i>N,N</i> -Dimethylformamide
DNA.....	2-Deoxyribonucleic acid
Dppf.....	1,1'-Bis(diphenylphosphino)ferrocene
EE.....	1-Ethoxyethyl
FCC.....	Flash column chromatography
FDA	US Food and Drug Administration
GDP	Guanosine diphosphate
GTP.....	Guanosine triphosphate
HR-FABMS.....	High resolution fast-atom bombardment mass spectrometry
HMDS.....	bis(trimethylsilyl)amide
HRMS	high-resolution mass spectrometry

HWE	Horner-Wadsworth-Emmons
IBX.....	2-Iodoxybenzoic acid
IC ₅₀	Inhibition concentration: concentration of an inhibitor where the response (typically growth) is reduced by half
IR	Infrared
LAH	Lithium aluminum hydride
MDA	Microtubule-destabilizing agent
MSA.....	Microtubule-stabilizing agent
MTA.....	Microtubule-targeting agent
MTPA	α -Methoxy- α -trifluoromethylphenylacetic acid
NHC-cat.	<i>N</i> -heterocyclic carbene catalyzed
NHK	Nozaki-Hiyama-Kishi
NMR	Nuclear magnetic resonance
NOE.....	Nuclear Overhauser Effect
NOESY	NOE spectroscopy
ODS	Octadecasilyl
PAX.....	Paclitaxel
PCC.....	Pyridinium chlorochromate
PDC	Pyridinium dichromate
PE	Petroleum ether
PG	Protecting group
Piv.....	Pivaloyl (tert-butyloxycarbonyl)
PMB.....	<i>para</i> -Methoxybenzyl ether
PMP	<i>para</i> -Methoxyphenyl
PPTS.....	Pyridinium <i>para</i> -toluenesulfonate
ProPhenol.....	2,6-Bis[2-(hydroxydiphenylmethyl)-1-pyrrolidinylmethyl]-4-methylphenol
p-TsOH	p-Toluenesulfonic acid
RBF.....	Round-bottom flask
RCAER	Ruthenium-catalyzed Alder-Ene reaction
RCM.....	Ring-closing metathesis
Ref.....	Reference

Rf	Retention factor
RNA	Ribonucleic acid
SAR.....	Structure-activity relationship
SET	Single-electron transfer
SM	Starting material
S-TRIP	(S)-3,3'-bis(2,4,6-triisopropylphenyl)-1,1'-binaphthyl-2,2'-diylhydrogenphosphate
TBAF	Tetrabutylammonium fluoride
TBAI	Tetrabutylammonium iodide
TBDPS.....	<i>tert</i> -Butyldiphenylsilyl
TBS	<i>tert</i> -Butyldimethylsilyl
TCBC	2,4,6-Trichlorobenzoyl chloride
TEMPO.....	2,2,6,6-Tetramethylpiperidin-1-yl)oxyl
Teoc.....	Trimethylsilylethoxycarbonyl
TES	Triethylsilyl
THF	Tetrahydrofuran
THP	Tetrahydropyran
TLC.....	Thin-layer chromatography
TMA.....	Trimethylaluminum
TMEDA	<i>N,N,N',N'</i> -Tetramethylethylene-1,2-diamine
TMS	Trimethylsilyl
TPPO	Triphenylphosphine oxide
WHO	World Health Organization
ZAMP.....	Zampanolide

Cell Lines

1A9.....	Clone of the human ovarian carcinoma cell line, A2780
A2780.....	Human ovarian cancer cell line
A2780.....	Derived from A2780 cells, P-gp pump overexpressing
A-549	Adenocarcinomic human alveolar basal epithelial cell line
HCT-116	Human colon cancer cells
HT-29.....	Human colon adenocarcinoma cell line
MCF-7.....	Human breast adenocarcinoma cell line
NCI/ADR-RES.....	Derived from OVCAR-8, P-gp pump overexpressing
OVCAR-8.....	Human ovarian cancer cell line
P-388.....	Menogaril-resistant mouse leukaemia cells
PC-3.....	Human prostate cancer cell line
SKM-1.....	Human leukemic cell line
SK-MEL-28	Melanoma cell line
SK-OV-3	Human ovarian cancer cell line with epithelial-like morphology
U937	Human leukemic monocyte lymphoma cell line

Chapter 1: Introduction

1.1 Cancer: Motivation for this Work

In 2015, 8.8 million people died from cancer, as reported by the World Health Organization (WHO). This means that one in six deaths worldwide is caused by this disease, making cancer the second leading cause of death globally (after cardiovascular disease). However, cancer is not one single disease but rather describes a whole group of diseases that can affect any part of the human body. It is characterized by “rapid creation of abnormal cells that grow beyond their usual boundaries, and which can then invade adjoining parts of the body and spread to other organs, the latter process is referred to as metastasizing.”¹ The five deadliest types of cancer (in 2015) in decreasing order are lung cancer (1.69 million deaths), liver cancer (788 000 deaths), colorectal cancer (774 000 deaths), stomach cancer (754 000 deaths) and breast cancer (571 000 deaths).

1.2 Classes of Chemotherapeutic Drugs

The treatment options for cancer are highly dependent on the type and advancement of the respective cancer. The three most common treatment options for cancer include:

1. surgery (physical removal of a tumor);
2. radiotherapy (damage or destruction of cancer cells through exposure to high energy particles or waves);
3. chemotherapy (treatment with drugs).

Chemotherapy itself can be classified into different sub-groups using the way the medicine interacts with the cancer cells. The following groupings are based on the

classification of chemotherapeutic drugs as devised by the American Cancer Society.²

Alkylating agents: These drugs react with the DNA strands and alkylate them in all stages of the cell cycle, which causes permanent damage and keeps the cells from reproducing. The most prominent example of an alkylating agent used as cancer chemotherapeutic drug is *cis*-platin.³

Antimetabolites: Antimetabolites usually resemble nucleotides and interfere with DNA and RNA synthesis by being used as building blocks during the copying process of the chromosomes, rendering the DNA useless and therefore killing the afflicted cells. Examples of antimetabolites used in chemotherapy are 5-fluorouracil and 6-mercaptopurine.^{4,5}

Antitumour antibiotics: This type of chemotherapeutic is not to be confused with antibiotics used to treat infections. Anti-tumour antibiotics interfere with the normal cell cycle by inhibiting enzymes involved in copying DNA, which ultimately leads to cell death. Doxorubicin and mitomycin-C are examples of this class of chemotherapeutic.^{6,7}

Topoisomerase inhibitors: As the name suggests, these drugs interfere with an enzyme class called topoisomerases. These enzymes are involved in the separation of the strands of the DNA during the cell division process, so the DNA can be copied. Inhibition of these enzymes therefore interrupts cell division and leads to cell death. Well known topoisomerase inhibitors include topotecan and etoposide.^{8,9}

Mitotic inhibitors: This class of chemotherapeutic, often derived from natural products, acts by stopping cells from dividing by interfering with microtubule dynamics during the mitotic stage of the cell cycle, which leads to the death of the cell. The best-known chemotherapeutic drugs of this class are ixabepilone, a derivative of the natural product epothilone B, paclitaxel and its derivative docetaxel, as well as vinblastine.¹⁰ (-)-Zampanolide (1), the compound this work focuses on, exhibits the same mode of action in inducing cell death in cancer cells, therefore it is discussed in more detail, in **section 1.4**.

Alongside the aforementioned classes of chemotherapies, there are several more therapies worth mentioning. These therapies are more specific in targeting cancer cells over normal cells than most other chemotherapeutics, by using cancer cell specific features or markers.

Immunotherapy: This type of therapy uses drugs to boost the patient's immune system and “train” it to recognize and attack cancer cells more effectively. The main types of immunotherapy include monoclonal antibodies, immune checkpoint inhibitors and cancer vaccines.^{11,12}

Targeted therapies: Targeted therapy drugs are compounds that work by exploiting differences between normal cells and cancer cells. They specifically target and disrupt processes that cancer cells need to survive but are not present or less prevalent in normal cells, therefore killing the cancer cell without impacting normal cells. Examples of targeted therapy drugs are cetuximab and erlotinib.¹³⁻¹⁵

Hormone therapies: Hormone therapy focuses on the treatment of cancers of the breast, prostate and endometrium with compounds that deprive those tumours of

the hormones they need to grow. An example of a drug that is used to treat certain types of breast cancer is Tamoxifen.¹⁶

1.3 Microtubule-Targeting Agents

Microtubules are an essential part of the cytoskeleton and are in a constant equilibrium involving assembly and disassembly. One of the main functions of microtubules is to help migration of the chromosomes to opposite ends of the cell during mitosis. If the delicate dynamics of microtubule assembly and disassembly are disturbed the affected cell dies, and this can be achieved intentionally with microtubule-targeting agents (MTAs). MTAs have found broad application as not only chemotherapeutics, but also as pesticides and antiparasitics. Many chemicals affecting microtubule dynamics are produced by plants, and it is hypothesized that this might be a way for the plant to avoid predation.¹⁰

1.3.1 Microtubule Dynamics

Microtubules are polymeric clusters made from 13 protofilaments, which themselves consist of heterodimers containing α - and β -tubulin proteins (**Figure 1-1**). The β -tubulin portion in the heterodimer has a guanosine triphosphate (GTP) bound to it, which allows the heterodimers to assemble. The GTP is then hydrolyzed to guanosine diphosphate (GDP), which causes the stabilization of the straight microtubule formation. However, a cap of GTP-containing subunits is necessary to keep the protofilaments associated with each other. If this cap is lost or removed, the protofilaments peel outwards and the microtubule disintegrates.

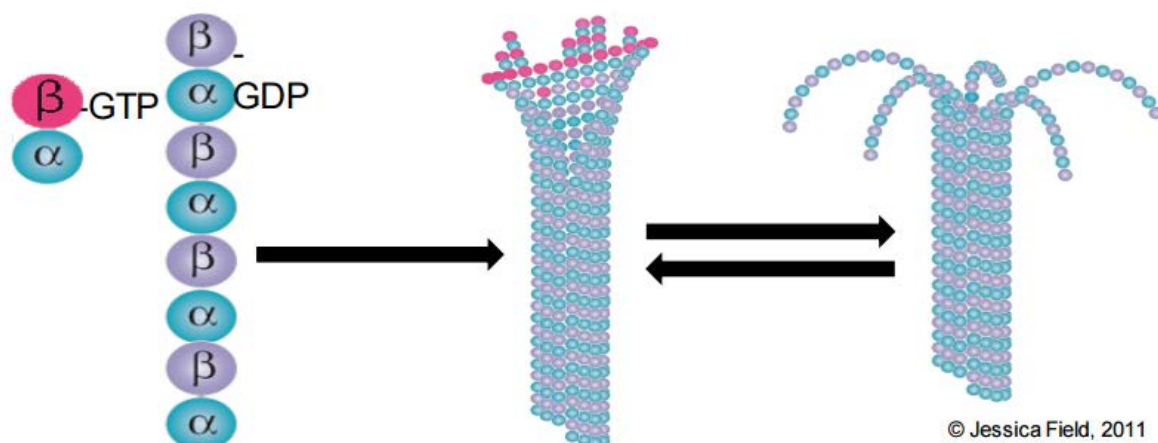


Figure 1-1 Assembly and disassembly of microtubules from α - and β -tubulin heterodimers. Unpublished. © Jessica Field 2011.

There are many natural products that interfere with the dynamics of microtubule assembly and disassembly, and these can be classified into microtubule-destabilizing agents (MDAs) and microtubule-stabilizing agents (MSAs). MDAs preferentially interact with the heterodimer, at the vinca-binding or colchicine-binding domain. Vinca-domain binder containing heterodimers are incorporated only at the end of the microtubule with the actual site located on the outside of the microtubule, while heterodimers that contain colchicine-site binders can be incorporated throughout the microtubule, with the location of the site also being on the outside of the microtubule.¹⁰ MSA's tend to bind to the paclitaxel-binding domain on the inside of the assembled polymer. Both MDAs and MSAs, through their respective mechanisms, lead to cell death and can be utilized as chemotherapeutics.¹⁷

1.3.2 Microtubule-Destabilizing Agents

The first class of MDAs identified was the group of vinca alkaloids more than 50 years ago.¹⁸ Other classes of compounds known to act as MDAs are the cryptophycins, colchicine and its analogues and many more, including the

dolastatins. Another example of an MDA is halichondrin B (**Figure 1-2**). It was first isolated from the marine sponge, *Halichondria okadai*, in 1986 and found to show promising anti-cancer activity.¹⁹ While halichondrin B (**2**) has not been used as a chemotherapeutic drug itself, the mesylate salt of its truncated synthetic analog eribulin (**3**) has been approved for the use in patients with breast cancer by the FDA in 2010, and for the treatment of liposarcoma in 2016.

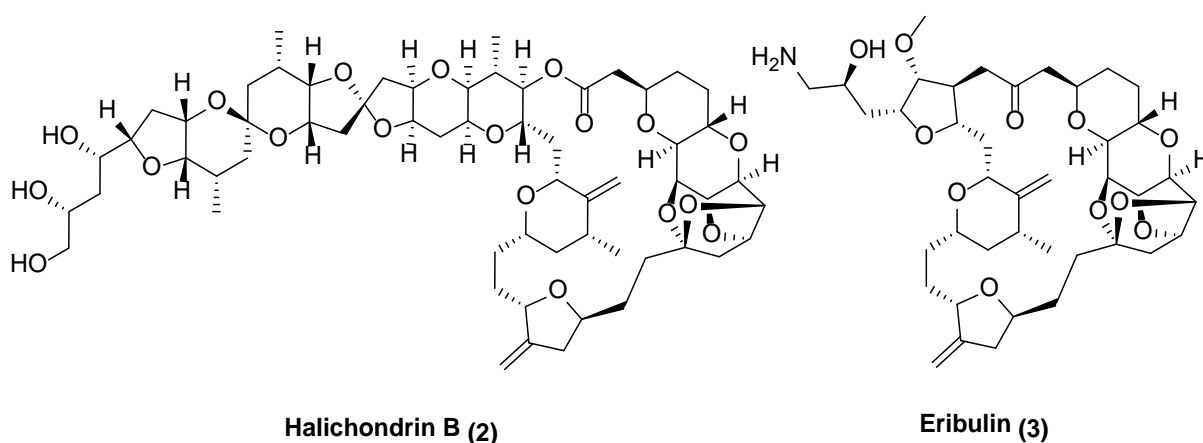


Figure 1-2 Chemical structures of halichondrin B (2) and eribulin (3).

Marine natural products, especially those from marine sponges, corals and algae (like halichondrin B) have distinct advantages over natural products found from terrestrial species. Marine life not only pre-dates terrestrial organisms by millions of years and therefore has had more time to allow greater evolutionary variation, but also because sponges, corals and algae are mostly immobile they produce secondary metabolites as a chemical defense against predation.²⁰ Since those metabolites are released into the water and therefore instantly diluted they have to possess very potent activities to be effective as a defense mechanism.

1.3.3 Microtubule-Stabilizing Agents: Paclitaxel, Docetaxel and the Epothilones

The first class of MSAs identified over 30 years ago were the taxanes, derived from the yew tree family; no plant compound in the field of therapeutic drugs discovered in the last three decades has received more public attention than paclitaxel (**4**).²¹ Paclitaxel (PAX) was discovered during a collaboration between the National Cancer Institute and the U.S. Department of Agriculture to identify natural products with anticancer activity²² and was the first compound to be identified as a non-covalent MSA in 1979.²³ Paclitaxel (**4**) as well as its semisynthetic analog docetaxel (**5**) were approved for and used in chemotherapy since the early 1990s.

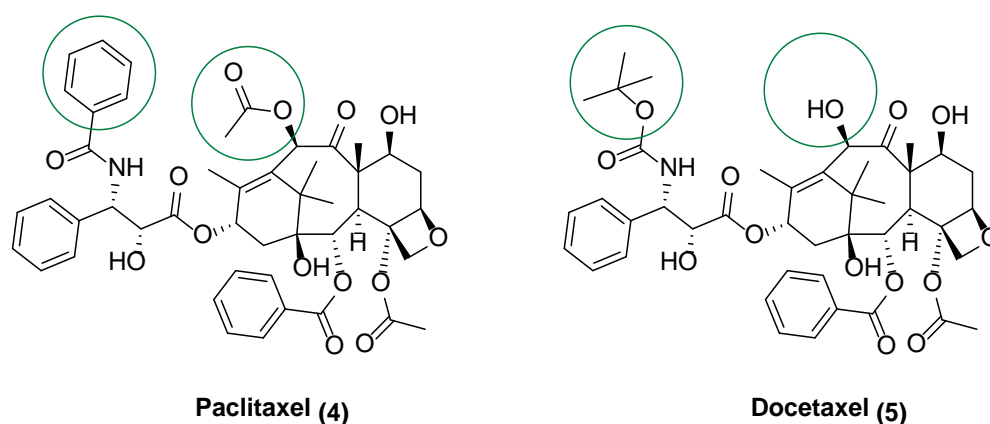


Figure 1-3 Chemical structures of paclitaxel (**4**) and its semi-synthetic analog docetaxel (**5**). The highlighted regions show the differences between the natural product and the analog.

Other well-known MSAs include the chemical families of the eleutherobins, the sarcodictyins and the epothilones. The isolation and investigation of epothilone B (**6**), the most potent member of the epothilone family isolated from the myxobacterium *Sorangium cellulosum*, has led to the development of a drug for breast cancer called ixabepilone (**7**) which has FDA approval. Interestingly, this compound exhibits potent cytotoxicity, even in paclitaxel-resistant cancer cells, although it acts in a similar fashion and interacts with the same binding-site as paclitaxel (**4**). This retention of activity is most likely because the epothilones do not seem to be substrates for the P-gp efflux pump, which is a major cause of

resistance against many chemotherapeutic and especially lipophilic drugs, including paclitaxel.¹⁰

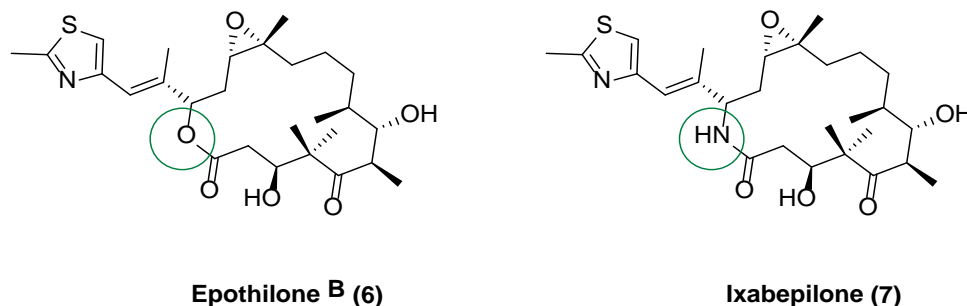


Figure 1-4 Chemical structures of epothilone B (6) and its semi-synthetic analog ixabepilone (7). The highlighted region shows the difference between the parent compound and the analog.

1.4 Zampanolide: A Novel Microtubule-Stabilizing Agent

1.4.1 Isolation and Structure Elucidation

(-)-Zampanolide (**Figure 1-5**) was first isolated in 1996 by Tanaka and Higa from the marine sponge *Fasciospongia rimosa* which was collected at Cape Zampa (Okinawa, Japan).²⁴ The sponge (480 g) was first extracted with acetone. Subsequent silica gel column chromatography and ODS HPLC yielded 3.9 mg of (-)-zampanolide (0.0008%). In 2009, Northcote and coworkers isolated the same compound from a different marine sponge, *Cacospongia mycofijiensis*, which was collected from 'Eua, Tonga.²⁵ The methanolic extract (from 341.0 g sponge) was purified *via* various normal- and reversed-phase columns and yielded 1.7 mg of (-)-zampanolide (0.0005%).

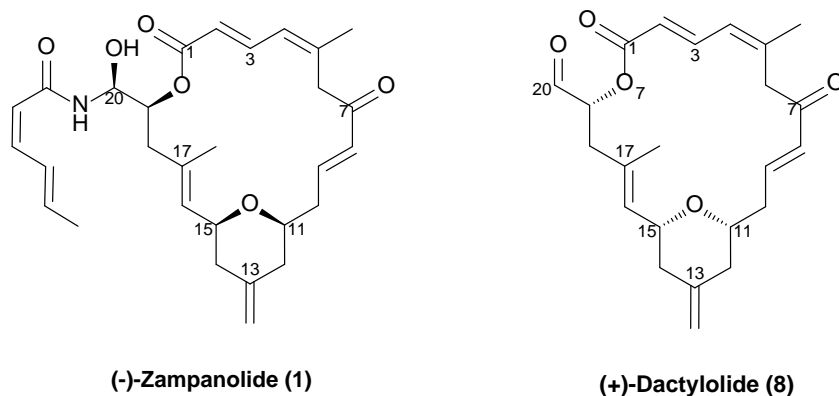


Figure 1-5 Structures of (-)-zampanolide (1, ZAMP) and (+)-dactylolide (8, DACT).

The structure of (-)-zampanolide was determined by Tanaka and Higa *via* 2D NMR spectroscopy and HR-FABMS and the relative configuration was assigned as $11R^*$, $15R^*$ and $19R^*$.²⁴ No conclusion about the configuration at C20 was made. Zampanolide contains four stereocenters and features a highly unsaturated, 20-membered macrolactone ring, a 2,6-*cis*-tetrahydropyran, and an *N*-acyl hemiaminal-containing sidechain. In 2001, Smith et al. reported the first total synthesis of zampanolide and established the relative and absolute stereochemistry of their synthetic (+)-zampanolide as $11R,15R,19R,20R$, which established the configuration of stereocenters as $11S,15S,19S,20S$ for the naturally occurring (-)-zampanolide.²⁶

A related compound, (+)-dactylolide (8, DACT), was isolated in 2001 by Cutignano et al. from a marine sponge of the *Dactylospongia* genus, which was collected off the coast of the Vanuatu islands.²⁷ In comparison to zampanolide, dactylolide lacks the *N*-acyl hemiaminal sidechain but features an aldehyde at C20 instead. Given their close structural relation, it would be reasonable to argue that dactylolide might be a degradation product of zampanolide, or alternatively, a direct biosynthetic precursor thereof. However, the core macrocycle of dactylolide was reported to exhibit the opposite sign of optical rotation than the naturally occurring (-)-zampanolide, suggesting the macrocycle is the mirror image of the one found in (-)-zampanolide. This was tested in 2002 by Smith and Safonov

through subjecting synthetic (+)-zampanolide to thermolysis, which led to the formation of (+)-dactylolide. This material had quite different magnitude of optical rotation compared to the natural product (synthetic $[\alpha]_D = +235$; natural $[\alpha]_D = +30$).²⁸ Uenishi and coworkers further studied the sign of optical rotation for the macrocycle of dactylolide and zampanolide by synthesizing (-)-zampanolide from (-)-dactylolide through treatment with CSA in the presence of (2Z,4E)-hexa-2,4-dienamide.²⁹ Thus, it is clear that the sign of optical rotation is consistent for a given absolute configuration in both compounds. Since the natural occurrence of both antipodes of a marine natural product is very rare, one would expect natural dactylolide and zampanolide to have the same absolute configuration. Hence, there might have been a mistake when the optical rotation of natural dactylolide was assigned, or the natural sample may have been contaminated. The isolation of both dactylolide and zampanolide from the same species and careful measurement of their optical rotation would afford conclusive evidence for solving these matters.

1.4.2 Biological Activity and Binding to Tubulin

The interest of the scientific community was sparked not only by the structure of (-)-zampanolide but also its remarkable biological activity. Tanaka and Higa's paper describing the isolation of (-)-zampanolide also outlined the first biological data, stating that (-)-zampanolide strongly inhibits the growth of P-388 (leukemia), A-549 (lung), HT-29 (colorectal) and SK-Mel-28 (melanoma) cancer cell lines with IC_{50} values in the range of 1-5 nM.²⁴ Natural dactylolide was first tested in 2001 when it was first isolated and exhibited a GI_{40} value of 3.2 $\mu\text{g/mL}$ against the SK-OV-3 (ovarian) line.²⁷ Interestingly, synthesized (-)-dactylolide exhibited a GI_{50} of 1.8 $\mu\text{g/mL}$ in the same cell line, which makes it roughly 2-4 more times more active than the natural antipode (+)-dactylolide.³⁰ Against the A-549, HT29 and SK-Mel-28 cell lines synthetic (-)-dactylolide exhibited activities roughly 100- to 1000-fold less potent than (-)-zampanolide, indicating that the N-

acyl hemiaminal sidechain plays an important role for the reported nanomolar activities.

The first paper investigating the mode of action by which zampanolide leads to cell death in cancer cells was published in 2009 by Miller's group at Victoria University of Wellington.²⁵ Zampanolide was found to exhibit microtubule-stabilizing activity in the nanomolar concentration range and to block cells in the G2/M phase of the cell cycle, which puts it into the same class of anticancer compounds as paclitaxel and the epothilones. **Figure 1-6** shows 1A9 human ovarian carcinoma cells that have been treated with (-)-zampanolide and paclitaxel at a concentration of 10 nM; microtubule bundle formation in interphase cells and formation of multiple spindle asters in mitotic cells are clearly visible with both zampanolide and paclitaxel treatment.

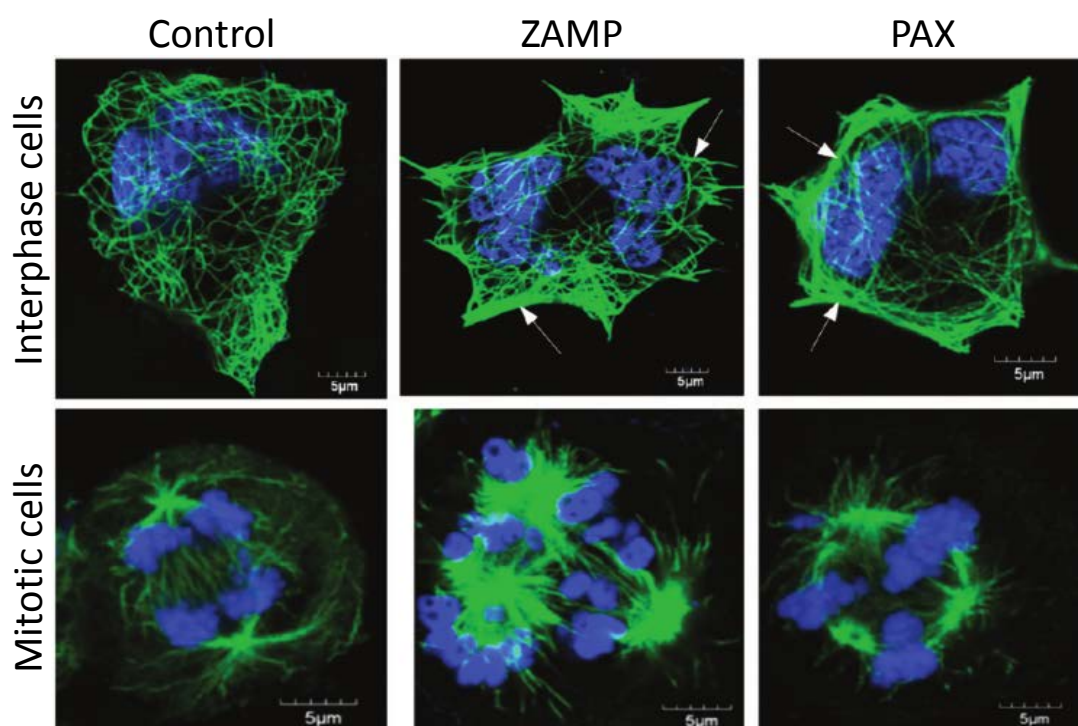


*Figure 1-6 Effects of 10 nM zampanolide (ZAMP) and 10 nM paclitaxel (PAX) on 1A9 human ovarian carcinoma cells after 12 hours. α -Tubulin was stained to visualize microtubules, revealing the formation of microtubule bundles in interphase cells (arrows), and multiple spindle asters in mitotic cells. Adapted with permission from *J. Med. Chem.* **52**, 7328–7332 (2009). Copyright (2018) American Chemical Society.*

Zampanolide was also tested for susceptibility to the P-gp efflux pump. That causes drug-resistance against many different chemotherapeutic drugs including paclitaxel. When tested in A2780 and A2780D human ovarian cancer cells, with the latter cell line overexpressing the P-gp efflux pump, zampanolide maintained its nanomolar activity (IC_{50} values 7.1 ± 2.0 nM and 7.5 ± 0.6 nM, respectively), while the activity of paclitaxel decreased many-fold, with IC_{50} values increasing from 2.8 ± 1.4 nM to 415 ± 48 nM. This suggests that zampanolide is not a substrate for the P-gp efflux pump. A second study compared natural and synthetic (-)-zampanolide and (-)-dactylolide with paclitaxel in the same two cell lines.³¹ Once again zampanolide mostly maintained its low nanomolar activity, while paclitaxel showed a significant loss of activity. (-)-Dactylolide showed a two-fold loss of activity. The results are summarized in **Table 1.1**.

Compound	A2780 (nM)	A2780D (nM)	R/S
Natural (-)-zampanolide	1.9 ± 0.2	2.2 ± 0.3	1.2
Synthetic (-)-zampanolide	1.4 ± 0.3	1.95 ± 0.4	1.1
(-)-Dactylolide	602 ± 100	1236 ± 180	2.1
Paclitaxel	0.46 ± 101	1065 ± 101	2315

Table 1.1 IC_{50} values of (-)-zampanolide (natural and synthetic), (-)-dactylolide and paclitaxel in ovarian carcinoma cells A2780 and P-gp overexpressing A2780AD cells. R/S is the relative resistance of the A2780D cell line and is obtained by dividing the IC_{50} of the resistant cell line by that of the parental A2780 cell line.

This same study by Field et al. investigated the binding mode of zampanolide and dactylolide using targeted mass spectrometry (MS) experiments, which revealed the peptide spanning 219-LTTPTYGDLNHLVSATMSGVTTCLR-243 on β -tubulin as the ZAMP- and DACT reactive sites in microtubules, confirming that both ZAMP and DACT interact with the Taxol luminal site located on the interior of the microtubule on the β -tubulin subunit.³¹ These experiments were followed by high-resolution mass spectrometry (HRMS) analyses to pinpoint the reactive residue. The most abundant fragment found indicated that zampanolide

covalently reacts with H229. Additionally, another, less abundant, fragment was found which indicated N228 can react as well. However, only one covalent bond between zampanolide and the protein can be formed at any one time. Docking studies using the NMR-determined bioactive conformation of DACT suggest that H229 most likely reacts at C9 of zampanolide, while N228 reacts at C3. Additionally, the studies of Field et al. strongly suggest that the paclitaxel luminal site exists in unassembled α - and β -tubulin heterodimers, not just in the fully assembled microtubules. This theory was proven correct only one year later, when Prota et al. reported a high-resolution crystal structure of α,β -tubulin in complex with (-)-zampanolide, confirming not only the binding occurring at the paclitaxel luminal site as predicted by Field et al., but also the covalent bond between C9 of (-)-zampanolide and H229 of the β -tubulin subunit (**Figure 1-7**).³² A covalent bond between N228 and C3 of (-)-zampanolide was not found. This does not necessarily mean that this bond is not formed at all, it could be simply due to a preference for crystallization of one compound over the other. Additionally, a possible explanation for the more potent microtubule-stabilizing activity of zampanolide in comparison to dactyloide was found. The hydroxy group at C20 and the acyl carbonyl of the sidechain of zampanolide interact with the M-loop of β -tubulin, which is responsible for lateral tubulin contacts in microtubules, thereby inducing structuring of the loop into a short helix and promoting microtubule assembly and stability. Dactyloide, lacking both these motifs, cannot, or only to a lesser extent, exhibit this stabilizing effect.

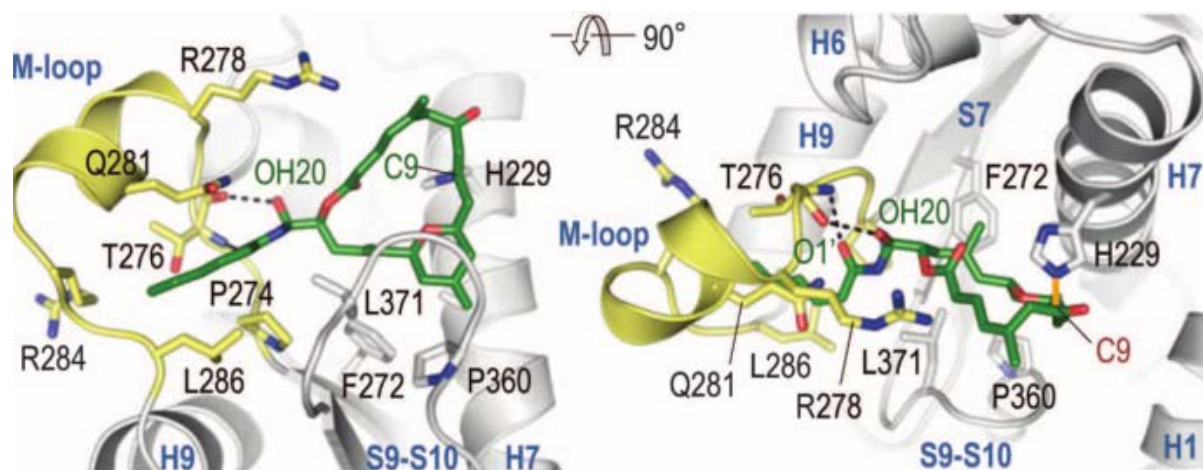
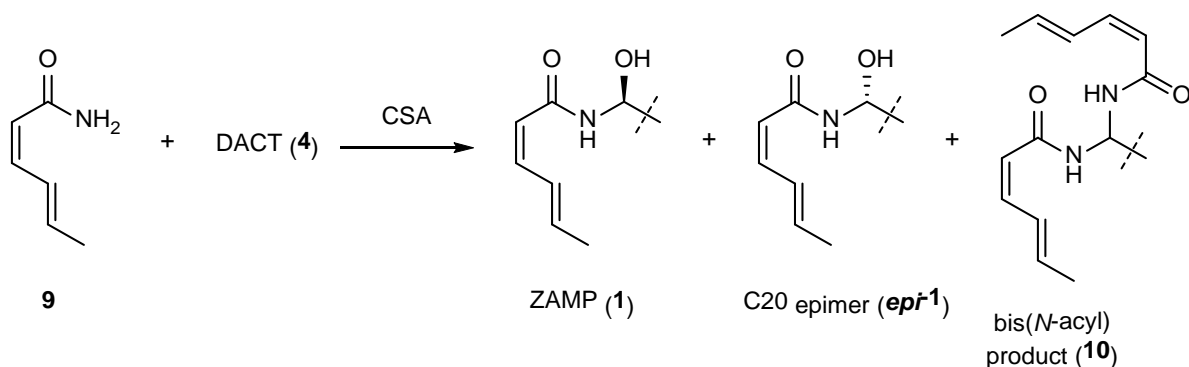


Figure 1-7 Crystal structure of the interaction between (-)-zampanolide and the β -tubulin subunit of the α - and β -tubulin heterodimers from two different angles. Hydrogen bonds are depicted with black dashed lines, while the covalent bond to C9 is represented as orange stick. From *Science*, **339**, 587–590 (2013). Reprinted with permission from AAAS.

1.5 Analogue and SAR Studies

1.5.1 Biological Testing of Uenishi's and Ghosh's Analogs

Although zampanolide is such a promising anticancer target, only very few analogs have been synthesized and tested so far. The first two analogs of zampanolide that were tested for their anticancer activity were formed as by-products in total syntheses conducted by Uenishi's as well as Ghosh's research groups in 2009 and 2013, respectively.^{29,33} One of the by-products tested was the C20 epimer of zampanolide *epi*-**1**, while the other one was the bis(*N*-acyl) product **10**, formed in the reaction of dactylolide (**4**) with (2*Z*,4*E*)-hexa-2,4-dienamide (**9**) promoted by CSA (**Scheme 1.1**).



Scheme 1.1 Uenishi's and Ghosh's formation of zampanolide (**1**), C20 epimer of zampanolide (**epi-1**) and the bis(*N*-acyl) product **10** from the CSA-promoted reaction of dactylolide (**4**) with (2*Z*,4*E*)-hexa-2,4-dienamide **10**.

Zampanolide, along with its C20 epimer **epi-1** and bis(*N*-acyl) product **10** were tested against various cancer cell lines (Table 1.2). While zampanolide and its epimer both exhibited activity in the nanomolar range in SKM-1 and U937 cells (albeit about 10-fold less potently in the case of the epimer), **10** was significantly less active. By comparison, in MCF-7, OVCAR 8 and NCI/ADR-RES cells, **epi-1** as well as **10** lose significant amounts of activity, while zampanolide maintained its low nanomolar activity. It is worth mentioning that in NCI/ADR-RES cells, which are overexpressing the P-gp efflux pump, therefore rendering them insensitive to paclitaxel, zampanolide as well as its analogs retained similar activity to that found in MCF-7 and OVCAR 8 cells.

Cell line	PAX (4)	ZAMP (1)	Epi- 1	10
SKM-1 (leukemia) ²⁹		1.1	10	490
U937 (lymphoma) ²⁹		2.9	27	950
MCF-7 (breast) ³³	2 ± 0	4.0 ± 0.5	200 ± 0	430 ± 200
OVCAR 8 (ovarian) ³³	7.5 ± 2	20 ± 0	250 ± 70	300 ± 0
NCI/ADR-RES (ovarian, P-gp efflux pump overexpressing) ³³	>5000	25 ± 7	750 ± 200	750 ± 400

Table 1.2 IC_{50} values (in nM) of paclitaxel (**4**), zampanolide (**1**), the C20 epimer of zampanolide (**epi-1**) and the bis(*N*-acyl) product (**10**) in various cancer cell lines, including the P-gp efflux pump-overexpressing cell line NCI/ADR-RES.

1.5.2 Altmann's Structure-Activity Relationship Studies

In 2010 and 2012, Altmann's research group reported the syntheses of (-)-dactylolide and (-)-zampanolide, respectively.^{34,35} These syntheses are discussed in more detail in **Chapter 2.1.12**. Alongside the natural product, the syntheses of several analogs for structure-activity relationship (SAR) studies were reported and the obtained analogs were tested for their antiproliferative activity in four different cancer cell lines, A549 (lung), MCF-7 (breast), HCT116 (colon) and PC-3 (prostate).

Altmann's analogs include the C20 epimer of zampanolide (**epi-1**), a whole range of analogs with varying residues and oxidation states at C20 (**11-14**), two desmethylene analogs (**15** and **16**), as well as three compounds where the tetrahydropyran ring was replaced with a simple ether functionality (**17-19**). Analogues are classified according to their modifications and are shown in **Figure 1-8**.

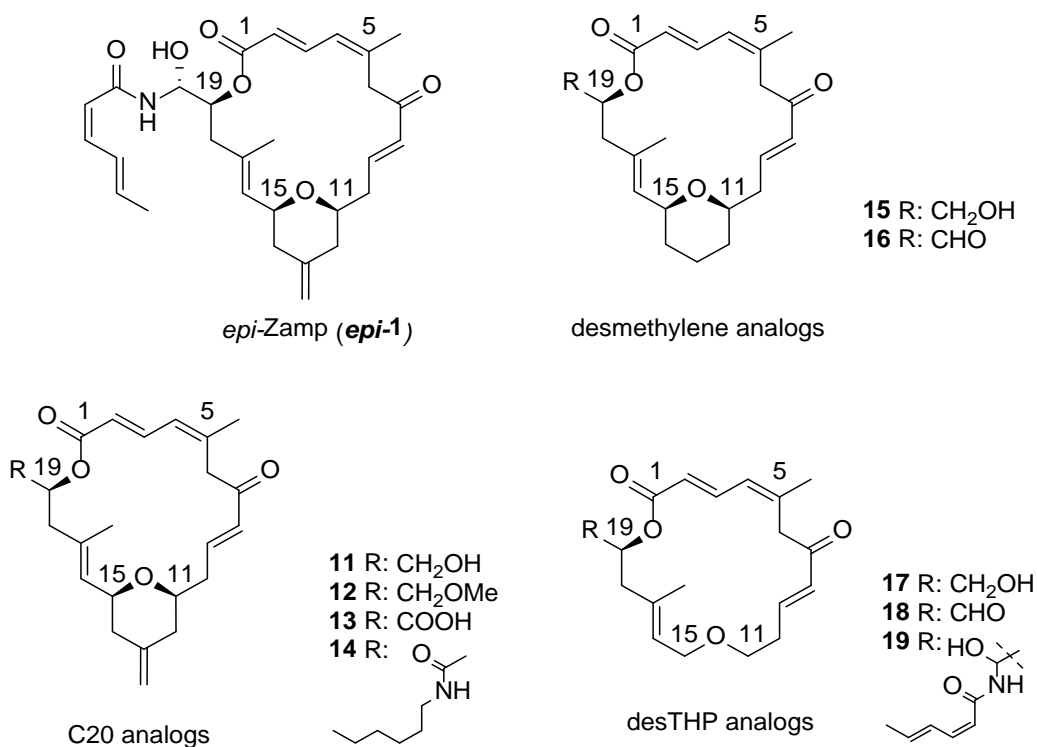


Figure 1-8 Structures of the analogs synthesized by Altmann's research group and classified according to their modifications.

Firstly, it has to be mentioned that the respective IC₅₀ values of zampanolide (**1**) and dactylolide (**8**) as well as their analogs are consistent across all tested cell lines, and the IC₅₀ values are listed in **Table 1.3**. The next apparent conclusion that can be drawn is that the sidechain plays an important role for the activity of (-)-zampanolide. As mentioned above, the IC₅₀ value for *epi-1* is approximately one order of magnitude higher than for the natural product. A complete absence of the sidechain, like in (-)-dactylolide (*ent-8*), decreases the activity by another order of magnitude across all cell lines.

Compound	A549	MCF-7	HCT116	PC-3
1	3.2 ± 0.4	6.5 ± 0.7	7.2 ± 0.8	2.9 ± 0.4
<i>epi</i> 1	53 ± 5.9	42 ± 9.3	88 ± 5.1	50 ± 11.7
8	301 ± 4.3	247 ± 2.6	210 ± 4.7	751 ± 69
Desmethylene Analogs				
15	189 ± 19.3	114 ± 10.2	74 ± 1.5	104 ± 4.1
16	149 ± 12.8	68 ± 5.6	249 ± 28	n.d.
C20 analogs				
11	127 ± 2.9	106 ± 3.6	155 ± 2.1	320 ± 26
12	1072 ± 103	1489 ± 83	1603 ± 122	1274 ± 117
13	9732 ± 260	7624 ± 303	12733 ± 379	9338 ± 242
14	973 ± 90	1138 ± 72	1204 ± 63	829 ± 27
DesTHP Analogs				
17	2378 ± 70	3891 ± 102	1845 ± 92	3051 ± 178
18	3821 ± 216	2894 ± 144	2653 ± 68	4021 ± 102
19	n.d.	165 ± 13	309 ± 47	218 ± 7

Table 1.3 IC₅₀ values in nM for zampanolide, dactylolide and analogs synthesized by the Altmann group in four different cell lines, adapted from Ref. ³⁵.

The loss of the exomethylene group does not seem to have much of an effect on the IC₅₀ values in any cell line. Analogs **15** and **16** are both lacking the sidechain and the exomethylene functionality and still exhibit activities similar to the activity of dactylolide, which suggest the exomethylene group is not required for the biological activity of dactylolide.

Looking at the C20 analogs, the data seem to suggest that the aldehyde moiety in dactylolide is not necessary for its antiproliferative activity, as **11** features an alcohol at the C20-position while exhibiting an even slightly higher activity than dactylolide. However, methylation of this alcohol in **12** results in a drastic increase in IC₅₀ value. It can be hypothesized that this loss in activity might occur due to the loss of hydrogen bonding capacity and therefore loss of the ability to effectively modulate the M-loop of β -tubulin to form a helix, as described in **Chapter 1.4.2**.

Oxidizing the alcohol function in **13** results in an even bigger increase in IC₅₀ value. Zurwerra et al. speculate that this result might be caused by poor cell penetration due to the negatively charged carboxyl group. Interestingly, installing an amide at C20 with a similar chain length in **14** results in a slight regain of activity with respect to compounds **12** and **13**. This is encouraging because it suggests that antiproliferative activity could be improved by fine-tuning the sidechain.

The most intriguing observation made in this study concerns the desTHP analogs. While the deletion of the THP ring and substitution with an ether function leads to a drastic increase in IC₅₀ values in compounds **17** and **18**, both lacking the zampanolide sidechain, relative to DACT, compound **19** is only 25- to 80-fold less active than its parent zampanolide (for the tested cell lines). This result is remarkable, as the deletion of the THP removes two of the four stereocenters of zampanolide, as well as a rigidifying structural element. Additionally, the authors of the study emphasize that **19** is a “1.6:1 mixture of diastereoisomers at C18; in light of the results obtained for **1** and *epi***1** it is tempting to speculate that the IC₅₀ values for **19** could in fact be lower than those observed for the mixture.”

Chapter 2: Previous Synthetic Work and Retrosynthetic Approach

2.1 Published Syntheses of Zampanolide and Dactylolide

Between 2001 and 2017, twelve research groups have published papers on the successful total synthesis of the macrocyclic core of zampanolide/dactylolide, and five research groups have completed the synthesis of zampanolide. The major disconnections and strategies are shown in **Figure 2-1**.

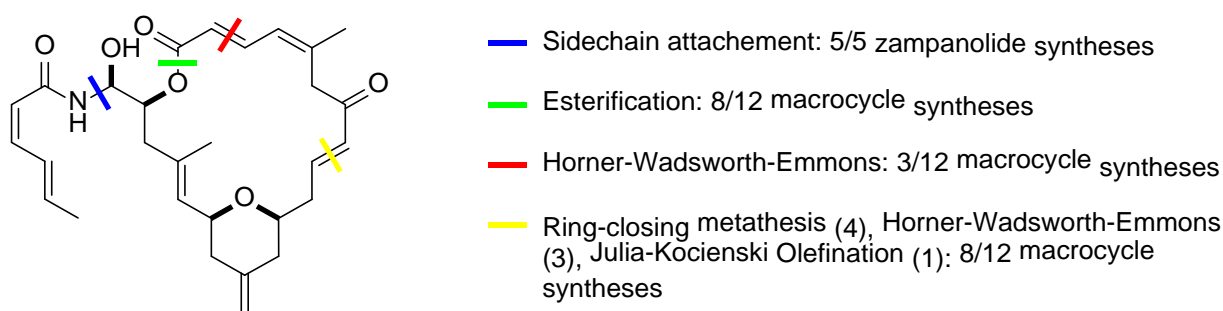


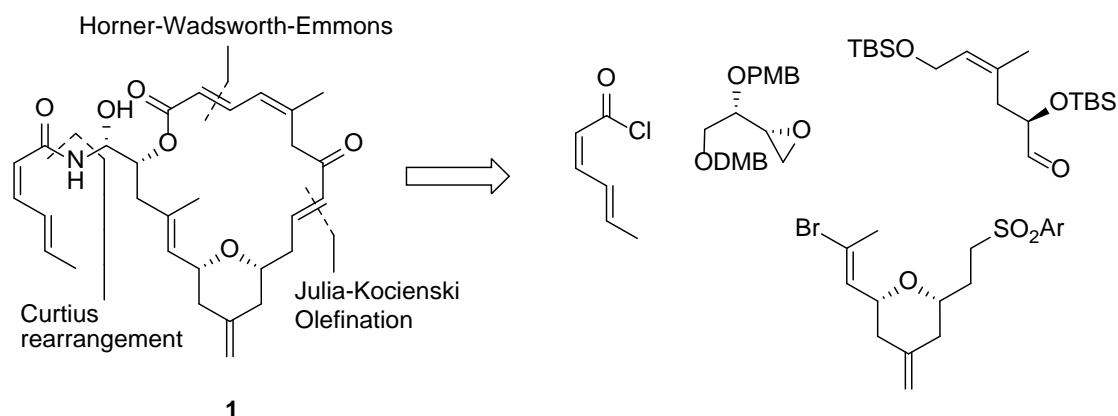
Figure 2-1 The main disconnection points utilized in the synthesis of the zampanolide macrocycle and natural product.

All zampanolide syntheses have installed the side chain by bond formation between the nitrogen and C20, although different methodologies have been used. These are discussed further in the following chapters. The ester at C19 is an obvious disconnection point and has been chosen by eight research groups for bond formation, with a variety of methods used for the esterification reaction. In two cases, the macrolactonization was performed this way. Furthermore, a Horner-Wadsworth-Emmons (HWE) reaction at C2-C3 was used by three research groups, and eight syntheses involved a connection at the C8-C9 alkene through three distinct methods, namely four ring-closing metatheses, three HWE reactions and one Julia-Kocienski olefination.

Many different methods for the synthesis of the tetrahydropyran ring have been employed and are therefore not shown in the above figure. However, they are discussed in more detail in the following chapters.

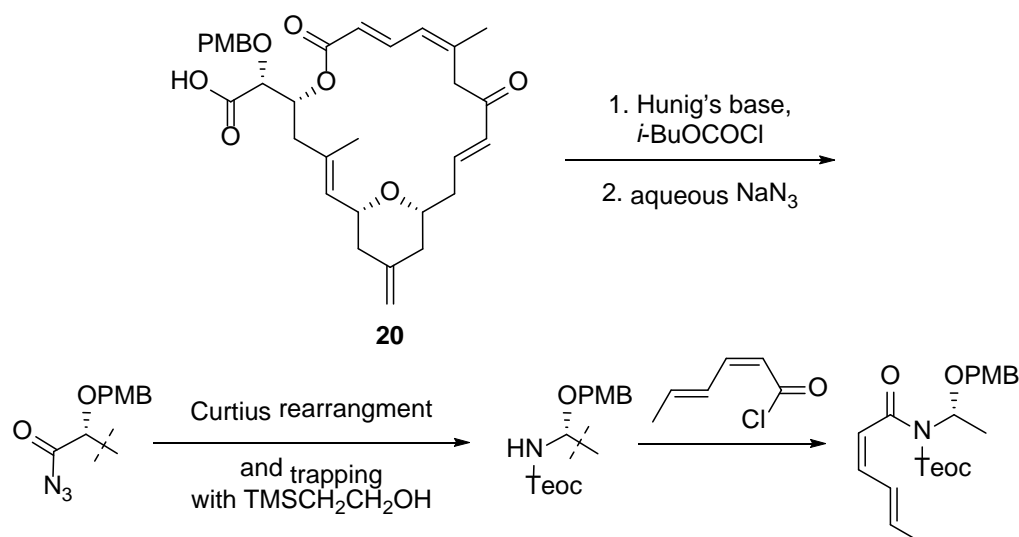
2.1.1 Smith's Total Synthesis of (+)-Zampanolide (2001)

In 2001 Smith and co-workers reported the first total synthesis of (+)-zampanolide and solved the absolute stereochemistry of the natural product.²⁶ The synthetic strategy involved connecting C8-C9 *via* a Julia-Kocienski olefination, an epoxide opening with a cuprate to obtain the stereocenter at C20 and a Horner-Wadsworth-Emmons reaction as the macrolactonization step (**Scheme 2.1**). The side chain was installed *via* a Curtius rearrangement.



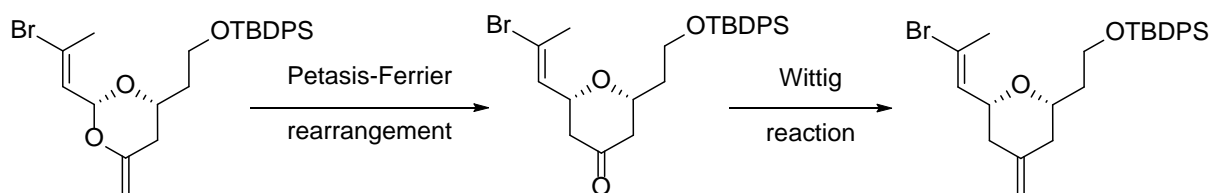
Scheme 2.1 Smith's total synthesis of (+)-zampanolide (*ent*-11), featuring a HWE reaction as macrolactonization step, a Julia-Kocienski reaction to form the C8-C9 bond and a Curtius rearrangement to generate the hemiaminal sidechain.

After intermediate **20** was treated with base and sodium azide, which allowed for the Curtius rearrangement to take place, the resulting isocyanate was trapped, and the newly formed amide nitrogen was acylated (**Scheme 2.2**).



Scheme 2.2 Installation of the sidechain of zampanolide in Smith's synthesis through a Curtius rearrangement and subsequent acylation.

The *cis*-THP ring in Smith's zampanolide synthesis was formed through a Petasis-Ferrier rearrangement, followed by a Wittig reaction (**Scheme 2.3**). The Petasis-Ferrier rearrangement is an acid-catalyzed ring opening-ring closure sequence. A Lewis acid, in Smith's case Me_2AlCl , is used to open the acetal, followed by formation of the ketone and ring-closure through the alkene. The ketone is then transformed into the *exo*-methylene group through a Wittig reaction.



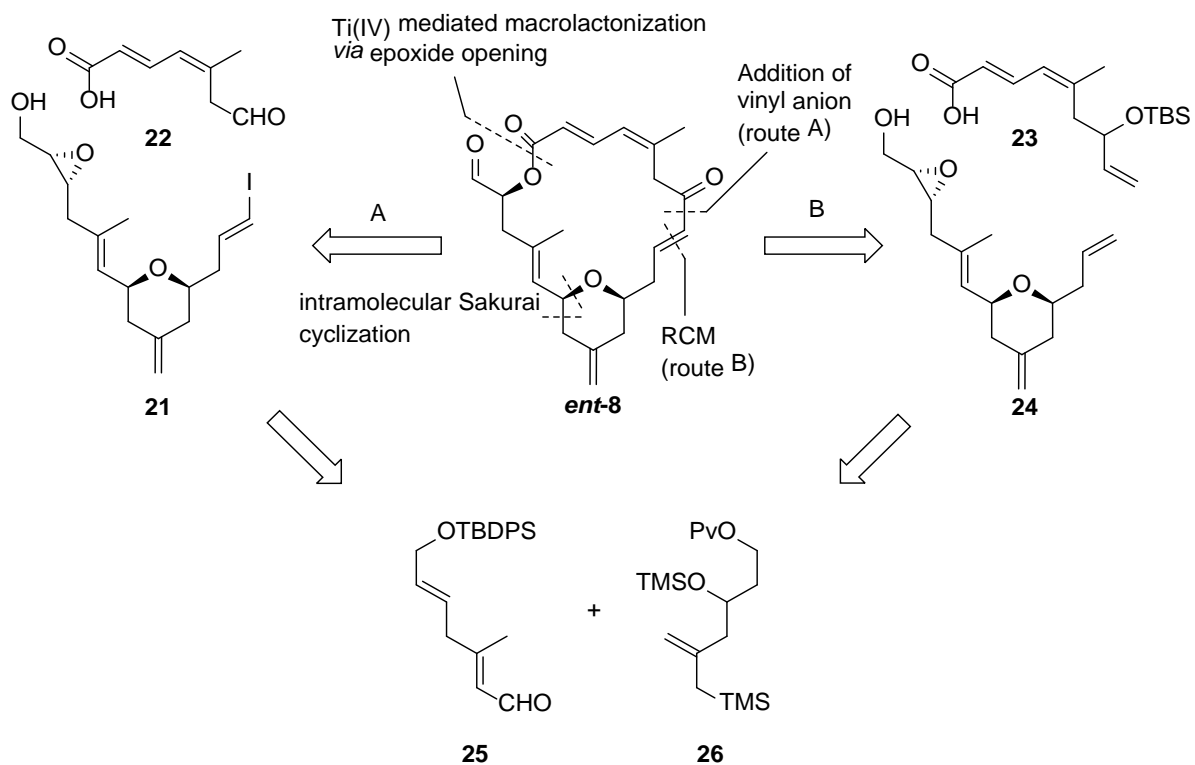
*Scheme 2.3 Petasis-Ferrier rearrangement leading to the synthesis of the *cis*-THP ring in Smith's zampanolide synthesis.*

A year later Smith's research group employed the same strategy for the synthesis of (+)-dactylolide, and showed that (+)-zampanolide degrades into (+)-dactylolide

when it is heated, first showing that the macrocyclic cores of natural zampanolide and dactyloide are antipodes to each other (assuming the published optical rotations for the two natural products were correct, see **Chapter 1.4.1**).²⁸

2.1.2 Hoye's Total Synthesis of (-)-Dactyloide (2003)

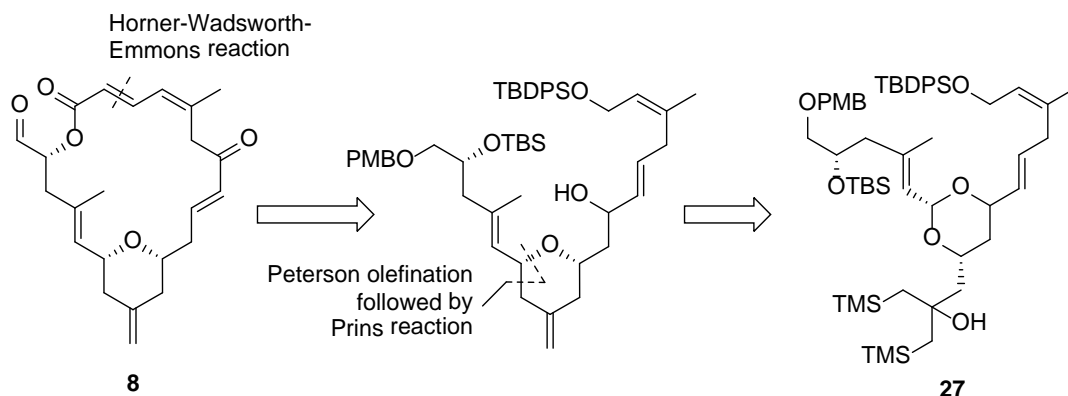
Hoye and coworkers reported the synthesis of (-)-dactyloide in 2003, following a different strategy that featured a novel Ti(IV)-mediated macrocyclization through opening of epoxide **21** with acid **22** (route A, **Scheme 2.4**).³⁶ They also reported a complimentary strategy employing a RCM as the cyclization step (route B, **Scheme 2.4**). In route A (**Scheme 2.4**), the connection between C7-C8 was formed *via* addition of the vinyl anion (derived from the iodide **21**) to the aldehyde **22**, yielding a 1:1 epimeric mixture at C7. The ring was then closed by using the newly developed Ti(IV)-mediated macrocyclization. In route B, the ester was formed first by reaction of **23** and **24**, followed by an RCM to close the macrocycle. In both routes, the *cis*-THP ring was formed through an intramolecular Sakurai reaction between aldehyde **25** and allyl silane **26** (**Scheme 2.4**).



*Scheme 2.4 Hoyer's total synthesis of (-)-dactylolide featuring two distinct macrocyclization strategies: a novel Ti(IV)-mediated macrolactonization of epoxy-acid and a complementary RCM macrocyclization. The *cis*-THP is formed via an intramolecular Sakurai cyclization.*

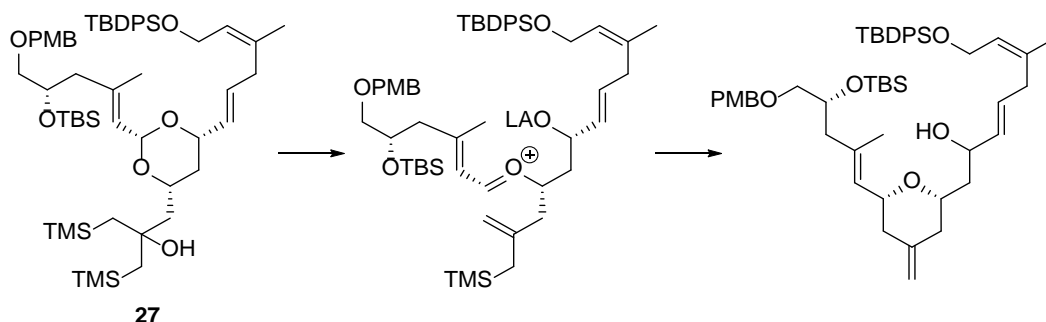
2.1.3 Floreancig's Total Synthesis of (+)-Dactylolide (2005)

Floreancig and coworkers reported their total synthesis of (+)-dactylolide in 2005.³⁷ For the closure of the macrocycle the group used a Horner-Wadsworth-Emmons (HWE) reaction to form the lactone, as had been established by Smith's group in 2001 (**Scheme 2.5**).²⁶ The *cis*-THP was formed through a Peterson olefination followed by a spontaneous Prins reaction of cyclic acetal **27**.



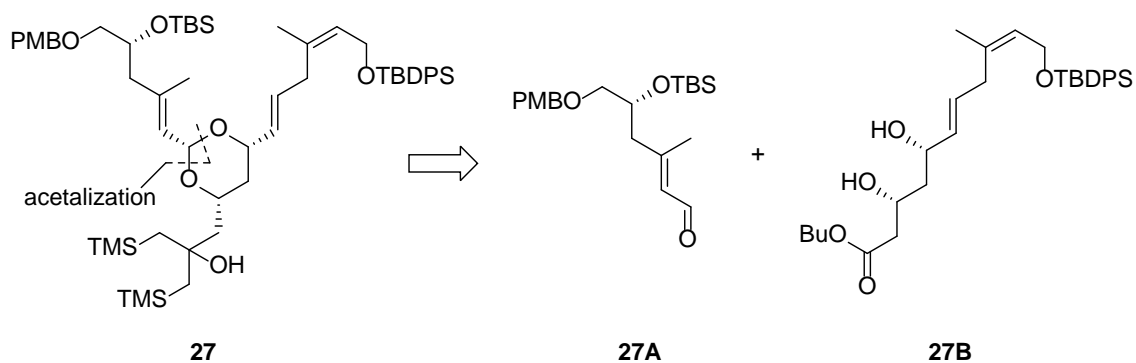
Scheme 2.5 Floreancig's total synthesis of (+)-dactyloide using a Peterson olefination and Prins reaction to generate the *cis*-THP ring, and a HWE reaction to close the macrocycle.

In the Peterson-Prins sequence, an elimination takes place, which effectively leads to the expulsion of TMSOH, forming a terminal double bond. Lewis acid-promoted opening of the cyclic acetal results in formation of the oxonium cation, which triggers the ring closure to the *cis*-THP ring and subsequent elimination of the second TMS group, as shown in **Scheme 2.6**.



Scheme 2.6 Formation of the *cis*-THP ring through a Peterson olefination followed by a Prins reaction.

The cyclic acetal intermediate **27** itself was formed through a reaction between two large fragments, **27A** and **27B** (**Scheme 2.7**), which contain most of the carbon skeleton of dactyloide.

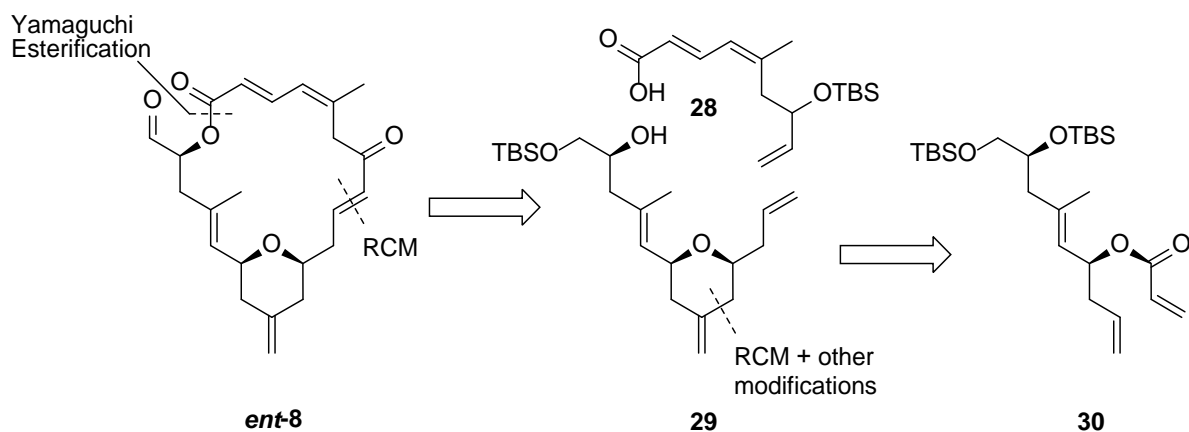


*Scheme 2.7 Formation of acetal intermediate **27** from two advanced synthetic fragments.*

2.1.4 Jennings' Total Synthesis of (-)-Dactylolide (2005)

Jennings and Ding reported a total synthesis of (-)-dactylolide in 2005.³⁰ They used a Yamaguchi esterification between intermediates **28** and **29** to establish the connection at C1 and a RCM as ring-closing step at C8-C9 (**Scheme 2.8**).

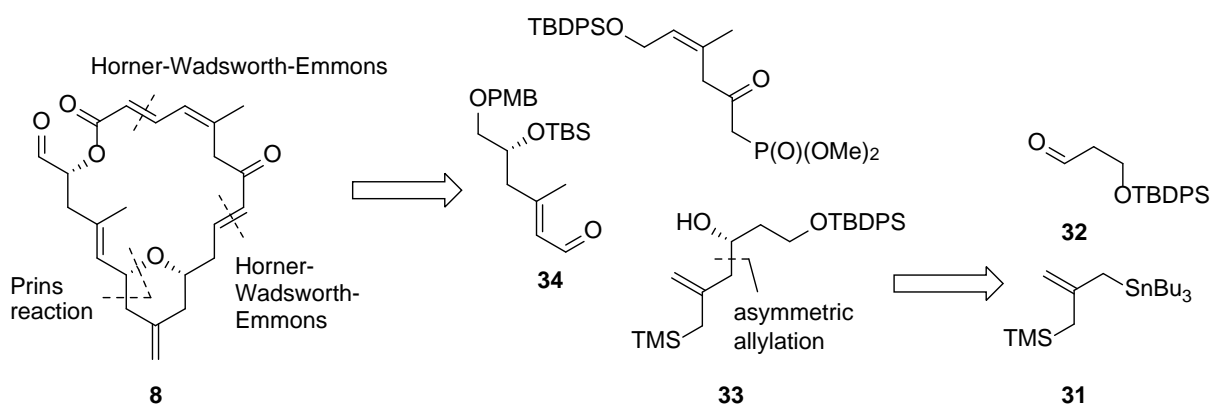
For the formation of the THP-ring a RCM was performed on **30**, followed by an epoxidation of the newly formed double bond, selective epoxide opening and transformation of the formed hydroxyl group into the exomethylene. Subsequently, the allyl group attached to the THP ring of **29** was installed by reaction of the ester carbonyl with allylmagnesium bromide, dehydration and reduction of the formed alkene.



*Scheme 2.8 Jennings' total synthesis of (-)-dactylolide, using a Yamaguchi esterification to connect building blocks **28** and **29**, and a RCM as ring-closing step.*

2.1.5 Keck's Total Synthesis of (+)-Dactylolide (2005)

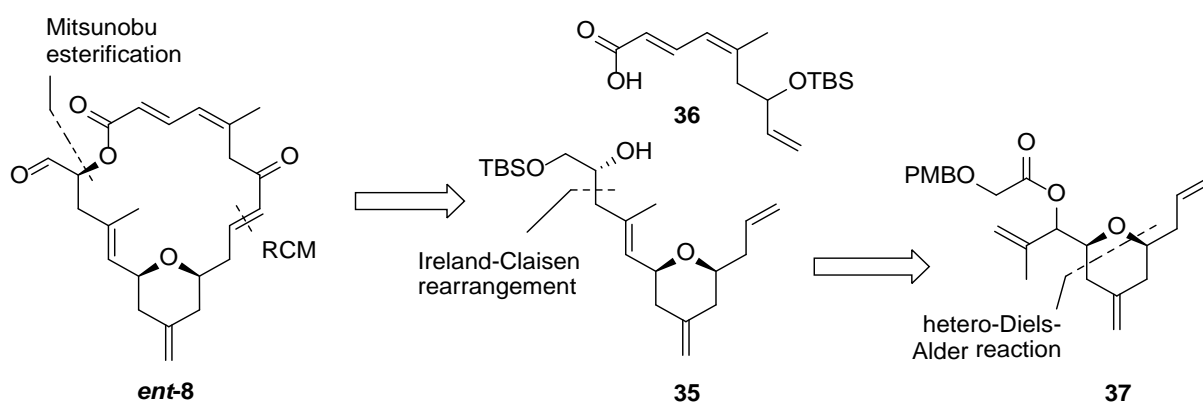
Keck and Sanchez reported a synthesis of (+)-dactylolide in 2005.³⁸ Their strategy involved a HWE reaction as the ring-closing step at C2-C3 alongside a second HWE reaction to form the C8-C9 bond (**Scheme 2.9**). A catalytic asymmetric allylation reaction between stannane **31** and aldehyde **32** led to building block **33**, which was then subjected to a Prins reaction with aldehyde **34**.



*Scheme 2.9 Keck's total synthesis of (+)-dactylolide using HWE reactions for connecting two major fragments and closing the macrocycle, and a Prins reaction to form the *cis*-THP ring.*

2.1.6 McLeod's Total Synthesis of (-)-Dactylolide (2006)

In 2006 McLeod reported a synthesis of (-)-dactylolide using a convergent approach to connect two large fragments, **35** and **36**, *via* Mitsunobu esterification at C1, and a RCM as ring-closing step at C8-C9 (**Scheme 2.10**).³⁹ The *cis*-THP ring was generated by an asymmetric hetero-Diels-Alder reaction employing a chromium(III) catalyst leading to an excellent enantiomeric excess (ee) of 99%. The C16-C19 portion of **35** was installed by an Ireland-Claisen rearrangement of fragment **37**.

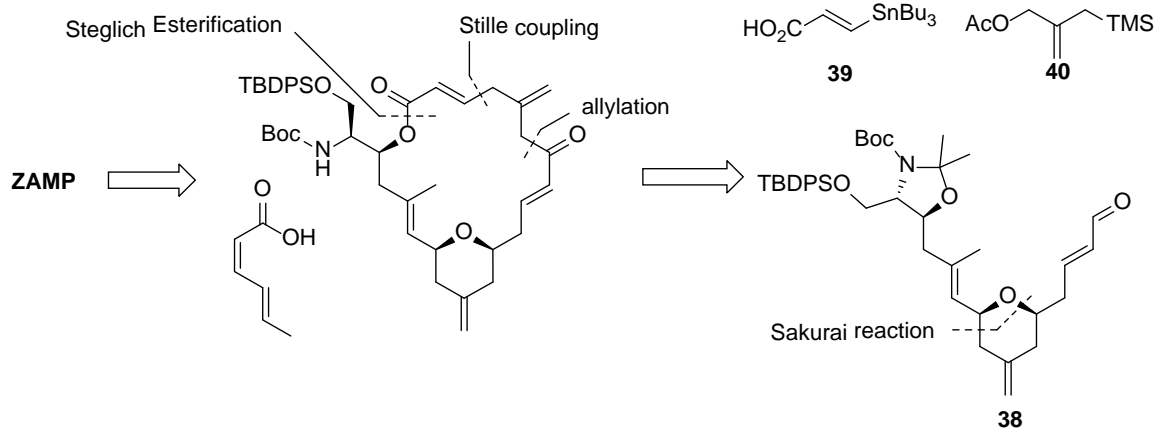


*Scheme 2.10 McLeod's total synthesis of (-)-dactylolide, featuring a Mitsunobu esterification as ring-closing step. The trisubstituted alkene at C16-C17 was installed through an Ireland-Claisen rearrangement. A hetero-Diels-Alder reaction was used to generate the *cis*-THP ring.*

2.1.7 Porco's Total Synthesis of the Macrocyclic Core of (-)-Zampanolide (2008)

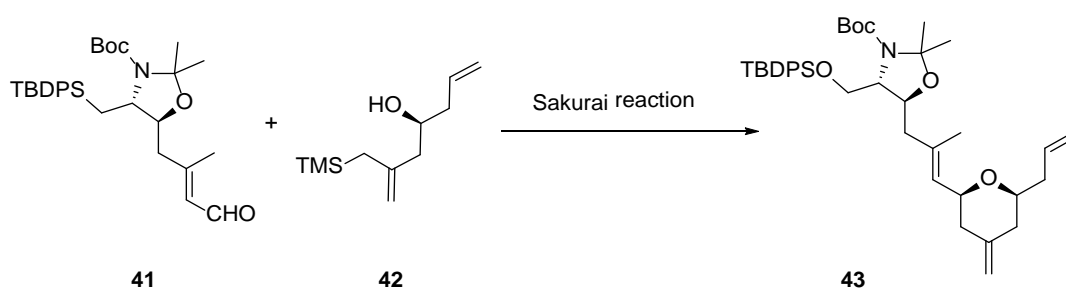
Porco and coworkers published a synthesis of the macrocyclic core of (-)-zampanolide in 2008.⁴⁰ The ester moiety at C1 was installed using a Steglich esterification connecting the alcohol derived from protected aminoalcohol **38** and stannane **39**, and the bond between C6-C7 was formed *via* allylation of the

aldehyde of **38** with allyl silane **40** (Scheme 2.11). The macrocycle was closed using a sp^2 - sp^3 Stille coupling.



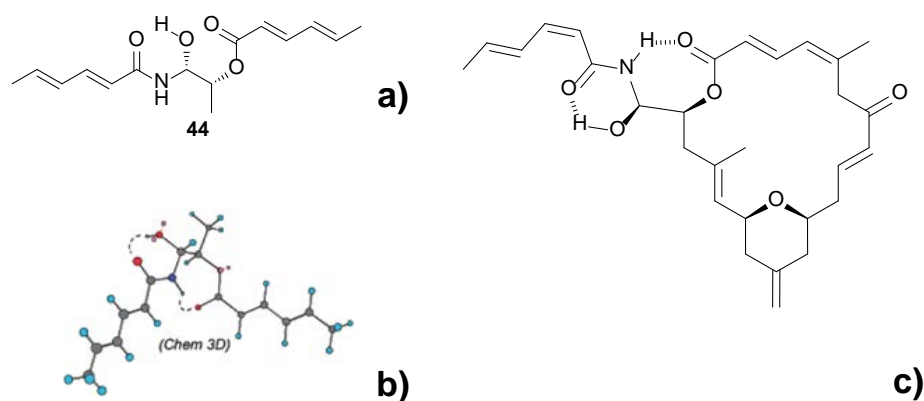
Scheme 2.11 Porco's total synthesis of (-)-zampanolide. A Steglich esterification is used to establish the ester moiety at C1, and the macrocycle is closed through a Stille coupling. The *cis*-THP ring is formed via a Sakurai reaction.

The *cis*-THP ring was formed using a Sakurai reaction, connecting aldehyde **41** and allyl silane **42** (Scheme 2.12). A subsequent crossmetathesis of **43** with acrolein led to building block **38**, ready for the subsequent allylation reaction mentioned above.



Scheme 2.12 Sakurai reaction used in Porco's synthesis of the macrocyclic core of (-)-zampanolide to form the *cis*-THP ring.

In 2002, Porco and coworkers published a paper investigating the synthesis of *N*-acyl hemiaminal model compounds related to zampanolide, as well as the importance of hydrogen bonding on the stability of the *N*-acyl hemiaminal side chain in zampanolide.⁴¹ One of the model compounds synthesized, **44**, is shown in part **A** of **Scheme 2.13**. This model system was subjected to ¹H NMR experiments and was found to exhibit hydrogen bonding between the amide carbonyl and the OH, as well as the ester carbonyl and amide NH as shown in part **B** of **Scheme 2.13**. The existence of these hydrogen bonds strongly suggests the existence of a similar network to stabilize the *N*-acyl hemiaminal sidechain in (-)-zampanolide, as shown in part **C** of **Scheme 2.13**.

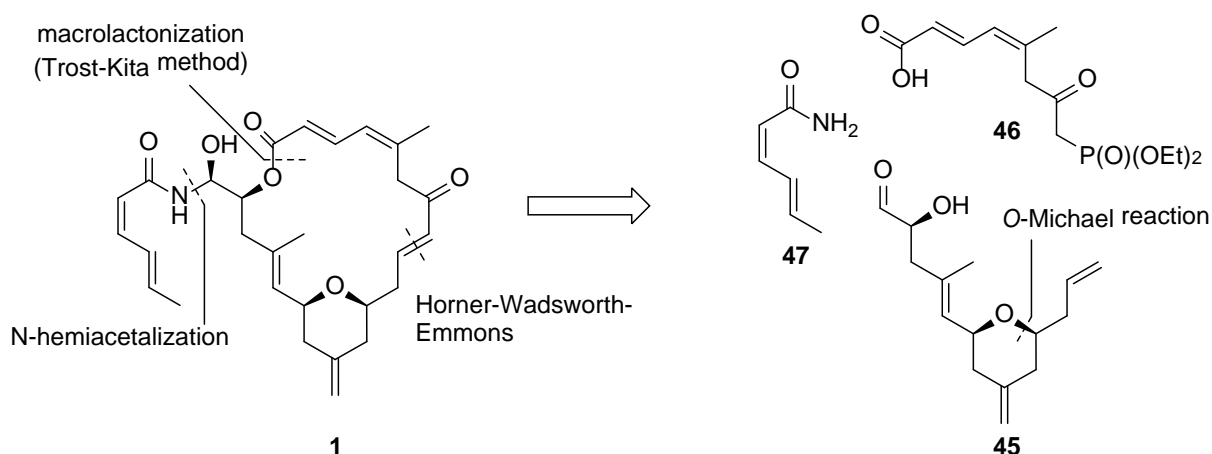


*Scheme 2.13 a) One of Porco's model compounds, which was used in ¹H NMR experiments to confirm the existence of a hydrogen bonding network as shown in b). These results strongly suggest the existence of a similar hydrogen-bonding network in (-)-zampanolide, c). Adapted with permission from Troast, D. M. & Porco Jr., J. A., *Org. Lett.* **4**, 991–994 (2002). Copyright 2018 American Chemical Society.*

2.1.8 Uenishi's Total Synthesis of (-)-Zampanolide (2009)

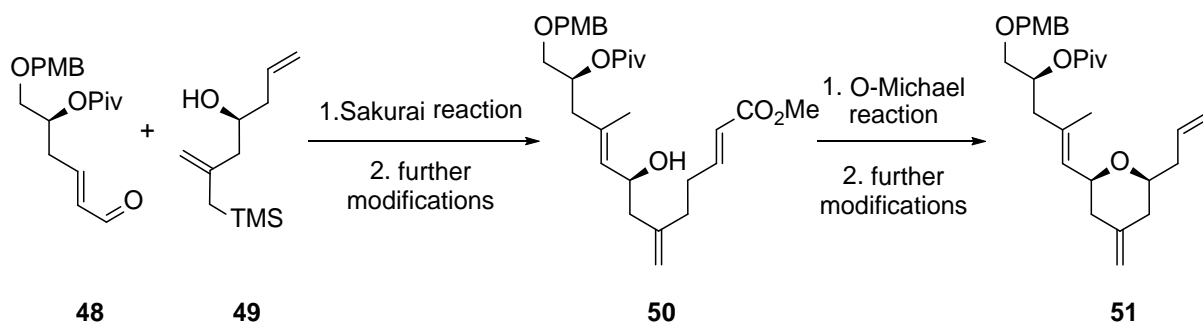
Uenishi and coworkers published a total synthesis of (-)-zampanolide in 2009.²⁹ Their synthesis featured a new method to close the macrocyclic ring of zampanolide, namely a Ru(II) catalyzed esterification using the Trost-Kita method (**Scheme 2.14**). This method works under non-basic conditions by subjecting a hydroxy acid, derived from HWE reaction of phosphonate **46** with aldehyde **45**,

and ethoxyacetylene to $[\text{RuCl}_2(\text{p-cymene})]_2$ and acid to form an ethoxyvinyl ester, which undergoes transesterification under expulsion of ethyl acetate and forms the desired macrocycle.⁴² The connection between building blocks **45** and **46** at C8-C9 was formed *via* a HWE reaction. The sidechain was installed by an acid-catalyzed *N*-acyl hemiacetal formation by treating dactylolide with CSA in the presence of **47**.



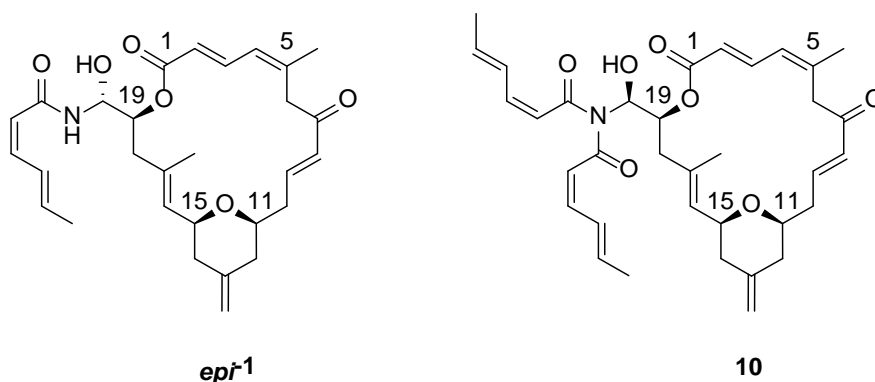
*Scheme 2.14 Uenishi's synthesis of (-)-zampanolide, featuring a *N*-hemiacetalization, an HWE reaction and a new method for the macrolactonization using the Trost-Kita method for esterifications.*

The *cis*-THP ring in this synthesis was formed by a Sakurai reaction between aldehyde **48** and allyl silane **49**, followed by several modifications to the homoallylic alcohol to install the methyl ester in **50** (Scheme 2.15). This compound then underwent a base-catalyzed *O*-Michael reaction to form the ring and several other modifications to produce building block **51**.



Scheme 2.15 Uenishi and coworkers employed a Sakurai reaction and subsequent O-Michael reaction to form the cis-THP ring of (-)-zampanolide.

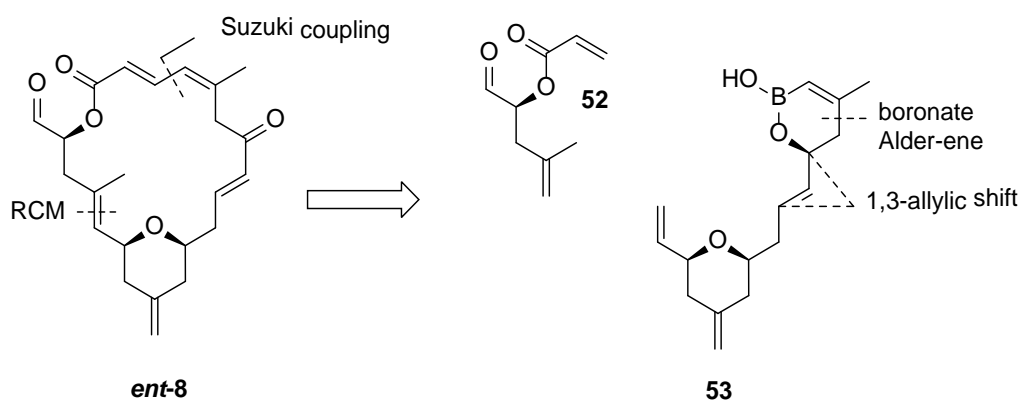
In the formation of the *N*-hemiacetalization reaction of dactylolide with **47** catalyzed by CSA to form (-)-zampanolide, two byproducts were formed as shown in **Scheme 2.16**. Both the C20-epimer of (-)-zampanolide *epi*-**1** as well as the bis(*N*-acyl)product **10** were biologically tested for their antiproliferative activity. Compound *epi*-**1** was found to be approximately 10-fold less active than zampanolide, while **10** was found to be up to 500-fold less active. These results are shown in **Chapter 1.5.1**.



*Scheme 2.16 Byproducts formed in the reaction of dactylolide with sidechain **47**, catalyzed by CSA.*

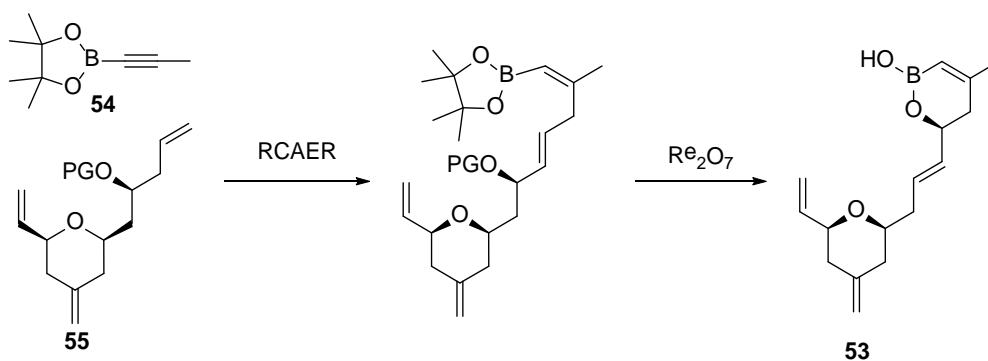
2.1.9 Lee's Total Synthesis of (-)-Dactylolide (2010)

The total synthesis of (-)-dactylolide in Lee's research group in 2010 relied heavily on transition metal-catalyzed reactions.⁴³ The building blocks **52** and **53** were connected *via* Suzuki coupling at C3-C4, and the macrocycle was formed using an RCM at C16-C17 (**Scheme 2.17**).



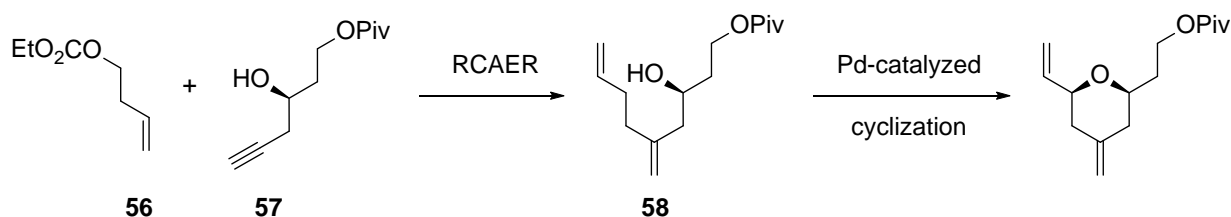
Scheme 2.17 Lee's total synthesis of (-)-dactylolide featuring a Suzuki coupling to connect building blocks **52** and **53**, and a RCM to close the macrocycle.

The boronic acid half ester **53** was synthesized through a RCAER (ruthenium-catalyzed Alder-ene reaction) of alkynyl boronate **54** with the least hindered double bond of **55**, followed by deprotection of the boronic acid pinacol ester and a 1,3-transposition of the protected allyl alcohol with rhenium oxide (**Scheme 2.18**).



Scheme 2.18 Formation of boronic half ester **53**.

The *cis*-THP ring in this synthesis was formed by another RCAER between fragments **56** and **57** leading to alcohol **58** (**Scheme 2.19**). The cyclization was achieved through a palladium catalyzed ring-closure.

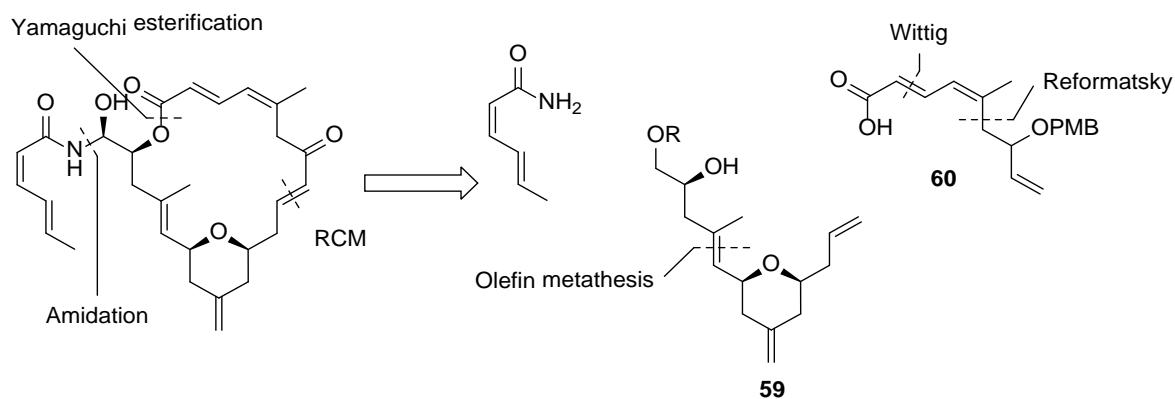


RCAER: ruthenium-catalyzed Alder-ene reaction

Scheme 2.19 Lee and coworkers used a RCAER (ruthenium-catalyzed Alder-ene reaction to connect fragments **56** and **57** and to form the exomethylene group, followed by a Pd-catalyzed cyclization to form the *cis*-THP ring.

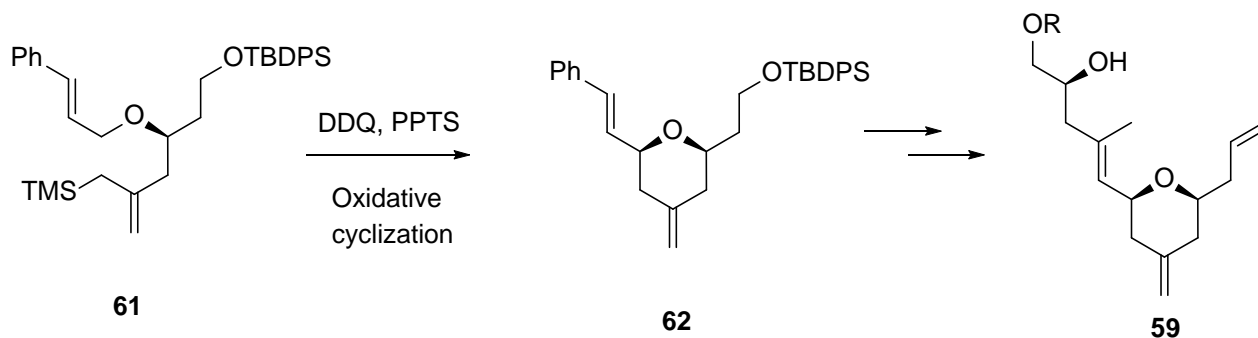
2.1.10 Ghosh's Total Synthesis of (-)-Zampanolide (2011)

Ghosh's research group reported their synthesis of (-)-zampanolide in 2011.⁴⁴ The macrocycle was closed using a RCM at C8-C9, after building blocks **59** and **60** were connected at C1 *via* Yamaguchi esterification (**Scheme 2.20**).



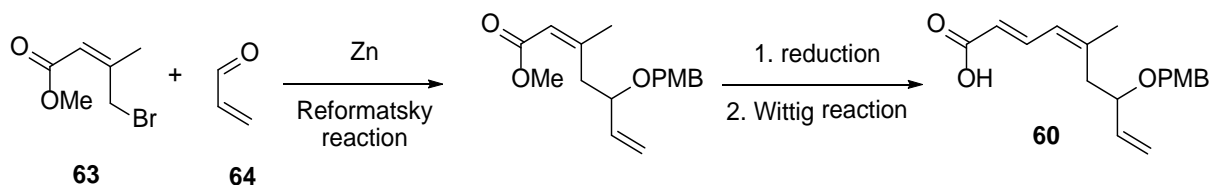
Scheme 2.20 Ghosh's total synthesis of (-)-zampanolide. A Yamaguchi esterification was used to connect the two major building blocks **59** and **60** at C1, followed by a RCM to close the macrocycle at C8-C9.

The *cis*-THP ring of building block **59** was synthesized *via* an oxidative cyclization of compound **61** to **62** using DDQ and PPTS, followed by multiple steps including a cross-metathesis to install the trisubstituted alkene at C16-C17 (**Scheme 2.21**).



Scheme 2.21 Formation of the *cis*-THP ring leading to fragment **59**.

Building block **60** was synthesized by reacting allylic bromide **63** with Zn to form a organozinc intermediate, which was then treated with acrolein **64** to form the C5-C6 bond *via* a Reformatsky reaction. Building block **60** is subsequently reduced to the aldehyde and a Wittig reaction was performed to install the acid functionality of **60**.



Scheme 2.22 Synthesis of Ghosh's C1-C8 fragment **60**.

However, the highlight of this synthesis was the formation of the *N*-acyl hemiaminal sidechain. Ghosh's group introduced a chiral phosphoric acid, (S)-TRIP (**Figure 2-2**), to promote the moderately diastereoselective amidation of C20. Although it is not a particularly novel reaction, it had considerable impact on the synthetic progress for (-)-zampanolide as it is more stereoselective than any other reported method for the sidechain installation. The two by-

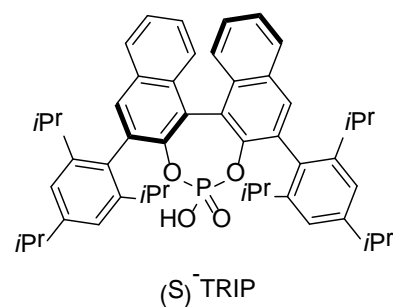


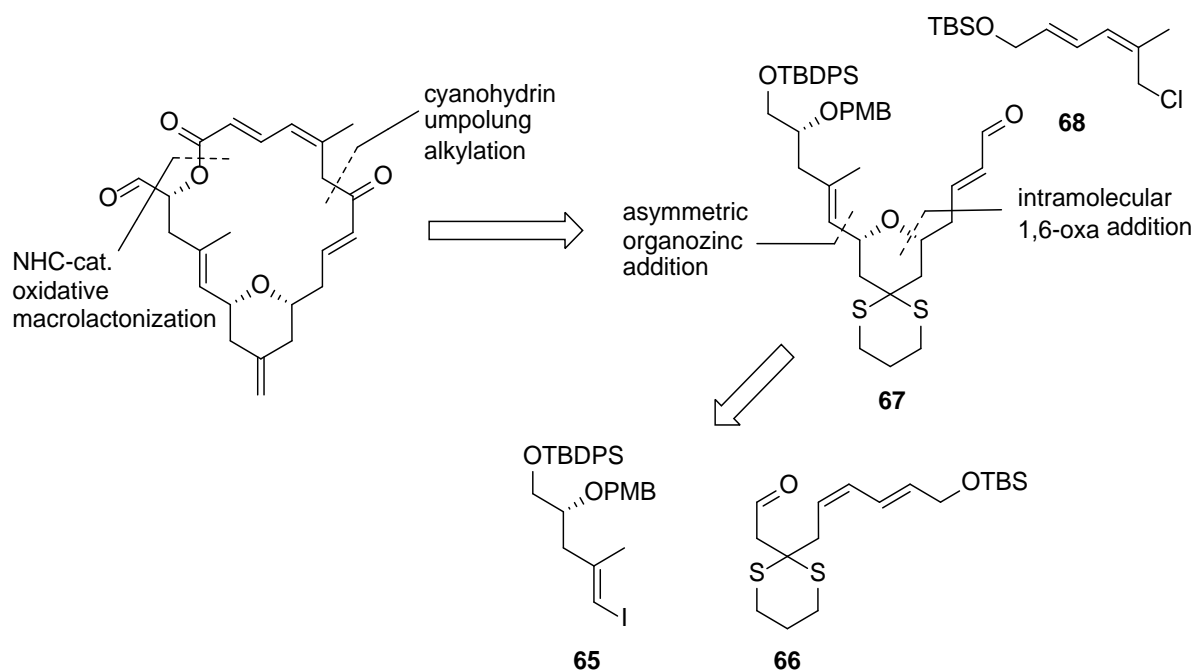
Figure 2-2 Chemical structure of the chiral phosphoric acid *S*-TRIP used by Ghosh's group to install the *N*-acyl hemiaminal functionality of (-)-zampanolide.

products previously observed in Uenishi's zampanolide synthesis, *epi*-**1** and **10**, were again observed but in decreased proportions (**Scheme 2.16**); these were included in tests for antiproliferative activity and evaluated in different cancer cell lines than reported by Uenishi.²⁹ However, the overall trends were the same, with both *epi*-**1** and **10** being at least 10-fold less active than zampanolide. These results are shown in **Chapter 1.5**.

2.1.11 Hong's Total Synthesis of (+)-Dactylolide (2012)

Hong and his research group published a total synthesis of (+)-dactylolide in 2012.³³ In this synthesis, the C16-C20 portion was installed *via* an asymmetric organozinc addition between iodide **65** and aldehyde **66**, and the tetrahydropyran moiety was formed subsequently *via* an intramolecular 1,6-oxa-Michael addition (**Scheme 2.23**). Building block **67** was then connected to the chloride **68** using a

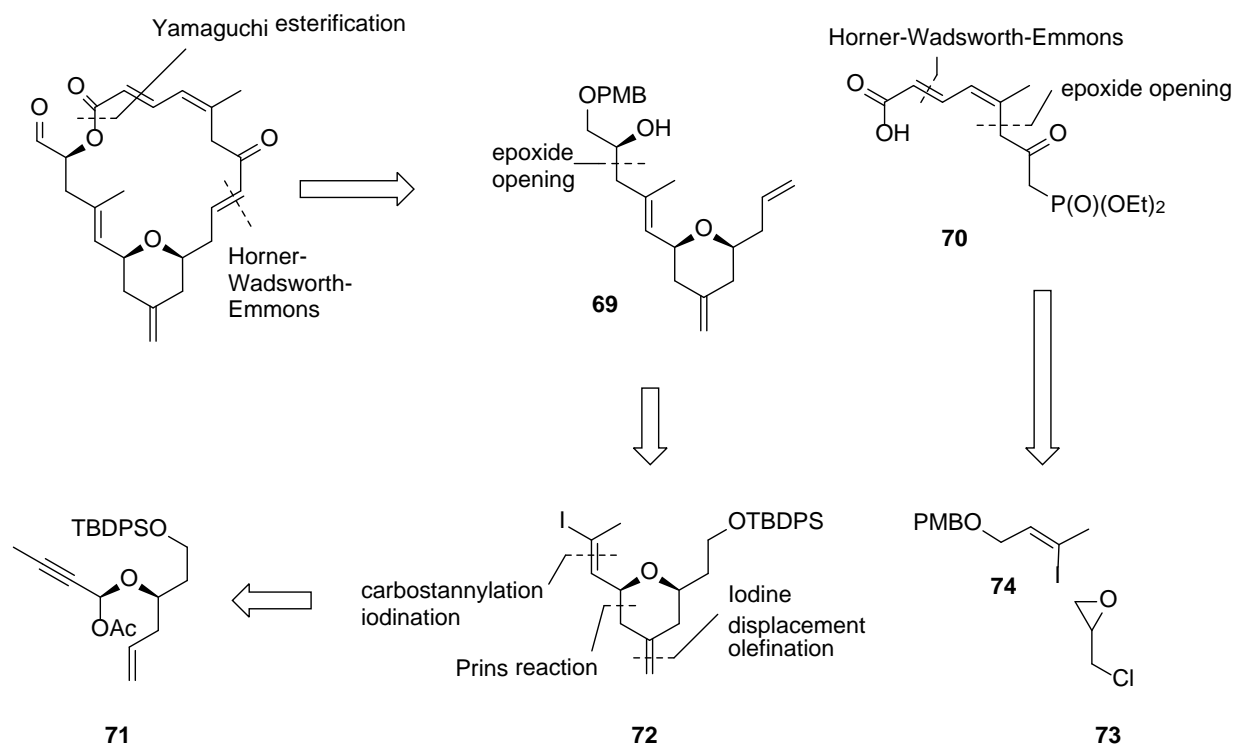
cyanohydrin umpolung alkylation reaction. Finally, the macrocycle was formed through a *N*-heterocyclic carbene-catalyzed (NHC-cat.) oxidative macrolactonization.



Scheme 2.23 Hong's total synthesis of (+)-dactylolide, using a NHC-catalyzed reaction as the ring-closing step. The bond between C6-C7 is formed through a cyanohydrin umpolung alkylation. The *cis*-THP ring is formed through an asymmetric organozinc addition, followed by an *O*-Michael reaction.

2.1.12 Altmann's Total Synthesis of (-)-Dactylolide (2010), (-)-Zampanolide And Analogs Thereof (2012)

Altmann and his group published a total synthesis of (-)-dactylolide in 2010.³⁴ Building blocks **69** and **70** were connected by a Yamaguchi esterification, followed by a HWE reaction to close the macrocycle (**Scheme 2.24**). Altmann's group was the first to use a HWE reaction between C8-C9 to form the macrocycle, although this reaction had been used in an intermolecular sense at this position in previous syntheses of the macrocyclic core of zampanolide.



*Scheme 2.24 Altmann's total synthesis of (-)-dactylolide. Building blocks **69** and **70** are connected via Yamaguchi esterification. A HWE reaction is used to close the macrocycle. The *cis*-THP is formed through a Prins reaction, followed by iodine displacement olefination and carbostannylation/iodination reaction.*

Building block **69** was synthesized from precursor **71**, which was subjected to a Prins reaction promoted by TMSI yielding the *cis*-THP ring containing compound **72**. The resulting iodine was then displaced to give the exomethylene in four steps. A carbostannylation reaction and quench with iodine was used to install the trisubstituted alkene in compound **72**, which was then used to selectively open a simple epoxide, leading to the formation of building block **69**.

Building block **70** was synthesized by reacting epichlorohydrin (**73**) with protected *Z*-vinyl iodide (**74**), followed by conversion to a new oxirane, which was then opened with lithiated diethylphosphite. The acid functionality of **70** was installed by means of a HWE reaction and saponification.

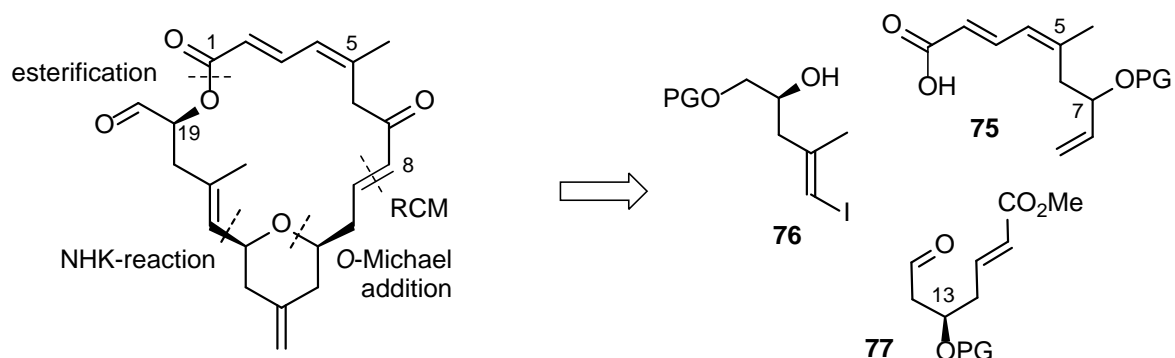
In 2012 another paper was published by Altmann's research group, describing the synthesis of (-)-zampanolide and several (-)-dactylolide derivatives for a SAR study.³² The strategy used for these syntheses differed slightly from the one previously used, but the major disconnections stayed the same. Structures of the synthesized derivatives are shown in **Figure 1-8** and the results of the antiproliferative tests are discussed in **Section 1.5.2**.

2.2 Previous Work in the Harvey group

Previous work on the zampanolide system in Joanne Harvey's group was conducted by Samuel Ting, Claudia Gray and Jingjing Wang. Ting mainly focused on synthesizing necessary fragments to form the macrocyclic core (discussed in **Chapter 2.2.1**), while Gray explored methods to synthesize sidechain analogs (discussed in **Chapter 2.2.2**). Wang's PhD thesis focused on advancing the synthesis of zampanolide itself and generating the fragment for the synthesis of the C5-desmethyl analog (**Chapter 2.2.3**).⁴⁵ At the same time, Wang explored the Bestmann ylid linchpin as an efficient approach to generate the dienolate motif of zampanolide and conducted studies to expand the scope of the method (**Chapter 2.2.4**).

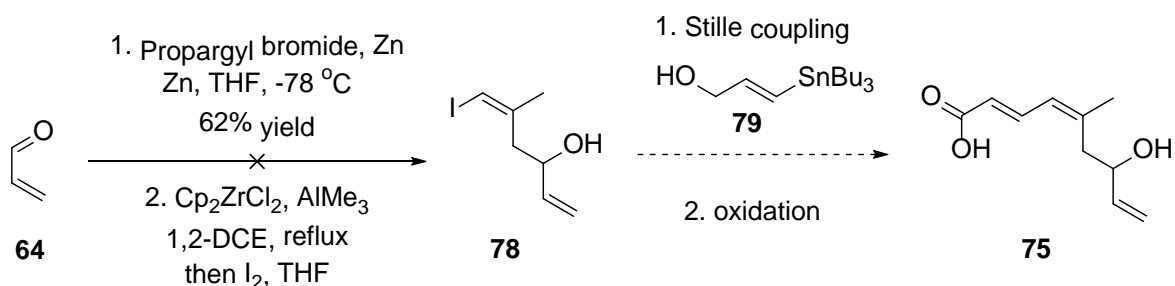
2.2.1 Ting's Work on Fragments

Ting's work as a research assistant focused on the synthesis of fragments for the zampanolide macrocycle, following the retrosynthetic plan outlined in **Scheme 2.25**. The ring-closure was planned to be achieved by either esterification at the C1 position between fragment **75** and **76**, or RCM at C8/C9, both well-established methods in the synthesis of zampanolide and dactylolide. To connect iodide **76** and aldehyde **77** and set the desired configuration at C15, a stereoselective Nozaki-Hiyama-Kishi (NHK) reaction was envisioned, followed by the formation of the THP ring by *O*-Michael addition.



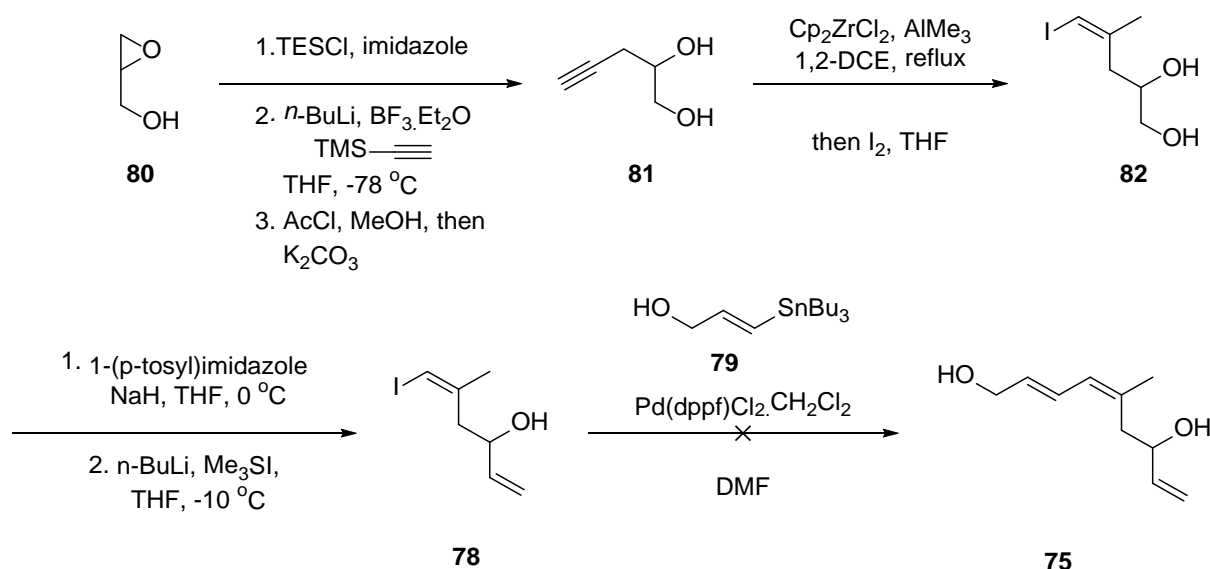
Scheme 2.25 Ting's retrosynthetic strategy featuring a NHK-reaction, esterification and RCM as major disconnections.

The synthesis of the C1-C8 fragment started with the addition of propargyl bromide to acrolein (**64**) using Barbier conditions, which proceeded with a moderate yield of 62% (the product is highly volatile) (**Scheme 2.26**). A subsequent carboalumination/iodination sequence was envisaged to reduce the alkyne to the trisubstituted alkyne. Iodide **78** would then be subjected to a Stille coupling with compound **79**, and the alcohol would be oxidized to acid **75** to prepare for the subsequent esterification. However, the *anti*-carboalumination/iodination was found to not be a feasible method even after countless optimization efforts. Trimethylaluminum (TMA) easily degrades and is hard to handle and the reaction outcome was not reproducible, therefore this route was abandoned.



Scheme 2.26 Ting's attempted synthesis of the C1-C8 fragment, using a carboalumination/iodination reaction followed by a Stille coupling.

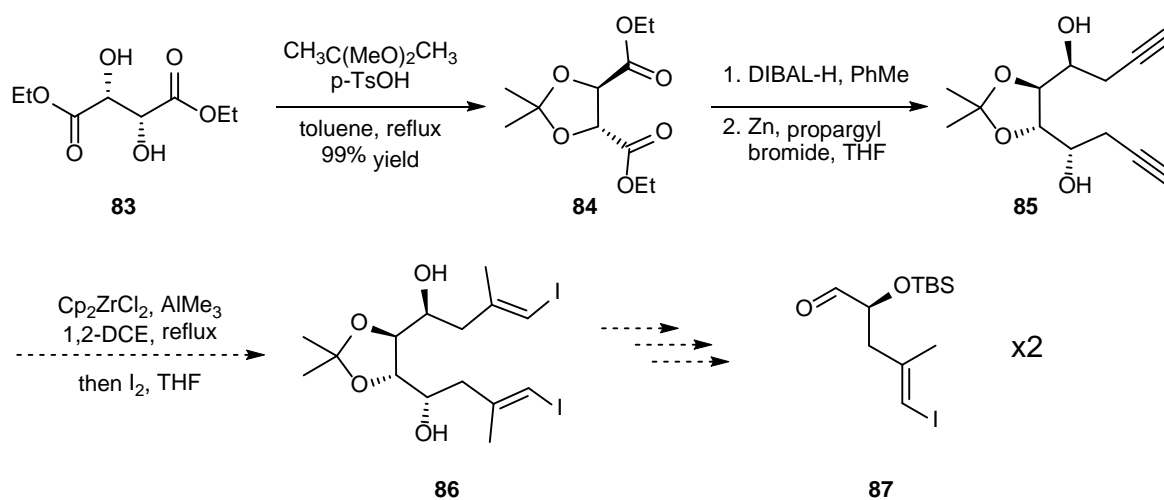
An attempt was made to synthesize the dienoate fragment from glycidol (**80**), which by using enantiopure glycidol would allow the synthesis of C7-hydroxy analogs of zampanolide with varying stereochemical configuration at C7 (**Scheme 2.27**). The alcohol of glycidol was protected as a TES ether and the epoxide was opened with TMS-acetylene. The TMS and TES groups were then easily removed by using AcCl in MeOH, followed by the addition of potassium carbonate producing diol **81**. The subsequent carboalumination and iodination yielded iodide **82**, albeit in low yields. The primary alcohol was then transformed into a terminal alkene in two steps. The key step however, the Stille coupling of compound **78** with alcohol **79** failed, therefore this route was abandoned.



Scheme 2.27 Ting's alternative synthesis of the top fragment in seven steps. The sequence failed in the last step, the Stille coupling.

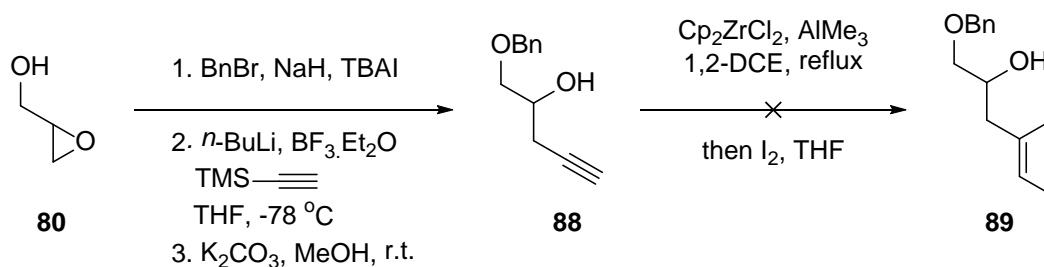
For the synthesis of the protected vinyl iodide **76**, Ting envisioned a synthesis starting from diethyl tartrate (**83**), which is a readily available source of chirality (**Scheme 2.28**). The diol was protected as cyclic acetal **84**, and both ester functionalities were reduced to the aldehyde, which allowed a Barbier reaction using propargyl bromide similar to the first step in **Scheme 2.26**. It was hoped that this reaction would produce **85** as a single stereoisomer, which could then be

subjected to a *cis*-carboalumination/iodination sequence to yield iodide **86**. Several modifications including a periodate cleavage would then result in two moles of fragment **87** for every mole of diethyl tartrate used, which could make this route highly efficient. However, this strategy was quickly abandoned after it became clear that the Barbier reaction did not proceed with the desired stereoselectivity.



Scheme 2.28 Ting's strategy for the synthesis of the C16-C20 fragment.

Using a similar strategy as in the attempted synthesis of the C1-C8 fragment, Ting resorted to using glycidol (**80**) as a starting material for the synthesis of the C16-C20 fragment, which again would allow for the introduction of defined configuration through a chiral pool reagent (Scheme 2.29). The alcohol was protected with benzyl bromide, the epoxide opened using TMS-acetylene and the TMS protecting group subsequently removed using potassium carbonate in MeOH to produce alcohol **88**. However, the key step in the sequence, the carboalumination/iodination sequence, did not result in the formation of desired iodide **89**.

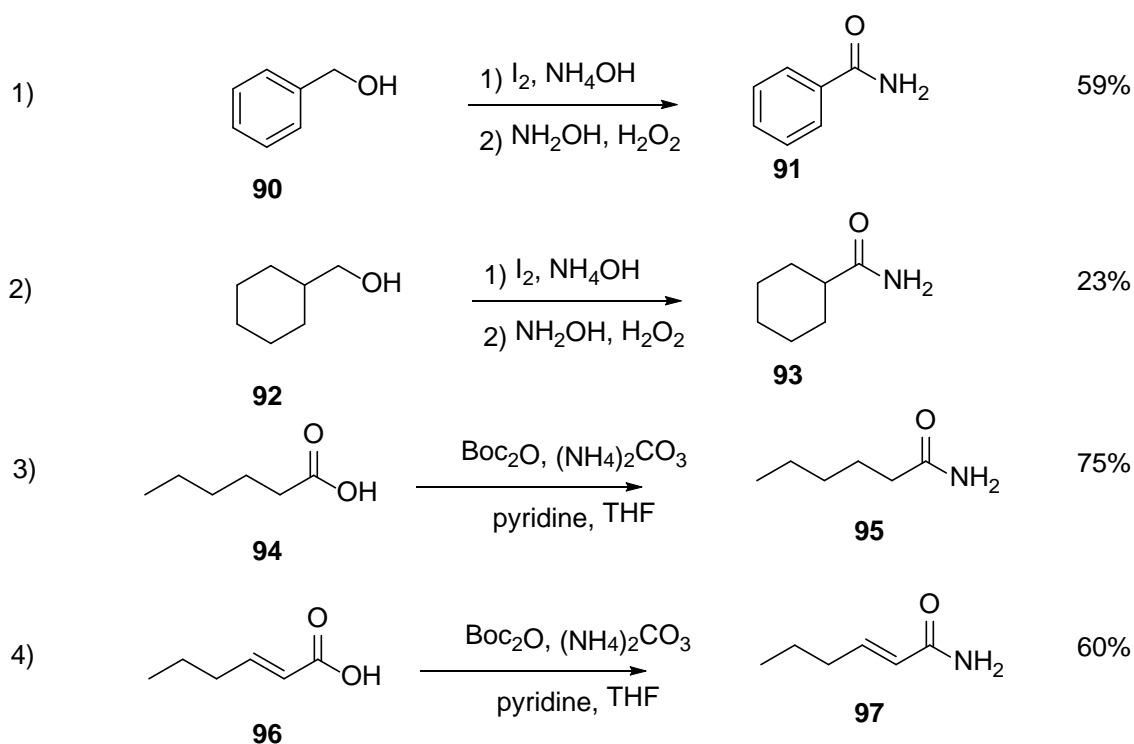


Scheme 2.29 Ting's second attempt at the synthesis of the C16-C20 fragment using glycidol as starting material.

Ting's difficulty in synthesizing precursors for the NHK reaction and the failure of the carboalumination/iodination sequence for the synthesis of the northern fragment led to a change in the retrosynthetic strategy in the course of Wang's thesis, and is briefly described in this work in **Chapter 2.4**.

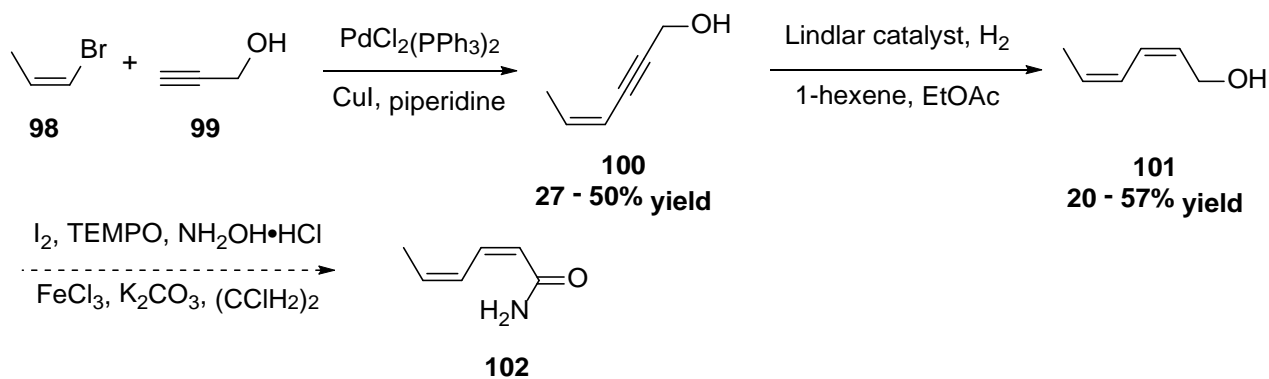
2.2.2 Gray's Work on Fragments for the Synthesis of Sidechain Analogs

Claudia Gray, who was a previous member of Joanne Harvey's research group, conducted preliminary studies on the synthesis of the various amide sidechains (**Scheme 2.30**). These amide sidechains, as typical in the zampanolide system, could then be attached to the macrocycle by reaction with the aldehyde moiety of dactylolide (**8**). The amidation of primary alcohols *via* oxidation with iodine in the presence of ammonia gave a reasonable yield for the oxidation of benzylic alcohol **90** to **91**, while the reaction of saturated **92** to **93** delivered poor yields. A second method investigated by Gray was the amidation of carboxylic acids using *t*-butyl dicarbonate (Boc_2O) to activate the acid in the presence of ammonium carbonate. This method proved to be more effective in the synthesis of saturated amide **95** from acid **94**, and gave a good yield for the synthesis of alkenyl amide **97** from conjugated acid **96**.



Scheme 2.30 Gray's synthesis of sidechain analogs using two different methods.

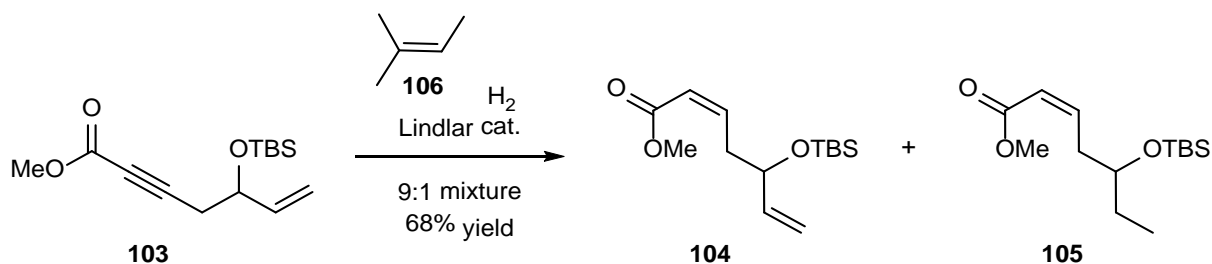
Gray also explored the synthesis of (2*Z*,4*E*)-hexa-2,4-dienamide (**102**), which is necessary for the synthesis of natural occurring (-)-zampanolide, (**Scheme 2.31**). The synthesis started with a Sonogashira coupling, connecting bromide **98** and propargylic alcohol **99** to form enyne **100**. However, the reduction of the alkyne to the alkene using Lindlar's catalyst resulted in partial over-reduction of **100**, and the isolation of desired product **101** as a mixture with partially saturated byproducts that could not be separated. Therefore the subsequent amidation has not been attempted yet.



Scheme 2.31 Proposed synthesis for Fragment D.

2.2.3 Wang's Synthesis of the C5-Desmethyl Fragment

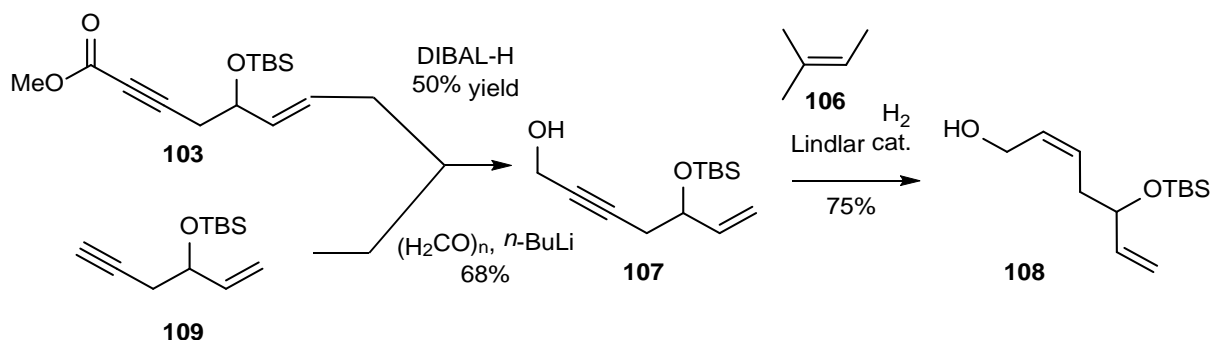
One of the proposed analogs is the C5-desmethyl version of zampanolide. In her thesis, Wang investigated methods to get to the necessary building block. She started from **103** and reduced the alkyne to *cis*-alkene **104** using H₂ and Lindlar catalyst. However, this led to an inseparable mixture of the desired product **104** and the over-reduced product **105**, despite addition of sacrificial alkene **106** (Scheme 2.32).



Scheme 2.32 Wang's attempted synthesis of the C5-desmethyl building block.

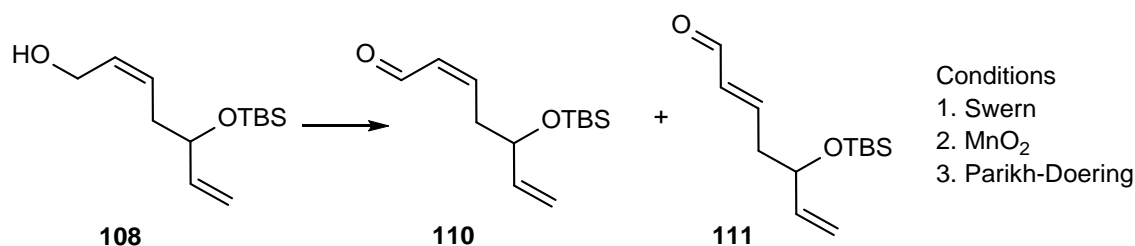
Hoping that the alkyne in a propargylic alcohol, which is more electron rich than in the corresponding ester, would be reduced significantly faster than the terminal alkene, Wang reduced ester **103** to alcohol **107** using DIBAL-H. The yield of this

reaction was only 50%; however, the subsequent Lindlar reaction produced alcohol **108** in 75% yield without any over-reduction when enough sacrificial **106** was included. In an effort to shorten the reaction sequence, Wang synthesized **107** directly from **109** using paraformaldehyde in DMF, which delivered alcohol **107** in a reasonable 68% yield (**Scheme 2.33**).



Scheme 2.33 Wang's successful reactions leading to the desired configuration of the C4-C5 alkene.

To get to the C5-desmethyl fragment, alcohol **108** had to be oxidized to aldehyde **110**. Wang tried various methods, including Swern oxidation, oxidation using manganese dioxide and Parikh-Doering conditions. She found that Swern and manganese dioxide oxidation resulted in inseparable mixtures of the *Z* and *E* enal, **110** and **111**, respectively. Parikh-Doering oxidation on a mixture of starting materials did not show any sign of the undesired alkene isomerization, and therefore remained the method of choice for this oxidation (**Scheme 2.34**).



Scheme 2.34 Different conditions tested by Wang for the oxidation of alcohol **108** to C5-desmethyl fragment **110** and byproduct **111**.

2.2.4 Wang's Scope Studies on the Bestmann Ylid Linchpin

Wang, alongside Ting's approach of forming the connection at C1 using a Yamaguchi esterification, investigated an alternative methodology to form the conjugated ester *via* a Bestmann ylid cascade. Wang conducted studies on the scope of the Bestmann ylid cascade in the synthesis of $\alpha,\beta,\gamma,\delta$ -unsaturated esters, using mostly cinnamic aldehyde as a model aldehyde and coupling it with various alcohols to find ideal conditions to be used in the zampanolide system. The results are summarized in her paper.⁴⁶ With these results in hand, Wang proceeded to test the Bestmann ylid cascade on macrocycle fragments for the synthesis of zampanolide. Both the reactions of PMB and TBDPS protected alcohol fragment (**112** and **113**, respectively) gave better yields in refluxing toluene than THF when reacted with Bestmann ylid **114** and *E*-cinnamaldehyde **115** (Table 2.1).

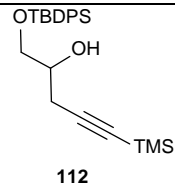
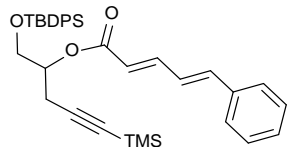
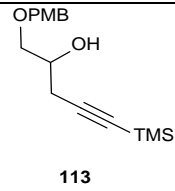
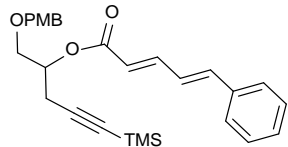
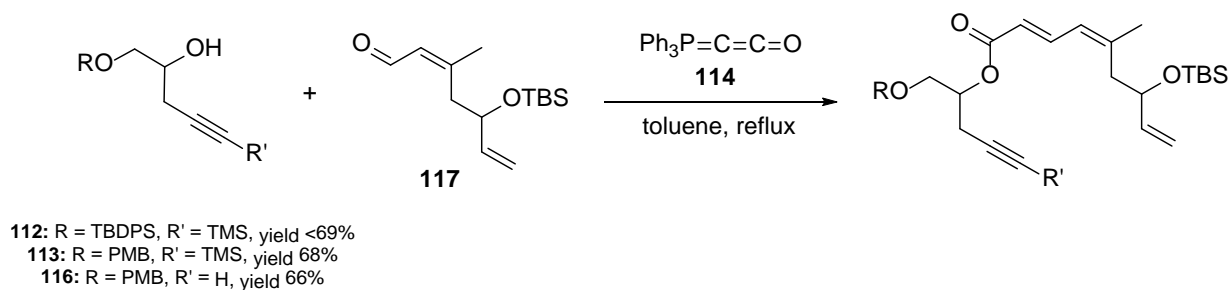
Entry	Alcohol	Conditions	Product	Yield
1	 112	THF, 68 °C, 3.5 h		<36% ^a
		Toluene, 110 °C, 2 h		<49% ^a
2	 113	THF, 68 °C, 8 h		42%
		Toluene, 110 °C, 4 h		70%

Table 2.1 Bestmann ylid cascade reaction of the zampanolide fragments **112** and **113** with *E*-cinnamaldehyde **115** in refluxing THF or toluene. ^aThe product was contaminated with the regioisomer resulting from silyl migration and esterification of the primary alcohol.

The reaction of the zampanolide fragments **112**, **113** and **116** with aldehyde **117**, the C3-C8 fragment for the synthesis of zampanolide, gave yields between 66% and 69% when they were conducted in refluxing toluene (Scheme 2.35).



Scheme 2.35 Bestmann ylid cascade reaction to connect the C16-C20- fragment (**112**, **113** and **116**) with the C3-C8 aldehyde fragment **117**.

2.3 Aim of This Thesis

The aim of this research was to further develop a new method for the total synthesis of (-)-zampanolide as well as prepare analogs thereof. As explained in **Chapter 1**, (-)-zampanolide exhibits activities in the nanomolar range against various cancer cell lines, including MDR pump overexpressing cells, which might allow for application in cancer patients that have developed a resistance against paclitaxel and other chemotherapeutic drugs.

The synthetic strategy should be concise, modular and allow the easy generation of analogs. This would facilitate development of an analog library and subsequent subjection of the synthesized compounds to structure-activity relationship studies in various cell lines. Guided by previously published biological results as well as the binding interactions found through the solved crystal structure of the zampanolide-tubulin complex, the proposed modifications would include the installation of different sidechains including aromatic and alkyl variations (**118-122**), sequential deletion of methyl groups located on the macrocycle (**123** and **124**) and removal as well as oxidation state changes of the exomethylene (**125** and **126**), summarized in **Figure 2-3**.

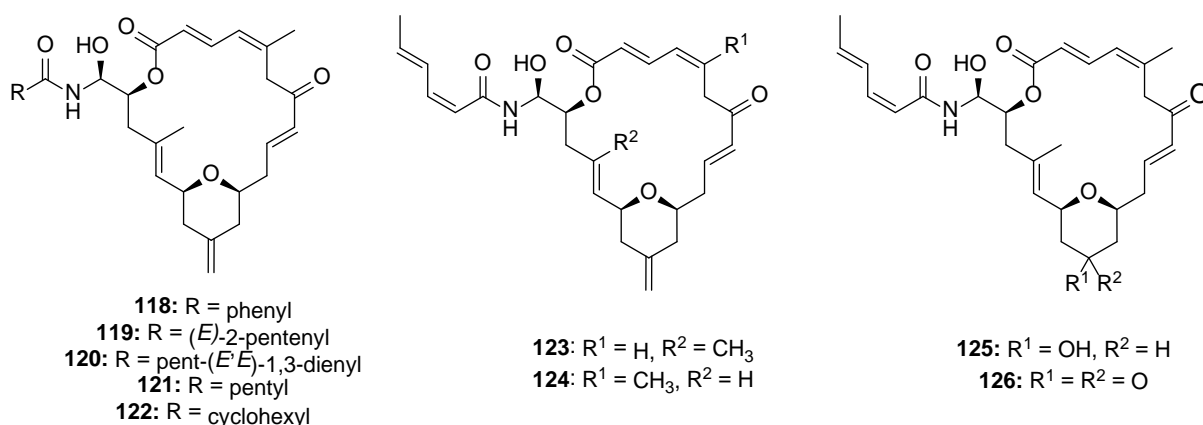
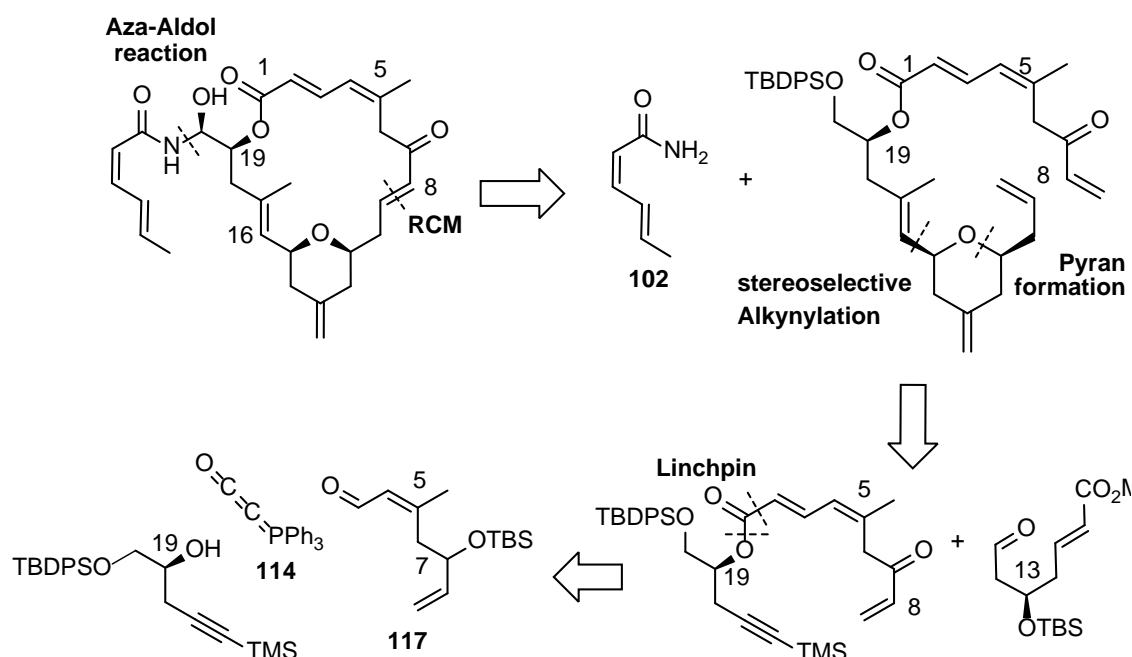


Figure 2-3 Structures of proposed analogs.

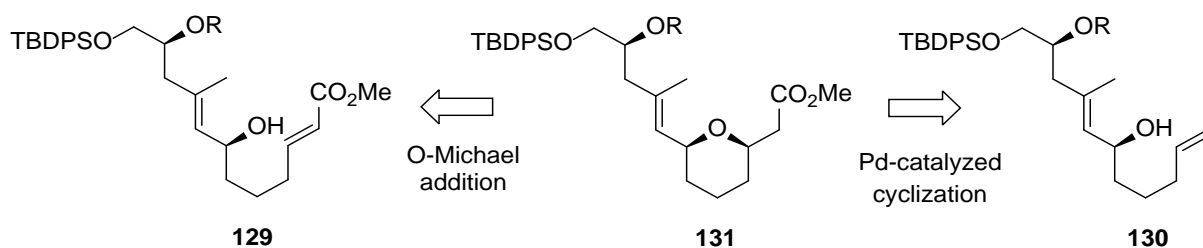
2.4 First Generation Retrosynthetic Approach Based on Wang's Thesis

When this project began on the zampanolide system, the synthetic approach as devised by Wang entailed a late stage installation of the side chain and three major disconnections within the macrocycle. The retrosynthetic approach is shown in **Scheme 2.36**. The side chain contains a hemi-aminal functionality which may be installed using an aza-aldol reaction between amide **102** and the aldehyde functionality of dactylolide. The formation of the macrocycle using an RCM at C8/C9 has been shown in the zampanolide system before and is well established.^{26,29,35,36,44} The two other major disconnections are a Bestmann ylid linchpin to form the dienoate motif of **127** as described by Wang,^{45,46} and a stereoselective alkynylation to connect fragment **127** and **128** and install the correct configuration at C15. In a first outline the protecting group strategy only involves silyl protecting groups, however it could easily be modified and adjusted as needed while the synthesis was progressing. By using five small fragments, which can be easily modified for the generation of analogs, and a convergent synthetic strategy, namely connecting fragments in a late stage of the synthesis, this approach would allow for a ready and rapid generation of compounds similar to zampanolide for subsequent biological screening.



Scheme 2.36 Retrosynthetic approach as devised by Wang.

The formation of tetrahydropyran (THP) rings is well explored in the scientific literature, and multiple different methods have been used to form the THP moiety in zampanolide, as discussed in **Chapter 2.1**. For our synthetic approach, two methods are particularly applicable, an *O*-Michael addition or a Pd-catalyzed carboxylative cyclization. Even though the two methods require slightly different precursors, **129** and **130**, as shown in **Scheme 2.37**, they yield the same product **131**, which could then be modified for use in the RCM. However, the use of an *O*-Michael addition is the preferred method, as it uses less expensive reagents, is less sensitive to air and moisture and requires shorter reaction times than the Pd-catalyzed reaction. An alternative method to form the THP ring would be an iodoetherification reaction, which uses the same precursor **130** as the Pd-catalyzed carboxylative cyclization, but which would then have to include a sp^2 - sp^3 Heck coupling to install the additionally required two carbon unit to set up for the RCM. Heck couplings of this type are known to be hard to control, as they are prone to elimination and only very few examples have been reported in the literature.



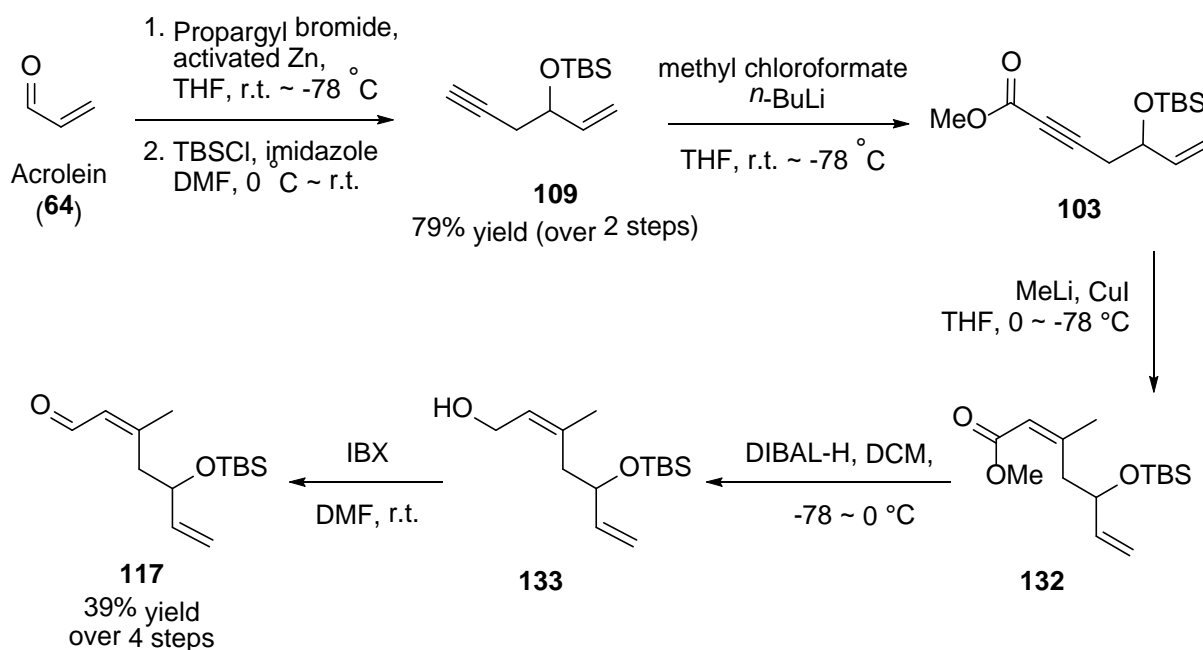
Scheme 2.37 Suggested methods to form the pyran ring.

For the installation of the methyl group at C17 and the selective reduction of the alkyne to the *E*-alkene a one-pot reaction using vitride followed by the addition of an alkyl halide was envisaged, as established by Jamison.⁴⁷ This method allows for the substituent at C15 to be exchanged without having to alter the methodology used. Alternatively, if the reductive methylation with vitride or the stereoselective alkynylation to connect fragments **127** and **128** were to fail, Ting's approach of using Cp_2ZrCl_2 and AlMe_3 could be revisited to install the C17 methyl group and reduce the alkyne first before coupling the resulting iodide with aldehyde **128** *via* an NHK reaction.

Chapter 3: Fragment Synthesis and Second Generation Retrosynthetic Approach

3.1 Synthesis of the C3-C8 Fragment

The reaction sequence for the synthesis of this fragment was established by Wang and has been repeated and optimized with regard to number of purification steps in this work. While the overall yield remained similar, the number of necessary columns was reduced from a total of five to only two columns in the sequence, which saves time and minimizes waste as well as required resources. An overview of the reaction sequence with current yields and indication of necessary purifications can be found in **Scheme 3.1**.



Scheme 3.1 Reaction scheme for the synthesis of fragment 117.

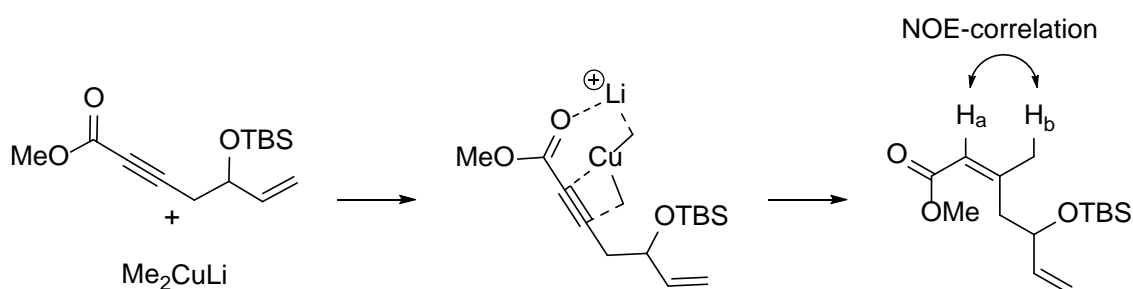
The first reaction in the synthesis of this fragment is a Barbier reaction performed on acrolein (**64**) as a substrate. The Barbier reaction is similar to the Grignard reaction, however the reactive metal species does not have to be generated in a separate step, which allows the Barbier reaction to be performed as a one-pot synthesis. This reaction has been known for over a hundred years and can be performed with various metals, including zinc, indium, samarium and aluminum amongst others. The mechanism most likely involves a single electron transfer (SET).⁴⁸

The reaction between the very volatile and toxic acrolein and propargylic bromide proceeds readily and in a clean manner when activated Zn powder is used. The product of the reaction is very volatile, so special care has to be taken when the solvent is reduced after the work up to minimize product loss. Evaporation of the solution to dryness is not necessary, and subsequent work can be done on the concentrated ethereal solution. While Wang used a short silica plug to purify the alcohol, no purification was needed in this work prior to performing the TBS protection, and a yield of 79% over two steps was achieved. The TBS protected alcohol **109** is still volatile but less so than the precursor and is therefore handled more easily and subjected to a silica column for purification.

In the next step, methyl chloroformate is reacted with the alkyne moiety of **109** under basic conditions to yield **103** in an 85% yield, and **103** was used without further purification. However, it was found that the yield and purity of the crude product of this reaction (as determined by NMR) is greatly dependent on the quality of the reagents, and the best yields have been achieved when newly opened bottles of *n*-BuLi and methyl chloroformate were used.

The reduction and methylation of the alkyne of **103** to the trisubstituted *E*-alkene was achieved by use of the Gilman reagent, which can easily be generated *in situ* by reacting freshly purified CuI with MeLi in THF at 0 °C to generate Me₂CuLi.

Gilman reagents are known to react *via* a 1,4-addition with conjugated carbonyl compounds, with regioselectivity being achieved through coordination of the Li to the carbonyl oxygen, as seen in **Scheme 3.2**. The generation of the *Z*-alkene **132** was confirmed by Wang through a strong NOE correlation between the alkene proton H_a and the protons of the methyl group H_b, and the data reported in this work matched her findings. The obtained product **132** can be used in the next step without any further purification.

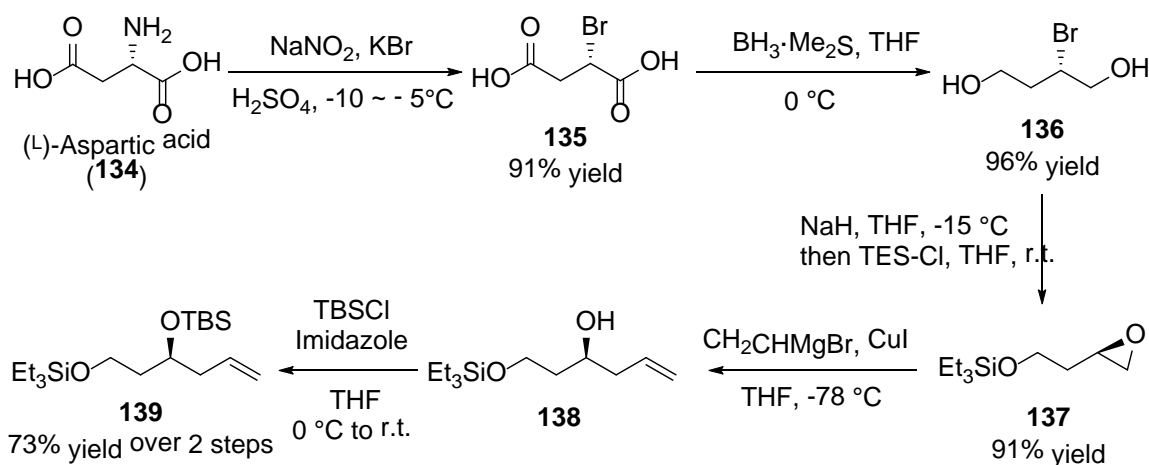


Scheme 3.2 Transition state of the reductive methylation using Gilman's reagent and NOE correlation used to confirm the correct product **132**.

To obtain fragment **117**, the ester functionality had to be converted to the corresponding aldehyde. Wang showed that a direct reduction to the aldehyde is not easily achievable, due to temperature sensitivity of the reaction and the stability of the intermediate, and that a reduction-oxidation sequence is more feasible. Therefore, the ester functionality was then reduced to alcohol **133** with 2.8 eq of DIBAL-H in good yields, before being reoxidized to aldehyde **117**. For the oxidation to the aldehyde IBX was used, which was synthesized following Sputore's method using Oxone to produce what was defined as "analytical grade IBX" in the paper.⁴⁹ The purity of the synthesized IBX was not analyzed and it was directly used in the oxidation reaction to yield aldehyde **117** in 39% yield over four steps after purification by column chromatography.

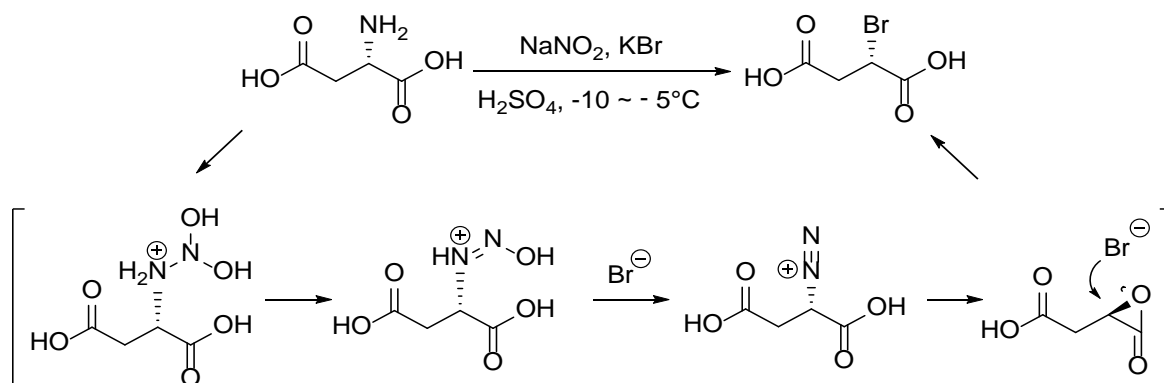
3.2 Synthesis of the C9-C15 Fragment

The synthesis of this fragment had been investigated by Ting (but featuring a different protecting group strategy) as well as by Wang (featuring the current protecting group strategy) and has been previously described in the literature.⁵⁰ However, in this work yields were improved while the number of purification steps needed was reduced. An overview of the reaction sequence with improved yields can be found in **Scheme 3.3**.



Scheme 3.3 Reaction scheme for the synthesis of compound **139**, which serves as precursor for building block **128**.

The sequence started with substitution of the amino group of (L)-aspartic acid (**134**) with a bromide in a Sandmeyer-type reaction, which proceeds *via* the diazonium salt with double inversion of the configuration, thereby retaining the configuration of the stereocenter overall (**Scheme 3.4**).

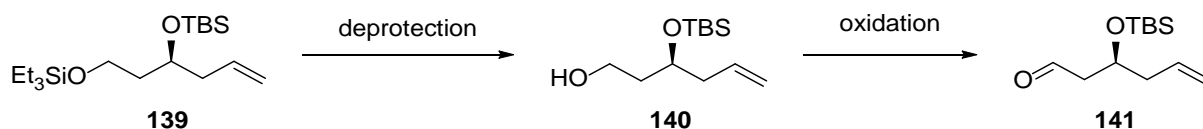


Scheme 3.4 Mechanism for the retention of configuration in the Sandmeyer-type reaction of 134 to 135.

This reaction proceeded with high yields and the formed product did not require further purification. Diacid **135** was then subjected to a double reduction with borane to afford the diol **136** again in excellent yields and in a clean manner, therefore no purification was needed to conduct the next step. A Williamson ether synthesis-type reaction was then used to form epoxide **137** and the remaining alcohol functionality protected *in situ* with a TES protecting group. At this stage, **137** was subjected to a silica column for purification for the first time in the sequence, and the yields achieved were usually 90% and above.

In the next step, the epoxide of **137** was opened regioselectively with vinylmagnesium bromide under assistance of copper(I) iodide to give compound **138**. When freshly purified copper(I) iodide and a new bottle of vinylmagnesium bromide were used, and all reagents were added very carefully, the reaction exclusively produced the desired product, which was then subjected to TBS protection without previous purification. Protected diol **139** was produced in 73% over two steps. If, however, the vinylmagnesium bromide solution was added too quickly, the temperature is not strictly kept at -78 °C during addition or the reaction mixture was allowed to warm up above 0 °C before the aqueous quench, some of the epoxide was opened with the undesired regioselectivity.

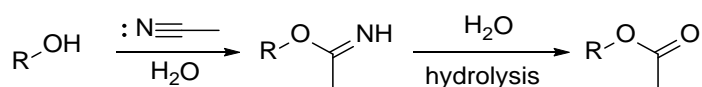
To obtain a substrate to be used in the stereoselective alkynylation, the primary alcohol has to be deprotected selectively to give alcohol **140**, which then has to be oxidized to aldehyde **141** (**Scheme 3.5**).



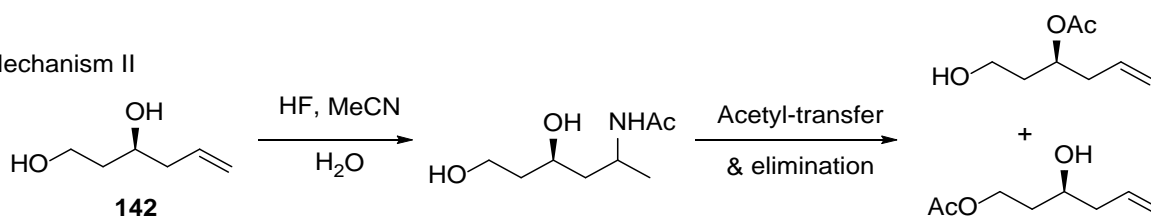
*Scheme 3.5 Deprotection and oxidation to convert protected dial **139** into aldehyde **141**.*

For the selective deprotection of the primary alcohol of **139**, initially a method using HF-pyridine in acetonitrile was used, which in initial attempts yielded the desired product in less than 10% yield, and mostly yielded double deprotected product **142**. The yield was improved by about six-fold by decreasing the reaction time from overnight to three hours, and close monitoring by TLC. Another rather unexpected problem, in addition to the double deprotection encountered by Wang, was that when analytical grade acetonitrile instead of distilled acetonitrile was used, acetylation of either and/or both hydroxy groups occurred. Two plausible mechanisms of how acetylation can occur are shown in **Scheme 3.6**.

Mechanism I



Mechanism II



Scheme 3.6 Proposed mechanisms for acetylation of the hydroxy group in the presence of water.

Mechanism I could occur if acetonitrile was protonated by HF in the presence of water, which would facilitate the attack by either hydroxy group of the doubly deprotected alcohol **142** to produce an imine. The imine would then be hydrolyzed in the presence of water, which would explain the acetylation of either hydroxy group, or both.

Mechanism II could occur *via* a Ritter reaction and subsequent acetyl-transfer and elimination of ammonia. The terminal alkene can be protonated and form the most stable carbenium ion, which is then attacked by the nitrogen of the nitrile group and water adds to the imine intermediate, resulting in an overall addition of an NHAc group to the terminal alkene. The acetyl group can then be transferred onto the secondary hydroxy group *via* a six-membered transition state, or onto the primary alcohol *via* an eight-membered transition state. The last step is the elimination of ammonia to regenerate the terminal alkene.

The fact that the expulsion of ammonia under the very acidic conditions is rather unlikely, as well as the consideration that the eight-membered transition state is not particularly favored but significant amounts of the doubly acetylated product and mono-acetylated product at the primary hydroxyl were isolated, led to the conclusion that mechanism I is more likely to occur under the given conditions.

HF-pyridine is a highly toxic reagent and very unpleasant to work with, therefore alternative deprotection strategies were explored. An alternate method to deprotect the primary alcohol using PPTS in MeOH was investigated. An initial attempt yielded the desired product in 26% yield in an overnight reaction at room temperature with 1.1 eq PPTS, along with double deprotected material. Optimization studies were conducted as shown in **Table 3.1**, and the ratios of mono deprotected product to double deprotected material of the crude mixture were determined by NMR spectroscopy. As entry 3 proved most promising, the reaction

was repeated under those conditions and afforded the desired product in 67% yield.

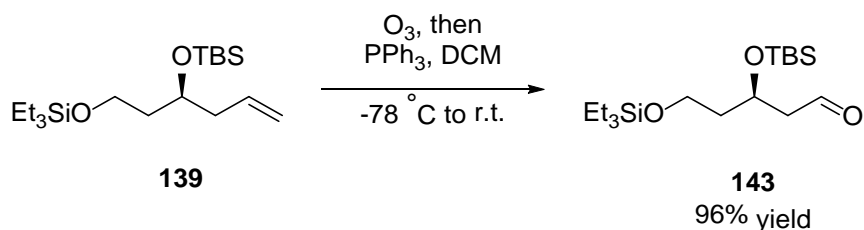
Entry	Eq. PPTS	Temperature (°C)	Ratio 140 : 142 ^a
1	0.1	4	1.1:1
2	1	-20	1.3:1
3	0.1	-20	7.7:1

*Table 3.1 Optimization conditions for the deprotection of the primary TES group using PPTS in MeOH. ^aThe ratio of **140** to **142** was determined by analysis of the ¹H NMR spectrum of the crude mixture.*

With **140** in hand, the next step was to oxidize the primary alcohol to the aldehyde to set up the fragment for the subsequent alkynylation reaction, which proved more difficult than expected. The first conditions tested were standard Swern oxidation conditions in accordance with literature, which yielded only small amounts of aldehyde and various byproducts according to the ¹H NMR spectrum of the crude reaction mixture. Alternative conditions tested included oxidation using PDC and IBX, again only yielding small quantities of aldehyde, multiple different aldehyde products and/or various byproducts, while the desired product was never isolated after purification. Oxidation was then attempted using TEMPO/BAIB. The ¹H NMR spectrum of the crude mixture showed the desired aldehyde **141** alongside with benzyl iodide, a byproduct of the reaction, and residual TEMPO impurities. However, upon purification by silica chromatography the aldehyde fully autoxidized to the acid, and clean aldehyde **141** could not be isolated. As it was crucial to obtain the aldehyde as a single, clean product to test the subsequent stereoselective alkynylation reaction, this route was abandoned and an alternative route was devised.

Instead of selectively deprotecting the primary alcohol and performing subsequent oxidation, an ozonolysis under standard conditions was performed. This reaction

yielded aldehyde **143** in an excellent yield of 96%, which was stable enough to be purified *via* FCC and stored in the fridge (**Scheme 3.7**).



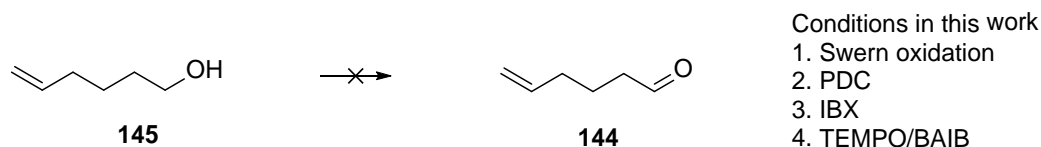
*Scheme 3.7 Ozonolysis of **139** to afford fragment **143** ready for stereoselective alkynylation reactions.*

Aldehyde **143** can be used to investigate stereoselective alkynylation conditions, however to subsequently form the pyran ring *via* *O*-Michael addition or Pd-catalyzed carboxylative cyclization and perform the ring-closing metathesis, further modifications have to be made (see **Chapter 2.4**). The TES group has to be removed and the primary alcohol needs to be oxidized to the aldehyde. To prepare for the Pd-catalyzed carboxylative cyclization, a Wittig reaction can be performed to install the terminal alkene, while to prepare for the *O*-Michael reaction a Wittig reaction with methyl 2-(triphenylphosphanyl)acetate can be performed

3.2.1 Synthesis of the C12 Desmethylene Fragment

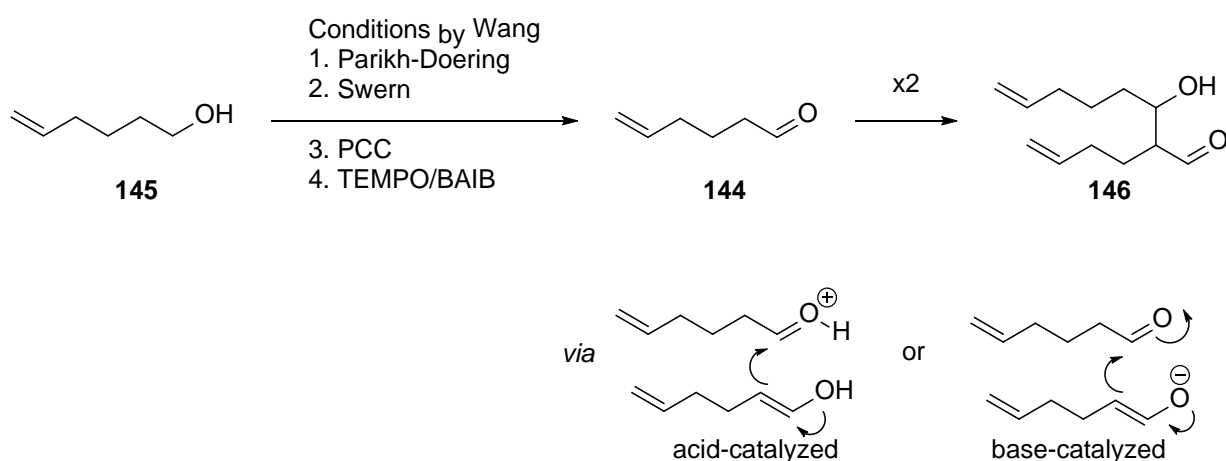
Along with the synthesis of fragment **143**, attempts were made to synthesize aldehyde **144** from commercially available 5-hexen-1-ol (**145**), not only to provide access to C13-desmethyl analogs but also to be used as an easily accessible model system for testing of conditions for the stereoselective alkynylation reaction. First attempts to obtain the desired aldehyde *via* various oxidation conditions failed (**Scheme 3.8**). Either the reactions were very messy, or the produced aldehyde degraded during purification *via* silica chromatography. The best results were obtained by oxidation using TEMPO/BAIB, as NMR analysis of the crude mixture

showed the desired aldehyde alongside iodobenzene and traces of TEMPO degradation products. However, **144** could not be isolated after purification.



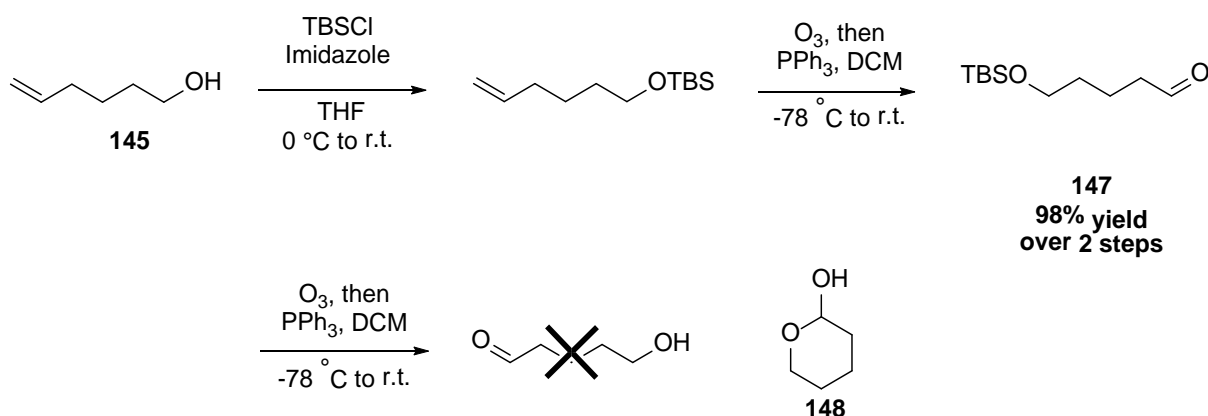
*Scheme 3.8 Oxidation conditions used in this work to oxidize **145** to **144**.*

Wang further investigated this reaction, using conditions such as Parikh-Doering, Swern, PCC and TEMPO/BAIB and different purification techniques including celite plugs, silica chromatography and vacuum distillation. She was not able to obtain the desired aldehyde; however, a dimerized byproduct was identified, which led to the conclusion that the purified aldehyde **144** is probably unstable and spontaneously dimerizes to product **146** *via* an aldol reaction as shown in **Scheme 3.9**.



*Scheme 3.9 Conditions used for the oxidation of **145** to **144** by Wang and possible mechanisms for the dimerization of the product *via* aldol reaction.*

As these issues were similar to the problems encountered in the synthesis of aldehyde **141**, the synthetic strategy was changed accordingly to obtain an aldehyde suitable for testing of stereoselective alkynylation conditions. Alcohol **145** was protected as a TBS ether and ozonolysis was performed, which yielded aldehyde **147** in a 98% yield. Direct ozonolysis of unprotected 5-hexen-1-ol only yielded lactol **148** (Scheme 3.10).



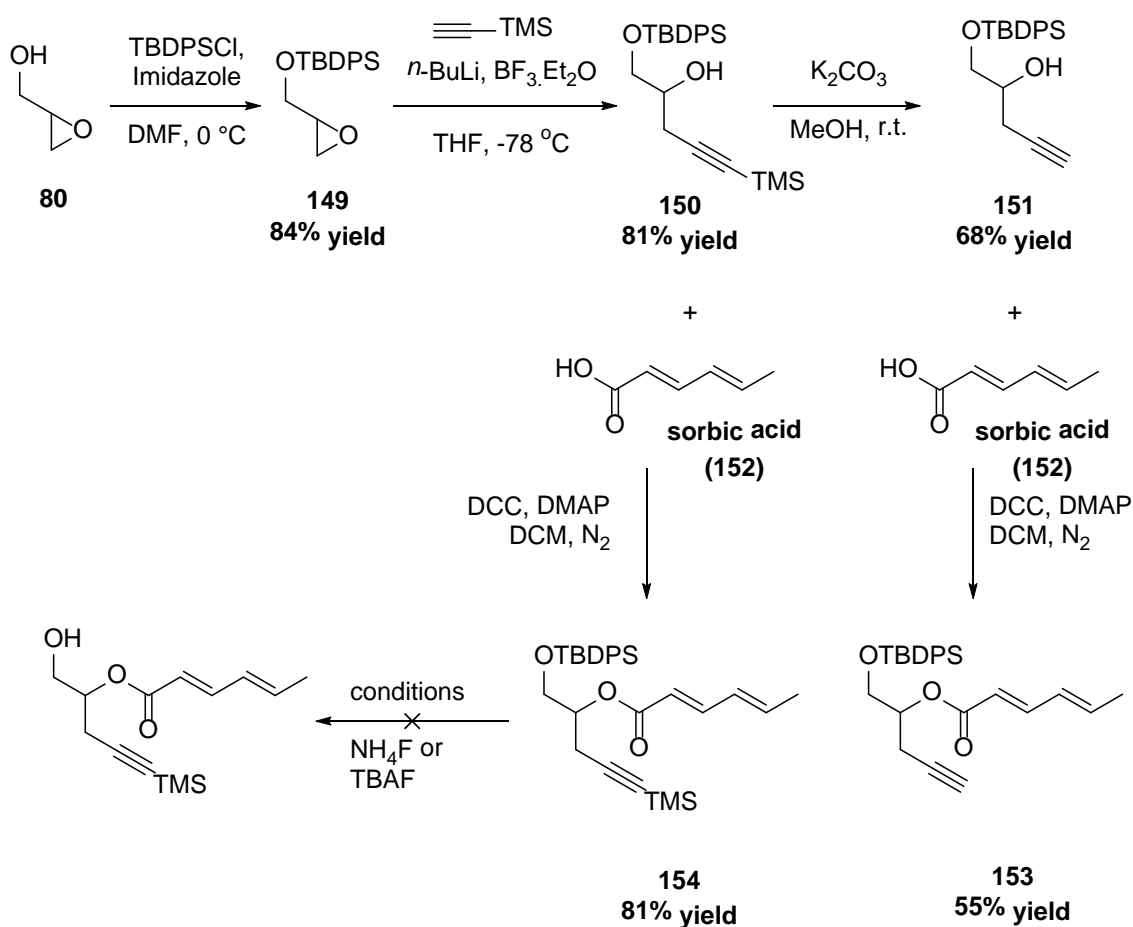
*Scheme 3.10 Synthesis for alternative aldehyde **147** through a protection/ozonolysis sequence.*

As seen before, aldehyde **147** was stable enough to be purified **via** FCC, and could be kept in the fridge for weeks before showing any sign of degradation or dimerization.

3.3 Synthesis of the C16-C20 Fragment and Model for Alkynylation

The synthesis of this fragment started from glycidol (**80**), which is readily available as a racemic mixture or as each enantiomer. To develop the synthesis racemic glycidol was used, while for the synthesis of enantiopure zampanolide (+)-glycidol was used.

As shown in **Scheme 3.11** and according to the first retrosynthetic approach based on Wang's thesis, glycidol was protected as the TBDPS ether in a good 84% yield, and the epoxide of **149** was subsequently opened with TMS-acetylene to yield compound **150** in 70% yield. In this step, it is crucial to use good quality boron trifluoride, as otherwise the yield drops significantly due to the formation of unidentified byproducts.



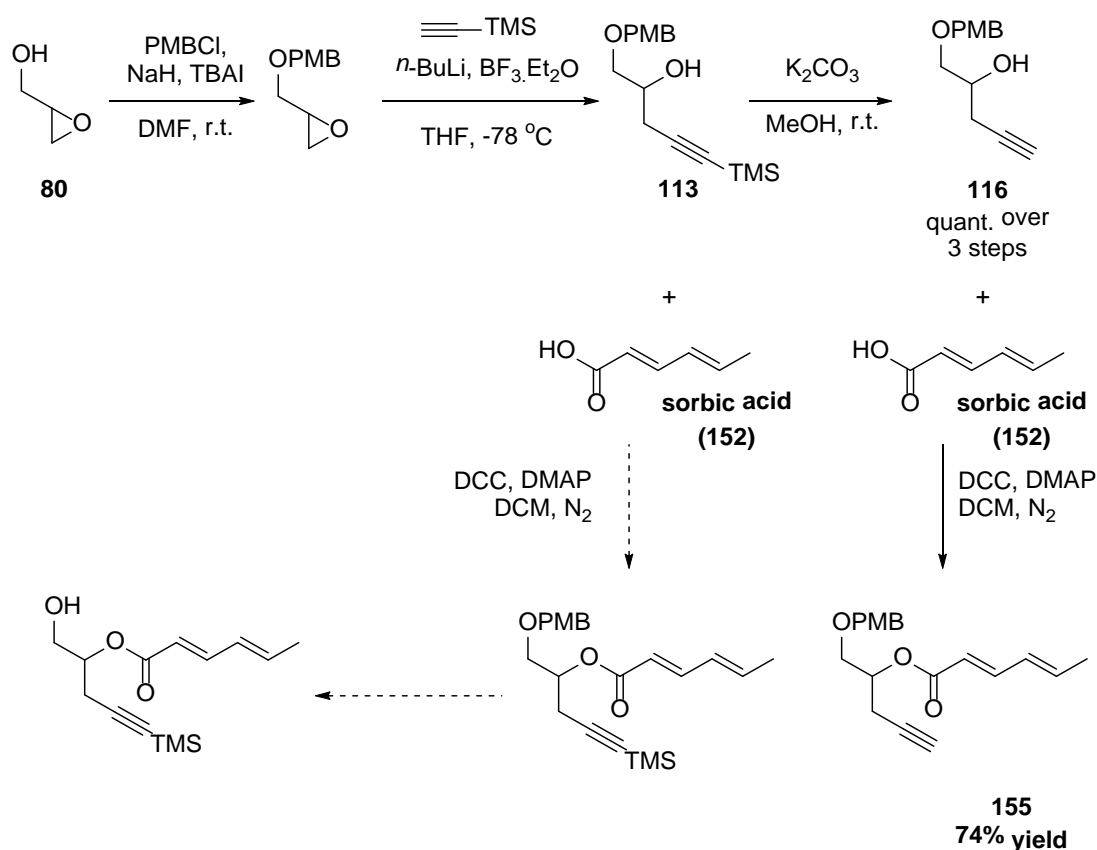
Scheme 3.11 Synthesis of compound **151** which serves as C16-C20 building block and model compounds **153** for alkylation, as well as the failed synthesis of a model for the sidechain attachment.

The TMS group was then removed by the use of potassium carbonate in MeOH in an overnight reaction, to afford fragment **151**. At this stage, sorbic acid (**152**) was

installed as an ester on compound **151** to mimic the C1-C5 portion of zampanolide and so created an easily accessible model to test various stereoselective alkynylation conditions. This was easily done using a Steglich esterification which yielded model compound **153** in a 55% yield. In a similar fashion, a sorbic acid ester was installed on compound **150** to obtain a model for testing different conditions to attach the sidechain contained in zampanolide.

Having the ester in place is critical in order to stabilize the hemiaminal sidechain through hydrogen bonding, as was shown by Porco⁴¹ and discussed in **Chapter 2.1.7**. The Steglich esterification proceeded with an 81% yield, however no conditions could be found to remove the TBDPS group of **154** without also cleaving the ester and/or TMS group.

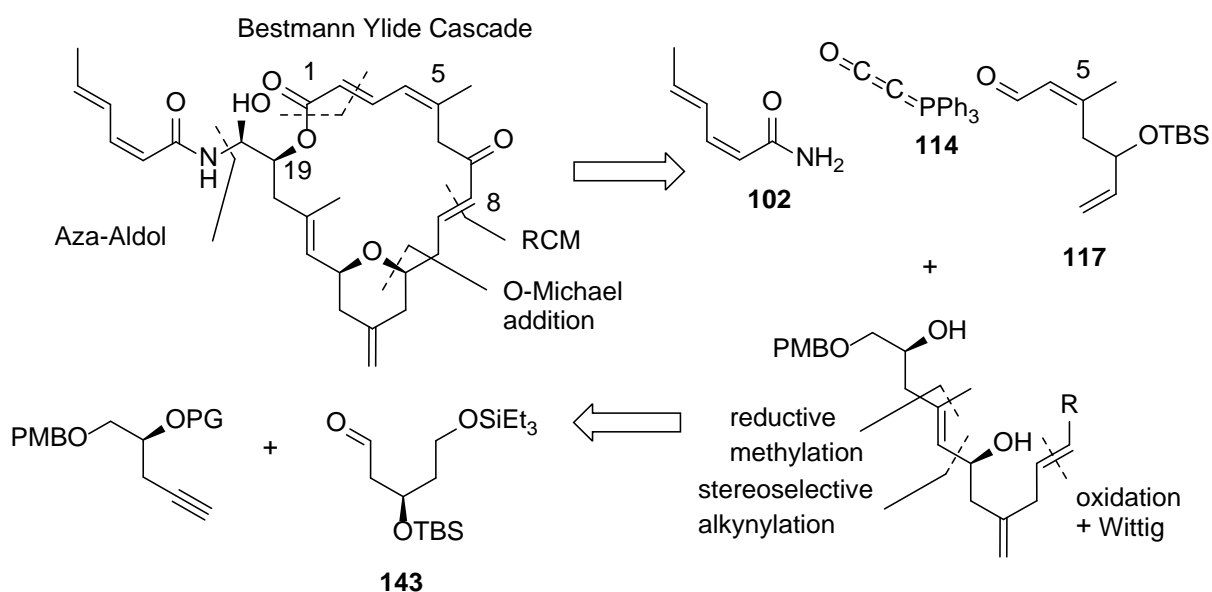
Although silyl migration was not observed in the course of this work, Wang found that TBDPS migration from the primary to the secondary alcohol of **151** could pose a problem, for instance in the basic conditions used for TMS removal. To avoid the migration, she attempted to protect the secondary alcohol as a PMB ether first, which only resulted in silyl migration, coupled with PMB protection of the freed primary alcohol. This suggests that protection of the C19 alcohol is tricky due to the bulkiness of the TBDPS group on C20. Additionally, and somewhat surprisingly, Wang also observed silyl migration during the Bestmann ylid cascade in a later stage, which indicated that the Bestmann ylid acts as a base in this process. Overall these findings led to the conclusion that the TBDPS is not the best choice for a protecting group for the purpose of this synthesis. Therefore, the protecting group strategy was changed, such that the C-20 hydroxyl would be protected as a PMB ether instead of a TBDPS ether to give compound **116**, and subsequently, **155**. PMB groups are not prone to base-catalyzed migration, and the change in protecting group allowed for purification steps to be omitted and improved yields as shown in **Scheme 3.12**, as well as allowing the Bestmann ylid cascade to proceed without difficulty.



Scheme 3.12 Yields for the synthesis of **155** which serves as C16-C20 building block with PMB ether instead of TBDPS ether as protecting group, along with **156**, which was used for subsequent alkylation studies.

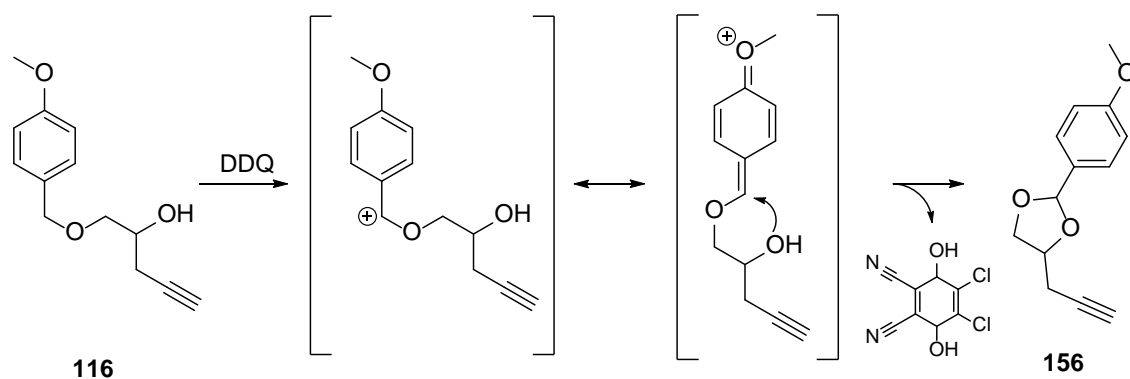
3.4 Second Generation Retrosynthetic Approach

After attempting various ways to perform the stereoselective alkylation, the sorbic acid ester proved to be unstable (see **Chapter 4.1**), therefore the synthetic strategy had to be revised. The updated retrosynthetic scheme is shown in **Scheme 3.13** and now includes a change in protecting group from TBDPS to PMB, the utilization of aldehyde **143** instead of aldehyde **128** or **141**, as well as the change in order of events from Bestmann ylid cascade followed by alkylation to protecting the secondary alcohol first, then alkylation, with deprotection of the C19 alcohol and the Bestmann ylid cascade being the last steps before the ring-closing metathesis.



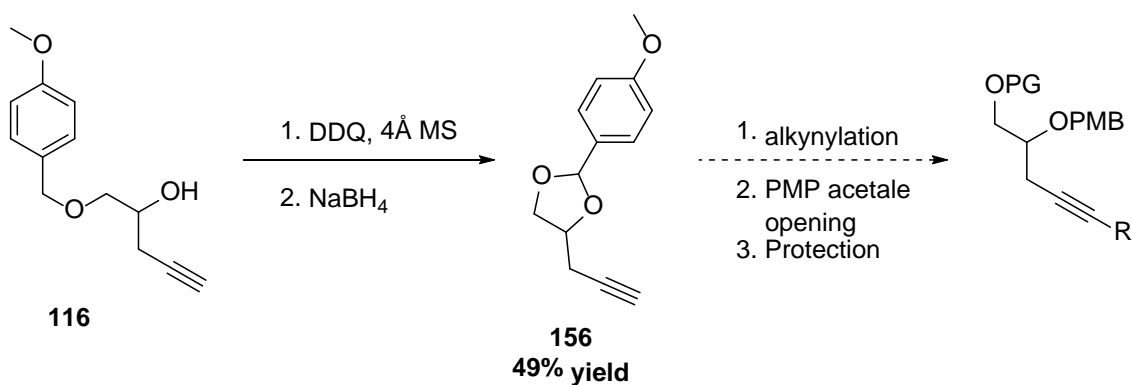
Scheme 3.13 Second generation retrosynthetic approach with revised protecting group strategy and order of events.

An additional advantage of choosing PMB over TBDPS as protecting group for the C20 alcohol revealed itself after the first alkylation attempts had been conducted and the synthetic plan had been adjusted as described above. As protection of the secondary alcohol of **116** became necessary, an elegant method to achieve protection was by using the already installed PMB ether to form the cyclic PMP acetal **156**. This protecting group has been developed by Yonemitsu's group in 1983 for their synthesis of macrolide and polyether antibiotics.⁵¹ He describes the formation of cyclic acetals to protect 1,2- as well as 1,3-diols, with 1,2-diols yielding varying ratios of both stereoisomers with respect to the benzylic carbon (depending on the conditions used), while protected 1,3-diols are isolated as a single stereoisomer. The diol can either be protected directly, or a PMB group can be installed first, as is the case in this synthesis, and then be transformed into the acetal by an oxidative cyclization pathway as suggested by Gamboni et al. and shown in **Scheme 3.14**.⁵²



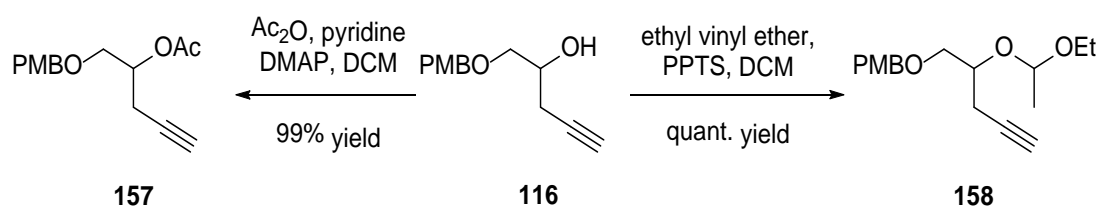
*Scheme 3.14 Mechanism of the oxidative cyclization pathway to from PMP acetal **156**, as proposed by Gamboni et al.*

Alcohol **116** was treated with DDQ in toluene to form acetal **156** as a near 1:1 mixture of diastereomers with respect to the benzylic carbon, in a 49% yield. However, the product was contaminated with anisaldehyde as a byproduct, which can be formed when there is water present in the reaction. In an effort to push the equilibrium to the product, additional anisaldehyde was added to the reaction. However, this did not improve the yield but made purification of the compound and removal of anisaldehyde that much harder. Unfortunately, the R_f values of anisaldehyde and the product are too similar to be separated sensibly *via* silica chromatography, therefore a different approach was chosen. The crude reaction mixture was treated with sodium borohydride in methanol to reduce any anisaldehyde to anisalcohol, which then allowed for an easier separation *via* FCC (**Scheme 3.15**).



Scheme 3.15 Oxidative PMP protection and planned subsequent reactions.

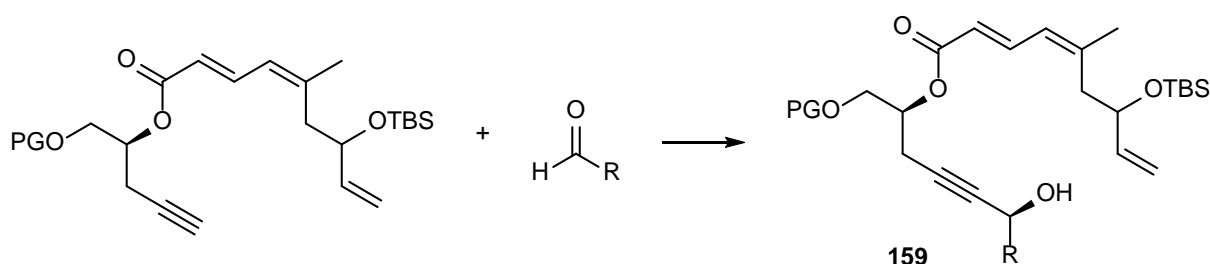
In light of the low yields and difficulties with purification it was decided that it was not feasible to use the PMP acetal as a protecting group, and to change the protecting group strategy once again. Therefore, the alcohol functionality of **116** was protected with an acetate group (**157**) and an ethoxyethyl ether (**158**) in excellent yield (**Scheme 3.16**).



*Scheme 3.16 Protection of alcohol 116 as acetate (**157**) or ethoxyethyl ether (**158**) in excellent yields.*

Chapter 4: Connecting C15-C16: Alkynylation

One of the key steps for the synthetic approach to be successful was to find a method for the synthesis of the chiral propargylic alcohol intermediate **159** (Scheme 4.1).



Scheme 4.1 The connection at C15 of (-)-zampanolide was envisaged to be performed via a stereoselective alkynylation reaction, also setting the desired stereochemistry at C15.

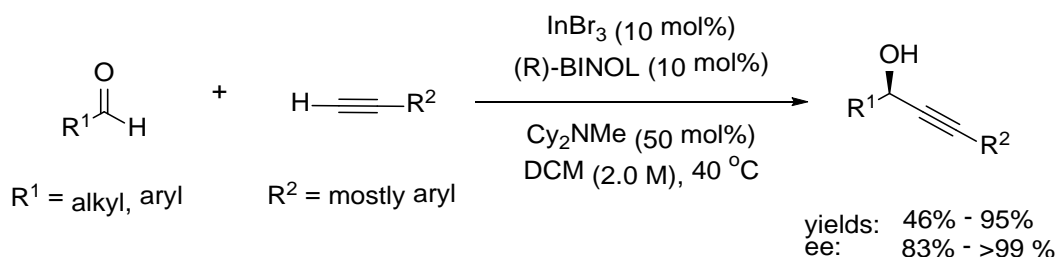
Propargylic alcohols in general, and chiral propargylic alcohols in particular, are very useful and versatile building blocks for the synthesis of a wide range of natural products, pharmaceuticals and other complex molecules. The reaction usually involves the addition of a metallated alkyne to a carbonyl group. The newly formed hydroxyl group can then be displaced or used as a synthetic handle, and the alkyne can be transformed into an allene, alkene, alkane, vinylsilane or even afford benzylic alcohols.⁵³ A review published by Trost and Weiss provides a comprehensive and detailed summary of different alkynylation methods.⁵³

4.1 Stereoselective Alkynylation

During the course of this work, many different methods to perform stereoselective alkynylation reactions were tested. Each method is briefly discussed and the respective results are presented. The corresponding conditions can be found in **Chapter 9.3.2**.

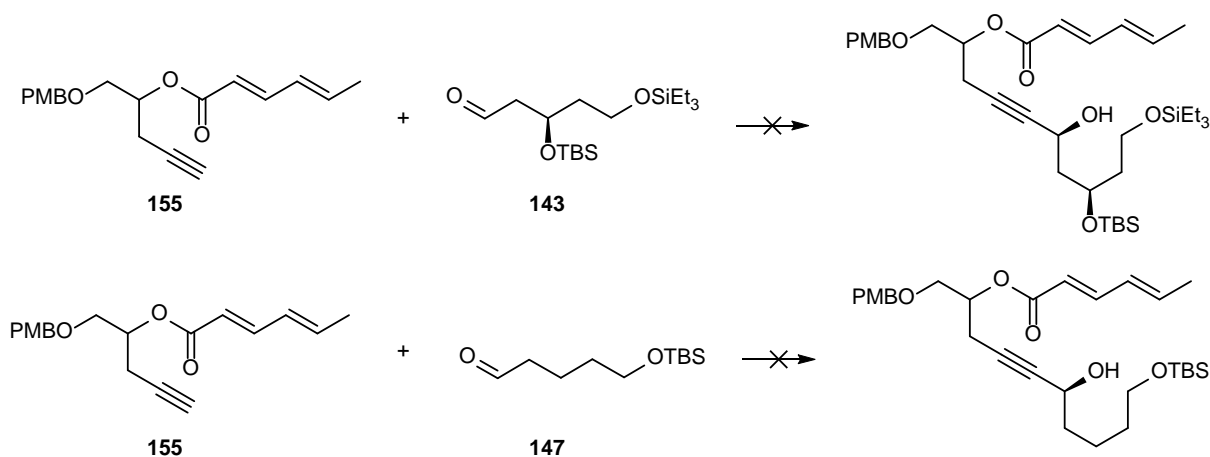
4.1.1 Shibasaki's Method Using Indium Bromide

In 2005, Shibasaki and coworkers developed a method for a stereoselective alkynylation which relies on dual activation of a soft nucleophile (terminal alkyne) and a hard electrophile (aldehyde or ketone),^{54,55} with BINOL as a chiral ligand. This reaction typically proceeds under very mild conditions and has been reported to deliver high yields and excellent enantioselectivities for both aromatic and aliphatic aldehydes (**Scheme 4.2**).



Scheme 4.2 Shibasaki's alkynylation method using InBr₃ and BINOL as chiral ligand.

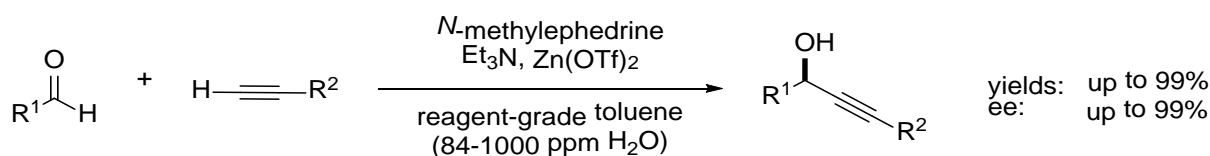
The above conditions were tested in the chosen model system, namely to combine C16-C20 model fragment **155** with aldehydes **143** or **147**, respectively (**Scheme 4.3**). Neither reaction yielded the desired product. NMR analysis of the crude mixtures of both reactions showed degradation of the aldehyde, as well as saponification of the ester functionality of starting material **155**.



Conditions: 2 eq alkyne, 1 eq aldehyde, 0.1 eq (R)-BINOL, 0.1 eq InBr_3 , 0.5 eq Cy_2NMe , DCM, stirred at 40 °C, overnight.
Scheme 4.3 Attempted stereoselective alkynylation using Shibasaki's method.

4.1.2 Carreira's Method Using Zinc Triflate

Carreira and coworkers described a method for a catalytic, non-stereoselective alkynylation using $\text{Zn}(\text{OTf})_2$ followed by a second paper describing a stereoselective alkynylation method using $\text{Zn}(\text{OTf})_2$ in combination with (+)-*N*-methylephedrine as a chiral ligand^{56–59}. Their scope for the stereoselective variant includes a broad range of alkynes, including acetylene, alkyl and aryl acetylenes, and various different aldehydes (**Scheme 4.4**).

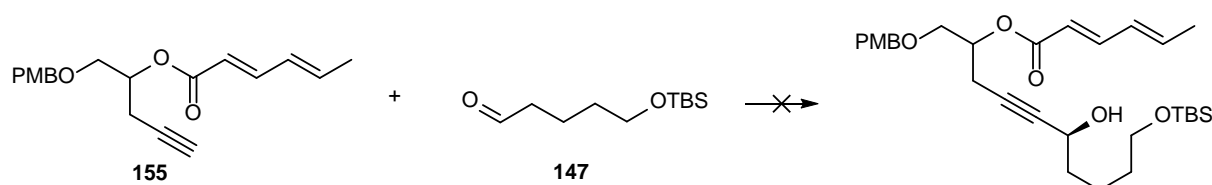


Scheme 4.4 Carreira's alkynylation method.

As *N*-methylephedrine is a strictly controlled substance in New Zealand and it is close to impossible to get even a small sample, an attempt was made to use (R)-BINOL as a chiral ligand instead, based on the assumption that the ligand is not necessary to achieve the formation of the new bond, which is supported by the fact that the reaction is reported to also be conducted non-stereoselectively. BINOL

was chosen as a ligand, because Pu and coworkers have previously reported the use of BINOL as a chiral ligand in Zn-mediated alkynylation reactions, as is discussed in **Section 4.1.3**.⁶⁰

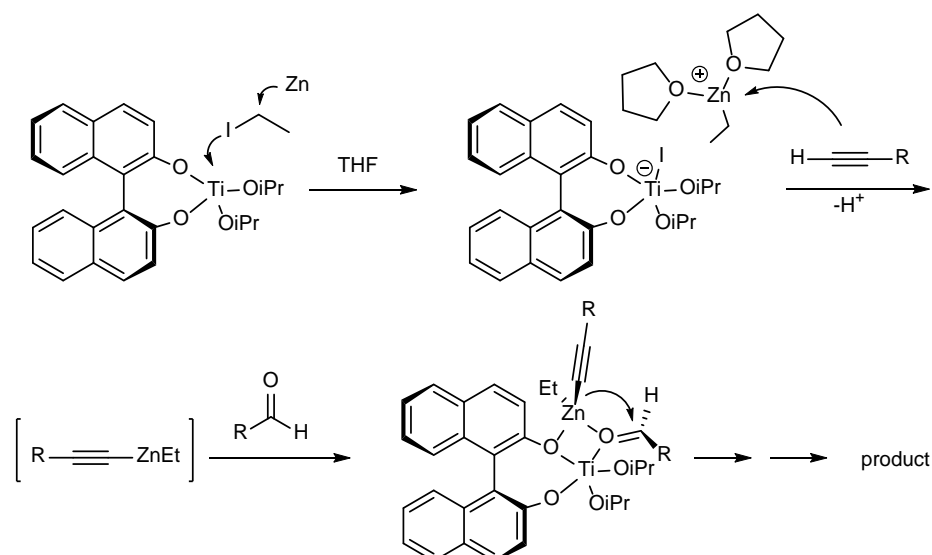
Unfortunately, the adaptation of Carreira's alkynylation reaction was not successful in the system at hand (**Scheme 4.5**), and the product was not isolated. NMR analysis of the crude mixture showed degradation of the aldehyde under the reaction conditions, but some of the alkyne starting material could be recovered without an apparent loss of the sorbic acid ester.



Conditions: 3 eq alkyne, 1 eq aldehyde, 0.2 eq Zn(OTf)₂ (homemade), 0.5 eq DIPEA, 0.8 eq (R)-BINOL, DCM, room temperature, 3 days

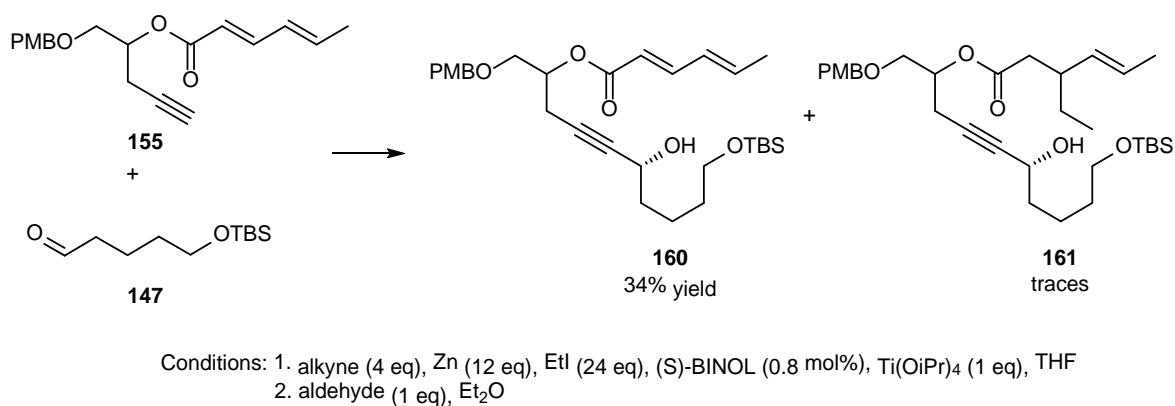
Scheme 4.5 Attempted stereoselective alkynylation using adaptation of Carreira's method.

In her thesis, Wang also reported an attempt of trying to use this stereoselective alkynylation on a similar model and found that there was no reaction when using homemade zinc triflate and conducting the reaction non-stereoselectively. However, when Wang used commercial zinc triflate, a 5% yield was achieved. Due to the low yield and the unavailability of Carreira's preferred chiral ligand, *N*-methylephedrine, a decision was made against pursuing this reaction any further.



Scheme 4.7 Pu's working hypothesis for the reaction of Zn, EtI, an alkyne and an aldehyde promoted by BINOL-Ti(OiPr)₄.

Hoping to avoid the direct usage of diethyl zinc for the previously mentioned reasons, Pu's method of generating diethyl zinc *in situ* and one-pot alkynylation was tested with the sorbic ester model. A first attempt to perform the reaction was conducted using an aged batch of activated zinc powder, and resulted in an estimated yield of 34% of product **160** in a mixture with BINOL. A byproduct that was formed in the reaction was identified as compound **161**, and could have formed by addition of an ethyl group to the β -position of the ester (Scheme 4.8).



Scheme 4.8 Stereoselective alkynylation using Pu's method, generating diethyl zinc *in situ*.

The clearest evidence for the formation of **160** in the proton NMR spectrum, apart from a more crowded alkane region and the very prominent TBS peaks, is the disappearance of the alkyne proton, as well as the appearance of a new oxymethine signal at 4.3 ppm, which corresponds to the newly formed tertiary center at position C1'' and can only appear if the connection between the building blocks had been formed. The shift of this signal is fairly consistent across all synthesized propargylic alcohols of this type (with varying protecting groups).

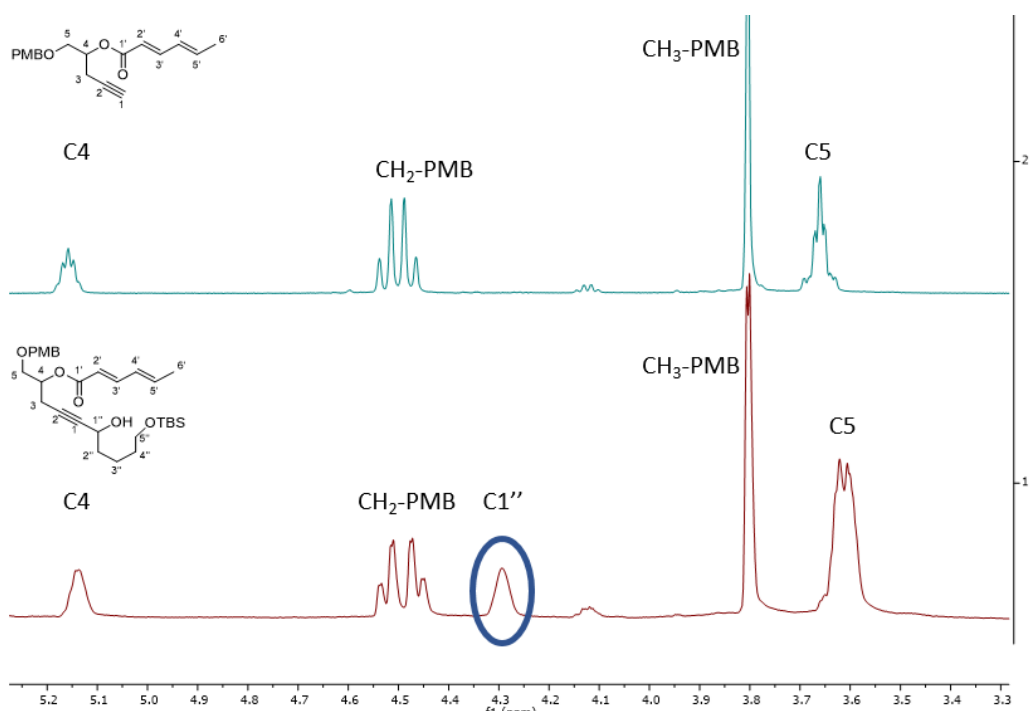


Figure 4-1 Comparison of the proton NMR spectra of **155** and **160**

Unfortunately, this positive result could not be repeated. All subsequent optimization attempts did not yield any product. All the reaction conditions tested are summarized in **Table 4.1**. Different equivalents and different batches of zinc were utilized, as well as unactivated zinc powder, with no success in repeating the first, positive result. (S)- as well as (R)-BINOL were tested to rule out failure of the reaction due to a matched/mismatched situation (**Table 4.1**, entries 1-8). One

main issue with the reaction seemed to be that the ester functionality was not stable even under these very mild reaction conditions.

155: R= sorbic acid 156: R= PMP		157: R= acetate 116: R= H		160: R= sorbic acid 163: R= PMP		162: R= acetate 164: R= H
#	R	BINOL	Zn batch	Zn eq	trapping	Result
1	155	S	original	12	-	34% product, unseparable from BINOL
2			new	12		saponification of SM
3			new	6		saponification of SM
4			old batch	6		saponification of SM
5		R	new	12		saponification of SM
6			new	6		saponification of SM
7			unactivated	6		saponification of SM
8			old batch	6		saponification of SM
9			new	6	TMSCl	degradation
10			new	6	TMSOTf	degradation
11	157	R	new	6		saponification of SM
12	156	R	new	6		no reaction
13	116	S	new	6		no reaction
14	156	R-H8	new	6		no reaction

Table 4.1 Reaction conditions tested for the stereoselective alkynylation following Pu's methodology.

Considering the high affinity titanium has for oxygen, re-coordination of the newly formed propargylic alcohol to the catalyst and reversal of the reaction was thought to be another possible issue. In an attempt to push the equilibrium towards the product and prevent re-coordination to titanium, conditions to trap the product as the TMS ether were tested, with no success (Table 4.1, entries 9 and 10).

Next, the general stability of ester groups under the reaction conditions was investigated. The reaction was performed with the acetylated alkyne instead of the sorbic acid ester. No reaction occurred, except for loss of the acetate, which confirms that ester groups are not stable under the reaction conditions (**Table 4.1**, entry 11).

With this knowledge, the synthetic strategy was changed as discussed in **Chapter 3.4 Second Generation Retrosynthetic Approach**. Instead of using a model to mimic the zampanolide system, the PMP protected alkyne was used with the intention to perform the Bestmann ylid linchpin as last step before closing the ring *via* RCM. While the PMP acetal proved to be stable under the alkynylation conditions, no reaction occurred (**Table 4.1**, entry 12).

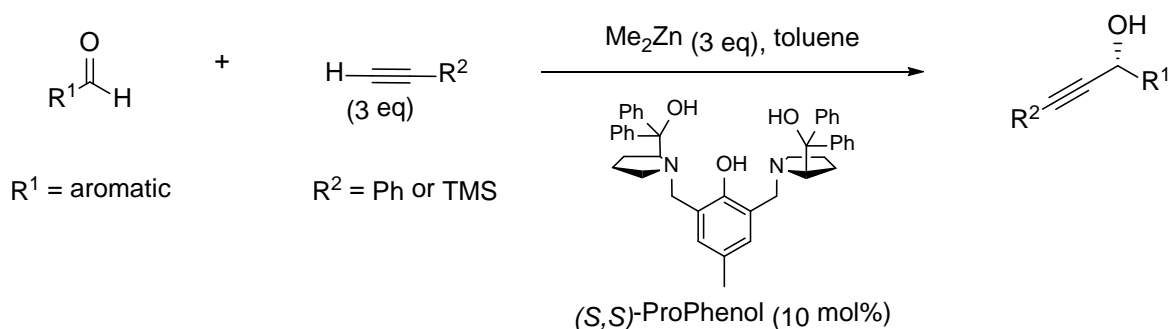
To test whether the groups on the alkyne were too bulky to coordinate successfully to the Ti-BINOL complex, the reaction was tested using the unprotected alkyne starting material **116**, but no reaction occurred (**Table 4.1**, entry 13).

Later in 2015, Pu's group published another article on the same type of reaction with optimized reaction conditions to further expand the substrate scope in comparison to the previously reported system.⁶³ BINOL was substituted by H8-BINOL and instead of using ethyl iodide isopropyl iodide was used. These new and improved conditions were also tested in the system at hand, however, again without success (**Table 4.1**, entry 14).

4.1.4 Trost's Method using Dialkyl Zinc and Prophenol

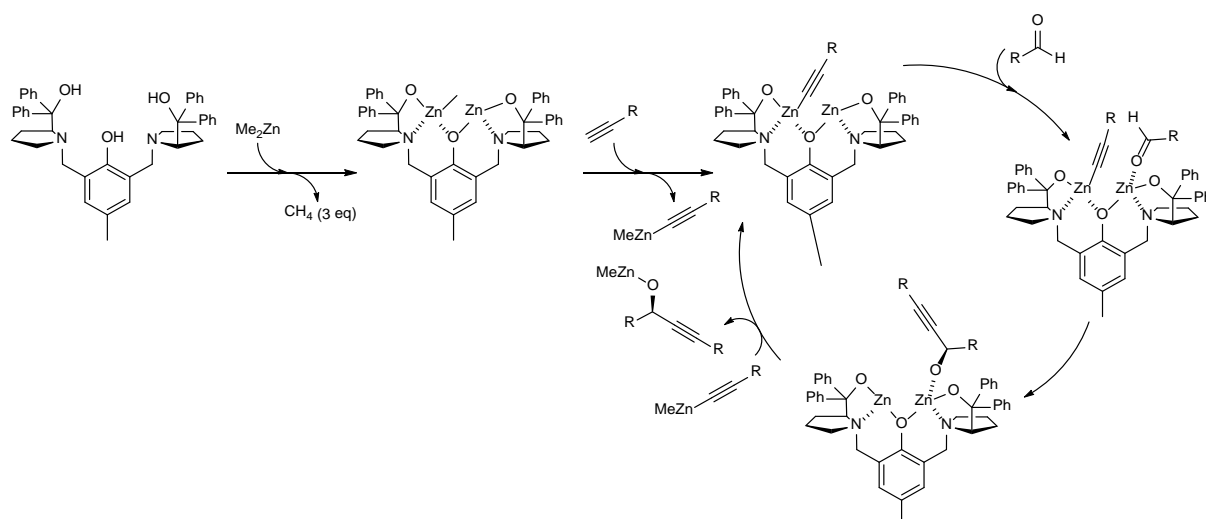
In 2005, Trost published a paper on asymmetric alkynylation, using the proline-derived bimetallic catalyst system which had previously been used by his group for a number of catalytic, enantioselective reactions including Henry, Mannich

and aldol reactions.⁶⁴ The alkyne component is premixed with Me_2Zn and the chiral proline-derived ligand (later made commercially available under the name ProPhenol) to form the zinc alkylidne-ProPhenol complex, after which the aldehyde is added. The aldehyde coordinates to the complex and reacts with the zinc alkynylid. The scope in this paper includes mostly aromatic aldehydes as well as a few α,β -unsaturated aldehydes and uses mainly phenyl- or TMS-acetylene as the alkyne component (**Scheme 4.9**).



Scheme 4.9 Trost's stereoselective alkynylation using Me_2Zn and ProPhenol.

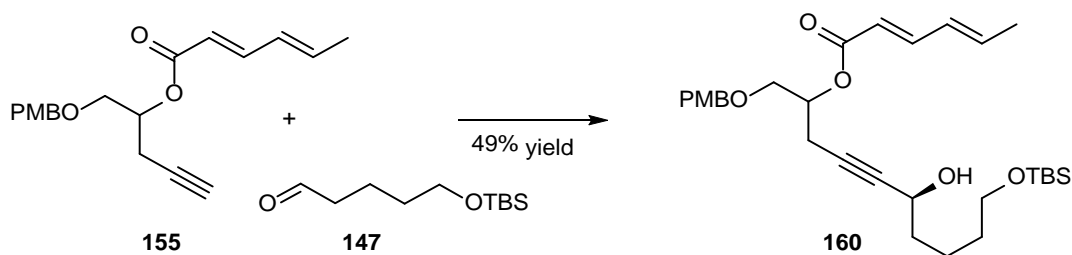
Seven years later, in 2012, Trost published another paper based on the same methodology, but expanding the substrate scope as well as testing different ligands for the reaction.⁶⁵ An updated version of the proposed mechanism was also provided and is shown in **Scheme 4.10**.



Scheme 4.10 Trost's proposed mechanism for the ProPhenol-catalyzed alkyne alkylation of aldehydes.

Additionally, it was found that acetate groups in the substrate enhanced enantioselectivity in the reaction, even if they were located far from the reacting alkyne terminus. The hypothesis was that due to their Lewis basicity, the acetate groups can coordinate to the dinuclear zinc catalyst and therefore enforce the chiral pocket. A variety of additives was screened to utilize this effect, and triphenylphosphine oxide was found to provide optimal results.

In this work, Trost's methodology was first tested on **155**, as a model for the top half of the zampanolide system (**Scheme 4.11**). For safety reasons, the stock solution of the highly flammable diethyl zinc was kept in the glovebox. The first attempt at the reaction was conducted in the glovebox for the duration of the reaction and removed immediately before quenching. In this first attempt, a yield of 49% of the desired product **160** was achieved (**Table 4.2**, entry 1).



Conditions: premix of: alkyne (2.8 eq), (R,R)-ProPhenol (0.2 eq), TPPO (0.4 eq) in toluene, Et_2Zn (1 M in hexane, 2.95 eq) added dropwise, stirred for 48 hours, then aldehyde (1 eq) in toluene added, stirred for another 24 hours.

Scheme 4.11 Stereoselective alkylation using Trost's method.

Due to limited space in the glovebox, the next attempt involved preparing the premix of the alkyne, diethyl zinc and ProPhenol in toluene in the glovebox, sealing the flask and letting it stir under a nitrogen atmosphere in the fumehood rather than the glovebox before addition of the aldehyde. This however, only resulted in degradation of both the alkyne and the aldehyde starting material (**Table 4.2**, entry 2). It is worth mentioning here that already two hours after the reaction mixture had been removed from the glovebox, it appeared to be a suspension rather than a clear solution, which indicates the formation of zinc hydroxide. Therefore, it was concluded that all future reactions had to be kept in the glovebox under inert atmosphere.

As the alkyne building block is a quite valuable building block, especially if the actual fragment of zampanolide was to be used, a reduction of equivalents needed in the reaction would be beneficial. Reduction of alkyne equivalents, however, only resulted in drastically reduced yields (**Table 4.2**, entries 3 and 4), which makes a reduction of alkyne equivalents not feasible.

Entry	eq alkyne	eq Zn	Premix time	Reaction time	Yield %	comment
1	2.8	2.95	48	24	49	Glovebox
2	2.8	2.95	48	24	-	Fumehood
3	1.4	1.48	48	24	18	
4	1	1.05	48	24	23	
5	2.8	2.95	96	24	-	
6	2.8	2.95	48	24	23	repeat 1
7	2.8	2.95	24	24	15	
8	2.8	2.95	o/n	24	24	

Table 4.2 Optimization conditions for the stereoselective alkylation between **155** and **147**.

Additionally, to further boost the yield of the reaction, optimization of the length of the premix time was attempted. Leaving the premix to react for 96 hours did not deliver any product (Table 4.2, entry 5), while leaving it for only 24 hours or overnight resulted in a reduced yield (Table 4.2, entries 7 and 8). To ensure that the reaction was still working as expected, the reaction was performed under the exact same conditions as entry 1, when a 47% yield had been achieved. Interestingly, in the repeated reaction only a 23% yield was achieved, which was the first indication that the reaction did not produce reliable results.

It was then decided to focus attention on using a different alkyne substrate, namely the PMP acetal and acetate protected alkyne, **156** and **157** respectively. In a first attempt using the original conditions and **156**, a 55% yield was achieved (Table 4.3, entry 1). Decreasing the time of the second step, the reaction of aldehyde **147** with the preformed catalyst and zinc alkynylide, resulted in a lower yield (Table 4.3, entry 2). Again, to ensure the reaction was still working properly, the conditions of entry 1 were repeated, but only yielded 11% of the desired product **163** (Table 4.3, entry 3). Since a different alkyne material was used, optimization

of the premix time was tackled once more, resulting in good results for increasing the reaction time to 72 hours (Table 4.3, entry 4), but significantly decreased yield for reduction of the premix time to just overnight (Table 4.3, entry 5). The conditions from entry 4 were then repeated multiple times with yields ranging from 28% to 93% yield (Table 4.3, entries 6-8). There seemed to be a correlation between the yield and the amount of toluene left in the storage bottle in the glovebox. The toluene is dispensed from a PureSolv system into a Schlenk flask, introduced into the glovebox, transferred to the storage bottle and kept over activated molecular sieves. When the bottle had been freshly filled, the yields were best, while they seemed to decrease with decreasing levels (and increasing age) of the toluene. No comprehensible explanation can be offered for this except for the aforementioned aging of the toluene.

Entry	eq alkyne	eq Zn	Premix time	Reaction time	Yield%	comment
1	2.8	2.95	48	24	55	
2	2.8	2.95	48	48	17	
3	2.8	2.95	48	24	11	repeat 1
4	2.8	2.95	72	40	50	
5	2.8	2.95	18	48	9	
6	2.8	2.95	72	40	93	full bottle of toluene
7	2.8	2.95	72	40	57	half bottle of toluene
8	2.8	2.95	72	40	28	near empty bottle of toluene

Table 4.3 Optimization conditions for the stereoselective alkylation between **156** and **147**.

The same trend was observed when using the acetate protected alkyne starting material **157** (Table 4.4, entries 1-3). To determine the enantioselectivity of the

reaction, the reaction was performed once more, but with enantiopure alkyne material derived from (R)-glycidol (**Table 4.4**, entry 4).

Entry	eq alkyne	eq Zn	Premix time	Reaction time	Yield%	comment
1	2.8	2.95	72	40	95	Full bottle toluene
2	2.8	2.95	72	40	40	half bottle toluene
3	2.8	2.95	72	40	68	Repeat 1, near full bottle
4	2.8	2.95	72	40	77	enantiopure SM

*Table 4.4 Optimization conditions for the stereoselective alkynylation between **157** and **147**.*

Evaluating the enantioselectivity of the reaction on acetate **162** rather than the PMP protected material **163** had the distinct advantage that a single set of diastereomers was produced, as the acetate material only contains two stereocenters.

Acetal **163** however contains three stereocenters with the stereocenter at the benzylic carbon being a mixture, which would have made a purification and subsequent Mosher ester analysis significantly more complicated. The possible diastereomers formed from the diastereomeric acetate mixture are shown in **Table 4.5**.

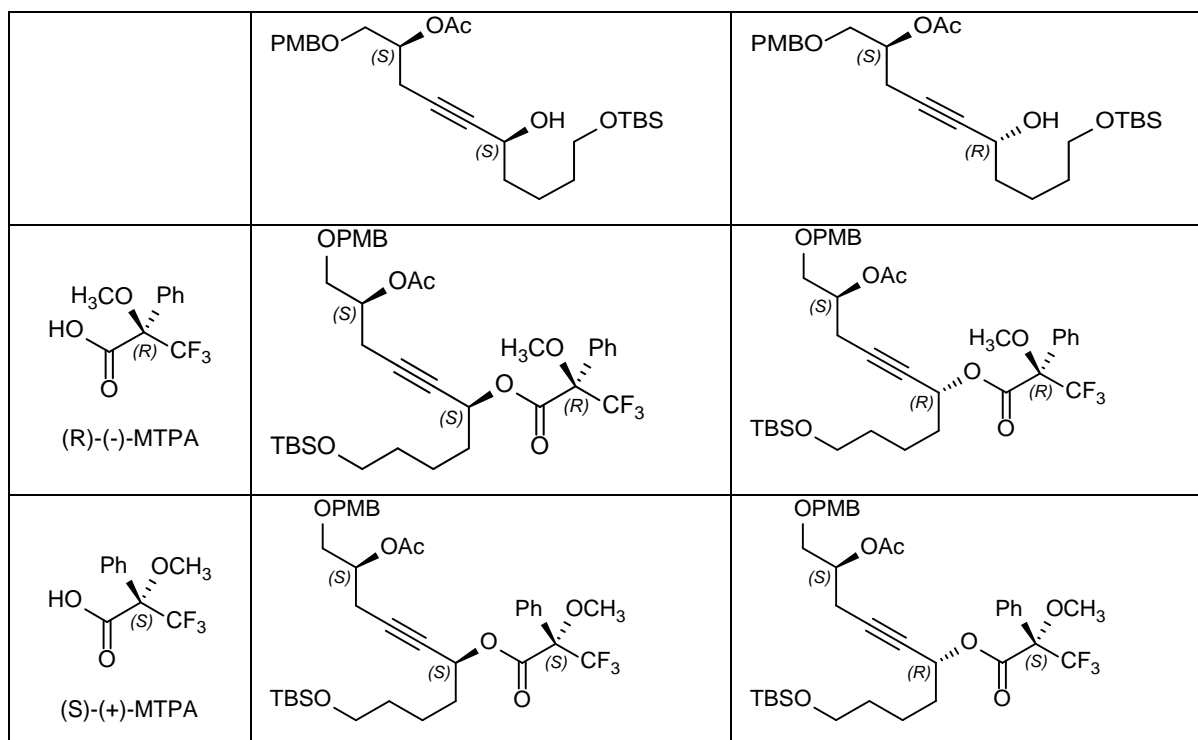


Table 4.5 Possible diastereomers generated in the reaction of the diastereomeric mixture of (*S,S*)-**162** and (*S,R*)-**162** with (*S*)- and (*R*)-MTPA respectively.

The (*R*)- as well as (*S*)-Mosher ester of the diastereomeric product mixture were formed using the Yamaguchi esterification method, which uses 2,4,6-trichlorobenzoyl chloride (TCBC), triethylamine and 4-DMAP to promote the esterification. Additionally to the products depicted above, in both reactions a byproduct, **165**, was formed which was identified as the TCBC ester of alcohol **162** (Scheme 4.12). The crude mixture was then subjected to purification by FCC, to try and separate the diastereomers and byproducts as well as possible.

4.2 Non-Stereoselective Alkynylation

After it had become clear that the tested stereoselective alkynylations either did not work, weren't consistent in their yields and additionally did not result in as high enantioselectivities as was envisaged, the decision was made to perform a non-stereoselective alkynylation instead, and attempt to achieve better enantioselectivities by an oxidation-reduction sequence at a later stage, or using Uenishi's method of separating the two diastereomers, and inverting the stereocenter of the undesired diastereomer by acetylating under Mitsunobu conditions and subsequent saponification.²⁹

The non-stereoselective alkynylation was performed following a standard procedure using MeLi to deprotonate the alkyne, and subsequent dropwise addition of a solution of aldehyde in THF.⁶⁶ The reaction was performed on three different alkyne materials, **156**, **157** and **116**, and the results are summarized in **Table 4.6**.

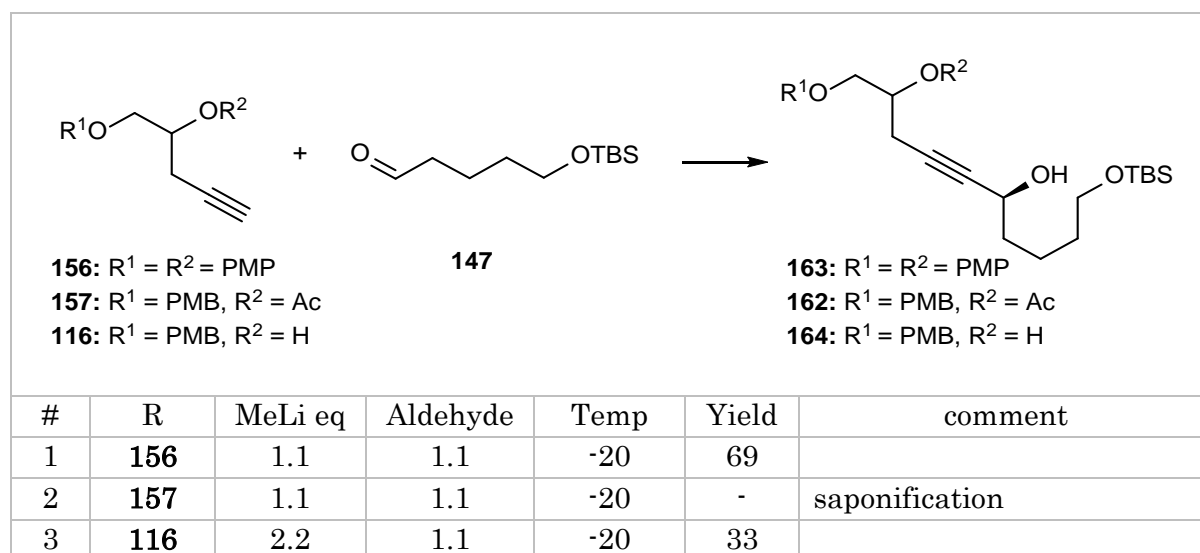


Table 4.6 Tested substrates for the non-stereoselective alkynylation.

While the PMP acetal **156** reacted with aldehyde **147** in good yield (**Table 4.6**, entry 1), using acetate **157** only resulted in saponification of the ester functionality (**Table 4.6**, entry 2). The reaction could however be successfully performed on alkyne **116** (**Table 4.6**, entry 3).

After the installation of the PMP protecting group was deemed to be not high yielding enough, and ester functionalities proved to be unstable under the conditions, the protecting group strategy was changed once again, this time to an ethoxyethyl (EE) acetal. After it was shown that the EE acetal group was stable under these alkynylation conditions and yielded product **166** (**Table 4.7**, entry 1), the reaction conditions were optimized with respect to the time between addition of the aldehyde and work up (**Table 4.7**, entries 1 and 2), the number of equivalents of methyl lithium used (**Table 4.7**, entries 2 and 3) and the temperature at which the alkyne was deprotonated (**Table 4.7**, entries 4 and 5). With exception of the reaction time, none of the other factors seems to have a major influence on isolated yield, therefore the more economic conditions (1.1 eq MeLi, room temperature) were chosen.

Since these reaction conditions are significantly less sensitive than any stereoselective alkynylation conditions tested, an attempt was made to use aldehyde **144** which had originally been intended for use. For this purpose, 5-hexen-1-ol (**145**) was oxidized using standard TEMPO/BAIB oxidation conditions as described in **Chapter 3.2.1 Synthesis of the C12 Desmethylene Fragment**. The crude mixture was analyzed by NMR and after confirmation that the aldehyde has indeed been successfully synthesized, the crude mixture was subjected to the alkynylation and yielded desired product **167** in a 16% yield (**Table 4.7**, entry 6).

Even though this yield is very low, using **144** instead of **147** would bring down the number of steps required to set up the C8-C10 portion of the C8-C15 fragment for the synthesis of the pyran ring and subsequent RCM. Therefore, attempts were

made to improve the yield of this reaction. Because aldehyde **144** can't be purified, it is uncertain how many equivalents are actually added to the alkyne-MeLi premix.

By increasing the equivalents of aldehyde **144** that were used in the oxidation with respect to the alkyne, the yield could be improved to 21% on a small scale (**Table 4.7**, entries 6-8). Luckily however, when the reaction was performed on a large scale (>2 g **158**), the yield was improved even more to give 53% of desired product **167**. Using enantiopure alkyne (**S**)-**158** on a slightly smaller scale yielded 30% product (**Table 4.7**, entry 10).

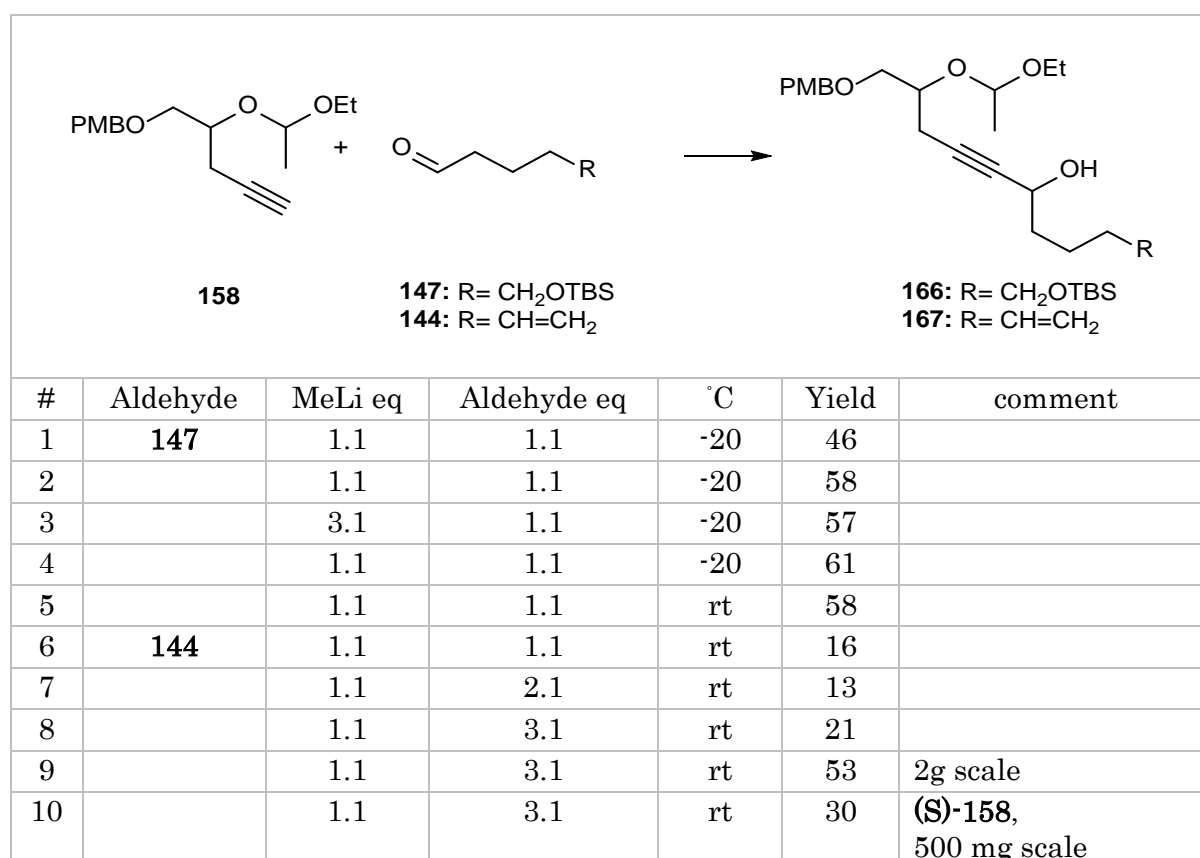


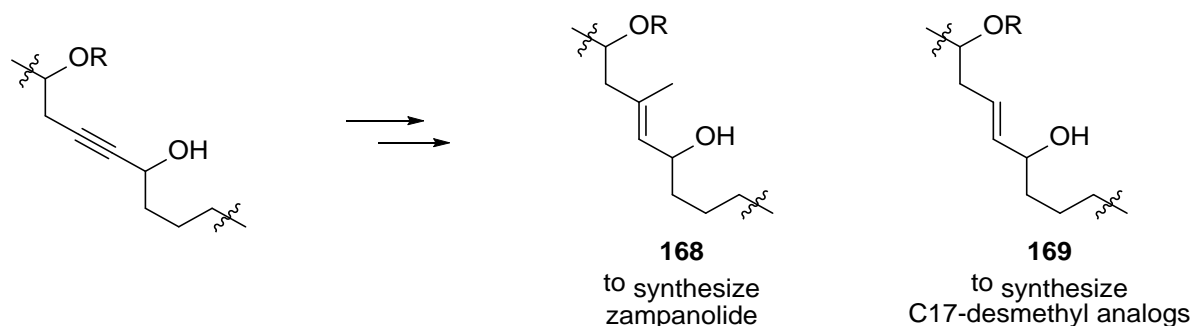
Table 4.7 Optimization conditions for the non-stereoselective alkylation using EE protected alkyne starting material.

4.3 Summary of Chapter 4: Connecting C15-C16: Alkynylation

In summary, four different methods for the stereoselective alkynylation were tested on various model systems and substrates in order to establish the C9-C20 carbon skeleton of zampanolide and establish the desired (S)-configuration of the C15 stereocenter. Due to low and/or irreproducible yields and poor diastereoselectivity the synthetic strategy was changed to include a simple non-stereoselective alkynylation instead, and the desired configuration of the stereocenter at C15 was set by an oxidation/stereoselective reduction sequence at a later stage of the synthesis.

Chapter 5: Conversion of the C16-C17 Alkyne to an Alkene: Reducti(ve methylati)on

For the synthesis of zampanolide, the alkyne of the propargyl alcohol moiety generated by the alkynylation reaction, had to be reduced and methylated to afford *trans*-product **168**. However, additionally to zampanolide itself, analogs lacking the C17 methyl-group were also targets, which meant the alkyne had to be reduced without methylation to afford *trans*-product **169** as well (**Scheme 5.1**).



Scheme 5.1 Necessary transformation to install the trans-alkene in zampanolide and C17-desmethyl analogs.

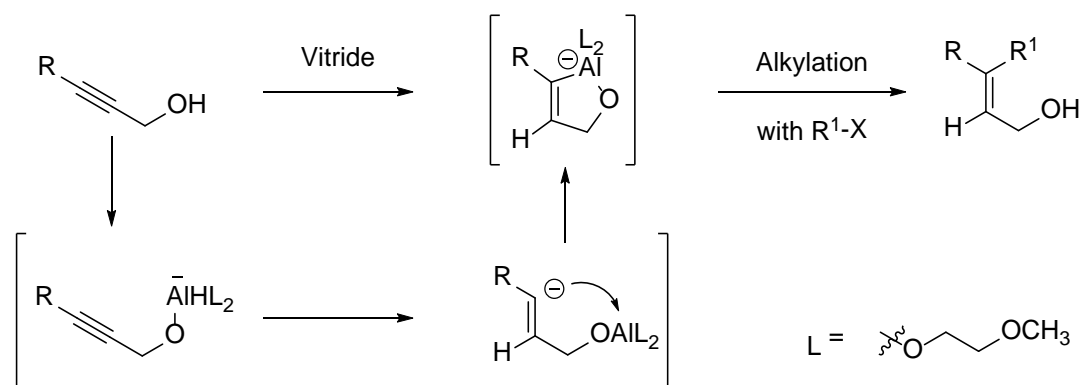
Many transformations of alkynes and propargylic alcohols to substituted alkenes have been reported in the literature, and are usually performed using hydrometallation reactions. Metals that have been used include boranes, silanes, stannanes, as well as copper, titanium or tin compounds. The most abundant metal used however is aluminum, often in combination with other metals used in only catalytic amounts such as titanium or zirconium. Most of these carbometallations proceed in a *syn*-manner, while *trans*-additions are less commonly seen.^{67,68,69}

5.1 Reductive Methylation of the Propargylic Alcohol

To synthesize compounds of type **168** and **169** (above) an *anti*-carbometallation reaction on an internal alkyne has to be performed. These reactions are fairly rare in comparison to *syn*-additions, but recent advances in the field have been made.⁷⁰ In this work mostly hydroaluminations of propargylic alcohols were investigated, as these reactions are most likely to undergo *anti*-addition. Each method is briefly discussed and the respective results are presented.

5.1.1 Jamison's Method Using Vitride®/MeLi/CuCl/RX

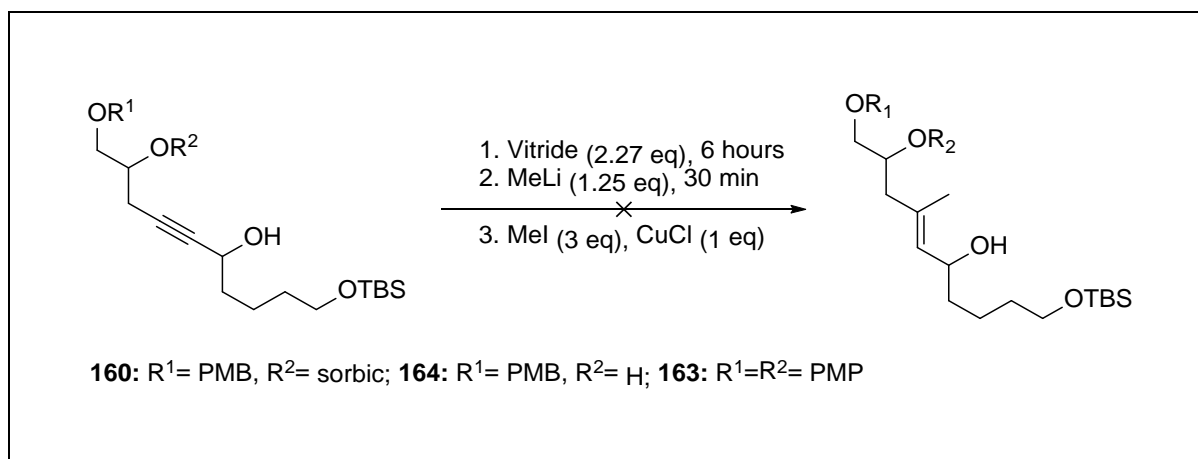
In 2006, Jamison published a paper for a one-pot synthesis of trisubstituted allylic alcohols *via* a *trans*-hydroalumination/alkylation sequence, which was the first of its kind.⁴⁷ Previously developed similar protocols yielded only the *cis*-hydroalumination/alkylation product. Jamison's group used Vitride® (also called Red-Al) to perform the *trans*-hydroalumination reaction, and then replaced the aluminate using MeLi as base, CuCl or CuI·POEt₃, and an alkyl bromide or iodide as the electrophilic component. Jamison gave no indication of a mechanism for the alkylation step, however the reaction mechanism for the *trans*-hydroalumination (for LAH) has been described in the literature before and is shown in **Scheme 5.2**.⁷¹ The *anti*-addition is achieved by the formation of a five-membered vinyl alanate, which then allows the aluminum to be replaced by an electrophilic group.



Scheme 5.2 Mechanism for trans-hydroalumination step.

Jamison's group optimized the reaction conditions for their new protocol using allyl bromide for the alkylation step, but in a later stage tested numerous other halides for the reaction, achieving good to excellent yields. However, they found that when using unactivated alkyl halides like methyl or ethyl iodide, full conversion to the trisubstituted alkene was not achieved due to a significant amount of proton quenching occurring during the reaction (1:1 ratio of methylated to proton-quenched product for the reaction with MeI).⁴⁷

In this work, the results for Jamison's method could not be successfully repeated with the materials at hand (**Table 5.1**). While using compound **160** only led to saponification of the ester, diol **164** (**Table 5.1**, entry 2) and the PMP acetal **163** did not react at all (**Table 5.1**, entries 2 and 3).



Entry	Alkyne	Result and Comment
1	160	Saponified SM
2	164	Recovered starting material
3	163	Recovered starting material

Table 5.1 Materials tested with Jamison's reductive methylation protocol.

In order to determine which part of the reaction was causing the problem, **164** was treated with three equivalents of Vitride® and samples for HRMS analysis were collected every 15 min for six hours, which is the time Jamison reported for the premix in his paper.⁴⁷ Each sample was quenched with a drop of water, which should result in the formation of the proton quenched compound featuring the *E*-alkene if the vitride had reacted with the alkyne. It was found that this product was already formed after the first 15 min of the reaction, while after 30 min there was no starting material left. After 60 min, the product seemed to be degrading as well. Hence it was decided to perform the premix for 30 min, rather than for six hours as reported by Jamison.

With this in mind, different substrates were subjected to the new protocol, allowing vitride to react with the propargyl alcohol for 30 min before being quenched with water, to establish which substrates were reactive. The results are summarized in **Table 5.2**. PMP acetal **164**, when allowed to react for 30 min followed by a quench of water gave quantitative yields of the proton-quenched product **170** (**Table 5.2**, entry 1). The acetate of **162** was cleaved (**Table 5.2**, entry

2), as was the sorbic ester in the previous set of reactions, which confirms that esters are not stable under the reaction conditions. Interestingly, if the homopropargylic alcohol in **164** was unprotected, no reaction occurred at all, even if the equivalents of Vitride® used were doubled to account for the hydroxy proton (Table 5.2, entry 3). In Jamison's paper, homopropargylic and bishomopropargylic alcohols (in the absence of a propargylic alcohol) had been tested as substrates and were found to be ineffective. Despite this result, it was not expected that the presence of a homopropargylic alcohol would prevent the propargylic alcohol from reacting.

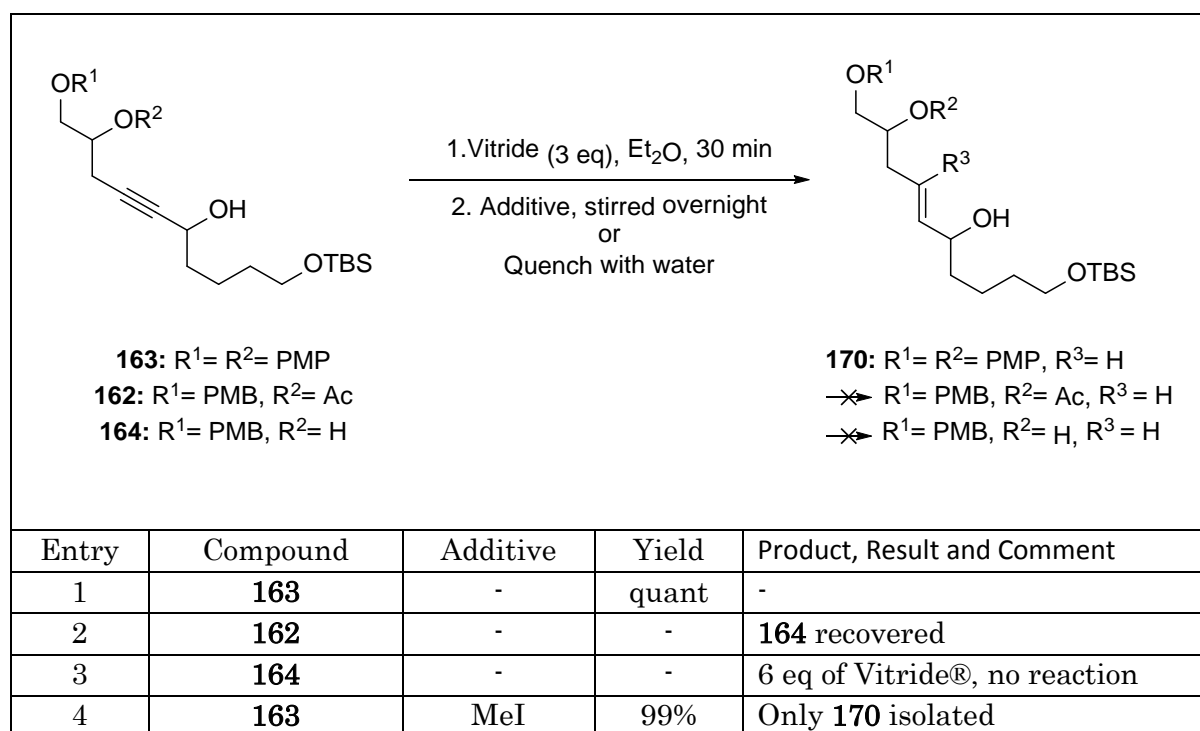


Table 5.2 Different substrates tested in the adapted *trans*-hydroalumination reaction.

The proton NMR spectrum of allylic alcohol **170** clearly shows the two alkene protons H1 and H2 formed in the reduction, at 5.61 and 5.68 ppm, respectively (Figure 5-1). H1 presents as a doublet of doublets, with coupling constants of 15.7 and 6.3 Hz. These coupling constants fit well with *trans*-coupling with H2 as well as the vicinal coupling with H1" in *E*-alkene **170**.

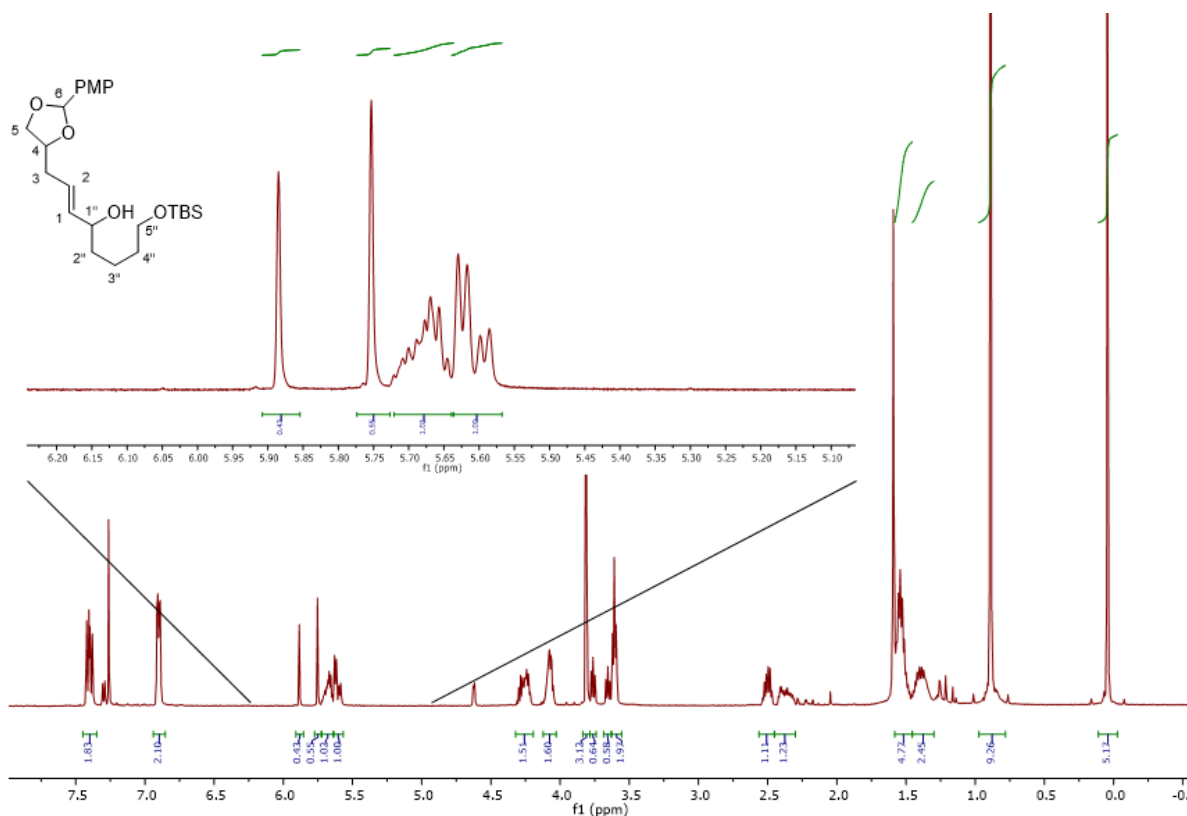
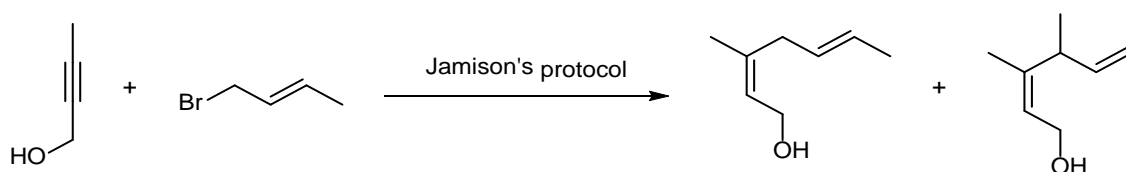


Figure 5-1 Proton NMR spectrum of **170**.

In 2016, at the same time this work was being conducted, Goswami's group reported that when they were applying Jamison's protocol to their chemistry using crotyl bromide as alkylation reagent, a significant amount of isomerization occurred (**Scheme 5.3**). This by itself is not a problem for substrates in this work, however their optimization attempts for this reaction showed that the *trans*-hydroalumination/alkylation sequence can be performed without additives by simply quenching the vinyl alanate with the alkyl halide reagent, crotyl bromide in their case.⁷²



Scheme 5.3 Goswami's attempt at a *trans*-hydroalumination/alkylation.

With this knowledge in mind, a reaction was attempted where the vinyl alanate formed was simply quenched by the addition of MeI and leaving the reaction mixture to stir overnight. However, this was found to be ineffective and only proton quenched **170** was recovered (**Table 5.2**, entry 4).

Knowing that Jamison had observed issues with proton quenches when trying to install a methyl group,⁴⁷ several different alkyl reagents were tested in the reaction. The EE protected compound **166** was used for this purpose, as ester protected materials **160** and **162** proved to be reduced under the conditions, the unprotected material **164** did not react and the PMP protected material **163** proved not to be feasible due to difficulty with its synthesis. The results are summarized in **Table 5.3**. A range of alkyl iodides were trialed (**Table 5.3**, entries 1-4), however, none of the trisubstituted alkenes could be isolated.

Entry	Additive	Yield	Result and Comment
1	Methyl iodide	-	60% 166
2	Ethyl iodide	32% (171)	15% 166
3	<i>Isopropyl</i> iodide	54% (171)	1% 166
4	<i>n</i> -Butyl iodide	41% (171)	13% 166
5	D ₂ O	36% (172), 14% (171)	26% 166 ,
6	Me ₂ SO ₄	-	degradation
7	Meerwein salt	-	degradation

Table 5.3 Different alkyl halides and other additives used for the trans-hydroalumination/alkylation reaction.

To determine if the proton quench occurred due to wet equipment, or if the alkyl halides were not reactive enough to replace the aluminum, the reaction was carried out as per usual, but quenched with deuterium oxide instead of water and stirred overnight before water was added for the work up (**Table 5.3**, entry 5). The main product was the deuterated species **172** with a yield of 36%, while there was also some starting material as well as proton quenched material recovered. This shows that at least a certain amount of the alanate is converted before the work up, however it also indicates that either the replacement of the aluminum with deuterium is really slow, or that the flask is not properly sealed and allows moisture to get into the reaction during the second step.

Other than reactivity issues with the alkyl halides, another reason that the deuterium oxide is able to replace the aluminum while none of the alkyl iodides seem capable to do so could be due to steric effects. It is possible that the iodide is simply too bulky to allow the alkyl residue to get close enough to the nucleophilic center to react. To test this theory, dimethylsulfate as well as Meerwein's salt, two other well-known methylating agents, were tested, which unfortunately resulted in degradation of the starting material rather than the formation of desired product **173** (**Table 5.3**, entries 6 and 7).

After the strategy for the alkynylation had been changed to using the non-stereoselective method, the reaction was also performed on EE protected compound **167** instead of **166**. First, the reaction was simply quenched after 30 min to confirm that the reaction was working well on this substrate (**Table 5.4**, entry 1). A 97% yield of **174** was achieved, which leads to the conclusion that the terminal double bond does not influence the reaction. A methylation was then attempted using tetramethylsilane, which only led to proton quenched product **174** instead of methylated product **175** (**Table 5.4**, entry 2). In a final attempt, allyl bromide was used, which is the same halide that Jamison used for his optimization studies and allowed for the highest yields. However, even using this activated halide only resulted in proton quenched product **174**.

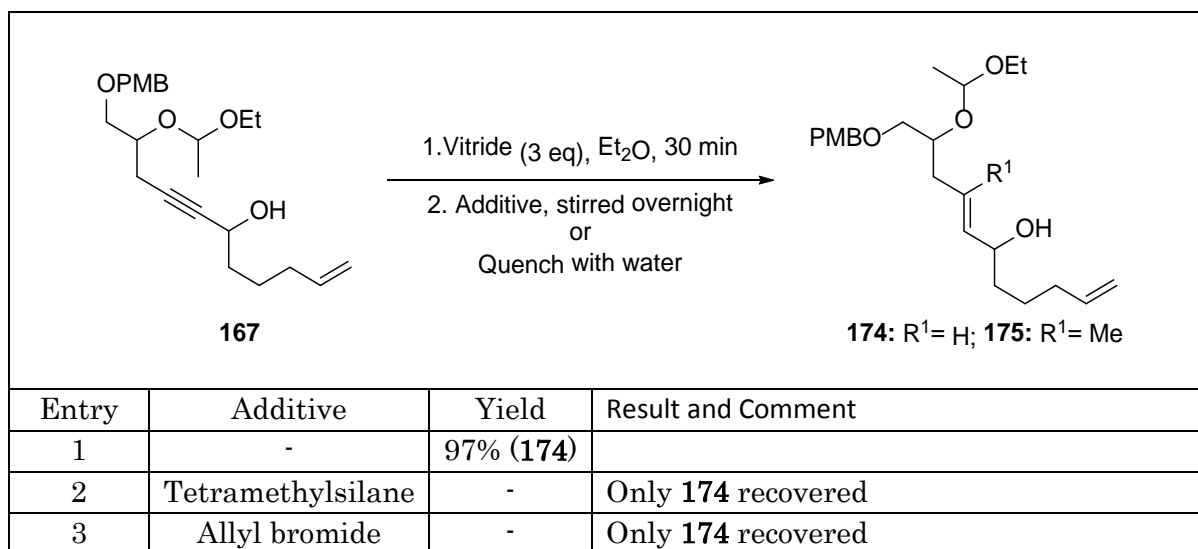
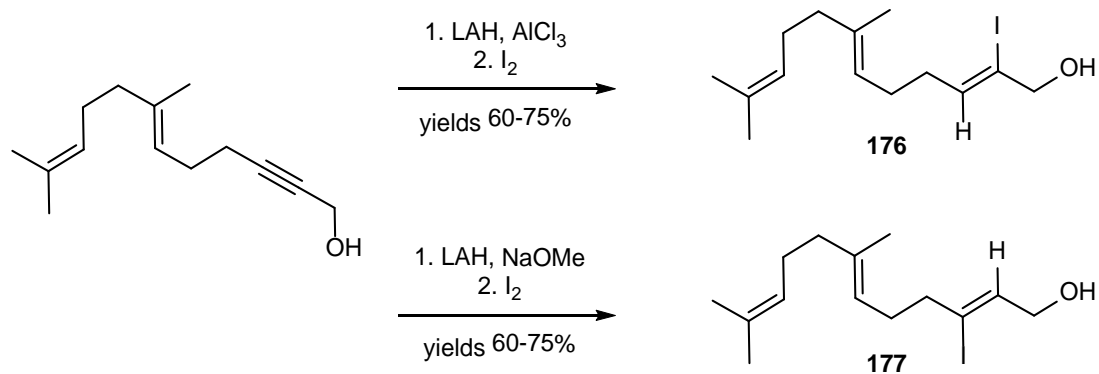


Table 5.4 Trans-hydroalumination/alkylation reactions performed on *EE* protected DB product.

In conclusion, using Vitride® as a reductant is a very quick and effective way to selectively reduce the propargylic alcohol to the *E*-alkene, which is useful for the synthesis of C17-desmethyl analogs of zampanolide. However, it does not allow for the installation of any alkyl residues at C17, which prevents the synthesis of zampanolide itself.

5.1.2 Corey's Method Using LAH/NaOMe

In 1967, Corey et al. reported a method to reduce propargylic alcohols to either 2-alkylated or 3-alkylated allylic alcohols by reducing the alkyne with LAH and quenching with iodine, which in a second step allowed them to substitute the iodine with Gilman's reagent. In either case, they exclusively observed *anti*-addition.^{73,74} Initially, they performed the reaction with only LAH which led to varying mixtures of β - and γ -substituted allylic alcohols. They screened several additives and found that addition of AlCl₃ exclusively produced the β -iodo alcohol **176**, while the addition of NaOMe led specifically to the γ -iodo alcohol **177** (Scheme 5.4). No explanation for these regioselectivities was given.



Scheme 5.4 Corey's method for reduction of an alkyne and iodination using LAH and an additive, followed by a quench with iodine.

In this work, the reductive iodination was first performed on PMP acetal **163**. This first reaction resulted in a 10% yield of the iodinated product **178** (confirmed by ¹H NMR and HRMS) and 35% yield of the proton quenched product **170** (Table 5.5, entry 1). However, the iodinated compound **178** degraded in the NMR tube before full characterization could be performed. Based on these poor results, coupled with the low yield obtained in forming the PMP acetal, a decision was made to abandon this protecting group. Therefore, the reduction part was next attempted on acetate **162**, which unsurprisingly resulted in the loss of the acetate group (Table 5.5, entry 2).

Once the alkynylation strategy had been changed to the non-stereoselective version, the reduction/iodination was attempted using the EE protected material **167**. A first attempt only resulted in degradation of the starting material without yielding any product (Table 5.5, entry 3).

To make sure that the sodium methoxide was not causing the problem in the reaction due to, for example, contamination with sodium hydroxide, the reaction was performed once more without the addition of sodium methoxide (Table 5.5, entry 4). The result of the reaction was once again degradation of the starting

material, suggesting that the terminal alkene and/or the EE group are not stable under the harsh reaction conditions.

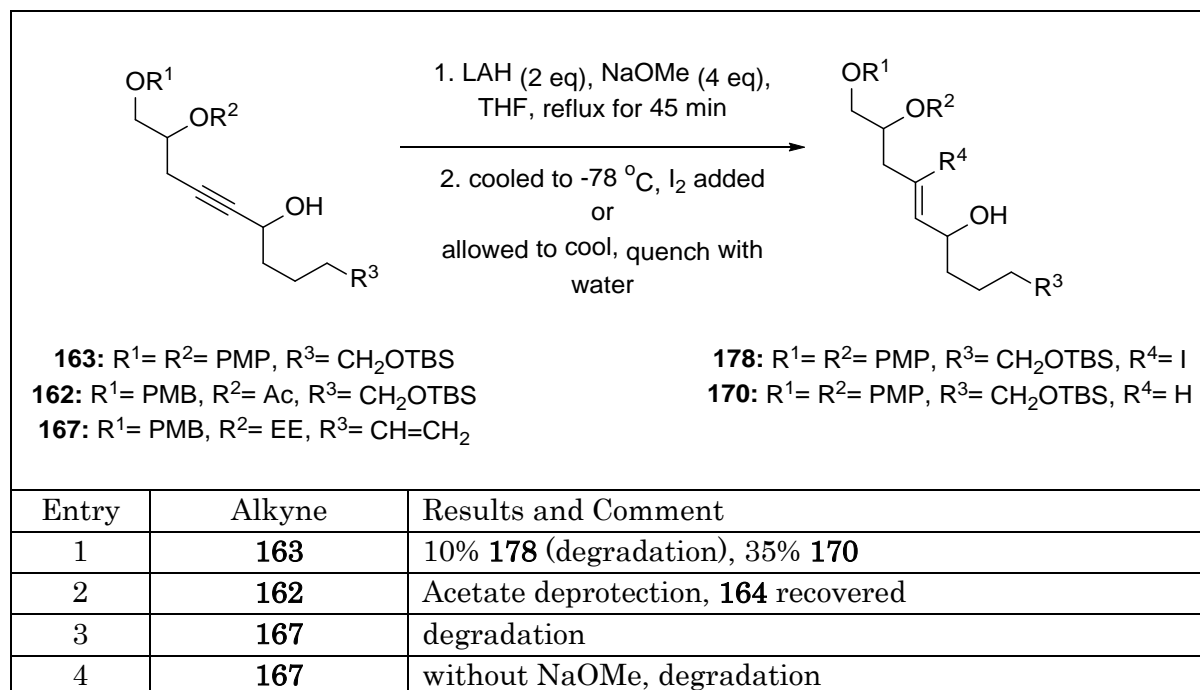
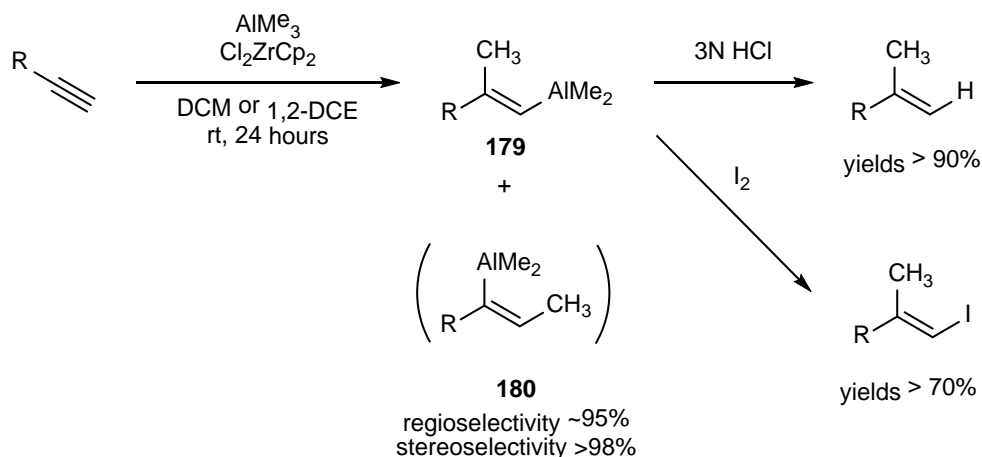


Table 5.5 Conditions and substrates used for the reductive iodination reaction with LAH and NaOMe.

5.1.3 Negishi's Method Using AlMe₃/Cl₂ZrCp₂

In 1985, Negishi published a method for the synthesis of trisubstituted alkenes from terminal alkynes using stoichiometric amounts of trimethylaluminum and catalytic amounts of Cl₂ZrCp₂, resulting in *anti*-addition to the alkyne and forming vinylalane **179**, which is then quenched with either acid or iodine (**Scheme 5.5**).⁷⁰ While small quantities of the regioisomer **180** were formed (about 5% for terminal alkynes), even lower amounts of the corresponding stereoisomer, generated by *syn*-addition, were found (usually less than 2%).



Scheme 5.5 Negishi's method to form trisubstituted alkenes from terminal alkynes using AlMe_3 and Cl_2ZrCp_2 .

Ting had previously attempted to use this chemistry for the generation of fragments for the total synthesis zampanolide without success, as described in **Chapter 2.2.1**. Since using Vitride® did not provide a method suitable to install the C17 methyl group and the reductive iodination with lithium did not yield satisfying results either, it was decided to revisit this methodology once again on differently protected materials (PMB instead of Bn protecting group). Using this strategy would employ an asymmetric NHK-reaction instead of the previously envisaged stereoselective alkynylation to form the C15-C16 bond of zampanolide and set the correct stereochemistry at C15.

A first attempt was made using alkyne **155** with the sorbic acid ester in place to mimic the top half of zampanolide. This reaction resulted in rapid degradation of the starting material, and no product could be recovered (**Table 5.6**, entry 1). Due to the instability of the sorbic ester encountered here, and in earlier stages of the synthesis, the reaction was then performed on the homopropargylic alcohol **116**. Again, the reaction failed to deliver product, this time, however, some starting material was recovered (**Table 5.6**, entry 2). The reaction was then attempted in distilled 1,2-DCE instead of in DCM taken from the PureSolv unit. Additionally the reaction was performed simultaneously inside the glovebox (**Table 5.6**, entry

3) and in the fumehood (**Table 5.6**, entry 4) to establish if the presence of traces of oxygen and moisture might stop the reaction from proceeding. It was found that the reaction performed in the glovebox had a more promising color at first when TMA was added to the Cl_2ZrCp_2 solution, however upon work up and NMR analysis of the crude mixture, no product was detected.

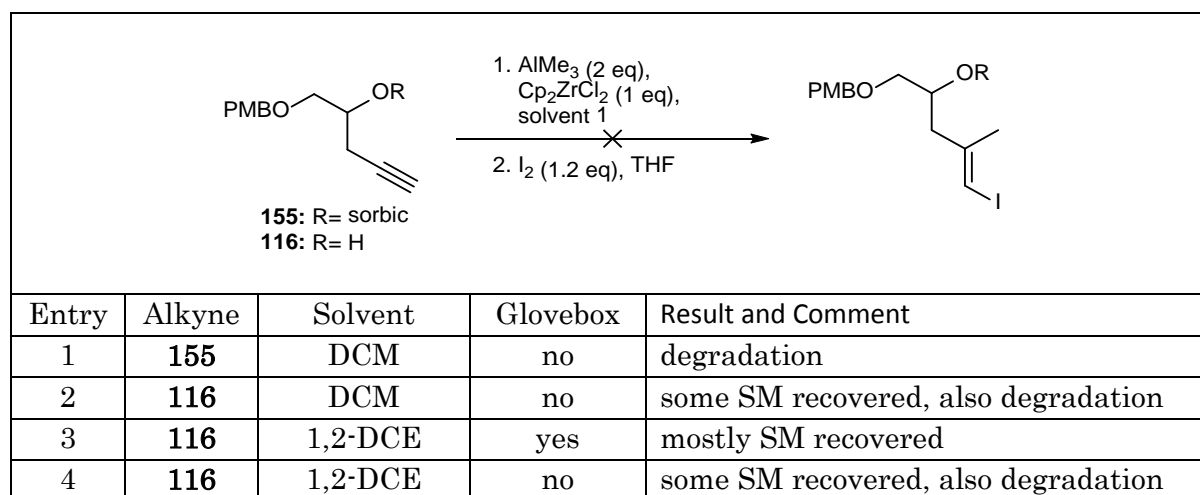
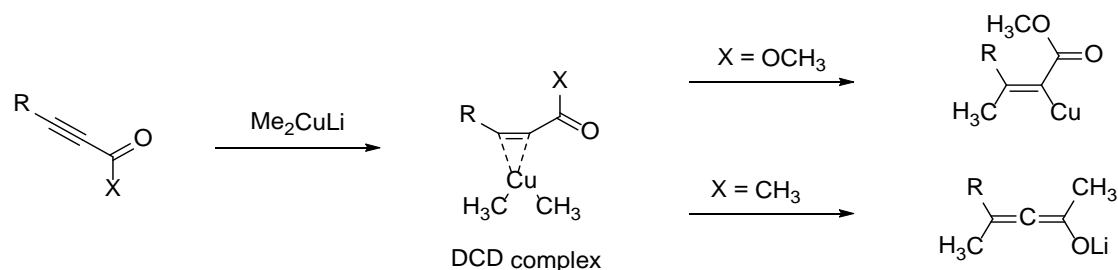


Table 5.6 Conditions and substrates tested for the reductive methylation/iodination following Negishi's procedure.

Since the next step, the asymmetric NHK-reaction, might also prove difficult it was decided to abandon this methodology and focus future efforts on synthesizing zampanolide analogs lacking the C17 methyl group and simultaneously trying to install the C17 methyl group through different chemistry.

5.2 Reductive Methylation of the Alkynone

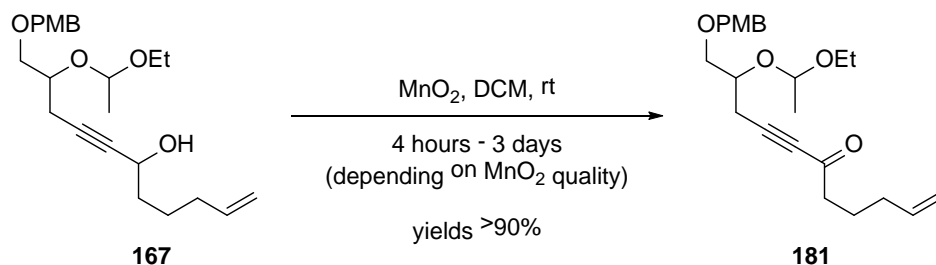
The 1,4-addition of the so called Gilman reagent ($\text{Alkyl}_2\text{CuLi}$, with the alkyl group often being methyl or ethyl) to α,β -unsaturated carbonyls is a very well-known reaction and can be used to produce trisubstituted alkenes from alkynes. This methodology was used earlier in this work, as described in **Chapter 3.1** to perform the reductive methylation on the propargylic methyl ester **103**, with the Gilman reagent performing a *cis*-carbocupration and therefore producing the *Z*-double bond rather than the *E*-alkene. The mechanism was long believed to go through a four-centered transition state as described previously, however Dewar–Chatt–Duncanson-type complexes have been identified by NMR spectroscopy in the addition of Me_2CuLi to electron-deficient alkynes. As shown below, this results in the formation of vinylcopper intermediates for the reaction of the Gilman reagent with ynoates, while allenes are formed when ynones are used (**Scheme 5.6**). It is not clear what causes this difference in reactivity.⁷⁵



Scheme 5.6 Reaction of ynoates and ynones with Gilman reagent.

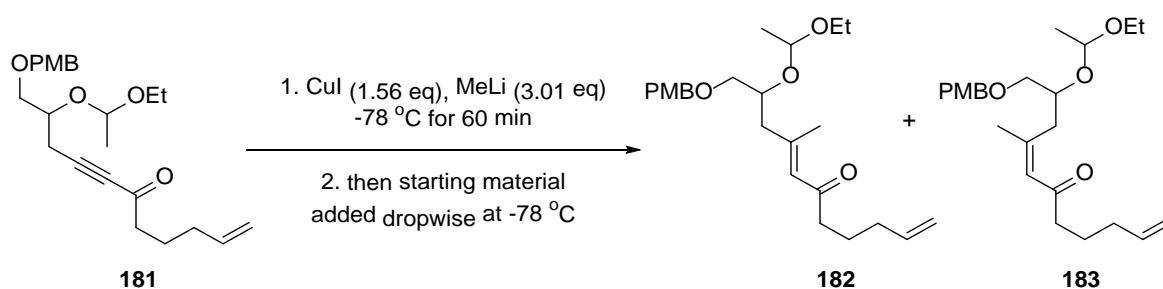
For this methodology to be useful for the reaction at hand and to install the methyl group at C17, alcohol **167** must be oxidized to the ketone to provide the conjugated system that is needed for the Gilman reagent to perform the addition reaction. The oxidation was achieved by stirring the starting material with freshly prepared manganese dioxide at room temperature and the reaction proceeded cleanly and with high yields to the desired product **181**. The reaction was monitored by TLC,

and if it was found to proceed slowly additional manganese dioxide was added as necessary (**Scheme 5.7**).



Scheme 5.7 Manganese dioxide oxidation of propargylic alcohol to the corresponding ynone.

With alkynone **181** in hand, the reductive methylation was attempted following the same procedure used for the methyl ester described in **Chapter 3.1**. The Gilman reagent was formed by adding MeLi to a suspension of CuI in THF at 0°C , and after 60 min the solution was cooled to -78°C and **181** in THF was added dropwise.



*Scheme 5.8 Reductive methylation of **181** using Gilman reagent.*

After work up and evaporation of the solvent, the crude mixture was analyzed by proton NMR and found to be a complicated mixture of multiple stereoisomers, most likely **182** and **183**. To simplify the analysis and confirm the geometry of the newly formed alkene, the EE group was removed using a large excess of PPTS in

first step of the reaction did probably not go to completion. NOESY analysis was performed on the isolated, single product (**Figure 5-2**).

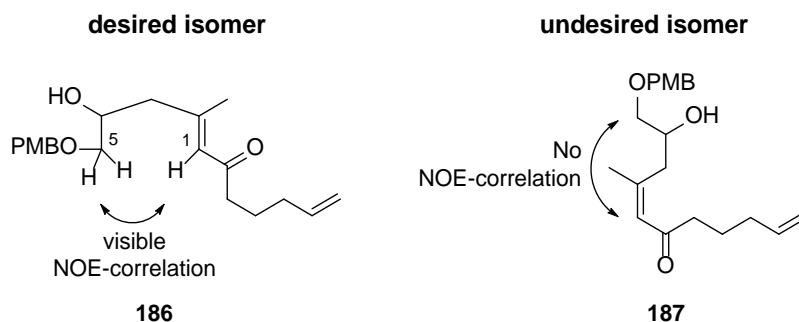


*Figure 5-2 NOESY correlation suggesting the main product is the desired *E*-isomer 186.*

A weak correlation between the newly introduced alkene proton H1 and protons H5a and H5b was found, which indicates that in this attempt mainly the desired *E*-isomer **186** was produced (**Figure 5-3**).

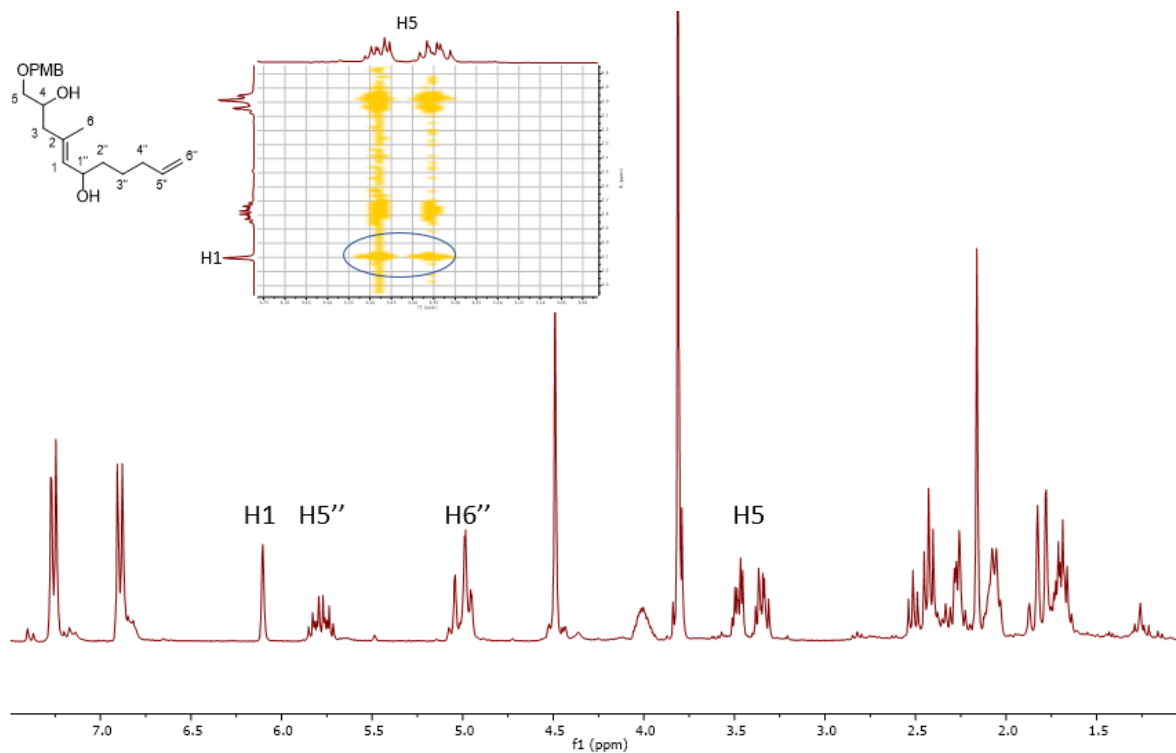
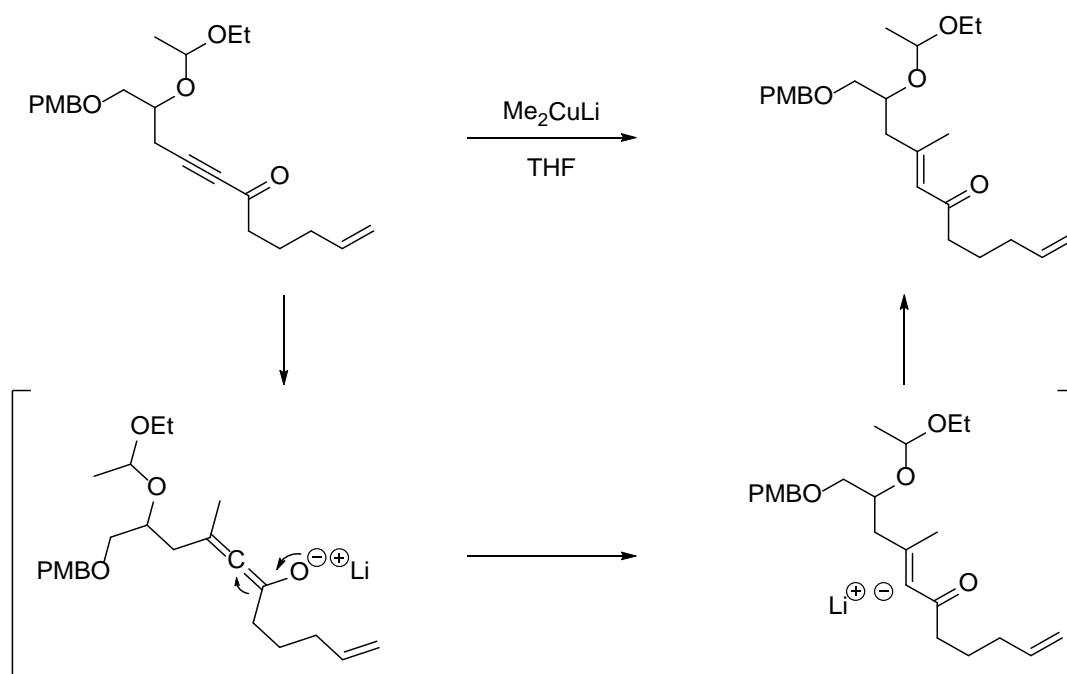


*Figure 5-3 Proton NMR of *E*-alkene 186 and NOE correlation between H1 and H5.*

In a paper published in 2011, Dai et al. reported that they were able to push the *E/Z* ratio of their conjugate addition of Gilman reagent to an ynoate towards the *E*-alkene by increasing the temperature from -78 to 0 °C, and using TMSCl as an additive.⁷⁶ This suggests that the difference in ratio between the first and second attempt at the reaction might be due to the Gilman reagent solution not being fully cooled to -78 °C when the solution of **181** was added, or that the addition was done faster in the second attempt, temporarily raising the temperature in the flask. This however should be further investigated, as well as the potential addition of TMSCl to push the reaction further and ensure a better *E/Z* ratio.

Another fact to consider is that ynones were found to produce allenes rather than vinyl cuprate intermediates.⁷⁵ A possible explanation for the preferred formation of the *E*-alkene over the *Z*-alkene could be that the allene oxy anion is formed first, which is then quenched during the aqueous work up to yield the *E*-alkene in what looks like an *anti*-addition (Scheme 5.10).

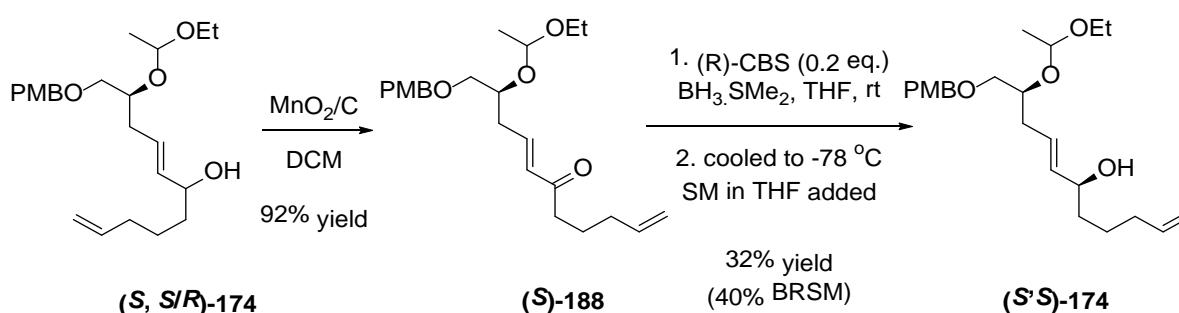


Scheme 5.10 Possible mechanism for the formation of the *E*-alkene over the *Z*-alkene via an allene intermediate.

In conclusion, using the Gilman reagent for the reductive methylation of the ynone seems to be a promising option but should be further investigated to optimize yield and *E:Z* ratio. Following the introduction of the *E*-alkene the ketone has to be reduced back to the alcohol and the stereochemistry at C15 must be set correctly, which can be done by CBS reduction. Successful enantioselective CBS reduction has been performed on similar materials reported in the literature before, with varying degrees of enantioenrichment.^{77,78} The CBS reduction of non-methylated product **174** is discussed in **Section 5.3**.

5.3 Setting the Configuration at C15

The stereoselective reduction was performed on the non-methylated product **174** and it was expected that (*R*)-CBS would provide the correct configuration.^{77,78} In order to perform the CBS-reduction, alcohol (***S,S/R***-**174**) has to be oxidized to the ketone first by treating **174** with manganese dioxide which yielded ketone **188** in a 92% yield (**Scheme 5.11**). The ketone was then stereoselectively reduced back to alcohol **174** in a 32% yield (40% BRSM, unoptimized) using (*R*)-CBS and borane.



Scheme 5.11 Manganese dioxide oxidation of diastereomeric alcohol (***S,S/R***-**174**) to ketone (***S***-**188**), followed by stereoselective CBS-reduction back to the now single diastereomeric alcohol (***S,S***-**174**).

In order to confirm the desired stereochemical configuration, Mosher's analysis was performed. **174** was esterified under Steglich conditions with (S)-(-)-MTPA and (R)-(+)-MTPA respectively. In order to facilitate analysis, the EE protecting group was immediately removed using PPTS in MeOH. It is noteworthy that in order to deprotect the (R)-MTPA product, ten times the amount of PPTS had to be used than for the deprotection of the (S)-MTPA product. After FCC, only one spot was isolated per reaction, which means that either only one diastereomer was formed in the CBS reduction or that the R_f values are too similar to separate the diastereomers. ^1H and ^{13}C NMR analysis showed that the latter was the case. The ratio of major to minor diastereomer was estimated to be about 7:1. However, an exact ratio cannot be determined at this point as there was most likely discrimination of formation of one diastereomer over the other due to differences in reaction rates.

The NMR spectra of the resulting product mixtures were then used to identify the configuration of the newly formed stereocenter, utilizing the shielding effect of the phenyl group on neighboring protons through space, and the de-shielding effect of the methoxy group, respectively, as shown in **Figure 5-4**.

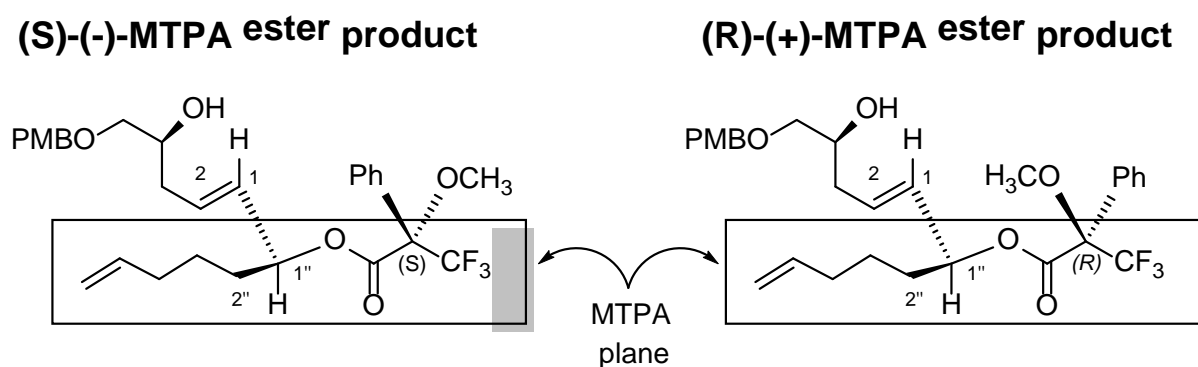


Figure 5-4 Shielding and deshielding effects on the protons in the (S)-(-)-MTPA ester and (R)-(+)-MTPA ester product.

Comparison of the proton NMR spectra of the (*S*)-(-)-MTPA and (*R*)-(+)-MTPA product shows a clear downfield shift of the protons in position 1 and 2 of the (*S*)-(-)-MTPA product in comparison to the (*R*)-(+)-MTPA product, while an upfield shift of the protons in position 2' is observed (Figure 5-5). The Mosher analysis relies on the assumption that the conformation of the alcohol and Mosher ester are the same, therefore the shielding and deshielding effect of the phenyl and methoxy group, respectively, can be directly correlated to their relative positions. If the conformations were exactly the same in the alcohol and the ester, no change to the multiplicity of the shifted signals would be observed. Unfortunately, in the example at hand, there seems to be a fairly significant change in the multiplicity of the shifted signals. While this could mean that the conformation of the alcohol and ester are not the same and therefore the Mosher analysis might not be accurate, this change in multiplicity could also result from underlying impurities. However, because the shift changes are as expected and CBS reduction for similar substrates yielded the desired configuration of the stereocenter, it is likely that the major diastereomer is the desired product (*S,S*)-174.

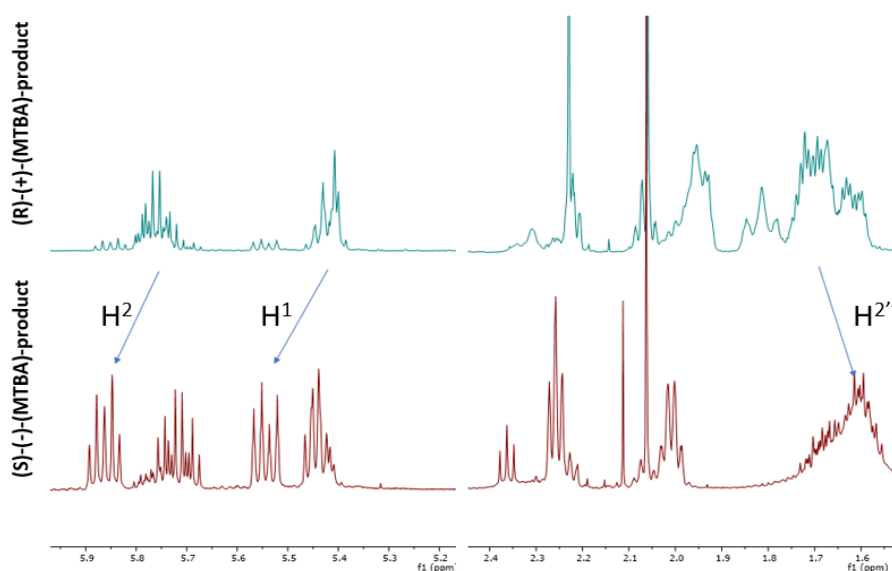
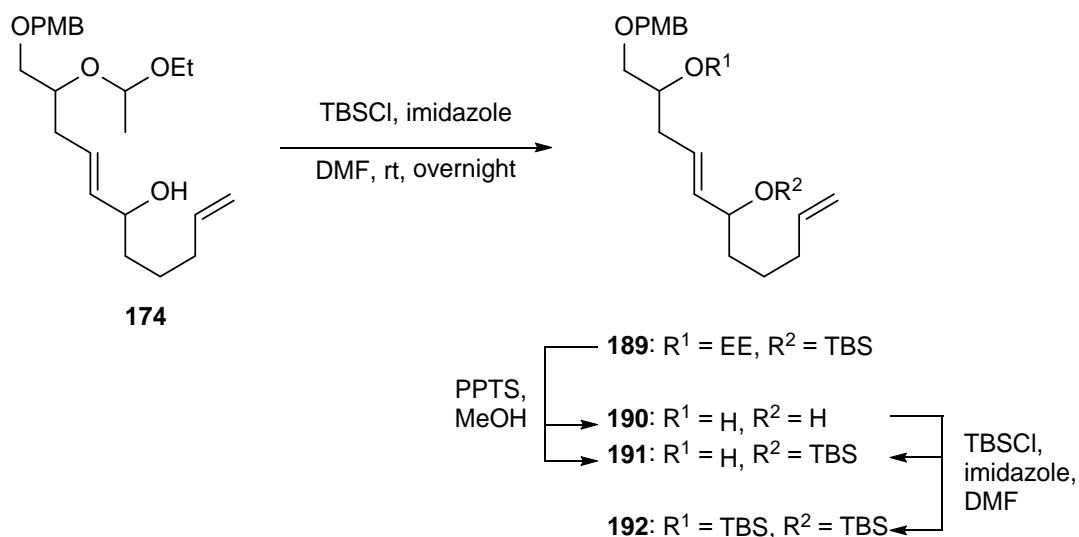


Figure 5-5 Comparison of the proton NMR spectra of the (*S*)-(-)-MTPA and (*R*)-(+)-MTPA product.

5.4 Protecting Group Adjustments

For subsequent reactions like the Bestmann ylid cascade, the protecting groups have to be adjusted. To perform the Bestmann ylid reaction and synthesize a non-THP analog of zampanolide, the free hydroxy group has to be protected while the EE group has to be removed from the other secondary alcohol (**Scheme 5.12**). To achieve this, compound **174** was protected with TBSCl overnight. This reaction resulted in a highly complicated TLC and even worse column chromatography, identifying four very similar products. To confirm that all these products were merely various diastereomers of the double-protected compound **189**, it was attempted to remove the EE group using a large excess of PPTS in MeOH. This however resulted in removal of the EE group as well as the TBS group (**190**), but confirmed that indeed all four spots were different diastereomers. In a second attempt, only one equivalent of PPTS was used and extra care was taken during the work up, which resulted in a 52% yield of mono-deprotected product **191** and only 12% of double deprotected material **190**. More optimization is needed with regards to reaction temperature and reaction time to improve the yield of the mono-protected species even further.



Scheme 5.12 Change of protecting groups to prepare for the Bestmann ylid cascade and subsequent synthesis of non-THP analogs.

It was then attempted to protect the allylic alcohol of the diol **190** selectively over the other secondary alcohol, utilizing the bulk of the PMB group to shield the latter. The reaction was performed using 1.1 eq. of TBSCl and imidazole in DMF, which resulted in a 40% yield of monoprotected **191** and recovered starting material after stirring for three hours. The reaction was repeated, using the same amount of TBSCl, but the reaction was stirred overnight. This however resulted in the formation of only double-protected material **192**. Further investigations to produce the mono-protected material have to be undertaken, however **192** also proved to be a valuable substrate in the pyran formation, as described in **Section 6.2.1**.

5.5 Summary of Chapter 5: Conversion of the C16-C17 Alkyne to an Alkene: Reducti(ve methylati)on

In summary, although Jamison's protocol involving use of Vitride® failed to provide the desired trisubstituted alkene, Vitride® was successfully established as the method of choice to selectively reduce the propargylic alcohol to the *E*-alkene in near quantitative yields therefore providing access to building blocks for the synthesis of various C17-desmethyl analogs of zampanolide. Oxidation of the allylic alcohol to the ketone allowed for the subsequent stereoselective reduction with (*R*)-CBS and yielded the desired product with (*S*)-configuration at C15 as the major isomer (in an estimated 7:1 ratio with the (*R*)-isomer). Additionally, several hydroxyl-protected species have been synthesized which could either be used in Bestmann ylide linchpin reactions (**Chapter 7**) or be employed as substrates for cross-metathesis reactions and subsequent THP-formations (**Section 6.2.1**).

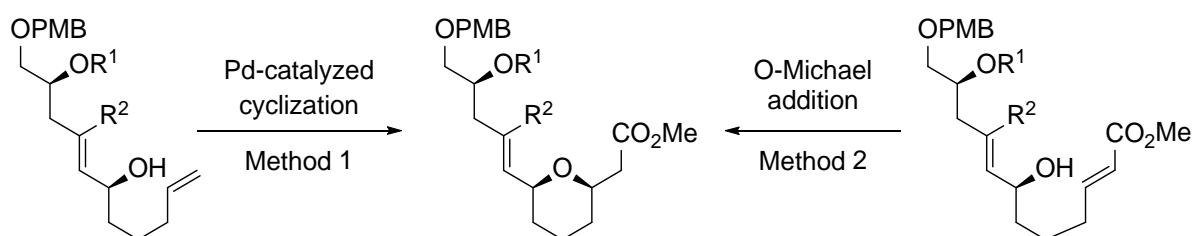
The Gilman reagent was successfully used to reduce the alkynone to the alkene and install the desired methyl group at C17 with varying ratios of *Z*:*E*-alkene.

Further investigations should be conducted to further increase the yields and push the ratio of diastereomers of this reaction towards the *E*-alkene.

Chapter 6: Formation of the *cis*-Tetrahydropyran Ring

Functionalized tetrahydropyran (THP) rings are a common motif in many bioactive natural products, including halichondrin B (**2**), eribulin (**3**), and of course zampanolide (**1**) and dactylolide (**8**). There are many ways a THP ring can be formed, including ester enolate Claisen rearrangements, ring expansions of tetrahydrofurans, iodolactonizations, hetero-Diels-Alder cyclizations, epoxide opening-ring closure reactions, *O*-Michael reactions or metal-catalyzed ring closures onto carbon-carbon double bonds, to name a few.^{79–81} Depending on whether the formation of a *cis*- or *trans*-THP ring is required and the functionalization of the ring, a method has to be chosen carefully.

For the synthesis of the THP ring in the zampanolide/dactylolide system, many different methods have been previously applied (see **Chapter 2.1**). The strategy in this work was to use either a Pd(II)-catalyzed oxidative cyclization and carboxylation sequence (method 1), or an *O*-Michael addition (method 2) similar to the reaction employed in Uenishi's published synthesis (**Chapter 2.1.8**)²⁹, as shown in **Scheme 6.1**.



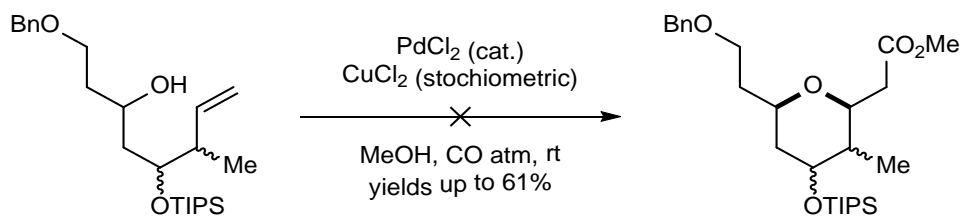
*Scheme 6.1 Proposed THP ring formation via Pd-catalyzed carboxylative cyclization or *O*-Michael reaction.*

The advantage of using method 1 is that it only delivers the *cis*-THP, while method 2 is less stereoselective and was reported to only give an approximately 2:1 ratio of *cis*- to *trans*-product in Uenishi's work.²⁹ Additionally, no modification of the material has to be performed after the reductive methylation to prepare for method 1, while a cross-metathesis is required to activate the double bond in preparation for ring-closure using method 2. On the other hand, method 1 not only requires the use of expensive palladium(II) catalysts in up to stoichiometric amounts, which makes this approach uneconomical, but also requires the use of highly toxic carbon monoxide. In contrast, method 2 is performed by simply adding base to the solution of the substrate.

Ultimately, it was decided to test the Pd(II)-catalyzed carboxylative cyclization first since it is a novel method for the formation of the THP ring in the zampanolide system and can give better stereoselectivity, but with the intention to investigate the *O*-Michael addition approach as well. The results are presented below.

6.1 Pd(II)-Catalyzed Tetrahydropyran Formation

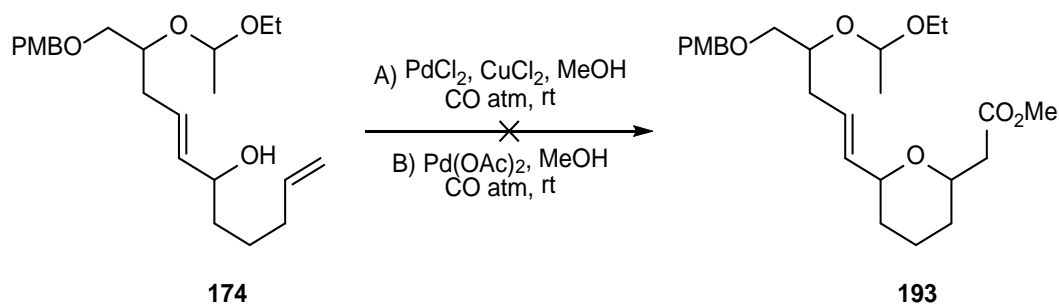
In 1999, White et al. published a paper on a method for intramolecular Pd(II)-catalyzed carboxylative cyclizations of substituted THP rings using catalytic palladium(II) chloride and stoichiometric copper(II) chloride as co-oxidant (**Scheme 6.2**). The reaction was performed under an atmosphere of carbon monoxide with MeOH as solvent and yielded only *cis*-THPs functionalized as methyl esters in moderate yields.⁸²



Scheme 6.2 White's Pd-catalyzed carboxylative cyclization to form substituted THP rings.

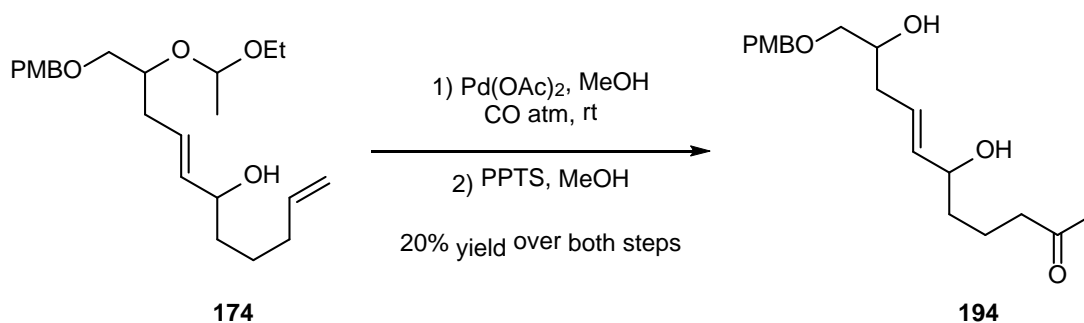
Over a decade later, the same group improved their previously published method during their synthesis of the marine toxin phorboxazole A.⁸³ After initial attempts using the old protocol, which took several days and still resulted in disappointing yields, they adjusted their protocol. Instead of solely using methanol as the solvent, a mixture of methanol and acetonitrile was used, which they found decreased the amount of reduction of the palladium catalyst. Additionally, instead of catalytic amounts of palladium(II) chloride, an excess of three equivalents of palladium(II) acetate was used.

In this work, both methods described above were tested as shown in **Scheme 6.3**. Method A used a catalytic amount of Pd(II) and stoichiometric amounts of CuCl_2 , but only resulted in degradation of the starting material **174**. Method B used quantitative Pd(II) and therefore did not need a co-oxidant, and yielded a clean compound after being purified by FCC, which did not correspond to the expected NMR spectra of the desired product **193**.



Scheme 6.3 Two initial attempts at the Pd-catalyzed carboxylative cyclization using PdCl_2 (Method A) and Pd(OAc)_2 (Method B).

The NMR spectra of this compound were very difficult to interpret due to the presence of multiple diastereomers, which led to the decision that it would be sensible to deprotect the secondary alcohol and therefore remove the stereocenter of the EE group in order to reduce the number of isomers. This was done simply by stirring the product with PPTS in MeOH overnight. After purification *via* FCC, the product was found to be ketone **194**, as shown in **Scheme 6.4**, and was isolated in 20% yield over two steps.



*Scheme 6.4 Ketone **194** formed in the Pd-catalyzed carboxylative cyclization/deprotection sequence.*

The “acetone-like” peaks in the proton and carbon NMR spectrum at 2.13 ppm and 209.2 ppm respectively, were first mistaken as acetone (**Figure 6-1**). However, upon closer examination of the exact shifts and correlations in 2D NMR spectroscopic data ketone **194** was identified, which was also confirmed by HRMS.

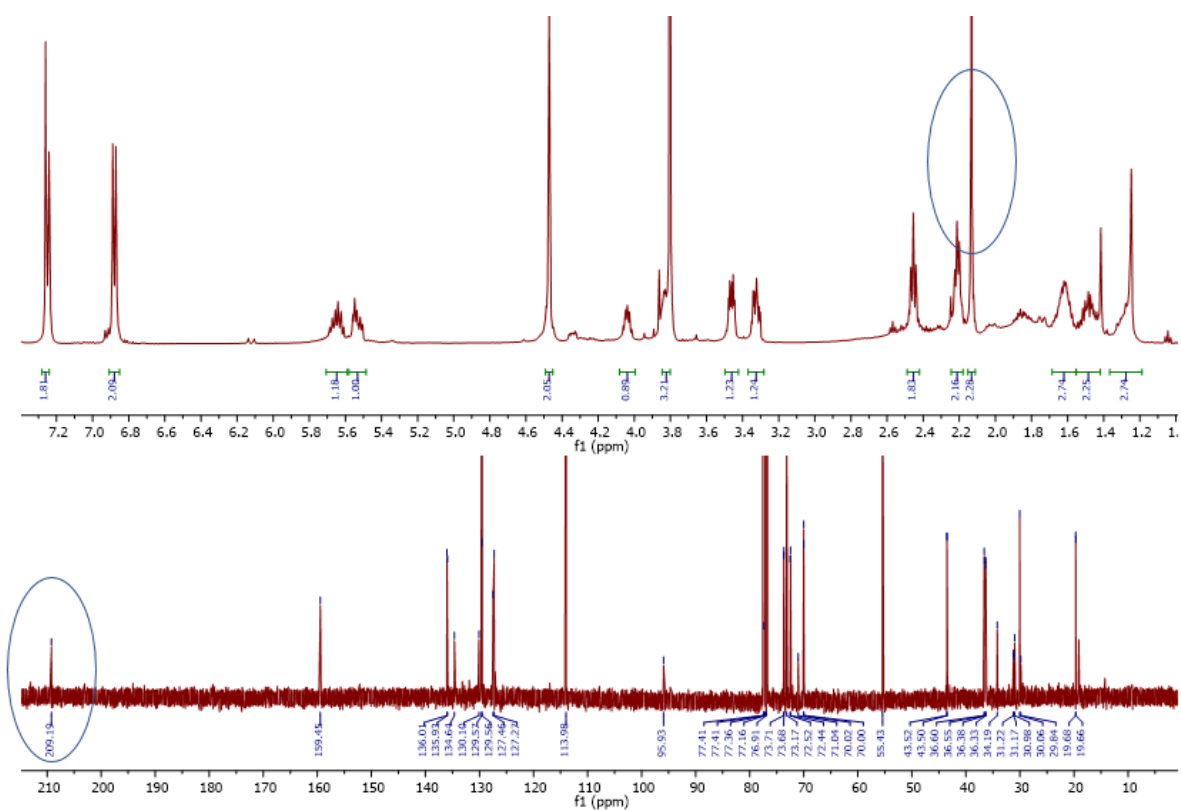
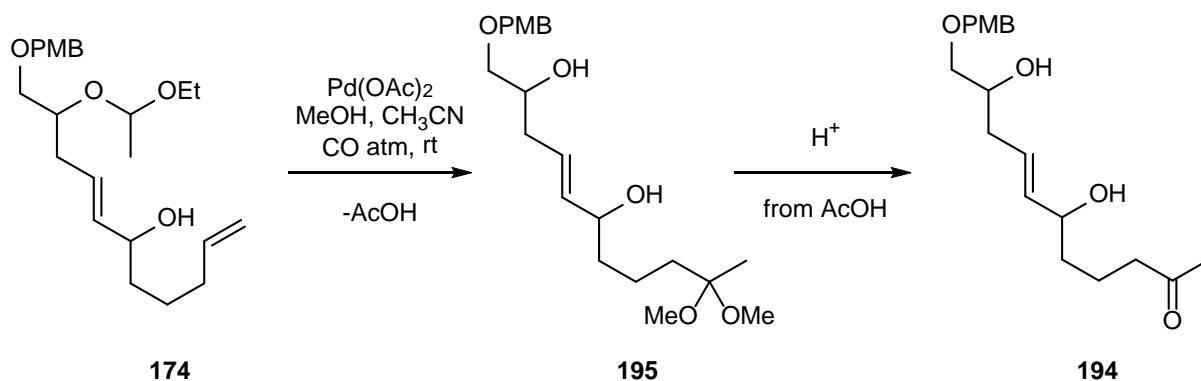


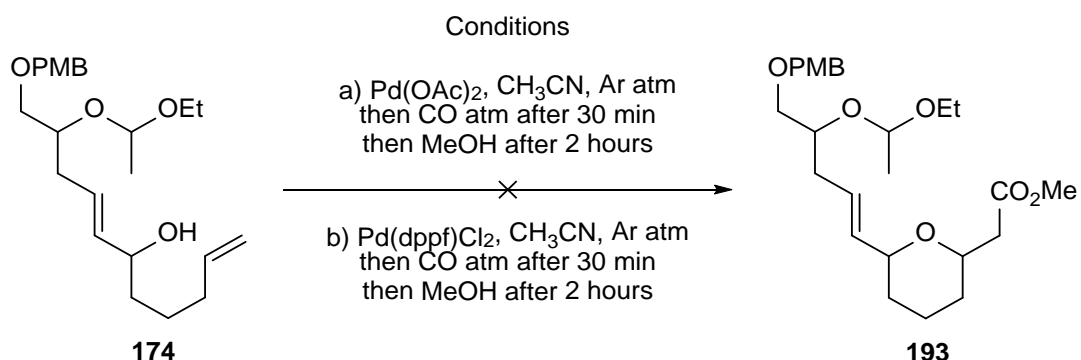
Figure 6-1 Proton and carbon NMR spectra of ketone **194**.

Ketone **194** would most likely have formed through a Wacker-type reaction. The Wacker reaction uses Pd(II)-catalysts, and either water or alcohols can act as a nucleophile. If water is the nucleophile, the ketone is the product, while with an alcohol an acetal is formed. Usually the Wacker reaction uses catalytic Cu(II) salts and molecular oxygen to regenerate the Pd catalyst. However, in the case at hand three equivalents of palladium(II) acetate were used, which explains why no co-oxidants were needed. Additionally, since it is highly unlikely there was this much water in the reaction, the most plausible cause for the formation of the ketone is that initially methanol reacted as nucleophile producing the methyl acetal **195**, which was then cleaved by the acetic acid formed upon filtering the reaction mixture through silica and washing the plug with wet DCM (**Scheme 6.5**).



*Scheme 6.5 Proposed mechanism for the formation of Wacker product **195** and deprotection of the formed acetal to give ketone **194**.*

In an attempt to avoid the Wacker reaction, the palladium catalyst was allowed to react with **174** first under argon atmosphere with only acetonitrile as the solvent to prevent the alcohol nucleophile from interfering with the palladium(II)-double bond complex. The argon was then exchanged for carbon monoxide and the reaction stirred for two hours to allow for the insertion of carbon monoxide to occur. Only then methanol was added to perform the last step, the formation of the ester, in an effort to obtain desired product **193** (Scheme 6.6). Unfortunately, these conditions only led to degradation of the starting material, and neither the desired product nor the Wacker product were detected.



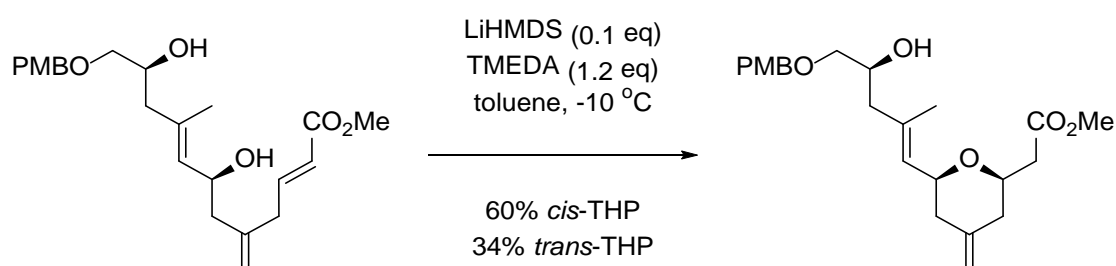
Scheme 6.6 Adjusted conditions to avoid the Wacker reaction.

Additionally, to the catalysts described in the literature, the reaction was attempted with a different palladium(II) catalyst, Pd(dppf)Cl₂. This catalyst is very stable and mild, which would hopefully allow for avoidance of degradation and would result in the formation of the desired product. Disappointingly this catalyst did not show any reactivity at all and only starting material was recovered (**Scheme 6.6**).

At this point, all efforts were refocused towards the implementation of the previously mentioned *O*-Michael reaction as the method to form the *cis*-THP ring.

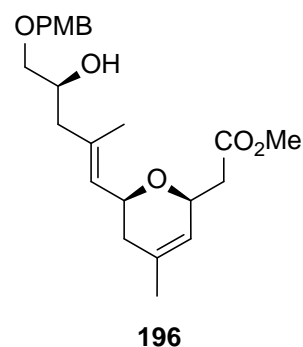
6.2 Tetrahydropyran Formation via *O*-Michael Reaction

The formation of the *cis*-THP ring in the zampanolide system by *O*-Michael reaction has been accomplished by Uenishi and coworkers in 2009.²⁹ They found that the cyclization proceeded with excellent overall yields of >90% when LiHMDS and TMEDA were used at -10 °C; however, a near 2:1 ratio of *cis* : *trans* THP product was formed (**Scheme 6.7**), with the desired *cis*-product being the thermodynamic product.



Scheme 6.7 Uenishi's method for the cis-THP formation in the zampanolide system.

Raising the temperature above $-10\text{ }^{\circ}\text{C}$ resulted in formation of byproduct **196**, with the exomethylene rearranging to an internal alkene (**Figure 6-2**). Even though the stereoselectivity of the reaction is not overwhelming, the silver lining is that Uenishi showed that the undesired *trans*-product can be converted into a 3:2 mixture of *cis*- and *trans*-product by treating it with NaHMDS, which can then be separated again and the process repeated if necessary. However, as the byproduct described in Uenishi's paper



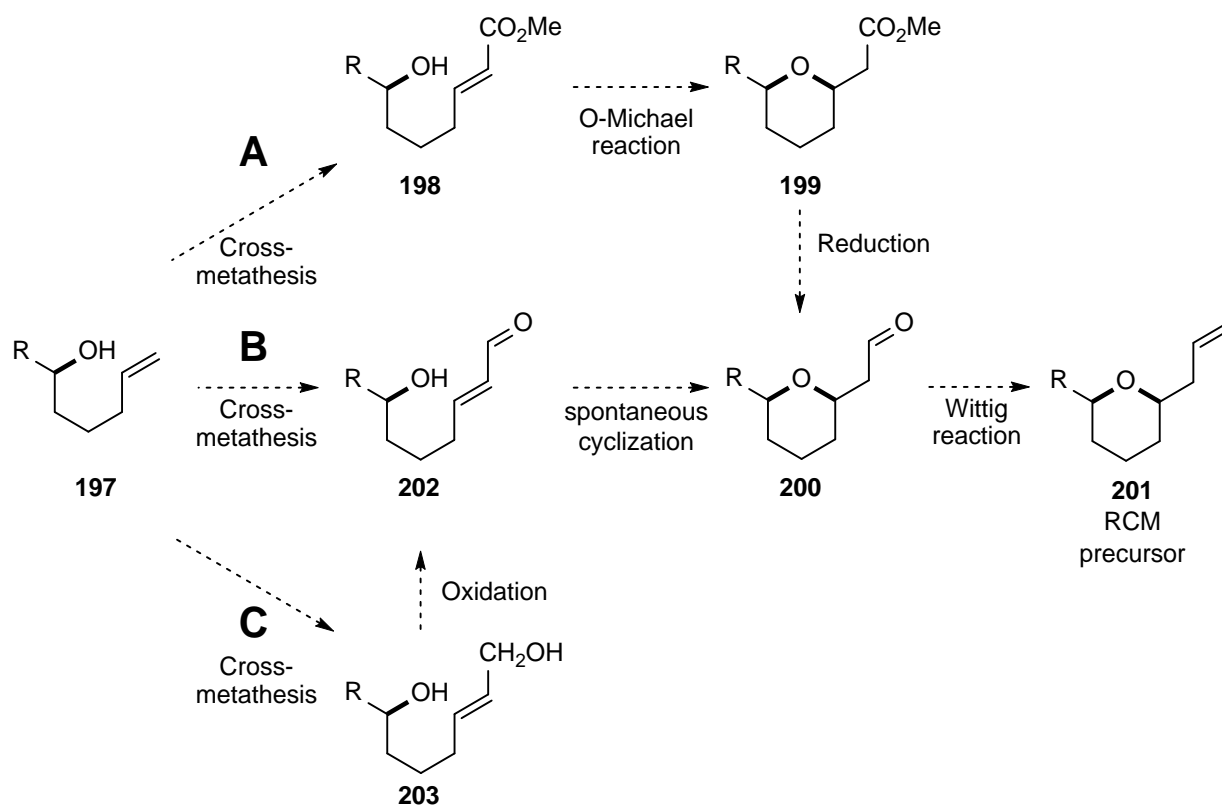
196
Figure 6-2 By-product of the O-Michael reaction of Uenishi and co-workers.

relates to a rearrangement of the exocyclic methylene double bond, which in this work was not planned to be installed until a later stage, increasing the temperature above $-10\text{ }^{\circ}\text{C}$ should be possible without formation of a byproduct and could favor formation of the thermodynamic *cis*-THP. Fuwa et al. reported an 11:1 ratio of *cis* to *trans*-THP rings when the reaction was performed in toluene at $135\text{ }^{\circ}\text{C}$.⁸⁴

To prepare for the *O*-Michael reaction, cross-metathesis of the alkyne-reduced species was necessary to install the required conjugated unsaturated carbonyl functionality. Once this is done, the cyclization could be performed to close the ring (**199** in A, or **200** in B and C) and subsequently the right-hand side of the molecule has to be modified to prepare for the ring-closing metathesis, including a one-carbon homologation. This can be achieved by first reducing ester **199** to aldehyde **200** followed by a Wittig reaction to give RCM precursor **201** (Pathway A, **Scheme 6.8**). However, instead of installing the ester through cross-metathesis and then reducing it to the aldehyde after the cyclization, with direct reduction of the ester to the aldehyde often proving difficult, there are several other suitable substrates for the *O*-Michael reaction which might facilitate the later preparation for the RCM and cut down the number of involved steps.

In pathway B (**Scheme 6.8**) the cross-metathesis was envisaged to be performed with acrolein (**64**), which should then lead to spontaneous cyclization of **202** due to

the increased reactivity of the aldehyde. If the cyclization to **200** does not occur spontaneously, addition of base should promote the *O*-Michael addition.



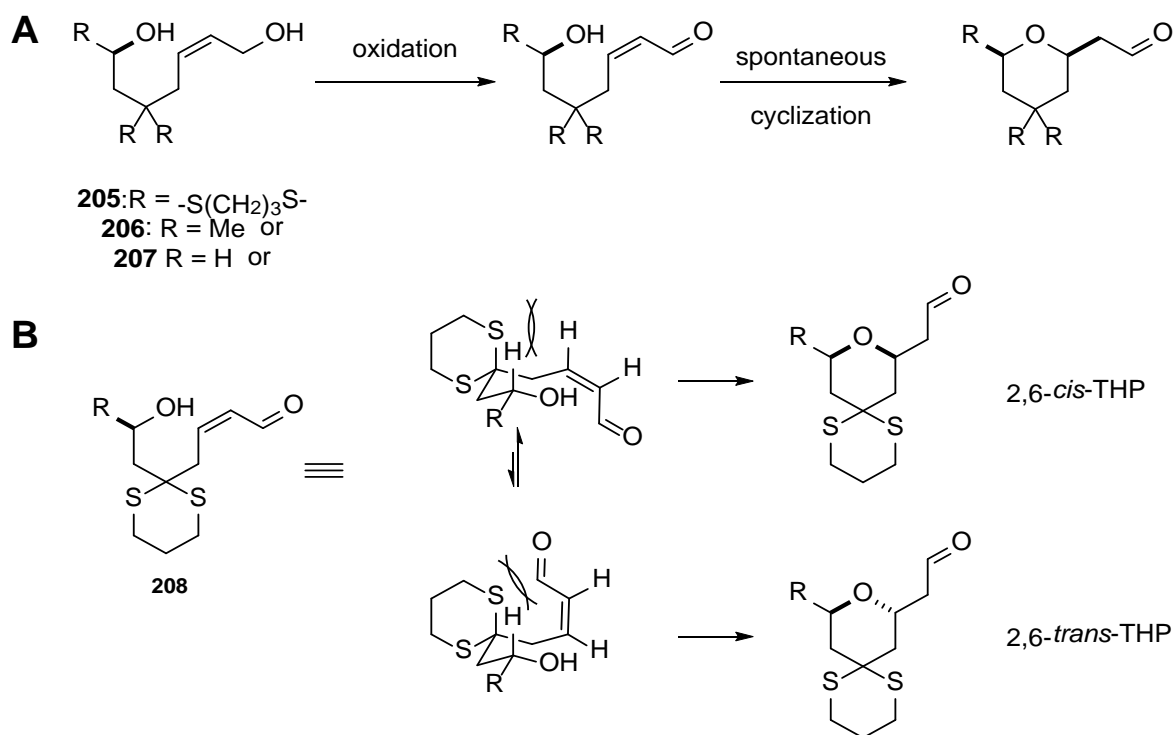
*Scheme 6.8 Possible options to synthesize RCM precursor **201** from the reductive methylation product **197** via three different pathways using cross-metathesis, cyclization and reduction/oxidation steps.*

For pathway C (**Scheme 6.8**), 2-buten-1,4-diol would be used in the cross-metathesis to yield diol **203**, followed by an oxidation step and spontaneous cyclization. Even though this route requires more synthetic steps, it has the advantage of avoiding the use of acrolein, a highly toxic compound. Additionally, the cross-metathesis with 2-buten-1,4-diol should proceed more easily than the cross-metathesis with acrolein.

The tandem allylic oxidation/oxa-Michael reaction has previously been described in the literature by Hong et al.⁸⁵ They found that this reaction achieves the best results when a bulky substituent is introduced to the ring that, through the Thorp-Ingold effect, would promote preorganization of the conformation of the substrate for the cyclization, like 1,3-dithiane **205** (Scheme 6.9, A). This is particularly relevant in this work because the fragment necessary for the synthesis of zampanolide has a substituent in the same position as Hong's dithiane substituent (in **205**) or methyl substituents (in **206**). Different methods for the oxidation step were tested, including the use of manganese dioxide and Parikh-Doering conditions, as well as substrates featuring a methyl substituent or no substituent. Hong et al. found that best results were achieved with bulkier substituents, achieving the best yields as well as the highest stereoselectivities as predicted.

Even though the substrate without a substituent, **207**, was least successful in Hong's studies, the reaction still resulted in an 83% yield and 7:1 ratio of *cis:trans*-THP, which is better stereoselectivity than Uenishi and coworkers achieved in their synthesis. The rationale for the better *cis*-selectivity when substrates with bulky substituents are used is shown in Scheme 6.9.

The 1,3-diaxial interaction of the dithiane with the bulky α,β -unsaturated aldehyde in **208** is highly disfavored, which results in the preferred formation of the *cis*-THP ring, which only exhibits minor steric hindrance between the dithiane and a hydrogen. In a compound without a substituent the 1,3-diaxial interaction would occur between the aldehyde with either hydrogen instead of the dithiane, which is less disfavored, therefore the *cis/trans*-selectivity is decreased.



Scheme 6.9 A. Hong's method for a tandem allylic oxidation/oxa-Michael reaction to form a cis-THP ring. B. Axial interactions leading to the preferred formation of the cis-THP over the trans-THP.

6.2.1 Cross-metathesis and *O*-Michael Reaction

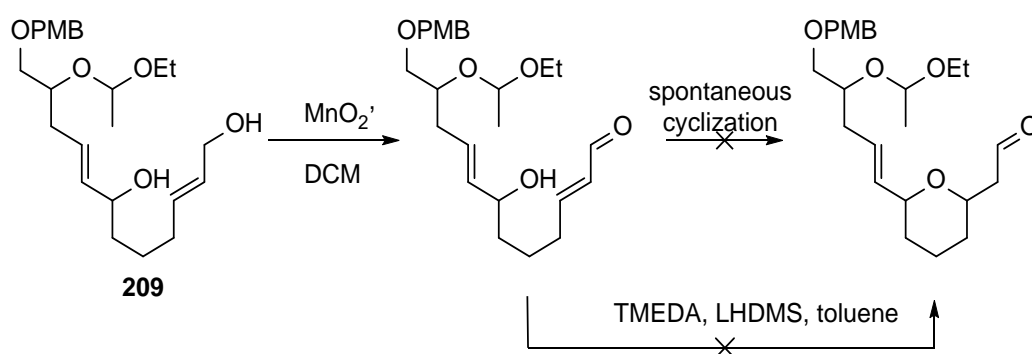
The cross-metathesis, as explained above, was performed on the reductive methylation product **174** and coupled with three different alkenes, namely 2-buten-1,4-diol, acrolein and methyl acrylate to yield alcohol **209**, aldehyde **210** and methyl ester **211**, respectively. The results are summarized in **Table 6.1**.

The reaction with 2-buten-1,4-diol (entry 1, **Table 6.1**) was performed using Grubbs-II catalyst and gave alcohol **209** in a yield of 23% (49% BRSM), which is moderate but a good basis for further optimization.

<p>174: R¹= EE, R²= H 192: R¹=R²= TBS</p> <p>209: R¹= EE, R²= H, R³= CH₂OH 210: R¹= EE, R²= H, R³= CO₂Me 211: R¹=R²= TBS, R³= CO₂Me</p>					
Entry	SM	Catalyst	Solvent	Reagent	yield
1	174	Grubbs II	0.16 M DCM	2-buten-1,4-diol	23% 209 (49% BRSM)
2	174	GH-II	0.05 M DCM	acrolein	-
3	174	Grubbs II	0.1 M PhMe	methyl acrylate	25% 210 (44% BRSM)
4	192	Grubbs II	0.1 M PhMe	methyl acrylate	83% of 211

Table 6.1 Cross-metathesis reactions performed to prepare for the O-Michael addition.

The product of the reaction, **209**, was then subjected to allylic oxidation using MnO₂ in DCM with stirring for 36 hours at room temperature, and the crude mixture was analyzed by NMR spectroscopy (**Scheme 6.10**).



Scheme 6.10 Attempt at a tandem allylic oxidation/O-Michael addition reaction.

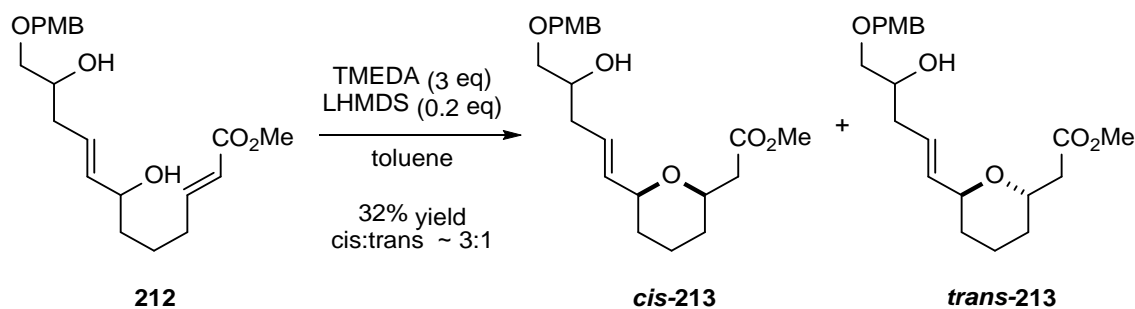
Several aldehyde peaks had appeared, but the number of peaks relating to double bonds suggested the α,β -unsaturated aldehyde was still present, indicating that

the ring closure had not been successful. A decision against further purification was made at this stage due to the small amount of material left. To attempt closing the ring, the crude reaction mixture was treated with TMEDA and LiHMDS in toluene at room temperature. However, no cyclized product was isolated.

The cross-metathesis using acrolein as coupling partner was attempted next, using Grubbs-Hoveyda II catalyst (entry 2, **Table 6.1**). This reaction resulted in mostly recovered starting material, and some of the starting material was deprotected during the reaction. No aldehyde was recovered, cyclized or otherwise.

Next, the cross-metathesis with methyl acrylate was attempted, using recrystallized Grubbs-II catalyst (entry 3, **Table 6.1**). The reaction yielded the desired product **210** in a yield of 25% (44% BRSM). However, it might be possible to optimize the reaction to achieve higher yields.

Additionally, the reaction was attempted on doubly TBS-protected material **211**, which was a by-product of an attempted selective TBS protection described in **Chapter 5.4**. This reaction proved to be the most successful attempt at a cross-metathesis, yielding 83% of the desired product (entry 4, **Table 6.1**). To perform the base-catalyzed *O*-Michael addition and form the THP ring, both TBS groups were removed using PPTS in methanol, which is a very mild method for TBS deprotection and can potentially be replaced by a faster method like using TBAF in THF. The diol **212** was then subjected to the same conditions that Uenishi used in his zampanolide synthesis²⁹, using sub-stoichiometric amounts of TMEDA and an excess of LHMDS to form the THP ring (**Scheme 6.11**).



Scheme 6.11 *cis*-THP formation using TMEDA and LHMDS.

The reaction gave a mixture of approximately 3:1 of *cis*- to *trans*-product (*cis*- and *trans*-213) in a 32% yield, as determined by the proton NMR spectrum of the crude reaction mixture. After FCC, clean *cis*-213 alongside some mixed fractions of *cis*-213 and *trans*-213 were obtained.

The stereochemical configuration was determined by comparison of the ¹H NMR spectra of the *cis*-product and *cis*/*trans*-product mixture with Uenishi's previously reported, very similar, compounds.²⁹ The results are summarized in **Table 6.2**. In comparison to the shifts of Uenishi's compounds, the signals for the compounds synthesized in this work are all shifted upfield. The signals for the relevant oxymethine protons in the *trans*-THP are both located significantly downfield of the corresponding protons in the *cis*-THP. The same is true for the THP-containing compounds synthesized in this work.

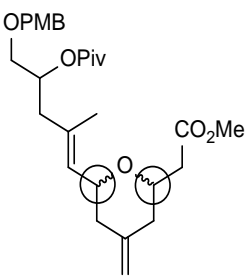
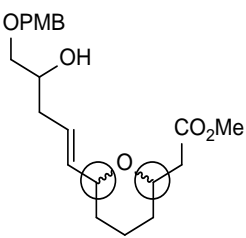
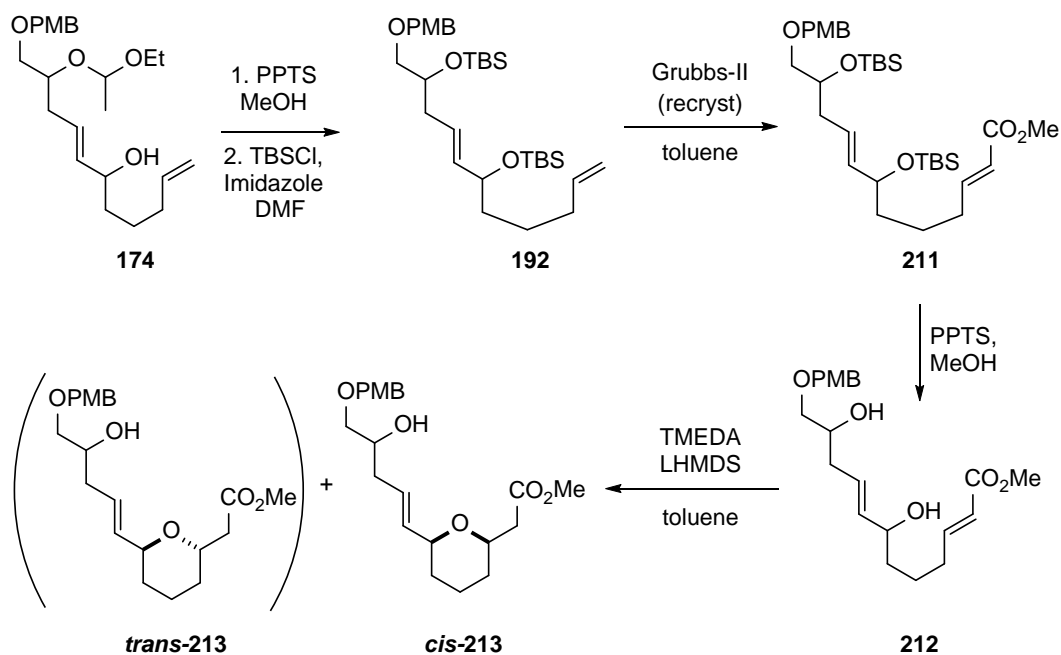
	Uenishi and coworkers ²⁹		This work	
				
<i>Cis</i> -THP	3.98	3.79-3.73	3.83-3.81	3.83-3.81
<i>Trans</i> -THP	4.52-4.46	4.22	4.36	4.16

Table 6.2 Comparison of ¹H-NMR shifts between Uenishi's *cis*- and *trans*-THP compound, and the THP-containing compounds synthesized in this work.

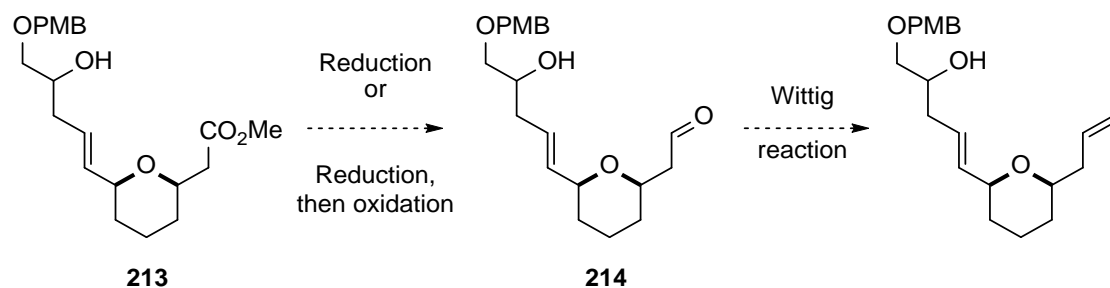
An overview of the transformations leading from the reduction product **174** to the THP containing *cis*-**213** are summarized in **Scheme 6.12**. The EE group of **174** was removed by stirring **174** in MeOH with PPTS overnight, and both hydroxy groups of the resulting diol were protected with TBSCl and imidazole in DMF to give **192**. Subsequently the cross-metathesis with methyl acrylate was performed and the TBS groups removed by again stirring with PTPS in MeOH overnight to produce diol **212**. The last step in this sequence consists of the base-promoted *O*-Michael reaction of **212** to form *cis*- and *trans*-**213** in a 32% yield.



Scheme 6.12 Overview of the transformations of the reduction product **174** to the *cis*-THP-containing compound **cis-213**, including all protection/deprotection steps.

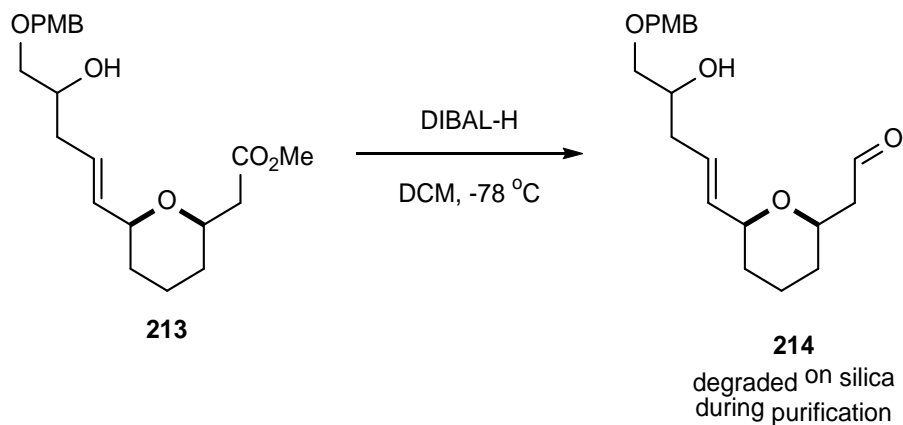
6.3 Modifications to Prepare for RCM

So far only a very small amount of THP compound **cis-213** had been produced due to time constraints, therefore not much work was achieved to prepare the molecule for the RCM. The ester would need to be reduced to the aldehyde, either through direct reduction to the aldehyde or reduction to the alcohol and re-oxidation to the aldehyde. Then a Wittig reaction could be performed in order to add one carbon to the molecule and install the terminal alkene, as shown in **Scheme 6.13**.



Scheme 6.13 Necessary transformation to set up for the subsequent RCM.

The first step was been attempted using DIBAL-H in DCM at -78°C (**Scheme 6.14**). The reaction was followed by TLC and seemed to proceed smoothly to aldehyde **214**, which was confirmed by a proton NMR of the crude mixture. However, after purification *via* silica FCC, all material seemed to have degraded. In order to avoid this in the future, the Wittig reaction should be performed on the crude mixture without purifying the aldehyde first.



*Scheme 6.14 Reduction of methyl ester **213** to aldehyde **214** in preparation for the Wittig reaction.*

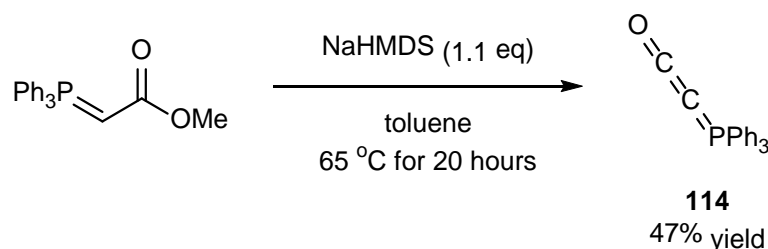
6.4 Summary of Chapter 6

Two types of methods were explored for the formation of a *cis*-THP ring, a palladium(II)-mediated carboxylative cyclization as well as a base-promoted *O*-Michael reaction. While the former method did not result in the desired product, the latter yielded the desired THP ring in an approximate 3:1 ratio of *cis*- and *trans*-THP product. With further optimization, this ratio could be pushed further toward the desired *cis*-product.

Future work should include the transformation of the methyl ester into a terminal alkene by reduction to the aldehyde and subsequent Wittig reaction, which is outlined above in **Section 6.3**. Once the C1-C9 portion of the zampanolide carbon skeleton is installed *via* Bestmann ylide linchpin, the building block is ready for the macrolactonization *via* RCM.

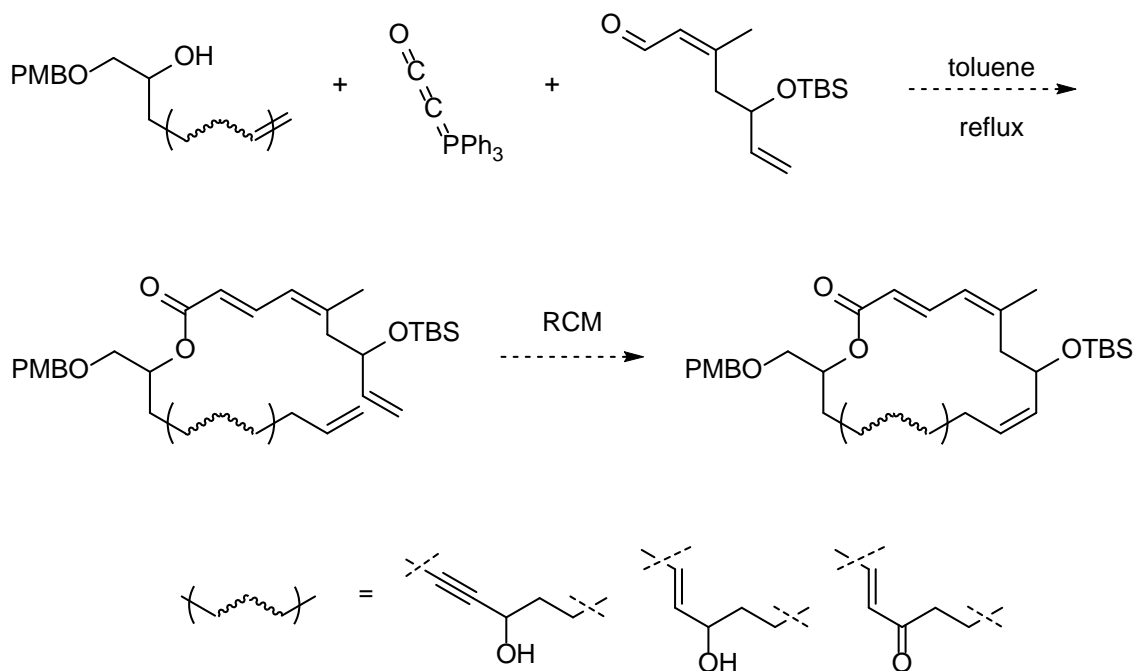
Chapter 7: Late Stage Connections: Bestmann Ylid Linchpin and Ring-Closing Metathesis

To synthesize the macrocycle, the top fragment of zampanolide has to be attached to the rest of the molecule, which was envisioned to be done by a Bestmann ylid linchpin. The Bestmann ylid reagent (**114**) is commercially available. Alternatively it can be easily prepared from commercially available (methoxycarbonylmethylene)triphenylphosphorane by heating it to 65 °C with NaHMDS in toluene for 20 hours (**Scheme 7.1**).⁸⁶ It is essential that all the equipment is dry, and that recrystallizations performed for purification purposes are done with dry toluene and under argon to avoid formation of the acid. The Bestmann ylid, if moisture is thoroughly excluded, is stable for long periods of time in a freezer.



Scheme 7.1 Synthesis of the Bestmann ylid reagent.

The use of 5-hexenal (**144**) in the non-stereoselective alkynylation would enable the synthesis of a whole range of analogs lacking the pyran ring by simply performing the Bestmann ylid linchpin and subsequent RCM without the necessity of performing any modifications to the C8-C10 portion of the molecules (**Scheme 7.2**). If aldehydes **143** or **147** were used, the silyl protected primary alcohol would have to be transformed into an alkene to allow for the RCM to be performed.



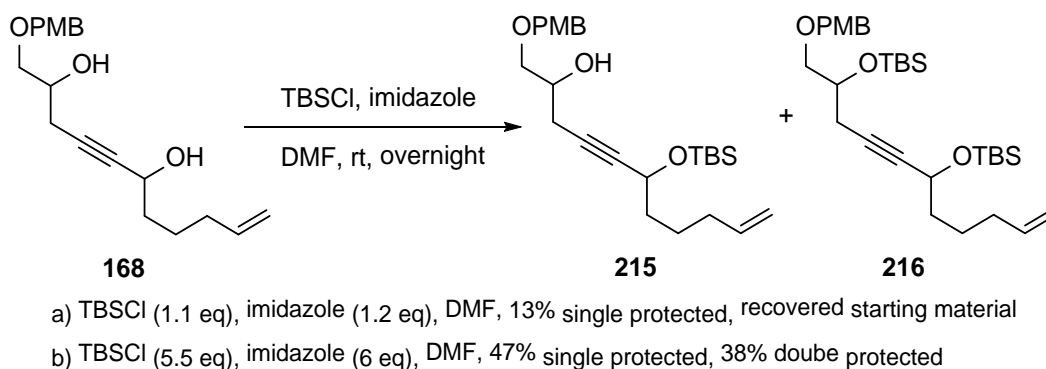
Scheme 7.2 Overview of the major late step connections, namely Bestmann ylid linchpin and RCM.

Each of the attempts to synthesize one of the non-THP analogs is described below and a summary is given at the end.

7.1 Analog 1: Non-THP Alkyne Analog

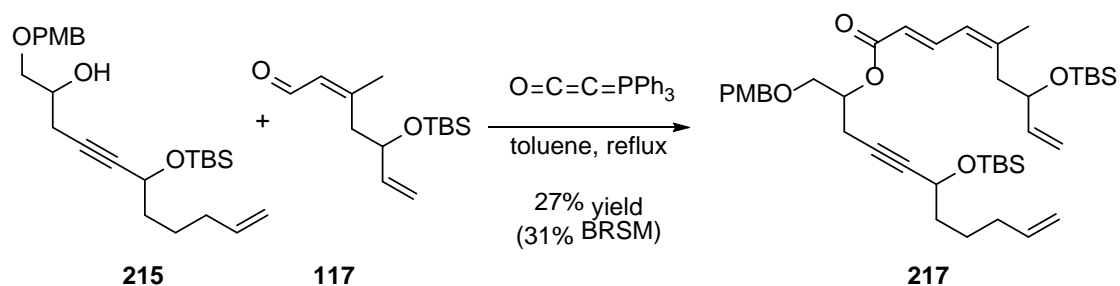
When the non-stereoselective alkylation was first successful in directly providing product **167** with the terminal alkene in place, the idea of an analog with a non-THP macrocycle featuring an alkyne instead of the trisubstituted alkene was born. Diol **168**, which was often produced as a byproduct in various reactions but can also be made directly, was mono-TBS protected at the propargylic alcohol position by using TBSCl and imidazole in DMF (**Scheme 7.3**). In a first attempt, 1.2 equivalents of TBSCl were used, which resulted in a very low yield (13%) of the monoprotected product **215**, and mostly recovered starting material. No doubly protected material was recovered. In a second attempt, 5.5 equivalents of TBSCl were used to encourage reaction, which resulted in a moderate 47% yield of the mono-protected compound **215** and 38% of the doubly protected compound **216**. No

further optimization attempts were made, however enough material was produced to attempt the Bestmann ylid linchpin and subsequent RCM.



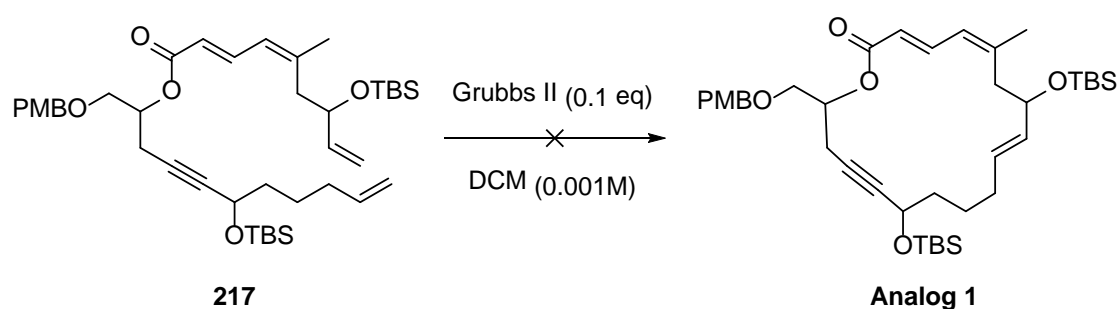
Scheme 7.3 Tested conditions for the mono-protection of the alkyne substrate in preparation for the Bestmann ylid coupling.

The mono-protected material was subjected to the Bestmann ylid linchpin, which yielded compound **217** in a 27% yield (31% BRSM, **Scheme 7.4**). Both starting materials seem to have degraded partially in the reaction. A solution to this could be as simple as lowering the temperature of the reaction, or changing the solvent from toluene to THF. Wang et al. published a paper on the preparation of conjugated dienoates with Bestmann ylid in 2015.⁴⁶ They found that when there was a high conversion rate but low yield in a reaction, conducting the reaction at lower temperatures or a change of solvent to THF was beneficial. This is also described in **Chapter 2.2.4**.



Scheme 7.4 Bestmann ylid linchpin performed on the mono-protected alkyne starting material.

The RCM was performed using Grubbs-II catalyst in DCM, and the reaction was allowed to stir overnight. No reaction occurred, and only starting material was recovered. This could be an indication that the system is very strained and might not be able to form the alkyne-containing macrocycle of **Analog 1**. No further attempts to synthesize this analog have been made so far; however, optimizations could be performed with regards to solvent, temperature and catalyst loading.

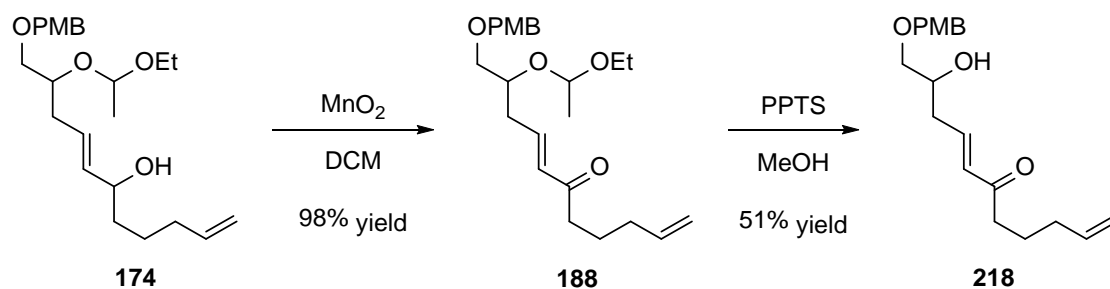


Scheme 7.5 Attempted RCM reaction to form Analog 1, a non-THP analog with an alkyne in place.

7.2 Analog 2: Non-THP C17-Desmethyl C15 Ketone Analog

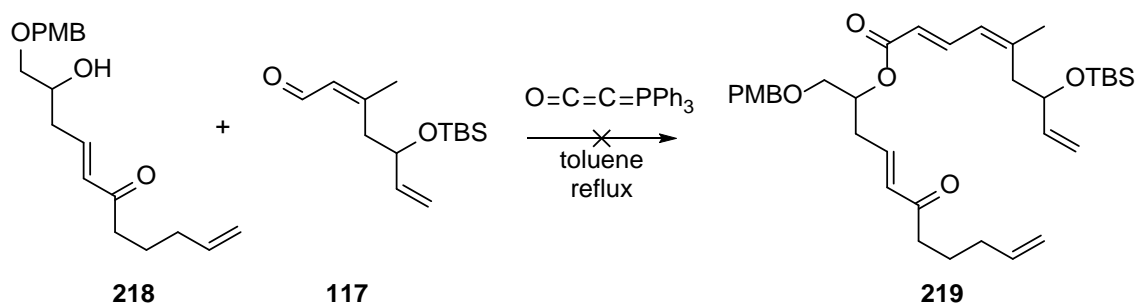
The synthesis of a non-THP analog lacking the C17 methyl group and featuring a ketone rather than an alcohol in the C15 position was attempted. The idea was that on the one hand, the ketone itself might be an interesting analog to test, but on the other hand the ketone can serve as somewhat of a “protecting group” for the alcohol as well as deactivating the C16-C17 alkene to truncative RCM. As mentioned in **Chapter 4.2**, the configuration at C15 has to be set after oxidation to the ketone by stereoselective reduction back to the alcohol. So, rather than using a protecting group on the alcohol, the idea was to oxidize alcohol **174** to ketone **188**, then remove the EE group, perform the Bestmann ylid linchpin on **218**, close the macrocycle and only then, if desired, stereoselectively reduce the ketone to the alcohol using a CBS reduction.

The allylic oxidation using manganese dioxide proceeded smoothly with excellent yield, and the protecting group was removed by simply stirring crude product **188** with PPTS in MeOH (**Scheme 7.6**).



Scheme 7.6 Transformations performed to synthesize the substrate for the Bestmann ylid linchpin.

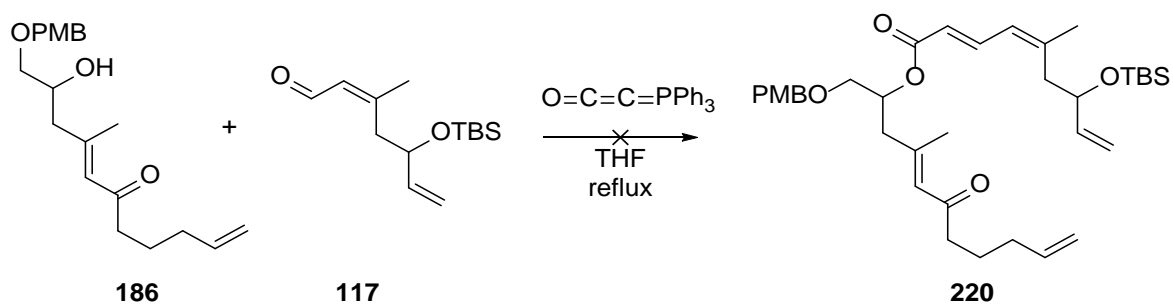
Crude product **218** was then subjected to the Bestmann ylid linchpin, using the same conditions as previously, namely refluxing all reagents in toluene overnight. Unfortunately, both starting materials severely degraded, and neither product nor starting materials were recovered (**Scheme 7.7**).



Scheme 7.7 Attempted Bestmann ylid linchpin to form the precursor for Analog 3.

7.3 Analog 3: Non-THP C15 Ketone Analog

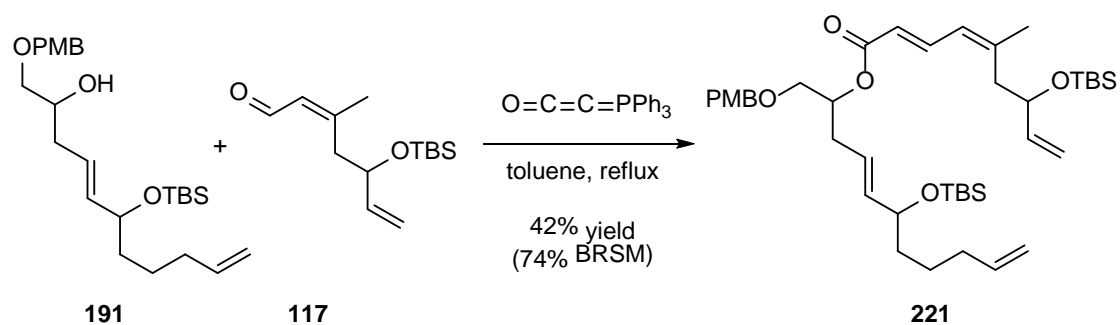
Next, the synthesis of an analog lacking the THP ring and featuring a C15 ketone as well as the C17 methyl group was attempted. In an effort to avoid the degradation of ketone **186**, the Bestmann ylide linchpin reaction was performed at reflux in THF instead of toluene. However, as seen in the attempted synthesis of **Analog 2**, ketone **186** degraded, while some of aldehyde **117** (used in excess) was recovered. These results strongly suggest that the α,β -unsaturated ketone moiety is not stable under the reaction conditions, and no further attempts were made to perform the Bestmann ylide linchpin reaction on substrates containing this motif.



Scheme 7.8 Attempted Bestmann ylid linchpin to form the precursor for Analog 4.

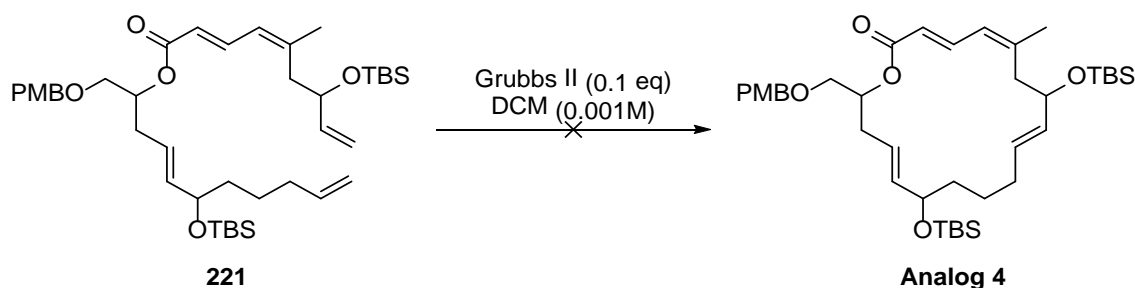
7.4 Analog 4: Non-THP C17-Desmethyl Analog

The next analog tackled consisted of a non-THP macrocycle featuring a *trans* double bond instead of the trisubstituted alkene. The mono-protected material **191** described in **Chapter 5.4** was used. The Bestmann ylid linchpin proceeded with moderate success, yielding desired product **221** in 42% yield (74% BRSM) using the standard conditions of refluxing all materials in toluene overnight (**Scheme 7.9**).



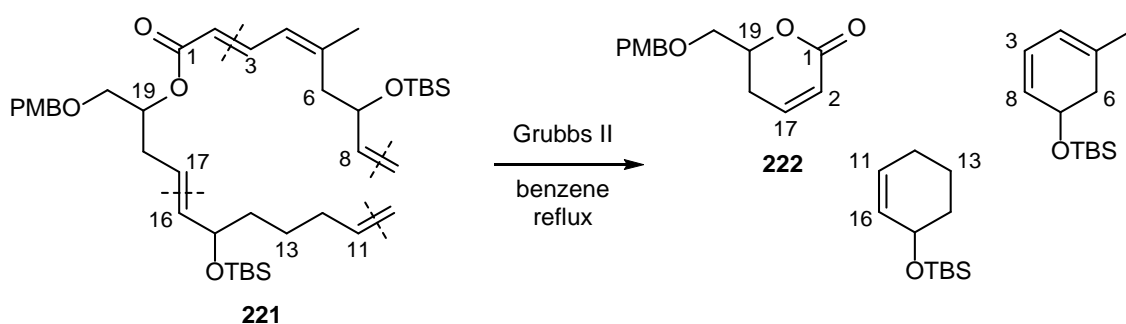
*Scheme 7.9 Bestmann ylid linchpin performed on the mono-protected starting material **191** with the *trans*-alkene in place.*

With the molecule set up for the RCM, two different methods were selected, both having been used in the synthesis of zampanolide before (**Scheme 7.10**). The first method involves stirring the precursor **221** with the catalyst in DCM at room temperature, as reported separately by Jennings and McLeod.^{87,39} This reaction seemed to have resulted in the desired product **Analog 4** (according to HRMS), however it could not be confirmed with certainty by NMR spectroscopy. The putative product obtained was not completely clean with purification proving to be problematic. The substrate as well as the product are highly non-polar and do not separate on silica. Additionally, the amount of “product” was too small to gather meaningful 2D NMR data. The reaction was repeated on a similar scale and again, no significant amounts of product-like material could be detected by NMR.



Scheme 7.10 Attempted methods for the RCM reaction to produce the non-THP C17-desmethyl analog.

The second attempt at achieving the RCM was inspired by Hoye's synthesis of dactylolide in 2002.³⁶ The conditions applied involved treating substrate **221** with Grubbs-II catalyst in boiling benzene. No product or starting material were recovered, however one of the degradation products was identified to be compound **222**. It seems that under these conditions the nearly completed macrocycle disintegrates into three six-membered rings, completely unraveling the molecule probably starting from position 10, as shown in **Scheme 7.11**.



Scheme 7.11 Proposed unraveling of the nearly completed macrocycle into three six-membered rings.

The reason that precursor **221** used in this work might be less stable and more prone to side reactions than the substrates used in the synthesis of zampanolide could be that the lack of the C17-methyl group provides better access than the trisubstituted alkene in zampanolide precursors. Additionally, the system has a higher degree of freedom, rather than being more constrained by attachment of the substituents to the 2- and 6-positions of a THP ring. Therefore, under alkene metathesis conditions, the initially formed terminal Ru-carbene between the catalyst and the C10-C11 alkene can fold readily into a six-membered ring through reaction with C16-C17 alkene, rather than reacting with the second terminal alkene to form the macrocycle.

Chapter 8: Conclusion and Future Work

Over the course of this thesis work, significant progress towards the synthesis of (-)-zampanolide and the syntheses of “zampanalogues” has been made. The synthesis of precursors for building blocks corresponding to the C3-C8, C9-C15 and C16-C20 regions has been achieved based on the first-generation synthetic plan and previous work. Substantial improvements to these syntheses have been made in comparison with previous work by reducing the number of purification steps, therefore making these syntheses more economic and time-efficient. Additionally, the synthesis of an analog building block corresponding to the C9-C15 region of zampanolide has been devised, which was used as an easy-to-access model system but which can also serve as a building block for the generation of non-THP analogs.

The protecting group strategy of the C16-C20 building block was been adjusted several times to allow for the successful application of an alkynylation reaction to form the bond at C15-C16, and avoid silyl migration during the Bestman ylid linchpin reaction. Substrates protected at C20 with three different groups and at C15 with four different groups have been synthesized and were tested in alkynylation reactions. In total, four stereoselective methods for alkynylation were tested, with the Trost conditions delivering the coupled product. Inconsistent yields and unsatisfactory diastereoselectivity of this reaction led to a decision to resort to a simple base-mediated non-stereoselective alkynylation to form the C15-C16 bond instead, with subsequent oxidation and stereoselective reduction to exert the desired stereochemical control at C15.

The C16-C17 alkyne was reduced to the *E*-alkene in near-quantitative yields by using the propargylic alcohol as a functional handle and Vitride® as reductant, after multiple attempts and adaptation of the literature protocol. This should

enable the future synthesis of C17-desmethyl analogs, while the reaction of the corresponding alkynone with the Gilman reagent Me_2CuLi led to the successful installation of the trisubstituted alkene, featuring the methyl group at C17 that is present in zampanolide. An oxidation-reduction sequence was shown to be successful in installing the desired (*S*)-configuration at C15 of zampanolide in an estimated 7:1 ratio with the (*R*)-isomer.

Studies on the formation of the *cis*-THP ring featured in zampanolide were conducted. While a Pd(II)-mediated carboxylative cyclization failed to deliver the desired product, a base-mediated *O*-Michael addition yielded the THP-ring product in a 3:1 ratio of *cis*:*trans* isomers. This ratio can most likely be augmented towards the *cis*-product. However, this remains to be further investigated in future research, along with transformation of the ester functionality of the product into a terminal alkene to prepare for the macrocyclization step.

A Bestmann ylid linchpin reaction was successfully performed on two compounds and produced two coupled species containing the full carbon skeleton of monocyclic zampanalogs ready for macrolactonization by alkene metathesis. In contrast, the two failed Bestman ylid reactions on ketone-containing starting materials clearly indicated that they are incompatible with the reaction. Subsequently, a RCM was tested as a macrocyclization step.

Preliminary explorations of the RCM to form monocyclic zampanalogs have been conducted. While the alkyne-containing precursor **217** did not react at all, possibly because the resulting macrocycle would be strained, the reaction of **218** gave mixed results. Subjecting **218** to alkene metathesis conditions in hot benzene resulted in the degradation of the starting material, while the reaction in DCM at room temperature led to the formation of **Analog 4** according to HRMS analysis. However, at this stage no NMR spectroscopic data is available to support this finding and further optimization is necessary to confirm this result.

Altering and combining of the methods for the reduction, reductive methylation and pyran formation presented in this thesis should allow for the generation of multiple analogs, provided that the difficulties with the RCM can be overcome.

Exchanging the simplified C9-C15 building block **141** for compound **144** (Section 3.3) enables the synthesis of various analogs (Figure 8-1). Monocyclic analogs with various groups at C11 (**223**) will be accessible, as well as analogs containing the full carbon framework present in zampanolide (**224**). Global deprotection will be necessary, followed by oxidation of the C9 and C20 hydroxy groups, which then allows for the installation of various sidechains and groups replacing the exomethylene (**225**) and, ideally, also a new synthesis of (-)-zampanolide (**1**) itself.

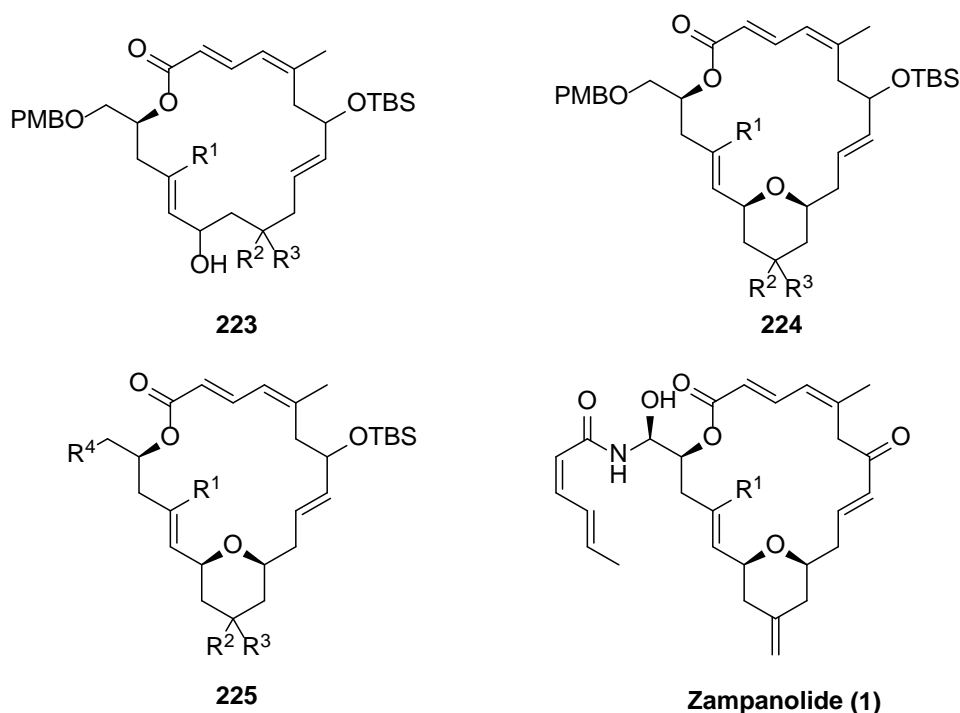


Figure 8-1 Potential analogs resulting from the research conducted in this thesis.

Chapter 9: Experimental

9.1 General Experimental Data

Unless otherwise stated, all reactions were carried out in flame-dried glassware under a positive pressure of nitrogen or argon, delivered *via* a balloon or manifold. Dry tetrahydrofuran, dichloromethane and toluene were obtained from a PureSolv MD 5 solvent purification system (Innovative Technology). Analytical grade solvents were used for aqueous work-up and column chromatography (petroleum ether, ethyl acetate, diethyl ether, methanol and dichloromethane). Column chromatography was performed on silica gel 60 Å (Pure Science, 40–63 µm) with the eluent mixtures as stated in the corresponding procedures. Thin-layer chromatography was performed on silica-coated plastic plates (Macherey-Nagel, POLYGRAM® Sil G/UV254). All compounds were detected under UV irradiation ($\lambda = 254$ nm), followed by visualization with various staining solutions. All other chemicals were purchased from Pure Science, Acros, Sigma-Aldrich, Panreac, Merck and AK Scientific and used without further purification unless stated in **Section 9.2**.

Infra-red (IR) spectra were collected on an ALPHA FT-IR spectrometer (Bruker) fitted with attenuated total reflectance (ATR). The intensities of signals are defined as: br = broad, s = strong, m = medium, w = weak. Mass spectra were collected on an Agilent 6530 Accurate-Mass Q-TOF LC/MS high-resolution mass spectrometer (HRMS). The specific rotations were collected on an AUTOPOL II automatic polarimeter (Rudolph Research Analytical), and the reported values are an average of ten measurements, temperature is reported in °C and concentrations are reported in g/100 mL.

Nuclear magnetic resonance (NMR) spectra were obtained in deuterated chloroform (CDCl_3) using Varian Inova instruments operating at 300 or 500 MHz for proton and 125 MHz for carbon. Proton and carbon chemical shifts are reported in parts per million (ppm) relative to residual CHCl_3 [$\delta_{\text{H}} = 7.26$ ppm] and CDCl_3 [$\delta_{\text{C}} = 77.0$ ppm], respectively. Signals are defined as: s = singlet, d = doublet, t = triplet, q = quartet, p = pentet, m = multiplet. Coupling constants (J) are reported in Hertz (Hz). *Ortho*, *meta* and *para* are assigned with respect to the CH_2 -group of PMB. Assignments were determined by two-dimensional NMR experiments (COSY, HSQC, and HMBC).

9.2 Reagent Synthesis and Purification

Activation of Zn Dust

Zn dust (10.0 g) was stirred in aq. HCl (10%, 50 mL) for 1 h and then collected on a Buchner funnel. The filter cake was then washed with water (3 x 20 mL), MeOH (3 x 20 mL) and diethyl ether (3 x 20 mL) and dried *in vacuo* to afford activated Zn as a grey powder (6.9 g, 69% recovery).

Recrystallisation of Copper(I) iodide

Impure Cu(I)I (5 g) was added to a boiling solution of NaI in water (35 g in 25 mL water) over approximately one h. The solution was then cooled to 0 °C and diluted with water to precipitate CuI. The solid was filtered off and washed sequentially with water, EtOH, EtOAc, diethyl ether, PE and dried *in vacuo* to afford Cu(I)I as a slightly pink solid (3.8 g, 76% recovery).

Trimethylsilyl trifluoromethanesulfonate

A 10 mL one-necked RBF equipped with a septum and stir bar was set under nitrogen and charged with trifluoromethanesulfonic acid (1.5 g, 9.8 mmol, 1 eq.) and tetramethylsilane (1.1 g, 12 mmol, 1.3 eq.) and the reaction stirred for two h. Tetramethylsilane was then removed under reduced pressure to afford the title compound as an orange liquid (1.6 g, 73%)

$^1\text{H NMR}$ (500 MHz, CDCl_3): δ 0.50 (s, 9H, $\text{Si}(\text{CH}_3)_3$).

Synthesis of IBX

A 500 ml one-necked RBF was charged with oxone (37.2 g, 0.061 mol, 3 eq.) and water (20 ml) added. 2-Iodobenzoic acid (5.0 g, 0.020 mol, 1 eq.) was added at once and the suspension heated to 70 °C for 3 h before being cooled down to 0 °C for 30 min. The solid was filtered off and washed with water (6 x 10 ml) and acetone (2 x 10 mL) and dried *in vacuo* overnight to yield the product as a colorless solid (4.4 g, 75%). The filtrate was treated with Na_2SO_3 and neutralized with 1 M NaOH before it was disposed of.

Synthesis of Activated MnO_2 on Carbon

A solution of KMnO_4 (5.0 g) in water was heated to reflux, and activated charcoal (1.56 g) added portion wise to keep the effervescence under control. The suspension was stirred at reflux until the purple color disappeared and the solid filtered off on a Buchner funnel. The black solid was dried in the oven overnight.

Distillation of Boron Trifluoride Diethyl Etherate

A solution boron trifluoride diethyl etherate was distilled over CaH_2 under a stream of nitrogen at $126\text{ }^\circ\text{C}$.

9.3 General Procedures

9.3.1 Oxidations

Swern Oxidation

A one-necked RBF equipped with a septum and stir bar was set under nitrogen and charged with DMSO (3 eq.) and DCM (0.18 M with respect to starting material), cooled to $-78\text{ }^\circ\text{C}$ and oxalyl chloride (1.5 eq.) was added dropwise. After 10 min, the starting material dissolved in DCM (0.18 M) and was added dropwise to the reaction and stirring continued for 60 min, before triethylamine (3 eq.) was added dropwise. The reaction was allowed to warm up to $0\text{ }^\circ\text{C}$ before it was quenched with water. DCM was added and the aqueous layer was extracted with DCM (2x). The combined organic layers dried over magnesium sulfate, filtered, and the solvent was removed under reduced pressure.

IBX Oxidation

A one-necked RBF equipped with a septum and stir bar was charged with IBX (3 eq.) and set under nitrogen, and DMSO (0.7 M with respect to starting material) was added. Upon complete dissolving, the alcohol (1 eq.) was added and stirring continued for three hours at room temperature or until TLC analysis showed full consumption of the starting material. The reaction was quenched by adding water and the aqueous layer was extracted with EtOAc (3x). The combined organic layers were dried over magnesium sulfate, filtered and the solvent was removed under reduced pressure.

PDC oxidation

A one-necked RBF equipped with a septum and stir bar was charged with alcohol (1 eq.) and set under nitrogen. PDC (1.5 eq.) in DCM (0.6 M with respect to the alcohol) was added at once and the reaction stirred for 36 hours at room temperature. The solvent was evaporated and the residue dissolved in diethyl ether, filtered through a silica plug and the solvent was removed under reduced pressure.

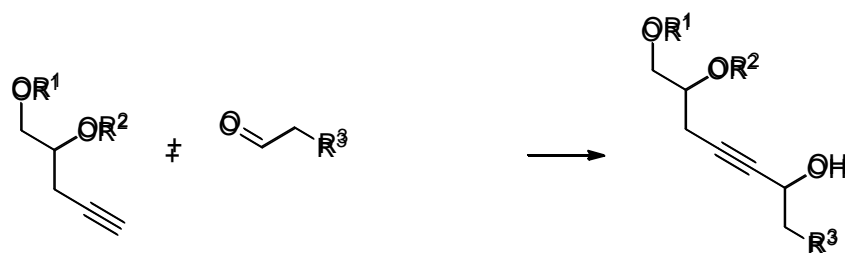
TEMPO/BAIB oxidation

A one-necked RBF equipped with a septum and stir bar was charged with alcohol (1 eq.), TEMPO (0.1 eq.) and BAIB (1.1 eq.) and set under nitrogen. DCM (1M with respect to the alcohol) was added. Stirring was continued for three hours at room temperature or until TLC analysis showed full consumption of the starting material. The reaction was diluted by adding more DCM and the organic layer was washed with sodium thiosulfate solution. The aqueous layer was extracted with DCM (3x) and the combined organic layers were washed with sodium bicarbonate solution and were dried over magnesium sulfate, filtered and the solvent was removed under reduced pressure.

Manganese dioxide oxidation

A one-necked RBF was charged with the the alcohol in DCM (0.1 M with respect to the alcohol) and MnO₂ (700 w/w%) were added. If the reaction did not finish after being stirred overnight, more MnO₂ was added and the reaction continued until TLC analysis showed full conversion of the starting material. The reaction mixture was filtered through celite and the solvent was removed under reduced pressure.

9.3.2 Alkynylations



Alkynylation using InBr₃/BINOL

A 10 mL one-necked RBF was equipped with a septum and stir bar was charged with (*S*)-BINOL (1.8 mg, 0.01 mmol, 0.1 eq.) and indium(III)bromide (2.2 mg, 0.01 mmol, 0.1 eq.) and set under nitrogen. The aldehyde (0.06 mmol, 1 eq.) in DCM (0.1 mL) was added and the mixture stirred for 15 min, before dicyclohexylmethylamine (6 mg, 0.03 mmol, 0.5 eq.) was added. After 10 min of stirring, a solution of the alkyne in DCM (0.1 mL) was added, the reaction mixture warmed to 40 °C and the reaction stirred at this temperature overnight. On the next day, the reaction was quenched with sat. aq. NH₄Cl, the phases separated and the aqueous layer extracted with Et₂O (3x). The combined organic layers were then dried with magnesium sulfate, filtered, and the solvent was removed under reduced pressure.

Alkynylation using Zn(OTf)₂/BINOL

A 10 mL one-necked RBF equipped with a septum and stir bar was charged with ZnOTf (10 mg, 0.03 mmol, 0.2 eq.) and (*S*)-BINOL (32 mg, 0.11 mmol, 0.8 eq.) and set under nitrogen. The alkyne (0.42 mmol, 3 eq.) in DCM (0.3 mL) was added as well as DIPEA (0.01 mL, 0.07 mmol, 0.5 eq.) and the reaction mixture stirred at room temperature for 30 min before the aldehyde (0.14 mmol, 1 eq.) in DCM (0.3 mL) was added. The resulting solution was stirred at room temperature for two days before the reaction was quenched with sat. aq. ammonium chloride

solution. The phases were separated and the aqueous layer extracted with DCM (3x). The combined organic layers were washed with brine, dried with magnesium sulfate, filtered, and the solvent was removed under reduced pressure.

Alkynylation using EtI/Zn/BINOL

A 5 mL one-necked RBF equipped with a septum and stir bar was charged with activated Zn (6 eq.) and BINOL (0.8 eq.) and set under nitrogen. EtI (0.12 eq.), alkyne (0.21 mmol, 1.5 eq.) in THF (0.5M with respect to the alkyne) and Ti(O*i*Pr)₄ (2 eq.) were added and the reaction mixture stirred for 24 hours. Et₂O (0.05 M with respect to the alkyne) were added and the reaction stirred for 15 min before aldehyde (0.14 mmol, 1 eq.) in Et₂O (1 mL) was added. Stirring was continued for another twelve hours and the reaction quenched with sat. aq. ammonium chloride solution. The phases were separated and the aqueous layer extracted with DCM (3x). The combined organic layers were then dried with magnesium sulfate, filtered, and the solvent was removed under reduced pressure.

Alkynylation using i-PrI/Zn/H8-BINOL

A 10 mL one-necked RBF equipped with a septum and stir bar was charged with activated Zn (6 eq.) and BINOL (0.8 eq.) and set under nitrogen. EtI (12 eq.), alkyne (1.5 eq.) in THF (0.5M with respect to the alkyne) and Ti(O*i*Pr)₄ (2 eq.) were added and the reaction mixture stirred for 24 h. Et₂O (0.05M with respect to the alkyne) were added and the reaction stirred for 15 min before the aldehyde (1 eq.) in Et₂O (1 mL) was added. Stirring is continued for another twelve hours and the reaction quenched with sat. aq. ammonium chloride solution. The phases were separated and the aqueous layer extracted with DCM (3x). The combined organic layers were then dried with magnesium sulfate, filtered, and the solvent was removed under reduced pressure

Alkynylation using Zn(alkyl)₂/ProPhenol/TPPO

In the glovebox under nitrogen atmosphere, a sample vial was charged with ProPhenol (0.2 eq.) and TPPO (0.4 eq.). Alkyne (2.8 eq.) in toluene (0.38 M with respect to the alkyne) was added, followed by dimethyl zinc or diethyl zinc (1M in hexane, 2.95 eq.). The reaction was stirred in the glovebox for 8-48 hours, before aldehyde (1 eq.) in toluene (0.38 M with respect to the aldehyde) was added. The reaction was left to stir for another 24 h before it was taken out of the glovebox and quenched with aq. Ammonium chloride solution. Ethyl acetate was added, the layers separated and the aqueous layer extracted with ethyl acetate (3x). The combined organic layers were then dried over magnesium sulfate, filtered, and the solvent was removed under reduced pressure.

Alkynylation using MeLi

A 25 mL one-necked RBF equipped with a septum and stirbar is charged with the alkyne (1 eq.) and set under nitrogen. THF (0.1M with respect to the alkyne) is added and the reaction stirred at -20 °C/0 °C/room temperature, respectively. MeLi (3M in 1,2-diethoxyethane, 1.1 eq.) was added dropwise. After 30 min, a solution of aldehyde (1.1 eq.) in THF (1 mL) was added dropwise and stirring was continued for two hours at low temperature. The reaction was then quenched with sat. aq. ammonium chloride solution and the aqueous layer extracted with diethyl ether (3x). The combined organic layers were dried over magnesium sulfate, filtered and the solvent is removed under reduced pressure.

9.3.3 Alkyne Transformations

Alkyne Reduction and Iodination Using Cl₂ZrCp₂

A one-necked RBF equipped with a stir bar and septum was charged with Cl₂ZrCp₂ (1 eq.) and activated MS and set under argon. DCE or DCM (0.4 M with respect to

alkyne) was added to the mixture and TMA (2 eq.) was added. Upon complete dissolution the alkyne (1 eq.) was added and the reaction was stirred for 24 hours at room temperature. An solution of iodine (0.8 M, 1.2 eq.) in THF was added and stirring continued for 30 min before the reaction was quenched with water and diethyl ether. The aqueous layer was extracted with diethyl ether (3x). the combined organic layers were washed with sodium thiosulfate solution, dried over magnesium sulfate, filtered and the solvent was removed under reduced pressure.

Alkyne Reduction Using LiAlH₄/NaOMe

A one-necked RBF equipped with a stir bar and septum was charged with the alkyne (1 eq.), LiAlH₄ (2 eq.) and NaOMe (4 eq.) and set under argon. Degassed THF (0.05 M with respect to the alkyne) was added and the reaction refluxed for 45 min. The reaction was either quenched with iodine (2 eq.) and stirred for another 60 min or quenched with water. A solution of Rochelle's salt was added and the aqueous layer extracted with diethyl ether (3x). The combined organic layers were dried over magnesium sulfate, filtered and the solvent was removed under reduced pressure.

Alkyne Reduction Using Vitride®® (Jamison)

A one-necked RBF was charged with a solution of the propargylic alkyne (1 eq.) in Et₂O (0.5 M with respect to the alkyne) and cooled to 0 °C. Vitride®® (65 w/w% in toluene, 3 eq.) was added dropwise and the cold bath was removed and stirred for six hours before the solution was cooled back to 0 °C and MeLi (3 M in diethoxymethane, 1.25 eq.) was added dropwise. The reaction was allowed to come to room temperature and stirred for 75 min before it was cooled to -78 °C. THF (0.2 M with respect to the alkyne) was added followed by MeI (3 eq.) and CuI (1 eq.). The reaction was stirred for 20 hours and allowed to slowly warm to room temperature. The reaction was then quenched with Rochelle's salt solution and EtOAc added. The aqueous layer was extracted with EtOAc (3x), the combined

organic layers dried over magnesium sulfate, filtered and the solvent removed under reduced pressure.

Alkyne Reduction Using Vitride®® (adapted)

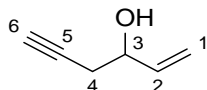
A one-necked RBF was charged with the propargylic alcohol (1 eq.) in Et₂O (0.1 M with respect to the alkyne) and Vitride®® (65 w/w% in toluene, 3 eq.) was added dropwise. The reaction mixture was either quenched with water, or a halide (3 eq.) was added to replace the aluminum and allowed to stir overnight. A saturated aq. solution of Rochelle's salt was then added and the aqueous layer was extracted with Et₂O (3x). The combined organic layers were dried over magnesium sulfate, filtered and the solvent was removed under reduced pressure.

Alkyne Reduction Using Gilman Reagent

A 1 NRBF equipped with a septum was set under nitrogen and charged with CuI (1.56 eq.) in THF (0.2 M with respect to the alkyne). The suspension was cooled to 0 °C and MeLi (2.8 M in THF, 3 eq.) was added dropwise. Stirring was continued for one hour at 0 °C before the mixture was cooled to -78 °C and the alkyne (1 eq.) in THF (0.1M with respect to the alkyne) was added dropwise. After three hours of stirring at this temperature the reaction was quenched with sat. aq. NH₄Cl solution, allowed to warm to room temperature and the aqueous layer extracted with diethyl ether (3x). The combined organic layers were dried over MgSO₄, filtered and the solvent was removed under reduced pressure.

9.4 Chapter 3: Fragment Synthesis and Second Generation Retrosynthetic Approach

Hex-1-en-5-yn-3-ol



A 100 ml one-necked RBF equipped with a septum and a stir bar was charged with activated Zn dust (982 mg, 15 mmol) and set under nitrogen. First THF (25 ml) was added and then propargyl bromide (1.8 ml, 16 mmol, 2.1 eq.) was added drop wise. This suspension was stirred for 1.5 hours at room temperature before being cooled to $-78\text{ }^{\circ}\text{C}$. Another portion of activated Zn dust (410 mg, 6.27 mmol) was added before acrolein (0.5 ml, 7.5 mmol, 1 eq.) in THF (4.2 ml) was added drop wise. The reaction was first stirred at $-78\text{ }^{\circ}\text{C}$ for one hour and then allowed to come to room temperature and stirred for another two hours. The reaction was quenched with sat. NH_4Cl solution (20 ml) and filtered through celite. The layers were separated and the aqueous layer extracted with diethyl ether (3 x 50 ml). The combined organic layers are dried over MgSO_4 , filtered and the solvent was partly and very cautiously removed under reduced pressure (product is highly volatile). The crude product was purified *via* a silica plug (15 g silica, PE/EtOAc = 3/1) to afford the title compound as a colorless liquid in mixture with EtOAc.

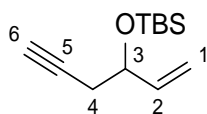
TLC: R_f (PE/EtOAc = 4/1) = 0.30.

$^1\text{H NMR}$ (500 MHz, CDCl_3): δ 5.99 – 5.87 (m, 1H, H2), 5.33 (d, $J = 17.2$ Hz, 1H, H1a), 5.19 (d, $J = 10.7$ Hz, 1H, H1b), 4.29 (m, 1H, H3), 2.41 (d, $J = 17.2$ Hz, 2H, H4a), 2.32 (s, $J = 17.2$ Hz, 1H, H4b), 2.06 (s, 1H, H6).

$^{13}\text{C NMR}$ (125 MHz, CDCl_3): δ 139.0 (CH, C2), 116.0 (CH_2 , C1), 80.3 (C, C5), 71.0 (CH, C6), 27.5 (CH_2 , C4).

These data were consistent with those reported previously.^{45,46}

tert-Butyl(hex-1-en-5-yn-3-yloxy)dimethylsilane - 109



A 100 ml one-necked RBF equipped with septum and stir bar was charged with hex-1-en-5-yn-3-ol (crude in EtOAc from previous reaction, 0.5 ml, 7.5 mmol, 1 eq.) and imidazole (620 mg, 9.11 mmol, 1.2 eq.) and set under nitrogen. DMF (9 ml) was added and the solution was cooled to 0 °C. TBSCl (1.24 g, 8.25 mmol, 1.1 eq.) in DMF (9 ml) was added dropwise, the cool bath removed and the reaction mixture stirred overnight at room temperature. On the next day diethyl ether (50 ml) was added and the solution washed with water (3 x 50 ml) and brine (50 ml). The combined organic layers were dried over MgSO₄, filtered and the solvent was cautiously removed under reduced pressure (product is still volatile). The crude product can be used as crude mixture or alternatively can be purified *via* FCC (30 g silica, PE/EtOAc = 10/1) to afford the title compound as a colorless liquid (1.25 g, 79% over two steps).

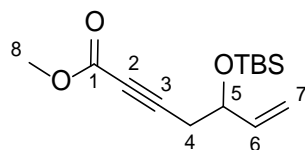
TLC: R_f (PE/EtOAc = 9/1) = 0.65.

¹H NMR (500 MHz, CDCl₃): δ 5.9 (m, 1H, H₂), 5.25 (d, *J* = 17.5 Hz, 1H, H_{1a}), 5.11 (d, *J* = 10.8 Hz, 1H, H_{1b}), 4.26 (m, 1H, H₃), 2.40 (d, *J* = 16.6 Hz, 1H, H_{4a}), 2.32 (d, *J* = 16.6 Hz, 1H, H_{4b}), 1.98 (s, 1H, H₆), 0.89 (s, 9H, TBS), 0.09 (s, 3H, TBS), 0.05 (s, 3H, TBS).

¹³C NMR (125 MHz, CDCl₃): δ 140.0 (CH, C₂), 114.9 (CH₂, C₁), 81.4 (C, C₅), 72.4 (CH, C₆), 70.1 (CH, C₃), 28.5 (CH₂, C₄), 25.9 (CH₃, TBS), 18.4 (C, TBS), -4.4 (CH₃, TBS), -4.7 (CH₃, TBS).

These data were consistent with those reported previously.^{45,46}

Methyl 5-tert-butyltrimethylsilyloxy-6-hepten-2-ynoate - 103



A 100 mL 1 one-necked RBF equipped with stir bar and septum was set under nitrogen charged with **109** (1.25 g, 6.0 mmol, 1 eq.) in THF (60 mL) and cooled to -78 °C. *n*-BuLi (1.8 M in cyclohexane, 3.7 mL, 6.6 mmol, 1.1 eq.) was added dropwise and the reaction mixture stirred at -78 °C. After 45 min, methyl chloroformate (0.92 ml, 11.9 mmol, 2 eq.) was added dropwise and stirring continued for 3h at the same temperature. The reaction mixture was then quenched with sat. aq. NH₄Cl solution (35 mL), allowed to come to room temperature and phases were separated. The aqueous layer was washed with diethyl ether (3 x 35 mL), the combined organic layers dried over MgSO₄, filtered and the solvent was removed under reduced pressure. The crude mixture can be used directly in the next step or alternatively can be purified *via* FCC (20 g silica, PE/EtOAc = 20/1) to afford the title compound as a yellow liquid (1.35 g, 85%).

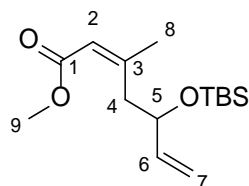
TLC: R_f (PE/EtOAc = 30/1) = 0.16.

¹H NMR (500 MHz, CDCl₃): δ 5.86 (m, 1H, H6), 5.26 (dt, *J* = 17.4, 1.4 Hz, 1H, H7a), 5.13 (dt, *J* = 10.5, 1.4 Hz, 1H, H7b), 4.30 (m, 1H, H5), 3.47 (s, 3H, H8), 2.53 (dd, *J* = 16.9, 6.6 Hz, 1H, H4a), 2.46 (dd, *J* = 16.9, 6.4 Hz, 1H, H4b), 0.89 (s, 9H, TBS), 0.09 (s, 3H, TBS), 0.05 (s, 3H, TBS).

¹³C NMR (125 MHz, CDCl₃): δ 154.1 (C, C1), 139.4 (CH, C6), 115.4 (CH₂, C7), 86.5 (C, C3), 74.2 (C, C2), 71.5 (CH, C5), 52.6 (CH₃, C8), 28.6 (CH₂, C4), 25.7 (CH₃, TBS), 18.2 (C, TBS), -4.6 (CH₃, TBS), -5.0 (CH₃, TBS).

These data were consistent with those reported previously.^{45,46}

Methyl 5-(tert-butyltrimethylsilyloxy)-3-methyl-2,6-heptadienoate - 132



A 50 mL 1 NRBF equipped with a septum was set under nitrogen and charged with CuI (1.50 g, 7.85 mmol, 1.56 eq.) in THF (30 mL). The suspension was cooled to 0 °C and MeLi (2.8 M in THF, 5.4 mL, 15.15 mmol, 3 eq.) added dropwise. Stirring was continued for 1 h at 0 °C before the mixture was cooled to -78 °C and **103** (1.35 g, 5.03 mmol, 1 eq.) in THF (3 mL) was added dropwise. After 1.5 h of stirring at this temperature the reaction was quenched with sat. aq. NH₄Cl solution (25 mL), allowed to warm to room temperature and the aqueous layer extracted with diethyl ether (3 x 40 mL). The combined organic layers were dried over MgSO₄, filtered and the solvent was removed under reduced pressure. The crude product can be used directly in the next step or alternatively can be purified *via* FCC (30 g silica, PE/EtOAc = 20/1) to afford the title compound as a colorless liquid (1.29 g, 90%).

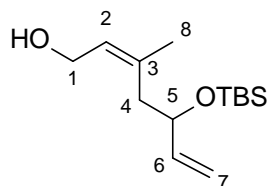
TLC: R_f (PE/EtOAc = 30/1) = 0.21.

¹H NMR (500 MHz, CDCl₃): δ 5.84 (ddd, *J* = 17.1, 10.3, 5.9 Hz, 1H, H6), 5.72 (m, 1H, H2), 5.18 (d, *J* = 17.1 Hz, 1H, H7a), 5.02 (d, *J* = 10.3 Hz, 1H, H7b), 4.41 (m, 1H, H5), 3.67 (s, 3H, H9), 2.86 (ddd, *J* = 12.2, 4.6, 0.7 Hz, 1H, H4a), 2.69 (dd, *J* = 12.2, 8.3 Hz, 1H, H4b), 1.94 (d, *J* = 1.2 Hz, 3H, H8), 0.87 (s, 9H, TBS), 0.00 (s, 3H, TBS), 0.00 (s, 3H, TBS).

¹³C NMR (125 MHz, CDCl₃): δ 186.7 (C, C1), 158.3 (C, C3), 141.3 (CH, C6), 116.9 (CH₂, C7), 113.7 (CH, C2), 73.6 (CH, C5), 50.8 (CH₃, C9), 41.9 (CH₂, C4), 27.5 (CH₃, C8), 25.9 (CH₃, TBS), 18.1 (C, TBS), -4.5 (CH₃, TBS), -4.9 (CH₃, TBS).

These data were consistent with those reported previously.^{45,46}

Z-5-((*tert*-Butyldimethylsilyloxy)-3-methylhepta-2,6-dien-1-ol - 133



A 25 ml 1 NRBF equipped with stir bar and septum was set under nitrogen and charged with methyl **132** (200 mg, 0.7 mmol, 1 eq.) in DCM (7.2 ml). This mixture was cooled to -78 °C, DIBAL-H (1M in hexane, 2.25 ml, 2.25 mmol, 3.2 eq.) added dropwise and the resulting mixture stirred for 30 min at -78 °C, 0 °C and room temperature. The reaction was quenched with a sat. aq. solution of Rochelle's salt (10 ml), stirred for one hour at room temperature and the phases were separated. The aqueous layer was extracted with DCM (3 x 10 ml) and the combined organic layers dried over MgSO₄, filtered and the solvent was removed under reduced pressure. The crude product can be used directly in the next step or alternatively can be purified *via* FCC (10 g silica, PE/EtOAc = 5/1) to afford the title compound as a colorless liquid (114 mg, 64%).

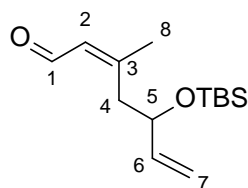
TLC: R_f (PE/EtOAc = 5/1) = 0.43.

¹H NMR (500 MHz, CDCl₃): δ 5.81 (ddd, *J* = 17.1, 10.3, 6.4 Hz, 1H, H6), 5.64 (t, *J* = 7.08 Hz, 1H, C2), 5.16 (dt, *J* = 17.3, 1.4 Hz, 1H, H7a), 5.05 (dt, *J* = 10.3, 1.2 Hz, 1H, H7b), 4.24 (m, 1H, H5), 4.10 (m, 1H, H1a), 4.00 (m, 1H, H1b), 2.49 (dd, *J* = 13.4, 8.8 Hz, 1H, H4a), 2.08 (dd, *J* = 13.2, 4.6 Hz, 1H, H4b), 1.96 (t, *J* = 5.6 Hz, 1H, OH), 1.76 (s, 3H, H8), 0.87 (s, 9H, TBS), 0.035 (s, 3H, TBS), 0.030 (s, 3H, TBS).

¹³C NMR (125 MHz, CDCl₃): δ 141.4 (C, C3), 136.8 (CH, C6), 127.1 (CH, C2), 114.1 (CH₂, C7), 72.1 (CH, C5), 58.6 (CH₂, C1), 42.0 (CH₂, C4), 25.9 (C, 3C, TBS), 23.9 (CH₃, C8), 18.3 (C, TBS), -4.5 (CH₃, TBS), -4.9 (CH₃, TBS)

These data were consistent with those reported previously.^{45,46}

(Z)-5-((*tert*-butyldimethylsilyl)oxy)-3-methylhepta-2,6-dienal - 117



A 25 mL one-necked RBF equipped with a stir bar was charged with IBX (464 mg, 1.66 mmol, 3 eq.) and DMSO (3.3 mL). A solution of **133** (142 mg, 0.55 mmol, 1 eq.) in DMSO (0.95 mL) was added and the reaction stirred overnight at rt. EtOAc was added, the suspension filtered and the solvent removed under reduced pressure. The crude product was purified *via* FCC (20 g silica, PE/EtOAc = 10/1) to afford the title compound as a colorless liquid (110 mg, 78%).

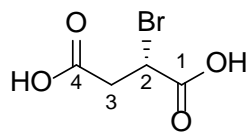
TLC: R_f (PE/EtOAc = 20/1) = 0.39.

¹H NMR (500 MHz, CDCl₃): δ 9.89 (d, *J* = 8.1 Hz, 1H, H1), 5.95 (m, 1H, H2), 5.87 – 5.75 (m, 1H, H6), 5.22 (d, *J* = 17.3 Hz, 1H, H7a), 5.10 (d, *J* = 10.3 Hz, 1H, H7b), 4.31 (m, 1H, H5), 2.96 – 2.80 (m, 1H, H4a), 2.53 (dd, *J* = 13.0, 4.3 Hz, 1H, H4b), 2.01 (d, *J* = 3.0 Hz, 3H, H8), 0.81 (s, 9H, TBS), 0.02 (s, 6H, TBS).

¹³C NMR (125 MHz, CDCl₃): δ 191.7 (CH, C1), 160.0 (C, C3), 140.7 (CH, C6), 130.5 (CH, C2), 115.1 (CH₂, C7), 72.8 (CH, C5), 41.6 (CH₂, C4), 26.3 (CH₃, C8), 26.0 (CH₃, TBS), 18.3 (C, TBS), -4.3 (CH₃, TBS), -4.7 (CH₃, TBS).

These data were consistent with those reported previously.^{45,46}

(S)-2-Bromosuccinic acid – 135



A 500 mL 3 NRBF equipped with a thermometer and a 250 mL dropping funnel and, *via* tubing, connected to a gas washing bottle containing 1M NaOH was charged with (L)-aspartic acid (9.4 g, 0.07 mol, 1 eq.) and KBr (36.3 g, 0.305 mol, 4.32 eq.). Then 2.5 M aq. H₂SO₄ (150 mL, 5.36 eq.) was added in one portion *via* the dropping funnel. The solution was cooled to -10 °C and a solution of NaNO₂ (8.3 g, 0.120 mol, 1.72 eq.) in water (20 mL) was added over a period of 15 min so that the temperature of the ice bath never exceeded -5 °C. The resulting mixture was stirred for two more hours at -5 °C and afterwards extracted with EtOAc (4 x 50 mL). The combined organic layers were washed with brine (50 mL), dried over MgSO₄, filtered and the solvent was removed under reduced pressure to afford the title compound as a colorless solid (12.6 g, 91%). The crude material was used without further purification.

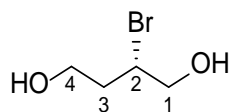
TLC: R_f (PE/EtOAc = 1/1 + 5% AcOH) = 0.52.

¹H NMR (500 MHz, D₂O): δ 4.59 (dd, *J* = 7.8, 6.7 Hz, 1H, H2), 3.18 (dd, *J* = 17.3, 7.8 Hz, 1H, H3a), 3.05 (dd, *J* = 17.3, 6.6 Hz, 1H, H3b).

¹³C NMR (125 MHz, D₂O): δ 173.9 (C, C4), 173.1 (C, C1), 39.3 (CH₂, C3), 39.2 (CH, C2).

These data were consistent with those reported previously.^{45,50}

***(S)*-2-Bromobutane-1,4-diol - 136**



A 250 mL 1 NRBF equipped with a stir bar and septum was set under nitrogen and charged with **135** (12.6 g, 0.064 mol, 1 eq.) in THF (125 mL) and cooled to 0 °C. A solution of borane dimethyl sulfide complex in THF (2 M, 90 mL, 0.180 mol, 3 eq.) was added dropwise over a period of 45 min, the cool bath was removed and after stirring at room temperature for 3 h the mixture was cooled back down to 0 °C and a sat. aq. solution of Rochelle's salt was added. The aqueous layer was extracted with EtOAc (3 x 60 mL), the combined organic layers were dried over MgSO₄, filtered and the solvent was removed under reduced pressure. The crude mixture can be used directly in the next step or it can be purified *via* FCC (60 g silica, PE/EtOAc/MeOH = 6/6/1) to afford the title compound as a slightly yellow oil (10.27 g, 96%).

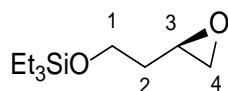
TLC: R_f (PE/EtOAc/MeOH = 6/6/1) = 0.34.

¹H NMR (500 MHz, CDCl₃): δ 4.34 (m, 1H, H2), 3.85 (m, 4H, H1 and H4), 2.62 (bs, 1H, OH), 2.12 (m, 2H, H3), 2.0 (bs, 1H, OH).

¹³C NMR (125 MHz, CDCl₃): δ 67.1 (CH₂, C1), 60.0 (CH₂, C4), 55.2 (CH, C2), 37.7 (C3).

These data were consistent with those reported previously.^{45,50}

Triethyl(2-[2R-oxiran-2-yl]ethoxy)silane - 137



A 10 mL 1 N RBF equipped with a septum and stir bar was charged with NaH (60% dispersion in mineral oil, 6.76 g, 169 mmol, 3 eq.) in THF (80 mL), set under nitrogen and cooled to -15 °C. Diol **136** (1.08 g, 6.4 mmol, 1 eq.) was dissolved in THF (80 mL) and added dropwise to the reaction flask. After 30 min of stirring at -15 °C TESCl (11.3 mL, 67.6 mmol, 1.2 eq.) was added dropwise, the cool bath removed and stirring continued for another 40 min. The reaction was then quenched with sat. aq. NH₄Cl solution (20 mL) and water (20 mL) and the aqueous layer extracted with EtOAc (3 x 50 mL). The combined organic layers were dried over MgSO₄, filtered and the solvent was removed under reduced pressure. The crude product was then purified *via* FCC (50 g silica, PE/EtOAc = 9/1) to afford the title compound as a colorless liquid (12.48 g, 91%).

TLC: R_f (PE/EtOAc = 9/1) = 0.41.

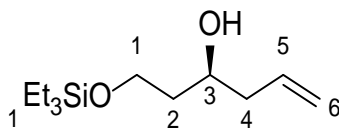
¹H NMR (500 MHz, CDCl₃): δ 3.67 (dt, 2H, *J* = 5.4, 1.2 Hz, H1), 3.04 (m, 1H, H3), 2.77 (dd, 1H, *J* = 4.8, 4.1 Hz, C5a), 2.51 (dd, 1H, *J* = 5.0, 2.8 Hz, C5b), 1.78 (m, 1H, C3a), 1.69 (m, 1H, C3b), 0.95 (t, 9H, *J* = 7.8 Hz, TES), 0.60 (q, 6H, *J* = 7.8 Hz, TES).

¹³C NMR (125 MHz, CDCl₃): δ 59.7 (CH₂, C1), 49.9 (CH, C3), 47.2 (CH₂, C4), 35.9 (CH₂, C2), 6.73 (CH₃, TES), 4.33 (CH₂, TES).

[α]_D^{24°C} = 13.9 (c = 1.15, DCM).

These data were consistent with those reported previously.⁴⁵

(S)-1-((Triethylsilyl)oxy)hex-5-en-3-ol - 138



A 50 ml 1 NRBF equipped with a septum and stir bar was set under nitrogen, charged with vinylmagnesium bromide (1M in THF, 11.7 ml, 11.7 mmol, 3 eq.) and cooled to -78 °C. CuI (0.08 g, 0.4 mmol, 0.1 mmol) was added in one portion and the reaction mixture stirred for 10 min before **137** (0.79 g, 3.9 mmol, 1 eq.) in THF (20 mL) was added. The cold bath was removed and the reaction allowed to warm to 0 °C over 60 min before it was quenched with sat. aq. NH₄Cl solution (16 mL), water (6 mL). After 15 min, 33% aq. NH₄OH solution (5 mL) was added. The aqueous layer was extracted with EtOAc (3 x 50 ml), the combined organic layers dried over MgSO₄, filtered and the solvent was removed under reduced pressure. The crude mixture can be used directly in the next step or it can be purified *via* FCC (30 g silica, PE/EtOAc = 10/1) to afford the title compound as a colorless liquid (720 mg, 80%).

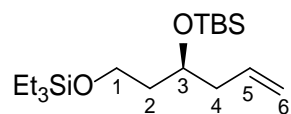
TLC: R_f (PE/EtOAc = 10/1) = 0.32.

¹H NMR (500 MHz, CDCl₃): δ 5.83 (m, 1H, H5), 5.19 (m, 2H, H6), 3.89 (m, 2H, H1), 3.80 (m, 1H, H3), 3.42 (d, *J* = 2.2 Hz, 1H, OH), 2.24 (m, 2H, H4), 1.66 (m, 2H, H2), 0.95 (t, *J* = 7.8 Hz, 9H, TES), 0.60 (q, *J* = 7.8 Hz, 6H, TES).

¹³C NMR (125 MHz, CDCl₃): δ 135.0 (CH, C5), 117.3 (CH₂, C6), 71.3 (CH, C3), 62.3 (CH₂, C1), 42.00 (CH₂, C4), 37.7 (CH₂, C2), 6.7 (CH₃, TES), 4.2 (CH₃, TES).

These data were consistent with those reported previously.⁴⁵

(S)-5-Allyl-9,9-diethyl-2,2,3,3-tetramethyl-4,8-dioxa-3,9-disilaundecane - 139



A 50 ml one-necked RBF equipped with a septum and stir bar was charged with **138** (2.0 g, 8.7 mmol, 1 eq.) and imidazole (0.71 g, 10.4 mmol, 1.2 eq.), set under nitrogen and DMF (21 mL) added. The reaction was cooled to 0 °C and TBSCl (1.44 g, 9.6 mmol, 1.1 eq.) was added. The cool bath was then removed and stirring continued overnight at room temperature. On the next day, the reaction was quenched with water and the aqueous layer extracted with ethyl acetate (3x). The combined organic layers were dried over MgSO₄, filtered and the solvent was removed under reduced pressure. The crude product was purified *via* FCC (30 g silica, PE/EtOAc = 10/1) to afford the title compound as a colorless oil (2.57 g, 86%).

TLC: R_f (PE/EtOAc = 10/1) = 0.75.

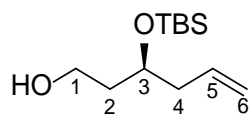
¹H NMR (500 MHz, CDCl₃): δ 5.81 (m, 1H, H5), 4.86 (m, 2H, H6), 3.85 (m, 1H, H3), 3.66 (m, 2H, H1), 2.23 (m, 2H, H4), 1.66 (m, 2H, H2), 0.94 (t, *J* = 8.1 Hz, 9H, TES), 0.88 (s, 9H, TBS), 0.58 (q, *J* = 8.1 Hz, 6H, TES), 0.04 (s, 6H, TBS).

¹³C NMR (125 MHz, CDCl₃): δ 135.1 (CH, C5), 116.7 (CH₂, C6), 68.7 (CH, C1), 59.8 (CH, C3), 42.1 (CH₂, C4), 39.7 (CH₂, C2), 25.8 (CH₃, TBS), 18.2 (C, TBS), 6.8 (CH₃, TES), 6.3 (CH₂, TES), -4.8 (CH₃, TBS), -5.4 (CH₃, TBS).

[α]_D²⁴ = 9.82 (c = 1.12, DCM).

These data were consistent with those reported previously.⁴⁵

(S)-3-((*tert*-Butyldimethylsilyl)oxy)hex-5-en-1-ol - 140



A 25 ml one-necked RBF equipped with a septum and stir bar was charged with 139 (138 mg, 0.40 mmol, 1 eq.) and set under nitrogen. Dry CH₃CN (6.6 mL) was added and the solution cooled to 0 °C before a 4% solution of HF.pyridine in CH₃CN (16 mL) was added at once. The reaction was stirred at 0 °C for three hours before it was quenched with sat. aq. sodium bicarbonate solution and diluted with ethyl acetate. The organic layer was separated and the aqueous layer extracted with ethyl acetate (3x). The combined organic layers were dried over MgSO₄, filtered and the solvent was removed under reduced pressure. The crude product was purified via FCC (2 g silica, gradient elution PE/EtOAc = 10/1, then 0/1) to afford the title compound as a colorless oil (56.3 mg, 61%) and the diol as a colorless oil (18.9 mg, 20%).

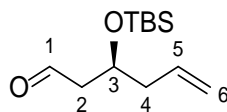
TLC: R_f (PE/EtOAc = 10/1) = 0.48.

¹H NMR (500 MHz, CDCl₃): δ 5.76 (m, 1H, H5), 5.05 (m, 2H, H6), 3.96 (m, 1H, H3), 3.82 (m, 1H, H1a), 3.71 (m, 1H, H1b), 2.29 (m, 3H, H4 and OH), 1.80 (m, 1H, H2a), 1.65 (m, 1H, H1b), 0.89 (s, 9H, TBS), 0.10 (s, 3H, TBS), 0.09 (s, 3H, TBS).

¹³C NMR (125 MHz, CDCl₃): δ 134.5 (CH, C5), 117.4 (CH₂, C6), 71.3 (CH, C3), 60.2 (CH₂, C1), 41.6 (CH₂, C4), 37.6 (CH₂, C2), 25.8 (CH₃, TBS), 18.0 (C, TBS), -4.4 (CH₃, TBS), -4.8 (CH₃, TBS).

These data were consistent with those reported previously.⁸⁸

(S)-3-((*tert*-Butyldimethylsilyl)oxy)hex-5-enal- 141

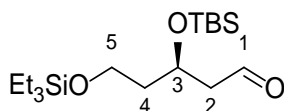


Prepared according to the general procedure for **TEMPO/BAIB oxidation** using **140** as starting material, yielding the title compound in a mixture with iodobenzene. The crude mixture was used without purification.

$^1\text{H NMR}$ (500 MHz, CDCl_3): δ 9.82 (t, $J = 2.3$ Hz, 1H, H1), 5.86 – 5.72 (m, 1H, H5), 5.15 – 5.06 (m, 2H, H6), 4.28 (p, $J = 5.9$ Hz, 1H, H3), 2.58 – 2.53 (m, 2H, H4), 2.33 (t, $J = 6.5$ Hz, 2H, H2), 0.89 (s, 9H TBS), 0.10 (s, 3H, TBS), 0.08 (s, 3H, TBS).

These data for **141** in the crude mixture were consistent with those reported previously.⁸⁸

(R)-3-((*tert*-Butyldimethylsilyl)oxy)-5-((triethylsilyl)oxy)pentanal - 143



A 50 mL one-necked RBF equipped with a septum and stir bar was charged with **139** (500 mg, 1.45 mmol, 1 eq.), set under nitrogen and DCM was added. The solution was cooled to -78 °C and ozone was bubbled through *via* a pasteur pipette until the solution turned blue, which indicated saturation with ozone. Triphenylphosphine (457 mg, 1.74 mmol, 1.2 eq.) was added and stirring continued for 15 min before the cool bath was removed. Stirring was continued at room temperature overnight and on the next day the solvent was removed under reduced pressure. The crude product was purified *via* FCC (30 g silica, PE/EtOAc = 10/1) to afford the title compound as a colorless oil (483 mg, 96%).

TLC: Rf (PE/EtOAc = 10/1) = 0.72.

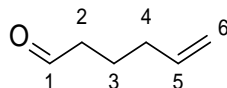
¹H NMR (500 MHz, CDCl₃): δ 9.8 (s, 1H, H1), 4.35 (m, 1H, H3), 3.71-3.65 (m, 2H, H5), 1.85-1.68 (m, 2H, H4), 0.94 (t, *J* = 8.1 Hz, 9H, TES), 0.86 (s, 9H, TBS), 0.58 (q, *J* = 8.1 Hz, 6H, TES), 0.06 (d, *J* = 4.6 Hz, 6H, TBS).

¹³C NMR (125 MHz, CDCl₃): δ 202.3 (CH, C1), 65.6 (CH, C3), 58.9 (CH₂, C5), 51.0 (CH₂, C2), 40.6 (CH₂, C4), 25.7 (CH₃, TBS), 18.0 (C, TBS), 6.8 (CH₃, TES), 4.4 (CH₂, TES), -4.6 (CH₃, TBS), -4.73 (CH₃, TBS).

[α]_D^{24°C} = -12.96 (c = 1.08, DCM).

HRMS (ESI⁺): calculated for C₁₇H₃₈O₃Si₂ [M+H]⁺: 347.2462. Found 347.2443, Δ = 3.22 ppm.

Hex-5-enal- 144

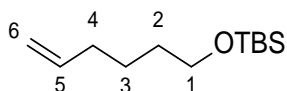


Prepared according to the general procedure for **TEMPO/BAIB oxidation** using 5-hexen-1-ol as starting material, yielding the title compound in a mixture with iodobenzene. The crude mixture was used without purification.

¹H NMR (500 MHz, CDCl₃): δ 9.78 (s, 1H, H1), 5.78 (ddt, *J* = 16.9, 10.1, 6.7 Hz, 1H, H5), 5.09 – 4.98 (m, 2H, H6), 2.46 (t, *J* = 7.9 Hz, 2H, H2), 2.11 (q, *J* = 7.1 Hz, 2H, H4), 1.75 (p, *J* = 7.3 Hz, 2H, H3).

These data for **144** in the crude mixture were consistent with those reported previously.⁸⁹

tert-Butyl(hex-5-en-1-yloxy)dimethylsilane



A 25 mL 1 NRBF was charged with 5-hexen-1-ol (500 mg, 5.00 mmol, 1 eq.) and imidazole (408 mg, 5.99 mg, 1.2 eq.) and the flask set under nitrogen. DMF (12 ml) was added to the reaction and the solution cooled to 0 °C. TBSCl (828 mg, 5.50 mmol, 1.1 eq.) was added in one portion and the reaction was allowed to warm to room temperature and stirred overnight. On the next day, the reaction was quenched with water, EtOAc added and the organic layer washed with aq. sat. sodium bicarbonate solution (1x), water (1x) and brine (1x). The organic layer was then dried with magnesium sulfate, filtered, and the solvent was removed under reduced pressure to afford the title compound as a colorless liquid. The crude material can be used without further purification or purified *via* FCC (30 g silica, PE/EtOAc = 10/1) to afford the title compound as a colorless liquid (946 mg, 88%).

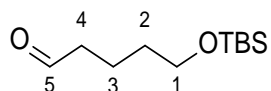
TLC: R_f (PE/EtOAc = 10/1) = 0.33.

¹H NMR (500 MHz, CDCl₃): δ 5.80 (m, 1H, H5), 4.99 (d, *J* = 17.1 Hz, 1H, H6a), 4.93 (d, *J* = 10.3 Hz, 1H, H6b), 3.60 (t, *J* = 6.4 Hz, 2H, H1), 2.05 (m, 2H, H4), 1.52 (m, 2H, H3), 1.41 (m, 2H, H2), 0.88 (s, 9H, TBS), 0.04 (s, 6H, TBS).

¹³C NMR (125 MHz, CDCl₃): δ 139.0 (CH, C5), 114.3 (CH₂, C6), 63.1 (CH₂, C1), 33.5 (CH₂, C4), 32.3 (CH₂, C2), 26.0 (CH₃, TBS), 25.1 (CH₂, C3), 18.4 (C, TBS), -5.3 (CH₃, TBS).

These data were consistent with those reported previously.⁹⁰

5-((tert-Butyldimethylsilyl)oxy)pentanal - 147



A 50 mL 1 N RBF was charged with *tert*-butyl(hex-5-en-1-yloxy)dimethylsilane (500 mg, 2.33 mmol, 1 eq.) and the flask set under nitrogen. DCM (30 mL) was added and the solution cooled to -78°C . Ozone (excess) was bubbled through the solution *via* a pasteur pipette until the solution turned light blue, which indicates the solution is saturated with ozone. PPh_3 (735 mg, 2.80 mmol, 1.2 eq.) was added at once and stirring is continued at low temperature for 10 min. The cold bath is then removed and the reaction mixture was allowed to come to room temperature and stirred overnight. On the next day, the solvent was removed under reduced pressure. The crude product was purified *via* FCC (30 g silica, PE/EtOAc = 10/1) to afford the title compound as a colorless liquid (480 mg, 95%).

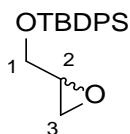
TLC: R_f (PE/EtOAc = 10/1) = 0.57.

$^1\text{H NMR}$ (500 MHz, CDCl_3): δ 9.76 (s, 1H, H5), 3.61 (t, $J = 6.2$ Hz, 2H, H1), 2.44 (t, $J = 7.32$ Hz, 2H, H4), 1.69 (m, 2H, H2), 1.53 (m, 2H, H3), 0.88 (s, 9H, TBS), 0.03 (s, TBS).

$^{13}\text{C NMR}$ (125 MHz, CDCl_3): δ 202.7 (CH, C5), 62.6 (CH_2 , C1), 43.6 (CH_2 , C4), 32.1 (CH_2 , C2), 26.0 (CH_3 , TBS), 18.6 (CH_2 , C3), 18.3 (C, TBS), -5.3 (CH_3 , TBS).

These data were consistent with those reported previously.⁹¹

2-(tert-Butyldiphenylsilyloxy)methyloxirane - 149



A 10 mL 1 NRBF equipped with a septum and stir bar was set under N₂ and charged with glycidol (rac., 100 mg, 1.35 mmol, 1 eq.), imidazole (120 mg, 1.76 mmol, 1.3 eq.) and DMF (1.4 mL). The reaction mixture was then cooled to 0 °C and TBDPSCl (0.4 mL, 1.55 mmol, 1.15 eq.) added dropwise. Stirring was continued for another 4 h at 0 °C before the reaction was quenched with water (8 mL) and diluted with diethyl ether (15 mL). Phases were separated and the organic layer washed with sat. aq. NaHCO₃ solution (2 x 10 mL), H₂O (10 mL) and brine (10 mL). The combined organic layers were dried over MgSO₄, filtered and the solvent was removed under reduced pressure. The crude product was purified *via* FCC (12 g silica, PE/EtOAc = 50/1) to afford the title compound as a colorless oil (0.25 g, 60%).

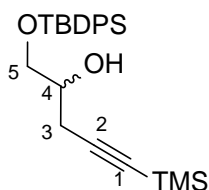
TLC: R_f (PE/EtOAc = 50/1) = 0.18.

¹H NMR (500 MHz, CDCl₃): δ 7.65-7.70 (m, 4H, TBDPS), 7.35-7.45 (m, 6H, TBDPS), 3.84 (dd, *J* = 12.0, 3.4 Hz, 1H, H1a), 3.70 (dd, *J* = 12.0, 4.9 Hz, 1H, H1b), 3.12 (m, 1H, H2), 2.74 (dd, *J* = 5.1, 4.2 Hz, 1H, H3a), 2.60 (dd, *J* = 5.7, 2.7 Hz, 1H, H3b), 1.05 (s, 9H, TBDPS).

¹³C NMR (125 MHz, CDCl₃): δ 135.6 (CH, 4C, TBDPS), 133.3 (C, 2C, TBDPS), 129.7 (CH, 2C, TBDPS), 127.7 (CH, 4C, TBDPS), 64.3 (CH₂, C1), 52.3 (CH, C2), 44.5 (CH₂, C3), 26.7 (CH₃, TBDPS), 19.2 (CH₃, TBDPS).

These data were consistent with those reported previously.^{45,46}

1-(tert-Butyldiphenylsilyloxy)-5-trimethylsilyl-4-pentyn-2-ol - 150



A 10 mL 1 NRBF equipped with a septum was set under nitrogen, charged with ethynyltrimethylsilane (0.1 mL, 0.74 mmol, 1.2 eq.) in THF (2.5 mL) and cooled to $-78\text{ }^{\circ}\text{C}$. *n*-BuLi (2 M in cyclohexane, 0.44 mL, 0.89 mmol, 1.45 eq.) was added dropwise and the reaction stirred for 25 min at $-78\text{ }^{\circ}\text{C}$ before a solution of **149** (200.0 mg, 0.62 mmol, 1 eq.) in THF (0.5 mL) was added dropwise. Stirring was continued for 10 min before boron trifluoride diethyl etherate (0.09 mL, 0.74 mmol, 1.2 eq.) was added dropwise. After 2.5 h of stirring at $-78\text{ }^{\circ}\text{C}$ the reaction mixture was allowed to warm up to $0\text{ }^{\circ}\text{C}$ and was then quenched with sat. aq. NH_4Cl solution (5 mL). The aqueous layer was extracted with diethyl ether (3 x 10 mL), the combined organic layers dried over MgSO_4 , filtered and the solvent was removed under reduced pressure. The crude product was purified *via* FCC (silica 10 g, PE/EtOAc = 20/1) to afford the title compound as a colorless oil (223 mg, 88%).

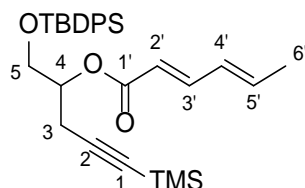
TLC: R_f (PE/EtOAc = 20/1) = 0.23.

$^1\text{H NMR}$ (500 MHz, CDCl_3): δ 7.65 (m, 4H, TBDPS), 7.41 (m, 6H, TBDPS), 3.88 (m, 1H, H4), 3.74 (dd, $J = 10.3, 4.4$ Hz, 1H, H5a), 3.68 (dd, $J = 10.3, 5.9$ Hz, 1H, H5b), 2.50 (m, 2H, H4), 1.06 (s, 9H, TBDPS), 0.10 (s, 9H, TMS).

$^{13}\text{C NMR}$ (125 MHz, CDCl_3): δ 135.5 (CH, TBDPS), 132.6 (C, TBDPS), 129.8 (CH, TBDPS), 127.8 (CH, TBDPS), 103.5 (C, C2), 91.8 (C, C1), 70.2 (CH_2 , C5), 66.6 (CH, C4), 26.9 (CH_3 , TBDPS), 24.7 (CH_2 , C3), 19.6 (C, TBDPS), 0.0 (CH_3 , TMS).

These data were consistent with those reported previously.^{45,46,92}

(2E,4E)-1-((tert-Butyldiphenylsilyl)oxy)-5-(trimethylsilyl)-pent-4-yn-2-yl hexa-2,4-dienoate - 154



A 10 mL 1 NRBF equipped with a stir bar and septum was charged with 4-DMAP (0.9 mg, 0.01 mmol, 0.1 eq.) and sorbic acid (37 mg, 0.30 mmol, 4 eq.) and set under nitrogen. DCM (1 mL) was added and the suspension cooled to 0 °C before DCC (57 mg, 0.27 mmol, 2 eq.), sorbic acid ester was added in one portion. Stirring is continued for 3 h at room temperature before this mixture was transferred to a 10 mL one-necked RBF charged with **150** (30 mg, 0.07 mmol, 1 eq.). This suspension was then stirred for 24 hours and directly applied to FCC (3 g silica, PE/EtOAc = 20/1) to afford the title compound as a colorless oil (30 mg, 81%).

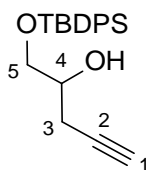
TLC: R_f (PE/EtOAc = 20/1) = 0.23.

¹H NMR (500 MHz, CDCl₃): δ 7.67 (m, 4H, *ortho*-TBDPS), 7.39 (m, 6H, *m* and *p*-TBDPS), 7.27 (dd, *J* = 15.4, 10.8 Hz, 1H, H3'), 6.16 (m, 2H, H4' and H5'), 5.77 (d, *J* = 14.9 Hz, 1H, H2'), 5.12 (m, 1H, H4), 3.88 (dd, *J* = 10.7, 4.6 Hz, 1H, H5a), 3.83 (dd, *J* = 11.0, 4.1 Hz, 1H, H5b), 2.73 (dd, *J* = 16.8, 9.8 Hz, 1H, H3a), 2.64 (dd, *J* = 16.9, 11.0 Hz, H3b), 1.86 (d, *J* = 6.6 Hz, 3H, H6'), 1.05 (s, 9H, TBDPS), 0.12 (s, 9H, TMS).

¹³C NMR (125 MHz, CDCl₃): δ 166.4 (C, C1'), 145.4 (CH, C3'), 139.5 (CH, C5'), 135.5 (CH, *ortho*-TBDPS), 133.3 (CH, C4'), 129.8 (CH, *para*-TBDPS), 129.7 (C, *ipso*-TBDPS), 127.7 (CH, *meta*-TBDPS), 118.8 (CH, C2'), 102.1 (C, C2), 86.8 (C, C1), 71.9 (CH, C4), 63.7 (CH₂, C5), 26.7 (CH₃, TBDPS), 21.9 (CH₂, C3), 19.3 (C, TBDPS), 18.7 (CH₃, C6'), 0.03 (CH₃, TMS).

HRMS (ESI⁺): calculated for C₃₀H₄₀O₃Si₂ [M+H]⁺: 505.2589. Found 505.2591, Δ = 0.53 ppm.

1-((tert-butyldiphenylsilyl)oxy)pent-4-yn-2-ol - 151



A vial was charged with **150** (200 mg, 0.49 mmol, 1 eq.) and K_2CO_3 (337 mg, 2.43 mmol, 5 eq.) and MeOH (5 ml) added. This suspension is stirred at room temperature overnight. On the next day K_2CO_3 is filtered off and the solvent is removed under reduced pressure to afford the title compound as a colorless oil. The material can be used without further purification or be purified *via* FCC (10 g silica, PE/EtOAc = 10/1) (112 mg, 68%).

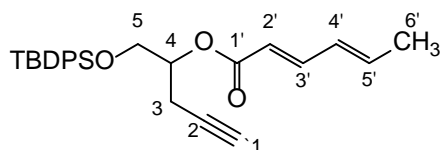
TLC: Rf (PE/EtOAc = 10/1) = 0.31.

1H NMR (500 MHz, $CDCl_3$): δ 7.66 (m, 4H, *ortho*-TBDPS), 7.40 (m, 6H, *meta*- and *para*-TBDPS), 3.88 (m, 1H, H4), 3.75 (dd, $J = 10.3, 4.4$ Hz, 1H, H5a), 3.75 (dd, $J = 10.3, 5.9$ Hz, 1H, H5b), 2.49 (d, $J = 5.4$ Hz, 1H, H3), 2.46 (d, $J = 6.4, 2.7$ Hz, 1H, H3), 2.07 (t, $J = 2.7$ Hz, 1H, H1), 1.06 (s, 9H, TBDPS).

^{13}C NMR (125 MHz, $CDCl_3$): δ 135.5 (CH, *ortho*-TBDPS), 133.0 (C, *ipso*-TBDPS), 129.8 (CH, *para*-TBDPS), 127.8 (CH, *meta*-TBDPS), 80.3 (CH, C2), 70.4 (CH_2 , C5), 70.2 (C, C1), 66.3 (CH, C4), 26.8 (CH_3 , TBDPS), 23.2 (CH_2 , C3), 19.3 (C, TBDPS).

These data were consistent with those reported previously.^{45,46,92}

(2E,4E)-1-((tert-Butyldiphenylsilyloxy)pent-4-yn-2-yl hexa-2,4-dienoate - 153



A 5mL one-necked RBF equipped with a septum and stir bar was charged with sorbic acid (57 mg, 0.51 mmol, 4 eq.) and DMAP (16 mg, 0.01 mmol, 0.1 eq.) and set under nitrogen. DCM (1 ml) was added and this suspension cooled to 0 °C before DCC (52 mg, 0.25 mmol, 2 eq.) was added. Stirring was continued for three hours before **151** (43 mg, 0.13 mmol, 1 eq.) in DCM (0.8 ml) was added. The reaction was then stirred at room temperature overnight. On the next day, the reaction was quenched with water and the aqueous layer extracted with EtOAc (3 x 5 ml). The combined organic layers were dried over MgSO₄, filtered and the solvent was removed under reduced pressure. The crude product was purified *via* FCC (5 g silica, PE/EtOAc = 20/1) to afford the title compound as a slightly yellow oil (31 mg, 55%).

TLC: R_f (PE/EtOAc = 20/1) = 0.25.

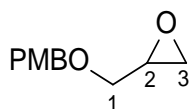
¹H NMR (500 MHz, CDCl₃): δ 7.66 (m, 4H, m-TBDPS), 7.37 (m, 6H, o-and p-TBDPS), 7.26 (dd, *J* = 15.4, 10.3 Hz, 1H, H3'), 6.16 (m, 2H, H4' and H5'), 5.76 (d, *J* = 15.4 Hz, 1H, H2'), 5.11 (m, 1H, H4), 3.86 (dd, *J* = 10.7, 4.6 Hz, 1H, H5a), 3.82 (dd, *J* = 10.7, 4.4 Hz, 1H, H5b), 2.70 (ddd, *J* = 16.8, 6.6, 2.7 Hz, 1H, H3a), 2.61 (ddd, *J* = 16.6, 5.9, 2.7 Hz, 1H, H3b), 1.95 (t, *J* = 2.7 Hz, 1H, H1), 1.86 (d, *J* = 6.1 Hz, 3H, H6'), 1.04 (s, 9H, TBDPS).

¹³C NMR (125 MHz, CDCl₃): δ 166.5 (C, C1'), 145.6 (CH, C3'), 139.7 (CH, C4'), 135.6 (CH, TBDPS), 133.2 (CH, TBDPS), 129.8 (CH, TBDPS), 127.7 (CH, C5'), 118.7 (CH, C2'), 79.7 (C, C2), 71.7 (CH, C4), 70.3 (CH, C1), 63.6 (CH₂, C5), 26.7 (CH₃, TBDPS), 20.5 (C3), 19.3 (CH₃, C6'), 18.7 (C, TBS).

IR (neat) cm⁻¹: 3296, 2958, 2858, 1716, 1112.7, 703, 505.

HRMS (ESI⁺): calculated for C₂₇H₃₂O₃Si [M+H]⁺: 433.2194. Found 433.2205, Δ = 2.67 ppm.

2-(((4-Methoxybenzyl)oxy)methyl)oxirane



A 250 ml one-necked RBF equipped with septum and stir bar was charged with NaH (1.4 g, 0.035 mol, 1.3 eq.) and set under nitrogen. DMF (23 mL) was added and this suspension cooled to -60 °C. Glycidol (**80**) (2.0 g, 0.027 mol, 1 eq.) in DMF (11 ml) was added and stirring continued for 1h, before TBAI (60 mg, cat.) and PMBCl (4.75 ml, 0.035 mol, 1.3 eq.) was added dropwise. After 2.5 h, the reaction was quenched with water and the aqueous layer extracted with diethyl ether. The combined organic layers were washed with water (1x) and brine (1x), dried over MgSO₄, filtered and the solvent removed under reduced pressure. The crude mixture can be used directly in the next step or it can be purified *via* a short silica plug (PE/EtOAc = 5/1) to afford the title compound as a colorless liquid (6.1 g, quant.).

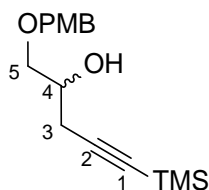
TLC: R_f (PE/EtOAc = 5/1) = 0.27.

¹H NMR (500 MHz, CDCl₃): δ 7.26 (d, *J* = 8.5 Hz, 2H, *ortho*-PMB), 6.87 (d, *J* = 8.54 Hz, 2H, *meta*-PMB), 4.54 (d, *J* = 11.5 Hz, 1H, CH₂-PMBa), 4.48 (d, *J* = 11.5 Hz, 1H, CH₂-PMBb), 3.8 (s, 3H, CH₃-PMB), 3.72 (dd, *J* = 11.5, 2.9 Hz, 1H, H1a), 3.41 (dd, *J* = 11.5, 5.9 Hz, 1H, H1b), 3.17 (m, 1H, H2), 2.79 (dd, *J* = 4.5, 4.2 Hz, 1H, H3a), 2.60 (dd, *J* = 4.9, 2.7 Hz, 1H, H3b).

¹³C NMR (125 MHz, CDCl₃): δ 159.3 (C, *para*-PMB), 129.4 (CH, *ortho*-PMB), 128.6 (C, *ipso*-PMB), 113.78 (CH, *meta*-PMB), 73.0 (CH₂, CH₂-PMB), 70.5 (CH₂, C1), 55.2 (CH₃, CH₃-PMB), 50.9 (CH, C2), 44.3 (CH₂, C3).

These data were consistent with those reported previously.^{19,70,72}

1-((4-Methoxybenzyl)oxy)-5-(trimethylsilyl)pent-4-yn-2-ol - 113



A 250 ml one-necked RBF equipped with a stir bar, septum and dropping funnel was set under nitrogen. Trimethylsilylacetylene (4.6 mL, 0.032 mol, 1.2 eq.) in THF (100 mL) was added and the solution cooled to -78°C . *n*-BuLi (2M in cyclohexane, 19.5 mL, 0.039 mol, 1.45 eq.) was added dropwise and the mixture stirred for 25 min before a solution of 2-(((4-methoxybenzyl)oxy)methyl)oxirane (0.027 mol, 1 eq.) in THF (35 mL) was added dropwise. The reaction was stirred for 10 min and $\text{BF}_3 \cdot \text{Et}_2\text{O}$ (4.0 mL, 0.032 mol, 1.2 eq.) was added slowly. Stirring at -78°C was continued for 2.5 h before the reaction was allowed to come to room temperature and quenched with sat. aqu. ammonium chloride solution. The aqueous layer was extracted with diethyl ether (3x) and the combined organic layers dried over magnesium sulfate, filtered and the solvent was removed under reduced pressure to afford the title compound as colorless liquid (quant.) The product was used as crude in the next step.

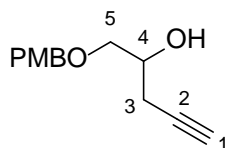
TLC: R_f (PE/EtOAc = 5/1) = 0.38.

$^1\text{H NMR}$ (500 MHz, CDCl_3): δ 7.25 (d, $J = 8.8$ Hz, 2H, *ortho*-PMB), 6.88 (d, $J = 8.5$ Hz, 2H, *meta*-PMB), 4.49 (s, 2H, CH_2 -PMB), 3.92 (m, 1H, H4), 3.80 (s, 3H, CH_3 -PMB), 3.57 (dd, $J = 9.5, 3.9$ Hz, 1H, H5b), 3.46 (dd, $J = 9.5, 6.6$ Hz, 1H, H5a), 2.47 (m, 2H, H3).

$^{13}\text{C NMR}$ (125 MHz, CDCl_3): δ 159.3 (C, *para*-PMB), 130 (C, *ipso*-PMB), 129.4 (CH, *ortho*-PMB), 113.8 (CH, *meta*-PMB), 102.5 (C, C2), 87.2 (C, C1), 73.0 (CH_2 , C5), 72.4 (CH_2 , CH_2 -PMB), 68.8 (CH, C4), 55.7 (CH_3 , CH_3 -PMB), 25.0 (CH_2 , C3), 0.0 (CH_3 , TMS).

These data were consistent with those reported previously.⁴⁶

1-((4-Methoxybenzyl)oxy)pent-4-yn-2-ol - 116



A 250 ml one-necked RBF equipped with a stir bar is charged with **113** (0.027 mol, 1 eq.), potassium carbonate (18.7 g, 0.135 mol, 5 eq.) and MeOH (100 mL) were added and the suspension was stirred overnight. On the next day, excess potassium carbonate was filtered off and solvent was removed under reduced pressure. The crude product was purified *via* FCC (silica, 150 g, gradient elution PE/EtOAc = 5/1, then 3/1, then 1/1) to afford the title compound as a slightly yellow oil (5.95 g, quant.).

TLC: R_f (PE/EtOAc = 5/1) = 0.12.

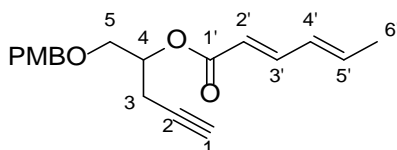
¹H NMR (500 MHz, CDCl₃): δ 7.25 (d, *J* = 8.8 Hz, 2H, *ortho*-PMB), 6.88 (d, *J* = 8.6 Hz, 2H, *meta*-PMB), 4.49 (s, 2H, CH₂-PMB), 3.95 (m, 1H, H₄), 3.8 (s, 3H, CH₃-PMB), 3.58 (dd, *J* = 9.5, 3.9 Hz, 1H, H_{5a}), 3.47 (d, *J* = 9.5, 6.6 Hz, 1H, H_{5b}), 2.44 (dd, *J* = 2.7, 1.0 Hz, 1H, H_{3a}), 2.43 (dd, *J* = 2.7, 1.2 Hz, 1H, H_{3b}), 2.01 (t, *J* = 2.7 Hz, 1H, H₁).

¹³C NMR (125 MHz, CDCl₃): δ 159.3 (C, *para*-PMB), 129.8 (C, *ipso*-PMB), 129.4 (CH, *ortho*-PMB), 113.9 (CH, *meta*-PMB), 80.2 (C, C₂), 73.1 (CH₂, PMB), 72.5 (CH₂, C₅), 70.6 (CH, C₁), 68.7 (CH, C₄), 55.3 (CH₃, PMB), 23.5 (CH₂, C₃).

[α]_D^{24°C} = 9.92 (c = 1.41, DCM) for (*S*)-**116**.

These data were consistent with those reported previously.⁴⁶

***(2E,4E)*-1-((4-Methoxybenzyl)oxy)pent-4-yn-2-yl hexa-2,4-dienoate - 155**



A 250 mL one-necked RBF equipped with a septum and stir bar was charged with DCC (2.06 g, 9.99 mmol, 1.1 eq.), 4-DMAP (0.11 g, 0.91 mmol, 0.1 eq.) and sorbic acid (2.04 g, 18.2 mmol, 2 eq.) and the flask was set under nitrogen. DCM (100 mL) was added and the resulting suspension stirred for three hours. **116** (2.00 g, 9.08 mmol, 1 eq.) in DCM (30 mL) was added and the reaction mixture stirred overnight. On the next day, the suspension was filtered through a sintered funnel and the solvent removed under reduced pressure. The crude product was purified *via* FCC (silica, 100 g, gradient elution PE/EtOAc = 5/1, then 3/1) to afford the title compound as a colorless oil (2.12 g, 74%).

TLC: R_f (PE/EtOAc = 5/1) = 0.33

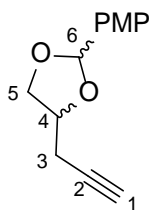
¹H NMR (500 MHz, CDCl₃): δ 7.27 (m, 3H, *ortho*-PMB and C3'), 6.88 (d, *J* = 6.8 Hz, 2H, *meta*-PMB), 6.17 (m, 2H, H4' and H5'), 5.80 (d, *J* = 15.4 Hz, 1H, H2'), 5.16 (m, 1H, H4), 4.53 (d, *J* = 11.7 Hz, CH₂, 1H, CH₂-PMB), 4.48 (d, *J* = 11.7 Hz, 1H, CH₂-PMB), 3.80 (s, 3H, CH₃-PMB), 3.66 (m, 2H, H5), 2.61 (m, 2H, H3), 1.97 (s, 1H, H1), 1.87 (d, *J* = 5.1 Hz, 3H, H6').

¹³C NMR (125 MHz, CDCl₃): δ 166.5 (C, C1'), 159.2 (C, *para*-PMB), 145.7 (CH, C3'), 139.8 (CH, C5'), 130.0 (C, *ipso*-PMB), 129.7 (CH, C4'), 129.3 (CH, *ortho*-PMB), 118.6 (CH, C2'), 113.8 (CH, *meta*-PMB), 79.5 (C, C2), 73.0 (CH₂, C5), 70.4 (CH, C4), 70.3 (CH₂, C2), 69.3 (CH, C1), 55.3 (CH₃, PMB), 20.9 (CH₂, C3), 18.7 (CH₃, C6').

IR (neat) cm⁻¹: 2932, 2837, 1698, 1511, 1245, 1032, 759.

HRMS (ESI⁺): calculated for C₁₉H₂₂O₄ [M+Na]⁺: 337.1410. Found 337.1397, Δ = 3.86 ppm.

2-(4-Methoxyphenyl)-4-(prop-2-yn-1-yl)-1,3-dioxolane – 156



A 50 mL one-necked RBF equipped with a septum and stir bar was charged with **116** (500 mg, 2.27 mmol, 1 eq.) and activated molecular sieves (4A, 500 mg) in toluene (15 mL). This mixture was cooled to 0 °C before a solution of DDQ (781 mg 3.404 mmol, 1.5 eq.) in toluene (10 mL) was added dropwise. The reaction was stirred for an hour before being put in the fridge overnight. On the next day, the molecular sieves were filtered off and the organic layer washed with 2 M NaOH solution (2x), water (1x) and brine (1x). The combined organic layers were dried over magnesium sulfate, filtered and the solvent was removed under reduced pressure. If the crude product was contaminated with anisaldehyde (which is inseparable from the product by FCC) it was dissolved in MeOH, cooled to 0 °C and NaBH₄ (1.1 eq to anisaldehyde) added. The reaction mixture was stirred for 30 min before it was quenched with acetone. The solvent is then removed under reduced pressure. The crude product was purified *via* FCC (silica, 50 g, gradient elution PE/EtOAc = 3/1, then 1/1) to afford the title compound as a colorless oil (239 mg, 48%, mixture of diastereomers).

TLC: R_f (PE/EtOAc = 3/1) = 0.68.

¹H NMR (500 MHz, CDCl₃): δ 7.41 (dd, *J* = 16.1, 8.4 Hz, 4H, *ortho*-PMP), 6.90 (d, *J* = 6.6 Hz, 4H, *para*-PMP), 5.94 (s, 1H, H6 diastereomer 1), 5.77 (s, 1H, H6 diastereomer 2), 4.44 – 4.40 (m, 1H, H4 diastereomer 1), 4.40 – 4.35 (m, 1H, H4 diastereomer 2), 4.35 – 4.29 (m, 1H, H5a diastereomer 1), 4.13 (dd, *J* = 13.6, 5.7 Hz, 1H, H5a diastereomer 2), 4.01 (dd, *J* = 8.1, 5.2 Hz, 1H, H5b diastereomer 1), 3.87 (t, *J* = 7.5 Hz, 1H, H5b diastereomer 2), 3.81 (s, 6H, CH₃-PMB), 2.63 (d, *J* = 16.6 Hz, 2H, H3a diastereomer 1 and H3a diastereomer 2), 2.55 (ddd, *J* = 14.8, 7.5,

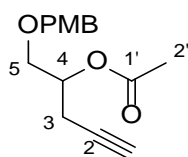
3.8 Hz, 2H, H3b diastereomer 1 and H3b diastereomer 2), 2.04 (s, 2H, H1 diastereomer 1 and H1 diastereomer 2).

¹³C NMR (125 MHz, CDCl₃): δ 160.4 (C, para-PMB diastereomer 1), 160.3 (C, para-PMB diastereomer 2), 129.7 (C, ipso-PMB diastereomer 1), 129.1 (C, ipso-PMB diastereomer 2), 128.0 (CH, ortho-PMB diastereomer 1), 127.7 (CH, ortho-PMB diastereomer 2), 113.7 (CH, meta-PMB diastereomer 1), 113.6 (CH, meta-PMB diastereomer 2), 104.5 (CH, C6' diastereomer 1), 103.7 (CH, C6' diastereomer 2), 79.5 (C, C2 diastereomer 1) 79.4 (CH, C2 diastereomer 2), 74.3 (CH, C4 diastereomer 1), 73.9 (CH, C4 diastereomer 2), 70.5 (CH, C1 diastereomer 1), 70.2 (CH, C1 diastereomer 2), 69.8 (CH₂, C5 diastereomer 1), 69.4 (CH₂, C5 diastereomer 2), 55.2 (CH₃, PMB), 23.9 (CH₂, C3 diastereomer 1), 23.1 (CH₂, C3 diastereomer 2).

IR (neat) cm⁻¹: 3287, 2936, 1711, 1614, 1304, 1247, 1171, 1076, 1031, 829.

HRMS (ESI⁺): calculated for C₁₃H₁₄O₃ [M+H]⁺: 219.1016. Found 219.1010, Δ = -2.74 ppm.

1-((4-Methoxybenzyl)oxy)pent-4-yn-2-yl acetate– 157



A 10 mL one-necked RBF equipped with a stir bar and septum was charged with **116** (500 mg, 2.27 mmol, 1 eq.) and set under nitrogen. DCM (2.5 mL) was added and the solution cooled to 0 °C before acetic anhydride (0.33 mL, 3.40 mmol, 1.5 eq.) and pyridine (0.3 mL, 3.63 mmol, 1.6 eq.) and DMAP (14 mg, 0.114 mol, 0.05 eq.) were added. The reaction was stirred for 60 min at 0 °C before it was quenched with sat. aqu. ammonium chloride solution. The aqueous layer was extracted with DCM (3x) and the combined organic layers were dried over magnesium sulfate, filtered and the solvent was removed under reduced pressure. The crude product

was purified *via* FCC (silica, 30 g, PE/EtOAc = 3/1) to afford the title compound as a colorless oil (591 mg, 99%).

TLC: R_f (PE/EtOAc = 3/1) = 0.49.

¹H NMR (500 MHz, CDCl₃): δ 7.25 (d, *J* = 7.6 Hz, 2H, *ortho*-PMB), 6.88 (d, *J* = 7.9 Hz, 2H, *meta*-PMB), 5.12 – 5.06 (m, 1H, H4), 4.52 (d, *J* = 11.7 Hz, 1H, CH₂-PMB), 4.47 (d, *J* = 11.7 Hz, 1H, CH₂-PMB), 3.81 (s, 3H, CH₃-PMB), 3.66 – 3.57 (m, 2H, H5), 2.60 (ddd, *J* = 16.9, 6.5, 1.5 Hz, 1H, H3a), 2.53 (ddd, *J* = 16.8, 5.8, 1.6 Hz, 1H, H3b), 2.08 (s, 3H, H2'), 1.97 (s, 1H, H1).

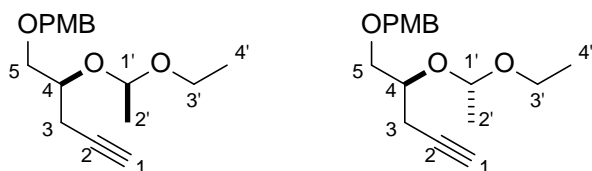
¹³C NMR (125 MHz, CDCl₃): δ 170.4 (C, C1'), 159.3 (C, *para*-PMB), 129.9 (C, *ipso*-PMB), 129.3 (CH, *ortho*-PMB), 113.8 (CH, *meta*-PMB), 79.3 (C, C2), 73.0 (CH₂, PMB), 70.5 (CH, C4), 70.4 (CH, C1), 69.2 (CH₂, C5), 55.3 (CH₃, PMB), 21.1 (CH₂, C3), 20.9 (CH₃, C2').

IR (neat) cm⁻¹: 3288, 2935, 2861, 1736, 1512, 1234, 1094, 1032, 818, 637.

[α]_D²⁴ = 7.20 (c = 1.25, DCM) for (**S**)-**157**.

HRMS (ESI⁺): calculated for C₁₅H₁₈O₄ [M+Na]⁺: 285.1097. Found 285.1085, Δ = 4.21 ppm.

1-(((2-(1-Ethoxyethoxy)pent-4-yn-1-yl)oxy)methyl)-4-methoxybenzene- 158



A 25 mL one-necked RBF equipped with a septum and stir bar was charged with **116** (200 mg, 0.91 mmol, 1 eq.) and set under nitrogen. DCM (9 mL) is added followed by ethyl vinyl ether (0.88 mL, 8.08 mmol, 10 eq.) and PPTS (256 mg,

0.1 mmol, 1.1 eq.). The reaction is stirred for 45 min before it was quenched with sat. aq. sodium bicarbonate solution. The aqueous layer is extracted with DCM (3x) and the combined organic layers were dried over magnesium sulfate, filtered and the solvent is removed under reduced pressure. The crude product (mixture of diastereomers) was used without further purification (266 mg, quant.)

TLC: Rf (PE/EtOAc = 3/1) = 0.68.

¹H NMR (500 MHz, CDCl₃): δ 7.25 (m, 2H, *ortho*-PMB), 6.88 (d, *J* = 6.8 Hz, 2H, *meta*-PMB), 4.86 (m, 1H, H1'), 4.49 (s, 2H, CH₂-PMB), 3.92 (m, 1H, H4), 3.81 (s, 3H, CH₃-PMB), 3.66 (m, 1H, H5a), 3.61-3.46 (m, 3H, H5b and H3'), 2.46-2.39 (m, 2H, H3), 1.97 (s, 1H, H1), 1.33 (t, *J* = 5.4 Hz, 3H, H4'), 1.17 (m, 7.0 Hz, 6H, H2').

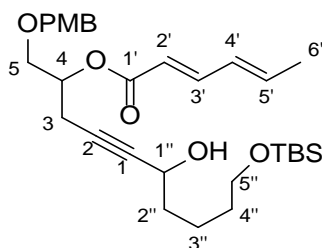
¹³C NMR (125 MHz, CDCl₃): δ 159.3 (C, *para*-PMB), 130.4 (C, *ipso*-PMB), 129.4 (CH, *ortho*-PMB), 113.9 (CH, *meta*-PMB), 100.0 (CH, C1' diastereomer 1), 99.7 (CH, C1' diastereomer 2), 81.1 (C, C2), 73.2 (CH₂, PMB), 73.0 (CH, C4), 71.5 (CH₂, C3' diastereomer 1), 71.4 (CH₂, C3' diastereomer 2), 70.0 (CH, C1), 60.6 (CH₂, C5 diastereomer 1), 60.4 (CH₂, C5 diastereomer 2), 55.4 (CH₃, PMB), 22.7 (CH₂, C3 diastereomer 1), 22.2 (CH₂, C3 diastereomer 2), 20.7 (CH₃, C2' diastereomer 1), 20.6 (CH₃, C2' diastereomer 2), 15.4 (CH₃, C4').

IR (neat) cm⁻¹: 3289, 2975, 2933, 1612, 1512, 1245, 1083, 819, 637.

HRMS (ESI⁺): calculated for C₁₇H₂₄O₄ [M+Na]⁺: 315.1567. Found 315.1552, Δ = -4.76 ppm.

9.5 Chapter 4: Connecting C15-C16: Alkynylation

(2E,4E)-10-((*tert*-Butyldimethylsilyl)oxy)-6-hydroxy-1-((4-methoxybenzyl)oxy)dec-4-yn-2-yl hexa-2,4-dienoate – 160



Prepared according to the general procedure for the **Alkynylation using Zn(alkyl)-*2*/ProPhenol/TPPO** using **155** (152 mg, 0.53 mmol, 1 eq.) and **147** (122 mg, 0.39 mmol, 2.8 eq.) as starting material. The crude material was subjected to FCC (10 g silica, gradient elution PE/EtOAc = 10/1 then 3/1 then 0/1) to yield the title compound as a colorless oil of inseparable diastereomers (36 mg, 49% yield, 97% BRSM).

TLC: R_f (PE/EtOAc = 3/1) = 0.56.

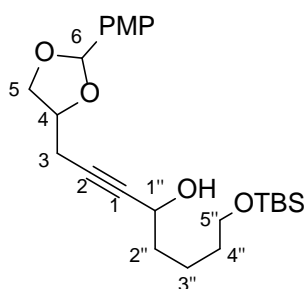
¹H NMR (500 MHz, CDCl₃): δ 7.26 (m, 3H, *ortho*-PMB and H3'), 6.87 (d, *J* = 8.5 Hz, 2H, *meta*-PMB), 6.24 – 6.09 (m, 2H, H4' and H5'), 5.78 (d, *J* = 15.1 Hz, 1H, H2'), 5.17 – 5.09 (m, 1H, H4), 4.49 (dd, *J* = 31.0, 11.6 Hz, 2H, CH₂-PMB), 4.29 (m, 1H, H1''), 3.81 (s, 3H, CH₃-PMB), 3.61 (m, 4H, H5 and H5''), 2.68 – 2.54 (m, 2H, H3), 1.86 (d, *J* = 3.7 Hz, 3H, H6'), 1.74 – 1.40 (m, 6H, H2'' and H3'' and H4''), 0.89 (s, 9H, TBS), 0.04 (s, 6H, TBS).

¹³C NMR (125 MHz, CDCl₃): δ 166.7 (C, C1'), 159.4 (C, *para*-PMB), 145.8 (CH, C3'), 140.0 (CH, C5'), 130.1 (C, *ipso*-PMB), 129.9 (CH, C4'), 129.5 (CH, *ortho*-PMB), 118.8 (CH, C2'), 113.9 (CH, *meta*-PMB), 83.5 (C, C1), 80.6 (C, C2), 73.1 (CH₂, PMB), 70.7 (CH₂, C5), 69.5 (CH, C4), 63.2 (CH₂, C5''), 62.7 (CH, C1''), 55.4 (CH₃, PMB), 37.8 (CH₂, C2''), 32.5 (CH₂, C4''), 26.1 (CH₃, TBS), 21.6 (CH₂, C3''), 21.4 (CH₂, C3), 18.9 (C, TBS), 18.5 (CH₃, C6'), -5.1 (CH₃, TBS).

IR (neat) cm^{-1} : 3411, 2930, 2858, 1717, 1518, 1245, 1172, 1092, 1032, 833, 775.

HRMS (ESI⁺): calculated for $\text{C}_{30}\text{H}_{46}\text{O}_6\text{Si}$ $[\text{M}+\text{Na}]^+$: 553.2956. Found 553.2983, $\Delta = 4.88$ ppm.

8-((tert-Butyldimethylsilyloxy)-1-(2-(4-methoxyphenyl)-1,3-dioxolan-4-yl)oct-2-yn-4-ol – 163



Prepared according to the general procedure for the **Alkynylation using Zn(alkyl)-₂/ProPhenol/TPPO** using **156** (30 mg, 0.14 mmol, 1 eq.) and **147** (85 mg, 0.39 mmol, 2.8 eq.) as starting material. The crude material was subjected to FCC (10 g silica, gradient elution PE/EtOAc = 3/1 then 1/1) and yielded the title compound as a colorless oil and usually as mixture of inseparable diastereomers (56 mg, 93% yield). A small fraction was subjected to careful FCC to separate the diastereomers for characterization purposes.

HRMS (ESI⁺): calculated for $\text{C}_{24}\text{H}_{38}\text{O}_5\text{Si}$ $[\text{M}+\text{H}]^+$: 435.2561. Found 435.2566, $\Delta = 1.15$ ppm.

Diastereomer 1

TLC: R_f (PE/EtOAc = 3/1) = 0.29.

¹H NMR (500 MHz, CDCl_3): δ 7.39 (d, $J = 8.6$ Hz, 2H, *ortho*-PMPs), 6.90 (d, $J = 8.5$ Hz, 2H, *meta*-PMPs), 5.92 (s, 1H, H6), 4.37 (m, 2H, H4 and H1''), 4.31 (dd,

$J = 8.0, 6.5$ Hz, 1H, H5a), 3.88 – 3.81 (m, 1H, H5b), 3.81 (s, 3H, CH₃-PMP), 3.62 (m, 2H, H5''), 2.66 (dd, $J = 16.7, 4.8$ Hz, 1H, H3a), 2.57 (dd, $J = 16.6, 7.4$ Hz, 1H, H3b), 1.92 (s, 1H, OH), 1.71 (m, 2H, H2''), 1.59-1.46 (m, 4H, H3'' and H4''), 0.89 (s, 9H, TBS), 0.05 (s, 6H, TBS).

¹³C NMR (125 MHz, CDCl₃): δ 160.5 (C, *para*-PMB), 130.0 (C, *ipso*-PMB), 128.0 (CH, *ortho*-PMB), 113.9 (CH, *meta*-PMP), 103.9 (CH, C6), 83.7 (C, C1), 80.4 (C, C2), 74.3 (CH, C4), 70.1 (CH₂, C5), 63.1 (CH₂, H5''), 62.7 (CH, C1''), 55.5 (CH₃, CH₃-PMP), 37.8 (CH₂, C2''), 32.5 (CH₂, C4''), 26.1 (CH₃, TBS), 23.6 (CH₂, C3), 21.7 (CH₂, C3''), 18.5 (C, TBS), -5.1 (CH₃, TBS).

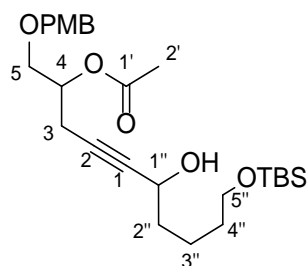
Diastereomer 2

TLC: R_f (PE/EtOAc = 3/1) = 0.26.

¹H NMR (500 MHz, CDCl₃): δ 7.39 (d, $J = 8.6$ Hz, 2H, *ortho*-PMPs), 6.90 (d, $J = 8.5$ Hz, 2H, *meta*-PMPs), 5.76 (s, 1H, H6), 4.37 (m, 2H, H4 and H1''), 4.12 (m, 1H, H5a), 3.99 (m, 1H, H5b), 3.81 (s, 3H, CH₃-PMP), 3.62 (m, 2H, H5''), 2.66 (dd, $J = 16.7, 4.8$ Hz, 1H, H3a), 2.57 (dd, $J = 16.6, 7.4$ Hz, 1H, H3b), 1.88 (s, 1H, OH), 1.71 (m, 2H, H2''), 1.59-1.46 (m, 4H, H3'' and H4''), 0.89 (s, 9H, TBS), 0.05 (s, 6H, TBS).

¹³C NMR (125 MHz, CDCl₃): δ 160.5 (C, *para*-PMB), 130.0 (C, *ipso*-PMB), 128.0 (CH, *ortho*-PMB), 113.9 (CH, *meta*-PMP), 104.5 (CH, C6), 83.2 (C, C1), 80.4 (C, C2), 74.6 (CH, C4), 69.5 (CH₂, C5), 63.1 (CH₂, C5''), 62.7 (CH, C1''), 55.5 (CH₃, CH₃-PMP), 37.7 (CH₂, C2''), 32.4 (CH₂, C4''), 26.0 (CH₃, TBS), 24.2 (CH₂, C3), 21.4 (CH₂, C3''), 18.4 (C, TBS), -5.3 (CH₃, TBS).

10-((tert-Butyldimethylsilyl)oxy)-6-hydroxy-1-((4-methoxybenzyl)oxy)dec-4-yn-2-yl acetate – 162



Prepared according to the general procedure for **Alkynylation using Zn(alkyl)₂/ProPhenol/TPPO** using **157** (30 mg, 0.14 mmol) and **147** (102 mg, 0.34 mmol) as starting material. The crude material was subjected to FCC (10 g silica, gradient elution PE/EtOAc = 10/1 then 3/1 then 0/1) and yielded the title compound as a colorless liquid of inseparable diastereomers (63 mg, 95% yield).

TLC: R_f (PE/EtOAc = 2/1) = 0.41.

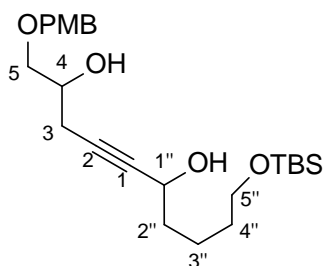
¹H NMR (500 MHz, CDCl₃): δ 7.26 (d, *J* = 8.2, 2H, *ortho*-PMB), 6.88 (d, *J* = 8.7 Hz, 2H, *meta*-PMB), 5.07 (m, 1H, H₄), 4.52 (d, *J* = 12.2 Hz, 1H, CH₂-PMB), 4.46 (d, *J* = 11.7 Hz, 1H, CH₂-PMB), 4.30 (m, 1H, H_{1''}), 3.81 (s, 3H, CH₃-PMB), 3.66 – 3.53 (m, 4H, H₅ and H_{5''}), 2.58 (m, 2H, H₃), 2.08 (s, 3H, H_{2'}), 1.81 – 1.37 (m, 6H, H_{2''} and H_{3''} and H_{4''}), 0.9 (s, 9H, TBS), 0.1 (s, 6H TBS).

¹³C NMR (125 MHz, CDCl₃): δ 170.6 (C, C_{1'}), 159.4 (C, *para*-PMB), 130.0 (C, *ipso*-PMB), 129.5 (CH, *ortho*-PMB), 113.9 (CH, *meta*-PMB), 83.5 (C, C₁), 80.4 (C, C₂), 73.1 (CH₂, CH₂-PMB), 70.9 (CH, C₄), 69.4 (CH₂, C₅), 63.2 (CH₂, C_{5''}), 62.7 (CH, C_{1''}), 55.4 (CH₃, CH₃-PMB), 37.8 (C_{2''}), 32.5 (C_{4''}), 26.1 (CH₃, TBS), 21.7 (CH₂, C_{3''}), 21.3 (CH₃, C_{2'}), 21.3 (CH₂, C₃), 18.5 (C, TBS), -5.1 (CH₃, TBS).

IR (neat) cm⁻¹: 3433, 2930, 2857, 1740, 1513, 1239, 1093, 1034, 833, 774.

HRMS (ESI⁺): calculated for C₂₆H₄₂O₆Si [M+H]⁺: 479.2823. Found 479.2801, Δ = -4.59 ppm.

10-((Tert-butyltrimethylsilyloxy)-1-((4-methoxybenzyl)oxy)dec-4-yne-2,6-diol –
164



Prepared according to the general procedure for **Alkynylation using MeLi** at room temperature using **116** (100 mg, 0.45 mmol, 1 eq.) and **147** (108 mg, 0.50 mmol, 1.1 eq.) as starting material. The crude material was subjected to FCC (10 g silica, gradient elution PE/EtOAc = 10/1 then 3/1 then 0/1) and yielded the title compound as a colorless oil of inseparable diastereomers (66 mg, 33% yield, 80% BRSM).

TLC: R_f (PE/EtOAc = 2/1) = 0.17.

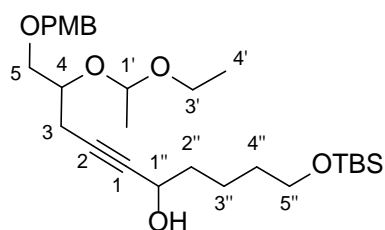
¹H NMR (500 MHz, CDCl₃): δ 7.27 (d, *J* = 11.2 Hz, 2H, *ortho*-PMB), 6.89 (d, *J* = 11.2 Hz, 2H, *meta*-PMB), 4.50 (s, 2H, CH₂-PMB), 4.35 (m, 1H, H1''), 3.92 (m, 1H, H4), 3.82 (s, 3H, CH₃-PMB), 3.65-3.59 (m, 2H, H5''), 3.59 – 3.53 (m, 1H, H5a), 3.49-3.43 (m, 1H, H5b), 2.46 (m, 2H, H3), 1.85 – 1.44 (m, 6H, H2'' and H3'' and H4''), 0.90 (s, 9H, TBS), 0.06 (s, 6H, TBS).

¹³C NMR (125 MHz, CDCl₃): δ 159.5 (C, *para*-PMB), 130.0 (C, *ipso*-PMB) 129.6 (CH, *ortho*-PMB), 114.0 (CH, *meta*-PMB), 83.7 (C, C1), 81.1 (C, C2), 73.2 (CH₂, CH₂-PMB), 72.7 (CH₂, C5), 69.1 (CH, C4), 63.2 (CH₂, C5''), 62.7 (CH, C1''), 55.4 (CH₃, CH₃-PMB), 37.8 (CH₂, C2''), 32.5 (CH₂, C4''), 26.1 (CH₃, TBS), 23.9 (CH₂, C3) 21.7 (CH₂, C3''), 18.5 (C, TBS), -5.1 (CH₃, TBS).

IR (neat) cm⁻¹: 3402, 2929, 2857, 1513, 1248, 1096, 1035, 835, 776.

HRMS (ESI⁺): calculated for C₂₄H₄₀O₅Si: 459.2537. Found 459.2556. [M+Na]⁺, Δ = 4.08 ppm.

13-(((4-methoxybenzyl)oxy)methyl)-2,2,3,3,15-pentamethyl-4,14,16-trioxa-3-silaoctadec-10-yn-9-ol – 166



Prepared according to the general procedure for **Alkynylation using MeLi** at room temperature using **158** (40.0 mg, 0.14 mmol, 1 eq.) and **147** (38 mg, 0.15 mmol, 1.1 eq.) as starting material. The crude material was subjected to FCC (10 g silica, gradient elution PE/EtOAc = 10/1 then 3/1 then 0/1) and yielded the title compound as a colorless oil of inseparable diastereomers (43 mg, 58% yield).

TLC: R_f (PE/EtOAc = 1/1) = 0.81.

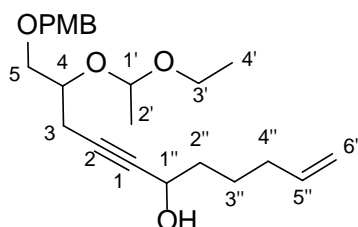
¹H NMR (500 MHz, CDCl₃): δ 7.28 (d, J = 8.0 Hz, 2H, ortho-PMB), 6.88 (dd, J = 8.5, 2.4 Hz, 2H, para-PMB), 4.90 – 4.83 (m, 1H, H1'), 4.49 (s, 2H, CH₂-PMB), 4.32 (t, J = 6.1 Hz, 1H, H1''), 3.89 (m, 1H, H4), 3.81 (s, 2H, CH₃-PMB), 3.70 – 3.46 (m, 6H, H5 & H3' & H5''), 2.58-2.41 (m, 1H, H3), 1.72-1.62 (m, 2H, H2''), 1.60 – 1.51 (m, 2H, H4''), 1.51-1.44 (m, 2H, H3''), 1.33 (t, J = 5.4 Hz, 3H, H2'), 1.23 – 1.13 (m, 3H, H4'), 0.90 (s, 9H, TBS), 0.06 (s, 6H, TBS).

¹³C NMR (125 MHz, CDCl₃): δ 159.2 (C, para-PMB), 130.3 (C, ipso-PMB), 129.3 (CH, ortho-PMB), 113.7 (CH, meta-PMB), 99.9 (C, C1 diastereomer 1), 99.5 (C, C1 diastereomer 2), 82.9 (C, C2 diastereomer 1), 81.7 (C, C2 diastereomer 2), 73.5 (CH, C4 diastereomer 1), 73.2 (CH, C4 diastereomer 2), 73.0 (CH₂, PMB), 71.4, 63.1 (CH₂, C5''), 62.5 (CH, C1''), 60.6 (CH₂, C3' diastereomer 1), 60.2 (CH₂, C3' diastereomer 2), 55.3 (CH₃, PMB), 37.7 (CH₂, C2''), 32.4 (CH₂, C4''), 26.0 (CH₃, TBS), 22.7 (CH₂, C3 diastereomer 1), 22.2 (CH₂, C3 diastereomer 2), 21.6 (CH₂, C3''), 20.6 (CH₃, C2' diastereomer 1), 20.5 (CH₃, C2' diastereomer 2), 18.4 (C, TBS), 15.3 (CH₃, C4'), -5.26 (CH₃, TBS).

IR (neat) cm^{-1} : 3449, 2930, 2857, 1720, 1513, 1248, 1093, 1035, 833, 775.

HRMS (ESI⁺): calculated for $\text{C}_{28}\text{H}_{48}\text{O}_6\text{Si}$ $[\text{M}+\text{Na}]^+$: 531.3112. Found 531.3107, $\Delta = -0.93$ ppm.

***(Z)*-7-(2-(1-Ethoxyethoxy)-3-((4-methoxybenzyl)oxy)propyl)tetradeca-1,7,13-triene-6,9-dione – 167**



Prepared according to the general procedure for **Alkynylation using MeLi** at room temperature using **158** (1.0 g, 3.42 mmol, 1 eq.) and **144** (crude product, 10.26 mmol, 3.1 eq.) as starting material. The crude material was subjected to FCC (10 g silica, gradient elution PE/EtOAc = 10/1 then 3/1 then 0/1) and yielded the title compound as a colorless oil of inseparable diastereomers (912 mg, 53% yield).

TLC: R_f (PE/EtOAc = 3/1) = 0.33.

¹H NMR (500 MHz, CDCl_3): δ 7.26 (d, $J = 7.5$ Hz, 2H, *ortho*-PMB), 6.88 (d, $J = 7.9$ Hz, 2H, *meta*-PMB), 5.80 (m, 1H, H5''), 4.99 (m, 2H, H6''), 4.85 (m, 1H, H1'), 4.48 (s, 2H, CH_2 -PMB), 4.32 (m, 1H, H1''), 3.88 (m, 1H, H4), 3.81 (s, 3H, CH_3 -PMB), 3.73 – 3.61 (m, 1H, H3'a), 3.60 – 3.43 (m, 3H, H3'b and H5), 2.56 – 2.50 (m, 2H, H3), 2.12 – 2.03 (m, 2H, H4''), 1.67 – 1.58 (m, 2H, H2''), 1.58 – 1.49 (m, 2H, H3''), 1.33 (t, $J = 5.2$ Hz, 3H, H4'), 1.17 (m, 3H, H2').

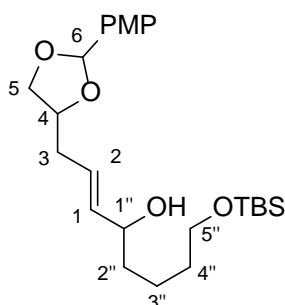
^{13}C NMR (125 MHz, CDCl_3): δ 159.2 (C, *para*-PMB), 138.4 (CH, C5''), 130.2 (C, *ipso*-PMB), 129.33 (CH, C5''), 129.27 (CH_2 , *ortho*-PMB), 114.8 (CH_2 , C6''), 113.7 (CH, *meta*-PMB), 99.9 (CH, C1' diastereomer 1), 99.5 (CH, C1' diastereomer 2), 82.8 (C, C1), 81.8 (C, C2), 73.4 (CH, C4), 73.0 (CH_2 , CH_2 -PMB), 71.3 (CH_2 , C5), 62.5 (CH, C1''), 60.6 (CH_2 , C3' diastereomer 1), 60.2 (CH_2 , C3' diastereomer 2), 55.3 (CH_3 , CH_3 -PMB), 37.4 (CH_2 , C2''), 33.3 (CH_2 , C4''), 24.4 (CH_2 , C3''), 22.7 (CH_2 , C3 diastereomer 1), 22.2 (CH_2 , C3 diastereomer 2), 20.6 (CH_3 , C2''), 15.3 (CH_3 , C4').

IR (neat) cm^{-1} : 2933, 2213, 1672, 1513, 1246, 1085, 1033, 819.

HRMS (ESI⁺): calculated for $\text{C}_{23}\text{H}_{34}\text{O}_5$ $[\text{M}+\text{NH}_4]^+$: 408.2745. Found 408.2741, $\Delta = -0.86$ ppm.

9.6 Chapter 5: Conversion of the C16-C17 Alkyne to an Alkene: Reducti(ve methylati)on

(E)-8-((*Tert*-butyldimethylsilyl)oxy)-1-(2-(4-methoxyphenyl)-1,3-dioxolan-4-yl)oct-2-en-4-ol – 170



Prepared according to the general procedure for **Alkyne Reduction Using Vitride®® (adapted)** using **163** (50 mg, 0.12 mmol, 1 eq.) as starting material. The crude material was subjected to FCC (10 g silica, gradient elution PE/EtOAc = 3/1 then 0/1) and yielded the title compound as a colorless oil of inseparable diastereomers (50 mg, quantitative yield).

TLC: Rf (PE/EtOAc = 3/1) = 0.26.

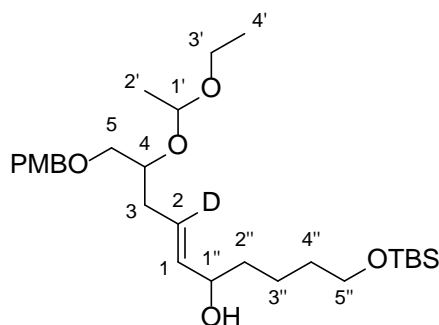
¹H NMR (500 MHz, CDCl₃): δ 7.40 (m, 2H, *ortho*-PMB), 6.90 (dd, *J* = 8.5, 3.4 Hz, 2H, *meta*-PMB), 5.88 (s, 1H, H6 diastereomer 1), 5.75 (s, 1H, H6 diastereomer 2), 5.68 (m, 1H, H2), 5.63 (m, 1H, H1), 4.25 (m, 2H, H4 and H5a diastereomer 1), 4.06 (m, 2H, H1'' and H5a diastereomer 2), 3.81 (s, 3H, CH₃-PMB), 3.76 (m, 1H, H5b diastereomer 2), 3.65 (m, 1H, H5b diastereomer 1), 3.61 (m, 2H, H5''), 2.50 (m, 1H, H3a), 2.38 (m, 1H, H3b), 1.62-1.47 (m, 4H, H2'' & H4''), 1.45 – 1.35 (m, 2H, H3''), 0.89 (s, 9H, TBS), 0.04 (s, 6H, TBS).

¹³C NMR (125 MHz, CDCl₃): δ 160.4 (C, *para*-PMB diastereomer 1), 160.3 (C, *para*-PMB diastereomer 2), 136.4 (CH, C1), 128.7 (C, *ipso*-PMB), 128.1 (CH, *ortho*-PMB), 126.0 (CH, C2), 113.7 (CH, *meta*-PMB), 104.1 (CH, C6 diastereomer 2), 103.3 (CH, C6 diastereomer 1), 75.5 (CH, C1''), 72.70 (CH, C4), 70.1 (CH₂, C5 diastereomer 1), 69.5 (CH₂, C5 diastereomer 2), 63.1 (CH₂, C5''), 55.3 (CH₃, CH₃-PMB), 36.9 (CH₂, C2''), 36.5 (CH₂, C3), 32.6 (CH₂, C4''), 26.0 (CH₃, TBS), 21.7 (CH₂, C3''), 18.4 (C, TBS), -5.3 (CH₃, TBS).

IR (neat) cm⁻¹: 3439, 2929, 2856, 1739, 1516, 1248, 1081, 1032, 829, 774.

HRMS (ESI⁺): calculated for C₂₄H₄₀O₅Si [M+K]⁺: 475.2277. Found 475.2291, Δ = -2.47 ppm.

Deuterated (E)-13-(((4-methoxybenzyl)oxy)methyl)-2,2,3,3,15-pentamethyl-4,14,16-trioxa-3-silaoctadec-10-en-9-ol – 172



Prepared according to the general procedure for **Alkyne Reduction Using Vitride®® (adapted)** using **166** (50.0 mg, 0.12 mmol, 1 eq.) as starting material and D₂O as reagent. The crude material was subjected to FCC (10 g silica, gradient elution PE/EtOAc = 5/1 then 3/1 then 0/1) and yielded the title compound as a colorless oil (13 mg, 29% yield) along with proton quenched material **171** (10 mg) as well as recovered starting material of inseparable diastereomers (12 mg).

TLC: R_f (PE/EtOAc = 1/1) = 0.76.

¹H NMR (500 MHz, CDCl₃): δ 7.25 (dd, *J* = 5.5, 3.4 Hz, 1H, *ortho*-PMB), 6.91 – 6.84 (m, 2H, *meta*-PMB), 5.55 – 5.48 (dd, *J* = 17.8 Hz, 6.6 Hz, 1H, H1), 4.83 (m, H1' diastereomer 1), 4.76 (q, *J* = 5.3 Hz, 0.5 H, H1' diastereomer 2), 4.50 – 4.42 (m, 2H, CH₂-PMB), 4.09-4.00 (m, 1H, H1'') 3.87-3.72 (m, 4H, CH₃-PMB and H4), 3.67-3.55 (m, 3H, H5'' and H3'a), 3.51 – 3.38 (m, 3H, H3'b and H5), 2.39 – 2.18 (m, 2H, H3), 1.56 – 1.48 (m, 4H, H2'' and H3''), 1.30 (t, *J* = 4.8 Hz, 3H, H4'), 1.16 (m, 3H, H2'), 0.88 (s, 9H, TBS), 0.04 (s, 6H, TBS).

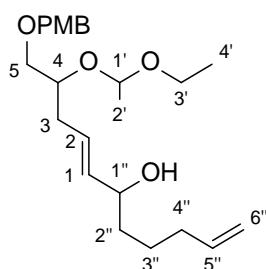
¹³C NMR (125 MHz, CDCl₃): δ 159.2 (C, *para*-PMB), 135.6 (CH, C1 diastereomer 1), 135.7 (CH, C1 diastereomer 2), 130.4 (c, *ipso*-PMB diastereomer 1), 130.3 (C, *ipso*-PMB diastereomer 2), 129.5 (CH, *ortho*-PMB diastereomer 1), 129.4 (CH, *ortho*-PMB diastereomer 2), 113.7 (C, *meta*-PMB diastereomer 1), 113.7 (C, *meta*-PMB diastereomer 2), 99.8 (CH, C1' diastereomer 1), 99.4 (CH, C1' diastereomer 2), 74.7 (CH, C4 diastereomer 1), 74.6 (CH, C4 diastereomer 2), 73.0 (CH₂, PMB), 72.8 (CH, C1''), 72.1 (CH₂, C3' diastereomer 1), 71.9 (CH₂, C3')

diastereomer 2), 60.5 (CH₂, C5 diastereomer 1), 60.0 (CH₂, C5 diastereomer 2), 55.4 (CH₃, CH₃-PMB), 36.9 (CH₂, C2''), 35.4, (CH₂, C3 diastereomer 1), 34.9 (CH₂, C3 diastereomer 2), 32.7 (CH₂, C4''), 26.0 (CH₃, TBS), 21.7 (CH₂, C3''), 20.5 (CH₃, C4'), 18.5 (C, TBS), 15.5 (CH₃, C2' diastereomer 1), 15.4 (CH₃, C2' diastereomer 2), -5.3 (CH₃, TBS).

IR (neat) cm⁻¹: 3454, 2930, 2857, 2363, 1738, 1514, 1249, 1096, 1036, 835, 776.

HRMS (ESI⁺): calculated for C₂₈H₄₉DO₆Si [M+NH₄]⁺: 529.3793. Found 529.3790, Δ = 1.2 ppm.

***(E)*-10-(1-Ethoxyethoxy)-11-((4-methoxybenzyl)oxy)undeca-1,7-dien-6-ol – 174**



Prepared according to the general procedure for **Alkyne Reduction Using Vitride®® (adapted)** using **167** (500 mg, 1.28 mmol, 1 eq.) as starting material. The crude material was subjected to FCC (10 g silica, gradient elution PE/EtOAc = 5/1 then 3/1 then 0/1) and yielded the title compound as a colorless oil of inseparable diastereomers (489 mg, 97% yield).

TLC: R_f (PE/EtOAc = 3/1) = 0.30.

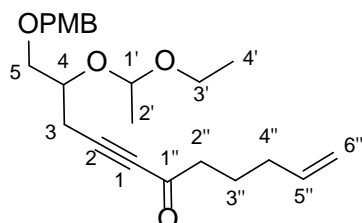
¹H NMR (500 MHz, CDCl₃): δ 7.24 (dd, J = 8.9, 3.3 Hz, 2H, ortho-PMB), 6.87 (dd, J = 8.9, 2.7 Hz, 2H, meta-PMB), 5.78 (m, 1H, H5''), 5.68-5.57 (m, 1H, H2), 5.5 (dd, J = 15.5, 6.5 Hz, 1H, H1), 5.03-4.92 (m, 2H, H6''), 4.82 (m, 1H, H1' diastereomer 1), 4.76 (m, 1H, H1' diastereomer 1), 4.44 (d, J = 5.8 Hz, 2H, CH₂-PMB), 4.02 (m, 1H,

H1''), 3.8 (s, 3H, CH₃-PMB), 3.79-3.73 (m, 1H, H4), 3.66-3.58 (m, 1H, H3'a), 3.51-3.37 (m, 3H, H3'b & H5), 2.36-2.19 (m, 2H, C3), 2.09-2.00 (m, 2H, H4''), 1.56-1.34 (m, 4H, H2'' & H3''), 1.29 (t, J = 5.1 Hz, 2H, H4''), 1.16 (dt, J = 12.9, 6.8 Hz, 3H, H2'').

¹³C NMR (125 MHz, CDCl₃): δ 159.3 (C, *para*-PMB diastereomer 1), 159.2 (C, *para*-PMB diastereomer 2), 138.6 (CH, C5''), 136.1 (CH, C1 diastereomer 1), 136.0 (CH, C1 diastereomer 2), 130.3 (C, *ipso*-PMB diastereomer 1), 130.0 (C, *ipso*-PMB diastereomer 2), 129.4 (CH, *ortho*-PMB diastereomer 1), 129.2 (CH, *ortho*-PMB diastereomer 2), 127.7 (CH, C2 diastereomer 1), 127.0 (CH, C2 diastereomer 2), 114.6 (CH₂, C6''), 113.9 (CH₂, CH₂-PMB diastereomer 1), 113.9 (CH₂, CH₂-PMB diastereomer 1), 99.8 (CH, C1' diastereomer 1), 99.4 (CH, C1' diastereomer 2), 74.7 (CH, C4 diastereomer 1), 74.6 (CH, C4 diastereomer 2), 73.5 (CH₂, C5 diastereomer 1), 73.0 (CH₂, CH₂-PMB), 72.8 (CH, C1''), 72.0 (CH₂, C5 diastereomer 2), 60.5 (CH₂, C3' diastereomer 1), 60.1 (CH₂, C3' diastereomer 2), 55.3 (CH₃, CH₃-PMB), 36.6 (CH₂, C2''), 35.6 (CH₂, C3), 33.5 (CH₂, C4''), 24.7 (CH₂, C3''), 20.4 (CH₃, C2''), 15.3 (CH₃, C4'').

HRMS (ESI⁺): calculated for C₂₃H₃₆O₆ [M+Na]⁺: 431.2404. Found 431.2421, Δ = 3.90 ppm.

10-(1-Ethoxyethoxy)-11-((4-methoxybenzyl)oxy)undec-1-en-7-yn-6-one – 181



Prepared according to the general procedure for **Manganese dioxide oxidation** using **167** (50 mg, 0.13 mmol, 1 eq.) as starting material. The crude material was subjected to FCC (10 g silica, gradient elution PE/EtOAc = 5/1 then 3/1 then 0/1)

and yielded the title compound as a colorless oil of inseparable diastereomers (43 mg, 87% yield).

TLC: Rf (PE/EtOAc = 3/1) = 0.67.

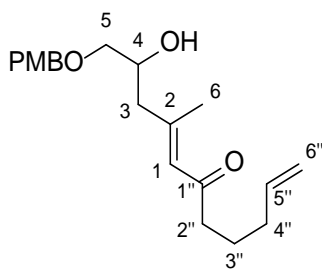
¹H NMR (500 MHz, CDCl₃): δ 7.25 (d, *J* = 8.2 Hz, 2H, *ortho*-PMB), 6.87 (dd, *J* = 8.6, 1.9 Hz, 2H, *meta*-PMB), 5.82 – 5.70 (m, 1H, H5''), 5.06 – 4.98 (m, 2H, H6''), 4.83 (q, *J* = 5.3 Hz, 1H, H1'), 4.48 (s, 2H, CH₂-PMB), 3.94 (m, 1H, H4), 3.80 (s, 3H, CH₃-PMB), 3.69 – 3.62 (m, 1H, H3'a), 3.61-3.58 (dd, *J* = 9.1, 5.1 Hz, 0.5 H, H5a diastereomer 1), 3.54-3.44 (m, 2.5 H, H3'b and H5b and H5a diastereomer 2), 2.77 – 2.66 (m, 1.5H, H5a diastereomer 1 and H5b), 3.62 (dd, *J* = 11.8, 5.9 Hz, 0.5 H, H5a diastereomer 2) 2.50 (t, *J* = 8.0 Hz, 2H, H2''), 2.07 (q, *J* = 7.2 Hz, 2H, H4''), 1.73 (p, *J* = 7.5 Hz, 2H, H3''), 1.35 – 1.29 (m, 3H, H2'), 1.17 (m, 3H, H4').

¹³C NMR (125 MHz, CDCl₃): δ 187.9 (C, C1''), 159.4 (C, *para*-PMB), 137.8 (CH, C5'' diastereomer 1), 137.8 (CH, C5'' diastereomer 2), 130.1 (C, *ipso*-PMB), 129.5 (CH, *ortho*-PMB diastereomer 1), 129.5 (CH, *ortho*-PMB diastereomer 2), 115.6 (CH₂, C6'' diastereomer 1), 115.6 (CH₂, C6'' diastereomer 2), 113.9 (CH, *meta*-PMB diastereomer 1), 113.9 (CH, *meta*-PMB diastereomer 2), 100.0 (CH, C1' diastereomer 1), 99.8 (CH, C1' diastereomer 2), 90.6 (C, C1), 82.1 (C, C2), 73.3 (CH₂, CH₂-PMB), 72.5 (CH, C4 diastereomer 1), 72.5 (CH, C4 diastereomer 2), 71.2 (CH₂, C5 diastereomer 1), 71.0 (CH₂, C5 diastereomer 2), 60.7 (CH₂, C3' diastereomer 1), 60.5 (CH₂, C3' diastereomer 2), 55.4 (CH₃, CH₃-PMB), 44.8 (CH₂, C2'' diastereomer 1), 44.8 (CH₂, C2'' diastereomer 2), 33.0 (CH₂, C4''), 23.3 (CH₂, C2'' diastereomer 1), 23.2 (CH₂, C3'' diastereomer 1), 23.2 (CH₂, C3'' diastereomer 2), 22.8 (CH₂, C2'' diastereomer 2), 20.6 (CH₃, C2', diastereomer 1), 20.5 (CH₃, C2', diastereomer 2), 15.4 (CH₃, H4' diastereomer 1), 15.4 (CH₃, H4' diastereomer 2).

IR (neat) cm⁻¹: 2932, 2363, 2214, 1738, 1673, 1513, 1366, 1248, 1094, 822.

HRMS (ESI⁺): calculated for C₂₃H₃₂O₅ [M+NH₄]⁺: 406.2588. Found 406.2600, Δ = 2.9 ppm.

(E)-10-Hydroxy-11-((4-methoxybenzyl)oxy)-8-methylundeca-1,7-dien-6-one
SOGE-186



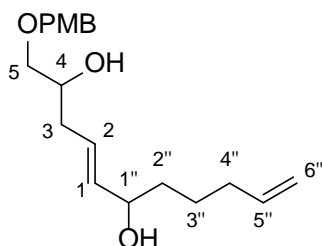
Prepared according to the general procedure for **Alkyne Reduction Using Gilman Reagent** using SOGE-133 (50.0 mg, 0.115 mmol, 1 eq.) as starting material. The crude material was then stirred with PPTS in MeOH at room temperature to remove the EE protecting group. Water and EtOAc are added and the aqueous layer was extracted with EtOAc (3x). The combined organic layers were dried over magnesium sulfate, filtered and the solvent was evaporated. The crude mixture was then subjected to FCC (silica, 10 g, PE/EtOAc = 3/1) to yield the title compound as colorless oil (28 % yield).

TLC: R_f (PE/EtOAc = 3/1) = 0.21.

¹H NMR (500 MHz, CDCl₃): δ 7.25 (d, *J* = 8.4 Hz, 2H, *ortho*-PMB), 6.89 (d, *J* = 8.7 Hz, 2H, *meta*-PMB), 6.10 (s, 1H, H1), 5.77 (m, 1H, H5''), 5.05 – 4.93 (m, 2H, H6''), 4.48 (s, 2H, CH₂-PMB), 4.01 (m, 1H, H4), 3.80 (s, 3H, CH₃-PMB), 3.51 – 3.43 (m, 1H, H5a), 3.34 (m, 1H, H5b), 2.45 – 2.38 (t, *J* = 7.5 Hz, 2H, H4''), 2.26 (t, *J* = 6.5 Hz, 2H, H3), 2.06 (p, *J* = 6.3 Hz, 2H, H4''), 1.82 (s, 1H, OH), 1.77 (s, 2H, H3''), 1.69 (m, 2H, H3'').

¹³C NMR (125 MHz, CDCl₃): δ 200.9 (C, C1''), 159.4 (C, *para*-PMB), 153.9 (C, C2), 138.2 (CH, C5''), 129.8 (C, *ipso*-PMB), 129.5 (CH, *ortho*-PMB), 125.5 (CH, C1), 115.1 (CH₂, C6), 113.9 (*meta*-PMB), 73.6 (CH₂, C5), 73.1 (CH₂, PMB), 68.3 (CH, C4), 55.3 (CH₃, PMB), 44.9 (CH₂, H3), 43.6 (CH₂, H2''), 33.2 (CH₂, H4''), 23.2 (H3''), 19.5 (CH₃, C6), 15.44.

(E)-1-((4-Methoxybenzyl)oxy)undeca-4,10-diene-2,6-diol – 190



A one-necked RBF was charged with a solution of the **174** (141 mg, 0.36 mmol, 1 eq.) in DMF (0.9 ml) and cooled to 0 °C. TBSCl (60 mg, 0.40 mmol, 1.1 eq.) and imidazole (30 mg, 0.43 mmol, 1.2 eq.) were added to the solution and the cold bath was removed. The solution was allowed to stir for two days at room temperature before it was quenched with water. EtOAc was added and the phases were separated. The aqueous layer was extracted with EtOAc (3x) and the combined organic layers were dried over MgSO₄, filtered and the solvent was removed under reduced pressure to yield the product as a crude mixture which was used directly in the next step. The double protected material was stirred with PPTS in MeOH overnight to remove the EE protecting group. Water and EtOAc were added to the solution and the phases were separated. The aqueous layer was extracted with EtOAc (3x) and the combined organic layers were dried over magnesium sulfate, filtered and the solvent was removed under reduced pressure. The crude mixture was purified *via* FCC (10 g silica, PE/EtOAc = 1/1) and yielded the title compound as a colorless oil of inseparable diastereomers (85 mg, 74% yield over 2 steps).

TLC: R_f (PE/EtOAc = 3/1) = 0.16.

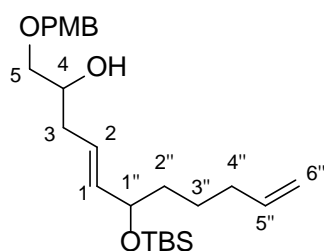
¹H NMR (500 MHz, CDCl₃): δ 7.25 (d, *J* = 6.7 Hz, 2H, *ortho*-PMB), 6.89 (d, *J* = 8.4 Hz, 2H, *meta*-PMB), 5.86 – 5.74 (m, 1H, H5''), 5.65 (dt, *J* = 12.6, 6.2 Hz, 1H, H2), 5.58 – 5.51 (m, 1H, H1), 4.97 (m, 2H, H6'), 4.48 (s, 2H, CH₂-PMB), 4.07 (m, 1H, H1''), 3.84 (m, 1H, H4), 3.81 (s, 3H, CH₃-PMB), 3.48 (dt, *J* = 9.3, 3.1 Hz, 1H, H5a), 3.36 – 3.29 (m, 1H, H5b), 2.23 (t, *J* = 6.5 Hz, 3H, H3), 2.07 (dd, *J* = 13.3, 6.8 Hz, 2H, H4''), 1.56 – 1.35 (m, 4H, H2'' and H3'').

^{13}C NMR (125 MHz, CDCl_3): δ 159.3 (C, *para*-PMB), 138.6 (CH, C5''), 136.2 (CH, C1), 129.9 (C, *ipso*-PMB), 129.4 (CH, *ortho*-PMB), 127.1 (CH, C2), 114.6 (CH_2 , C6''), 113.8 (CH_2 , CH_2 -PMB), 73.6 (CH_2 , C5), 73.0 (CH_2 , CH_2 -PMB), 69.9 (CH, C4), 55.3 (CH_3 , CH_3 -PMB), 36.6 (CH_2 , C2''), 36.2 (CH_2 , C3), 33.6 (CH_2 , C4''), 24.7 (CH_2 , C3'').

IR (neat) cm^{-1} : 3458, 2929, 2856, 1724, 1513, 1248, 1084, 1037, 835, 776.

HRMS (ESI⁺): calculated for $\text{C}_{19}\text{H}_{28}\text{O}_4$ $[\text{M}+\text{Na}]^+$: 343.1880. Found 343.1895, $\Delta = 4.39$ ppm.

(E)-6-((*Tert*-butyldimethylsilyl)oxy)-1-((4-methoxybenzyl)oxy)undeca-4,10-dien-2-ol – 191



A one-necked RBF was charged with **190** (85 mg, 0.27 mmol, 1 eq.) in DMF (1 mL) and cooled to 0 °C. TBSCl (44 mg, 0.29 mmol, 1.1 eq.) and imidazole (22 mg, 0.32 mmol, 1.2 eq.) were added and the solution was allowed to come room temperature and stirred at this temperature overnight. On the next day, the reaction was quenched with water and EtOAc was added. The phases were separated and the aqueous layer was extracted with EtOAc (3x). The combined organic layers were dried over magnesium sulfate, filtered and the solvent was removed under reduced pressure. The crude mixture was subjected to FCC (silica, 10 g, PE/EtOAc = 3/1) and yielded the title compound as a colorless oil of inseparable diastereomers (46 mg, 40% yield, 98% yield BRSM).

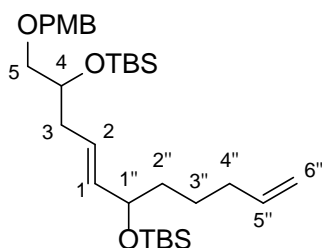
TLC: Rf (PE/EtOAc = 1/1) = 0.63.

¹H NMR (500 MHz, CDCl₃): δ 7.25 (m, 2H, *ortho*-PMB), 6.88 (d, *J* = 8.6 Hz, 2H, *meta*-PMB), 5.85 – 5.73 (m, 1H, H5''), 5.59 – 5.44 (m, 2H, H1 and H2), 5.03 – 4.90 (m, 2H, H6''), 4.48 (s, 2H, CH₂-PMB), 4.07 – 4.01 (m, 1H, H1''), 3.87 – 3.81 (m, 1H, H4), 3.81 (s, 3H, CH₃-PMB), 3.47 (ddd, *J* = 9.2, 5.7, 3.3 Hz, 1H, H5a), 3.36 – 3.28 (m, 1H, H5b), 2.24 – 2.18 (m, 2H, H3), 2.04 (m, 2H, H4''), 1.53 – 1.32 (m, 4H, C2'' and C3''), 0.88 (s, 9H), 0.03 (s, 3H, TBS), 0.01 (s, 3H, TBS).

¹³C NMR (125 MHz, CDCl₃): δ 159.4 (C, *para*-PMB), 139.0 (CH, C5''), 137.1 (CH, C1), 130.2 (*ipso*-PMB), 129.5 (CH, *ortho*-PMB), 125.3 (CH, H2), 114.6 (CH₂, C6''), 114.0 (CH, *meta*-PMB), 73.8 (CH₂, C5 diastereomer 1), 73.7 (CH₂, C5 diastereomer 2), 73.4 (CH, C1''), 73.2 (CH₂, CH₂-PMB) 70.2 (CH, C4 diastereomer 1), 70.2 (CH, C4 diastereomer 2), 55.4 (CH₃, CH₃-PMB), 37.9 (CH₂, C2''), 36.4 (CH₂, C3), 33.8 (CH₂, C4''), 26.1 (CH₃, TBS), 24.8 (CH₂, C3''), 18.4 (C, TBS), -4.1 (CH₃, TBS), -4.6 (CH₃, TBS).

HRMS (ESI⁺): calculated for C₂₅H₄₂O₄Si [M+NH₄]⁺: 452.3191. Found 452.3197, Δ = 1.42 ppm.

(*E*)-9-(((4-Methoxybenzyl)oxy)methyl)-2,2,3,3,11,11,12,12-octamethyl-5-(pent-4-en-1-yl)-4,10-dioxo-3,11-disilatridec-6-ene – 192



A one-necked RBF was charged with **190** (51.0 mg, 0.159, 1 eq.) in DMF (1 mL) and cooled to 0 °C. TBSCl (44 mg, 0.29 mmol, 1.8 eq.) and imidazole (22 mg, 0.32 mmol, 2.0 eq.) were added and the solution was allowed to come room

temperature and stirred at this temperature overnight. On the next day, the reaction was quenched with water and EtOAc was added. The phases were separated and the aqueous layer was extracted with EtOAc (3x). The combined organic layers were dried over magnesium sulfate, filtered and the solvent was removed under reduced pressure. The crude mixture was subjected to FCC (silica, 10 g, PE/EtOAc = 3/1) and yielded the title compound as a colorless oil of inseparable diastereomers (46 mg, 65% yield).

TLC: R_f (PE/EtOAc = 3/1) = 0.66.

¹H NMR (500 MHz, CDCl₃): δ 7.26 (d, *J* = 8.1 Hz, 2H, *ortho*-PMB), 6.88 (d, *J* = 8.4 Hz, 2H, *meta*-PMB), 5.80 (m, 1H, H5''), 5.55 (m, 1H, H2), 5.43 (dd, *J* = 15.4, 6.3 Hz, 1H, H1), 4.97 (m, 2H, H6''), 4.45 (m, 2H, CH₂-PMB), 4.02 (m, 1H, H1''), 3.85 (m, 1H, H4), 3.81 (s, 3H, CH₃-PMB), 3.35 (m, 2H, H5), 2.31 – 2.25 (m, 1H, H3a), 2.25 – 2.16 (m, 1H, H3b), 2.07 – 2.01 (m, 2H, H4''), 1.56-1.32 (m, 4H, H2'' and H3''), 0.89 (app. s, 18H, TBS), 0.06 (m, 12H, TBS).

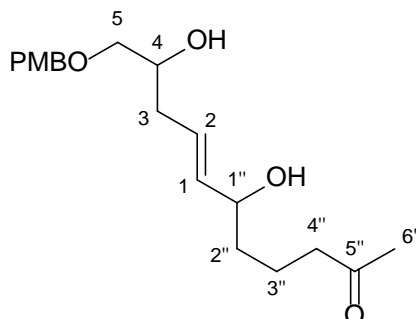
¹³C NMR (125 MHz, CDCl₃): δ 159.2 (C, *para*-PMB), 139.11 (CH, C5'' diastereomer 1), 139.09 (CH, C5'' diastereomer 2), 136.4 (CH, C1 diastereomer 1), 136.3 (CH, C1 diastereomer 2), 130.73 (C, *ipso*-PMB diastereomer 1), 130.70 (C, *ipso*-PMB diastereomer 2), 129.34 (CH, *ortho*-PMB diastereomer 1), 129.32 (CH, *ortho*-PMB diastereomer 2), 125.9 (CH, C2 diastereomer 1), 125.8 (CH, C2 diastereomer 2), 114.5 (CH₂, C6''), 113.8 (CH, *meta*-PMB), 73.9 (CH₂, C5), 73.6 (CH, C1'' diastereomer 1), 73.5 (CH, C1'' diastereomer 2), 73.1 (CH₂, CH₂-PMB), 71.48 (CH, C4 diastereomer 1), 71.46 (CH, C4 diastereomer 2), 55.4 (CH₃, CH₃-PMB), 38.0 (CH₂, C2''), 37.8 (CH₂, C3 diastereomer 1), 37.7 (CH₂, C3 diastereomer 2), 33.9 (CH₂, C4''), 26.1-26.0 (CH₃, TBS), 24.8 (CH₂, C3'' diastereomer 1), 24.7 (CH₂, C3'' diastereomer 2), 18.4-18.3 (C, TBS), -4.0- -4.6 (CH₃, TBS).

IR (neat) cm⁻¹: 2928, 2856, 2362, 2338, 1738, 1514, 1365, 1249, 1089, 936, 776.

HRMS (ESI⁺): calculated for C₃₁H₅₆O₄Si₂ [M+Na]⁺: 571.3609. Found 571.3634, Δ = 4.38 ppm.

9.7 Formation of the *cis*-Tetrahydropyran Ring

(E)-6,10-Dihydroxy-11-((4-methoxybenzyl)oxy)undec-7-en-2-one – 194



A one-necked 10 ml RBF was charged with a solution of starting material (67.9 mg, 0.17 mmol, 1 eq.) in a 1:1 mixture of CH₃CN and MeOH (6 mL) and Pd(OAc)₂ (99 mg, 0.43 mmol, 2.5 eq.) was added. The flask was set under CO atmosphere and allowed to stir for 2.5 days. The suspension was filtered through celite and the plug washed with DCM. The crude mixture was then subjected to FCC (silica, 15 g, gradient elution PE/EtOAc = 5/1 then 2/1 then 0/1) to yield the title compound, which was then treated with PPTS in MeOH and stirred overnight to remove the EE protecting group to simplify the NMR spectra. The solvent was removed under reduced pressure and the crude mixture subjected to FCC (silica, 10g, PE/EtOAc = 1/1) to yield the title compound as a colorless oil of inseparable diastereomers (11 mg, 20% yield).

TLC: R_f (PE/EtOAc = 1/1) = 0.13.

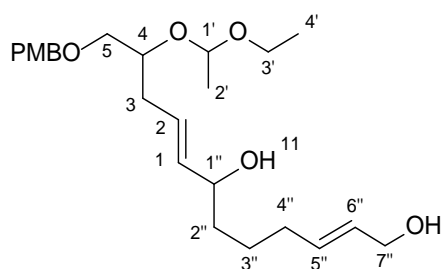
¹H NMR (500 MHz, CDCl₃): δ 7.26 (d, *J* = 8.0 Hz, 2H, *ortho*-PMB), 6.88 (d, *J* = 8.6 Hz, 2H, *meta*-PMB), 5.65 (m, 1H, H2), 5.58 – 5.48 (m, 1H, H1), 4.47 (s, 2H, CH₂-PMB), 4.04 (dt, *J* = 11.8, 6.3 Hz, 1H, H1''), 3.87-3.80 (m, 1H, H4), 3.80 (s, 3H, CH₃-PMB), 3.46 (dt, *J* = 9.3, 4.5 Hz, 1H, H5a), 3.37 – 3.28 (m, 1H, H5b), 2.45 (t, *J* = 7.0 Hz, 2H, H4''), 2.24 – 2.18 (m, 2H, H3), 2.13 (s, 3H, H6''), 1.69 – 1.55 (m, 2H, H3''), 1.55 – 1.42 (m, 2H, H2'').

^{13}C NMR (125 MHz, CDCl_3): δ 209.2 (C, C5''), 159.5 (C, *para*-PMB), 136.0 (CH, C1 diastereomer 1), 135.9 (CH, C1 diastereomer 2), 130.1 (C, *ipso*-PMB), 129.57 (CH, *meta*-PMB diastereomer 1), 129.56 (CH, *meta*-PMB diastereomer 2), 127.5 (CH, C2 diastereomer 1), 127.3 (CH, C2 diastereomer 1), 73.71 (CH_2 , C5 diastereomer 1), 73.68 (CH_2 , C5 diastereomer 1), 73.2 (CH_2 , PMB), 72.5 (CH, C1'' diastereomer 1), 72.4 (CH, C1'' diastereomer 2), 71.0 (CH, C4), 55.4 (CH_3 , CH_3 -PMB), 43.52 (CH_2 , C4'' diastereomer 1), 43.50 (CH_2 , C4'' diastereomer 2), 36.60 (CH_2 , C3'' diastereomer 1), 36.55 (CH_2 , C3'' diastereomer 1), 36.4 (CH_2 , C3 diastereomer 1), 36.3 (CH_2 , C3 diastereomer 2), 29.8 (CH_3 , C6''), 19.68 (CH_2 , C2'' diastereomer 1), 19.65 (CH_2 , C2'' diastereomer 2).

IR (neat) cm^{-1} : 3403, 2929, 2856, 2364, 2343, 1738, 1714, 1513, 1366, 1248.

HRMS (ESI⁺): calculated for $\text{C}_{19}\text{H}_{28}\text{O}_5$ $[\text{M}+\text{Na}]^+$: 359.1829. Found 359.1836, $\Delta = 1.86$ ppm.

(2E,8E)-11-(1-Ethoxyethoxy)-12-((4-methoxybenzyl)oxy)dodeca-2,8-diene-1,7-diol
– SOGE-117

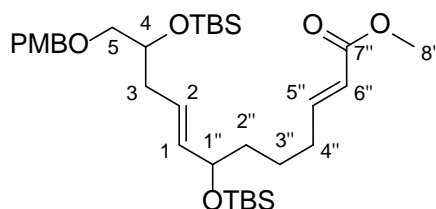


A 10 ml 1N RBF was charged with the starting material (42.0 mg, 0.1274 mmol, 1 eq.) in DCM (0.8 mL) and Grubbs-II catalyst (5.4 mg, 0.0064mmol, 0.05 eq.) was added to the solution. 2-buten-1,4-dial (44.9 mg, 0.5096 mmol, 4 eq.) was added to the solution and the reaction stirred at room temperature overnight. On the next day, the reaction was filtered through a plug of celite and the solvent was removed under reduced pressure. The mixture was used as crude in the next step.

TLC: Rf (PE/EtOAc = 1/1) = 0.25.

HRMS (ESI⁺): calculated for C₂₄H₃₈O₆: 445.2561. Found 445.2579. [M+Na]⁺, Δ = 4.22 ppm

Methyl (2E,8E)-7,11-bis((tert-butyldimethylsilyl)oxy)-12-((4-methoxybenzyl)oxy) dodeca-2,8-dienoate – 211



A solution of the **194** (57 mg, 0.10 mmol, 1 eq.) in toluene (1 mL) was added to a 10 mL one-necked RBF containing Grubbs II catalyst (8.7 mg, 0.01 mmol, 0.1 eq.). Methyl acrylate (0.96 ml, 10.7 mmol, 60 eq.) was added to the solution and the reaction was allowed to stir at room temperature for two hours. A drop of triethylamine was added and the reaction mixture was exposed to air for 1.5 hours, before being filtered through a plug of silica. The solvent was removed under reduced pressure and the crude mixture was subjected to FCC (silica, 10 g, PE/EtOAc = 20/1) to yield the title compound as a colorless oil of inseparable diastereomers (32 mg, 83% yield).

TLC: Rf (PE/EtOAc = 10/1) = 0.31.

¹H NMR (500 MHz, CDCl₃): δ 7.26 (d, J = 8.5 Hz, 2H, ortho-PMB), 7.03 – 6.90 (m, 1H, H5''), 6.88 (d, J = 8.6 Hz, 2H, meta-PMB), 5.82 (d, J = 16.4 Hz, 1H, H6''), 5.57 (m, 1H, H2), 5.42 (dd, J = 16.7, 7.6 Hz, 1H, H1), 4.45 (s, 2H, CH₂-PMB), 4.06 (m, 1H, H1''), 3.89 – 3.84 (m, 1H, H4), 3.82 (s, 3H, PMB), 3.74 (m, 3H, H8''), 3.35 (m, 2H, H5), 2.34 – 2.26 (m, 1H, H3a), 2.26-2.16 (m, 3H, H3b & H4''), 1.70-1.55 (m, 2H,

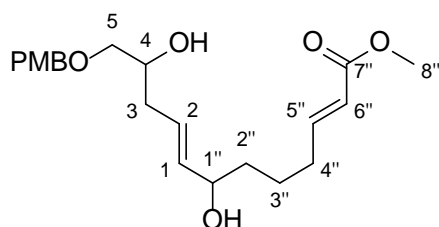
H3"), 1.55 – 1.38 (m, 2H, H2"), 0.89 (s, 18H, TBS), 0.06 (s, 3H, TBS), 0.05 (s, 3H, TBS), 0.04 (s, 3H, TBS), 0.02 (s, 3H, TBS).

¹³C NMR (125 MHz, CDCl₃): δ 167.2 (C, C7"), 159.0 (C, para-PMB), 149.7 (CH, C5"), 135.9 (CH, C1 diastereomer 1), 135.4 (CH, C1 diastereomer 2), 130.5 (C, ipso-PMB), 129.2 (ortho-PMB), 126.5 (CH, C2 diastereomer 1), 126.0 (CH, C2 diastereomer 2), 120.9 (CH, C6" diastereomer 1), 120.8 (CH, C6" diastereomer 2), 113.7 (CH, meta-PMB), 73.8 (CH₂, C5 diastereomer 1), 73.7 (CH₂, C5 diastereomer 2), 73.1 (CH, C1" diastereomer 1), 73.0 (CH₂, PMB), 72.7 (CH, C1" diastereomer 2), 71.3 (CH, C4 diastereomer 1), 71.2 (CH, C4 diastereomer 2), 55.3 (CH₃, PMB), 51.4 (CH₃, C8"), 37.8 (CH₂, C2"), 37.6 (CH₂, C3 diastereomer 1), 37.5 (CH₂, C3 diastereomer 2), 36.5 (CH₂, C3"), 32.2 (CH₂, C4"), 25.9 (CH₃, TBS), 25.8 (CH₃, TBS), 18.2 (C, TBS), -4.4 (CH₃, TBS), -4.5 (CH₃, TBS), -4.7 (CH₃, TBS).

IR (neat) cm⁻¹: 2951, 2929, 2855, 1725, 1513, 1248, 1086, 1037, 832, 775.

HRMS (ESI⁺): calculated for C₃₃H₅₈O₆Si₂ [M+Na]⁺: 629.3664. Found 629.3663, Δ = -0.19 ppm.

Methyl (2E,8E)-7,11-dihydroxy-12-((4-methoxybenzyl)oxy)dodeca-2,8-dienoate – 212



211 (52 mg, 0.09 mmol, 1 eq.) was treated with PPTS (64 mg, 0.26 mmol, 3 eq.) in MeOH (2 mL) for 16 hours at room temperature. The reaction was quenched with sat. aq. NaHCO₃ solution and diethyl ether was added to the mixture. The phases were separated and the aqueous layer was extracted with diethyl ether (3x). The

combined organic layers were dried over magnesium sulfate, filtered and the solvent was removed under reduced pressure. The crude mixture was subjected to FCC (silica, 10 g, gradient elution PE/EtOAc = 3/1 then 1/1) to yield the product as a colorless oil of inseparable diastereomers (32 mg, quant. yield).

TLC: Rf (PE/EtOAc = 3/1) = 0.34.

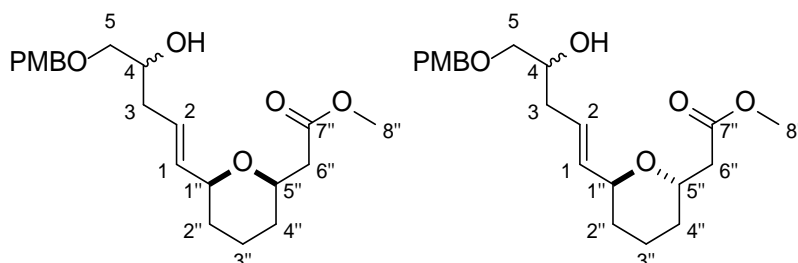
¹H NMR (500 MHz, CDCl₃): δ 7.24 (d, *J* = 7.9 Hz, 2H, *ortho*-PMB), 7.00 – 6.93 (dt, *J* = 15.9, 6.8 Hz, 1H, H5''), 6.91 (dd, *J* = 7.8 Hz, 2H, *meta*-PMB), 5.82 (d, *J* = 15.6 Hz, 1H, H6''), 5.70 – 5.60 (m, 1H, H2), 5.54 (dd, *J* = 15.3, 6.4 Hz, 1H, H1), 4.47 (s, 2H, CH₂-PMB), 4.06 (m, 1H, H1''), 3.83 (m, 1H, H4), 3.81 (s, 3H, CH₃-PMB), 3.72 (s, 3H, H8''), 3.50 – 3.44 (m, 1H, H5a), 3.32 (t, *J* = 9.0 Hz, 1H, H5b), 2.21 (m, 4H, C3 and C4''), 1.70-1.38 (m, 4H, C2'' and C3'').

¹³C NMR (125 MHz, CDCl₃): δ 167.2 (C, C7''), 159.5 (C, *para*-PMB), 149.3 (CH, C5''), 136.04 (CH, C1, diastereomer 1), 135.96 (CH, C1 diastereomer 2), 129.6 (C, *ipso*-PMB), 127.6 (CH, C2 diastereomer 1), 127.4 (CH, C2 diastereomer 2), 121.3 (CH, C6''), 114.0 (CH, *meta*-PMB), 73.70 (CH₂, C5 diastereomer 1), 73.68 (CH₂, C5 diastereomer 2), 73.2 (CH₂, CH₂-PMB), 72.72 (CH, C1'' diastereomer 1), 72.65 (CH, C1'' diastereomer 2), 70.04 (CH, C4 diastereomer 1), 70.01 (CH, C4 diastereomer 2), 55.4 (CH₃, CH₃-PMB), 51.6 (CH₃, C8''), 36.62 (CH₂, C3 diastereomer 1), 36.58 (CH₂, C3 diastereomer 2), 36.34 (CH₂, C2'' diastereomer 1), 36.30 (CH₂, C2'' diastereomer 2), 32.2 (CH₂, C4''), 24.1 (CH₂, C3'').

IR (neat) cm⁻¹: 3446, 2925, 2854, 1735, 1252, 1169, 1088, 1031.

HRMS (ESI⁺): calculated for C₂₁H₃₀O₆Si [M+NH₄]⁺: 396.2381. Found 396.2398, Δ = 4.34 ppm.

Methyl 2-((2*R,6*S**)-6-((*E*)-4-hydroxy-5-((4-methoxybenzyl)oxy)pent-1-en-1-yl)-3,4,5,6-tetrahydro-2*H*-pyran-2-yl)acetate – *cis*-213 and methyl 2-((2*S**,6*S**)-6-((*E*)-4-hydroxy-5-((4-methoxybenzyl)oxy)pent-1-en-1-yl)-3,4,5,6-tetrahydro-2*H*-pyran-2-yl)acetate - *trans*-213**



A flask was charged with a solution of **212** (32 mg, 0.09 mmol, 1 eq.) in toluene (1 mL), and TMEDA (0.06 mL, 0.41 mmol, 3 eq.) and LiHMDS (0.03 mL, 0.03 mL, 0.2 eq.) were added dropwise to the solution. The reaction was stirred for 90 min at room temperature, before it was quenched with sat. aq. NaHCO₃ solution. The aqueous layer was extracted with diethyl ether (3x) and the combined organic layers were washed with water and brine. The organic layer was then dried over magnesium sulfate, filtered and the solvent was removed under reduced pressure. The crude mixture was subjected to FCC (silica, 10 g, gradient elution PE/EtOAc = 3/1 then 1/1 then 0/1) which yielded the products as colorless oils (10 mg of clean *cis*-product, 6 mg of a mixture of *cis*-/*trans*-product, 32% total yield).

***cis*-213**

TLC: R_f (PE/EtOAc = 3/1) = 0.37

¹H NMR (500 MHz, CDCl₃): δ 7.25 (d, *J* = 8.0 Hz, 2H, *ortho*-PMB), 6.88 (d, *J* = 8.4 Hz, 2H, *meta*-PMB), 5.69 – 5.59 (m, 1H, H₂), 5.54 (dd, *J* = 15.9, 6.1 Hz, 1H, H₁), 4.47 (s, 2H, CH₂-PMB), 3.86-3.77 (m, 3H, H₄ and H_{1''} and H_{5''}), 3.81 (s, 3H, CH₃-PMB), 3.67 (s, 3H, H_{8''}), 3.47 (m, 1H, H_{5a}), 3.35 – 3.28 (m, 1H, H_{5b}), 2.60 (dd, *J* = 14.9, 7.5 Hz, 1H, H_{6''a}), 2.41 (dd, *J* = 15.0, 6.2 Hz, 1H, H_{6''b}), 2.21 (app. t, *J* = 6.3 Hz, 2H, H₃), 1.84 (m, 1H, H_{3''a}) 1.68-1.50 (m, 3H, H_{3''b} and H_{4''}), 1.25 (m, 2H, H_{2''}).

¹³C NMR (125 MHz, CDCl₃): δ 172.0 (C, C7''), 159.4 (C, *para*-PMB), 134.4 (CH, C1), 130.2 (C, *ipso*-PMB), 129.6 (CH, *ortho*-PMB), 126.8 (CH, C2), 114.0 (CH, *meta*-PMB), 78.1 (CH, C1''), 74.4 (CH, C5''), 73.8 (CH₂, C5), 73.2 (CH₂, CH₂-PMB), 70.0 (CH, C4), 55.4 (CH₃, CH₃-PMB), 51.8 (CH₃, C8''), 41.6 (CH₂, C6''), 36.6 (CH₂, C3), 31.4 (CH₂, C2''), 31.1 (CH₃, C4''), 23.4 (CH₂, C3'').

HRMS (ESI⁺): calculated for C₂₁H₃₀O₆Si [M+NH₄]⁺: 396.2381. Found 396.2398, Δ = 4.34 ppm.

trans-213 (characterized from a mixture with **cis-213**)

TLC: R_f (PE/EtOAc = 3/1) = 0.35

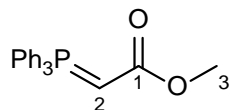
¹H NMR (500 MHz, CDCl₃): δ 7.25 (d, *J* = 7.4 Hz, 2H, *ortho*-PMB), 6.88 (d, *J* = 7.4 Hz, 2H, *meta*-PMB), 5.76 – 5.60 (m, 1H, H2), 5.54 (dd, *J* = 15.8, 5.7 Hz, 1H, H1), 4.48 (s, 2H, CH₂-PMB), 4.36 (m, 1H, H1''), 4.20 – 4.12 (m, 1H, H6''), 3.86 – 3.79 (m, 4H, H4 and CH₃-PMB), 3.67 (s, 3H, H8''), 3.52 – 3.44 (m, 1H, H5a), 3.41 – 3.28 (m, 1H, H5b), 2.60 (dd, *J* = 15.0, 7.6 Hz, 1H, H6''a), 2.41 (dd, *J* = 15.0, 6.8 Hz, 1H, H6''b), 2.27 (t, *J* = 6.3 Hz, 2H, H3), 1.76 – 1.69 (d, *J* = 12.8 Hz, 1H, H4''a), 1.68-1.51 (m, 3H, H4''b and H3''), 1.40-1.27 (m, 2H, H2'')

¹³C NMR (125 MHz, CDCl₃): δ 172.1 (C, C7''), 159.4 (C, *para*-PMB), 133.1 (CH, C1 diastereomer 1), 133.0 (CH, C1 diastereomer 2), 130.3 (C, *ipso*-PMB), 129.5 (CH, *ortho*-PMB), 128.5 (CH, C2 diastereomer 1), 128.4 (CH, C2 diastereomer 2), 114.0 (*meta*-PMB), 73.7 (CH₂, C5), 73.2 (CH₂, CH₂-PMB), 72.2 (CH, C1'' diastereomer 1), 72.2 (CH, C1'' diastereomer 2), 70.2 (CH, C4), 67.8 (CH, C6'' diastereomer 1), 67.8 (CH, C6'' diastereomer 2), 55.4 (CH₃, CH₃-PMB), 51.8 (CH₃, C8''), 40.3 (CH₂, C6'' diastereomer 1), 40.3 (CH₂, C6'' diastereomer 1), 36.9 (CH₂, C3 diastereomer 1), 36.9 (CH₂, C3 diastereomer 2), 30.6 (CH₂, C2''), 29.2 (CH₂, C4'' diastereomer 1), 29.1 (CH₂, C4'' diastereomer 1), 18.8 (CH₂, C3'').

HRMS (ESI⁺): calculated for C₂₁H₃₀O₆Si [M+NH₄]⁺: 396.2381. Found 396.2398, Δ = 4.34 ppm

9.8 Late Stage Connections: Bestmann Ylid Linchpin and Ring-Closing Metathesis

Methyl 2-(triphenylphosphaneylidne)acetate



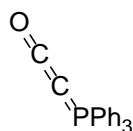
A 100 mL one-necked RBF was charged with a solution of PPh₃ (7.0 g, 0.0267 mol, 1.02 eq.) in toluene (30 mL). Methyl bromoacetate (4.0 g, 0.0261 mol, 1.0 eq.) in toluene (8 mL) was added to the flask and the reaction mixture stirred at room temperature for 20 hours. The white solid was then filtered off, redissolved in DCM (100 mL) and aqu. NaOH solution (60 mL, 0.5 M) and the aqueous layer extracted with DCM (3x). The combined organic layers were dried over magnesium sulfate, filtered and the solvent was removed under reduced pressure to yield the product as a white solid (6.75 g, 77% yield).

¹H NMR (300 MHz, CDCl₃): δ 7.72-7.40 (m, 15H, CH, PPh₃), 3.51 (s, 3H, CH₃, H3), 2.90 (s, 1H, CH, H2).

³¹P NMR (120 MHz, CDCl₃): δ 17.6.

These data were consistent with those reported previously.^{45,46}

2-(Triphenylphosphoranylide) ethenone (Bestmann Ylid) - 114



A 25 mL one-necked RBF fitted with a stir bar, condenser and septum was charged with methyl 2-(triphenylphosphoranylide) acetate (1.0 g, 3 mmol, 1 eq.) and set under nitrogen. Toluene (10 mL) and NaHMDS (0.6 M in toluene, 5.5 mL, 3.3

mmol, 1.1 eq.) were added and the resulting mixture was stirred at 65 °C and for 20 hours, before the hot solution was filtered through a thin celite pad. The solvent was removed under reduced pressure and the crude product was purified by recrystallization from hot toluene and cooling to 4 °C overnight to yield **114** as colorless solid (425 mg, 47%).

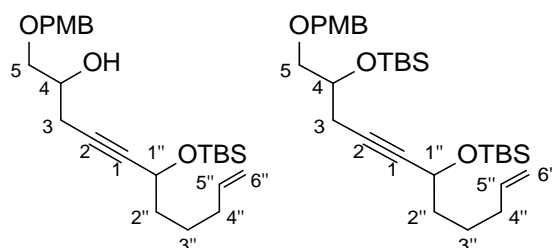
¹H NMR (500 MHz, CDCl₃): δ 7.68 (dd, *J* = 13.7, 7.6 Hz, 6H), 7.57 (t, *J* = 7.4 Hz, 3H), 7.49 (t, *J* = 6.8 Hz, 6H).

¹³C NMR (125 MHz, CDCl₃): δ 135.0 (d, *J* = 3.1 Hz), 133.3 (d, *J* = 10.7 Hz), 132.3 (d, *J* = 11.2 Hz), 130.4 (d, *J* = 12.9 Hz), 128.9 (d, *J* = 13.0 Hz). The signals for C1 and C2 were missing from the ¹³C NMR data. However, all other data agreed with those previously reported.

³¹P NMR (120 MHz, CDCl₃): 5.5.

These data were consistent with those reported previously.^{45,46}

6-((tert-Butyldimethylsilyl)oxy)-1-((4-methoxybenzyl)oxy)undec-10-en-4-yn-2-ol - 215 and 9-(((4-Methoxybenzyl)oxy)methyl)-2,2,3,3,11,11,12,12-octamethyl-5-(pent-4-en-1-yl)-4,10-dioxo-3,11-disilatridec-6-yne - 216



A RBF was charged with a solution of **168** (48 mg, 0.15 mmol, 1 eq.) in DMF (1 mL) and TBSCl (126 mg, 0.84 mmol, 5.5 eq.) and imidazole (91 mg, 1.33 mmol, 8.8 eq.) were added to the reaction. The solution was stirred at room temperature

overnight before the reaction was quenched with water and EtOAc was added. The phases were separated and the aqueous layer was extracted with EtOAc (3x). The combined organic layers were dried over magnesium sulfate, filtered and the solvent was removed under reduced pressure to yielded. The crude mixture was subjected to FCC (silica, 15 g, gradient elution PE/EtOAc = 5/1 then 3/1) which yielded **215** as a colorless oil of inseparable diastereomers (27 mg, 44%) along with **216**, which also presented as a colorless oil of inseparable diastereomers (27 mg, 33% yield).

215

TLC: R_f (PE/EtOAc = 3/1) = 0.33.

¹H NMR (500 MHz, CDCl₃): δ 7.26 (d, *J* = 6.8 Hz, 2H, *ortho*-PMB), 6.89 (d, *J* = 8.4 Hz, 2H, *meta*-PMB), 5.86 – 5.74 (m, 1H, H5''), 4.98 (m, 2H, H6''), 4.48 (s, 2H, CH₂-PMB), 4.32 (m, 1H, H1''), 3.92 (m, 1H, H4), 3.81 (s, 3H, CH₃-PMB), 3.60 (dd, *J* = 15.0, 8.1 Hz, 2H, H5a), 3.45 (m, 1H, H5b), 2.45 (m, 2H, H3), 2.06 (m, 2H, H4''), 1.63 (m, 2H, H2''), 1.50 (m, 2H, H3''), 0.90 (s, 9H, TBS), 0.10 (s, 3H, TBS), 0.10 (s, 3H, TBS).

¹³C NMR (125 MHz, CDCl₃): δ 159.3 (C, *para*-PMB), 138.7 (CH, C5''), 129.8 (C, *ipso*-PMB), 129.4 (CH, *ortho*-PMB), 123.8 (CH, C5''), 114.6 (CH₂, C6''), 113.8 (CH, *meta*-PMB), 84.3 (C, C1), 79.8 (C, C2), 73.1 (CH₂, CH₂-PMB), 72.7 (CH₂, C5), 69.4 (CH, C4), 62.9 (CH, C1''), 55.3 (CH₃, CH₃-PMB), 38.3 (CH₂, C2''), 33.3 (CH₂, C4''), 25.8 (CH₃, TBS), 24.6 (CH₂, C3''), 23.8 (CH₂, C3), 18.3 (C, TBS), -4.5 (CH₃, TBS), -4.99 (CH₃, TBS).

IR (neat) cm⁻¹: 3455, 2929, 2856, 2362, 1737, 1513, 1248, 1086, 1037, 836, 777.

HRMS (ESI⁺): calculated for C₂₅H₄₀O₄Si [M+Na]⁺: 455.2588. Found 455.2603, Δ = 3.31 ppm.

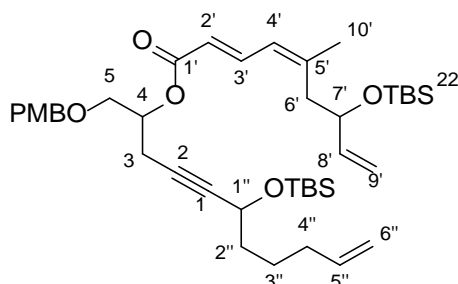
TLC: Rf (PE/EtOAc = 3/1) = 0.37.

¹H NMR (500 MHz, CDCl₃): δ 7.24 (m, 2H, *ortho*-PMB), 6.87 (d, *J* = 6.6 Hz, 2H, *meta*-PMB), 5.79 (m, 1H, H5''), 5.04 – 4.91 (m, 2H, H6''), 4.46 (s, 2H, CH₂-PMB), 4.31 (m, 1H, H1''), 3.91 (m, 1H, H4), 3.80 (s, 3H, CH₃-PMB), 3.49 (m, 1H, H5a), 3.41 (m, 1H, H5b), 2.46 (m, 1H, H3a), 2.36 (m, 1H, H3b), 2.04 (m, 2H, H4''), 1.62 (m, 4H, H2'' and H3''), 0.89 (s, 9H, TBS), 0.87 (s, 9H, TBS), 0.10 – 0.06 (m, 12H, TBS).

¹³C NMR (125 MHz, CDCl₃): δ 159.1 (C, *para*-PMB), 138.7 (CH, C5''), 130.5 (C, *ipso*-PMB), 129.1 (CH, *ortho*-PMB), 114.5 (CH₂, C6''), 113.7 (CH₂, *meta*-PMB), 83.4 (C, C1), 81.0 (C, C2), 73.4 (CH₂, C5), 73.0 (CH₂, CH₂-PMB), 70.4 (CH, C4), 63.0 (CH, C1''), 55.2 (CH₃, CH₃-PMB), 38.3 (CH₂, C2''), 33.4 (CH₂, C4''), 25.84 (CH, TBS), 25.81 (CH, TBS), 24.9 (CH₂, C3), 24.6 (CH₂, C3''), 18.3 - 18.1 (C, TBS), -4.4 (CH₃, TBS), -4.61 (CH₃, TBS), -4.76 (CH₃, TBS), -5.01 (CH₃, TBS).

IR (neat) cm⁻¹: 2951, 2929, 2856, 2363, 1739, 1463, 1248, 1086, 833, 775.

**6-((*tert*-Butyldimethylsilyl)oxy)-1-((4-methoxybenzyl)oxy)undec-10-en-4-yn-2-yl
(*2E,4Z*)-7-((*tert*-butyldimethylsilyl)oxy)-5-methylnona-2,4,8-trienoate– 217**



A 10 mL RBF was charged with a solution of **215** (31 mg, 0.07 mol, 1 eq.) and **114** (22 mg, 0.03 mmol, 1 eq.) in toluene (1 mL) and heated to reflux. A solution of **117** (19 mg, 0.07 mmol, 1 eq.) in toluene (0.5 mL) was added and the reaction mixture

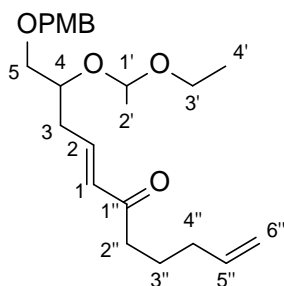
was kept at reflux overnight. On the next day, the solvent was removed under reduced pressure and the crude mixture was subjected to FCC (silica, 15 g, gradient elution PE/EtOAc = 5/1 then 3/1) to yield the title compound as a colorless oil of inseparable diastereomers (14 mg, 27% yield).

TLC: Rf (PE/EtOAc = 20/1) = 0.77.

¹H NMR (500 MHz, CDCl₃): δ 7.56 (dd, J = 15.0, 11.6 Hz, 1H, H3'), 7.24 (d, J = 7.9 Hz, 2H, ortho-PMB), 6.87 (d, J = 7.6 Hz, 2H, meta-PMB), 6.06 (d, J = 11.4 Hz, 1H, H2'), 5.85-5.72 (m, 3H, H4' and H8' and H5''), 5.17 (d, J = 16.6 Hz, 1H, H9'a), 5.12 (m, 1H, H4), 5.07-4.91 (m, 3H, H9'b and H6''), 4.51 (d, J = 11.7 Hz, 1H, CH₂-PMBa), 4.46 (d, J = 11.7 Hz, 1H, CH₂-PMBb), 4.30 (t, J = 6.05 Hz, 1H, H1''), 4.24 (m, 1H, H7'), 3.80 (s, 3H, CH₃-PMB), 3.65 (m, 2H, H5), 2.69-2.50 (m, 3H, H6' and H3a), 2.42-2.30 (m, 1H, H3b), 2.04 (m, 2H, H4''), 1.91 (s, 3H, H10'), 1.67-1.54 (m, 2H, H2''), 1.53 – 1.44 (m, 2H, H3''), 0.89 (s, 9H, TBS), 0.86 (s, 9H, TBS), 0.10 (s, 3H, TBS), 0.07 (s, 6H, TBS), 0.01 (s, 3H, TBS).

¹³C NMR (125 MHz, CDCl₃): δ 166.8 (C, C1), 159.2 (C, para-PMB), 146.6 (C, C5'), 141.7 (CH, C3'), 140.9 (CH, C8'), 138.7 (CH, C5''), 130.1 (C, ipso-PMB), 129.2 (CH, ortho-PMB), 126.1 (CH, C2'), 118.9 (CH, C4'), 114.5 (CH₂, C9'), 114.2 (CH₂, C6''), 113.8 (CH, meta-PMB), 83.9 (C, C1), 79.4 (C, C2), 73.0 (CH₂, CH₂-PMB), 72.8 (CH, C7'), 70.6 (CH, C4), 69.5 (CH₂, C5), 62.9 (C1''), 55.2 (CH₃, CH₃-PMB), 41.7 (CH₂, C3), 38.2 (CH₂, C2''), 33.3 (CH₂, C4''), 31.9 (CH₃, C10'), 25.8 (CH₃, TBS), 24.5 (CH₂, C3''), 21.2 (CH₂, C6'), 18.2 (C, TBS), -4.4 (CH₃, TBS), -4.6 (CH₃, TBS), -4.9 (CH₃, TBS), -5.0 (CH₃, TBS).

(E)-10-(1-Ethoxyethoxy)-11-((4-methoxybenzyl)oxy)undeca-1,7-dien-6-one – 188



Prepared following the general procedure for **Manganese dioxide oxidation** using **181** (81 mg, 0.21 mmol, 1 eq.) as starting material. The crude mixture was subjected to FCC (silica, 15g, gradient elution PE/EtOAc = 5/1 then 1/1) and yielded the title compound as a colorless oil of inseparable diastereomers (78 mg, 98% yield).

TLC: R_f (PE/EtOAc = 10/1) = 0.53.

¹H NMR (500 MHz, CDCl₃): δ 7.23 (dd, *J* = 8.7, 2.0 Hz, 2H, *ortho*-PMB), 6.86 (dd, *J* = 9.0, 2.5 Hz, 2H, *meta*-PMB), 6.83-6.73 (m, 1H, H₂), 6.14 – 6.07 (m, 1H, H₁), 5.77 (m, 1H, H₅"), 5.04 – 4.93 (m, 2H, H₆"), 4.82 (q, *J* = 5.3 Hz, 1H, H₁' diastereomer 1), 4.74 (q, *J* = 5.3 Hz, 1H, H₁' diastereomer 2), 4.44 (m, 4.4 Hz, 2H, CH₂-PMB), 3.91 – 3.82 (m, 1H, H₄), 3.79 (s, 3H, CH₃-PMB), 3.65 – 3.55 (m, 1H, H₃'a), 3.53-3.38 (m, 3H, H₅ and H₃'b), 2.54 – 2.39 (m, 4H, H₃ and H₄"), 2.06 (m, 1H, H₂"), 1.75 – 1.66 (m, 2H, H₃"), 1.32 – 1.26 (m, 3H, H₂'), 1.15 (m, 7.0, 5.7 Hz, 3H, H₄').

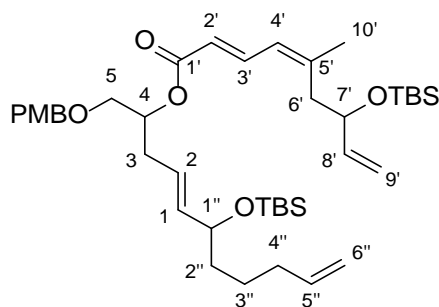
¹³C NMR (125 MHz, CDCl₃): δ 200.3 (C, C₁"), 159.2 (C, *para*-PMB), 143.2 (CH, C₂ diastereomer 1), 142.8 (CH, C diastereomer 2), 138.0 (CH, C₅"), 132.6 (CH, C₁ diastereomer 1), 132.4 (CH, C₁ diastereomer 2), 130.0 (C, *ipso*-PMB), 129.4 (CH, *ortho*-PMB diastereomer 1), 129.3 (CH, *ortho*-OMB diastereomer 2), 115.2 (CH₂, C₆"), 113.8 (CH, *meta*-PMB), 99.64 (CH, C₁' diastereomer 1), 99.59 (CH, C₁' diastereomer 2), 73.7 (CH, C₄ diastereomer 1), 73.6 (CH, C₄ diastereomer 2), 73.0 (CH₂, CH₂-PMB), 71.8 (CH₂, C₅), 60.4 (CH₂, C₃' diastereomer 1), 60.3 (CH₂, C₃' diastereomer 1), 55.3 (CH₃, CH₃-PMB), 39.1 (CH₂, C₄"), 35.9 (CH₂, C₃

diastereomer 1), 35.4 (CH₂, C3 diastereomer 2), 33.1 (CH₂, C2''), 23.2 (CH₂, C3''), 22.7 (CH₃, C2' diastereomer 1), 20.5 (CH₃, C2' diastereomer 1), 15.3 (CH₃, C4'), 15.2 (CH₃, C4').

IR (neat) cm⁻¹: 2974, 2933, 2364, 1672, 1513, 1248, 1094, 1034, 821.

HRMS (ESI⁺): calculated for C₂₃H₃₄O₅ [M+Na]⁺: 413.2299. Found 413.2312, Δ = 3.19 ppm.

(E)-6-((*Tert*-butyldimethylsilyl)oxy)-1-((4-methoxybenzyl)oxy)undeca-4,10-dien-2-yl (*2E,4Z*)-7-((*tert*-butyldimethylsilyl)oxy)-5-methylnona-2,4,8-trienoate – 221



A 10 mL RBF was charged with a solution of **191** (46 mg, 0.11 mol, 1 eq.) and **114** (32 mg, 0.11 mmol, 1 eq.) in toluene (0.5 mL) and heated to reflux. A solution of **117** (27 mg, 0.11 mmol, 1 eq.) in toluene (0.5 mL) was added and the reaction mixture was kept at reflux overnight. On the next day, the solvent was removed under reduced pressure and the crude mixture was subjected to FCC (silica, 15 g, gradient elution PE/EtOAc = 10/1 then 5/1 then 3/1) which yielded an inseparable mixture of diastereomers and by-products as colorless oil (80 mg, 42% yield, 47% BRSM).

TLC: R_f (PE/EtOAc = 20/1) = 0.79.

¹H NMR (500 MHz, CDCl₃): δ 7.59-7.48 (m, 1H, H3'), 7.24 (d, J = 8.5 Hz, 2H, ortho-PMB), 6.86 (d, J = 7.5 Hz, 2H, meta-PMB), 6.06 (d, J = 11.8 Hz, 1H, H2'), 5.86-5.66 (m, 3H, H4', H8', H5''), 5.51-5.42 (m, 2H, H1 and H2), 5.21-4.90 (m, 5H, H4 and H9' and H6''), 4.43 (s, 2H, CH₂-PMB), 4.24 (m, 1H, H7'), 4.01 (m, 1H, H1''), 3.80 (s, CH₃-PMB), 3.55-3.48 (m, 2H, H5), 2.61-2.51 (m, 1H, H6'a), 2.46-2.26 (m, 3H, H6'b and H3), 2.08-1.97 (m, 2H, H4''), 1.91 (s, 3H, H10), 1.49-1.30 (m, 4H, H2'' and H3'').

¹³C NMR (125 MHz, CDCl₃): δ 167.1-167.0 (C, C1' diastereomers), 159.3 (C, para-PMB), 146.5-146.1 (CH, C5' diastereomers), 141.5-141.4 (CH, C3' diastereomers), 141.2-141.0 (CH, C8'), 139.0 (CH, C8'), 138.6 (CH, C5''), 137.3 (C1 diastereomers), 131.2 (CH, C1), 130.3 (C, ipso-PMB), 129.4-129.3 (CH, ortho-PMB diastereomers), 126.2 (CH, C2'), 124.6-124.5 (CH, C2 diastereomers), 119.4 (CH, C4 diastereomers), 114.9-114.2 (CH₂, C9' diastereomers and C6'' diastereomers), 113.9 (CH, meta-PMB diastereomers), 73.4-73.3 (CH, C1'' diastereomers), 73.1 (CH, C7' diastereomers), 73.0 (CH₂, CH₂-PMB), 72.1-71.9 (CH, C4), 70.4-70.3 (CH₂, C5), 55.4 (CH₃, CH₃-PMB), 41.9 (CH₂, C6'), 37.9 (CH₂, C2''), 34.2-33.6 (CH₂, C3 and C4''), 26.0 (CH₃, TBS), 25.8 (CH₃, C10), 24.7 (CH₂, C3''), 18.4-18.3 (C, TBS), -4.1- -4.7 (CH₃, TBS).

HRMS (ESI⁺): calculated for C₄₁H₆₈O₆Si₂ [M+Na]⁺: 735.4447. Found 735.4456, Δ = 1.27 ppm.

References

1. WHO. Cancer Fact Sheet. *February* (2017). Available at: <http://www.who.int/mediacentre/factsheets/fs297/en/>.
2. American Cancer Society, X. How Chemotherapy Drugs Work. (2017). Available at: <https://www.cancer.org/treatment/treatments-and-side-effects/treatment-types/chemotherapy/how-chemotherapy-drugs-work.html>.
3. Dasari, S. & Tchounwou, P. B. Cisplatin in cancer therapy: molecular mechanisms of action. doi:10.1016/j.ejphar.2014.07.025
4. Longley, D. B., Harkin, D. P. & Johnston, P. G. 5-Fluorouracil: mechanisms of action and clinical strategies. *Nat. Rev. Cancer* **3**, 330–338 (2003).
5. SALSER, J. S. & BALIS, M. E. The Mechanism of Action of 6-Mercaptopurine. *Cancer Res.* **25**, 539–43 (1965).
6. Sanyakamdhorn, S., Agudelo, D. & Tajmir-Riahi, H. A. Review on the targeted conjugation of anticancer drugs doxorubicin and tamoxifen with synthetic polymers for drug delivery. *J. Biomol. Struct. Dyn.* **35**, 2497–2508 (2017).
7. Verweij, J. & Pinedo, H. M. Mitomycin C: mechanism of action, usefulness and limitations. *Anticancer. Drugs* **1**, 5–13 (1990).
8. Ormrod, D. & Spencer, C. M. Topotecan: a review of its efficacy in small cell lung cancer. *Drugs* **58**, 533–51 (1999).
9. Schmoll, H. Review of etoposide single-agent activity. *Cancer Treat. Rev.* **9 Suppl**, 21–30 (1982).
10. Dumontet, C. & Jordan, M. A. Microtubule-binding agents: a dynamic field of cancer therapeutics. *Nat. Rev. Drug Discov.* **9**, 790–803 (2010).
11. Khalil, D. N., Smith, E. L., Brentjens, R. J. & Wolchok, J. D. The future of

- cancer treatment: immunomodulation, CARs and combination immunotherapy. *Nat. Rev. Clin. Oncol.* **13**, 273–290 (2016).
12. Farkona, S., Diamandis, E. P. & Blasutig, I. M. Cancer immunotherapy: the beginning of the end of cancer? *BMC Med.* **14**, 73 (2016).
 13. Kirkpatrick, P., Graham, J. & Muhsin, M. Fresh from the pipeline: Cetuximab. *Nat. Rev. Drug Discov.* **3**, 549–550 (2004).
 14. Yazdi, M. H., Faramarzi, M. A., Nikfar, S. & Abdollahi, M. A Comprehensive Review of Clinical Trials on EGFR Inhibitors Such as Cetuximab and Panitumumab as Monotherapy and in Combination for Treatment of Metastatic Colorectal Cancer. *Avicenna J. Med. Biotechnol.* **7**, 134–44 (2015).
 15. Ganjoo, K. N. & Wakelee, H. Review of erlotinib in the treatment of advanced non-small cell lung cancer. *Biologics* **1**, 335–46 (2007).
 16. Hu, R., Hilakivi-Clarke, L. & Clarke, R. Molecular mechanisms of tamoxifen-associated endometrial cancer (Review). *Oncol. Lett.* **9**, 1495–1501 (2015).
 17. Diaz, J. F., Andreau, J. M. & Jimenez-Barbero, J. The Interaction of Microtubules with Stabilizers Characterized at Biochemical and Structural Levels. *Top Curr Chem* **11**, 13–35 (2013).
 18. Noble, R. L., Beer, C. T. & Cutts, J. H. Role of Chance Observations in Chemotherapy: Vinca Rosea. *Ann. N. Y. Acad. Sci.* **76**, 882–894 (1958).
 19. Hirata, Y. & Ljemura, D. Halichondrins—antitumor polyether macrolides from a marine sponge. *Pure Appl. Chem* **58**, 701–710 (1986).
 20. Miller, J. H., Jonathan Singh, A. & Northcote, P. T. Microtubule-stabilizing drugs from marine sponges: focus on peloruside A and zampanolide. *Mar. Drugs* **8**, 1059–1079 (2010).
 21. Kingston, D. G. I. The shape of things to come: Structural and synthetic studies of taxol and related compounds. *Phytochemistry* **68**, 1844–1854 (2007).

22. Weaver, B. A. How Taxol/paclitaxel kills cancer cells. *Mol. Biol. Cell* **25**, 2677–81 (2014).
23. Schiff, P. B., Fant, J. & Horwitz, S. B. Promotion of microtubule assembly in vitro by taxol. *Nature* **277**, 665–667 (1979).
24. Tanaka, J. & Higa, T. Zampanolide, a new cytotoxic macrolide from a marine sponge. *Tetrahedron Lett.* **37**, 5535–5538 (1996).
25. Field, J. J. *et al.* Microtubule-Stabilizing Activity of Zampanolide, a Potent Macrolide Isolated from the Tongan Marine Sponge *Cacospongia mycofiijiensis*. *J. Med. Chem.* **52**, 7328–7332 (2009).
26. Smith III, A. B., Safonov, I. G. & Corbett, R. M. Total Synthesis of (+)-Zampanolide. *J. Am. Chem. Soc.* **123**, 12426–12427 (2001).
27. Cutignano, A. *et al.* Dactylolide, a new cytotoxic macrolide from the Vanuatu sponge *Dactylospongia* sp. *Eur. J. Org. Chem.* 775–778 (2001).
28. Smith III, A. B. & Safonov, I. G. Total Synthesis of (+)-Dactylolide. *Org. Lett.* **4**, 635–637 (2002).
29. Uenishi, J., Iwamoto, T. & Tanaka, J. Total Synthesis of (-)-Zampanolide and Questionable Existence of (-)-Dactylolide as the Elusive Biosynthetic Precursor of (-)-Zampanolide in an Okinawan Sponge. *Org. Lett.* **11**, 3262–3265 (2009).
30. Ding, F. & Jennings, M. P. An Expedient Total Synthesis of (-)-Dactylolide and Formal Synthesis of (-)-Zampanolide. *Org. Lett.* **7**, 2321–2324 (2005).
31. Field, J. J. *et al.* Zampanolide, a Potent New Microtubule-Stabilizing Agent, Covalently Reacts with the Taxane Luminal Site in Tubulin α,β -Heterodimers and Microtubules. *Chem. Biol. (Oxford, U. K.)* **19**, 686–698 (2012).
32. Prota, A. E. *et al.* Molecular Mechanism of Action of Microtubule-Stabilizing Anticancer Agents. *Sci. (Washington, DC, U. S.)* **339**, 587–590 (2013).
33. Ghosh, A. K., Cheng, X., Bai, R. & Hamel, E. Total Synthesis of Potent

- Antitumor Macrolide (-)-Zampanolide: An Oxidative Intramolecular Cyclization-Based Strategy. *Eur. J. Org. Chem.* **2012**, 4130–4139 (2012).
34. Zurwerra, D., Gertsch, J. & Altmann, K.-H. Synthesis of (-)-Dactylolide and 13-Desmethylene(-)-dactylolide and Their Effects on Tubulin. *Org. Lett.* **12**, 2302–2305 (2010).
 35. Zurwerra, D. *et al.* Total synthesis of (-)-zampanolide and structure-activity relationship studies on (-)-dactylolide derivatives. *Chem. - Eur. J.* **18**, 16868–16883 (2012).
 36. Hoye, T. R. & Hu, M. Macrolactonization via Ti(IV)-Mediated Epoxy-Acid Coupling: A Total Synthesis of (-)-Dactylolide [and Zampanolide]. *J. Am. Chem. Soc.* **125**, 9576–9577 (2003).
 37. Aubele, D. L., Wan, S. & Floreancig, P. E. Total synthesis of (+)-dactylolide through an efficient sequential Peterson olefination and Prins cyclization reaction. *Angew. Chem., Int. Ed.* **44**, 3485–3488 (2005).
 38. Sanchez, C. C. & Keck, G. E. Total Synthesis of (+)-Dactylolide. *Org. Lett.* **7**, 3053–3056 (2005).
 39. Louis, I., Hungerford, N. L., Humphries, E. J. & McLeod, M. D. Enantioselective Total Synthesis of (-)-Dactylolide. *Org. Lett.* **8**, 1117–1120 (2006).
 40. Troast, D. M., Yuan, J. & Porco Jr., J. A. Studies toward the synthesis of (-)-zampanolide: preparation of the macrocyclic core. *Adv. Synth. Catal.* **350**, 1701–1711 (2008).
 41. Troast, D. M. & Porco Jr., J. A. Studies Toward the Synthesis of (-)-Zampanolide: Preparation of N-Acyl Hemiaminal Model Systems. *Org. Lett.* **4**, 991–994 (2002).
 42. Trost, B. M. & Chisholm, J. D. An Acid-Catalyzed Macrolactonization Protocol. *Org. Lett.* **4**, 3743–3745 (2002).
 43. Yun, S. Y. *et al.* Total Synthesis of (-)-Dactylolide. *Angew. Chem., Int. Ed.*

- 49, 4261–4263, S4261/1–S4261/21 (2010).
44. Ghosh, A. K. & Cheng, X. Enantioselective Total Synthesis of (-)-Zampanolide, a Potent Microtubule-Stabilizing Agent. *Org. Lett.* **13**, 4108–4111 (2011).
 45. Wang, J. Towards the Synthesis of Marine Natural Product (-)-Zampanolide and its Analogues. (Victoria University of Wellington, 2015).
 46. Wang, J., Ting, S. Z. Y. & Harvey, J. E. Preparation of conjugated dienoates with Bestmann ylide: Towards the synthesis of zampanolide and dactylolide using a facile linchpin approach. *Beilstein J. Org. Chem.* **11**, 1815–1822 (2015).
 47. Langille, N. F. & Jamison, T. F. trans-hydroalumination/alkylation: One-pot synthesis of trisubstituted allylic alcohols. *Org. Lett.* **8**, 3761–3764 (2006).
 48. Wang, Z. in *Comprehensive Organic Name Reactions and Reagents* (John Wiley & Sons, Inc., 2010). doi:10.1002/9780470638859.conrr047
 49. Frigerio, M., Santagostino, M. & Sputore, S. A User-Friendly Entry to 2-Iodoxybenzoic Acid (IBX). *J. Org. Chem.* **64**, 4537–4538 (1999).
 50. Wullschleger, C. W., Gertsch, J. & Altmann, K.-H. Stereoselective Synthesis of a Monocyclic Peloruside A Analogue. *Org. Lett.* **12**, 1120–1123 (2010).
 51. Oikawa, Y., Nishi, T. & Yonemitsu, O. Kinetic acetalization for 1,2- and 1,3-diol protection by the reaction of p-methoxyphenylmethyl methyl ether with DDQ. *Tetrahedron Lett.* **24**, 4037–4040 (1983).
 52. Mickel, S. J. *et al.* Large-Scale Synthesis of the Anti-Cancer Marine Natural Product (+)-Discodermolide. Part 3: Synthesis of Fragment C 15-21. *Org. Process Res. Dev.* **8**, 107–112 (2004).
 53. Trost, B. M. & Weiss, A. H. The Enantioselective Addition of Alkyne Nucleophiles to Carbonyl Groups. *Adv. Synth. Catal.* **351**, 963–983 (2009).
 54. Takita, R., Fukuta, Y., Tsuji, R., Ohshima, T. & Shibasaki, M. A New Entry in Catalytic Alkynylation of Aldehydes and Ketones: Dual Activation of Soft

- Nucleophiles and Hard Electrophiles by an Indium(III) Catalyst. *Org. Lett.* **7**, 1363–1366 (2005).
55. Takita, R., Yakura, K., Ohshima, T. & Shibasaki, M. Asymmetric Alkynylation of Aldehydes Catalyzed by an In(III)/BINOL Complex. *J. Am. Chem. Soc.* **127**, 13760–13761 (2005).
 56. Frantz, D. E., Fa, R. & Carreira, E. M. Catalytic in Situ Generation of Zn (II) -Alkynilides under Mild Conditions : A Novel C=N Addition Process Utilizing Terminal Acetylenes. *J. Am. Chem. Soc.* 11245–11246 (1999).
 57. Frantz, D. E., Fässler, R. & Carreira, E. M. Facile enantioselective synthesis of propargylic alcohols by direct addition of terminal alkynes to aldehydes [3]. *J. Am. Chem. Soc.* **122**, 1806–1807 (2000).
 58. Sasaki, H., Boyall, D. & Carreira, E. M. Facile, asymmetric addition of acetylene to aldehydes: In situ generation of reactive zinc acetylide. *Helv. Chim. Acta* **84**, 964–971 (2001).
 59. Boyall, D., Frantz, D. E. & Carreira, E. M. Efficient enantioselective additions of terminal alkynes and aldehydes under operationally convenient conditions. *Org. Lett.* **4**, 2605–2606 (2002).
 60. Moore, D. & Pu, L. BINOL-Catalyzed Highly Enantioselective Terminal Alkyne Additions to Aromatic Aldehydes. *Org. Lett.* **4**, 1855–1857 (2002).
 61. Gao, G., Moore, D., Xie, R.-G. & Pu, L. Highly Enantioselective Phenylacetylene Additions to Both Aliphatic and Aromatic Aldehydes. *Org. Lett.* **4**, 4143–4146 (2002).
 62. Chen, S. *et al.* A Lewis acid activated reaction of Zn with EtI to promote highly enantioselective alkyne additions to aldehydes. *Chem. Commun.* **51**, 358–361 (2015).
 63. Huang, W.-C., Liu, W., Wu, X.-D., Ying, J. & Pu, L. Enantioselective Alkyne Addition to Aliphatic, Aromatic, and Vinyl Aldehydes Using Zn, i PrI, H8BINOL, and Ti(OiPr)₄. *J. Org. Chem.* **80**, 11480–11484 (2015).

64. Trost, B. M., Weiss, A. H. & Jacobi von Wangelin, A. Dinuclear Zn-Catalyzed Asymmetric Alkynylation of Unsaturated Aldehydes. *J. Am. Chem. Soc.* **128**, 8–9 (2005).
65. Trost, B. M., Bartlett, M. J., Weiss, A. H., Vonwangelin, A. J. & Chan, V. S. Development of Zn-prophenol-catalyzed asymmetric alkyne addition: Synthesis of chiral propargylic alcohols. *Chem. Eur. J.* **18**, 16498–16509 (2012).
66. Schwartz, B. D. *et al.* Spiroacetal biosynthesis in insects from diptera to hymenoptera: The Giant Ichneumon wasp *Megarhyssa nortoni nortoni* Cresson. *J. Am. Chem. Soc.* **130**, 14853–14860 (2008).
67. Hoveyda, A. H., Evans, D. A. & Fu, G. C. Substrate-Directable Chemical Reactions. *Chem. Rev* **93**, 1307–1370 (1993).
68. Hudrlik, P. F. & Hudrlik, A. M. in *The Carbon–Carbon Triple Bond (1978)* 199–273 (John Wiley & Sons, Ltd., 1978). doi:10.1002/9780470771563.ch7
69. Normant, J. F. & Alexakis, A. Carbometallation (C-Metallation) of Alkynes: Stereospecific Synthesis of Alkenyl Derivatives. *Synthesis (Stuttg)*. **1981**, 841–870 (1981).
70. Negishi, E., Van Horn, D. E. & Yoshida, T. Carbometallation reaction of alkynes with organoalane-zirconocene derivatives as a route to stereo- and regiodefined trisubstituted alkenes. *J. Am. Chem. Soc.* **107**, 6639–6647 (1985).
71. Grant, B. & Djerassi, C. The Mechanism of Hydride Reduction of 1-Alkyn-3-ols. *J. Org. Chem.* **39**, 968–970 (1974).
72. Das, S., Paul, D. & Goswami, R. K. Stereoselective Total Synthesis of Bioactive Marine Natural Product Biselyngbyolide B. *Org. Lett.* 1908–1911 (2016). doi:10.1021/acs.orglett.6b00713
73. Corey, E. J., Katzenellenbogen, J. a. & Posner, G. H. New stereospecific synthesis of trisubstituted olefins. Stereospecific synthesis of farnesol. *J. Am. Chem. Soc.* **89**, 4245–4247 (1967).

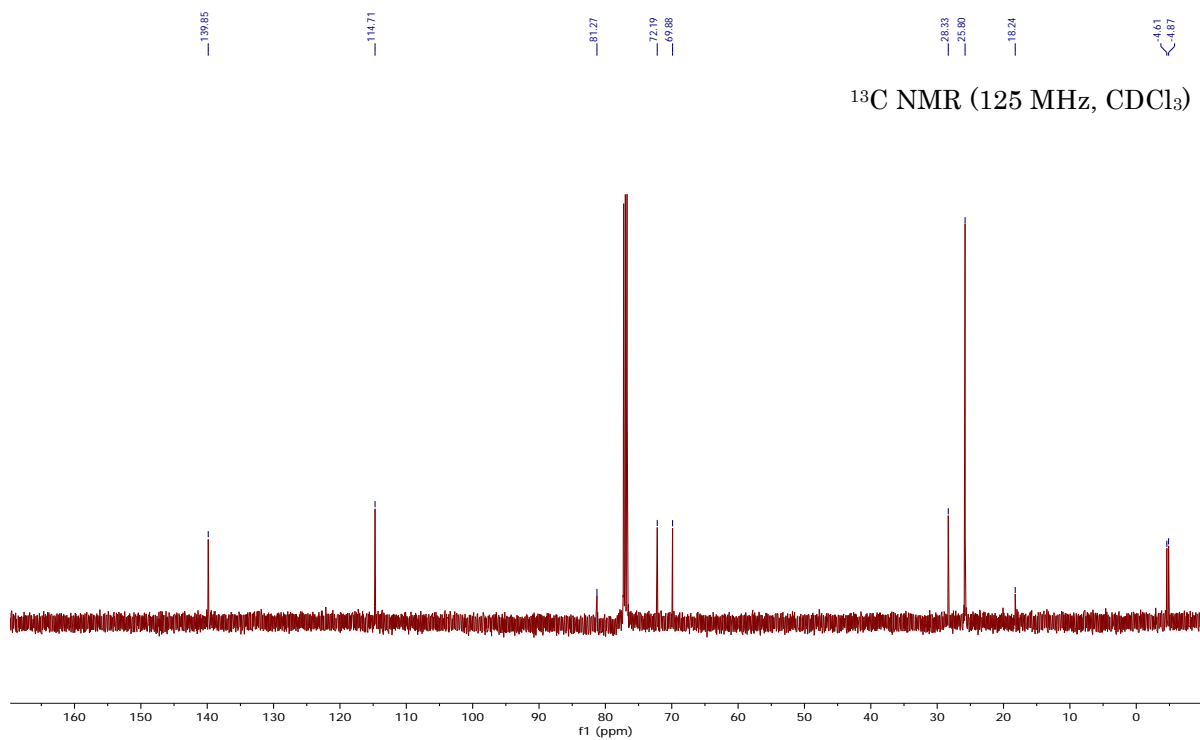
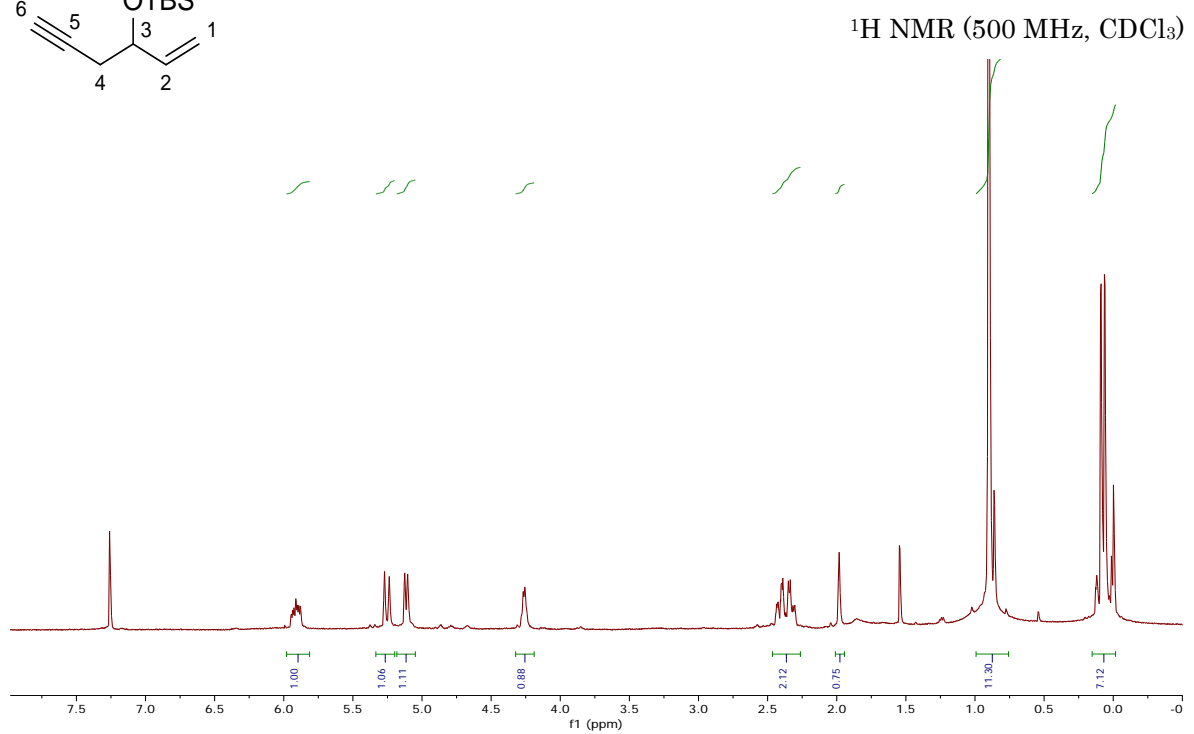
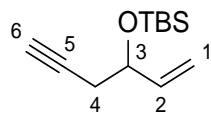
74. Corey, E. J., Katzenellenbogen, J. A., Gilman, N. W., Roman, S. A. & Erickson, B. W. Stereospecific Total Synthesis of the dl-C18 Cecropia Juvenile Hormone. *J. Am. Chem. Soc.* **5618–5620** (1968). doi:10.1021/ja01022a060
75. Mori, S. & Nakamura, E. in *Modern Organocopper Chemistry* 315–346 (Wiley-VCH Verlag GmbH, 2002). doi:10.1002/3527600086.ch10
76. Liu, Y., Feng, G., Wang, J., Wu, J. & Dai, W.-M. Synthesis of Two Diastereomers of Iriomoteolide-1a via a Tunable Four- Module Coupling Approach Using Ring-Closing Metathesis as the Key Step. *SYNLETT* **2**, 1774–1778 (2011).
77. Feng, C. & Kobayashi, Y. Allylic Substitution for Construction of a Chiral Quaternary Carbon Possessing an Aryl Group. *J. Org. Chem.* **78**, 3755–3766 (2013).
78. Takamura, H. *et al.* Stereoselective synthesis and absolute configuration of the C33–C42 fragment of symbiodinolide. *Tetrahedron* **65**, 7449–7456 (2009).
79. Boivin, T. L. B. Synthetic routes to tetrahydrofuran, tetrahydropyran, and spiroketal units of polyether antibiotics and a survey of spiroketals of other natural products. *Tetrahedron* **43**, 3309–3362 (1987).
80. Clarke, P. A. & Santos, S. Strategies for the Formation of Tetrahydropyran Rings in the Synthesis of Natural Products. *European J. Org. Chem.* **2006**, 2045–2053 (2006).
81. Larrosa, I., Romea, P. & Urpí, F. Synthesis of six-membered oxygenated heterocycles through carbon–oxygen bond-forming reactions. *Tetrahedron* **64**, 2683–2723 (2008).
82. White, J. D., Hong, J. & Robarge, L. A. Intramolecular palladium catalyzed alkoxy carbonylation of 6-hydroxy-1-octenes. Stereoselective synthesis of substituted tetrahydropyrans. *Tetrahedron Lett.* **40**, 1463–1466 (1999).
83. Kuntiyong, P., Lee, T. H., Kranemann, C. L. & White, J. D. Total synthesis

- of the marine toxin phorboxazole A using palladium(II)-mediated intramolecular alkoxyacylation for tetrahydropyran synthesis. *Org. Biomol. Chem.* **10**, 7884–7899 (2012).
84. Fuwa, H., Yamaguchi, H. & Sasaki, M. An enantioselective total synthesis of aspergillides A and B. *Tetrahedron* **66**, 7492–7503 (2010).
85. Kim, H., Park, Y. & Hong, J. Stereoselective Synthesis of 2,6-cis-Tetrahydropyrans through a Tandem Allylic Oxidation/Oxa-Michael Reaction Promoted by the gem-Disubstituent Effect: Synthesis of (+)-Neopeltolide Macrolactone. *Angew. Chemie Int. Ed.* **48**, 7577–7581 (2009).
86. Schobert, R. Preparation of (Triphenylphosphoranylidene)-Ketene From (Methoxycarbonylmethylene)-Triphenylphosphorane. *Org. Synth.* **82**, 140 (2005).
87. Ding, F. & Jennings, M. P. Total Synthesis of (-)-Dactylolide and Formal Synthesis of (-)-Zampanolide via Target Oriented b-C-Glycoside Formation. *J. Org. Chem.* **73**, 5965–5976 (2008).
88. Smith, A. B., Minbiole, K. P., Verhoest, P. R. & Schelhaas, M. Total Synthesis of (+)-Phorboxazole A Exploiting the Petasis-Ferrier Rearrangement. (2001). doi:10.1021/ja011604l
89. Hyugano, T., Liu, S. & Ouchi, A. Facile Photochemical Transformation of Alkyl Aryl Selenides to the Corresponding Carbonyl Compounds by Molecular Oxygen: Use of Selenides as Masked Carbonyl Groups. doi:10.1021/jo801730j
90. Bracca, A. B. J. & Kaufman, T. S. An alternative and convenient synthesis of oct-7-enal, a naturally-occurring aldehyde isolated from the Japanese thistle *Cirsium dipsacolepis*. *J. Braz. Chem. Soc.* **19**, 1125–1128 (2008).
91. Frankowski, K. J., Golden, J. E., Zeng, Y., Lei, Y. & Aubé, J. Syntheses of the *Stemona* Alkaloids (±)-Stenine, (±)-Neostenine, and (±)-13-Epineostenine Using a Stereodivergent Diels–Alder/Azido-Schmidt Reaction. *J. Am. Chem. Soc.* **130**, 6018–6024 (2008).

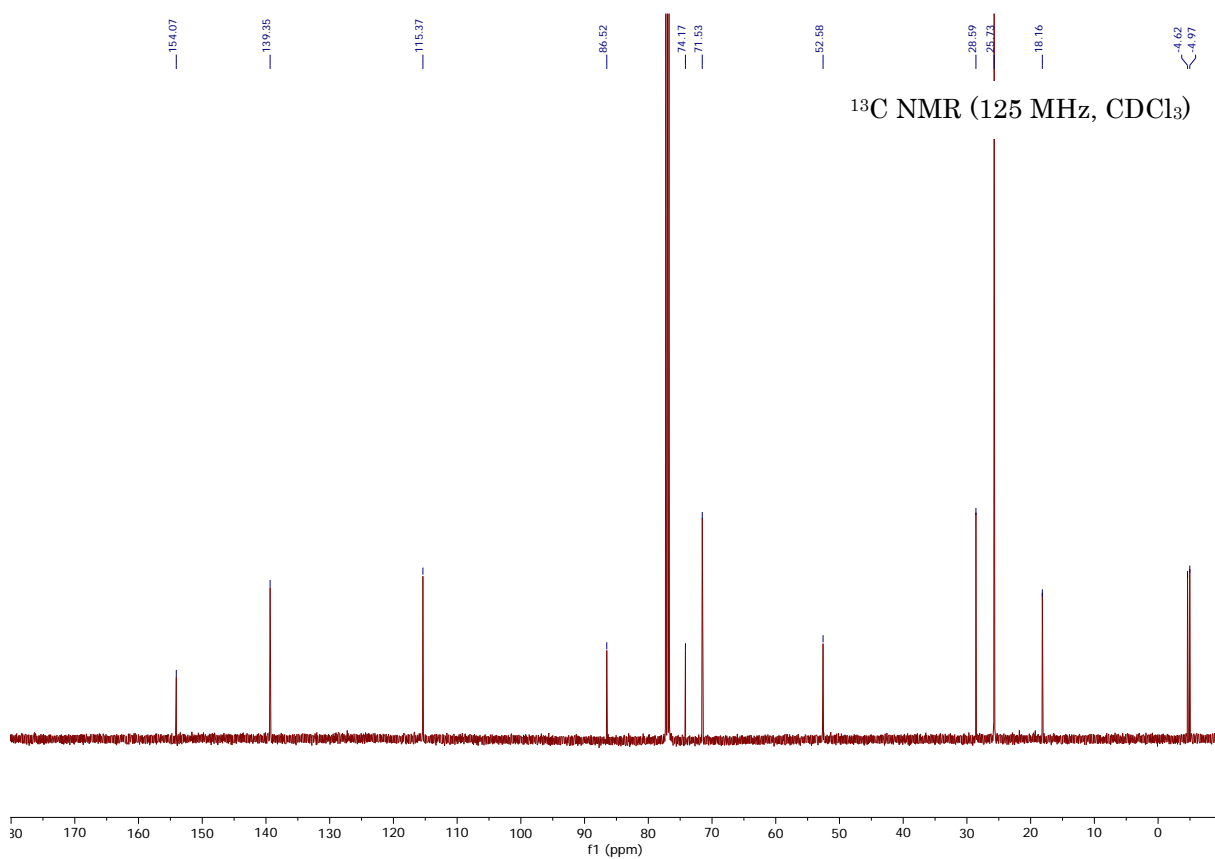
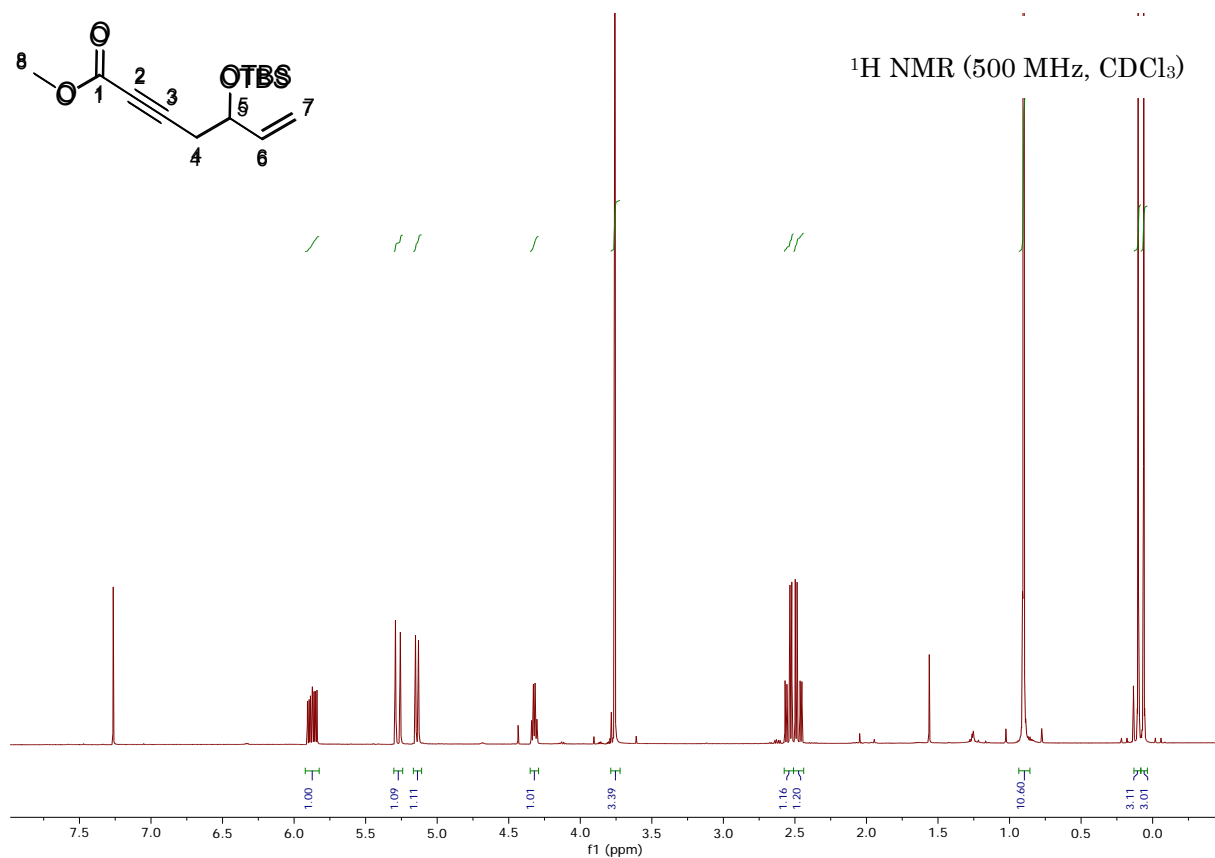
92. Ko, H. M. *et al.* Total Synthesis of (-)-Amphidinolide K. *Angew. Chemie Int. Ed.* **48**, 2364–2366 (2009).

Appendix

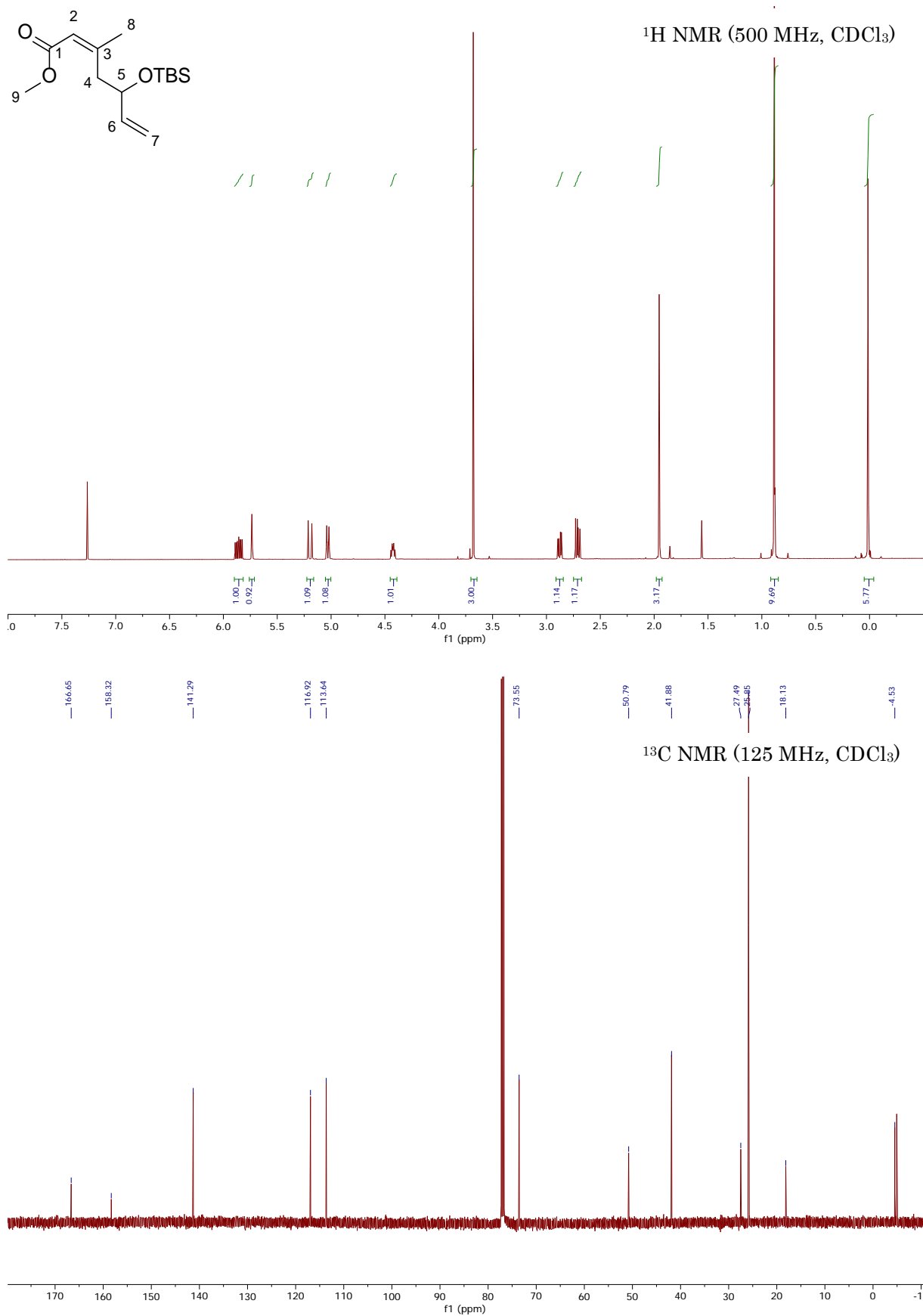
tert-Butyl(hex-1-en-5-yn-3-yloxy)dimethylsilane – 109



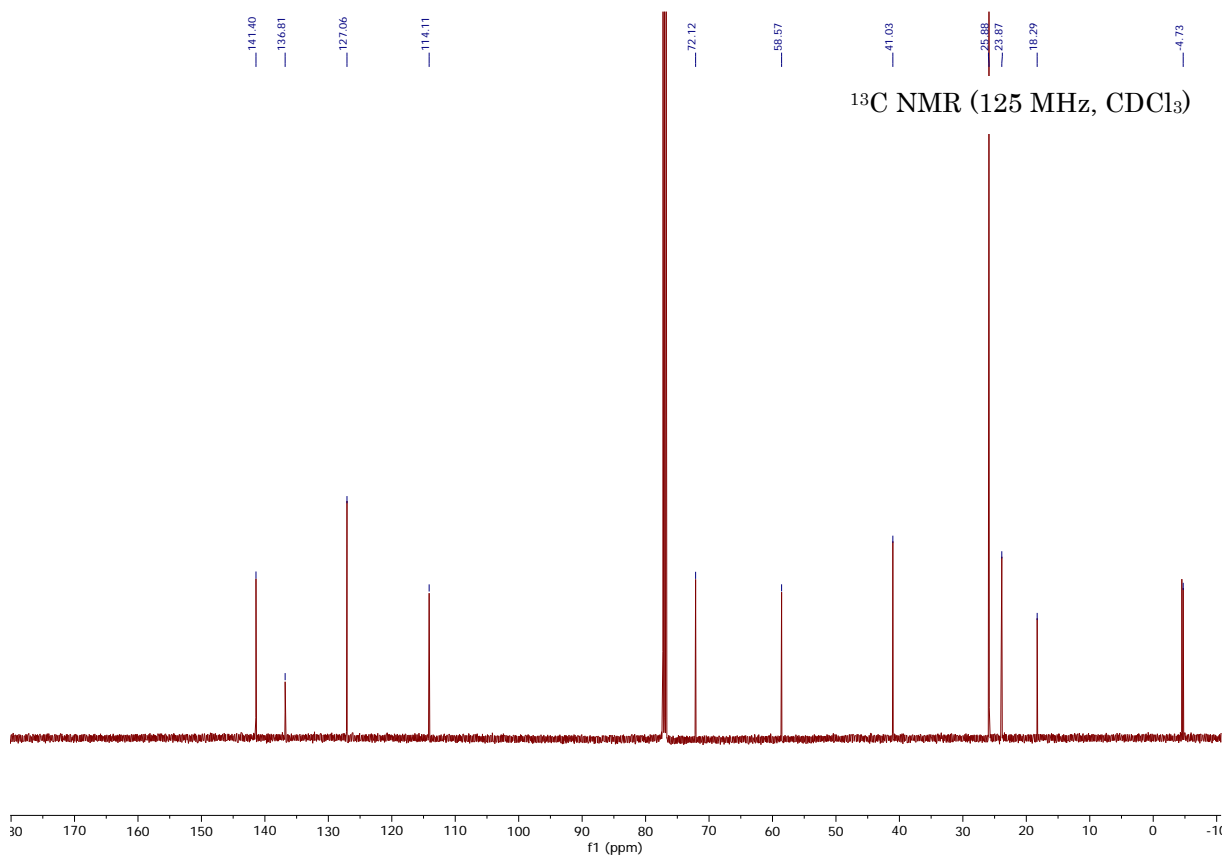
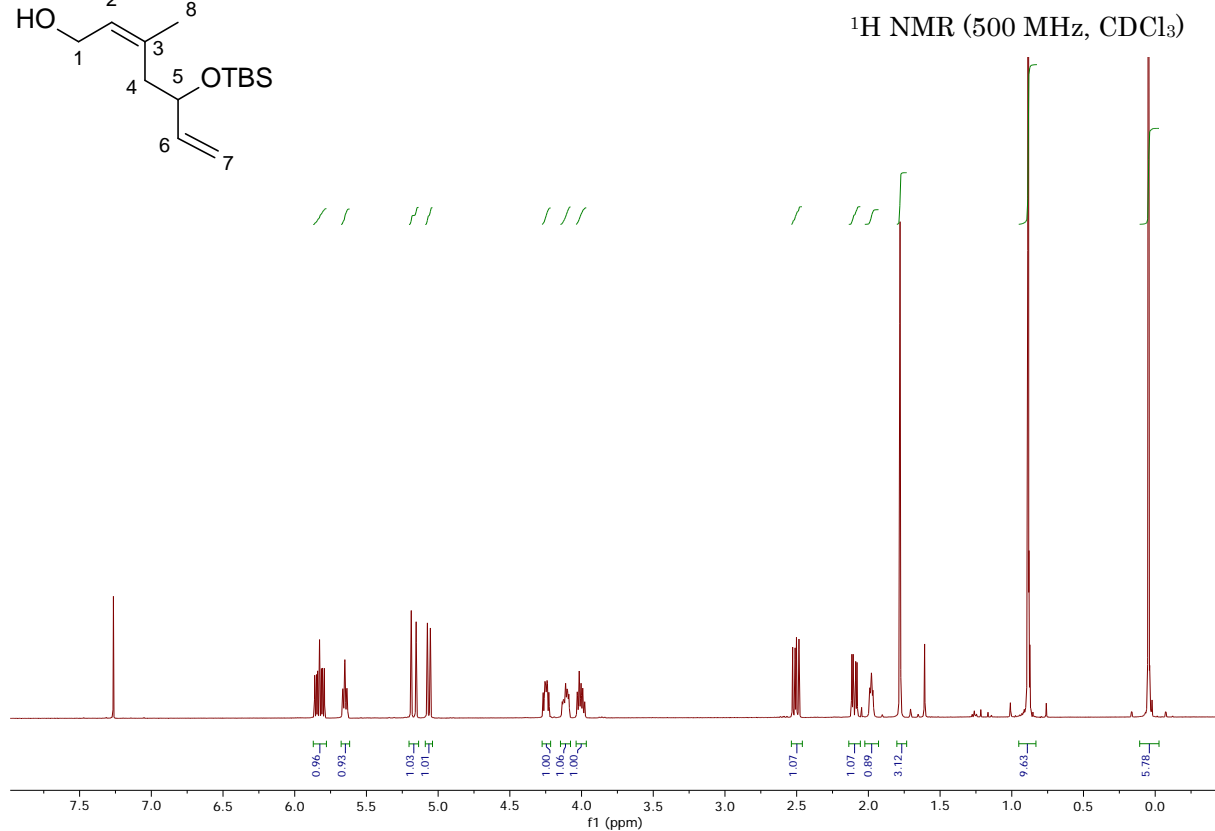
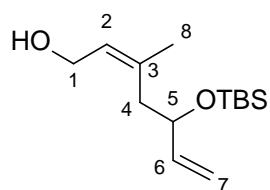
Methyl 5-tert-butyltrimethylsilyloxy-6-hepten-2-ynoate - 103



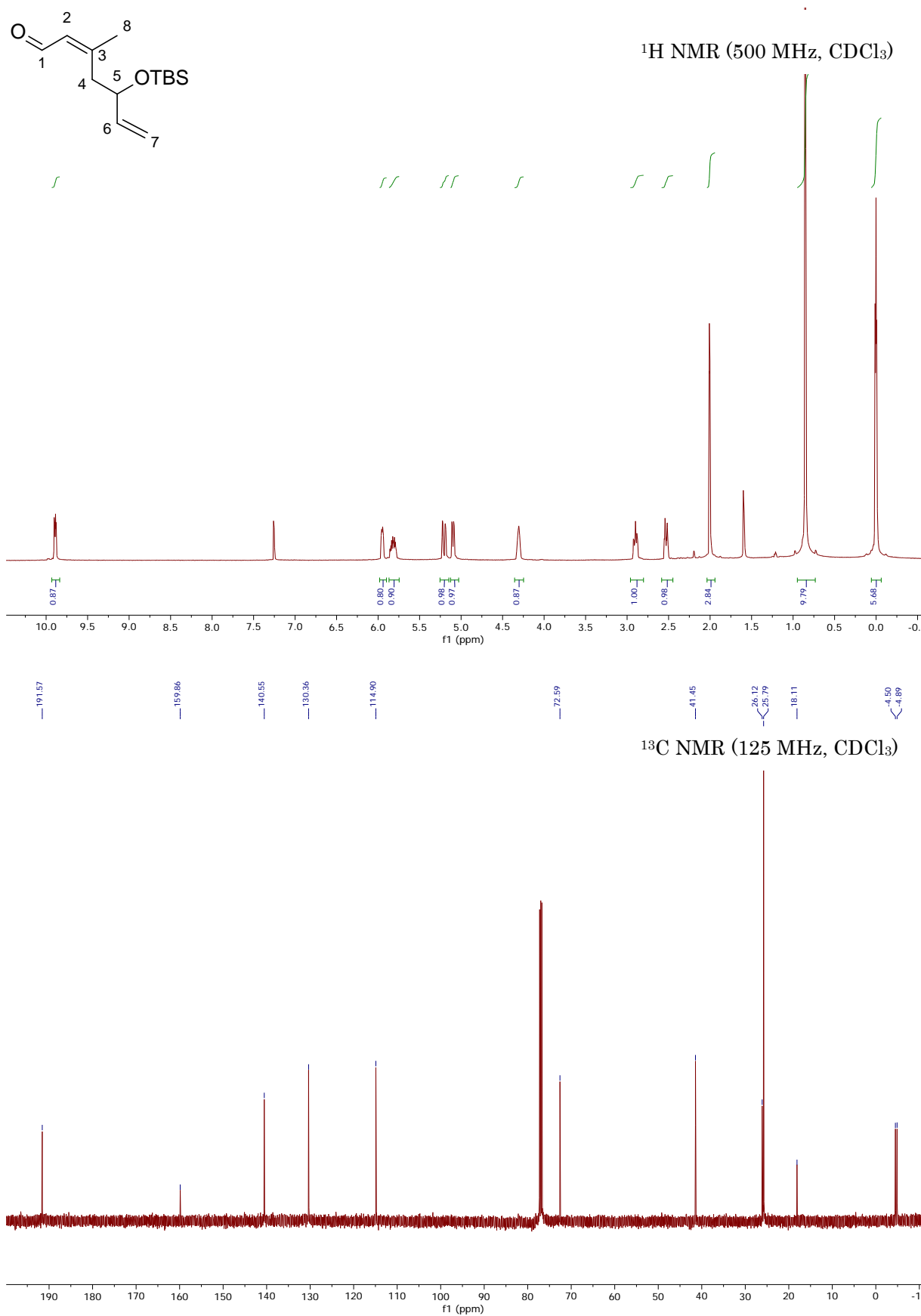
Methyl 5-(tert-butyldimethylsilyloxy)-3-methyl-2,6-heptadienoate - 132



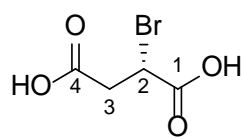
Z-5-((*tert*-Butyldimethylsilyl)oxy)-3-methylhepta-2,6-dien-1-ol - 133



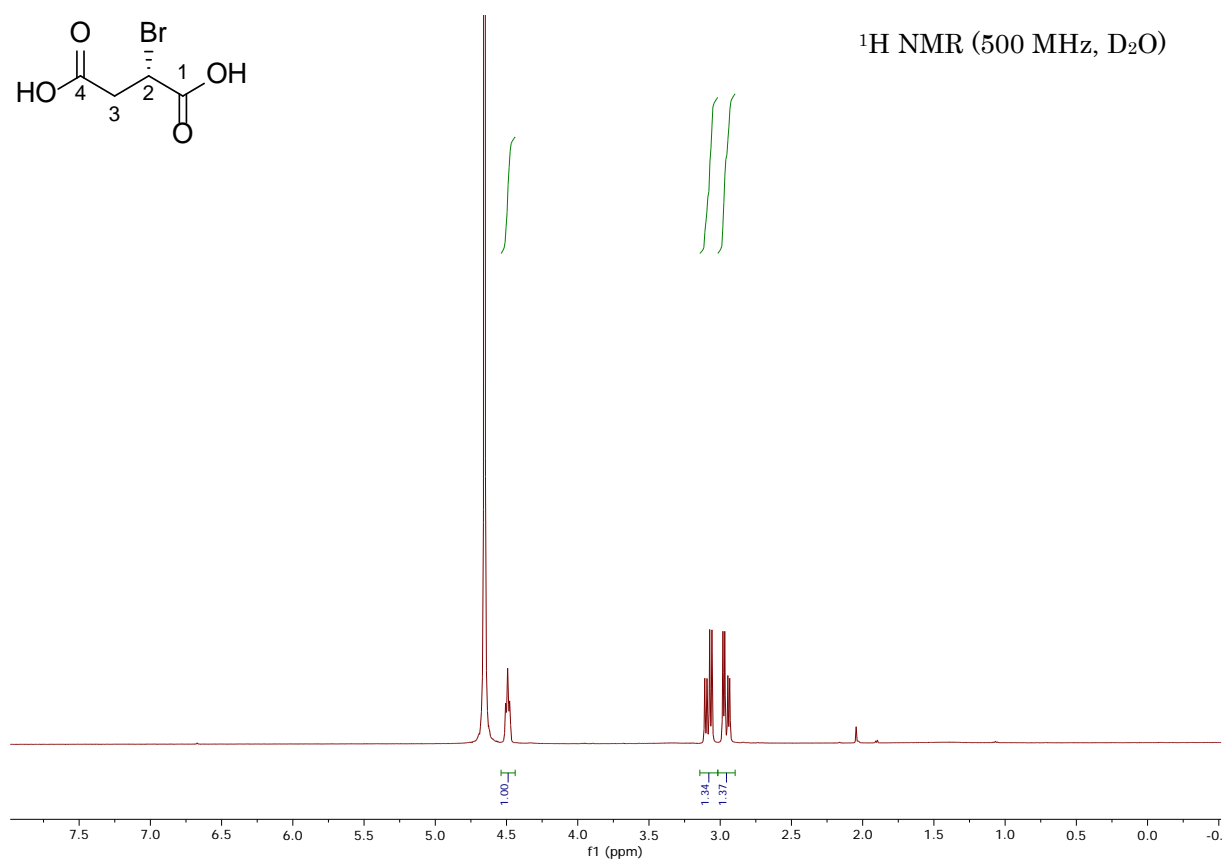
(Z)-5-((*tert*-Butyldimethylsilyloxy)-3-methylhepta-2,6-dienal - 117



(S)-2-Bromosuccinic acid – 135



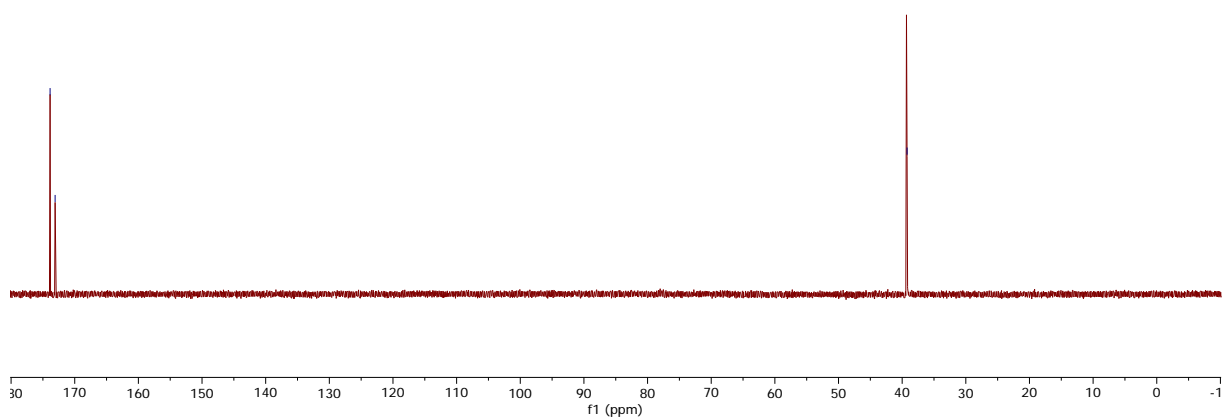
^1H NMR (500 MHz, D_2O)



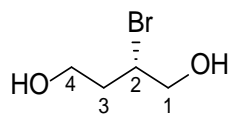
173.67
173.66

39.23

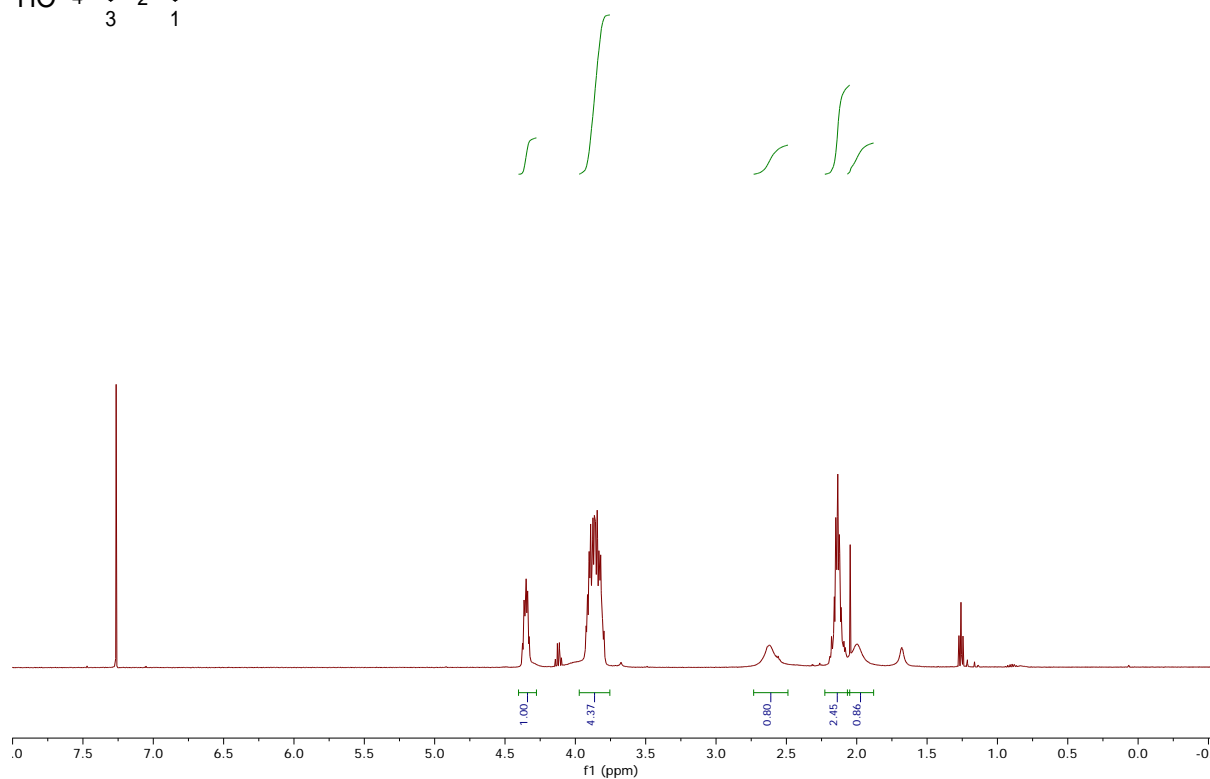
^{13}C NMR (125 MHz, D_2O)



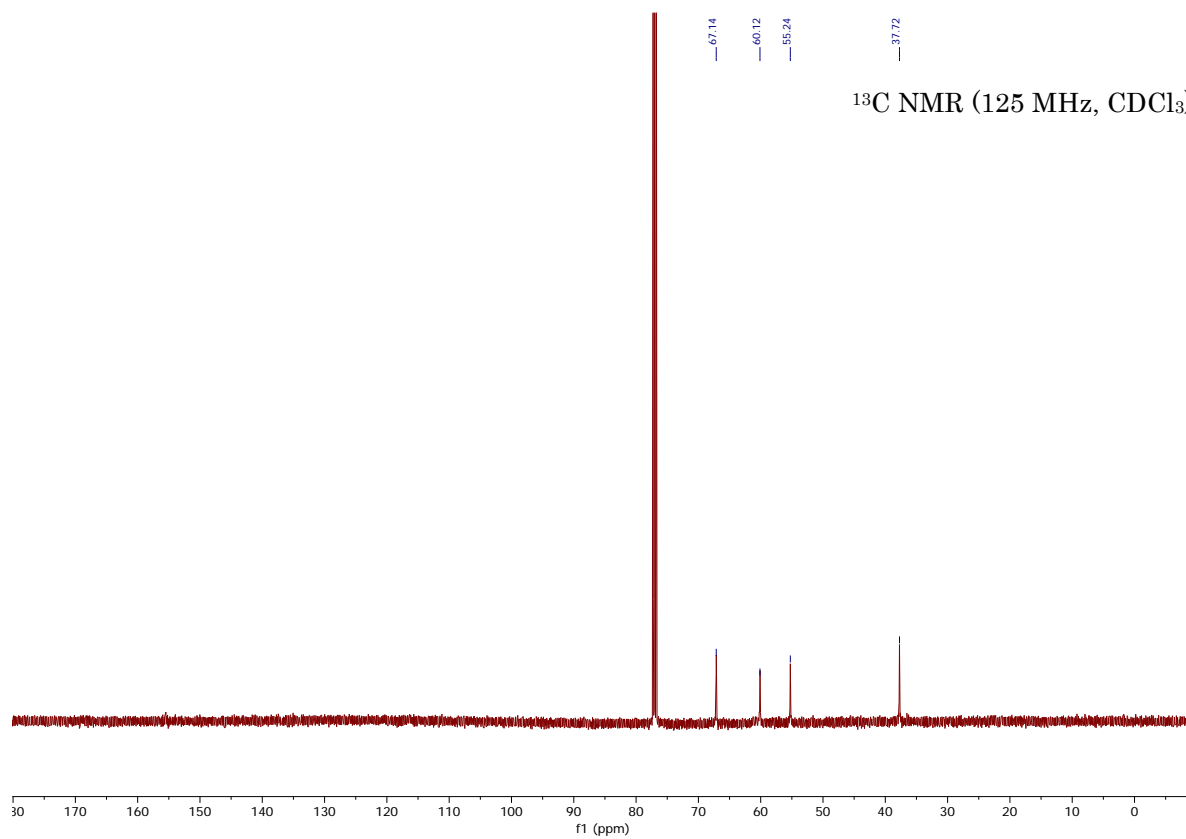
(S)-2-Bromobutane-1,4-diol – 136



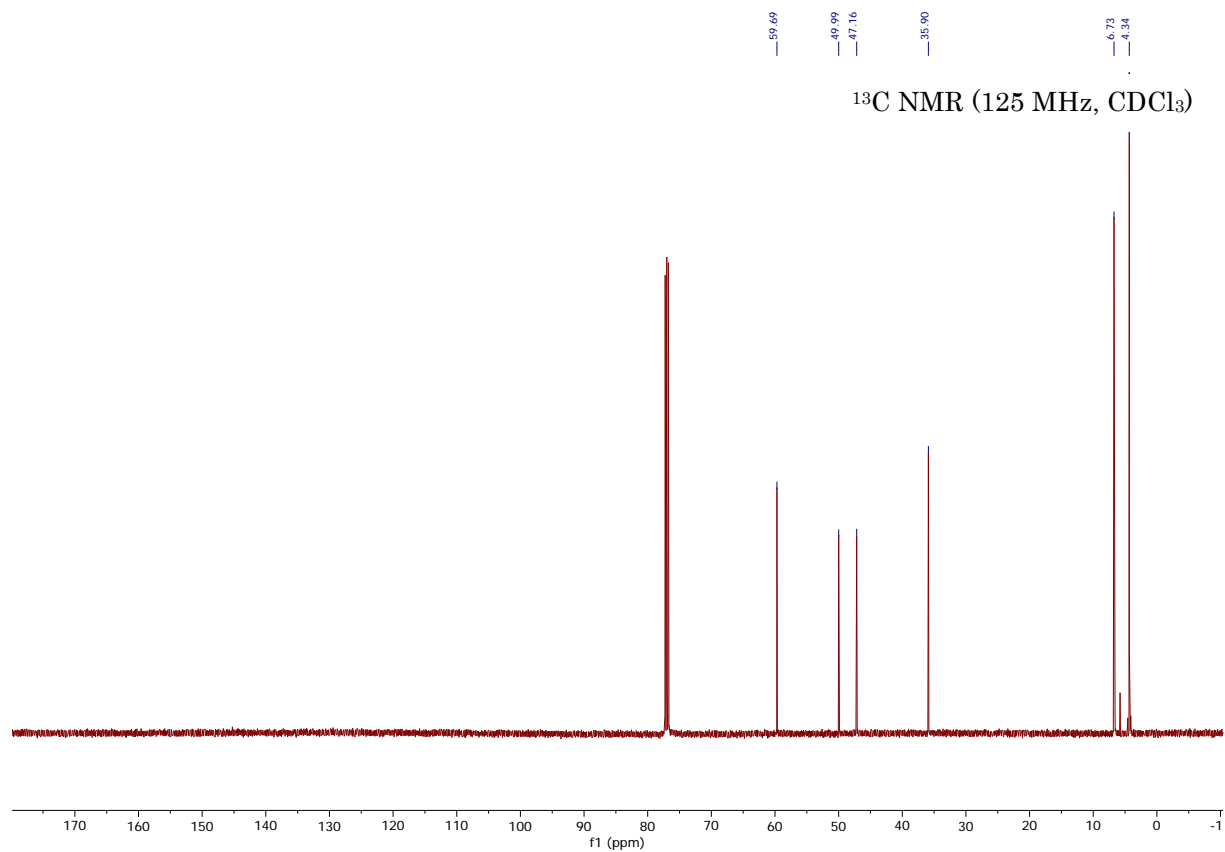
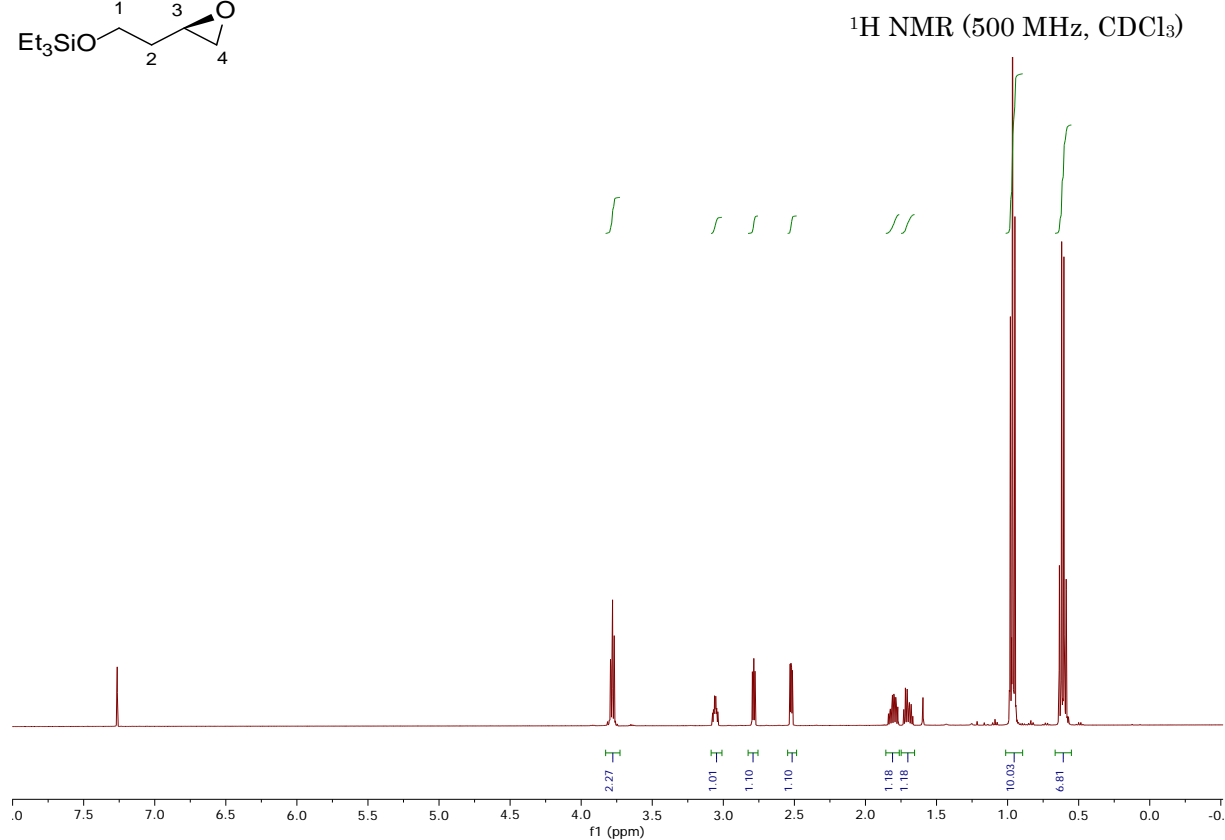
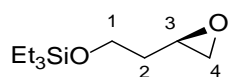
¹H NMR (500 MHz, CDCl₃)



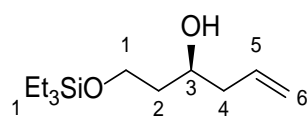
¹³C NMR (125 MHz, CDCl₃)



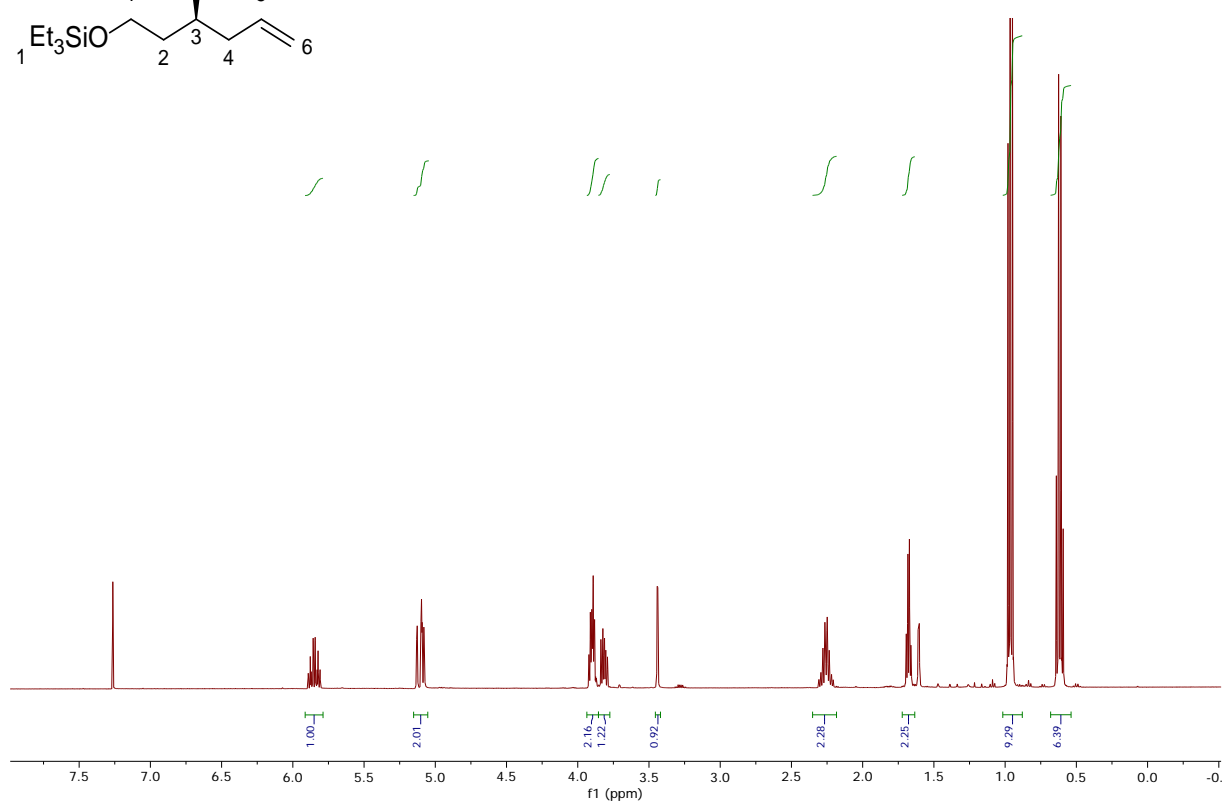
Triethyl-(2-[2R-oxiran-2-yl]ethoxy)-silane – 137



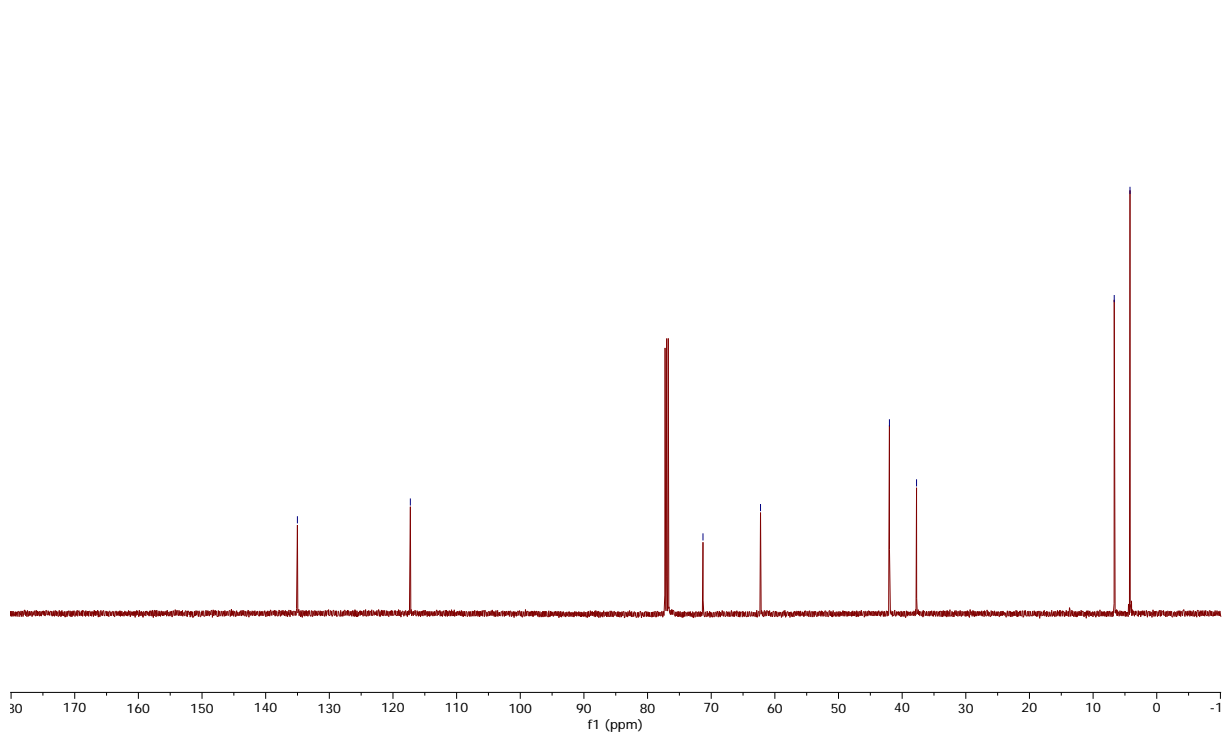
(S)-1-((Triethylsilyl)oxy)hex-5-en-3-ol - 138



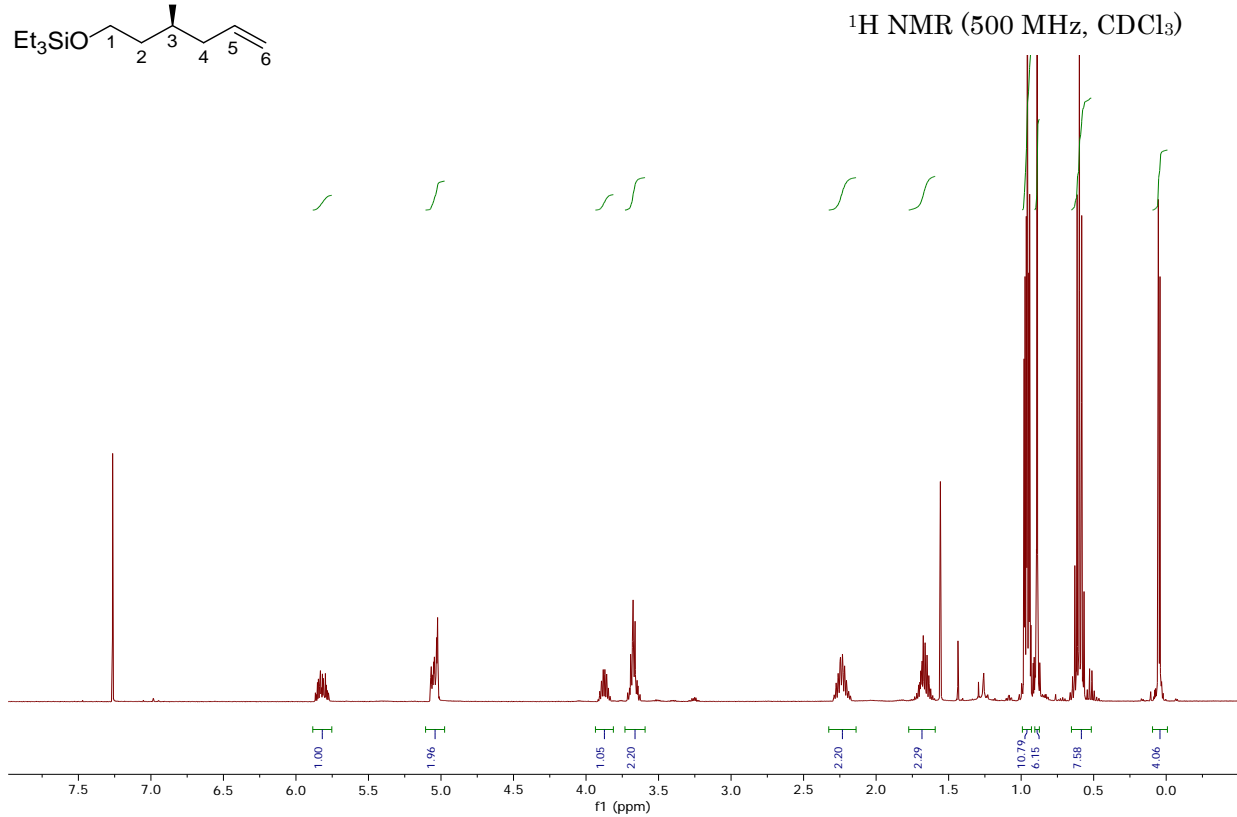
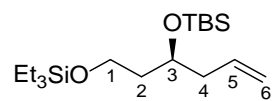
¹H NMR (500 MHz, CDCl₃)



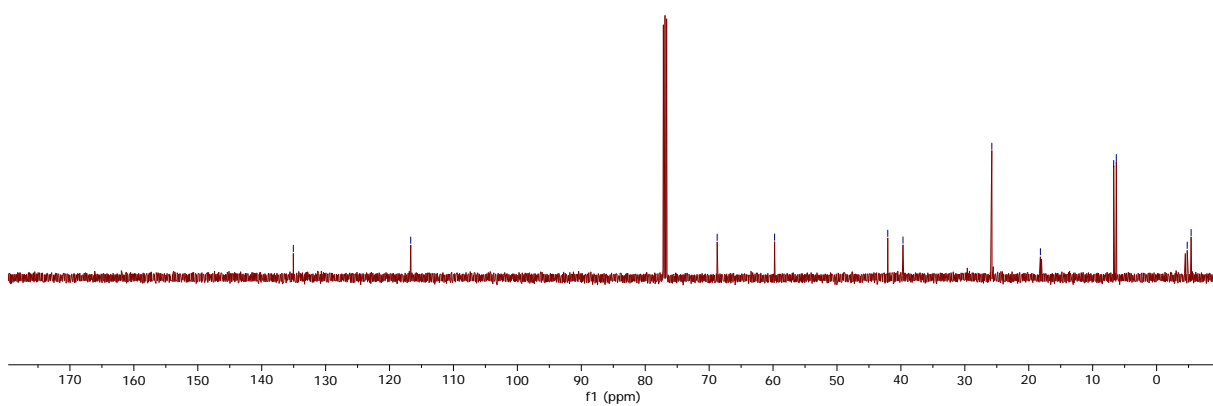
¹³C NMR (125 MHz, CDCl₃)



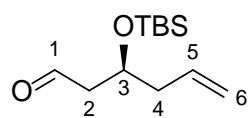
(S)-5-Allyl-9,9-diethyl-2,2,3,3-tetramethyl-4,8-dioxa-3,9-disilaundecane - 139



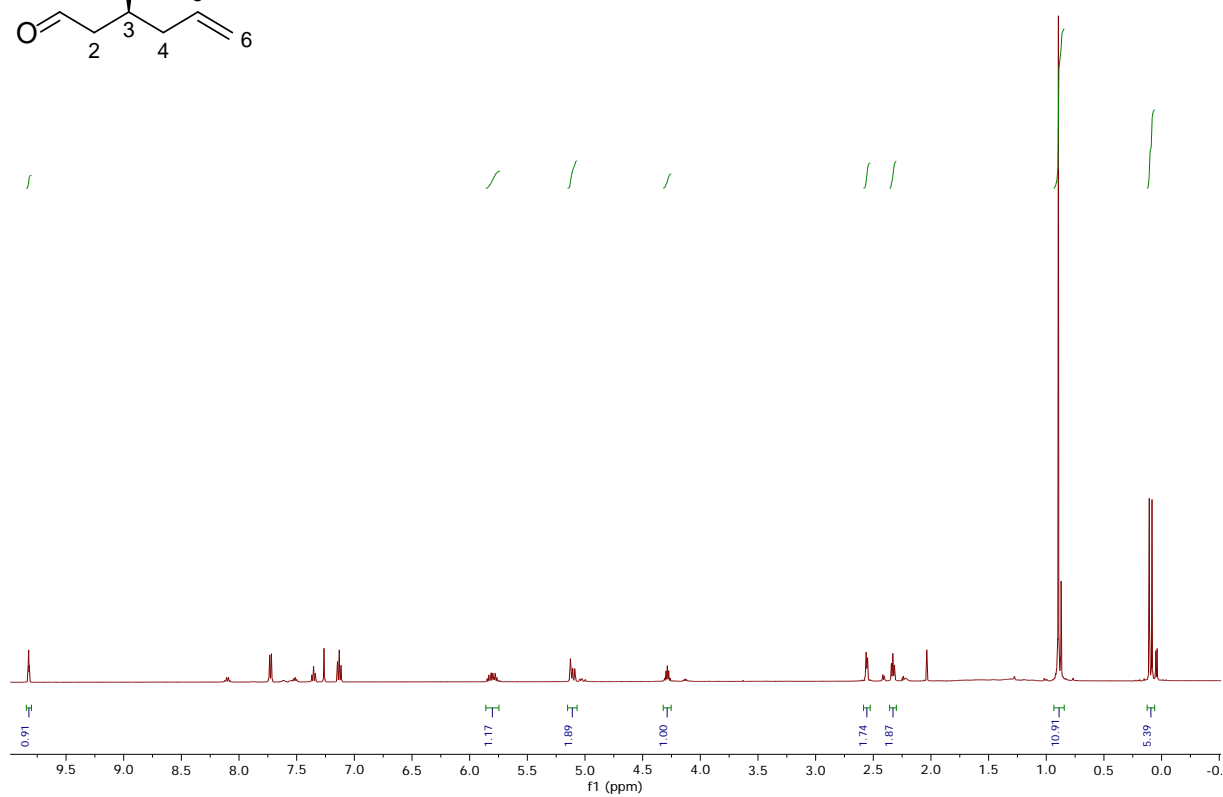
¹³C NMR (125 MHz, CDCl₃)



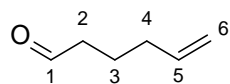
(S)-3-((*tert*-Butyldimethylsilyl)oxy)hex-5-enal- 141



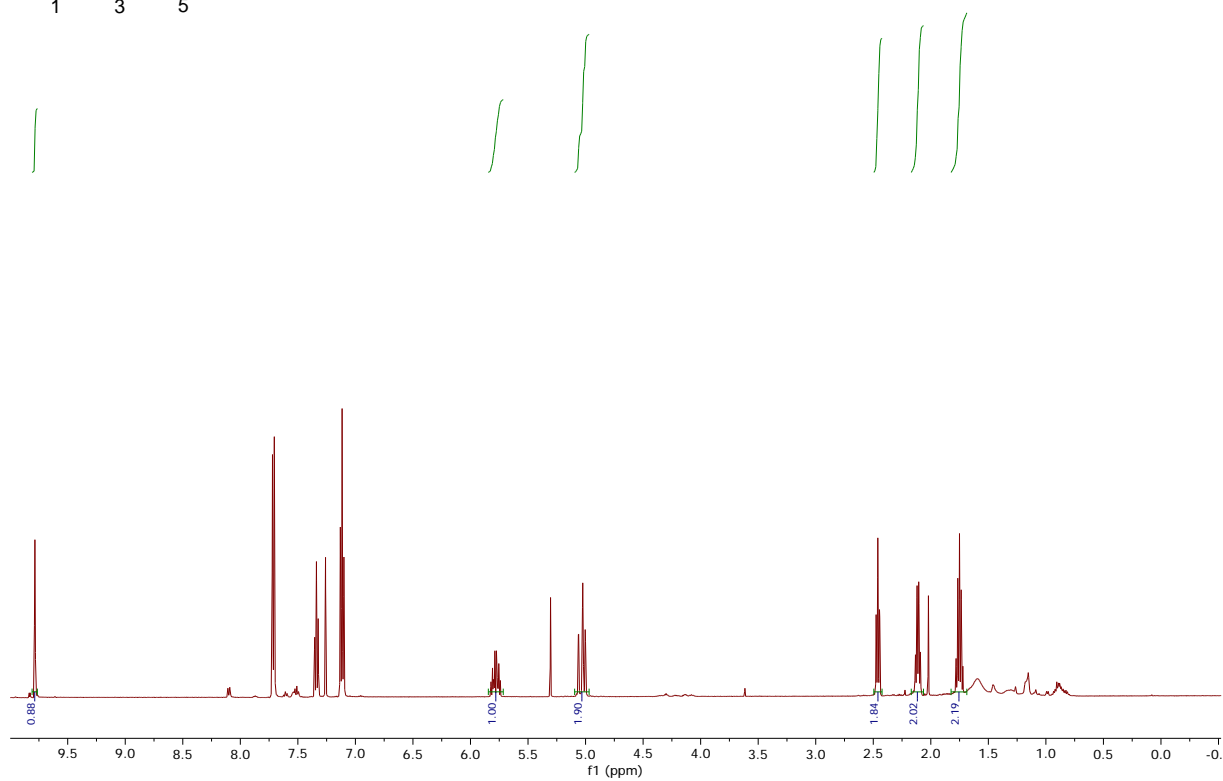
¹H NMR (500 MHz, CDCl₃)



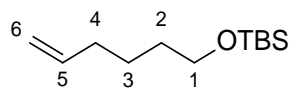
Hex-5-enal- 144



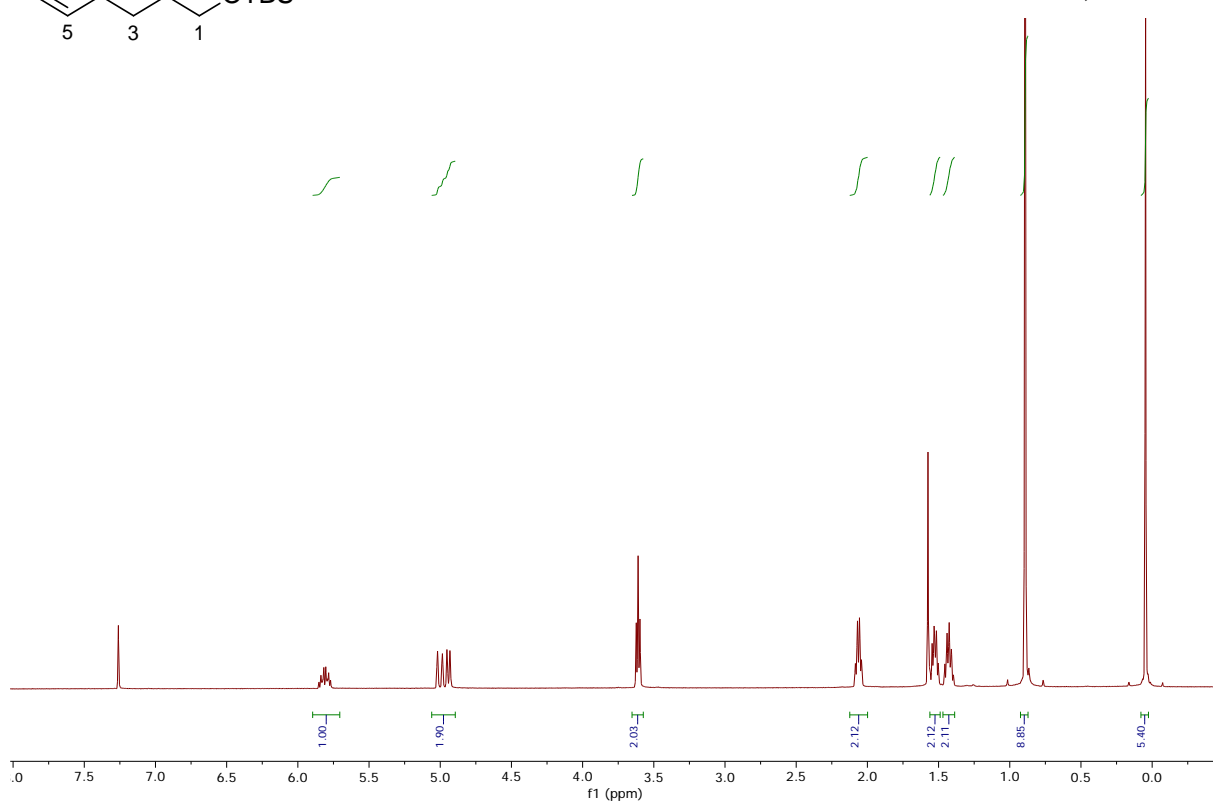
¹H NMR (500 MHz, CDCl₃)



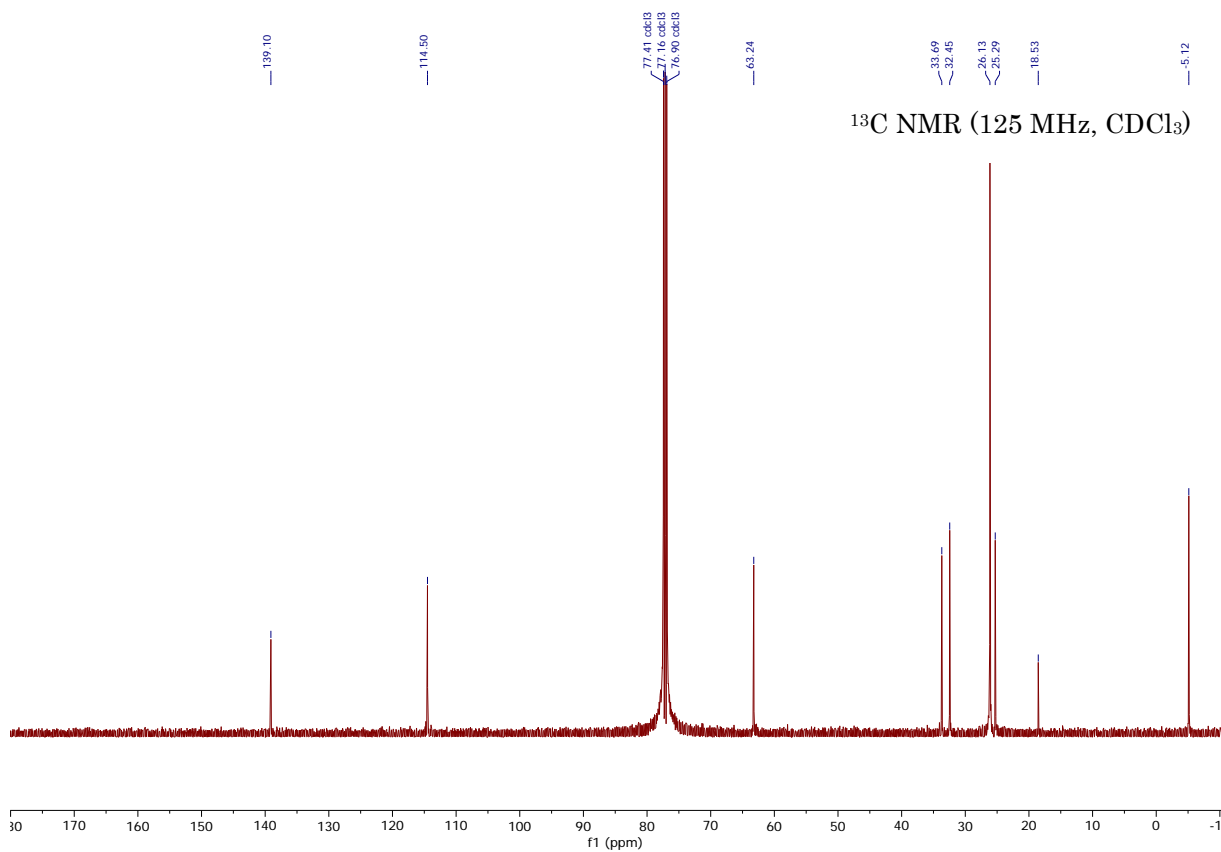
tert-Butyl(hex-5-en-1-yloxy)dimethylsilane



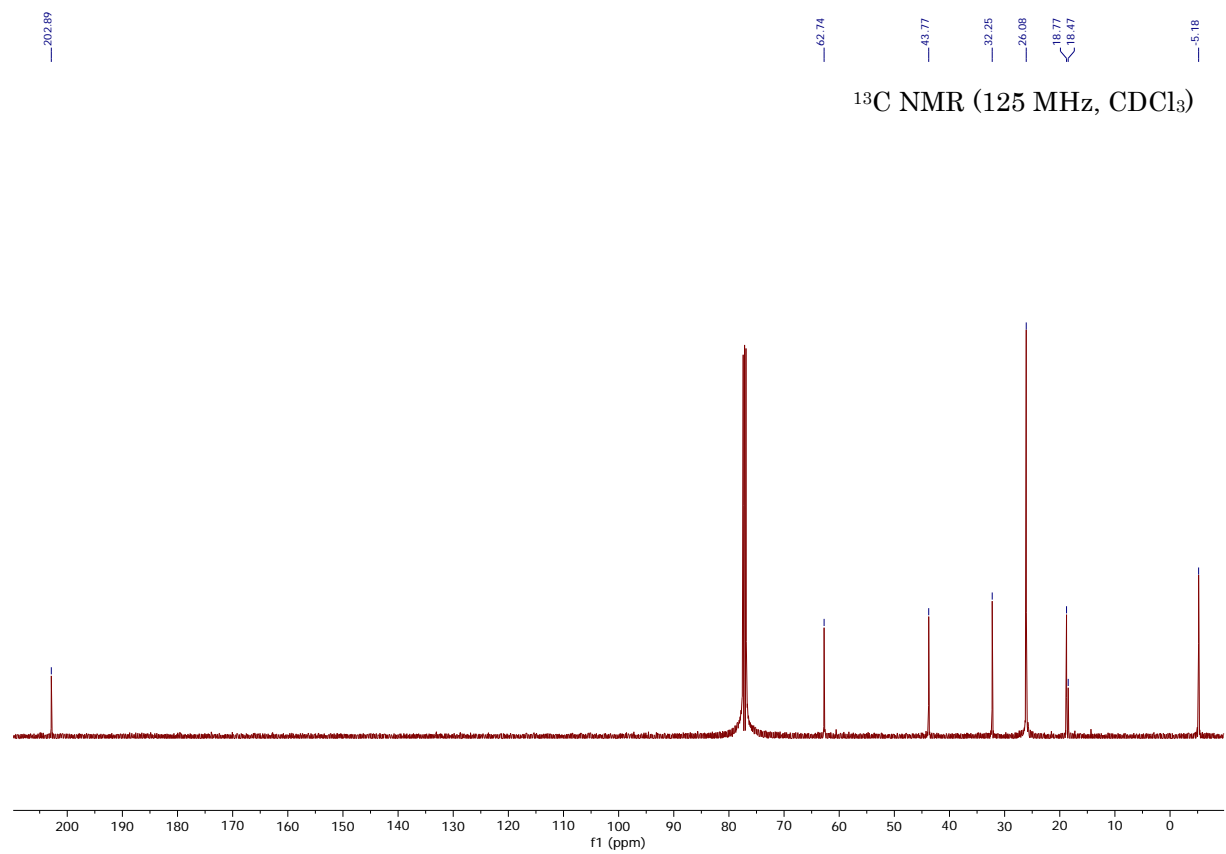
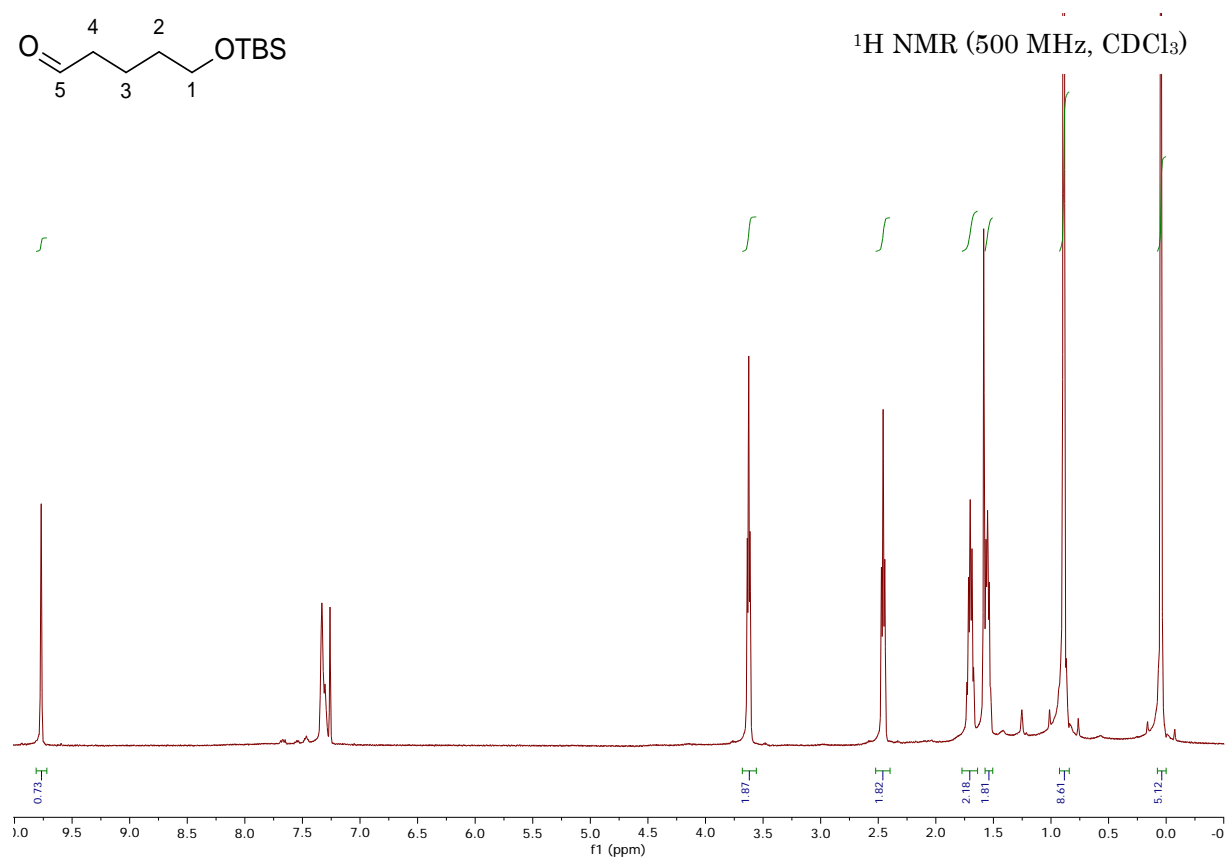
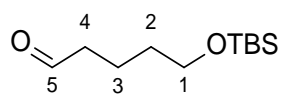
¹H NMR (500 MHz, CDCl₃)



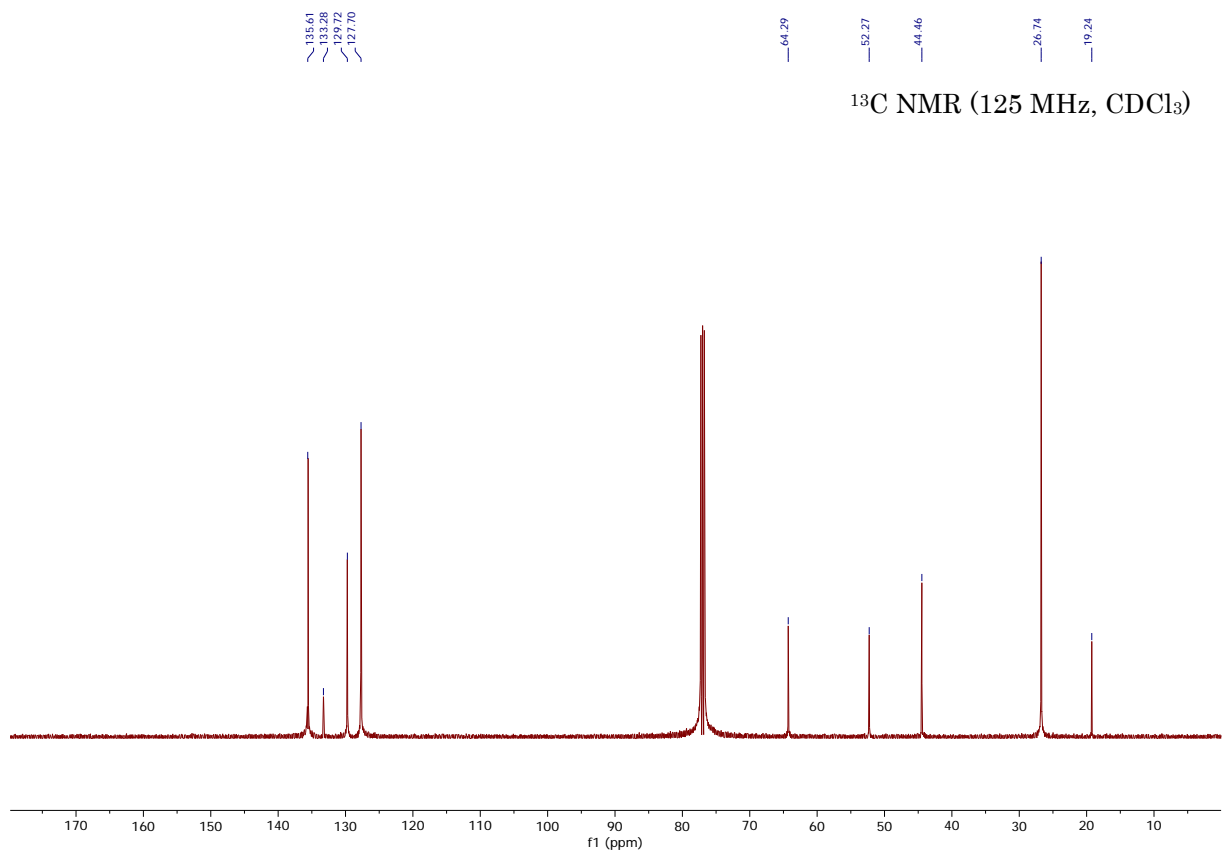
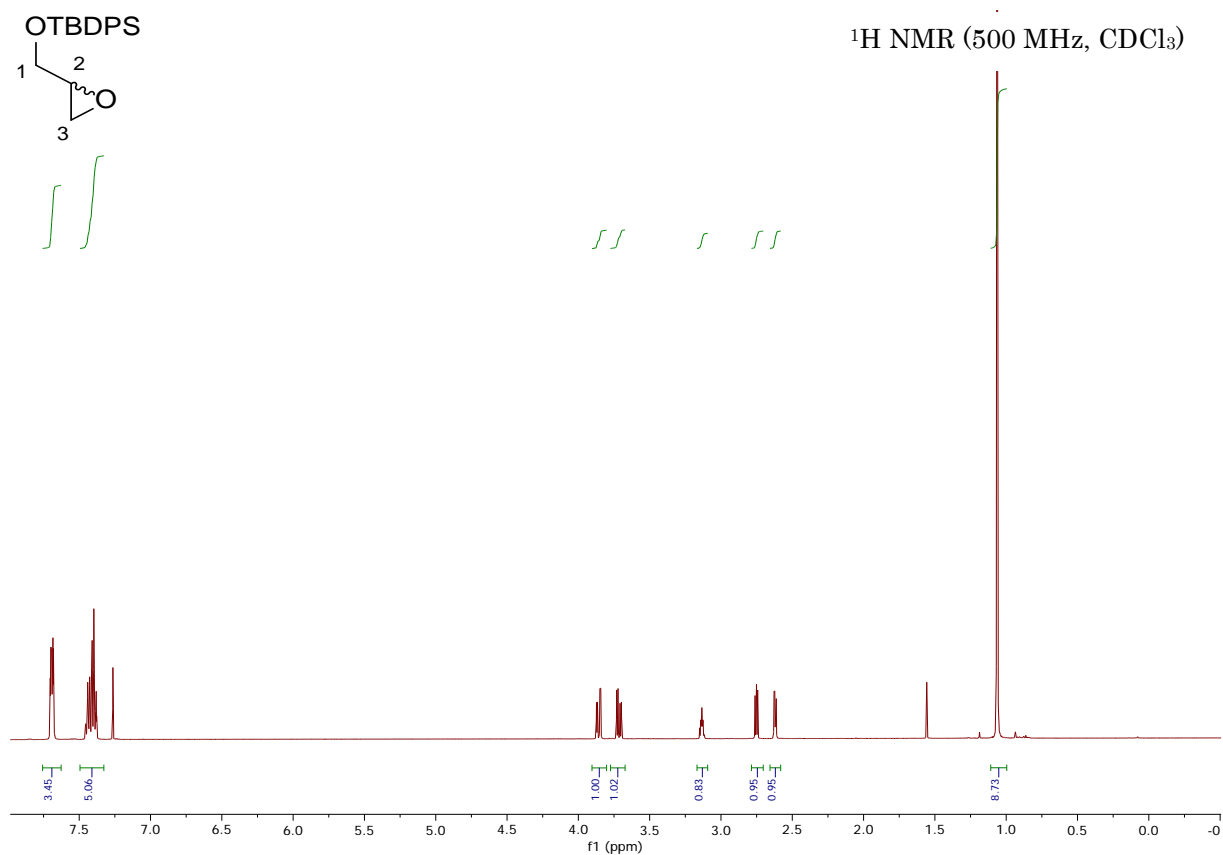
¹³C NMR (125 MHz, CDCl₃)



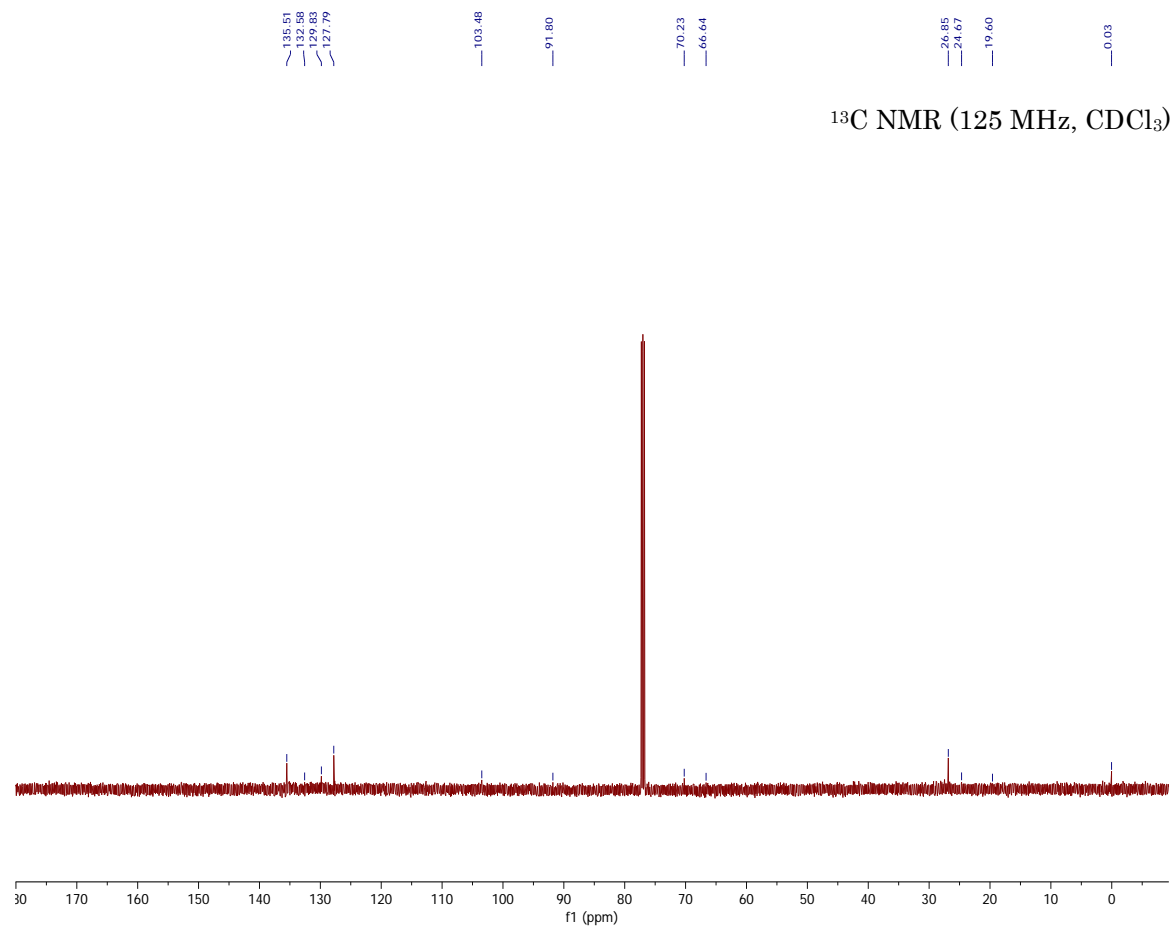
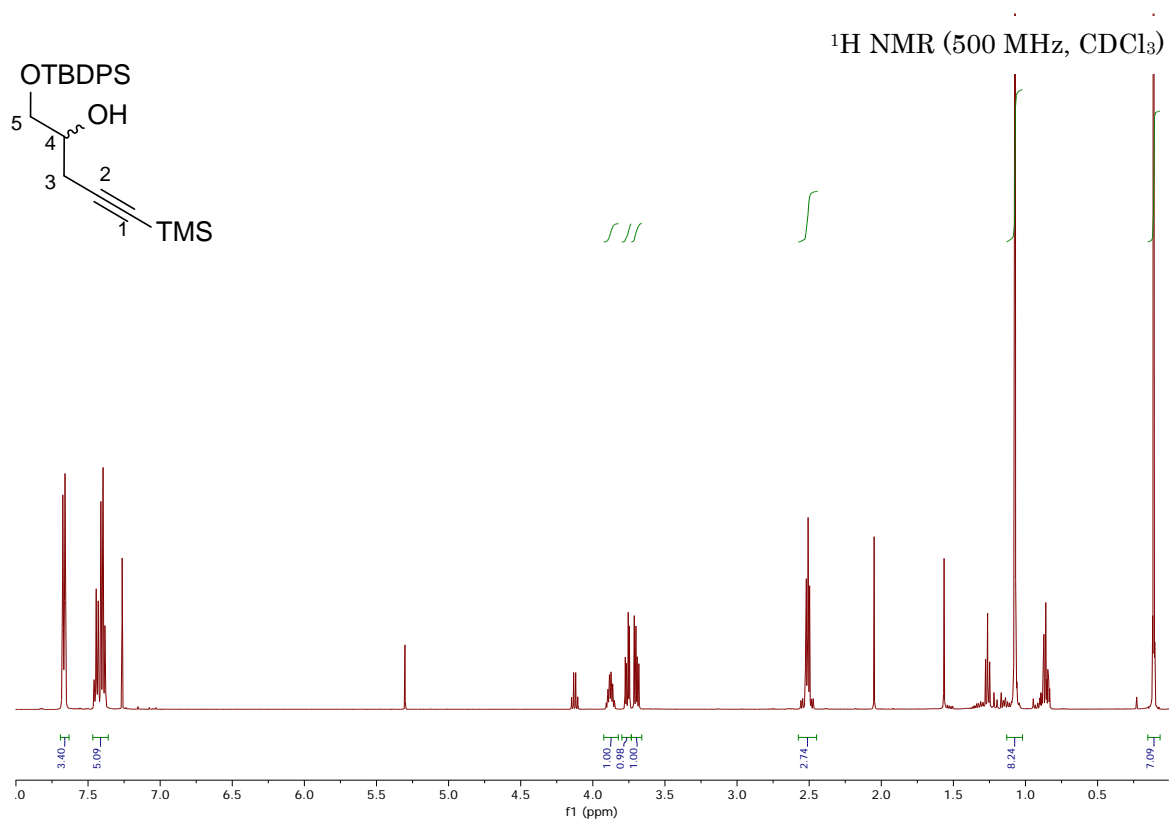
5-((*tert*-Butyldimethylsilyl)oxy)pentanal - 147



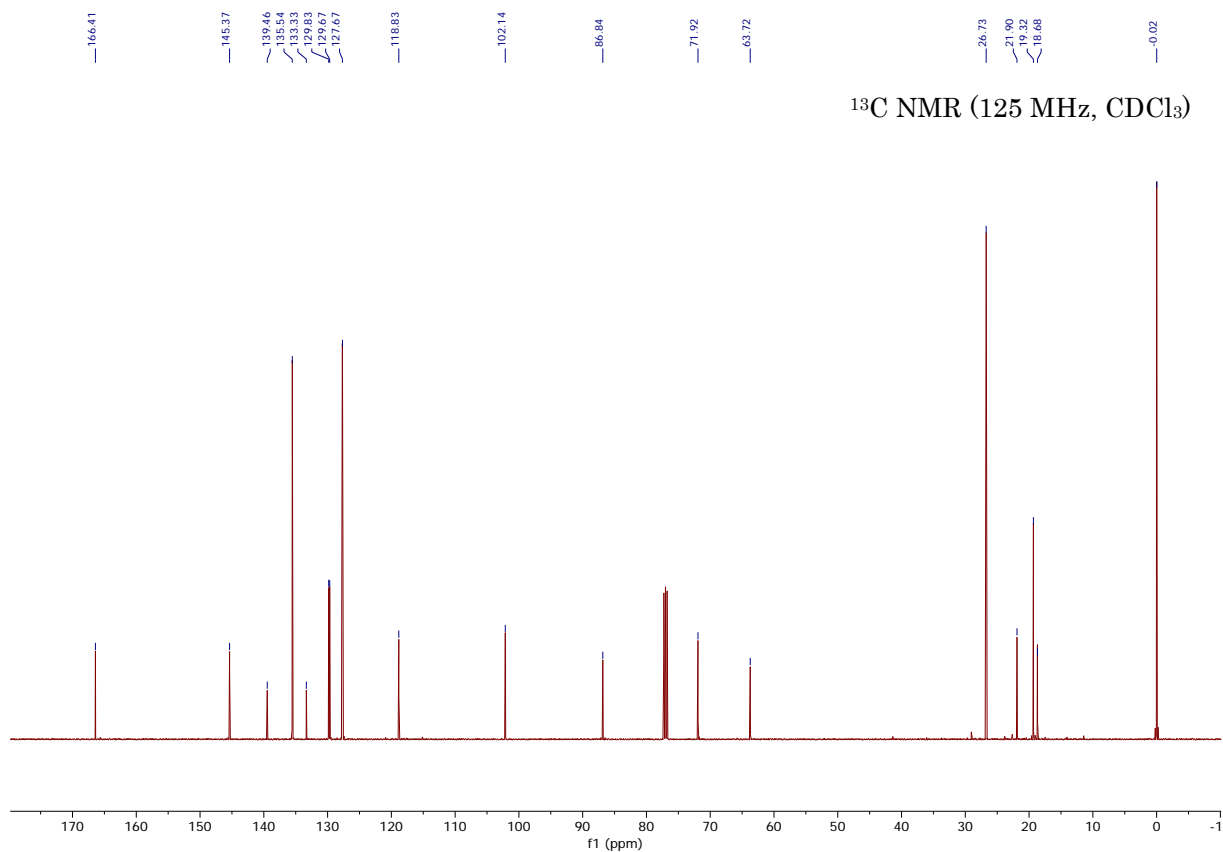
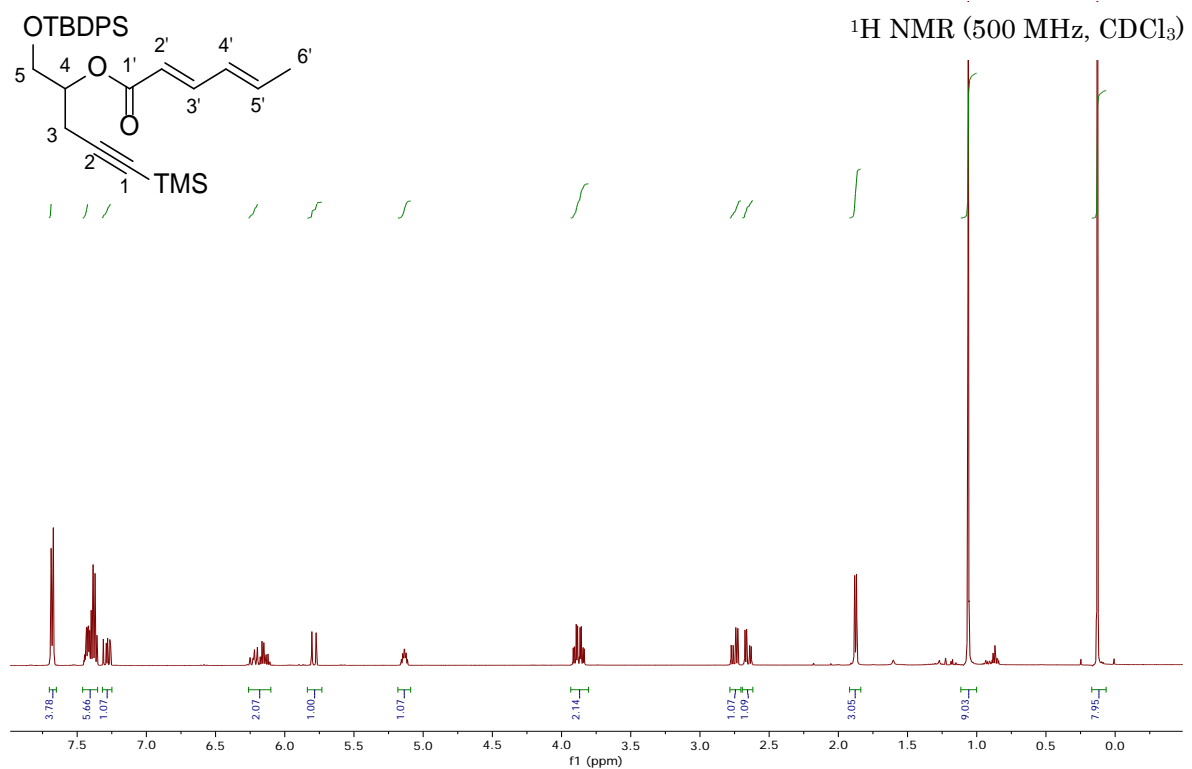
2-(tert-Butyldiphenylsilyloxy)methyloxirane - 149



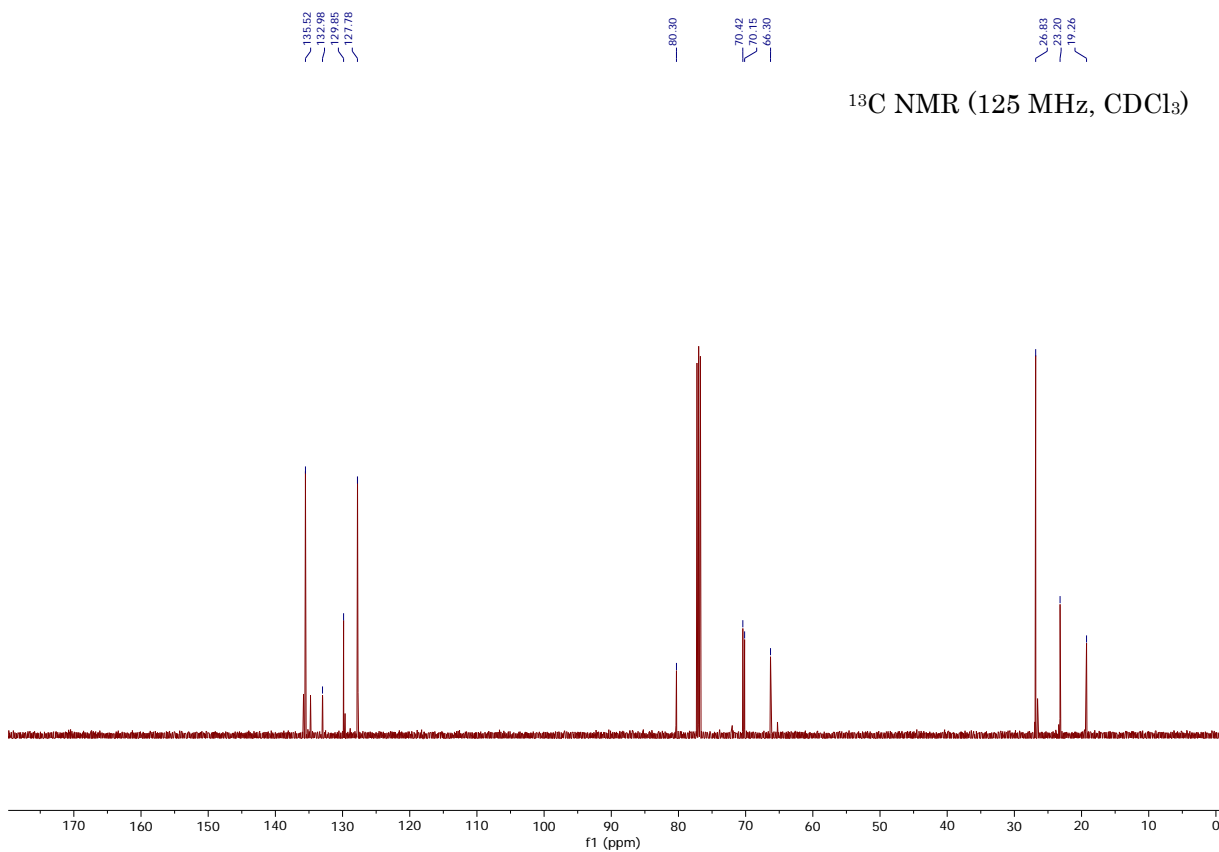
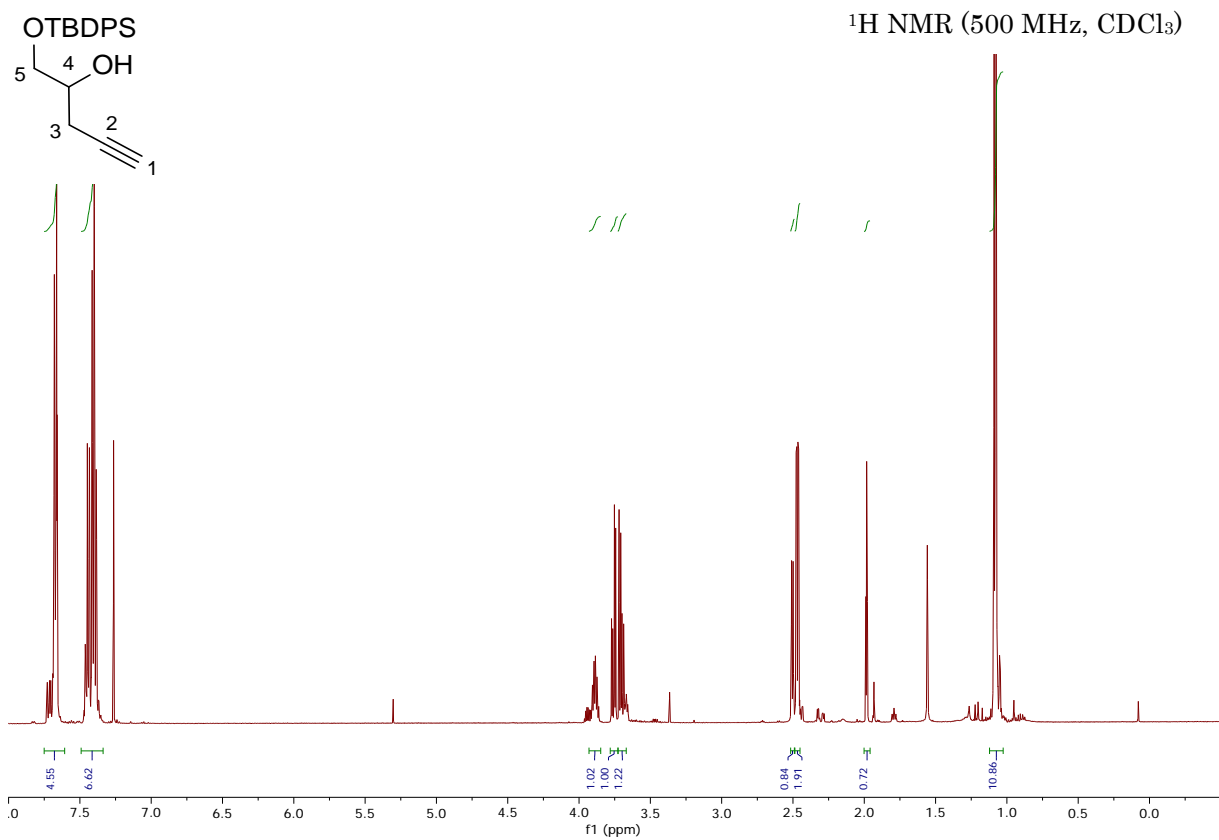
1-(tert-Butyldiphenylsilyloxy)-5-trimethylsilyl-4-pentyn-2-ol - 150



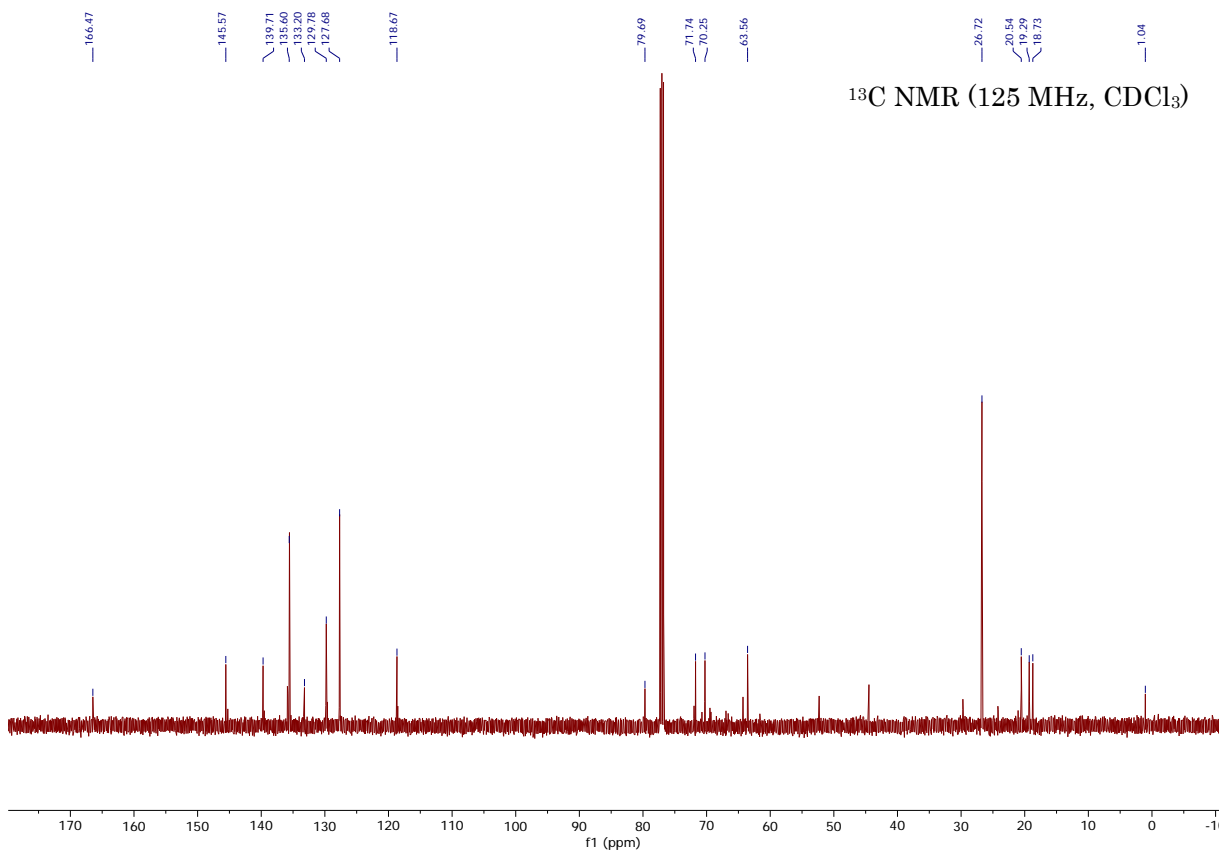
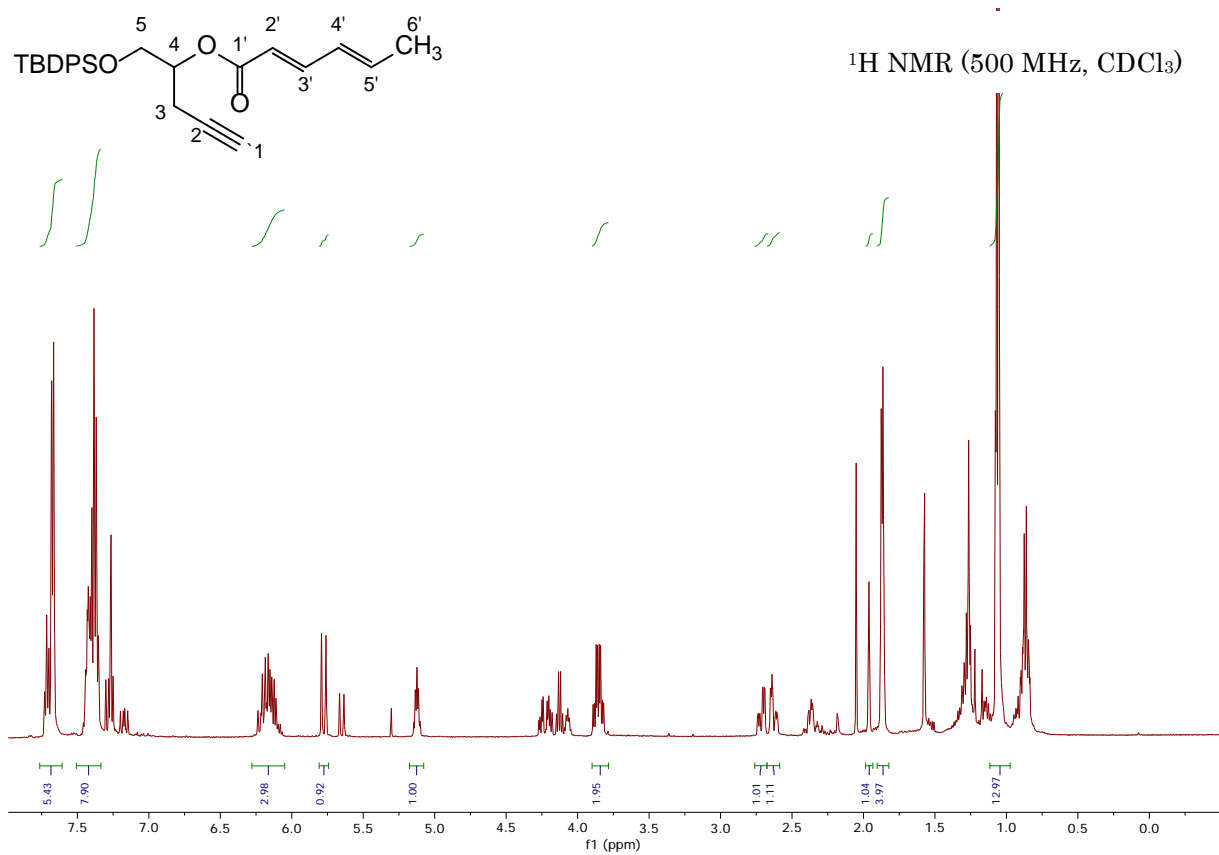
***(2E,4E)*-1-((*tert*-Butyldiphenylsilyl)oxy-5-(trimethylsilyl)-pent-4-yn-2-yl-hexa-2,4-dienoate - 154**



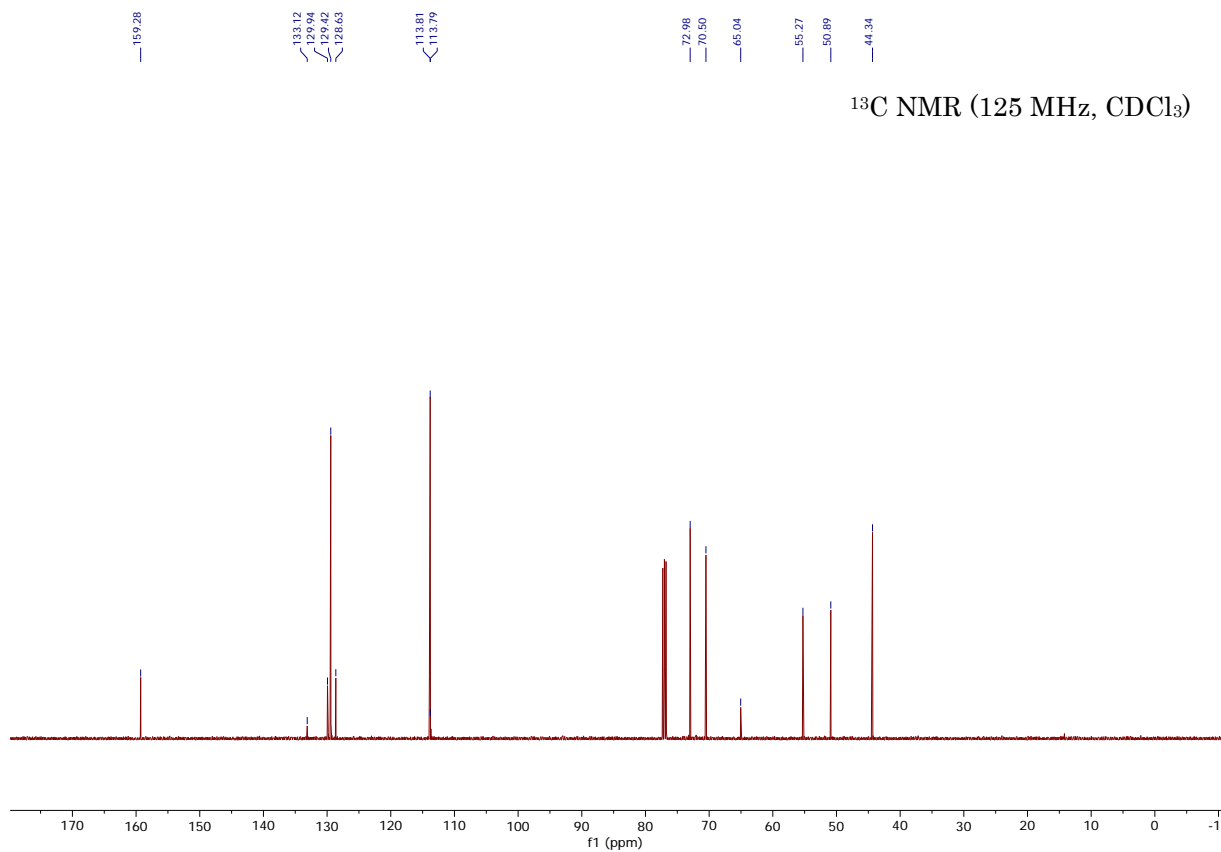
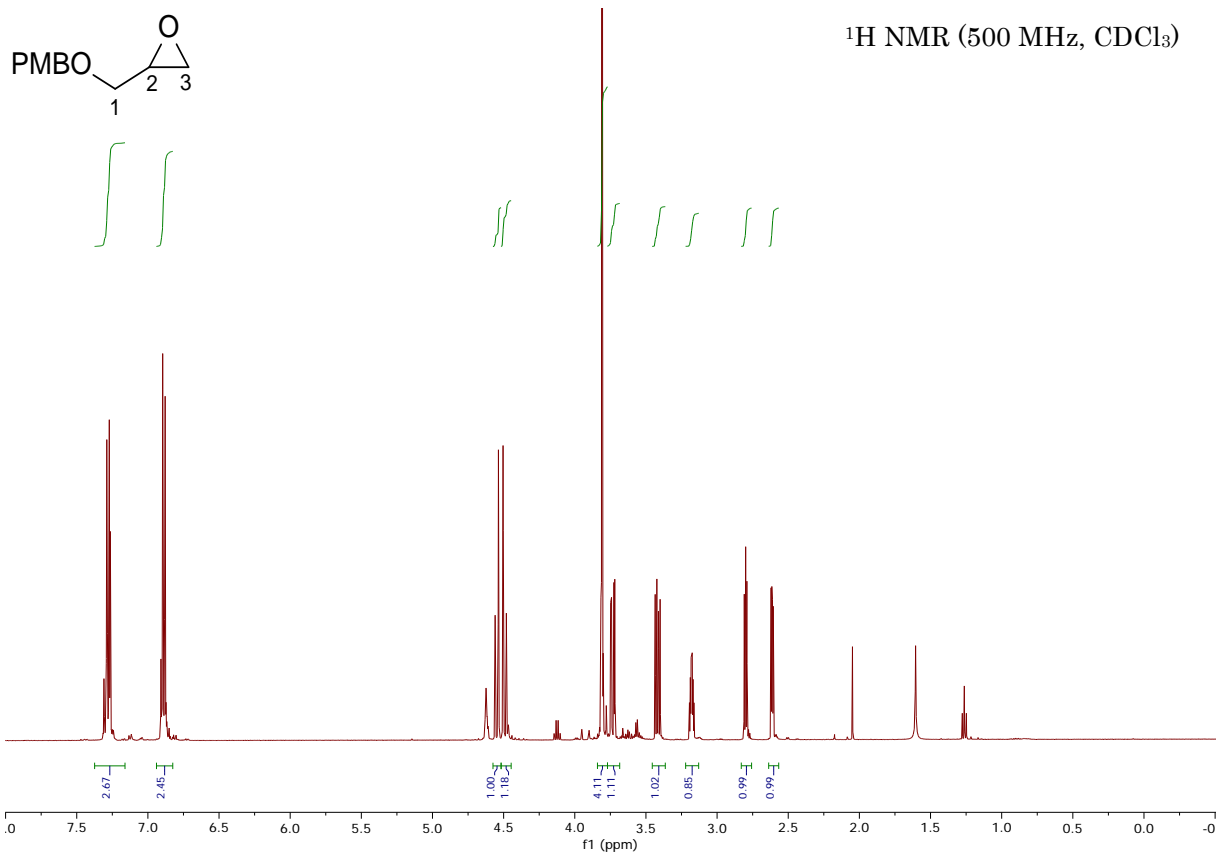
1-((tert-Butyldiphenylsilyl)oxy)pent-4-yn-2-ol - 151



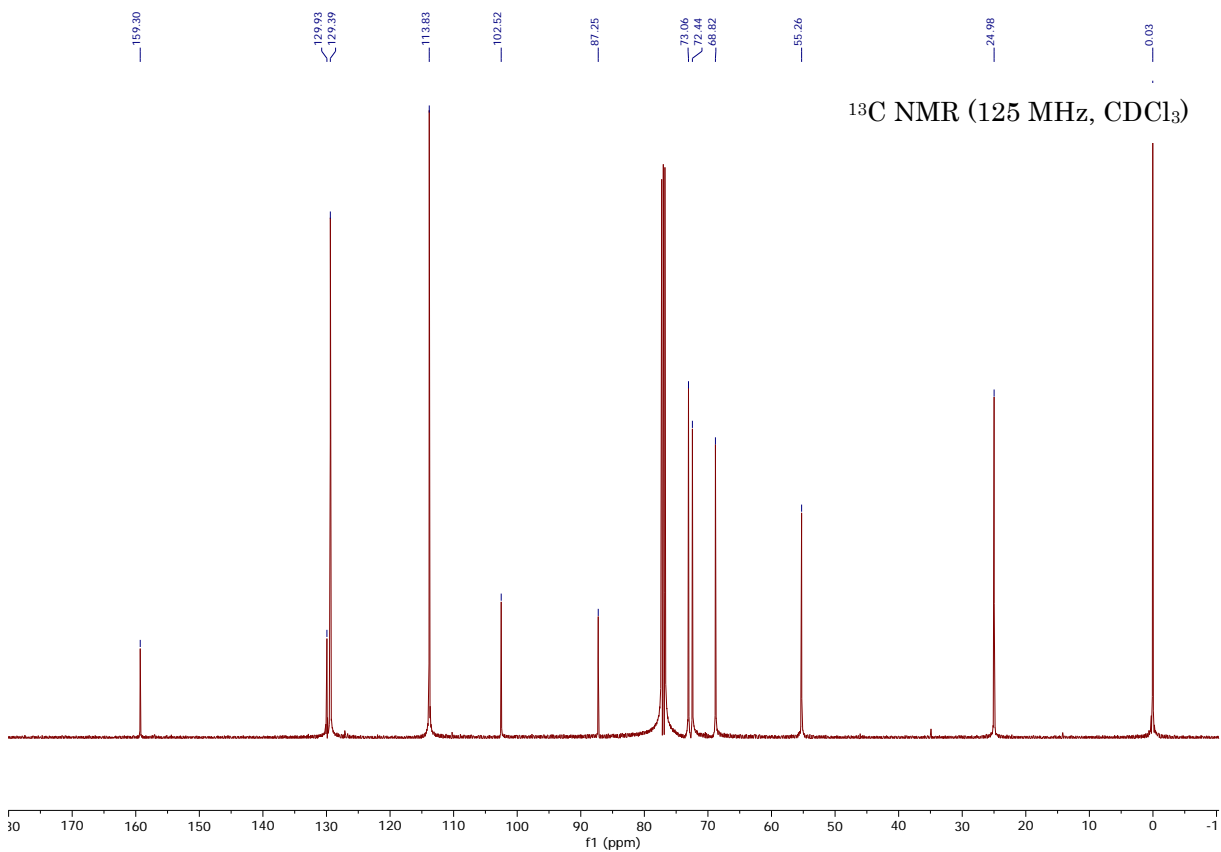
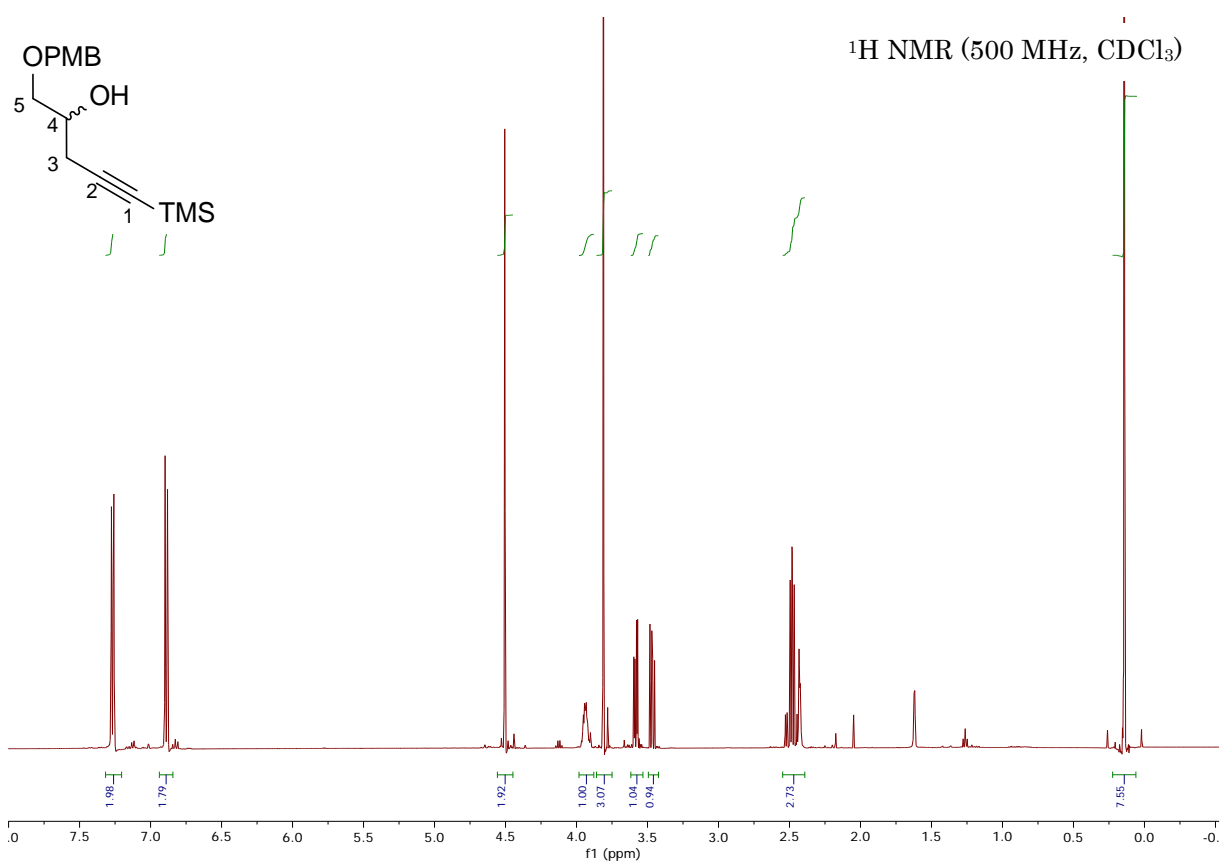
(2E,4E)-1-((*tert*-Butyldiphenylsilyl)oxy)pent-4-yn-2-yl hexa-2,4-dienoate - 153



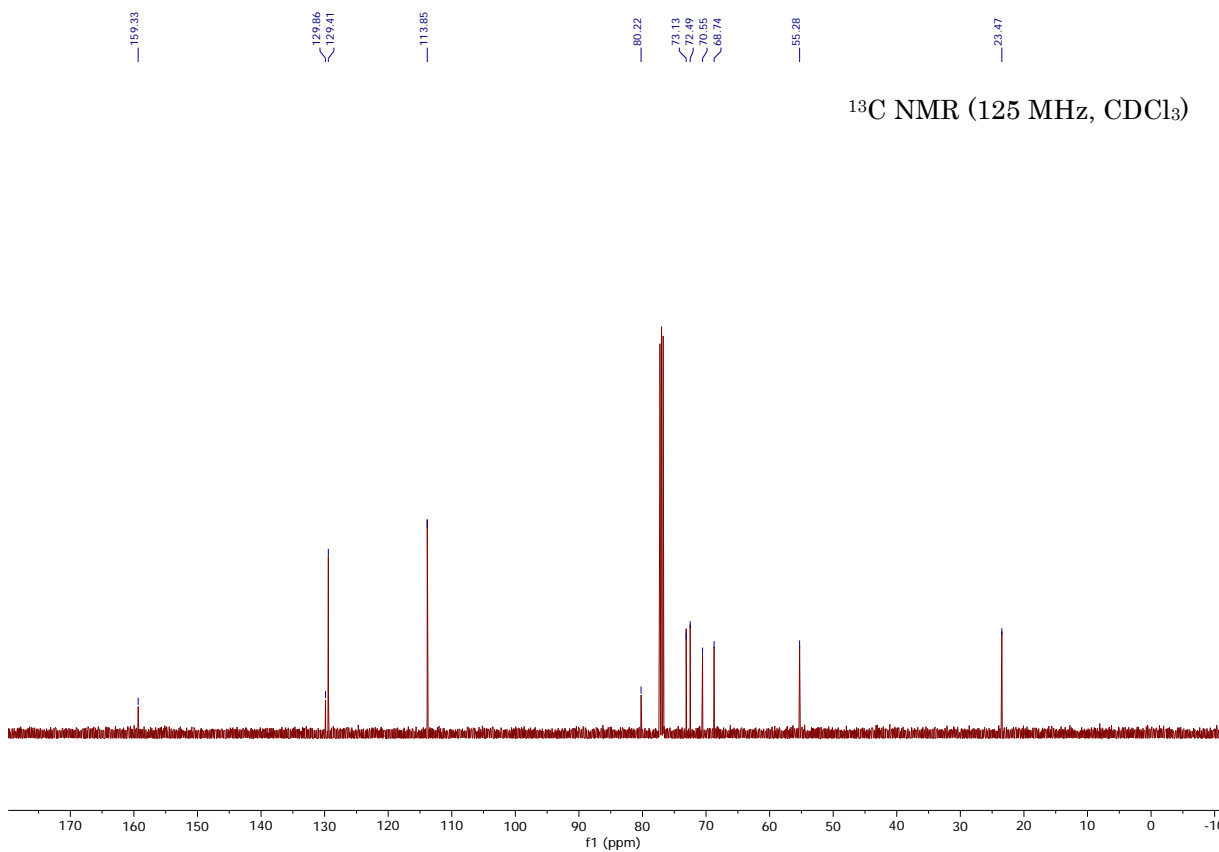
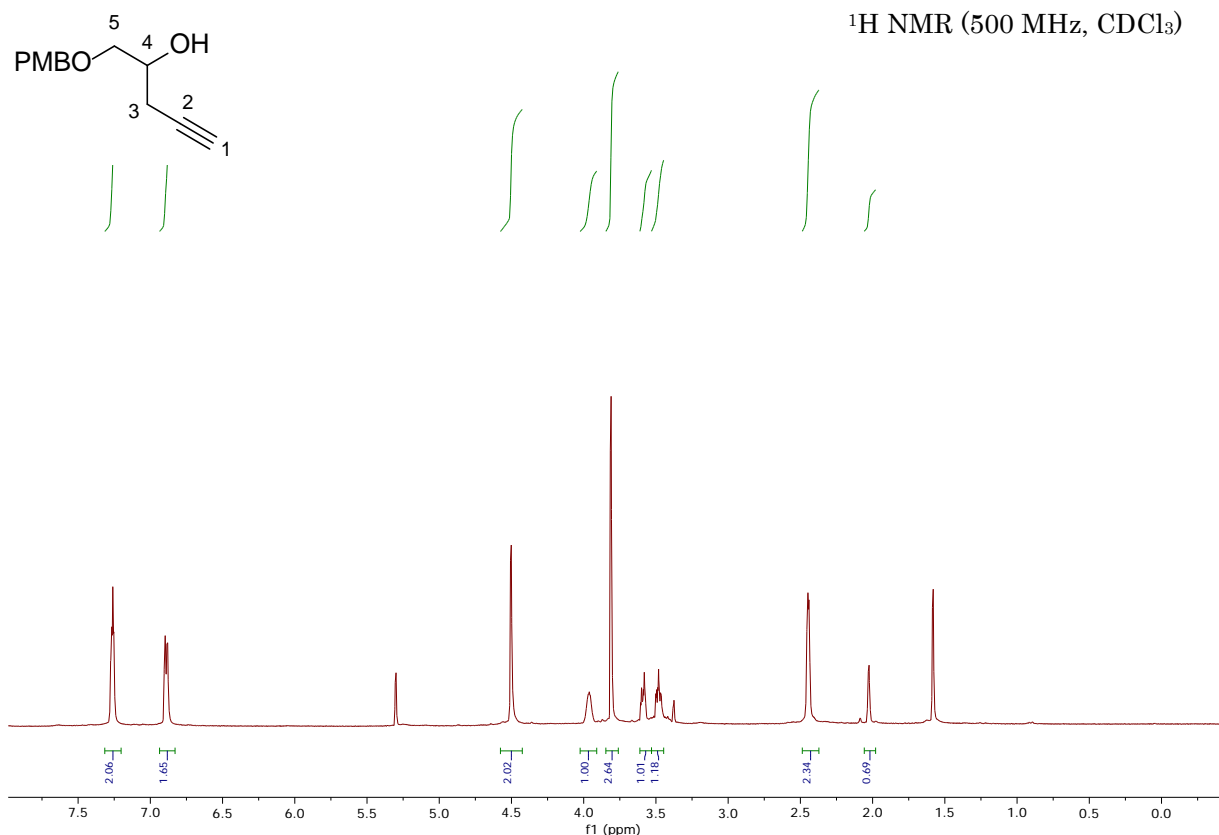
2-(((4-Methoxybenzyl)oxy)methyl)oxirane



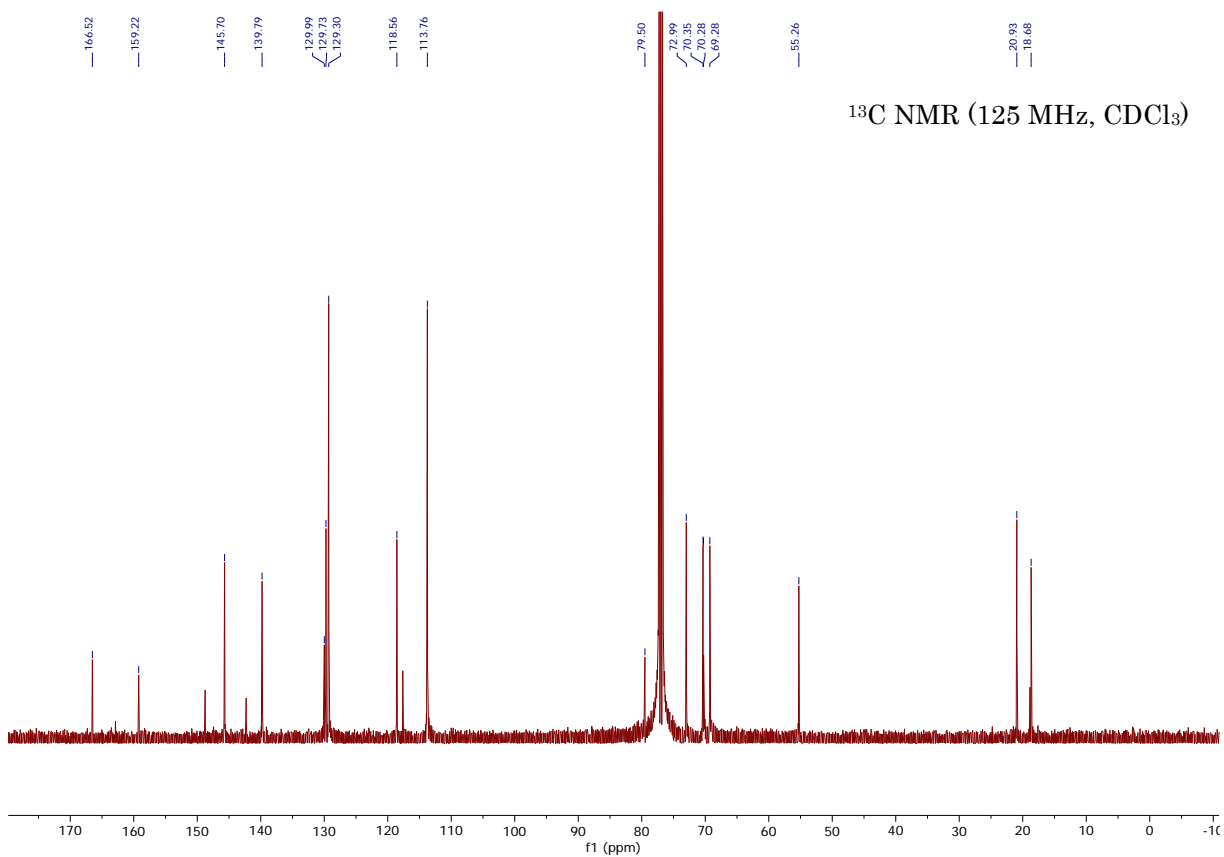
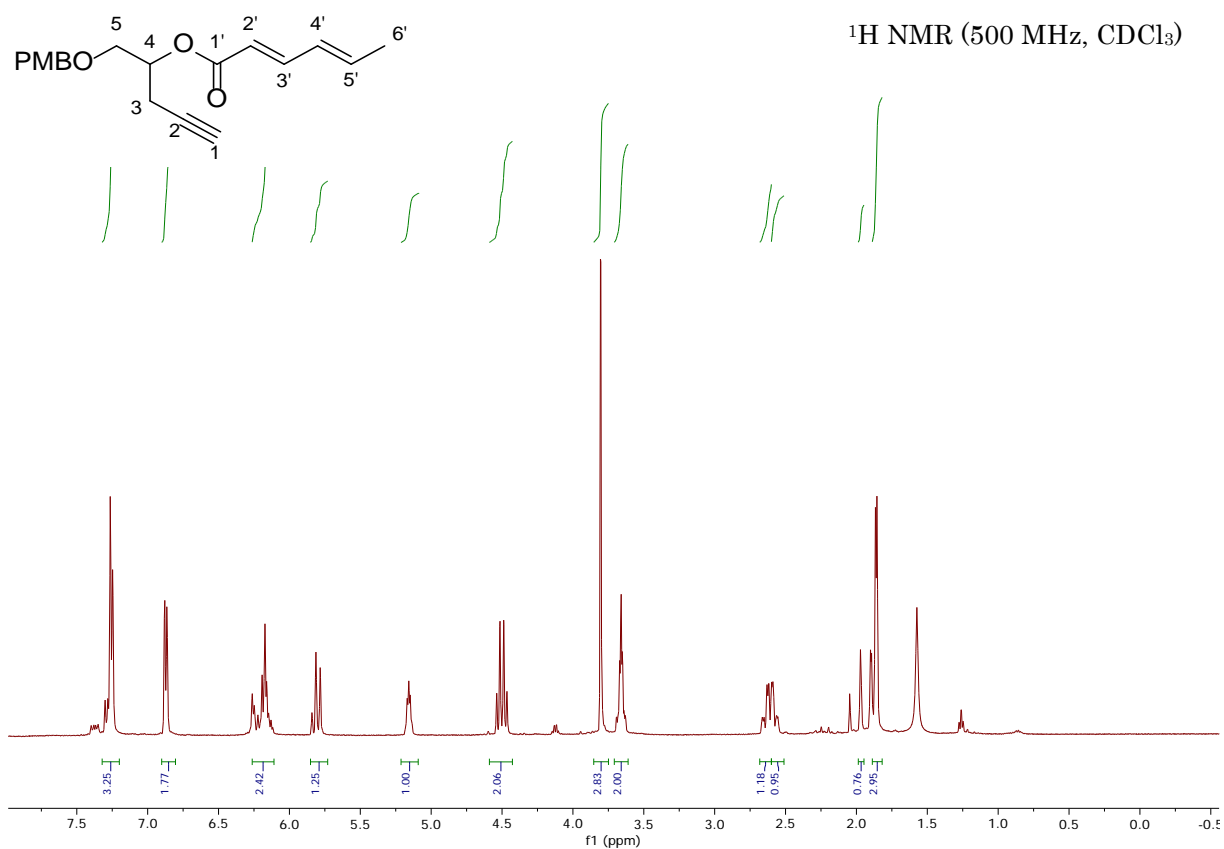
1-((4-Methoxybenzyl)oxy)-5-(trimethylsilyl)pent-4-yn-2-ol - 113



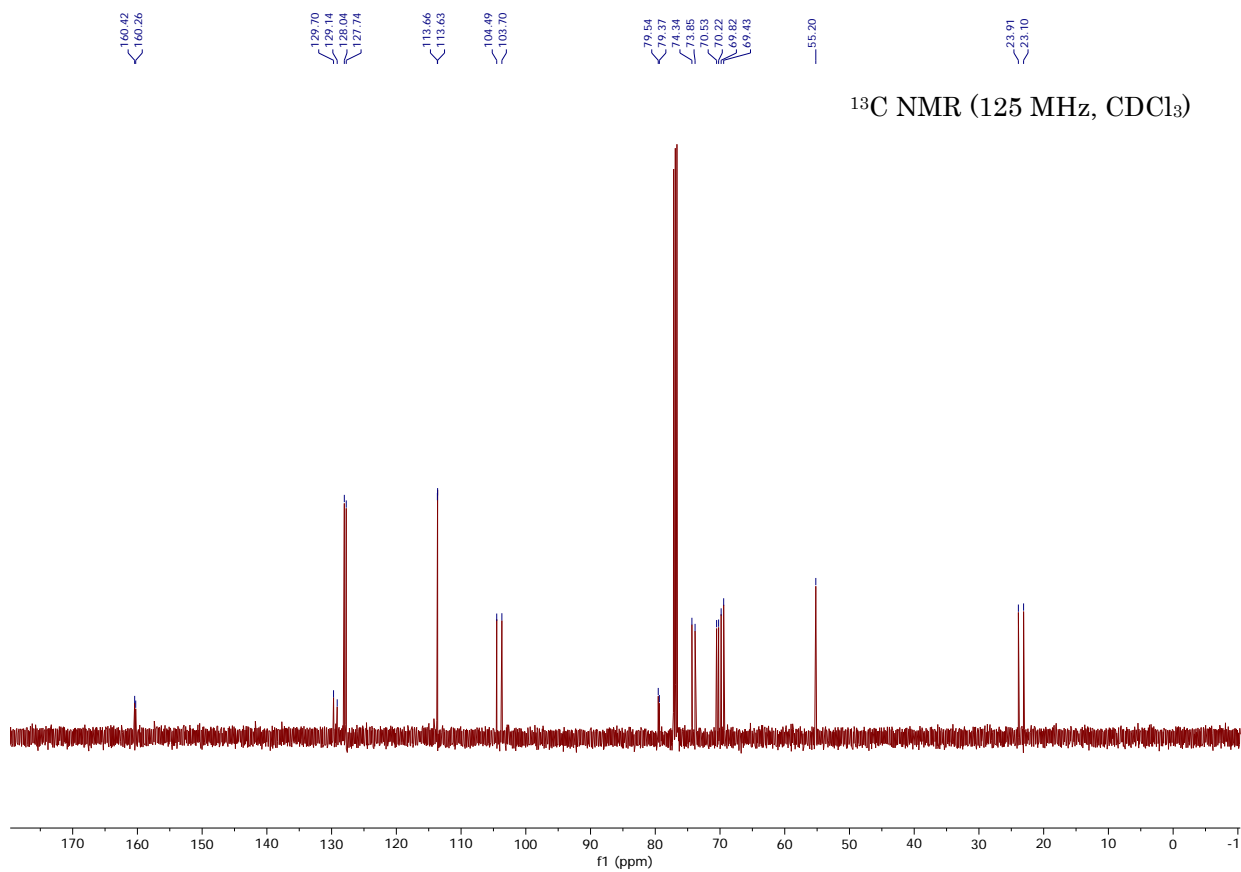
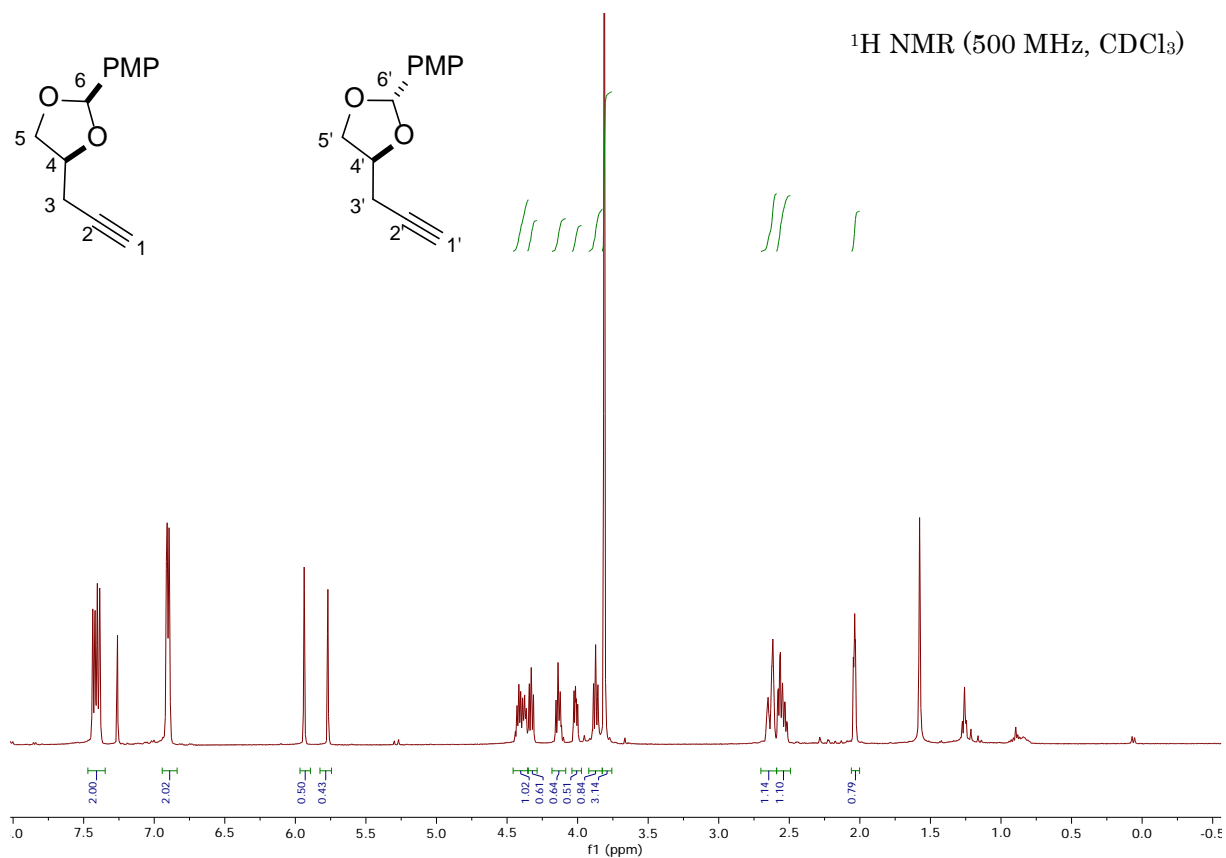
1-((4-Methoxybenzyl)oxy)pent-4-yn-2-ol - 116



(2E,4E)-1-((4-Methoxybenzyl)oxy)pent-4-yn-2-yl hexa-2,4-dienoate - 155

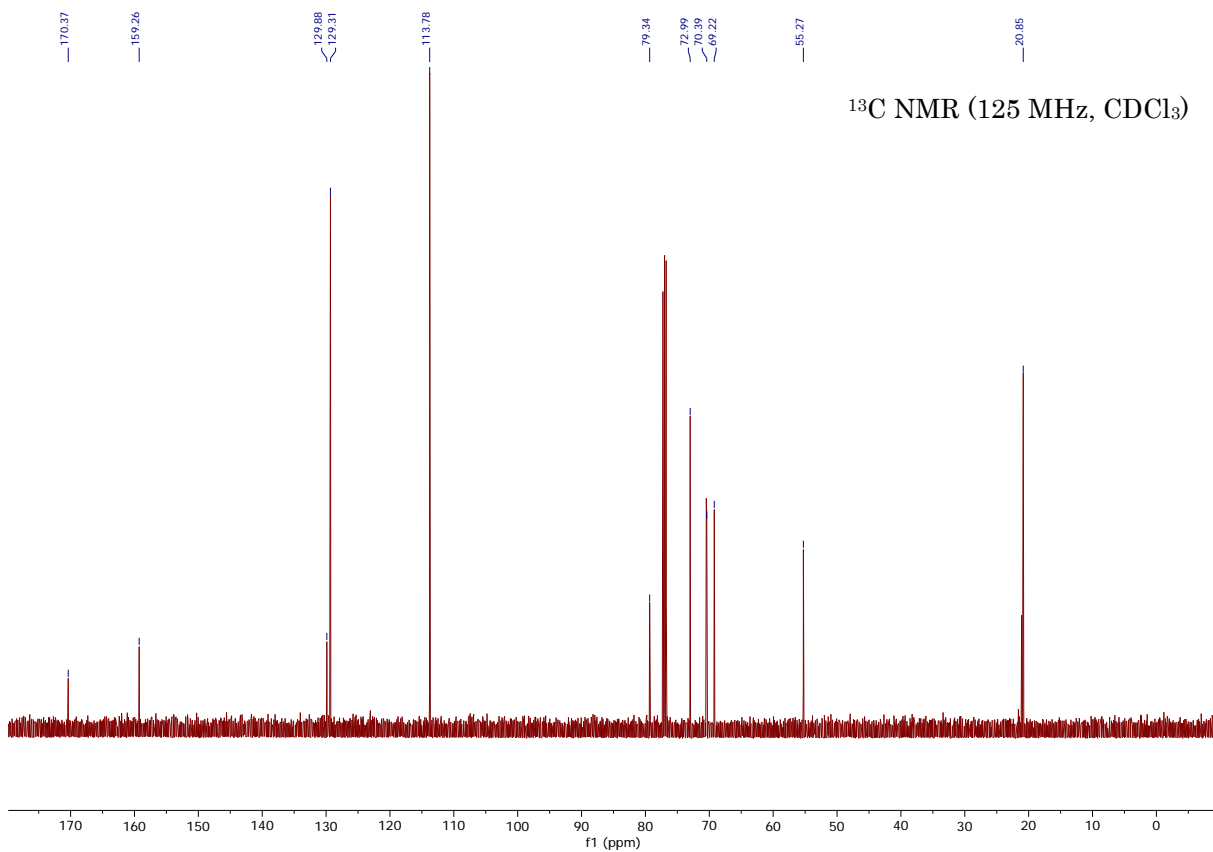
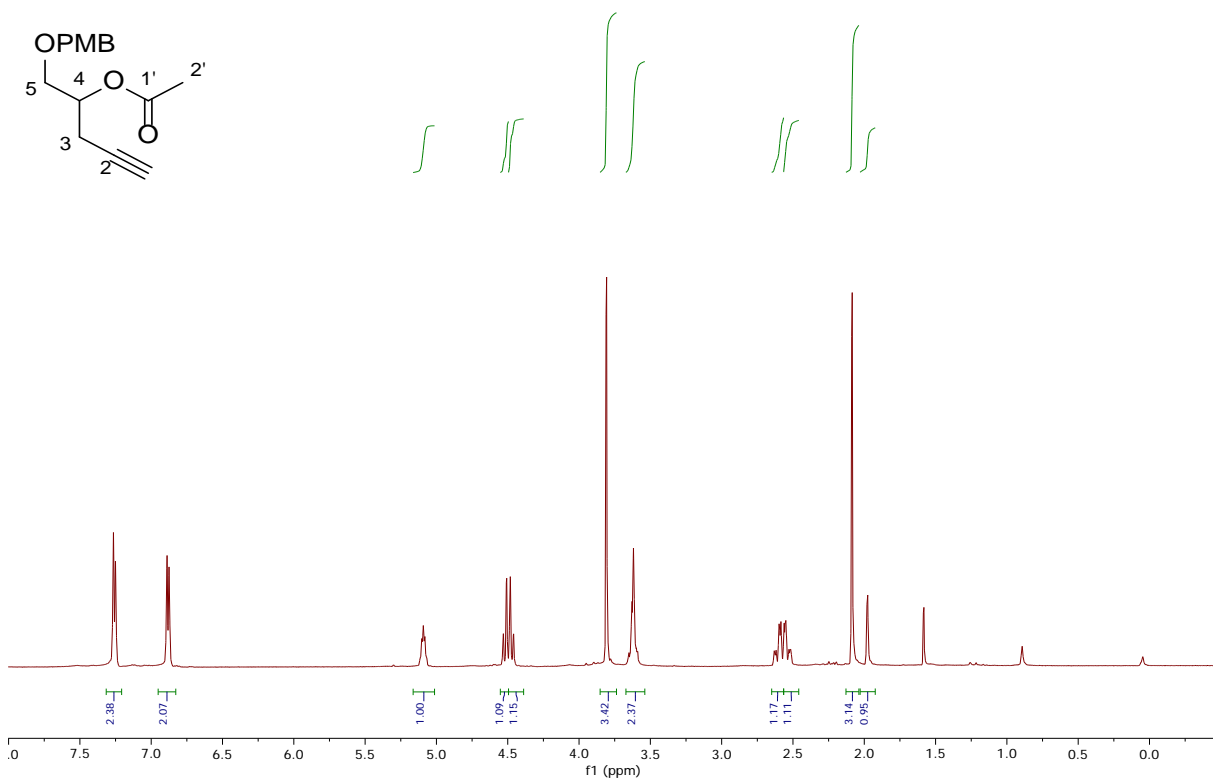


2-(4-Methoxyphenyl)-4-(prop-2-yn-1-yl)-1,3-dioxolane – 156

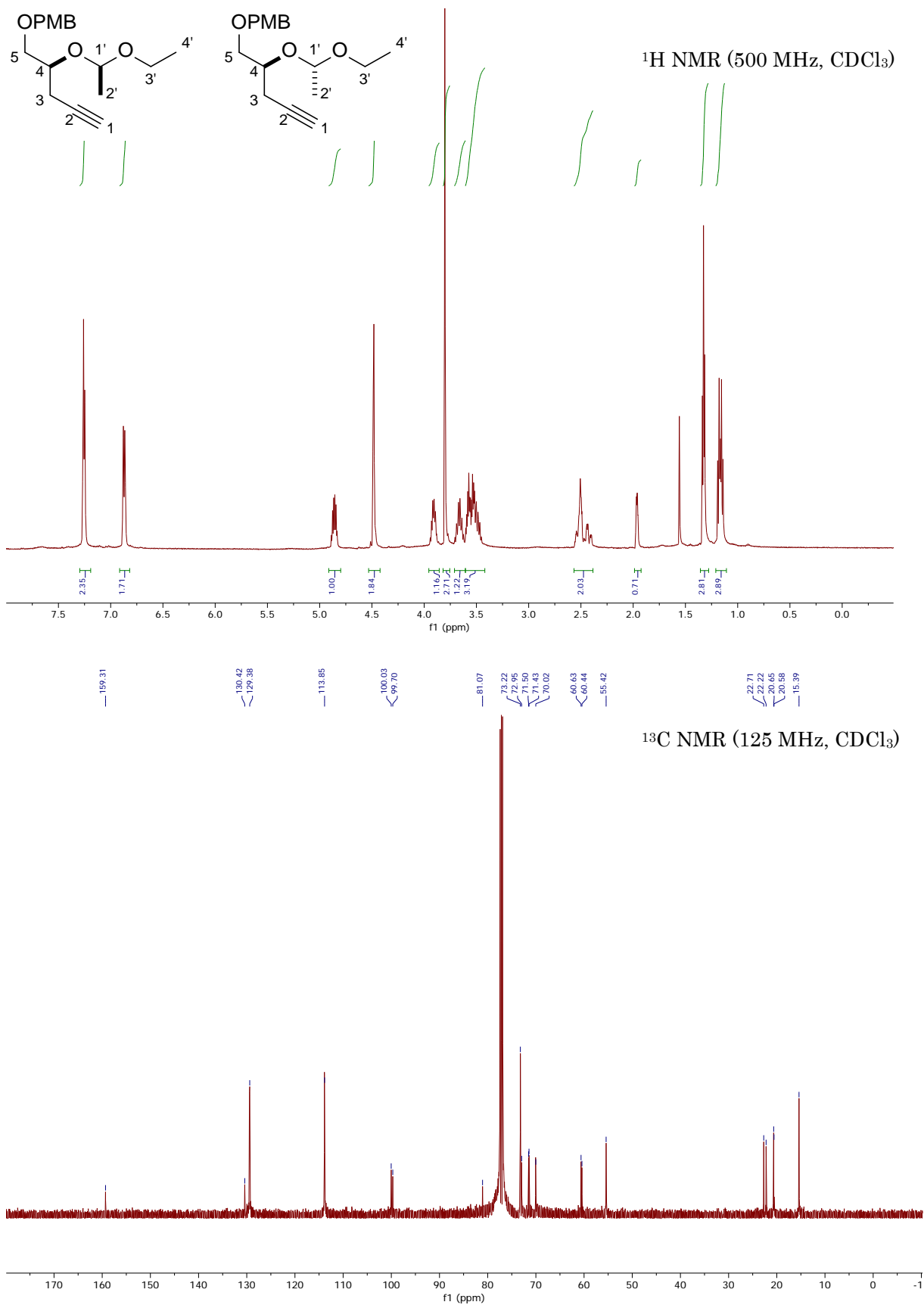


1-((4-Methoxybenzyl)oxy)pent-4-yn-2-yl acetate– 157

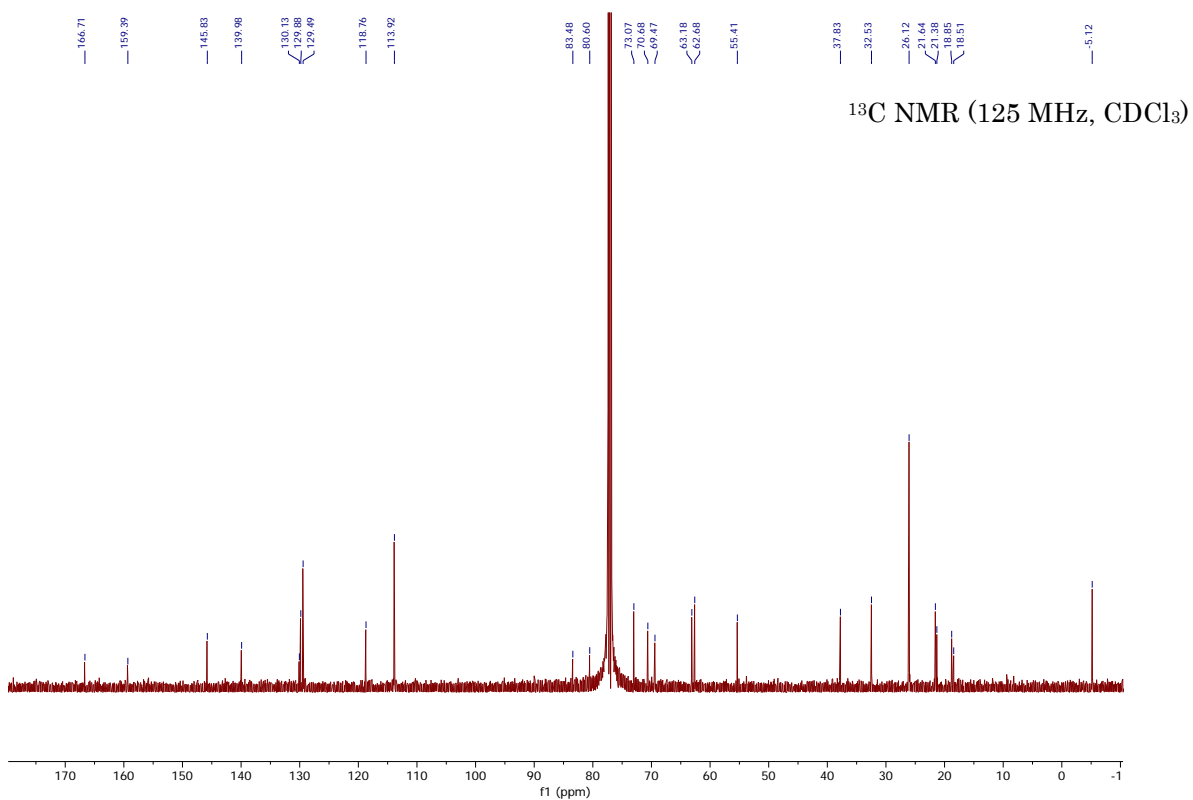
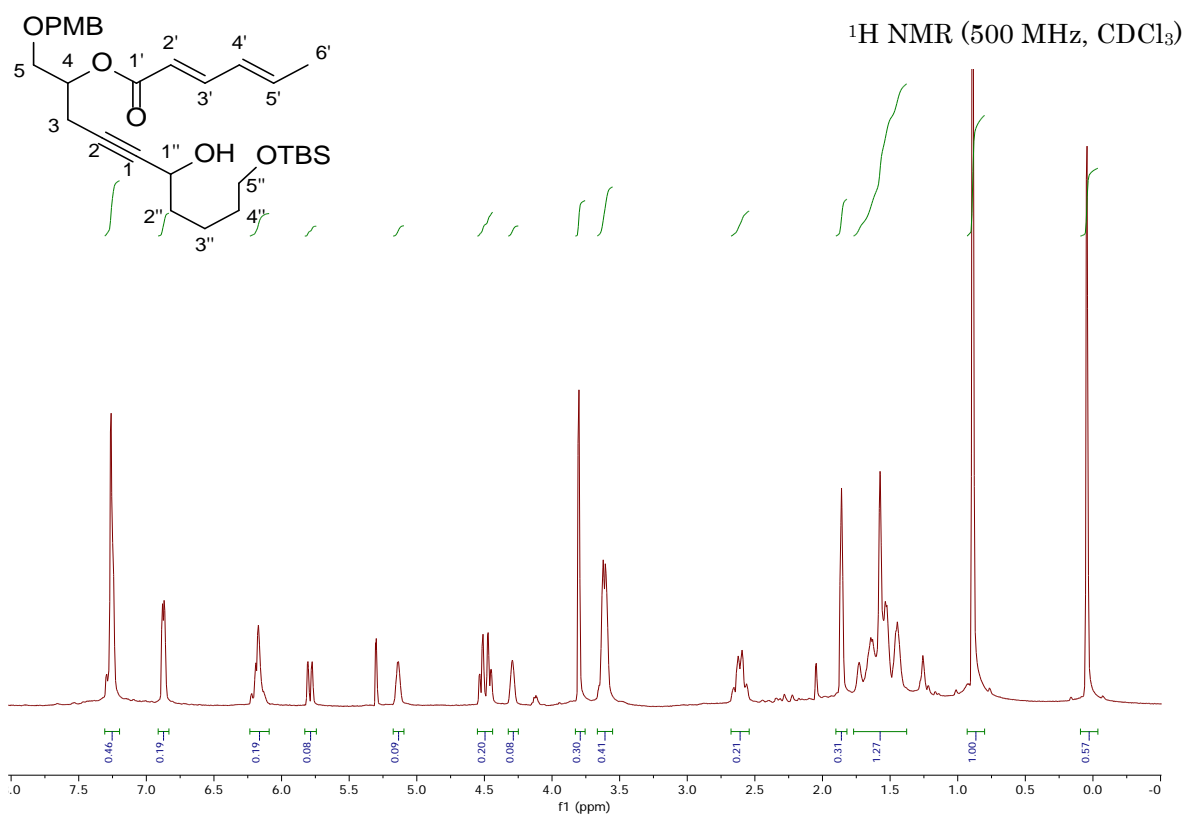
$^1\text{H NMR}$ (500 MHz, CDCl_3)



1-(((2-(1-Ethoxyethoxy)pent-4-yn-1-yl)oxy)methyl)-4-methoxybenzene- 158

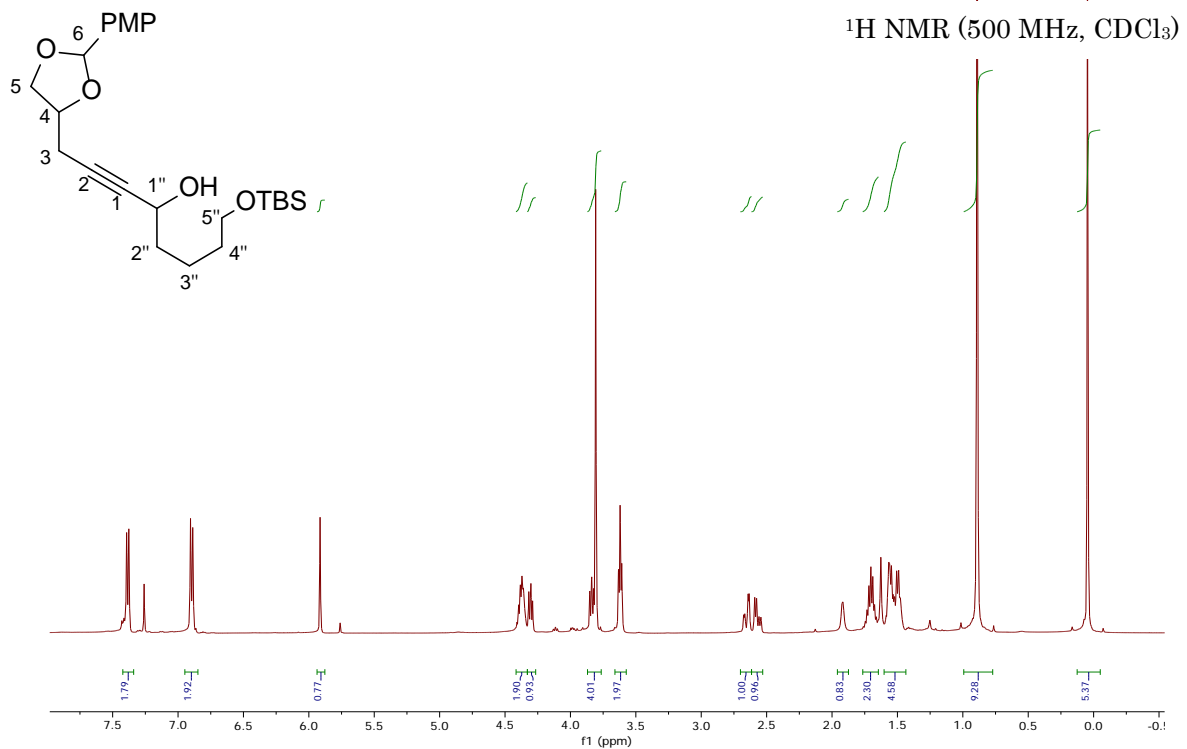


***(2E,4E)*-10-((*tert*-Butyldimethylsilyl)oxy)-6-hydroxy-1-((4-methoxybenzyl)oxy)dec-4-yn-2-yl hexa-2,4-dienoate – 160**

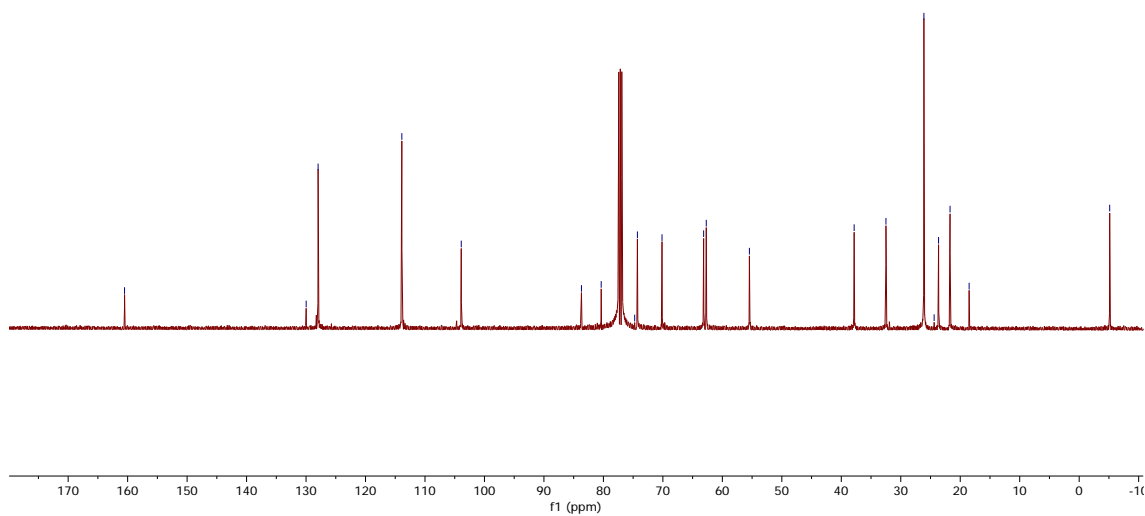


8-((tert-Butyldimethylsilyl)oxy)-1-(2-(4-methoxyphenyl)-1,3-dioxolan-4-yl)oct-2-yn-4-ol – 163

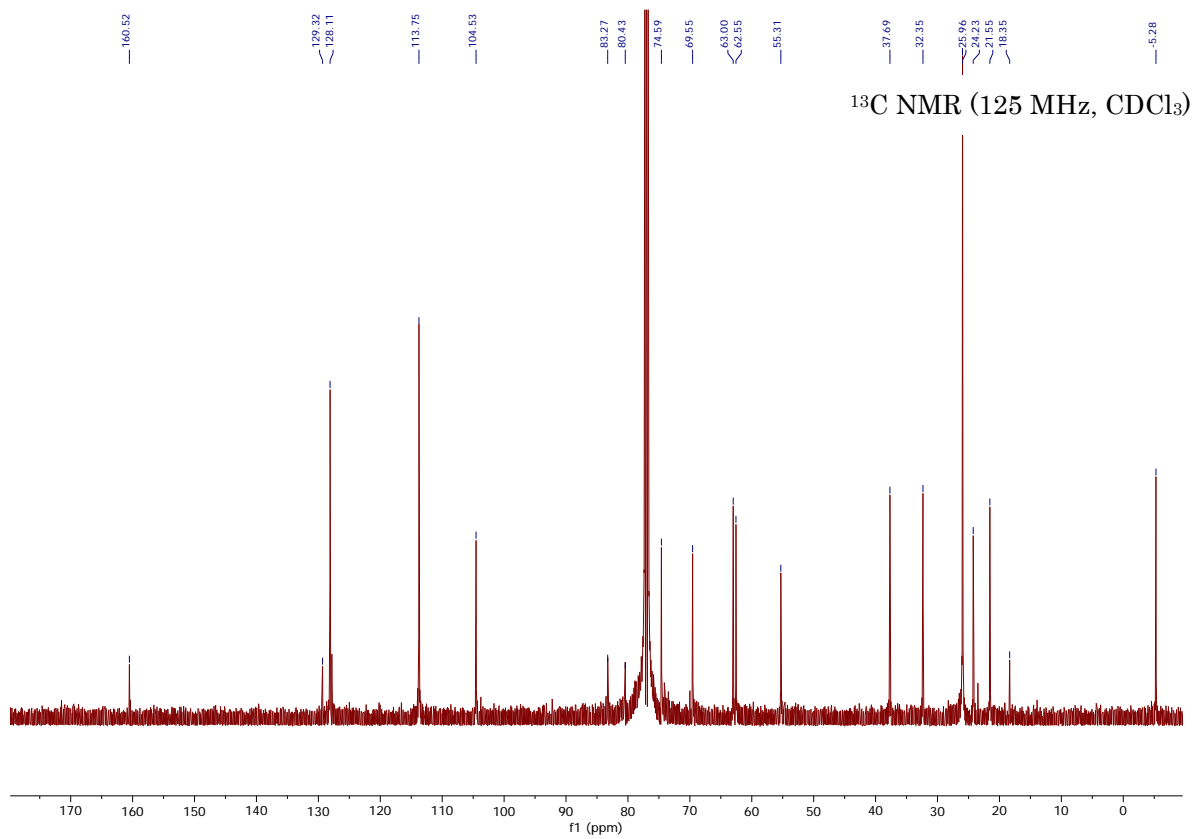
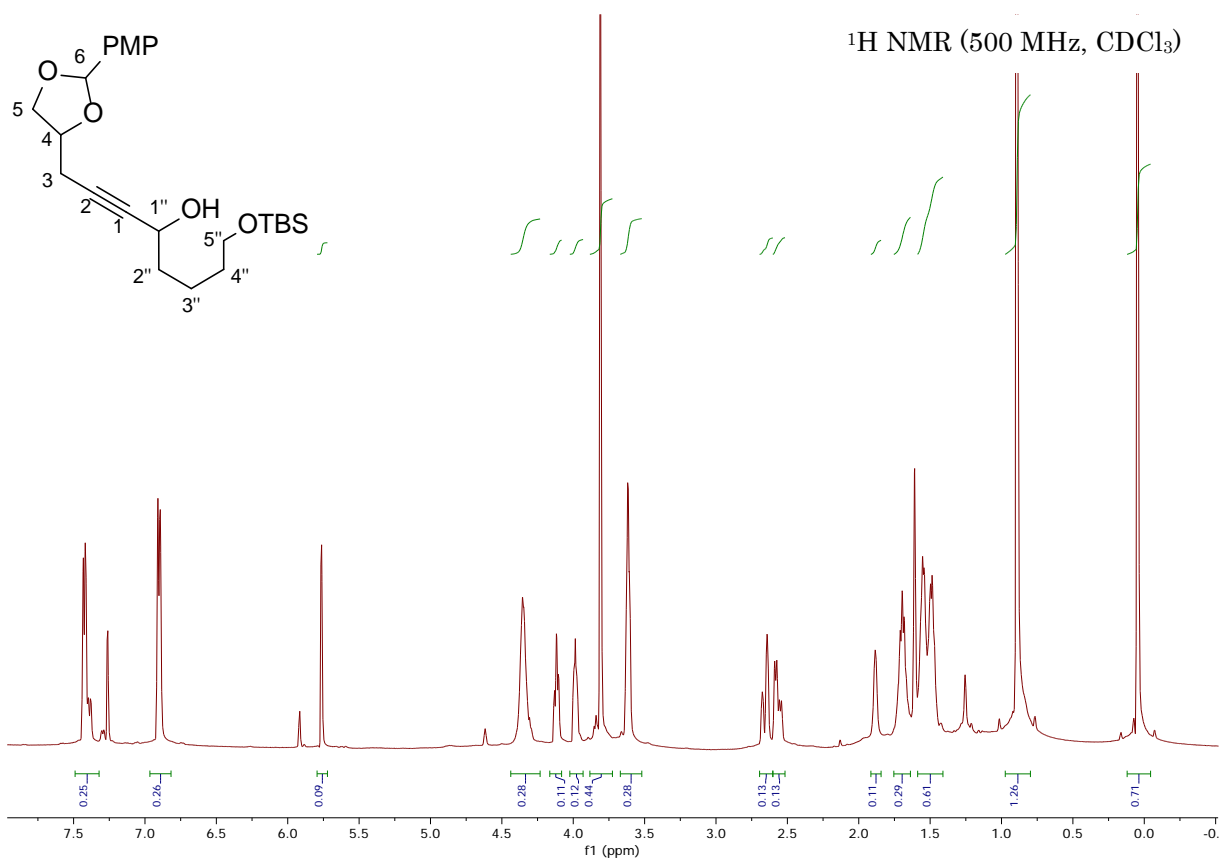
Diastereomer 1



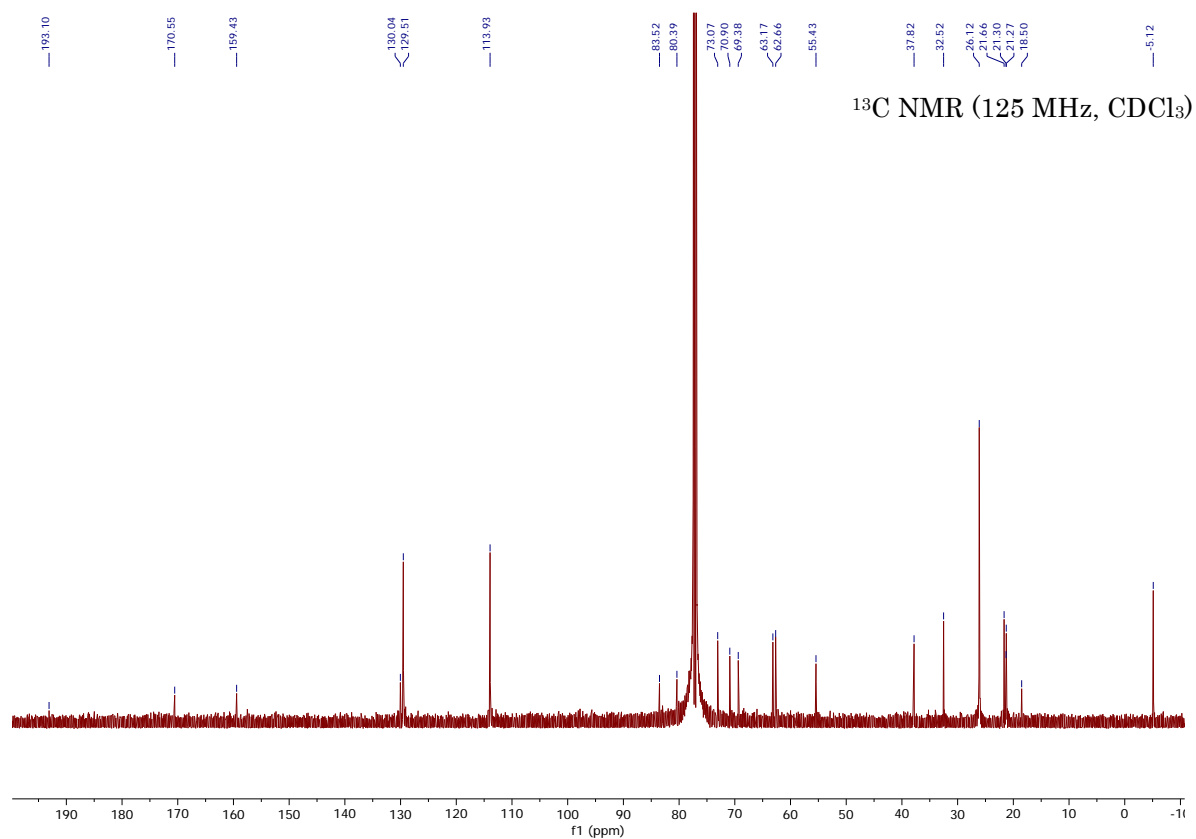
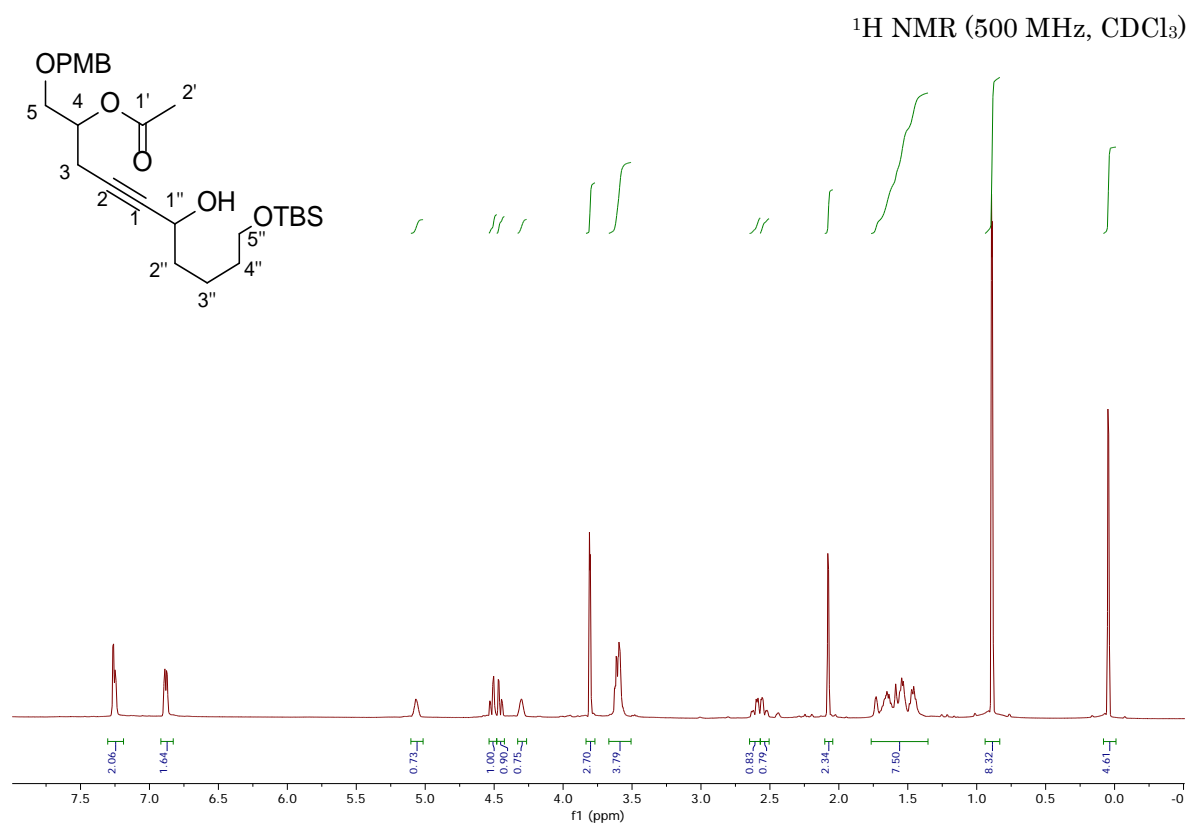
¹³C NMR (125 MHz, CDCl₃)



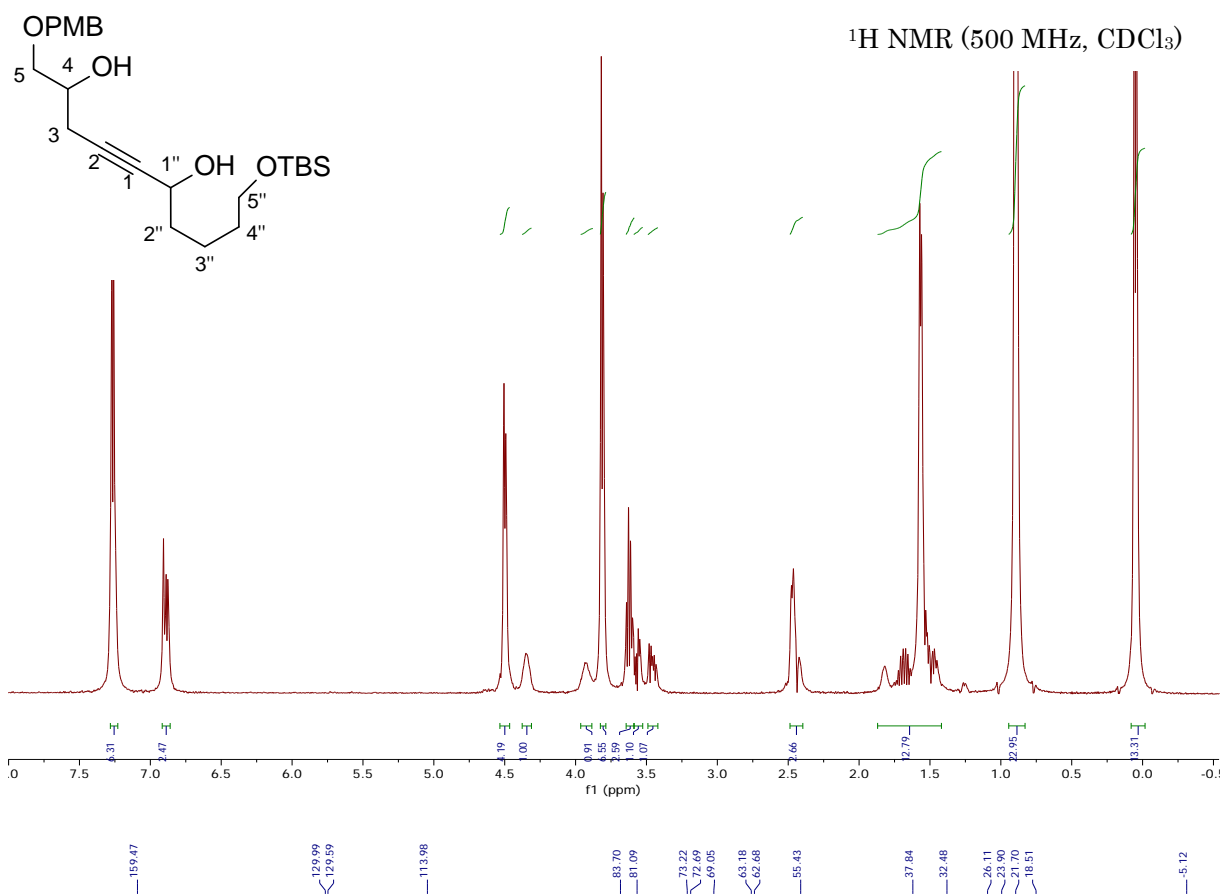
Diastereomer 2



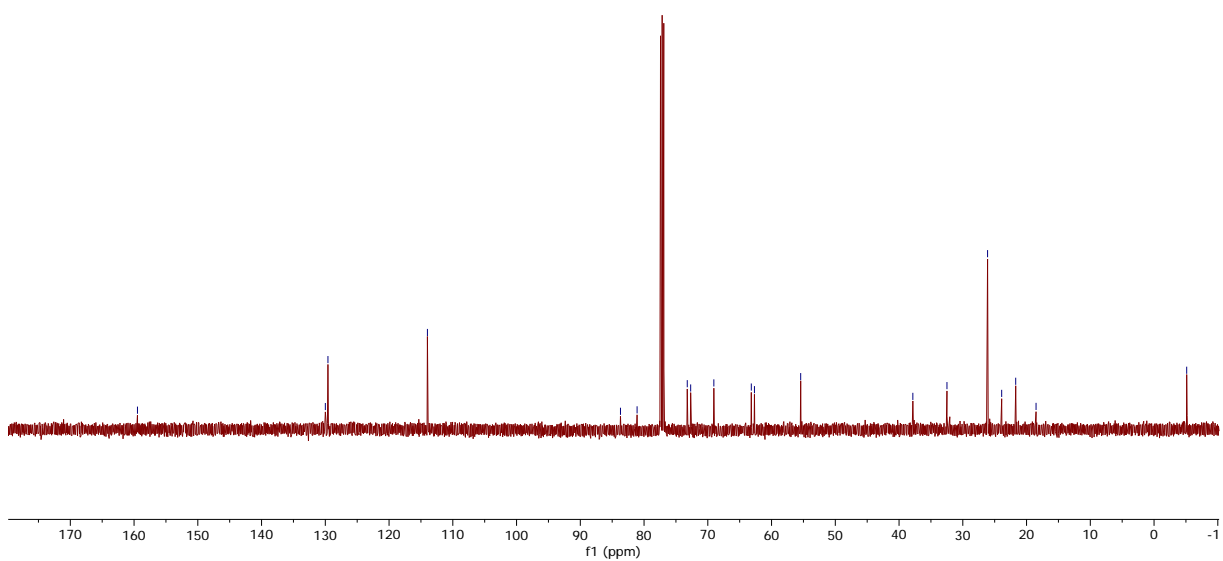
10-((tert-Butyldimethylsilyl)oxy)-6-hydroxy-1-((4-methoxybenzyl)oxy)dec-4-yn-2-yl acetate – 162



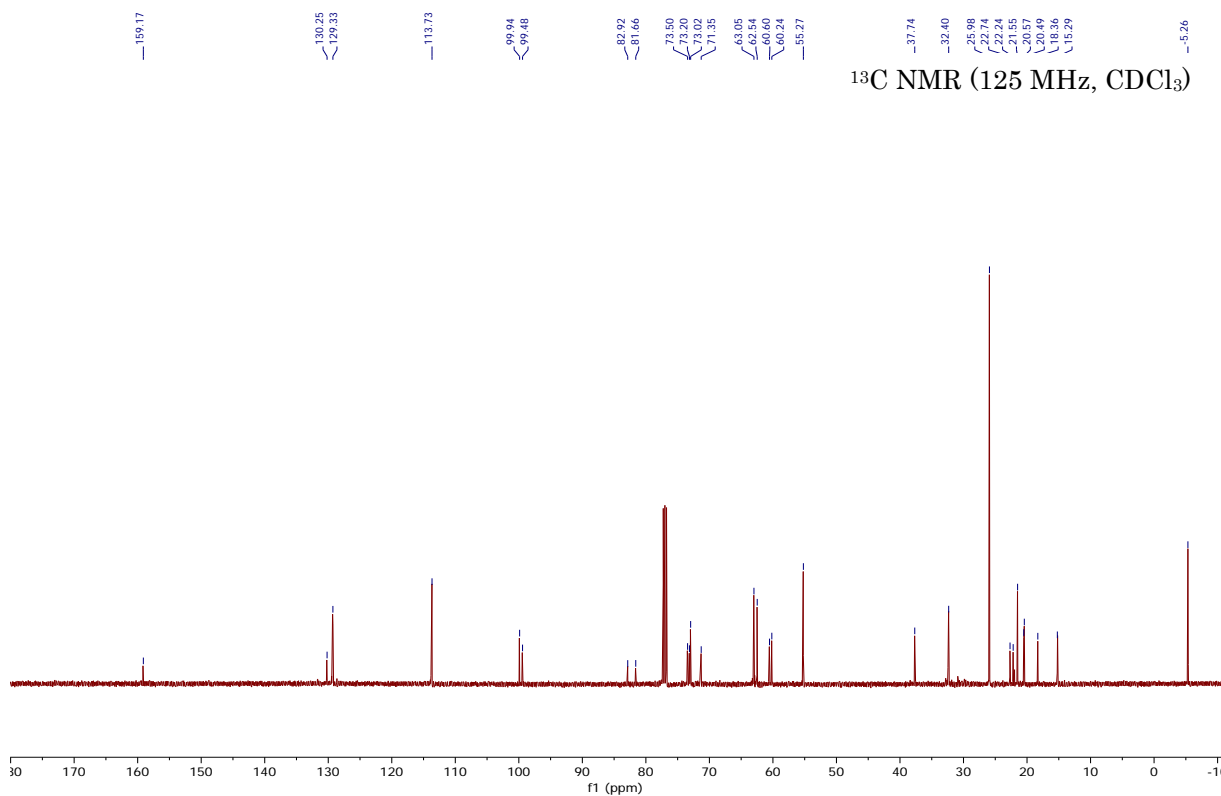
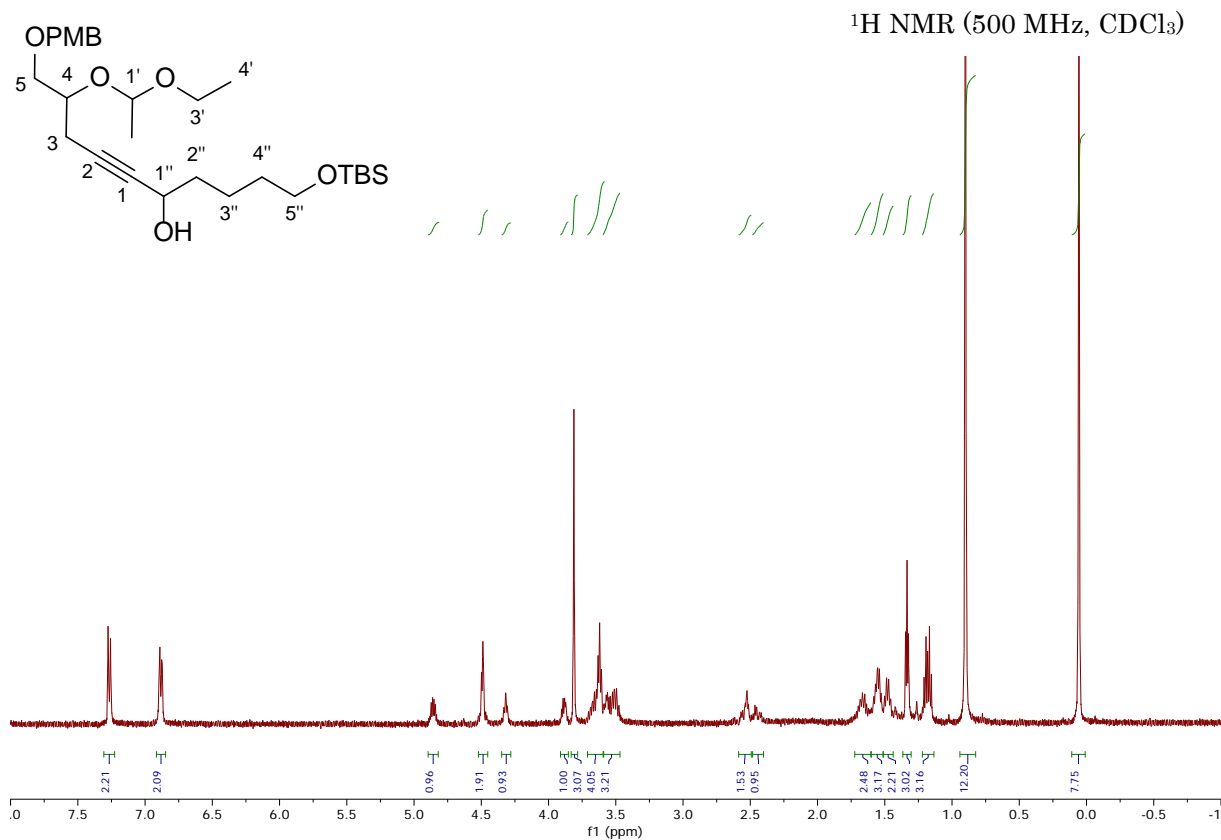
10-((tert-Butyldimethylsilyl)oxy)-1-((4-methoxybenzyl)oxy)dec-4-yne-2,6-diol —
 164



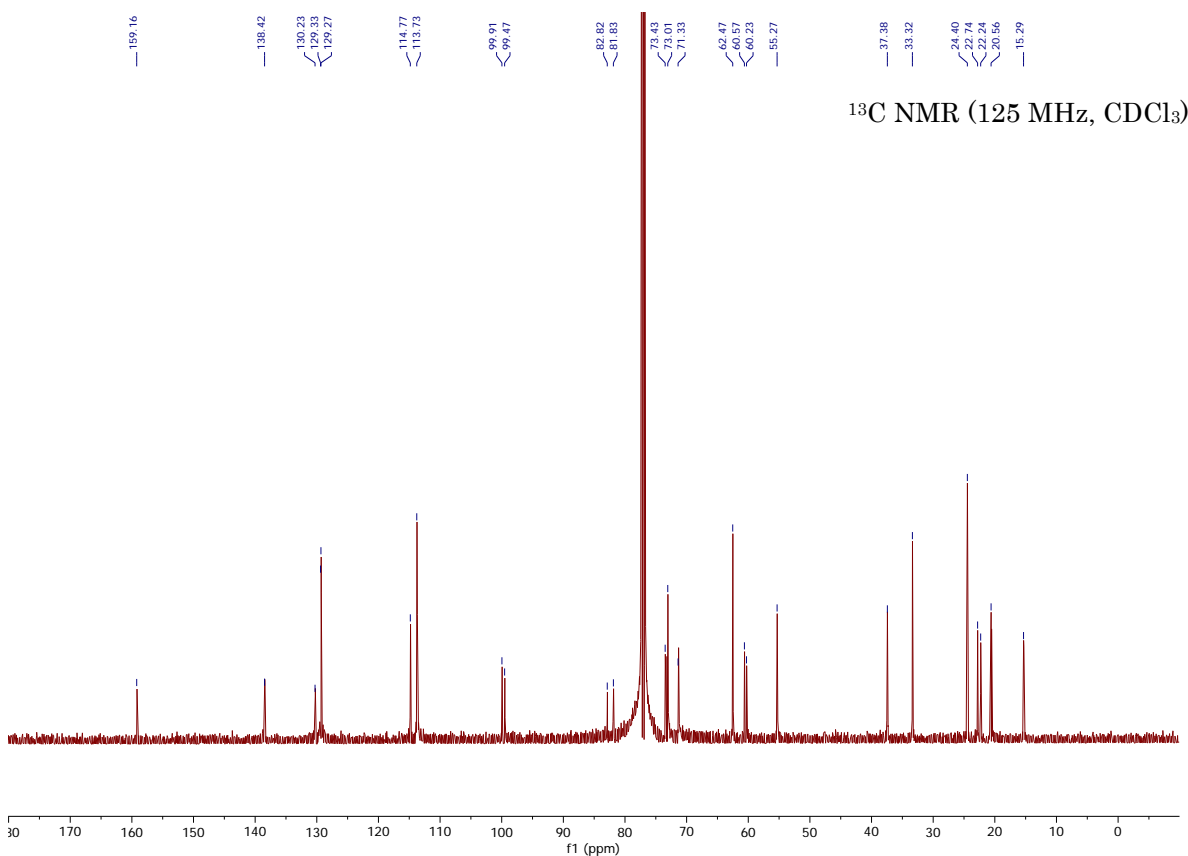
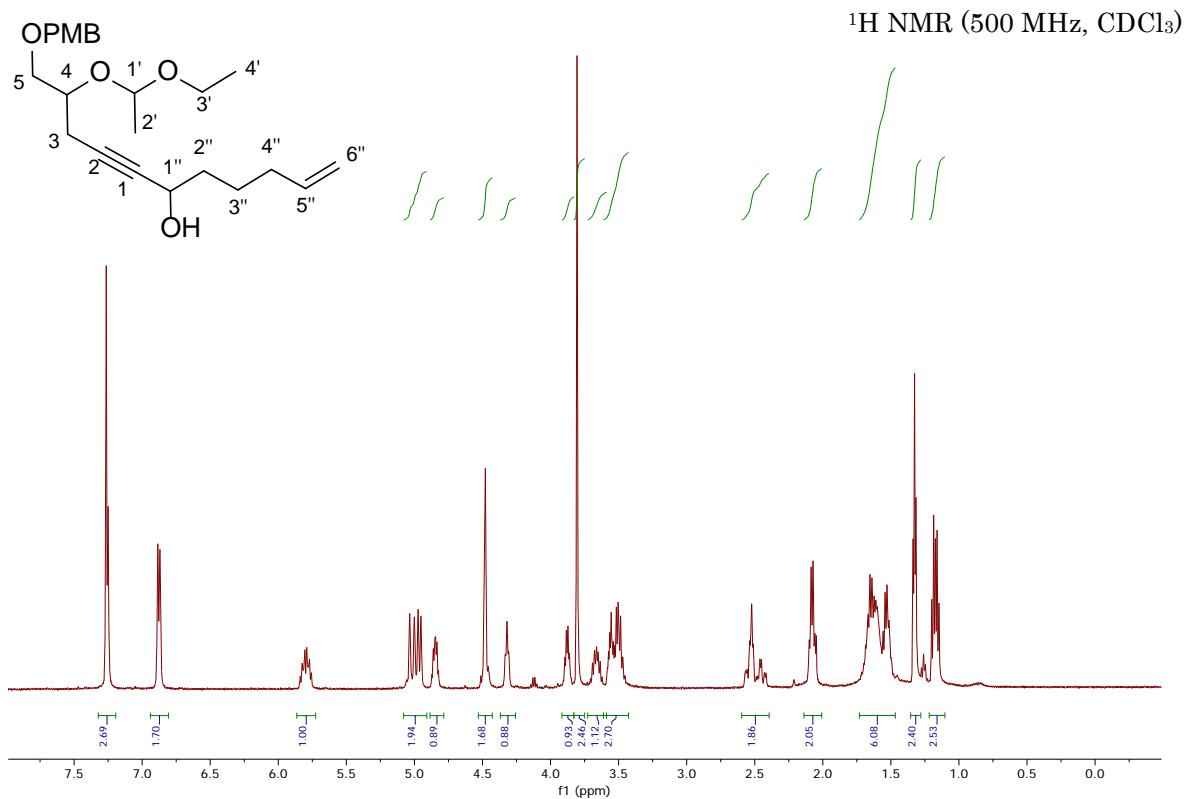
¹³C NMR (125 MHz, CDCl₃)



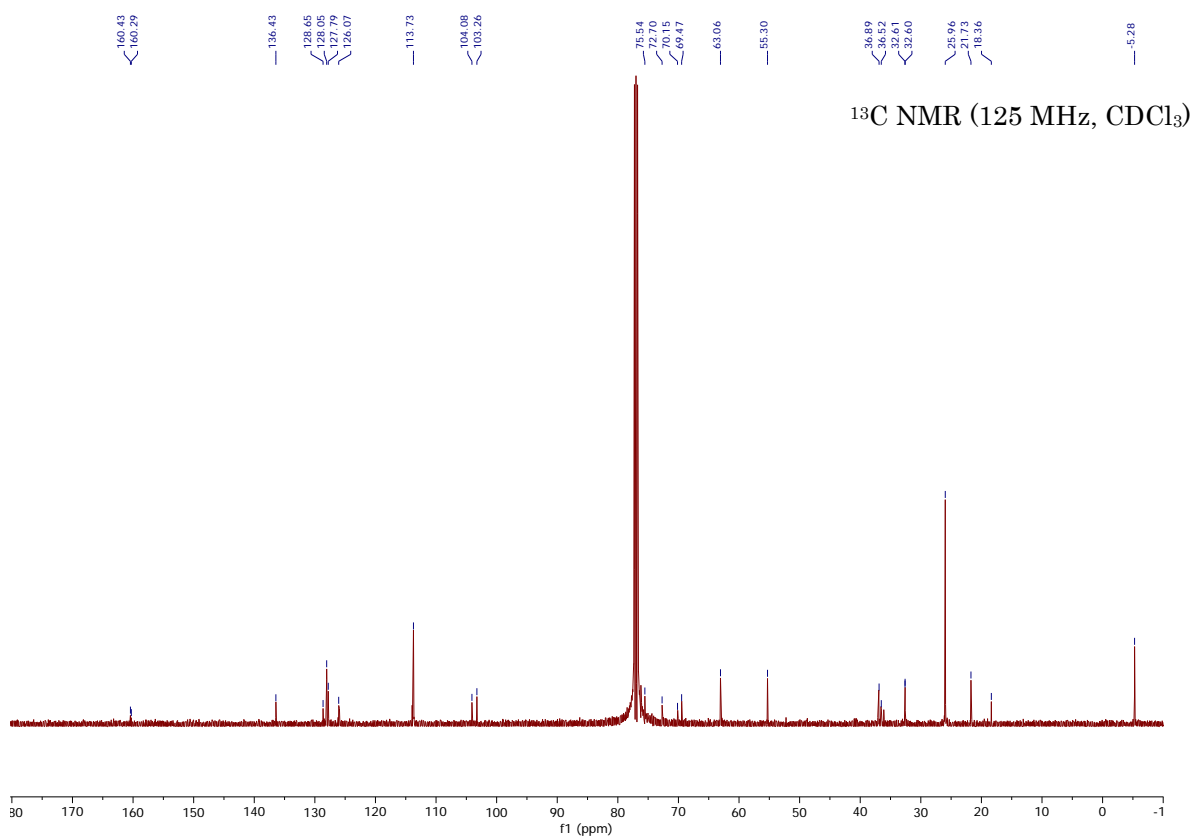
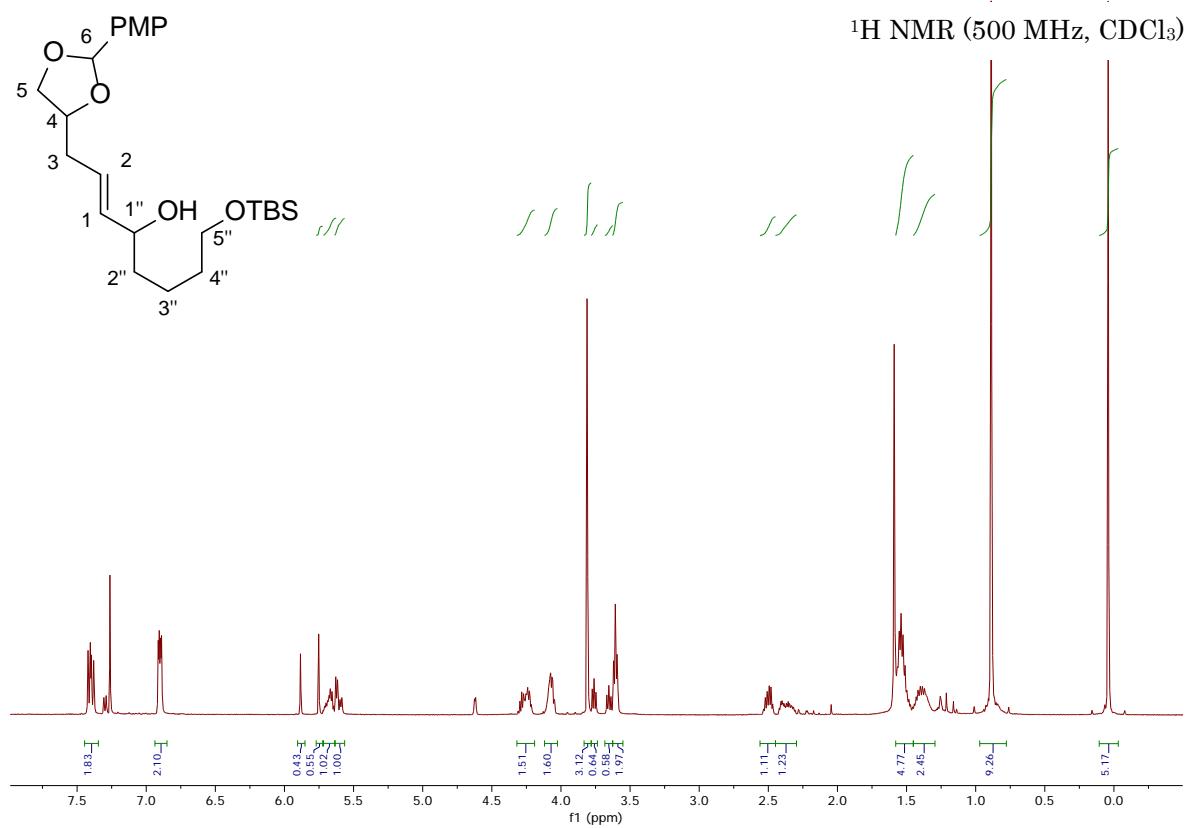
13-(((4-Methoxybenzyl)oxy)methyl)-2,2,3,3,15-pentamethyl-4,14,16-trioxa-3-silaoctadec-10-yn-9-ol – 166



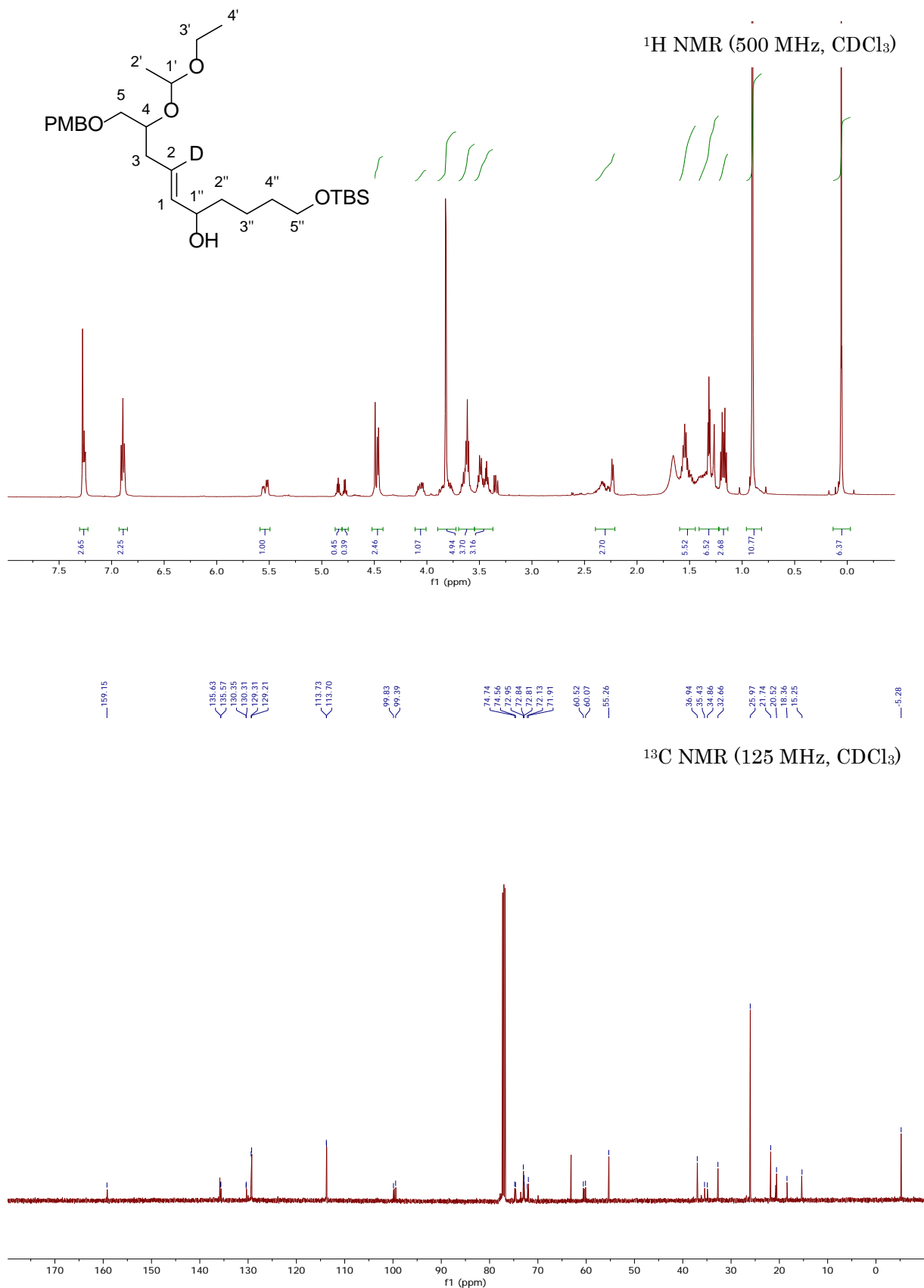
***(Z)*-7-(2-(1-Ethoxyethoxy)-3-((4-methoxybenzyl)oxy)propyl)tetradeca-1,7,13-triene-6,9-dione – 167**



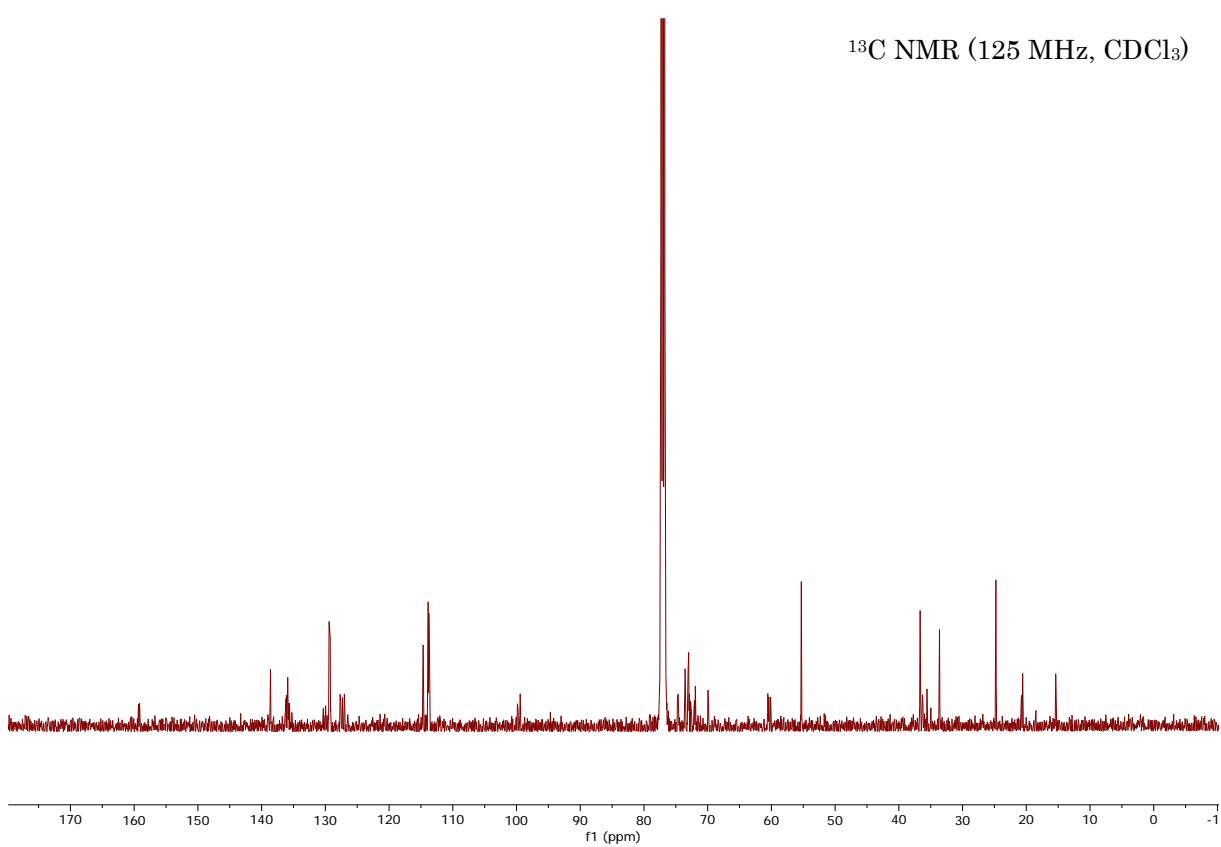
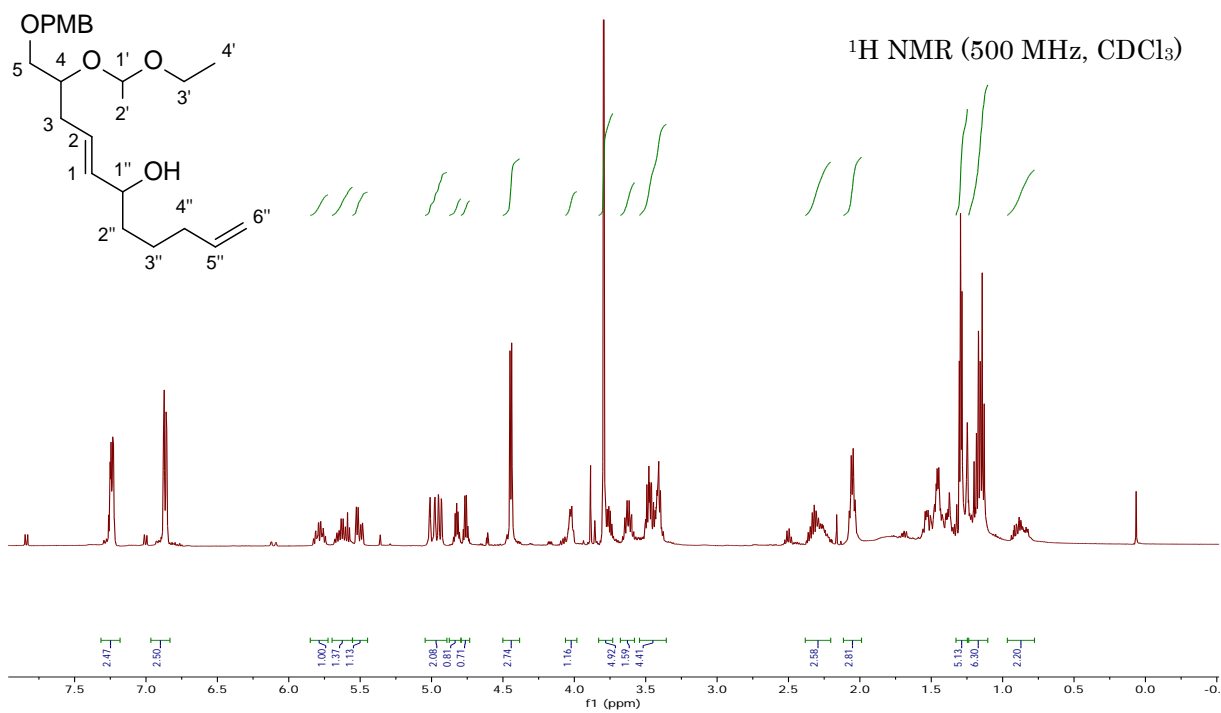
(E)-8-((*tert*-Butyldimethylsilyl)oxy)-1-(2-(4-methoxyphenyl)-1,3-dioxolan-4-yl)oct-2-en-4-ol – 170



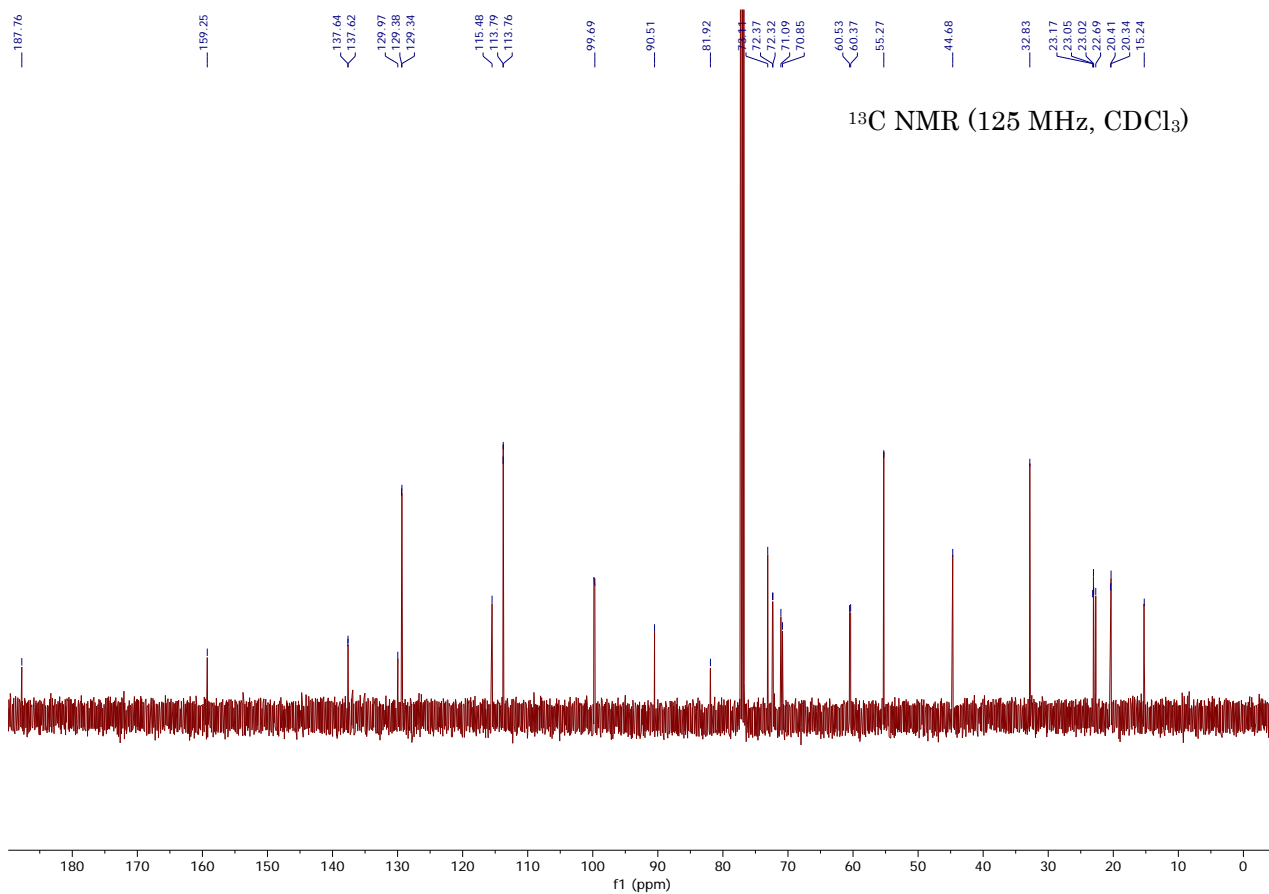
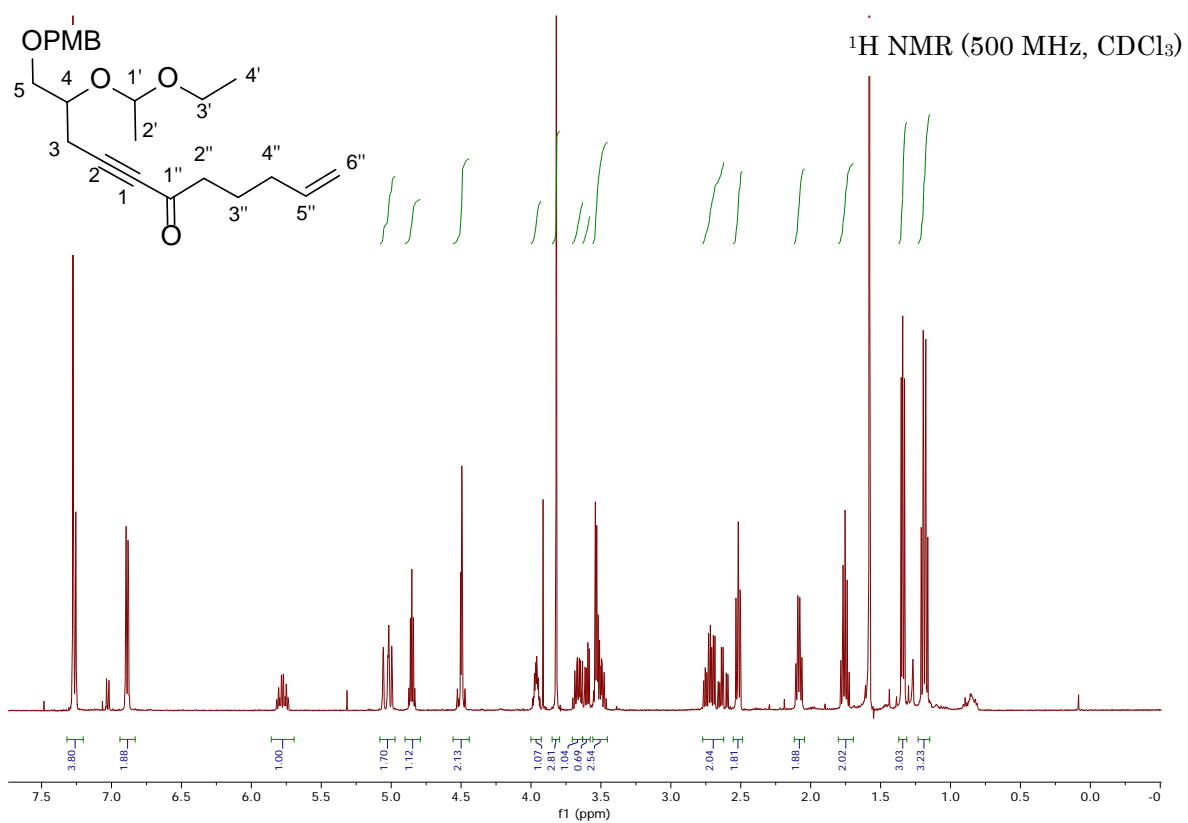
Deuterated (E)-13-(((4-Methoxybenzyl)oxy)methyl)-2,2,3,3,15-pentamethyl-4,14,16-trioxa-3-silaoctadec-10-en-9-ol – 172



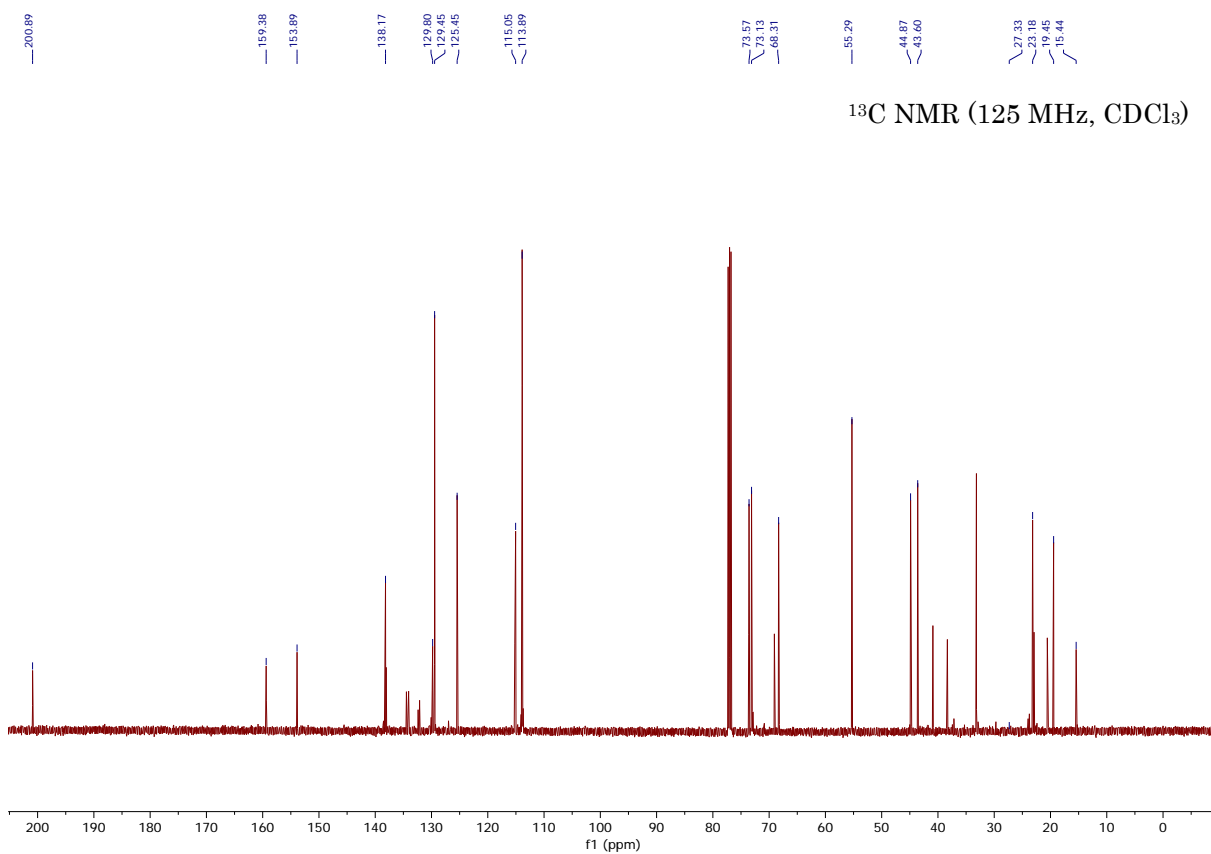
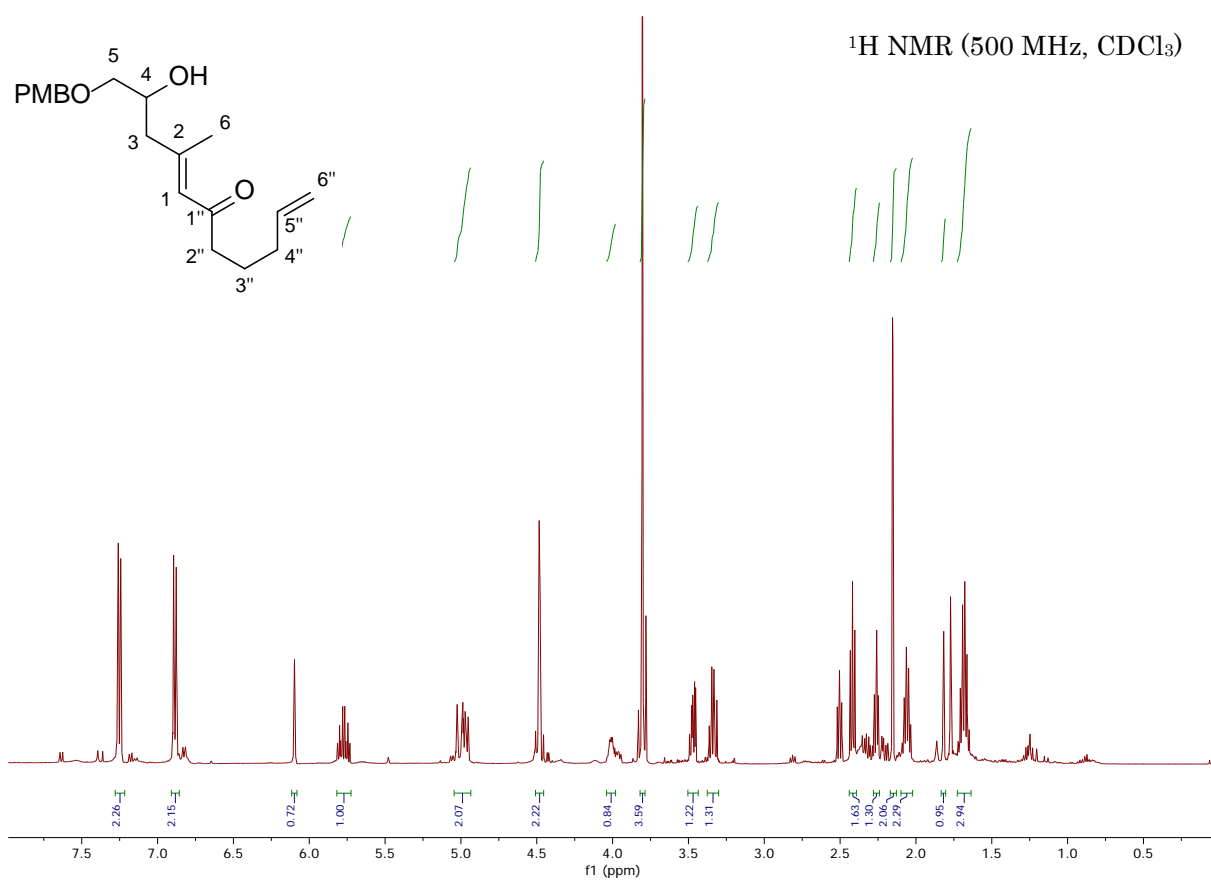
(E)-10-(1-Ethoxyethoxy)-11-((4-methoxybenzyl)oxy)undeca-1,7-dien-6-ol – 174



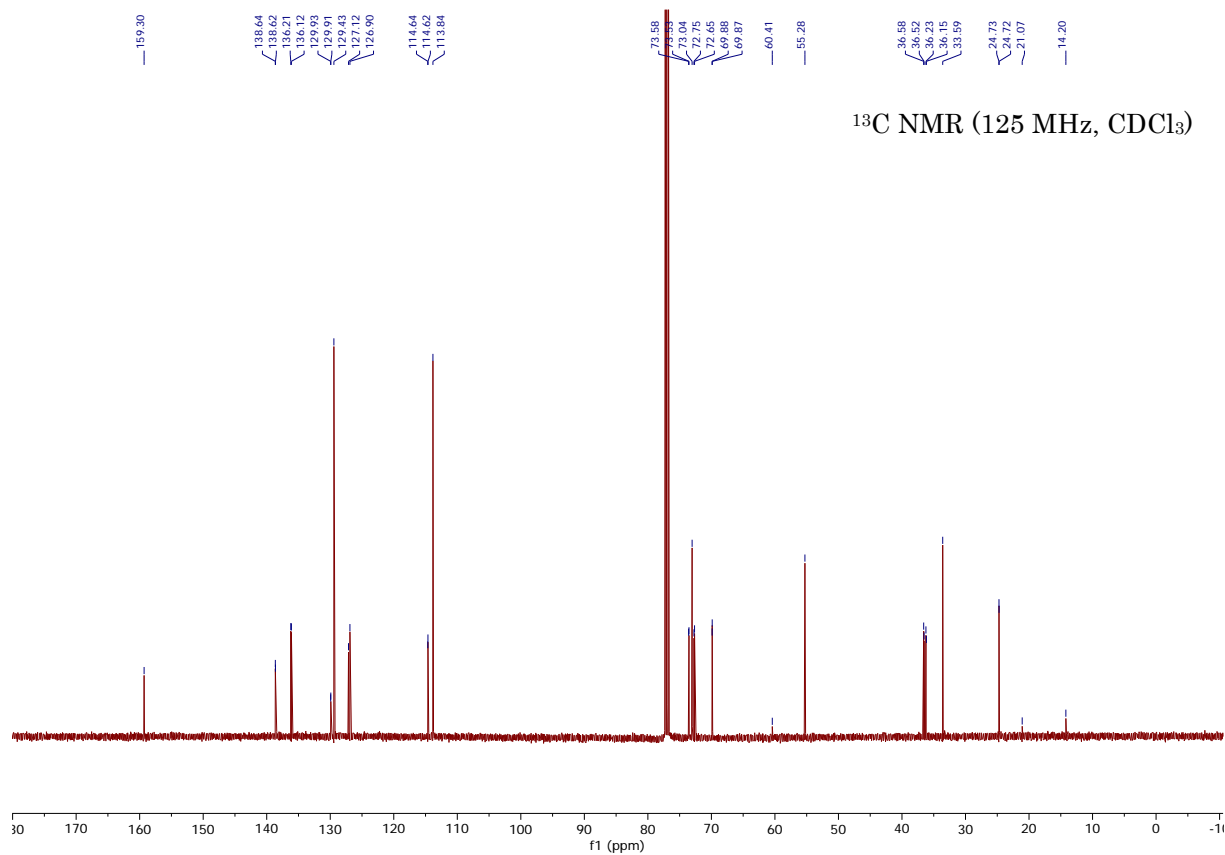
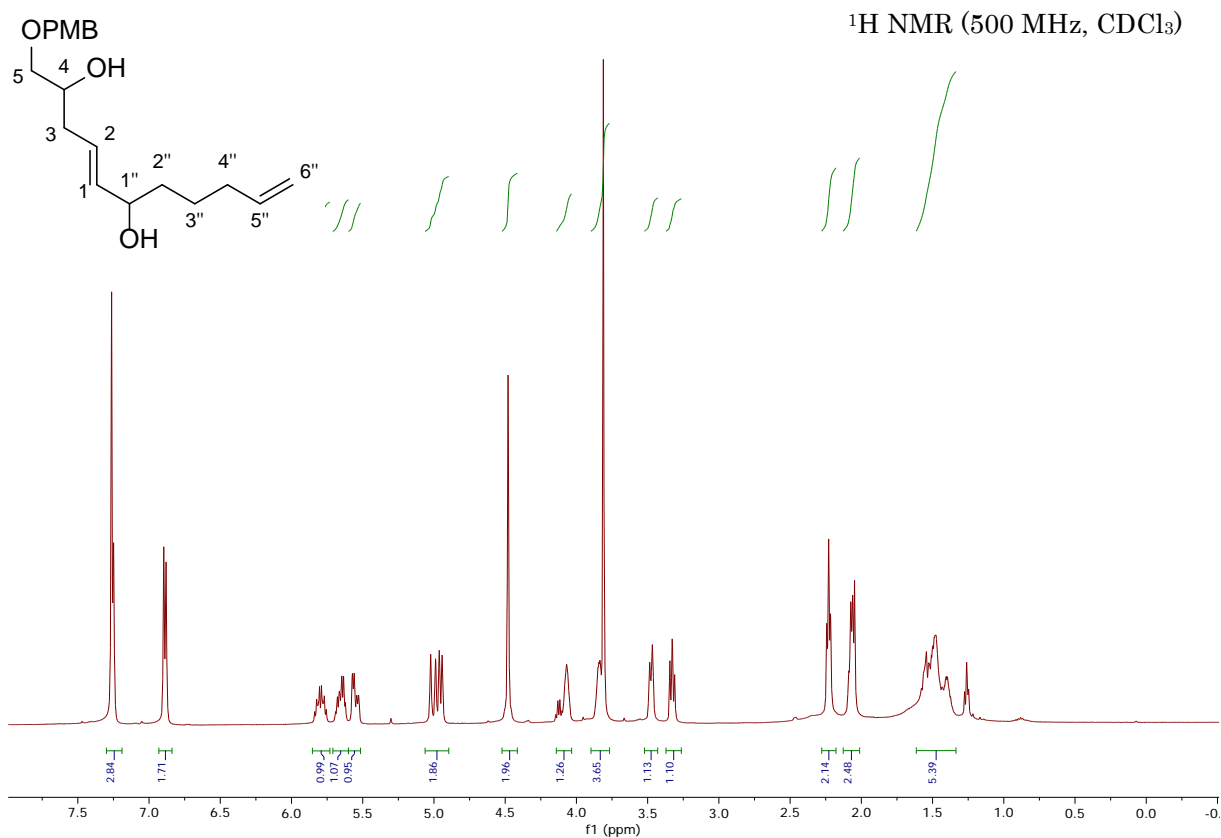
10-(1-Ethoxyethoxy)-11-((4-methoxybenzyl)oxy)undec-1-en-7-yn-6-one- 181



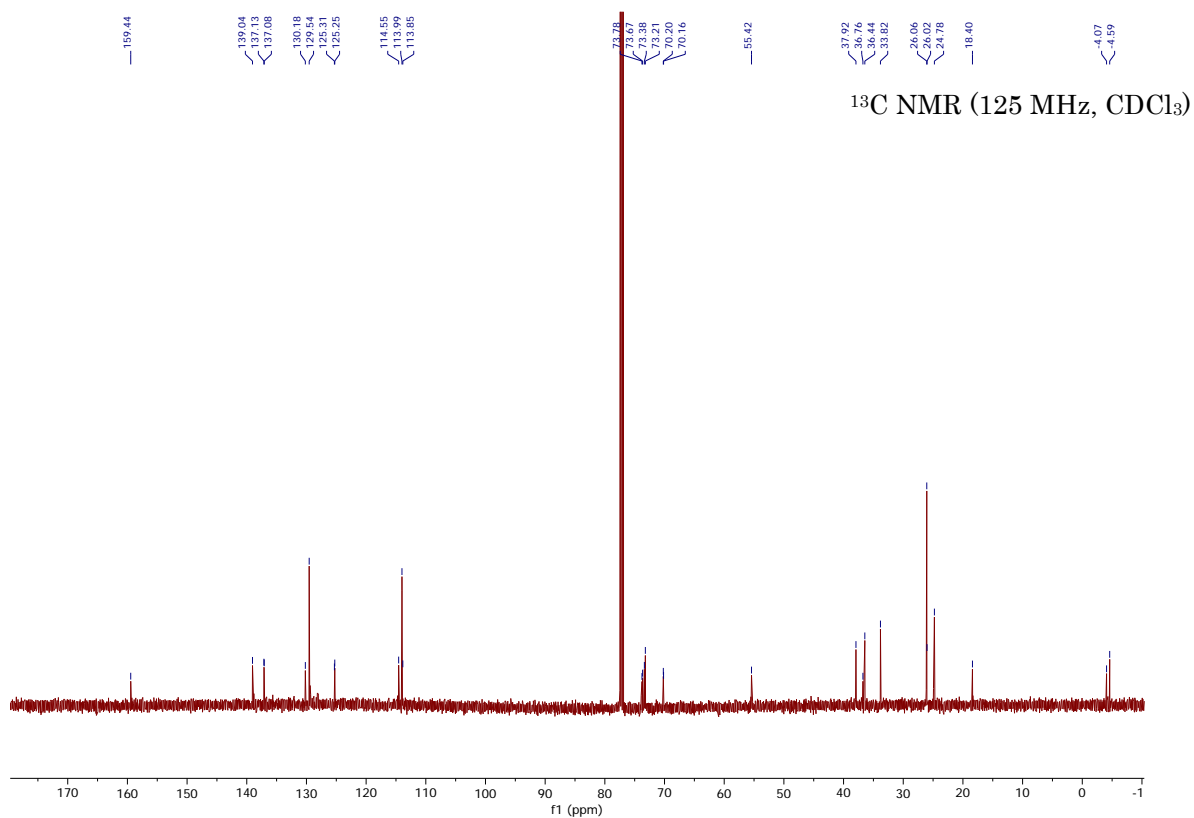
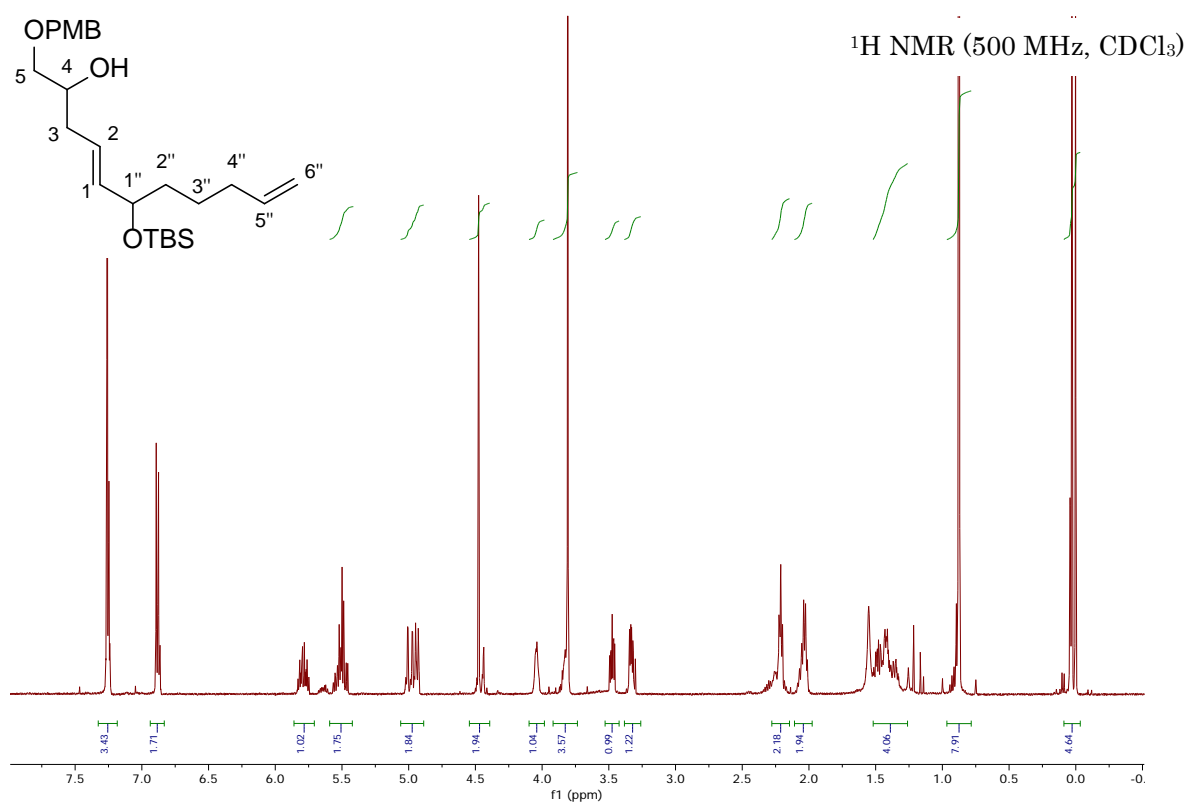
(E)-10-Hydroxy-11-((4-methoxybenzyl)oxy)-8-methylundeca-1,7-dien-6-one – 186



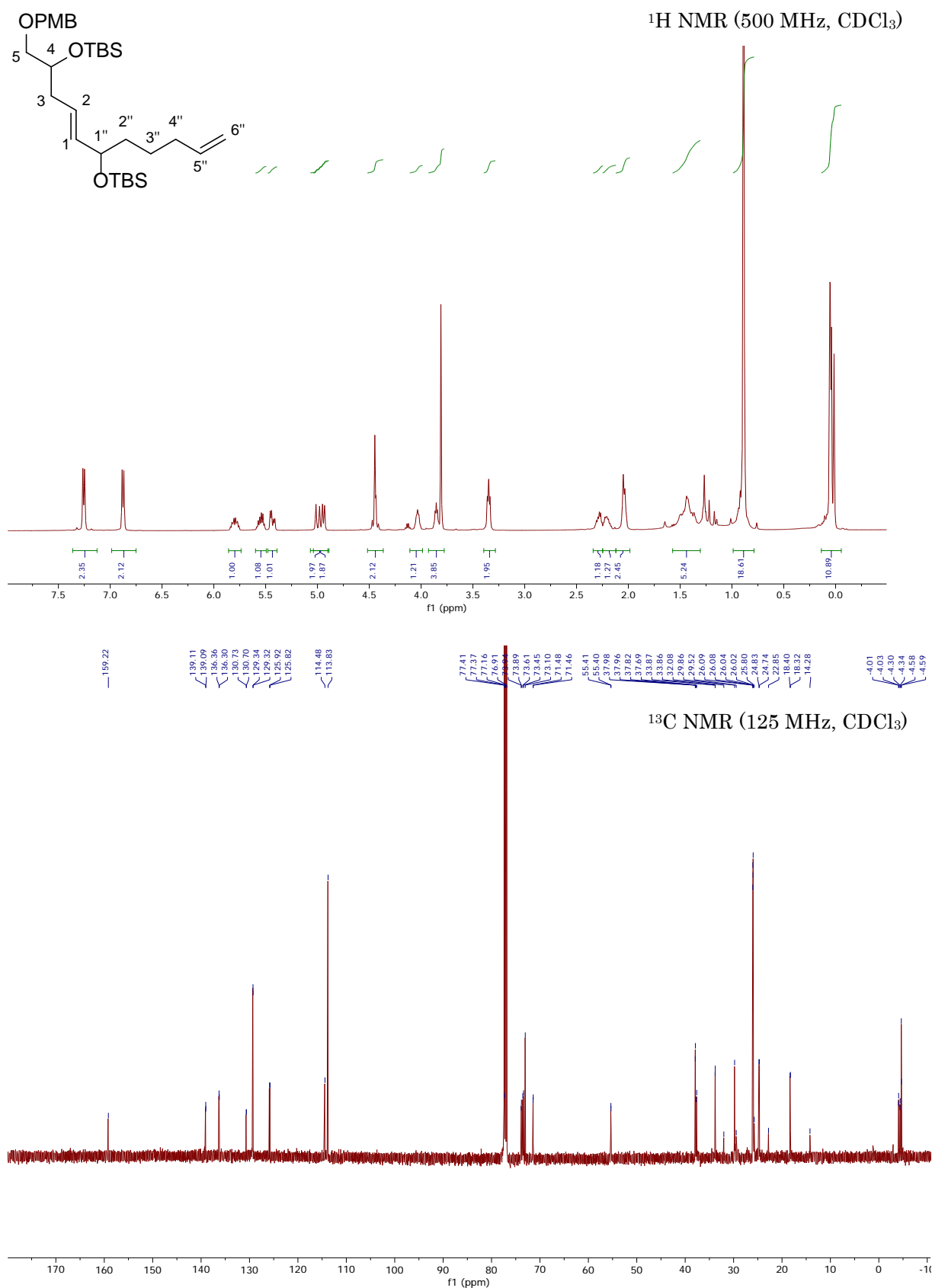
(E)-1-((4-Methoxybenzyl)oxy)undeca-4,10-diene-2,6-diol – 190



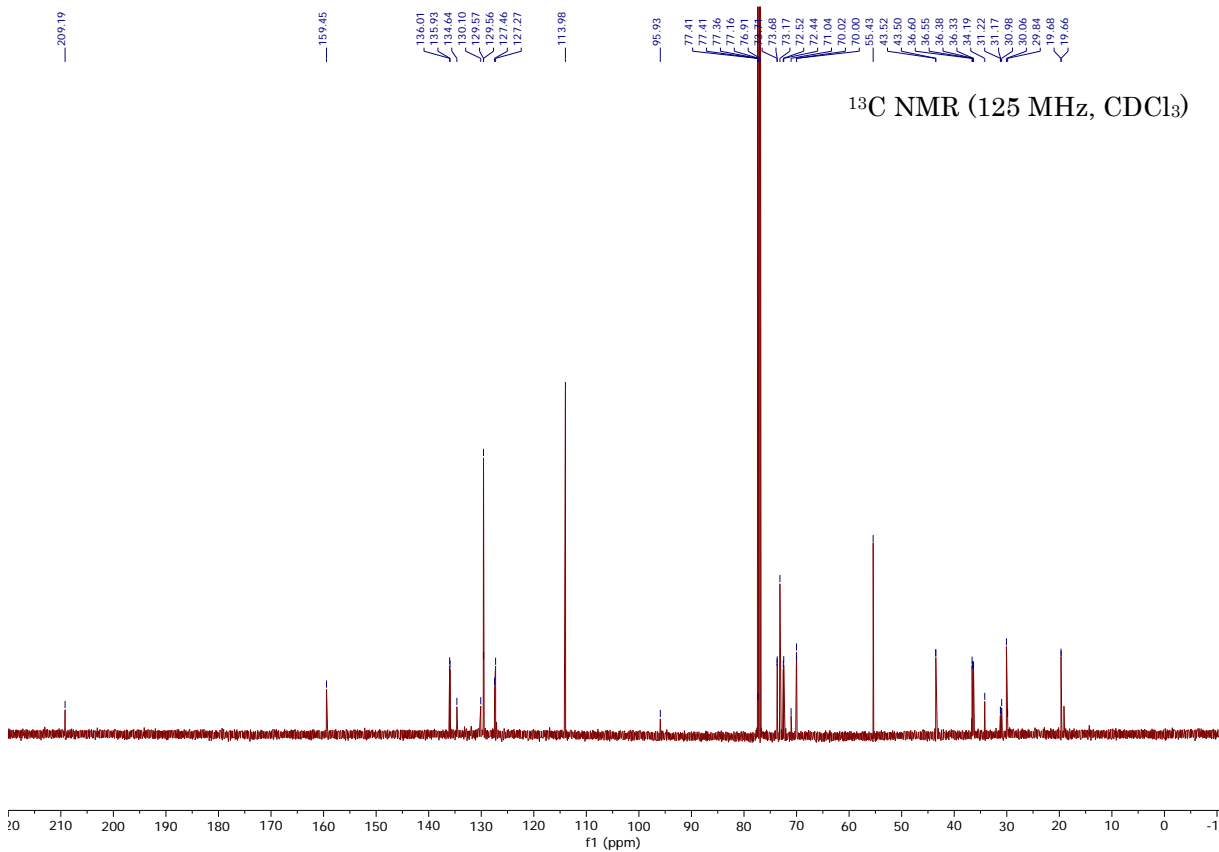
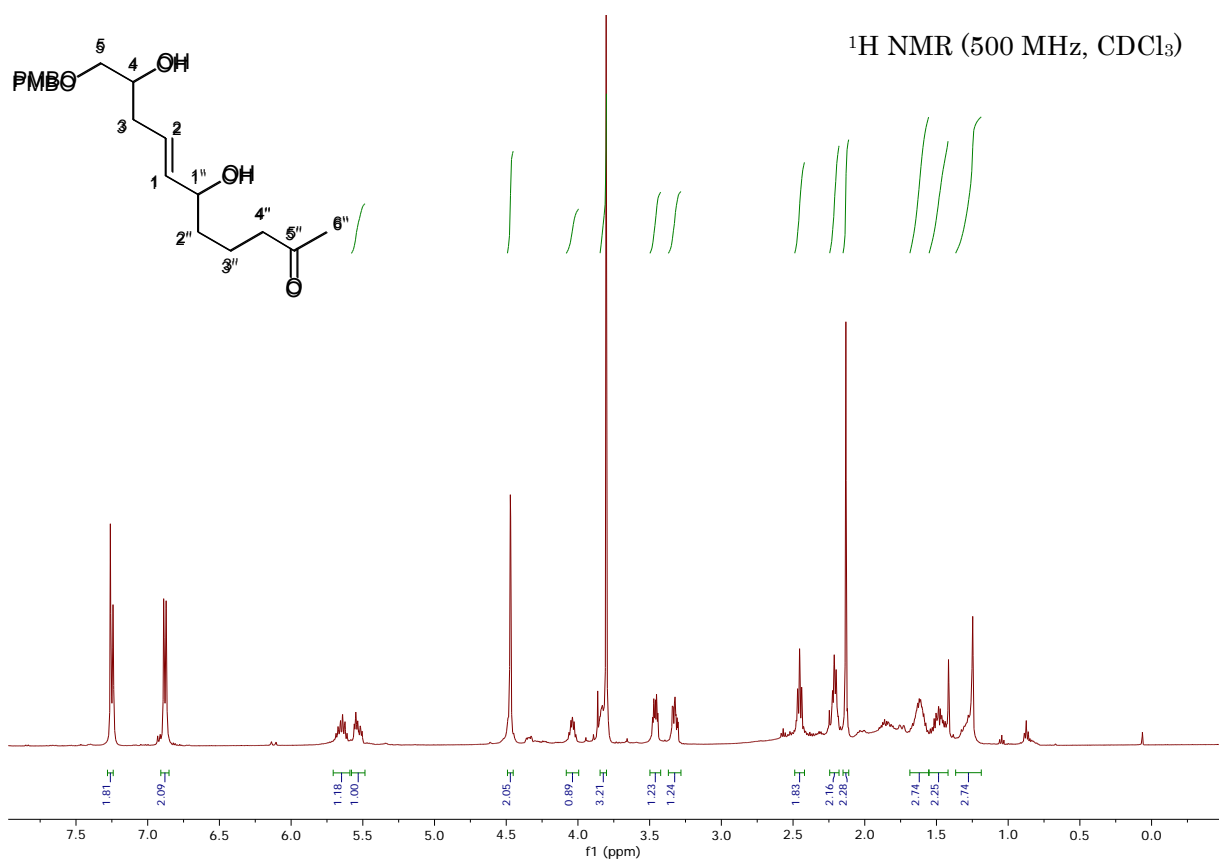
(E)-6-((*tert*-Butyldimethylsilyl)oxy)-1-((4-methoxybenzyl)oxy)undeca-4,10-dien-2-ol – 191



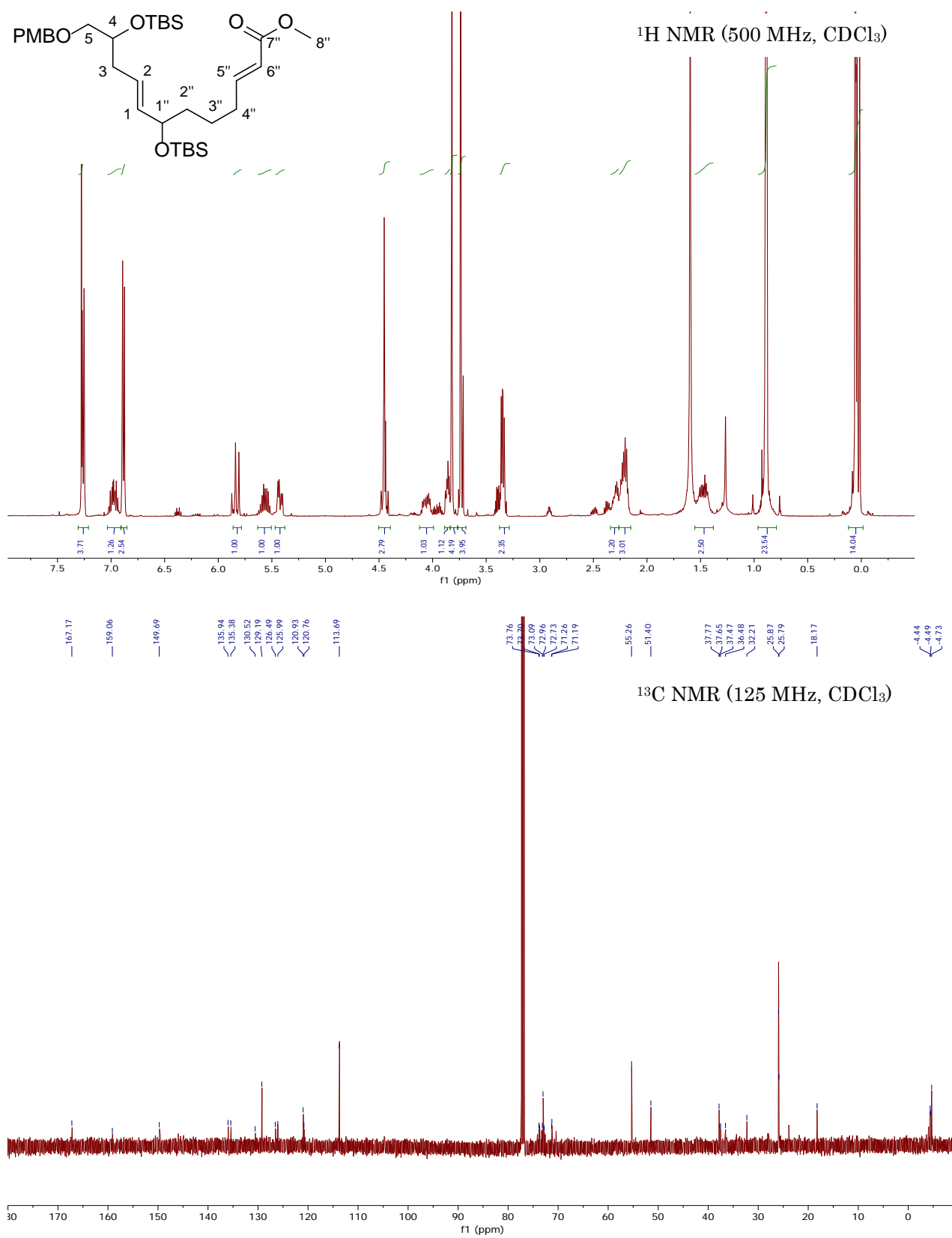
***(E)*-9-(((4-Methoxybenzyl)oxy)methyl)-2,2,3,3,11,11,12,12-octamethyl-5-(pent-4-en-1-yl)-4,10-dioxo-3,11-disilatridec-6-ene – 192**



(E)-6,10-Dihydroxy-11-((4-methoxybenzyl)oxy)undec-7-en-2-one – 194

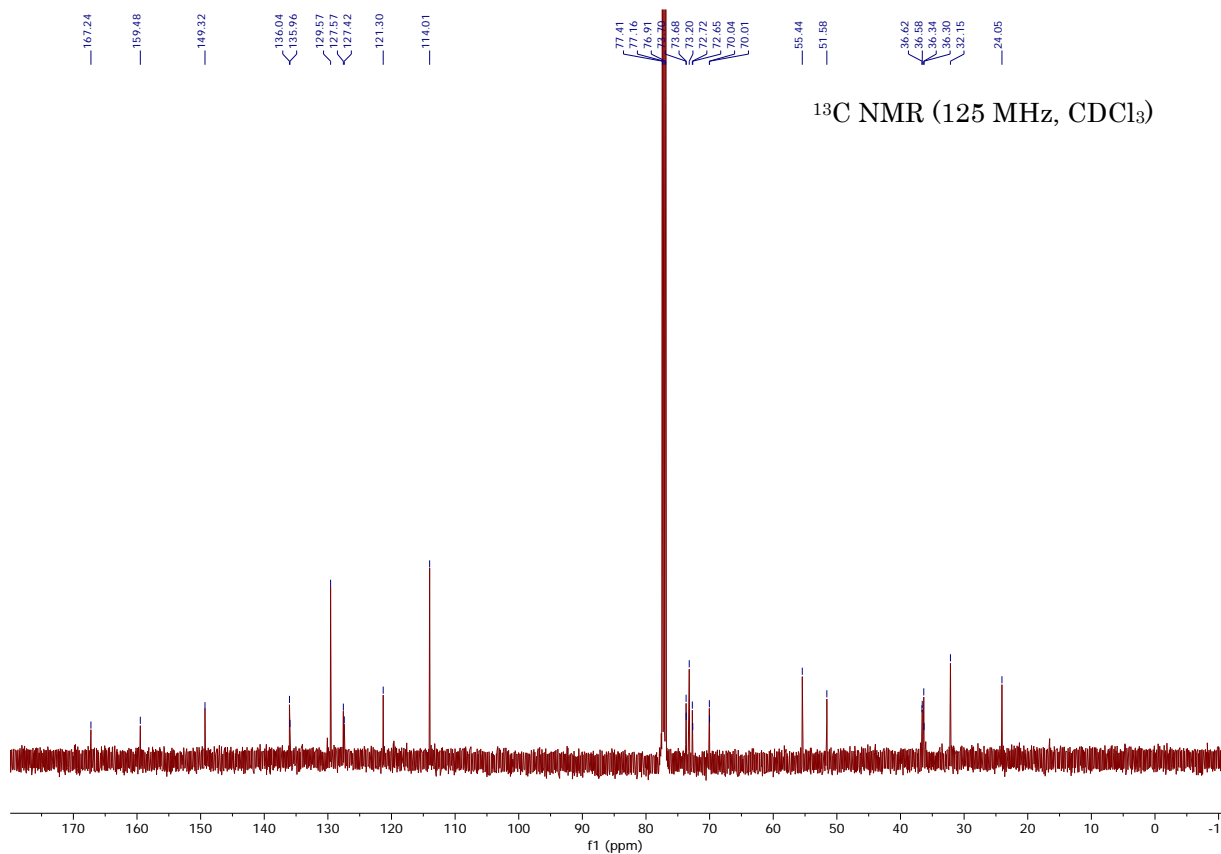
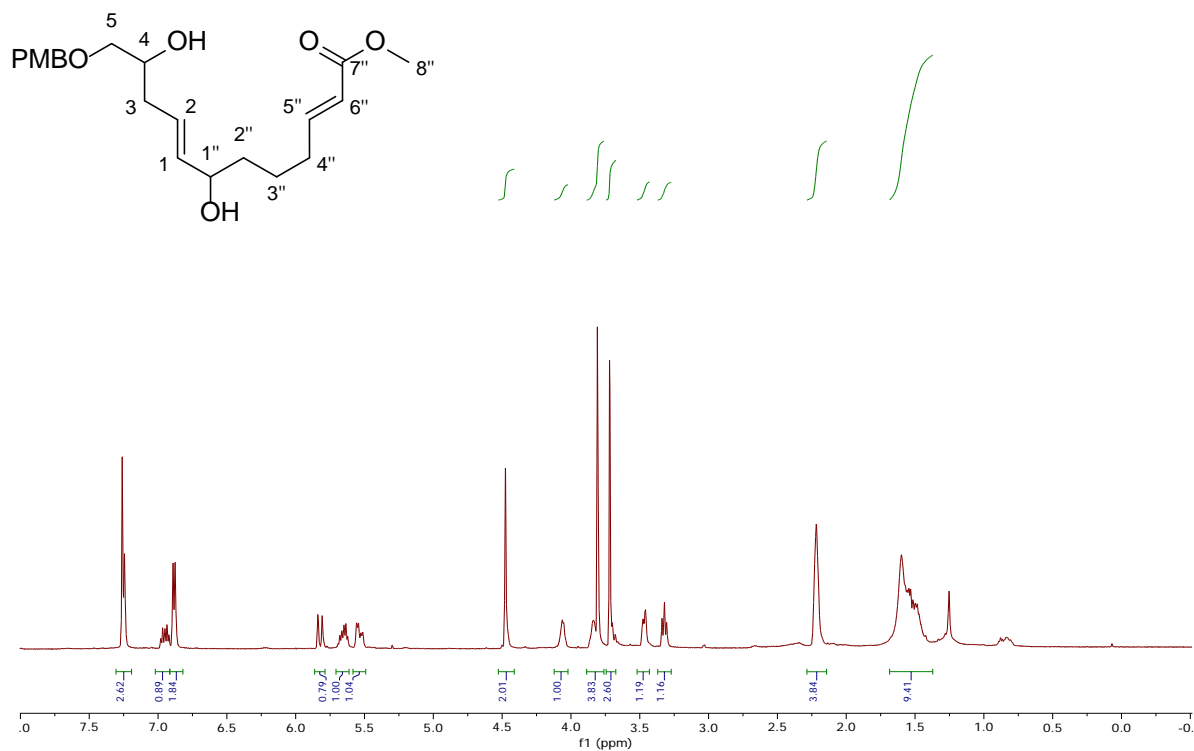


Methyl (2E,8E)-7,11-bis((tert-butyl dimethylsilyl)oxy)-12-((4-methoxybenzyl)oxy) dodeca-2,8-dienoate – 211

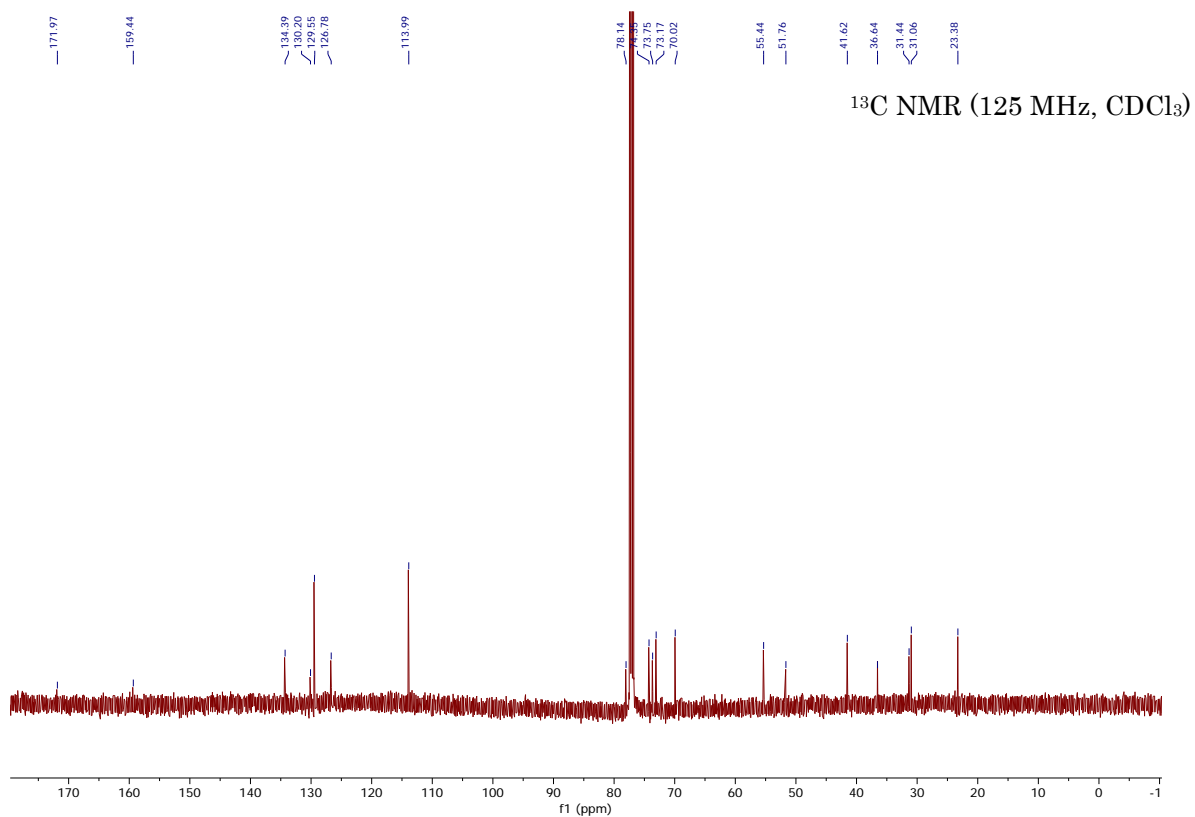
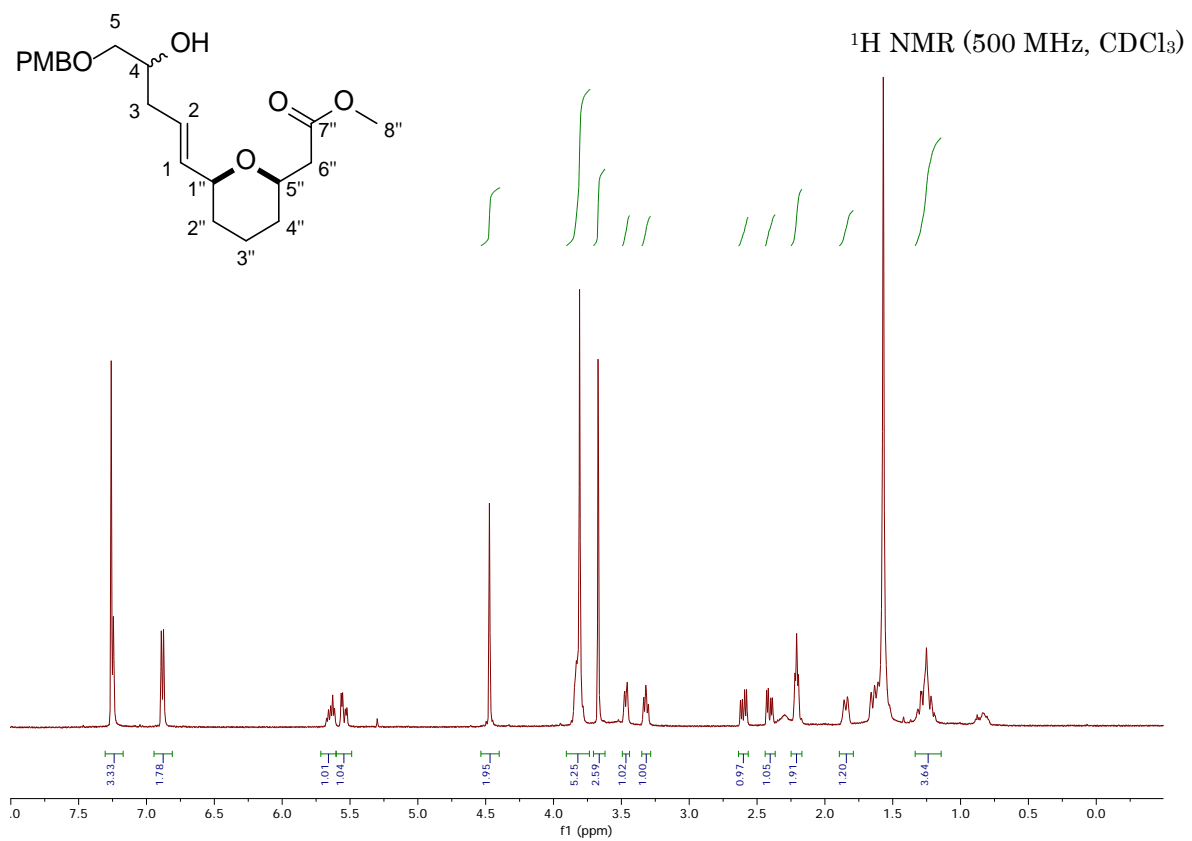


Methyl (2E,8E)-7,11-dihydroxy-12-((4-methoxybenzyl)oxy)dodeca-2,8-dienoate – 212

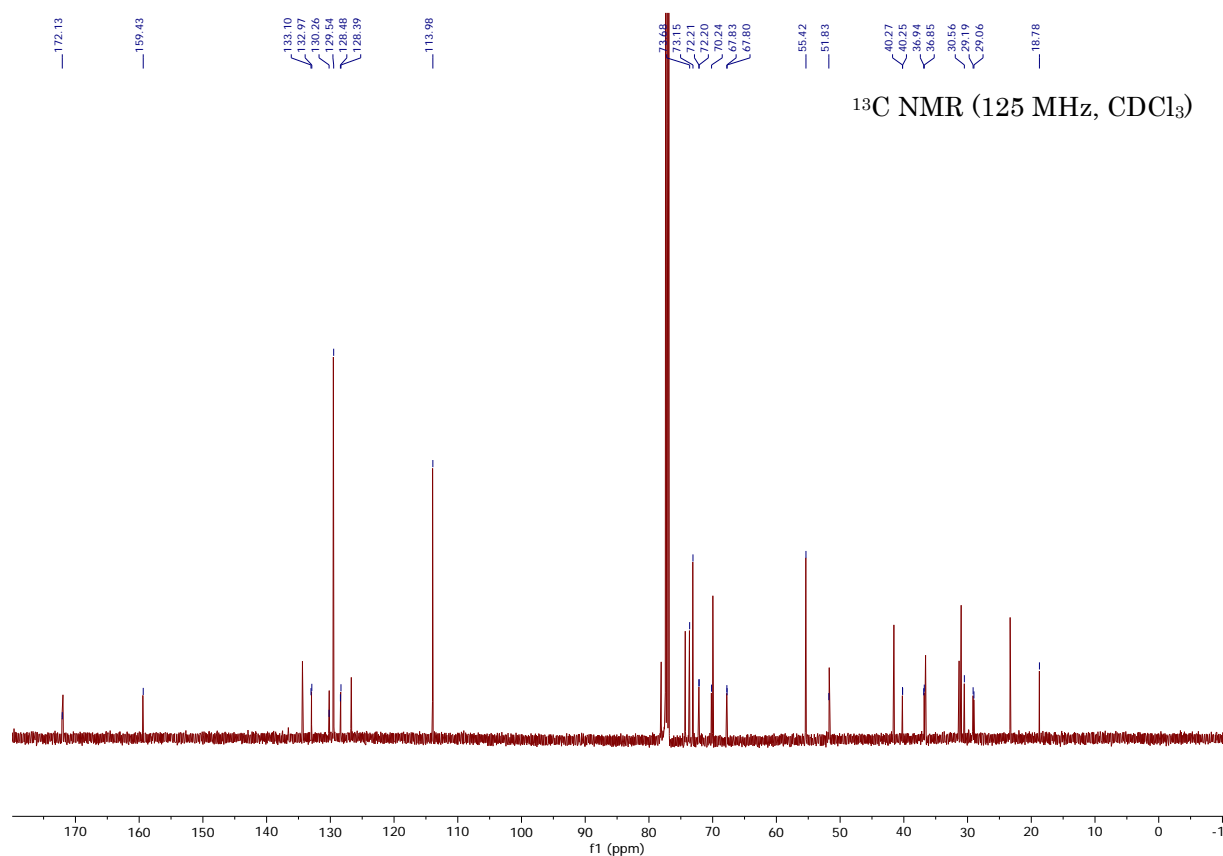
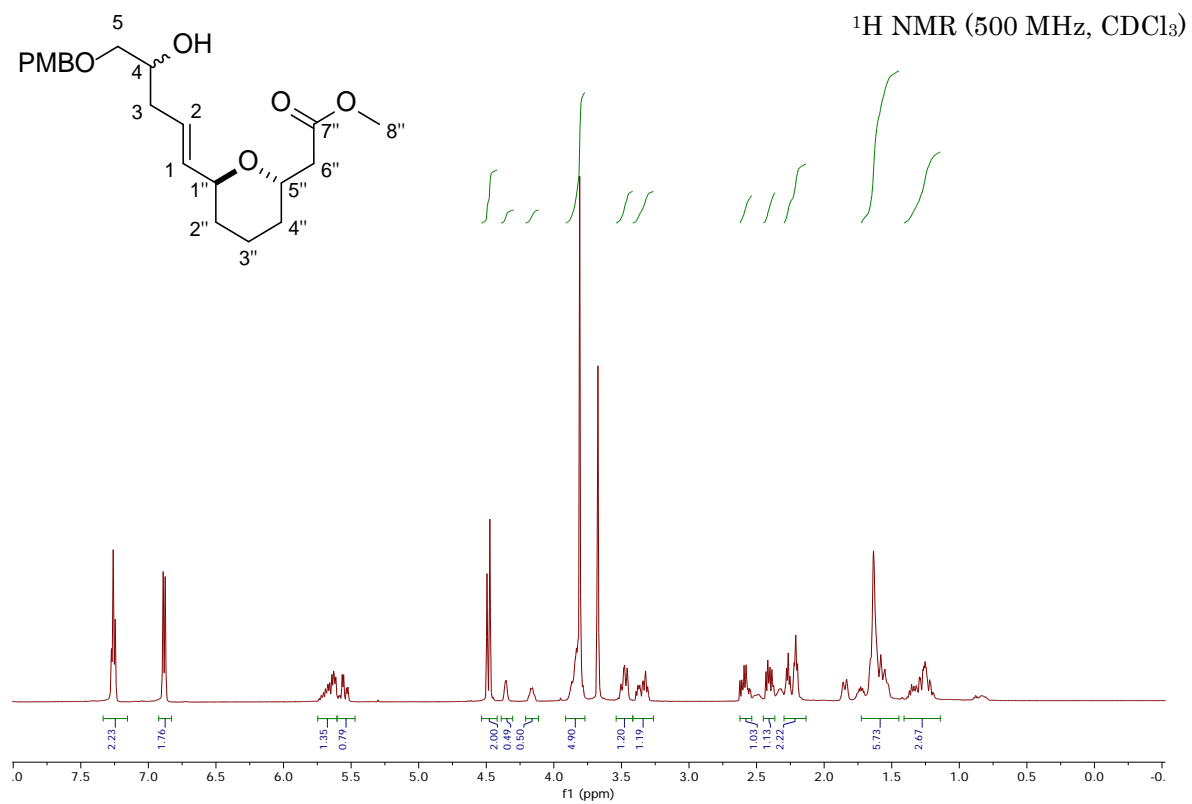
¹H NMR (500 MHz, CDCl₃)



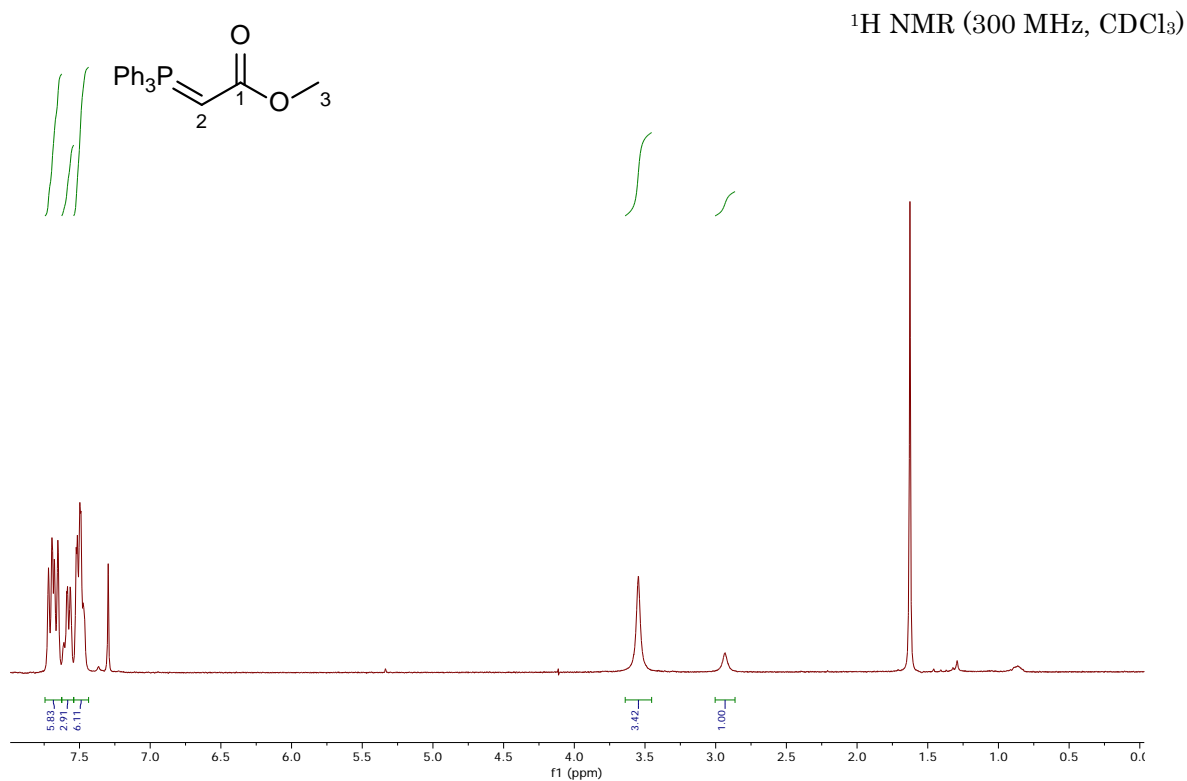
Methyl 2-((2R,6S)-6-((E)-4-hydroxy-5-((4-methoxybenzyl)oxy)pent-1-en-1-yl)3,4,5,6-tetrahydro-2H-pyran-2-yl)acetate – cis-213



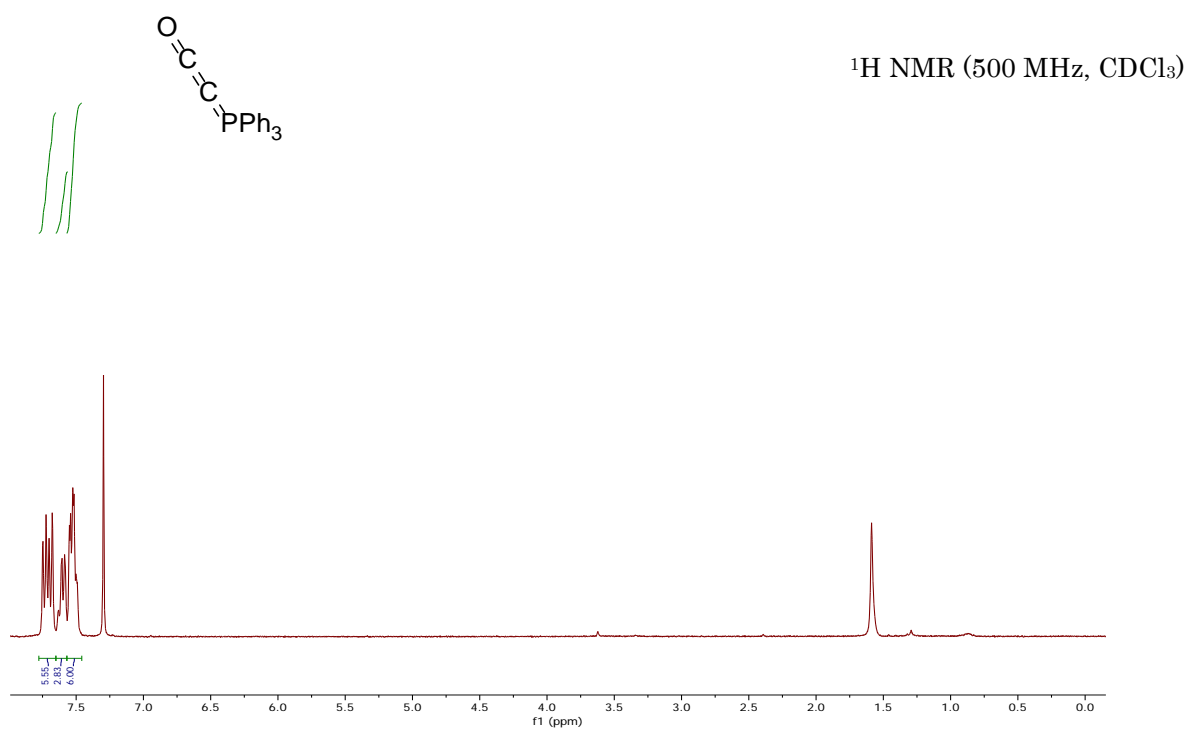
Methyl 2-((2S,6S)-6-((E)-4-hydroxy-5-((4-methoxybenzyl)oxy)pent-1-en-1-yl)tetrahydro-2H-pyran-2-yl)acetate - trans-213 in a mixture with trans-213



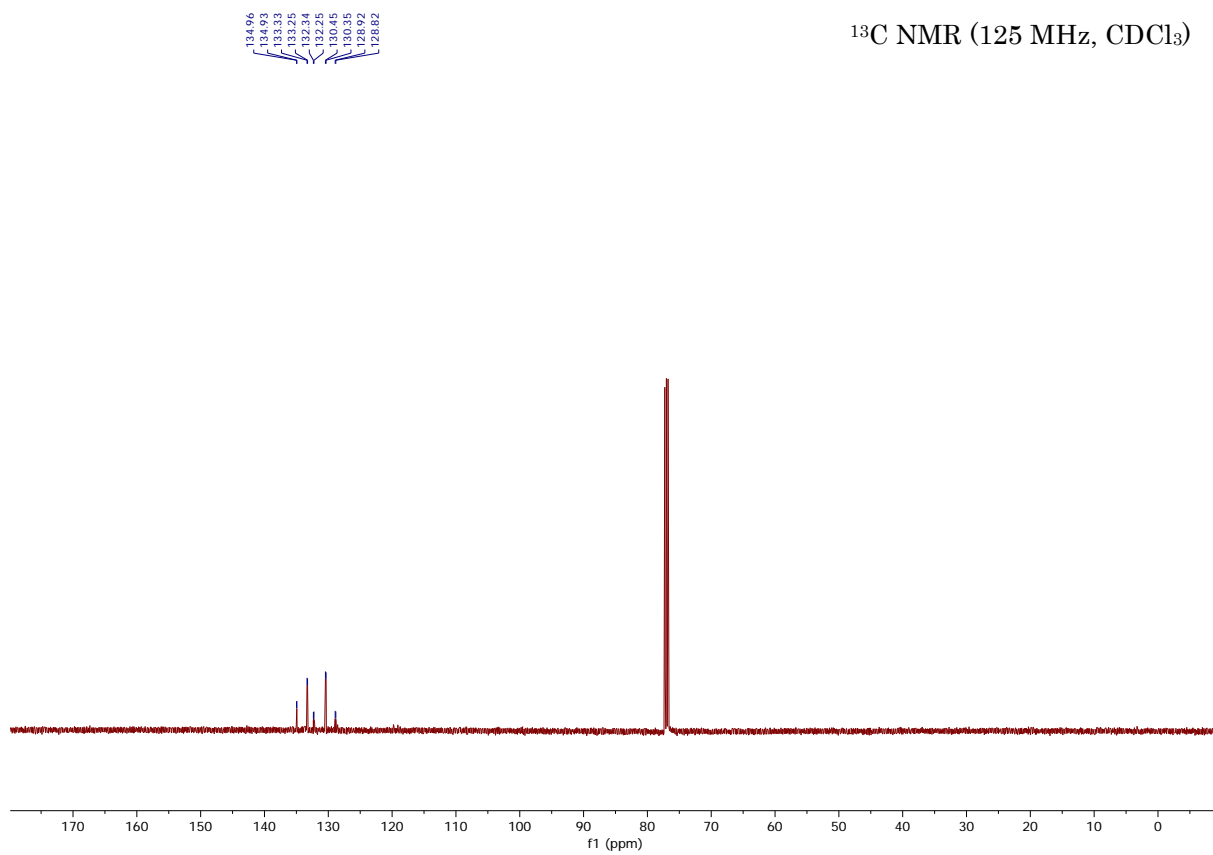
Methyl 2-(triphenylphosphaneylidne)acetate



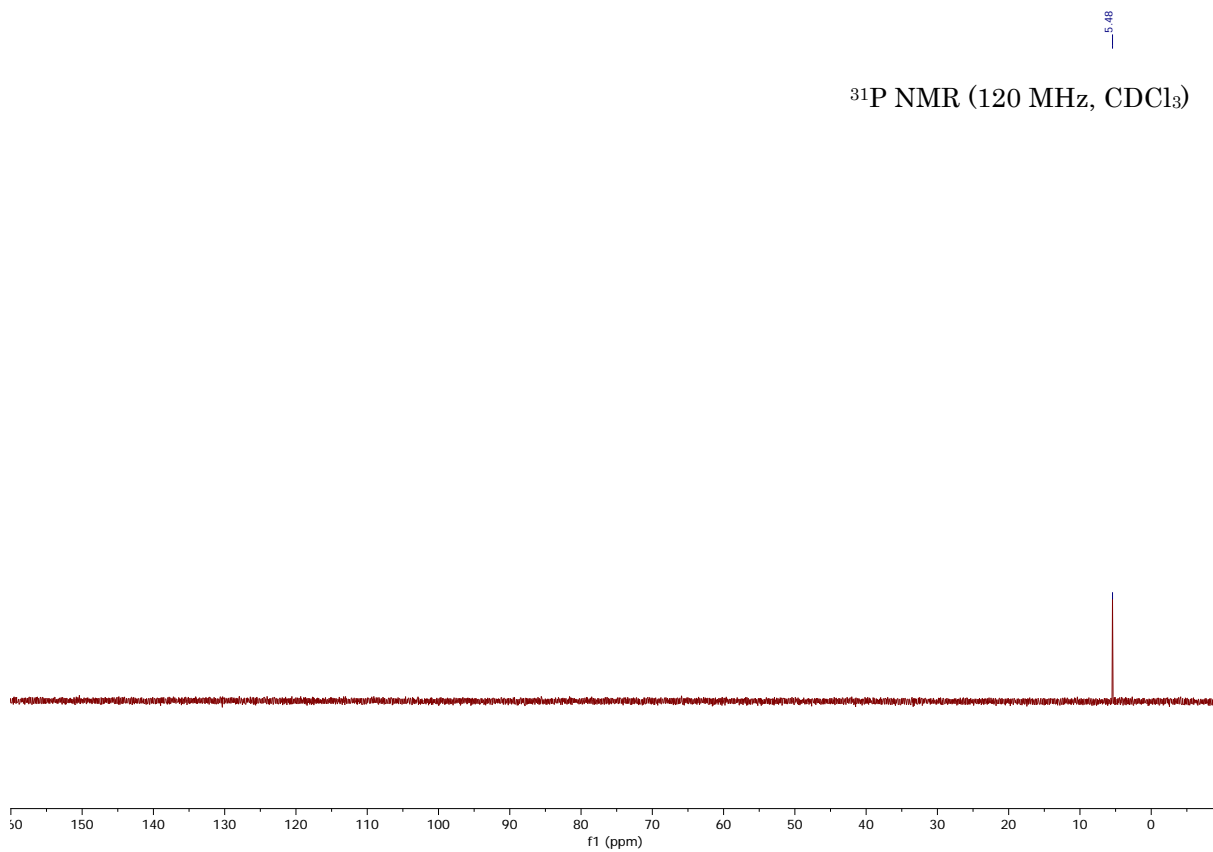
2-(Triphenylphosphoranylidne)ethenone (Bestmann Ylid) 114



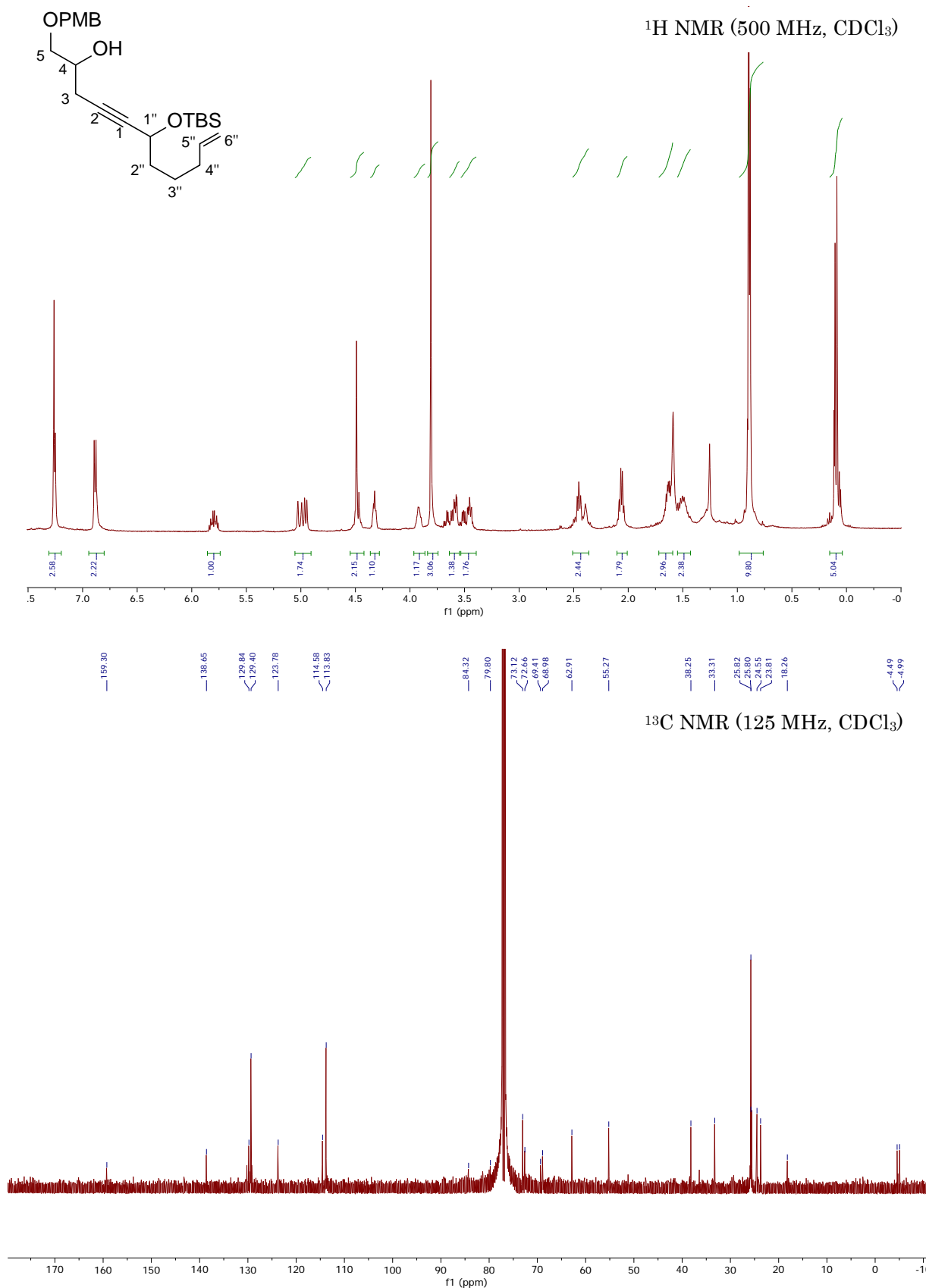
^{13}C NMR (125 MHz, CDCl_3)



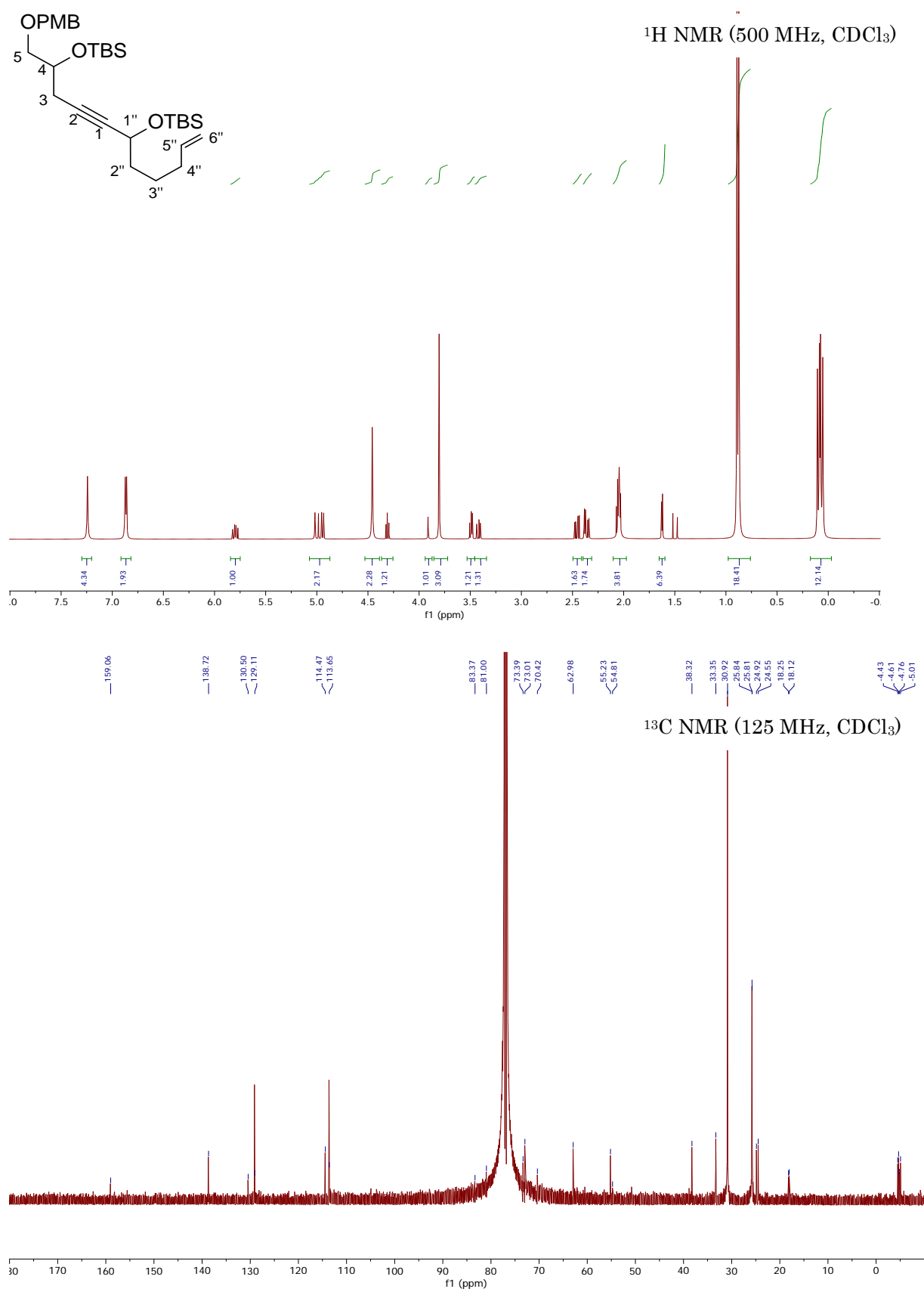
^{31}P NMR (120 MHz, CDCl_3)



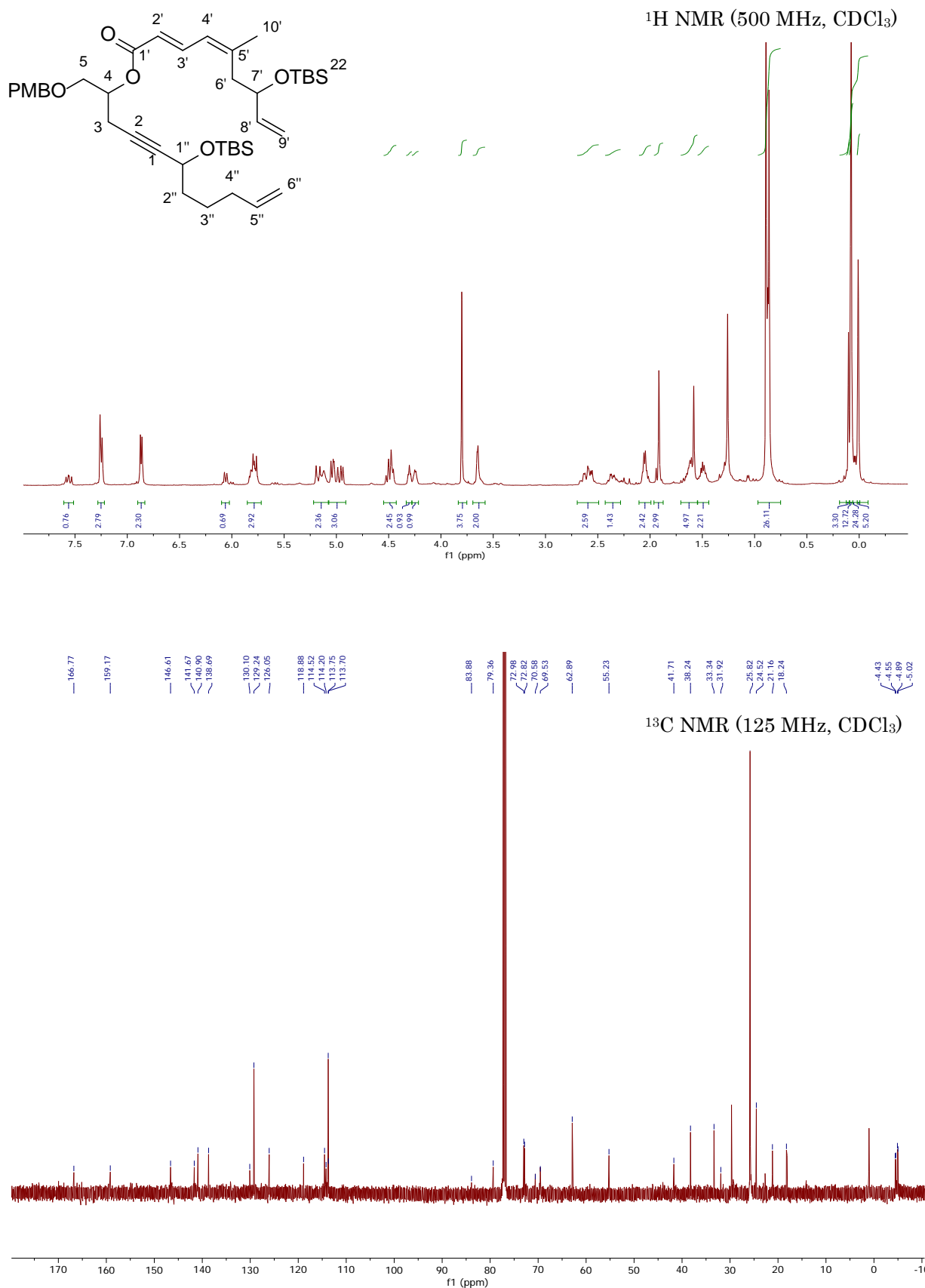
6-((*tert*-Butyldimethylsilyl)oxy)-1-((4-methoxybenzyl)oxy)undec-10-en-4-yn-2-ol - 215



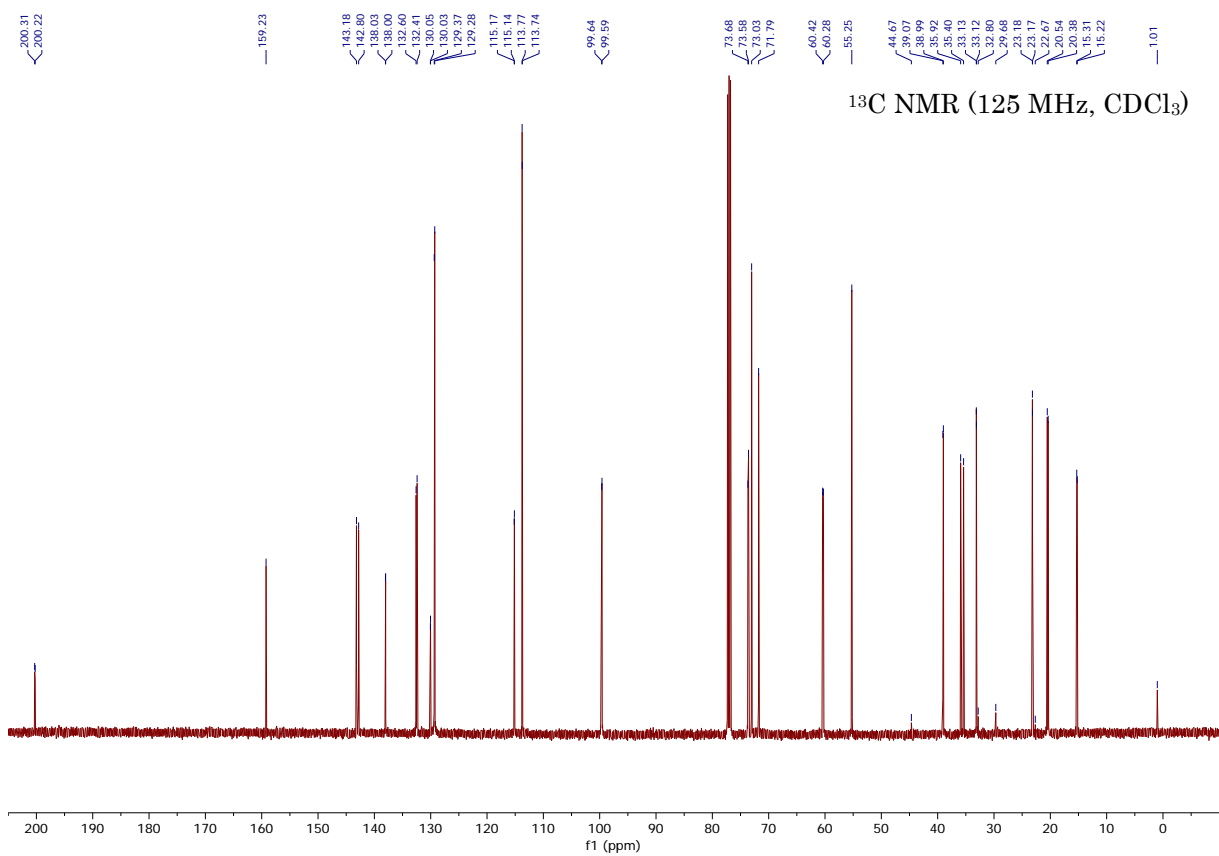
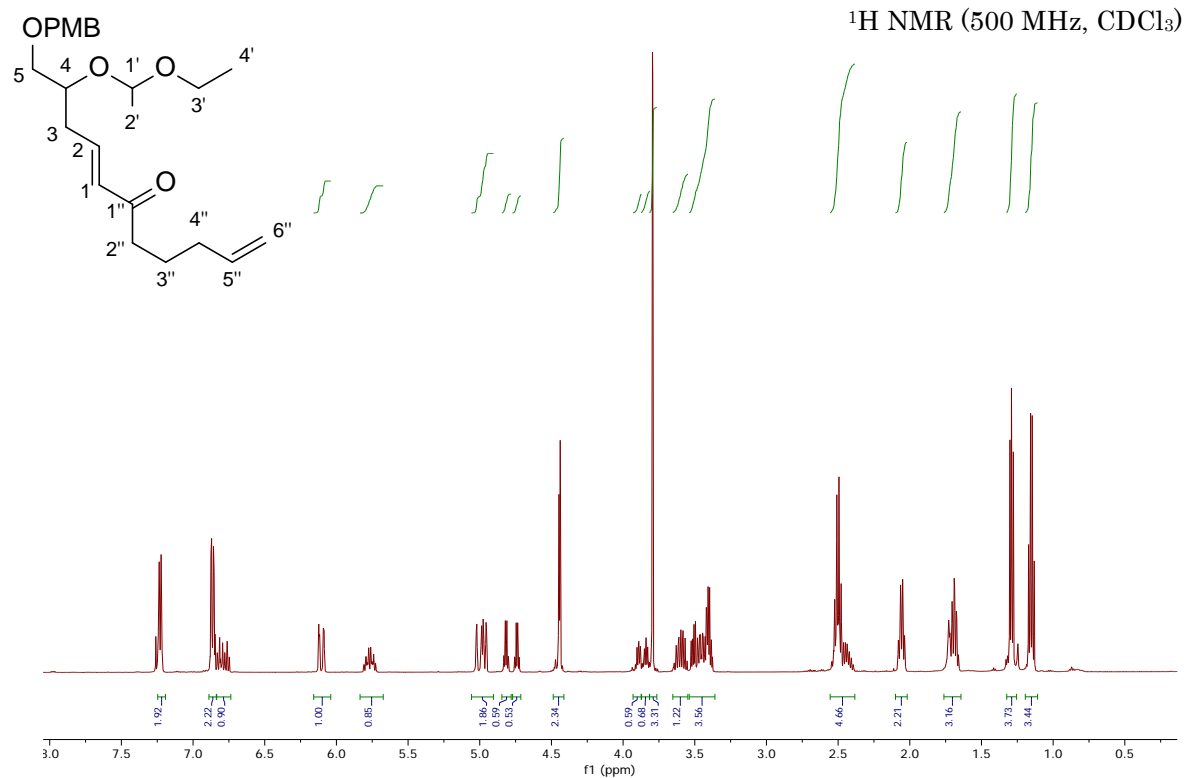
9-(((4-Methoxybenzyl)oxy)methyl)-2,2,3,3,11,11,12,12-octamethyl-5-(pent-4-en-1-yl)-4,10-dioxo-3,11-disilatriscylohex-6-yne - 216



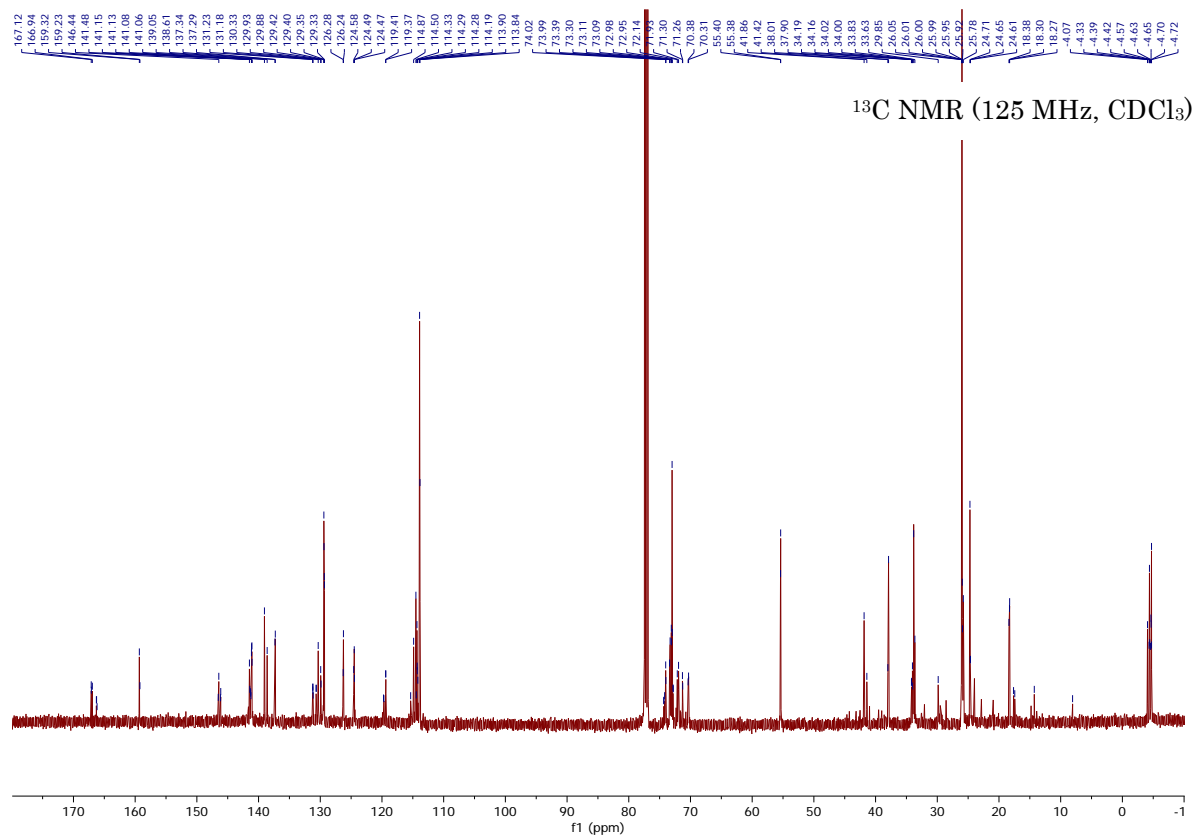
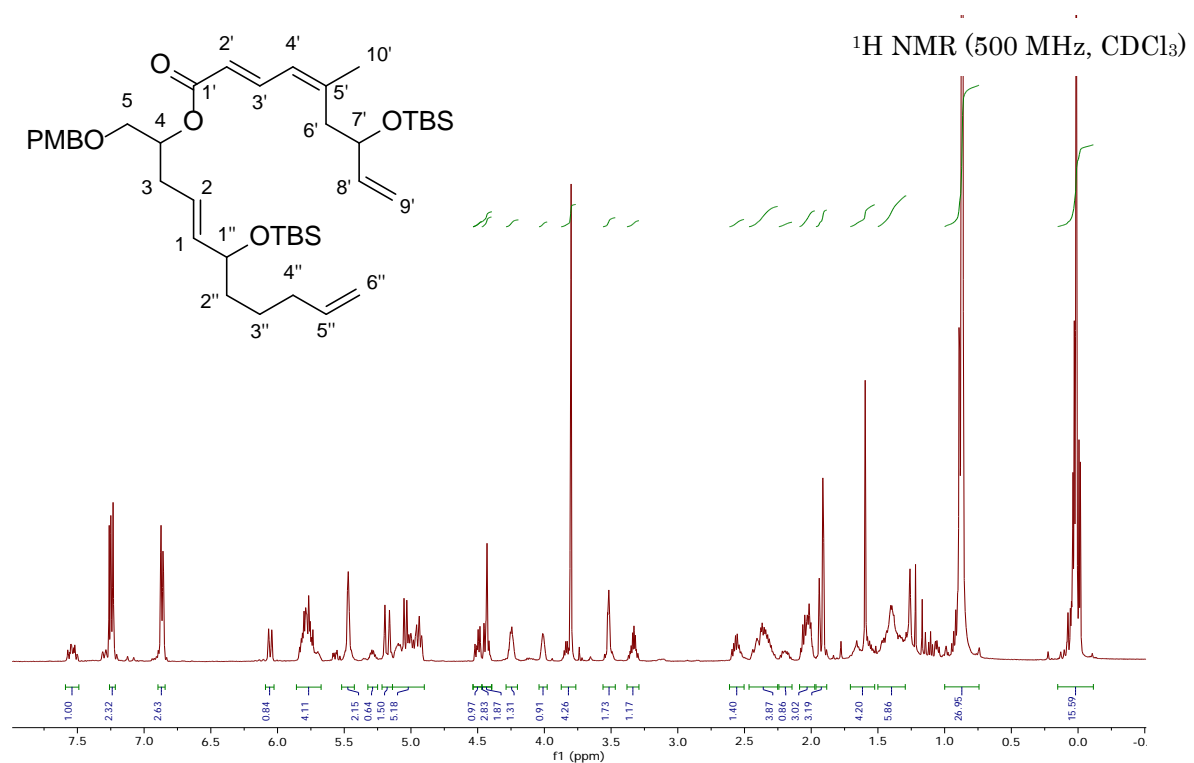
**6-((*tert*-Butyldimethylsilyl)oxy)-1-((4-methoxybenzyl)oxy)undec-10-en-4-yn-2-yl
(2*E*,4*Z*)-7-((*tert*-butyldimethylsilyl)oxy)-5-methylnona-2,4,8-trienoate– 217**



(E)-10-(1-Ethoxyethoxy)-11-((4-methoxybenzyl)oxy)undeca-1,7-dien-6-one – 188



(E)-6-((*tert*-Butyldimethylsilyl)oxy)-1-((4-methoxybenzyl)oxy)undeca-4,10-dien-2-yl (2*E*,4*Z*)-7-((*tert*-butyldimethylsilyl)oxy)-5-methylnona-2,4,8-trienoate – 221



Sophie Geyrhofer, MSc

Chetwode Grove, Wellington 6037, New Zealand

+64 22 150 2781

sophie.geyrhofer@gmail.com

Education

08/2014 – now

PhD Studies in Chemistry at Victoria University of Wellington (VUW)

- Advisor: Dr. Joanne Harvey (Victoria University of Wellington)
- Main focus: Total synthesis of natural products and their analogues, API, purification, spectroscopy, LC-MS
- Title: "Synthesis of New Zampanolide Analogues for SAR studies"

10/2011 – 06/2013

Master's Degree with Distinction in Chemistry at the University of Vienna

- Advisor: Dr. Marko Mihovilovic (Vienna University of Technology, VUT)
- Main focus: Medicinal chemistry, synthetic organic chemistry, purification, spectroscopy, HPLC
- Master's thesis: "Design and Synthesis of a Compound Library Exploiting 5-Methoxyleoligin as Angiogenic Lead Structure"

10/2008 – 07/2011

Bachelor's Degree in Chemistry at the University of Vienna

- Advisor: Emer. Prof. Johann Mulzer (University of Vienna)
- Main focus: Synthetic organic chemistry, natural product synthesis
- Bachelor's thesis: "Synthesis of a building block for total synthesis of Bielschowskysin"

Professional Experience

11/2017 – now

Science Advisor at Medsafe (Ministry of Health), Wellington, New Zealand

- Tasks: Evaluation of New and Changed Medicines Applications, particularly high-risk medicines

01/2015 – 10/2017

Deputy Lab Manager, Organic Synthesis Laboratory at VUW, Wellington, New Zealand (unpaid)

- Tasks: Maintaining a safe working environment, keeping the chemical inventory up to date

03/2015 – 05/2017

Demonstrator in the laboratory courses "Chemical Synthesis" and "Advanced Chemical Synthesis" and tutor in the course "Organic Chemistry" at VUW, Wellington, New Zealand

- Tasks: Supervising students during their laboratory work, teaching them safe working methods, marking reports, clarifying contents of the courses

01/2014 – 07/2014

Intern at Advanced Molecular Technologies Pty Ltd, Melbourne, Australia

- Specialist chemical manufacturer providing products and services to the chemical and pharmaceutical industries
- Tasks: Contract synthesis (mostly organoborons and halides), various purification techniques, routine use of HPLC and NMR for characterization, exact documentation of methods for development and commercialisation of new intellectual property

09/2013 – 12/2013

Intern at King Mongkut's Institute of Technology Ladkrabang, Bangkok, Thailand

- Tasks: Solid-phase synthesis of amide derivatives, supervision of students in a chemistry beginner's laboratory course

10/2012 – 06/2013

Tutor in the laboratory courses "Basics of Chemistry" and "Synthesis" at the Vienna University of Technology, Vienna, Austria

- Tasks: Supervising students during their laboratory work, maintaining a safe laboratory environment, keeping the laboratory clean and tidy

08/2010 – 08/2010

Internship at MA39 (in the chemistry lab of IFUM, laboratory for environmental medicine), Vienna, Austria

- Tasks: chemical and physical analysis, photometric determinations, sampling of ground, bathing and drinking water

Scholarships

08/2017 – 10/2017

Victoria Doctoral Submission Scholarship

08/2014 – 07/2017

Victoria University Doctoral Scholarship

10/2015 – 10/2017

e-fellows.net scholarship

Publications and Conferences

06/2017

Sophie Geyrhofer, Jingjing Wang, Samuel Z. Y. Ting, Joanne Harvey. **Zampanolide as an Anti-Cancer Lead: Towards the Synthesis of Analogs**; Acceptance to present a poster at the 18th Tetrahedron Symposium, Budapest, Hungary

08/2016

Sophie Geyrhofer, Jingjing Wang, Samuel Z. Y. Ting, Joanne Harvey. **Zampanolide as an Anti-Cancer Lead: Towards the Synthesis of "Zampanalogs"**; Lightning talk and poster presented at Queenstown Research Week, Drug Discovery Satellite, Nelson, New Zealand

07/2015

Zampanolide as an anti-cancer lead: towards the synthesis of zampanalogues; Talk presented at Centre for Biodiscovery Symposium, Wellington, New Zealand

- 11/2014 **Co-organiser of the 23rd Massey-Victoria Student Symposium,**
14. November 2014, Victoria University of Wellington
- 09/2014 Thomas Linder, Sophie Geyrhofer, Atanas Atanasov, Verena Dirsch Hermann Stuppner, Michael Schnürch, Marko D. Mihovilovic.
Synthetic Lignans Targeting Cardiovascular Diseases; Poster presented at EFMC XXIII International Symposium on Medicinal Chemistry and the 1st EFMC Young Medicinal Chemist Symposium, Lisbon, Portugal

Skills

Languages	German	Native	
	English	Fluent; IELTS (Academic, overall band score 8.0)	
	French	Good; DELF B2 (Diplôme d'études en langue française)	
Soft Skills	Excellent communication skills (verbal, written, interdisciplinary) Highly adaptable to new working environments Team player with good collaboration skills Self-motivated and driven with excellent time management skills		
Software/IT	MS Office	Symyx	MestreNova
	ChemDraw	Agilent Masshunter	Topspin
	ChemSketch	ACD	Spinworks
	Scifinder	Chromeleon	etc
Other	Driving license (full license for cars, restricted license for motorbikes) Certificate for "Basic Fire Equipment Handling", awarded by Wormald EBC*L (European Business Competence License, A level)		